Forest Science Project
Humboldt State University Foundation, Arcata, CA
(707) 825-7350

7761

The Forest Science Project is a non-profit trust that operates within the Humboldt State University Foundation, a 501C-3 corporation. The Forest Science Project is supported largely by donations from private landowners in Northern California concerned about ecological resources on managed landscapes

Regional Assessment of Stream Temperatures Across Northern California and Their Relationship to Various Landscape-Level and Site-Specific Attributes

by

T.E. Lewis, D.W. Lamphear, D.R. McCanne, A.S. Webb, J.P. Krieter, and W. D. Conroy

Forest Science Project

1 Harpst Street
Humboldt State University
Arcata, CA 95521
(707) 825-7350
(707) 825-7350 (FAX)
fsp@axe.humboldt.edu
http://www.humboldt.edu/~fsp/

About the Forest Science Project

The Forest Science Project was formed by private landowners in Northern California who are concerned about ecological resources on managed lands. The Project is supported largely by donations made by these private landowners. The Forest Science Project is a non-profit trust that operates within the Humboldt State University Foundation, a 501C-3 corporation.

Mission Statement

The Forest Science Project is dedicated to the acquisition, compilation, dissemination, and application of knowledge about the ecological systems in Northern California. The Forest Science Project contributes to a regional understanding of the ongoing processes of forest and habitat management. The Forest Science Project actively participates in regional decision-making regarding the ecological management of natural resources, and promotes a broader awareness of the importance of ecological relationships to human welfare.

ACKNOWLEDGMENTS

Many students at Humboldt State University, who have since moved on to good positions with private, public, and government organizations, contributed their talents in the analyses of the data that have gone into this report. We wish to thank Jason Butcher, Maia Cheli-Colando, Adam Deem, David Gibney, David Jones, Scott Leonard, Paul Meyer, Kareen Moriarty, and Brent Petrzak for their assistance, and wish them great success in their future endeavors.

David Cassell , Jack Lewis, and Trent McDonald provided invaluable statistical support and advice throughout the analyses and modeling of the data. To them we extend our sincere thanks and appreciation.

We greatly appreciate the critical reviews and helpful comments provided by John Bartholow, Alan Herlihy, George Ice, and Kate Sullivan.

We are indebted to Angie Brown for her assistance in technical editing, word processing, and general administrative support during the final stages of document preparation. We sincerely thank Joe Lance for his perseverance in preparing the CD-ROM version of the report.

We thank the Forest Science Project Board of Directors and Technical Committee for helpful suggestions and comments throughout the development of this regional stream temperature assessment.

We are grateful to the various organizations and individuals that were willing to provide data and collect additional information for this assessment. Without their generous contribution of both time and data, this report would not have been possible.

DISCLAIMER

The opinions, findings, conclusions, or recommendations expressed in this report are those of the authors and do not necessarily reflect the views of any data contributors, participants in, or committees of, the Forest Science Project. Mention of trade names or commercial products does not constitute endorsement or recommendation for use by the Forest Science Project.

Cite this report as:

T.E. Lewis, D.W. Lamphear, D.R. McCanne, A.S. Webb, J.P. Krieter, and W. D. Conroy. 2000. *Regional Assessment of Stream Temperatures Across Northern California and Their Relationship to Various Landscape-Level and Site-Specific Attributes*. Forest Science Project. Humboldt State University Foundation, Arcata, CA. 420 pp.

Table of Contents

Chapter 5 - Air and Water Temperature Relationships

Chapter 6 - Geographic Position and Stream Temperatures

Chapter 7 - Watershed Position and Stream Temperature

Chapter 8 - Influence of Site-Specific Attributes on Stream Temperature

Chapter 9 - Influence of Canopy on Stream Temperature

Chapter 10 - Empirical Modeling of Regional Stream Temperatures

Chapter 11 - Historical Perspectives

List of Figures

Chapter 1 - Introduction

Chapter 2 - Methods

Chapter 3 - Summary of the Statistical Attributes of Regional Stream Temperatures

Chapter 4 - Air Temperature

Chapter 5 - Air and Water Temperature Relationships

Chapter 6 - Geographic Position and Stream Temperatures

Chapter 7. Watershed Position and Stream Temperatures

Chapter 8. Influence of Site-Specific Attributes on Stream Temperature

Chapter 9. Influence of Canopy on Stream Temperature

Chapter 11 - Historical Perspectives

Appendix A - Chapter 2: Methods

Appendix B - Chapter 3: Summary of the Statistical Attributes of Regional Stream Temperatures

Appendix C - Chapter 5: Air and Water Temperature Relationships

Appendix D - Chapter 7: Watershed Position and Stream Temperature

Appendix E - Chapter 8: Influence of Site-Specific Attributes on Stream Temperature

List of Tables

Chapter 1 - Introduction

Chapter 2 - Methods

Chapter 4 - Air Temperature

Chapter 5 - Air and Water Temperature Relationships

Chapter 7 - Watershed Position and Stream Temperature

Chapter 8 - Influence of Site-Specific Attributes on Stream Temperatures

Chapter 9 - Influence of Canopy of Stream Temperatures

Chapter 10 - Empirical Modeling of Regional Stream Temperatures

Chapter 11 - Historical Perspectives

Appendix A - Chapter 2: Methods

Appendix B: Summary of the Statistical Attributes of Regional Stream Temperatures

Conversion Tables

Degrees Celsius to Degrees Fahrenheit: $°C = (5/9)(°F - 32)$

Degrees Fahrenheit to Degrees Celsius: $°F = (9/5)(°C) + 32$

Multiply Metric Units	BY	To Obtain English Units
Meters (m)	3.2839895	Feet (ft)
Meters (m)	0.0006213711922	Miles (mi)
Kilometers (km)	0.6213711922	Miles (mi)
Kilometers (km)	3280.839895	Feet (ft)
Square Meters (m^2)	0.0002471054	Acres (ac)
Square Meters (m^2)	0.0000003861003	Square Miles (mi^2)
Hectares (ha)	2.471054073	Acres (ac)
Hectares (ha)	0.00386107925111652	Square Miles (mi^2)
Hectares (ha)	107639.1042	Square Feet (ft^2)

List of Acronyms and Abbreviations

AE	Agriculture Exclusive
AFLUX	Average Diurnal Fluctuation
AOI	Area of Interest
AML	Arc Macro Language
AVGMAX	30-Year Average Maximum Monthly Air Temperature
CC	Coastal California (ESU)
CDF	Cumulative Distribution Function
CIMIS	California Irrigation Management Information System
cms	Cubic meters per second
CSP	California Coastal Steppe Province
DEM	Digital Elevation Model
DLG	Digital Line Graph
DRG	Digital Raster Graphic
DTF	Data Transfer Format
EPA	U.S. Environmental Protection Agency
ESRI	Earth Systems Research Institute
ESU	Evolutionarily Significant Unit
FFFC	Fish, Farm, and Forest Communities Forum
FSP	Forest Science Project
FTP	File Transfer Protocol
GIS	Geographic Information System
HUC	Hydrological Unit
IY1DI	Lowest Daily Minimum Temperature
LOGBFM	log10 Bankfull Width (meters)
LOGWA	log10 Watershed Area (hectares)
MWAT	Maximum Weekly Average Temperature
NOAA	National Oceanic and Atmospheric Administration
NRM	Natural Resource Management Corporation
OT	Optimal Growth Temperature
PG&E	Pacific Gas and Electric Company
PRISM	Parameter-Elevation Regressions on Independent Slopes Model
RCD	Resource Conservation District
SAS	Statistical Analysis System
SONCC	Southern Oregon Northern Coastal California
SQL	Structured Query Language
SSP	California Sierran Steppe-Mixed Forest-Coniferous Forest Province
STORET	U.S. Environmental Protection Agency's database of water quality information
SUMDEG24	Sum of Degrees over 24°C
SUMT24	Total Time Spent Above 24°C
TMDL	Total Maximum Daily Load
TPZ	Timber Protection Zone
UCIPM	University of California Statewide Integrated Pest Management Project
ULIT	Upper Lethal Incipient Temperature
USDA	United States Department of Agriculture
USGS	United States Geological Survey
UTM	Universal Transverse Mercator
W:A_RATIO	Water-to-Air Temperature Ratio
WRCC	Western Regional Climate Center
WSO	National Weather Service Office
XYA7DA	Highest Seven-Day Moving Average of the Daily Average

XYA7DX	Highest Seven-Day Moving Average of the Daily Maximum
XY1DX	Highest Daily Maximum Temperature
ZCI	Zone of Coastal Influence

EXECUTIVE SUMMARY

INTRODUCTION

Stream temperature has been and continues to be a concern in watersheds throughout Northern California. There has been heightened interest in the potential effects of altered stream temperatures on salmonids and other aquatic riparian species. Several regulatory measures have been promulgated to mitigate potential impacts of increased water temperatures on aquatic biota. Restoration activities have been initiated, conservation measures developed, and land use practices altered in an attempt to counteract possible alterations in stream temperatures throughout the state of California and the Pacific Northwest. Land stewards in the private and public sector have been gathering temperature data for several years. With the onset of continuous temperature sensor technology, large volumes of stream temperature data are now being assembled and analyzed. More and more state and federal agencies and private landowners are choosing continuous stream temperature monitoring devices over thermometers because of the need for diurnal and seasonal water temperature data.

Stream temperature is an important factor in aquatic ecosystems for several reasons. Water temperature directly and indirectly influences fish physiology and behavior in several ways:

- Metabolism
- Food requirements, appetite, and digestion rates
- Growth rates
- Developmental rates of embryos and alevins
- Timing of life-history events, including adult migrations, fry emergence, and smoltification
- Competitor and predator-prey interactions
- Disease-host and parasite-host relationships

Stream temperature may also influence other aquatic and riparian species such as reptiles, amphibians, and macroinvertebrates. Collection of stream temperature data is driven largely by the concern for aquatic biological resource protection. Monitoring of stream temperature to assess diurnal and seasonal variation is a prerequsite to assessing potential acute and chronic thermal impacts to aquatic biota. The seasonality of life histories of the species of interest must also be considered when monitoring stream temperatures. Thus, monitoring that captures the temporal trends in stream temperature is needed to assess thermal exposures of different life stages.

BACKGROUND

With the onset of continuous temperature sensor technology, large volumes of stream temperature data are available and are continuing to be gathered. Despite the hundreds of gigabytes of stream temperature data collected by various groups and agencies throughout the state, no regional synthesis and assessment of these data has been published and no clear understanding of temperature regimes and their association with land use practices exists. This regional stream temperature assessment focuses on a well-defined geographic area of interest (AOI), namely the California portion of the Southern Oregon Northern Coastal California (SONCC) and the Central California (CC) evolutionarily significant units (ESUs) for coho salmon (*Oncorhynchus kisutch*). It is unknown whether all streams in the AOI are temperature sensitive in relation to the California Forest Practice Rules or other pertinent land management treatments (i.e., Northwest Forest Plan). To identify sensitive streams in the AOI, characterization of

stream temperature regimes in the various watersheds, basins, and ecoregions comprising the AOI is essential. A characterization of contemporary thermal regimes across a broad geographic area was the primary goal of the Forest Science Project's regional stream temperature assessment.

State and federal agencies are lacking information on what range of stream temperatures are physically achievable in a stream reach, watershed, or basin, given the prevailing management prescriptions and climatic conditions. Provided with this information, agencies would be better able to (1) set reach- or watershed-specific temperature standards that are scientifically defensible, (2) assess the relative contributions of natural and human-induced factors to non-attainment of stream temperature standards, (3) identify and prioritize stream reaches that are grossly out of compliance and most in need of remediation, and (4) establish realistically attainable temperature-reduction goals for streams, watersheds, and basins that have naturally high water temperatures. The Forest Science Project's regional stream temperature assessment provides agencies, land stewards, and landowners with the information needed to make important decisions regarding adaptive management, remedial measures, and restoration goals.

SCOPE

The watersheds and basins within the California portion of the SONCC and Central California ESUs were defined as the geographic AOI. This area extends from the Oregon border south to San Francisco and eastward to the Central Valley.

This assessment report is based on data gathered by numerous private landowners, and various state and federal agencies. Land stewards that submitted data for the assessment collected stream temperature data under a multitude of objectives and assumptions. These diverse objectives can be grouped into three broad categories:

- Pre- and post-timber harvest plan monitoring
- Thermal reach monitoring
- Characterization of thermal refugia

Forest Science Project cooperators and other parties that submitted stream temperature data can be characterized as forested landowners and stewards. Therefore, the population of stream temperature monitoring locations all fell in predominately forested catchments or on lands zoned as Timber Protection Zone (TPZ) or Agriculture Exclusive (AE). Data from both private landowners and public resource management agencies were acquired. Thus, the land management prescriptions were dependent upon whether monitored streams were on private or public lands. Stream temperature records from 1087 sites spanning nine years were assembled and analyzed. Not all sites were monitored every year. Predominantly, results from analyses of 1998 data were included in the various chapters found in this report since 1998 was the most complete data set with which to work.

The assessment was restricted to data collected using continuous sensor technology. Snapshot (synoptic) data using hand-held thermometers or min-max thermometers were not included in statistical analyses in the regional assessment. Some synoptic data were used in qualitative comparisons of contemporary to historical stream temperatures. Hourly (or other time interval) data from continuous sensors were obtained from the various data contributors. Data that were aggregated to a particular temporal or spatial level prior to submission to the Forest Science Project were not used due to potential differences in statistical analytical procedures and aggregation approaches. Consistent data verification, validation, and spatial and temporal aggregation were deemed critical for increasing the likelihood of data comparability for statistical comparisons (i.e., comparing apples with apples).

The amount of site-specific information provided by data contributors was limited. In some instances, analyses on a reduced subset of the data were performed to explore important site-level or landscape-level relationships. In such

cases, the number of sites and their geographic distribution are illustrated for evaluation. In some instances, Geographic Information System (GIS)-derived data (e.g., elevation, distance to coast) or regional data (e.g., air temperature, flow, degree day) were used to perform analyses. As mentioned previously, 1998 had the most complete data set in terms of stream temperature and site-specific attribute data. Thus, many of the analyses presented in the report are based on 1998 data.

The majority of data contributors collected stream temperature data during the summer months (June through September). Some investigators allowed temperature recorders to remain in the stream for longer or shorter periods of time. Inasmuch as the preponderance of data was gathered during the summer season, the assessment report focused on summertime stream temperatures. The juvenile life stage of coho salmon and other anadromous species is the stage most commonly encountered during the summer. Thus, the report places stream temperature analyses in the context of potential thermal stress on summer juvenile coho salmon primarily, with some reference to other anadromous juvenile salmonids. This is not to imply that adult stages of various species are not present in the stream systems in the AOI during the summer months, e.g., chinook salmon and steelhead trout. However, juvenile stages are known to be the most sensitive to thermal stress, hence the reason for this focus.

OBJECTIVES

The objectives of this stream temperature assessment report were:

1. Compile available stream temperature data in a verified and validated database for purposes of regional assessment
2. Assess status and trends in stream temperatures across the region
3. Evaluate the influence of regional scale factors (e.g., climate, geographic location, watershed position, etc.) and site-specific factors (e.g., canopy closure, channel orientation, etc.) on status and trends in stream temperatures
4. Through the assessment process identify areas where improvements in existing protocols and analysis and synthesis are needed
5. Identify knowledge gaps in site-specific information that should be collected on a routine basis to improve our assessment capabilities and move us closer to a regional stream temperature sampling design
6. Identify knowledge gaps between stream temperature monitoring and information on the distribution of coho salmon and other aquatic species

SIGNIFICANT FINDINGS

A single stream temperature standard is difficult to apply across a broad region, such as the entire range of the coho salmon in Northern California, because streams differ markedly in size, drainage area, elevation, geographical location, prevailing climatic conditions, aspect, riparian vegetation, etc. These factors act directly or indirectly to influence water temperature by affecting the degree of shading or the ambient climatic conditions (air temperature, humidity, and solar radiation). For example, maximum water temperatures would be expected to differ markedly

between a wide, low-altitude, near-coastal stream in Southern Humboldt County as compared to a narrow, well-shaded mountain stream in northeastern California. Streams in diverse settings behave very differently, and temperature standards, whether narrative or numeric, should reflect those differences.

Regional Trends in Air Temperature (Chapter 4)

Air temperature is known to have a significant influence on stream temperatures. Bartholow (1989) and Sinokrot and Stefan (1994) ranked air temperature as the single most important parameter for predicting water temperature, followed by solar radiation. Most stream temperature models use air temperature as a driver to predict temporal change in water temperature. To determine the effects of air temperatures on mean stream temperature, acquisition of ***local*** air temperatures is particularly important. If one uses remote or approximate air temperature data, then one can only hope for remote or approximate stream temperature predictions.

Air temperatures did not follow expected adiabatic cooling trends across the entire study area. Near the coast, air temperature was more a function of distance from the coast rather than elevation. In the interior portion of the study area air temperatures follow the more expected trend: decreasing air temperature with increasing elevation. The relationship between air temperature and the two independent variables, distance from the coast and elevation varied seasonally. During the winter months air temperatures in the coastal portion of the study area conformed more to the expected negative relationship with elevation.

In addition to yearly data acquired from 72 remote air sites, 30-year long-term regional air temperature data were acquired from the Oregon State University Climate Analysis Service and the Oregon Climate Service at Oregon State University. These data were developed using PRISM (**P**arameter-**e**levation **R**egressions on **I**ndependent **S**lopes **M**odel). PRISM is a climate analysis system that uses point data, a digital elevation model (DEM), and other spatial datasets to generate gridded estimates of annual, monthly and event-based climatic parameters.

Examination of 30-year long-term average PRISM air temperature data revealed that air temperatures exhibit appreciable gradients within and across U.S. Geological Survey hydrologic units (HUCs) that comprise the range of the coho salmon in Northern California. Hydrologic units that are predominantly coastal have cooler air temperatures whereas those that have a somewhat southeasterly to northwesterly orientation show strong thermal gradients. Some HUCs are 10°C to 15°C warmer in the upper reaches than near the coast. Interior HUCs have warmer air temperatures throughout the drainage, with cooler air temperatures at higher elevations.

PRISM air temperature data sets were used to develop a relationship between the 30-year average maximum monthly air temperature (AVGMAX) and the inland extent of the coastal effect. The zone of coastal influence (ZCI) was derived from 30-year long-term PRISM air temperature data by defining the steepest rate of change in air temperature along transects at increasing distances from the coast. The ZCI is an approximation of the fog zone, which intuitively would have a cooling influence on water temperatures due to its associated cooler air temperatures and solar energy interception. Using the ZCI as a spatial coverage, stream temperature monitoring sites were stratified by whether they were inside or outside of the ZCI.

Spatial trends in air temperatures across the region must be understood in order to predict their influence on water temperatures. A useful air temperature database has been developed to characterize air temperature regimes across Northern California. In the future, acquisition of the monthly average PRISM air temperature data for individual water temperature years will greatly improve our understanding of the role air temperature plays in influencing water temperatures at large spatial scales.

Air and Water Temperature Relationships (Chapter 5)

Nearest-neighbor air stations were identified using a 12-dimensional Euclidian distance model. Air temperatures from these nearest-neighbor air stations, referred to as macroair temperatures, were found to show some correlation with water temperatures at a regional scale. Monthly minimum water temperatures were greater than monthly minimum macroair temperatures at most sites. Conversely, monthly maximum water temperatures were usually lower than monthly maximum macroair temperatures. Monthly mean water temperatures in the interior ecoprovince varied more closely with monthly mean macroair temperatures than water temperatures in the coastal ecoprovince.

The water-to-air temperature ratio increased with increasing distance from the watershed divide. The divide distance at which the ratio began to exceed unity varied by HUC, but generally fell between 6 km and 10 km. HUCs with tributaries that originate in the warm interior portions of the study area and drain into the zone of coastal influence exhibited greater numbers of sites with water-to-air ratios greater than one. HUCs that lie entirely within the interior portion of the study area exhibited fewer sites with water-to-air temperature ratios exceeding one.

The assessment report explores the correlations between water temperature and air temperatures measured at stream-side (microair) and at remote air monitoring sites (macroair).

Geographic Position and Stream Temperature (Chapter 6)

Stream temperatures across Northern California vary with geographic position. The variation in water temperature with respect to distance from the coast, UTM y-coordinate (a surrogate for latitude), ecoprovince, zone of coastal influence, and elevation was large for the highest 1998 values of the daily maximum (XY1DX) and the seven-day moving average of the daily average (XYA7DA) and daily maximum (XYA7DX) stream temperatures. Variation in lowest daily minimum temperature (IY1DI) in relation to various geographic position factors was not as great, with much clearer trends discernable. Geographic position factors are largely surrogates for air temperature. Since the daily minimum temperature, in this case the lowest 1998 daily minimum observed at each site, occurs at the time when solar radiation is absent, the reduced scatter in IY1DI values suggests that air temperature may be asserting more influence on this stream temperature metric than on those metrics that have more of a solar-heating and daily-maximum-air-temperature component. While air temperature is known to influence water temperatures, the large variation observed for XY1DX, XYA7DA, and XYA7DX suggests that other factors are important in explaining the observed variability across the region. These factors include canopy closure, watershed area, distance from the watershed divide, flow, gradient, and channel orientation.

Watershed Position and Stream Temperature (Chapter 7)

Water temperatures have a tendency to increase with increasing distance from the watershed divide and with increasing drainage area. Water temperature near the source is the coolest, normally close to groundwater temperature. Groundwater temperature is typically within 1 °C to 3 °C of mean annual air temperature. Using PRISM 30-year long-term air temperature data, the 30-year mean annual air temperature was computed at 4-km grid resolution. Mean annual air temperatures can serve as estimates of groundwater temperature throughout HUCs that comprise the range of the coho salmon in Northern California. Since groundwater temperatures vary with air temperature, large variability is also exhibited in estimated groundwater temperatures.

In some HUCs, estimated groundwater temperatures are within a few degrees of the maximum weekly average temperature (MWAT) threshold. Some headwater streams may originate in areas with warm groundwater temperatures. Well monitoring data is being acquired by the Forest Science Project to assess the accuracy of groundwater temperatures estimated from PRISM air temperature data.

Fourteen HUCs contained sufficient numbers of stream temperature monitoring sites to characterize the change in water temperature with watershed position. All HUCs exhibited a trend of increasing water temperature with increases in both watershed area and distance from the watershed divide. Streams that drain HUCs that are predominantly situated inland (i.e., away from the zone of coastal influence) showed much greater increases in stream temperature with increasing watershed area and divide distance.

Influence of Site-Specific Attributes on Stream Temperature (Chapter 8)

Channel Orientation

With an understanding of the hydrology and basin characteristics of Northern California it was not surprising to find that there were fewer streams in the 0° to 90° and 90° to 180° orientation classes. These are streams with northerly-to-northeasterly and southeasterly-to-southerly flows, respectively.

Graphical and statistical evaluations of the relationship between the highest 1998 daily maximum stream temperature (XY1DX) and the daily maximum on 26 June 1998 and channel orientation showed slight, albeit not significant, differences between channel orientation classes. Examination of canopy closure in relation to channel orientation did not show any significant differences between channel orientation class within each canopy class. Average daily maxima were slightly lower in the east-west orientation class for intermediate canopy classes, although they were not significantly different from the north-south orientation class.

Given all the other factors (e.g., canopy, air temperature) that have been shown to influence various stream temperatures metrics, such as the highest daily maximum, channel orientation appears to play a minor role. Due to a lack of significance in the interaction between canopy class and channel orientation, special canopy retention levels for certain channel orientations may not be warranted. However, GIS-derived channel orientation estimates may not be completely representative of the orientation of the entire stream reach.

All sites in our regional stream temperature analysis contained non-missing values for channel orientation due to our ability to derive this attribute in GIS. However, out of 548 sites with water temperature data available for regional analyses in 1998, only 207 of these were accompanied by canopy data. There was an even greater paucity of canopy data in years prior to 1998. Null data were a great impediment to our ability to discern regional status and trends in stream temperatures and the factors that control them. A statistically valid sampling design coupled with canopy measurements collected using a consistent protocol is needed to better address the interaction between channel orientation, canopy, and stream temperature.

Channel Gradient

There was a decreasing trend in water temperature with increasing gradient. This trend may have several underlying mechanisms. Generally, as gradient increases the distance from the watershed divide and drainage area decreases. Stream temperatures are expected to be cooler closer to the headwaters. Streams become narrower at higher gradients, thereby making riparian vegetation more effective in providing shade.

Habitat Type

While the Forest Science Project Stream Temperature Protocol (found in the Appendix of the full report) calls for placement of temperature sensors in well-mixed habitats, e.g., riffles and runs, many data contributors placed their sensors in pools. There was no overriding sampling design. Each organization had their own objectives for monitoring temperature, which often included characterization of the extent of cold water refugia. In 1998, temperature sensors were about equally divided into pools and riffles/runs. Generally, pools were cooler than

riffles runs. Statistical analysis revealed that shallow, medium, and deep pools could be combined, as well as riffles and runs, for subsequent modeling.

Influence of Canopy on Stream Temperatures (Chapter 9)

Canopy has been widely acknowledged as influencing stream temperature. It has been shown that forest harvesting or road building that removes riparian vegetation (canopy) increases the water temperature of the adjacent stream. In a comparison of stream temperature models by Washington's Timber, Fish, and Wildlife found that canopy, in some form, was included in all but one of the six stream temperature models that were evaluated.

Some cooperators estimated canopy closure optically. A canopy closure computer-generated card was provided to cooperators for use in 1998 in an attempt to increase the number of sites with non-null canopy values. The card served to calibrate the eye to different canopy levels. The card presented canopy closure in 10% increments, in three different crown geometries. The field person could visually match the canopy closure observed overhead to the nearest canopy closure image on the card.

Sullivan and coworkers (1991) developed the concept of *threshold distance*, that is the distance from the watershed divide at which streams become too wide for riparian vegetation to provide adequate shading. They found that streams seemed to reach an equilibrium temperature at approximately 40-50 km from the watershed divide. At this point, stream temperature was more a function of air temperature than canopy cover. This theoretical threshold distance is a function of stream width and riparian vegetation. Thus, the threshold distance will be different for different drainages and no single value should be applied to all streams.

The threshold distance concept was explored empirically using data gathered on streams throughout Northern California. At a divide distance greater than 70 km, there were no reported canopy closure values greater than 30%, and most were 10% or less. This suggests that 70 km may be the distance from the divide where streams become too wide for stream-side vegetation to have an effect on shading. However, the data were from many basins. Thus, this distance is considered the theoretical maximum threshold distance. The threshold distance for some basins may be less than the theoretical 70-km threshold. The lack of higher canopy values at distances greater than 70 km from the watershed divide may be a result of relatively few canopy closure measurements at greater distances from the divide and the lack of a sampling design. If a curve is fit to the outer most points, representing the maximum canopy closure potential for a given distance from watershed divide, a threshold distance becomes much more difficult to define.

A similar analysis was performed for canopy versus watershed area. Sites with watershed areas of approximately 63,000 ha (~243 sq. mi.) or larger had canopy closure values less than 20%.

There was a trend in higher canopy values or classes resulting in lower stream temperatures, even though the correlation was not high. Much of the variability will be taken into account by other variables that are explored in the stream temperature modeling chapter (Chapter 10).

Stream Temperature Empirical Modeling (Chapter 10)

The assessment report presents results of multivariate linear regression modeling development. Models were developed for all sites combined and for each ecoprovince. Backward selection was used in model development and Akaike's Information Criterion was used to select the model (using 1998 data) which contained the most information. Independent variables that proved to be highly influential on stream temperature throughout the preceding chapters were also found to be highly significant in empirical models.

Historical Perspectives (Chapter 11)

Historical stream temperature data were acquired from various sources: USGS, California Fish and Game Administrative Reports, the Pacific Gas and Electric's Potter Valley Project. More contemporary FSP sites were spatially matched with historical sites for comparisons. Unfortunately, most of the historical sites were located on mainstem systems. However, very interesting trends were found.

USEFUL TOOLS

In the appendixes of this report can be found many useful tools for collecting, processing, and analyzing stream temperature data. Arc macro language (AML) and Avenue script code are provided for deriving various site attributes. These can be adapted to meet individual analytical needs. The FSP's regional stream temperature protocol, field forms, and data formatting guidelines are including to assist other organizations in designing a stream temperature monitoring program.

Chapter 1

INTRODUCTION

Stream temperature has been and continues to be of concern in watersheds throughout Northern California. There has been a heightened interest in the potential effects of altered stream temperatures on salmonids and other aquatic/riparian species. Several regulatory measures have been promulgated to mitigate impacts of increased water temperatures on aquatic biota. Restoration activities have been initiated, conservation measures developed, and land use practices altered to minimize potential alterations in stream temperatures throughout the state of California and the Pacific Northwest. Land stewards in the private and public sector have been gathering temperature data for several years. With the onset of continuous temperature sensor technology, large volumes of stream temperature data are now being assembled and analyzed. More and more state and federal agencies and private landowners are choosing continuous stream temperature monitoring devices over thermometers because of the need for diurnal and seasonal water temperature data.

Stream temperature is an important factor in aquatic ecosystems for several reasons. Water temperature directly and indirectly influences fish physiology and behavior in several ways (Spence et al., 1996):

- Metabolism
- Food requirements, appetite, and digestion rates
- Growth rates
- Developmental rates of embryos and alevins
- Timing of life-history events, including adult migrations, fry emergence, and smoltification
- Competitor and predator-prey interactions
- Disease-host and parasite-host relationships

Stream temperature may also influence other aquatic and riparian species such as reptiles, amphibians, and macroinvertebrates. Collection of stream temperature data is driven largely by the concern for aquatic biological resource protection. Monitoring of stream temperature to assess diurnal and seasonal variation is a prerequisite to assessing potential acute and chronic thermal impacts to aquatic biota. The seasonality of life histories of the species of interest must also be considered when monitoring stream temperatures. Thus, monitoring that captures the temporal trends in stream temperature is needed to assess thermal exposures of different life stages.

Background

With the onset of continuous temperature sensor technology, large volumes of stream temperature data are available and are continuing to be gathered. Despite the hundreds of gigabytes of stream temperature data collected by various groups and agencies throughout California, no regional synthesis and assessment of these data has been published and no clear understanding of temperature regimes and their association with natural resource management exists. This regional stream temperature assessment focuses on a well defined geographic area of interest (AOI), namely the California portion of the Southern Oregon Northern Coastal California (SONCC) and the Central California (CC) evolutionarily significant units (ESUs) for coho salmon (*Oncorhynchus kisutch*). It is unknown whether all streams in the AOI are temperature sensitive in relation to the California Forest Practice Rules or other pertinent land management treatments (i.e., Northwest Forest Plan).

To identify sensitive streams in the AOI, characterization of stream temperature regimes in the various watersheds, basins, and ecoregions comprising the AOI is essential. A characterization of contemporary thermal regimes across a broad geographic area was the primary goal of the Forest Science Project's regional stream temperature assessment.

State and federal agencies are lacking information on what range of stream temperatures are physically achievable in a stream reach, watershed, or basin, given the prevailing management prescriptions and climatic conditions. Provided with this information, agencies would be able to (1) set reach- or watershed-specific temperature standards that are scientifically defensible, (2) assess the relative contributions of natural and human-induced factors to non-attainment of stream temperature standards, (3) identify and prioritize stream reaches that are grossly out of compliance and most in need of remediation, and (4) establish realistically attainable temperature-reduction goals for streams, watersheds, and basins that may have naturally high water temperatures. The Forest Science Project's regional stream temperature assessment provides agencies, land stewards, and landowners with the information needed to make important decisions regarding adaptive management, remedial measures, and restoration goals.

Scope

The watersheds and basins within the California portion of the SONCC and Central California ESUs were defined as the geographic area of interest. This area extends from the Oregon border south to San Francisco and eastward to the Central Valley (Figure 1.1).

This assessment report is based on data gathered by numerous private landowners, and various state and federal agencies. Approximately 1100 sites with stream temperature records spanning nine years were assembled and analyzed. Predominantly, results from analyses of 1998 data are included in the various chapters found in this report since 1998 was the most complete data set with which to work.

The assessment is restricted to data collected using continuous sensor technology. Snapshot (synoptic) data using hand-held thermometers or min-max thermometers were not included in statistical analyses in the regional assessment. Some synoptic data were used in qualitative comparisons of recent stream temperatures to historical stream temperatures. Hourly (or other time interval) data from continuous sensors were obtained from the various data contributors. Data that were aggregated to a particular temporal or spatial level prior to submission to the Forest Science Project were not used due to potential differences in statistical analytical procedures and aggregation approaches. Consistent data verification, validation, and spatial and temporal aggregation were deemed critical for increasing the likelihood of data comparability for statistical comparisons (i.e., comparing apples with apples).

The amount of site-specific information provided by data contributors was limited. In some instances, analyses on a reduced subset of the data were performed to explore important site-level or landscape-level relationships. In such cases, the number of sites and their geographic distribution are illustrated for evaluation. In some instances, Geographic Information System (GIS)-derived (e.g., elevation, distance to coast) or regional data (e.g., air temperature, flow, degree day) were used to perform analyses. As mentioned previously, 1998 had the most complete data set in terms of stream temperature and site-specific attribute data. Thus, many of the analyses presented in the report are based on 1998 data.

The majority of data contributors collected stream temperature data during the summer months (June through September). Some investigators allowed temperature recorders to remain in the stream for longer or shorter periods of time. Inasmuch as the preponderance of data was gathered during the summer season, the assessment report focused on summertime stream temperatures. The juvenile life stage of coho salmon and other anadromous species is the stage most commonly encountered during the summer. Thus, the report places stream temperature analyses in the context of potential thermal stress on summer juveniles of coho salmon primarily, with some reference to other anadromous juvenile salmonids. This is not to imply that juvenile and adult

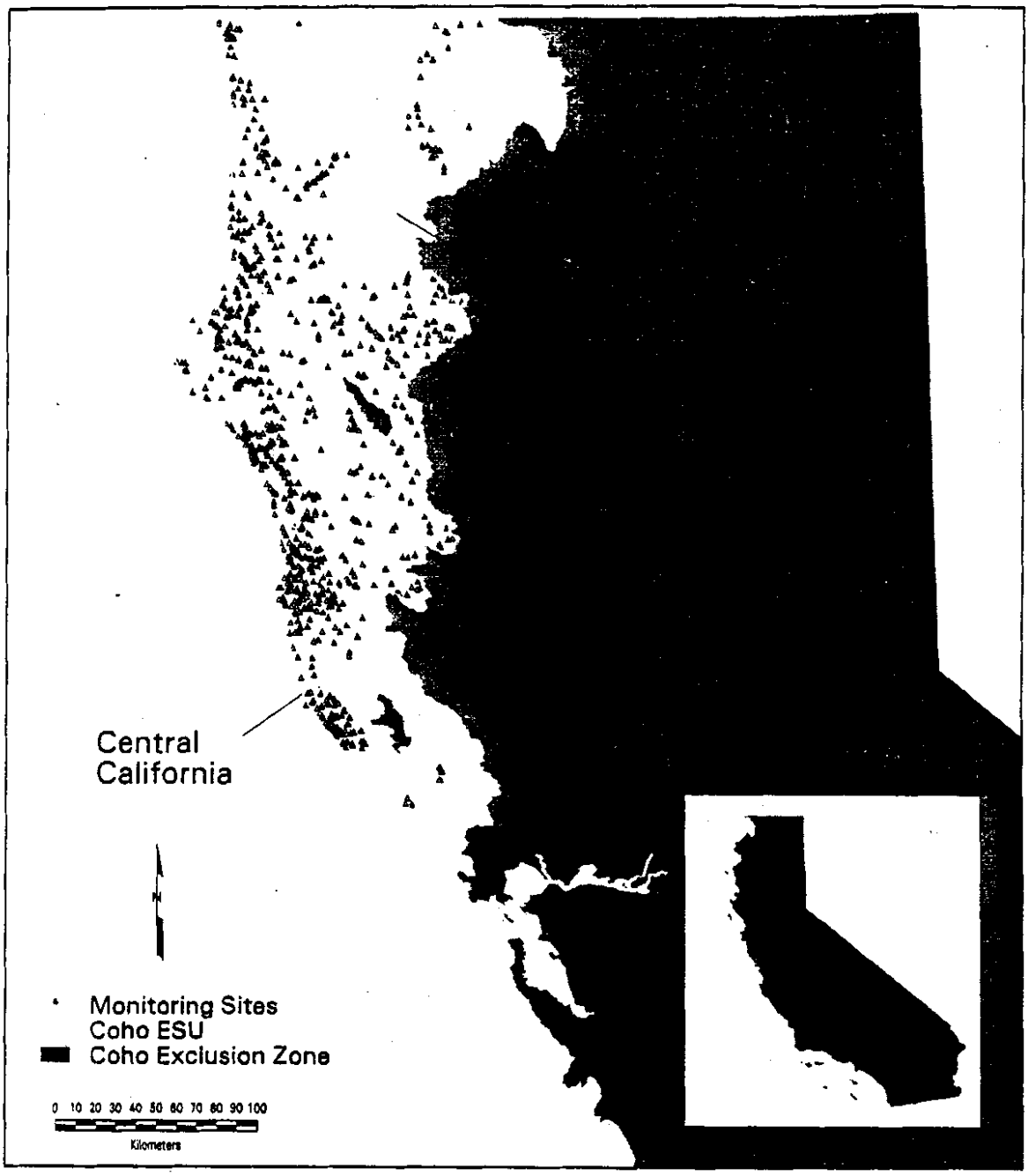

Figure 1.1. Area of interest for FSP's Regional Stream Temperature Assessment as defined by the Southern Oregon Northern Coastal California and Central California evolutionarily significant units.

Table 1.1. Seasonal Occurrence of Adult, Embryonic, and Juvenile Anadromous Salmonids in Freshwaters of Western Oregon and Washington. Modified from Everest et al. (1985).

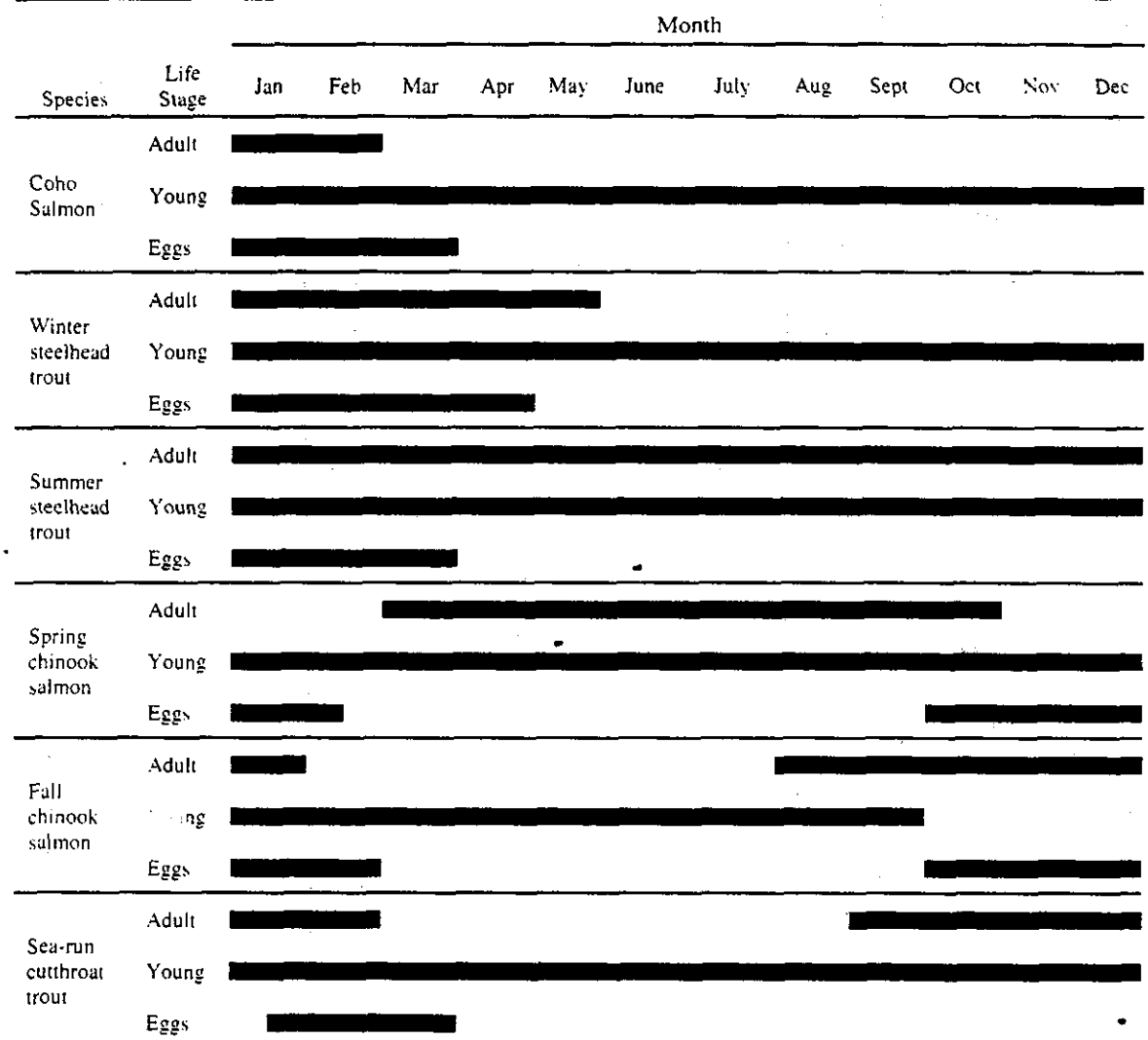

stages of various species are not present in the various systems in the AOI during the summer months. e.g., chinook salmon and steelhead trout. However, juvenile stages are known to be the most sensitive to thermal stress, hence the reason for this focus. Table 1.1 can be used as a reference tool to determine other species of interest and the life stages that may inhabit systems in the AOI during the summer temporal window of interest assessed in this report.

Objectives

The objectives of this stream temperature assessment report were:

1. Compile available stream temperature data in a verified and validated database for purposes of regional assessment

2. Assess status and trends in stream temperatures across the region

3. Evaluate the influence of regional scale factors (e.g., climate, geographic location, watershed position, etc.) and site-specific factors (e.g., canopy closure, channel orientation, etc.) on status and trends in stream temperatures

4. Through the assessment process identify areas where improvements in existing protocols and analysis and synthesis are needed

5. Identify knowledge gaps in site-specific information that should be collected on a routine basis to improve our assessment capabilities and move us closer to a regional stream temperature sampling design

6. Identify knowledge gaps between stream temperature monitoring and information on the distribution of coho salmon and other aquatic species

Chapter 2

METHODS

Study Design

There was no study design in place for this stream temperature assessment. Land stewards that submitted data for the assessment collected stream temperature data under a multitude of objectives and assumptions. These diverse objectives can be grouped into three broad categories:

- Pre- and post-timber harvest plan monitoring
- Thermal reach monitoring
- Characterization of thermal refugia

Forest Science Project cooperators and other parties that submitted stream temperature data can be characterized as forested landowners and stewards. Therefore, the population of stream temperature monitoring locations fell predominately in forested catchments or on lands zoned as Timber Protection Zone (TPZ) or Agriculture Exclusive (AE). Some mainstem river sites were exceptions. Data from both private landowners and public resource management agencies were acquired. Thus, the land management prescriptions were dependent upon whether monitored streams were on private or public lands.

Site Selection

The stream temperature data available for analysis and assessment were entirely dependent upon the willingness of the cooperator to provide the data. The data collected reflects a broad spectrum of climatic, hydrological, topographical, and ecophysiographical conditions. As a consequence, an array of sites reflecting a range of riparian conditions across the region allowed for post-stratification of variables by hierarchical spatial scales for statistical analyses. Site selection was not based on a probabilistic or random sampling design. Rather, the sites reflect a multitude of cooperator interests and monitoring objectives in a particular stream or watershed. Table 2.1 lists the various data contributors whose data were included in this assessment.

Data were accepted from contributors for inclusion in the assessment if they met all required criteria. Additionally, many data contributors submitted one or more of the optional criteria.

Required

- Stream temperature measured with a continuous monitoring device capable of taking an integrated or instantaneous reading every 2.5 hours (as opposed to a hand-held thermometer or max-min thermometer read infrequently)
- Site coordinates provided (lat/long, UTM, state plane, or hard copy maps)
- Monitors placed in Class I streams (data from some Class II streams were received)

Optional

- Air temperature measured simultaneously at the water temperature monitoring site
- Site-specific characteristics (e.g., slope, aspect, canopy closure, habitat type) measured for a (thermal) reach. Thermal reach defined as approximately 600 m for this study.

Table 2.1. Stream Temperature Data Sources for the Forest Science Project's Regional Stream Temperature Assessment.

	YEAR								
Source	**1990**	**1991**	**1992**	**1993**	**1994**	**1995**	**1996**	**1997**	**1998**
Barnum Timber Company								12	23
Bureau of Land Management							2		
CA Dept. Fish & Game								4	
Elk River Timber Company								6	4
Fruit Growers Supply								14	18
Georgia Pacific West. Inc.				63	54	66	64	64	75
Gualala Redwoods, Inc.					17	27	27	26	28
Humboldt County RCD							152	159	113
Humboldt State University									12
Jackson State Forest							49	34	27
Louisiana Pacific Corporation					16	15	53	36	
Mattole Salmon Group							16		
Natural Resources Cons. Serv.						11	14	13	4
NRM Corporation						3	15	23	26
Pacific Lumber Company					4	10	25	54	27
Pacific SW Experiment Station					7	7	13		
Pioneer Resources								41	39
Redwood National Park						1	1	11	10
Russ Ranch & Timber Company							2	4	9
Shasta-Trinity National Forest	15	18	17	10	23	14	6	16	13
Sierra Pacific Industries							14	24	17
Simpson Timber Company					40	30	10	29	44
Six Rivers National Forest				3	5	12	26	42	42
Soper/Soper-Wheeler Company					1				
Stimson Redwood Company					4		7	6	7
Timber Products Company							4	9	10
TOTAL	15	18	17	76	171	196	500	627	548

- Microclimatic data such as relative humidity, evaporation, sky cover, available in association with water temperature

The regional stream temperature assessment data base included 2168 site-years representing 1090 spatially unique continuous stream temperature monitoring sites. Site coordinates were available for all sites used in the assessment report. In most cases, coordinates were provided by the cooperator with the stream temperature data. In some cases, location of monitoring sites were denoted on maps that were provided by the cooperators. Coordinates were assigned to these sites using heads-up (interactive, on-screen) digitizing techniques and 1:24,000 scale digital raster graphic (DRG) topographic quadrangles. A spatial accuracy assessment was performed in January of 1999. The procedures used for the spatial accuracy assessment are described below.

Spatial Accuracy Assessment

Site coordinates provided by the project cooperators were evaluated using 1:24.000 scale DRG images. DRGs are an accurate, georeferenced digital representation of United States Geological Survey (USGS) topographic quadrangles. Note, USGS 1:24.000 scale data are purported to meet National Map Accuracy Standards for 1:20.000 or smaller scale, which state that 90% of well-defined features are within 40 ft of their true position.

An initial examination yielded varying degrees of displacement from the hydrographic component ranging from a few meters to 63 kilometers. The sources of these errors may include: base mapping sources other than USGS 1:24.000 quadrangles, transcription, digitizing and geocoding anomalies, projection and datum differences. While the potential problems arising from an error in position of 63 kilometers are quite obvious, errors of less than 10 meters can cause misleading analytical results. Small positional errors within a stream network, especially near a tributary confluence, can cause the incorrect association of a mainstem temperature site with a tributary site or visa versa. This leads to invalid relationships between sites, errors in drainage area and aspect computation, and other erroneous results. Large displacement errors will lead to the incorrect association of elevation, ownership, basin membership and other attributes necessary for spatial stratification and reporting which are critical to a regional assessment.

From the initial site survey, it was determined that a 100% site location validation strategy be developed. Stream temperature site locations were divided into groups by cooperating organization. ArcView projects consisting of site locations, DRG images, and other relevant geospatial data were developed for each group. Office visits with each cooperator were scheduled with the individual having the most knowledge of the site location to assist in the repositioning process.

There were 817 out of 1090 total sites that included both before and after site coordinate validation. The remaining 273 sites had their initial coordinates derived during office visits and were not used in the spatial accuracy analysis.

Examination of the horizontal displacement exposed 294 sites with errors greater than 50 m. A frequency distribution graph of the horizontal spatial error for 817 sites is shown in Figure 2.1. This level of spatial displacement can have severe adverse effects. Stream network position can be altered by changing a site's relationship to a tributary-mainstem confluence. Since many temperature sensors are located within 50 m of a confluence, many mainstem sites were incorrectly located above, below, or on the tributary. This will have deleterious effects when modeling the influence of a tributary's temperature input.

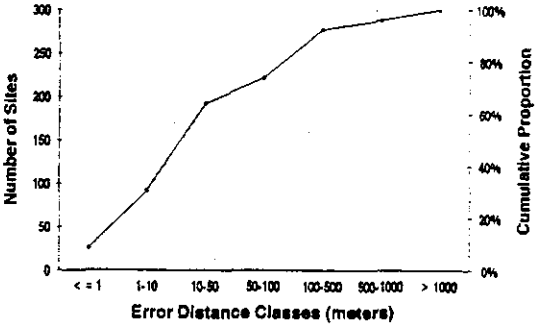

Figure 2.1. Frequency and magnitude of inaccuracies in the spatial location of stream temperature monitoring sites before site coordinate validation.

Of these 294 sensor sites, 62 sites had horizontal errors of greater than 500 m. These positional errors located many sites in the wrong drainage basin.

Upon completion of this process, the database was updated with the upgraded position and additional GIS-derived attributes.

Determining and Documenting Location

As discussed above, establishing and documenting the correct site location was critical. Key to this process was determining the required level of accuracy necessary for analysis. Digital data at a scale of 1:100,000 were found to be both lacking in spatial quality and quantity. Many stream temperature monitoring sites were located on streams represented only on 1:24,000 scale data. Hence, it was determined that the majority of GIS-based analyses would be undertaken at a scale of 1:24,000.

Two important considerations of site location are absolute positional accuracy and network topology. A high degree of absolute positional accuracy can be achieved by obtaining the site location coordinates using the Global Positioning System. This system of 28 satellites and a ground-based receiver can typically locate a site to within several meters of the true location. However, this will not ensure that a site's network topology is correctly established. Due to the spatial error in 1:24,000 scale data, a site with a high degree of absolute positional accuracy may well be incorrectly located within the network topology. Network topology describes a site's relative location within a network, in our case a hydrological network, e.g., the site is on the mainstem of the Mad River, 20 m downstream of confluence with Mill Creek.

Characterizing a site's network location with reference to well-defined features in addition to locating the site on a 1:24,000 scale topographic quadrangle will ensure that the spatial relationships between sites are maintained and that a site can be located and reestablished in the future.

GIS-Derived Variables

Once the spatial accuracy of stream temperature monitoring locations was confirmed, certain attributes were derived in GIS using standard overlay principles, raster modeling, and other methods facilitated by Arc macro language (AML) and Avenue script programs. The AML and Avenue script code can be found in Appendix A. The GIS- and Avenue-script-derived attributes were:

AML-derived
coho ESU
steelhead ESU
chinook ESU
ecoprovince
hydrologic unit (HUC)
CAL planning watershed
total maximum daily load (TMDL) Consent Decree Basin
elevation
shortest distance to coast
watershed area
distance to watershed divide

Avenue-derived
channel orientation
channel gradient
channel sinuosity

Watershed area and distance to divide were acquired by applying a simple hydrologic model to a compiled and edge-matched 1:24,000 scale digital elevation model (DEM). The compiled DEM was created by mosaicing more than 400 U.S. Geological Survey (USGS) 7.5-minute tiles. DEMs are generally available from the USGS in two distinct levels of quality. DEMs classified as Level I are created using a manual profiling procedure or the Gestalt Photo Mapper. Typically, Level I DEMs have inherent errors exhibited by elevation shifts in bands along the east-west axis. Level II DEMs are elevation data sets that have been processed for consistency and edited to remove identifiable systematic errors. Level II DEMs are created using hypsographic (contours) and hydrographic (streams) data which produce a somewhat smoother more continuous surface model. Where Level II DEMs did not exist, one of two procedures were used to create the necessary tiles. Several 30-meter DEMs were created in-house from 1:24,000 scale vector contour data while others were created by resampling USGS Level II 10-meter DEMs to a 30-meter spacing.

The compiled DEM was processed to remove spurious sinks, i.e., areas of undefined flow, by

filling these to a surrounding outlet elevation. The assembled DEM was evaluated for internal and along-tile boundary errors by computing a flow-direction and flow-accumulation model for each logical basin within the Area of Interest (AOI). Any break in flow within a logical basin before reaching the natural outlet (Pacific Ocean) was determined to be an error requiring an appropriate correction. Once a flow corrected DEM existed, upstream watershed (drainage) area and divide distance were derived for each temperature monitoring site.

Using 1:24,000 scale digital raster graphics (DRGs) and USGS 30-meter digital elevation models ArcView (Environmental Systems Research Institute, Redlands [ESRI], CA) combined with Avenue scripts were used to acquire the necessary information to compute the desired attributes. Channel orientation was calculated by tracing a 600-meter reach upstream of each temperature sensor location. From this point a straight-line distance and bearing was calculated back to the sensor location. Channel orientation represents this bearing in compass degrees where north equals 0 degrees. Elevation was acquired from the DEM for the sensor site and the location 600 meters upstream. Channel gradient was calculated as the difference in elevation between these two sites divided by the reach length. Channel sinuosity was calculated by dividing the reach length (600 meters) by the straight-line distance between the two locations. Very straight reaches yielded sinuosity values nearly equal to 1.

It is important to be aware of and understand the associated errors of these products and how these errors can affect results. For example, gradient values of less than or equal to zero were occasionally acquired from sites located along channels with little natural elevation change. While a negative upstream gradient may be disconcerting, these sites can confidently be described as very low gradient reaches. Since our application was at a regional scale and we were looking at general classifications (e.g., flat, sloped, very sloped, steep), the realized error was considered acceptable.

Calculated Water Temperature Metrics

Various water temperature metrics were calculated from the data. These metrics were considered important in characterizing the thermal regimes in water temperature across Northern California. These included:

- daily minimum
- daily mean
- daily maximum
- seven-day moving average of the daily minimum
- seven-day moving average of the daily mean
- seven-day moving average of the daily maximum

The above six metrics comprise the core set of statistics that were used throughout the regional assessment. Other metrics, representing both chronic and acute thermal stress, are presented in subsequent chapters and are therein defined.

Daily and weekly temperature metrics were further reduced to single statistics for each site for each year. For example, for a given site, the highest daily maximum temperature for the year was used as a temperature index that was compared to various climatic, landscape, and site-specific attributes. Similarly, the highest seven-day moving average of the daily average was compared to similar independent variables. A list of the yearly summary statistics calculated from the daily and weekly data and most commonly used in our analyses is presented in Table 2.2.

A naming convention was developed for assigning variable names to yearly temperature metrics. While the abbreviations may seem unwieldy upon first encounter, they become second nature once an understanding of the naming convention is acquired. The first letter denotes that the yearly statistic is the maXimum (**X**), Average (**A**), or mInimum (**I**) for the year. The second letter denotes that the statistic is a Yearly statistic (**Y**). While a complete year (i.e., January 1 through December 31) of temperature is not used to calculate the yearly statistic, the value

Table 2.2. Most Commonly Used Yearly Temperature Statistics Calculated from Daily and Weekly Data Sets.

Yearly Site-Level Statistic	Abbreviation
highest daily maximum	XY1DX
lowest daily minimum	IY1DI
highest seven-day moving average of the daily average	XYA7DA
highest seven-day moving average of the daily maximum	XYA7DX

represents the maximum, average, or minimum for the defined sampling window in a given year. Obviously, the minimum for the year is not captured in the defined sampling window. For seven-day moving averages, the third letter specifies that the statistic is the maXimum (**X**), Average (**A**), or mInimum (**I**). If the metric is based on a daily value, e.g., the daily average, daily minimum, or daily maximum, the third character in the variable name is a one ('1') and the fourth is a 'D' for Daily. If the statistic is based on a seven-day moving average the fourth and fifth characters in the variable denote this by '**7D**'. The last character specifies that the statistic is the daily value or seven-day moving average of the maXimum, Average, or mInimum.

Some examples will help clarify the naming convention. The maXimum (or highest) daily (**1 Day**) maXimum for the Year would be represented as **XY1DX**, where

X = maXimum for the year
Y = a Yearly statistic
1D = **1** Day or daily
X = maXimum.

The mInimum (or lowest) daily (**1 Day**) mInimum temperature for a site in a given Year would be denoted as **IY1DI**, where

I = mInimum for the year
Y = a Yearly statistic
1D = **1** Day or daily
I = mInimum.

The maXimum (or highest) **7-Day** moving Average of the daily Average for a site in a given Year would be encoded as **XYA7DA**, where

X = maXimum for the year
Y = a Yearly statistic
A = Average
7D = **7** Day moving average
A = Average.

Potential Errors in Calculating Water Temperature Metrics

In calculating summary statistics for the various temperature metrics it was found that a potential error was inherent in the data. The highest daily minimum and lowest daily maximum were influenced by daily records that did not contain a complete number of observations due to removal of anomalous readings, e.g., ambient air spikes. If only a portion of the daily observations were removed, an incomplete daily record resulted. For example, if the sampling frequency of a device was set to take an instantaneous reading every hour, 24 observations per day should be found for each daily observation. However, if anomalous readings were removed from the daily record, less than 24 observations were observed for certain days. When the daily minimum and daily maximum temperatures were calculated using Statistical Analysis System (SAS) (SAS, 1996), days that had an incomplete number of observations had elevated daily minimum and depressed daily maximum temperatures, depending on the time of day data were missing.

Due to errors introduced in the data due to missing observations, a SAS program was written to search the hourly data set for days where the number of observations was less than the maximum number of daily observations or the maximum number of daily observations minus one. The ***maximum minus one*** provision was used to compensate for sites where the

number of daily observations oscillated by one. This occurs when the device start time and sampling frequency results in the last observation of the day being very close to midnight. For example, depending on the start time, a monitoring device set at a 1.6- hr sampling frequency will have 15 daily observations on one day, then have 14 daily observations on the next day. When days with daily fragments were encountered the daily observation was left in the data set, however, the temperature values were set to missing. Without the ***maximum minus one*** provision, every other day (the day with 14 observations) would have had all the temperature values set to missing. The data set with daily fragments removed (set to missing) is henceforth referred to as the ***defragmented weekly data set***.

Additional temporal refinement was applied to the defragmented weekly data set for statistical analyses. Many multivariate analyses and modeling in this regional assessment were based on the highest daily maximum (XY1DX), the highest seven-day moving averages of both the daily average (XYA7DA) and the daily maximum (XYA7DX) for the year. Limiting the temporal window of the temperature data to June 1 through September 30 for all sites and all years helped ensure that stream temperatures across a consistent time frame were used in summary statistics. However, even with this precaution it became apparent that the "highest" value for a particular site may not necessarily have been captured if data were missing during the time the "true" highest stream temperatures occurred. Thus, the defragmented weekly data set converted daily and seven-day moving average temperature values to missing values for days with incomplete observations. It was deemed critical to refine the temporal window to the time period when the highest stream temperature metrics were most likely to occur. This time frame was determined from the defragmented weekly data set by calculating the mean and median day of year in which the highest seven-day moving average occurred.

To briefly summarize, there were 1090 spatially unique study sites monitored between 1990 and 1998 inclusive. The mean day of the year the XYA7DA and XYA7DX occurred was determined by running a series of queries. The mean value for the day of occurrence was 215, which corresponds to August 4. This calendar date may vary by one day, depending on whether or not a given year was a leap year. A 15-day period on either side of day 215 was used as the temporal window (day of year between 201 and 230 or approximately July 21 through August 19). Additionally, sites having five or more days within this period with missing values were removed from further analyses. This criterion represents about 85% of the days within the desired time frame required to have non-missing observations. This missing data criterion is the same as that used by the National Weather Service for inclusion of air temperature monitoring data in their data summaries. Of the 1090 study sites, 1034 sites had data within the 30-day window, with 1014 sites having data that met all criteria. The most data-rich year, that is existence of data for both stream temperature and many of the site-specific attributes, was 1998 – there were 518 sites for this year. This year was used predominantly throughout the report to explore relationships between stream temperature and various landscape and site-specific variables.

Temporal, Spatial, and Physical Stratification

The temporal delimiters placed on the data to remove errors in statistical analyses were discussed above. Certain spatial and physical criteria were also imposed on the data used in stream temperature analyses to render the data comparable within and between years. Table 2.3 lists the criteria used in data standardization. Figure 2.2 shows the spatial distribution of sites for each year and all years combined (1990-1998) that met the criteria shown in Table 2.3. As can be noted from the spatial displays in Figure 2.2, the spatial distribution of sites was not uniform across all years. The lack of uniformity in spatial coverage was taken into consideration when relationships between stream temperature and certain landscape- and site-level attributes were examined

The spatial qualifiers that were applied to the data ensured that data used in the regional assessment were gathered from the appropriate areas of interest. A spatial hierarchy was used to post-stratify the data by these areas of interest. The focus of this temperature assessment was on anadramous fish,

Table 2.3. Criteria Used to Standardize Stream Temperature Data Within and Between Years.

Criterion		Value	Description
Stream class	=	1	Class 1, fish-bearing streams
	=	5	Stream class not specified
	=	' '	Stream class missing
Site type	=	water	Water or air temperature. Relative humidity data were excluded from analyses.
		air	
Temporal	≥	21 July	Date was greater than or equal to 21 July for each year
	≤	19 Aug	Date was less than or equal to 19 August for each year
Spatial	Only sites that fell within the boundaries of the California portion of the Southern Oregon Northern Coastal California and Central California evolutionarily significant units		

namely coho salmon. Thus, the largest spatial boundary applied to the geographic distribution of sampling points was the combined SONCC and CC evolutionarily significant units for coho salmon (*O. kisutch*) (Figure 1.1). If in the assessment, status and trends in stream temperatures pertinent to coho salmon within one of the ESUs were of interest, the coho ESU boundary for that ESU was used to poststratify sampling points by this area of interest. Likewise, if relationships between stream temperature and certain landscape- and site-specific variables were explored by ecoprovinces (USDA, 1997), the spatial boundaries of these ecoprovinces were used to aggregate data by this area of interest.

Measurement Techniques and Data Processing

The measurement techniques used by the various data contributors and the Forest Science Project's methods of data processing are presented in Appendix A.

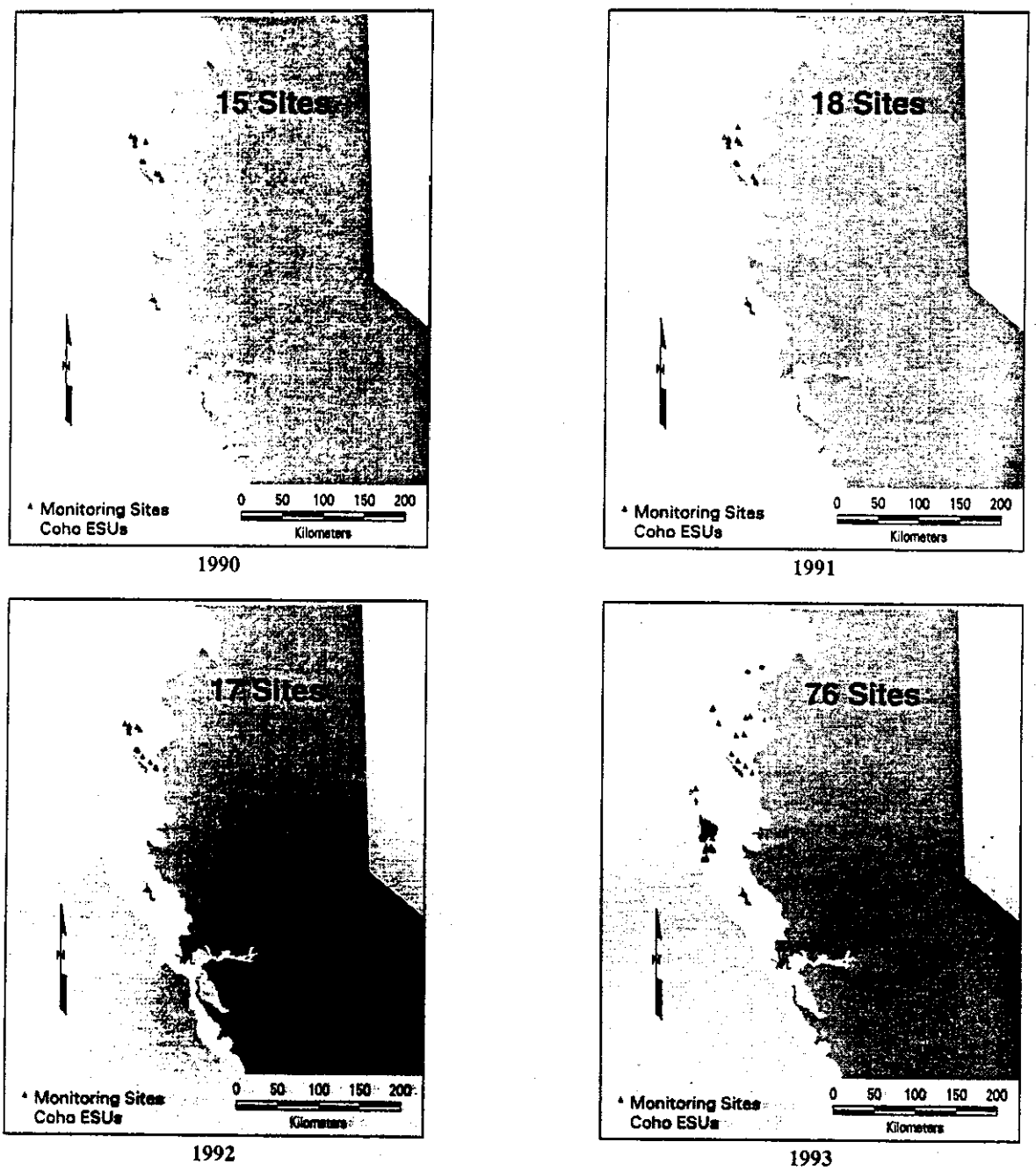

Figure 2.2. Location of stream temperature monitoring sites used in the Regional Stream Temperature Assessment.

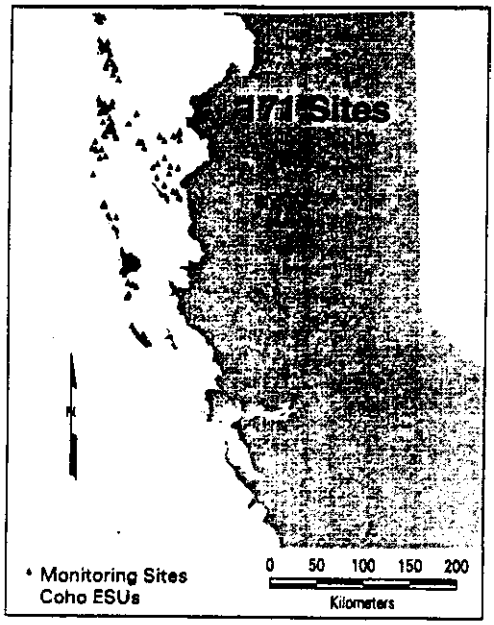

1994

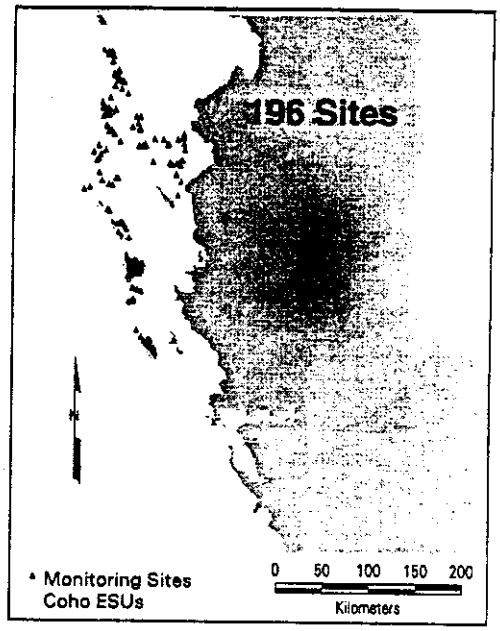

1995

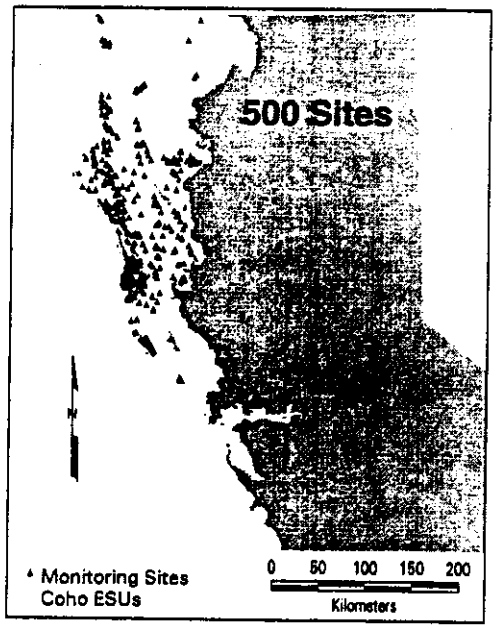

1996

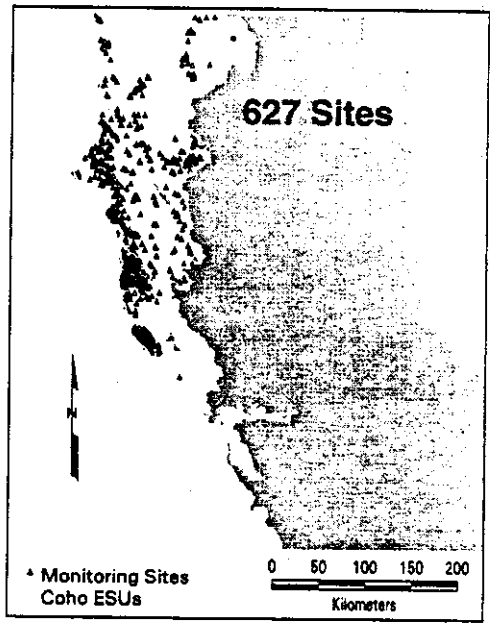

1997

Figure 2.2. (continued)

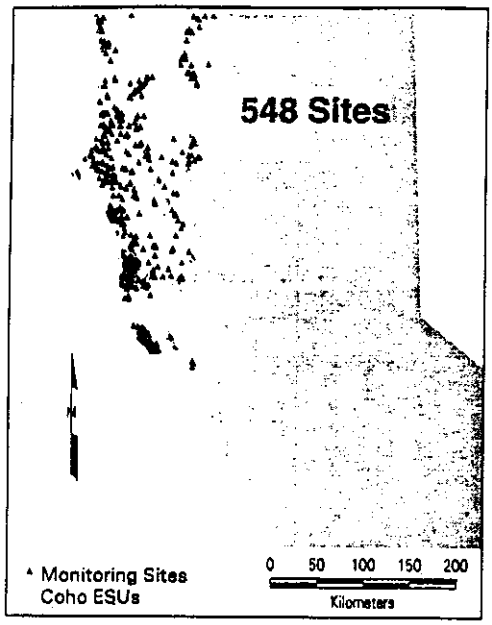

1998

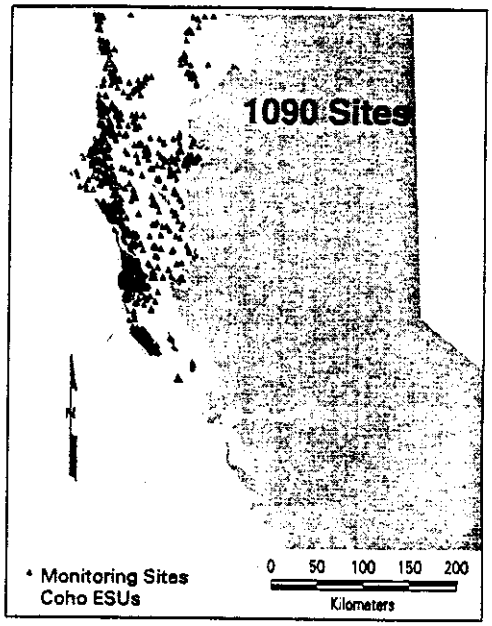

All Sites, All Years (1990-1998)

Figure 2.2. (continued)

Chapter 3

SUMMARY OF THE STATISTICAL ATTRIBUTES OF REGIONAL STREAM TEMPERATURES

Introduction

Summary statistics were calculated for data sets containing individual observations (henceforth referred to as the ***hourly data set***) and data sets containing the daily minimum, average, and maximum, and seven-day moving averages (henceforth referred to as the ***weekly data set***). The defragmented weekly data set was used to produce summary statistics, to avoid the inherent errors if days with missing observations were used to calculate summary statistics. The PROC UNIVARIATE procedure in SAS was used to generate summary statistics (SAS, 1985).

Sidebar #1

Interpreting Summary Statistics

A cautionary note is offered to the reader. Hourly and weekly summary statistics are only applicable to the sites monitored in a single year. The number of sites and their geographic distribution increased from 1990 to 1998. The sites are by no means consistent across all nine years. Therefore, inferences should not be made from yearly summary statistics as to whether stream temperatures showed increasing or decreasing trends across years.

Hourly Summary Statistics

Summary statistics were generated from the hourly data set containing the individual observations (e.g., hourly observations, 1.5-hr intervals, etc., depending on the sampling frequency of each device). The summary statistics of hourly data are presented in detail in Appendix B. The temporal window for which summary statistics were calculated was June 1 through September 30 of each year.

Daily and Weekly Stream Temperature Metrics Summary Statistics

Summary statistics were generated by year for the defragmented weekly data set for the following stream temperature metrics:

- daily minimum
- daily mean
- daily maximum
- seven-day moving average of the daily minimum
- seven-day moving average of the daily mean
- seven-day moving average of the daily maximum

The summary statistics for the daily stream temperature metrics are presented in Appendix B for years 1990 through 1998. A cautionary note is provided in Sidebar #1 that should be read before examining and interpreting yearly summary statistics.

The summary statistics for the weekly (seven-day moving average) temperature metrics are also presented in Appendix B for years 1990 through 1998. The highest seven-day moving average of the daily mean is often referred to as the Maximum Weekly Average Temperature or MWAT (Ferraro et al., 1978). Some state and federal agencies in California and other states have been referring to the highest seven-day moving average of the daily maximum as the MWAT value. The summary statistics for the seven-day moving average of the daily maximum are presented in Appendix B, Table B-10 through B-19.

Cumulative Distributions of Regional Stream Temperatures

The cumulative distribution function (CDF) graphical technique was used by the FSP as one method of presenting regional stream temperature analytical results. This introduction describes how to interpret a CDF graph. The effort to learn how to interpret the output from this graphical technique is modest, and the reward is substantial: many monitoring programs around the world use this simple, powerful, and informative graphical technique for presenting data summaries.

A CDF is better than a tabular summary for presenting an objective view of FSP data. Specifically, optimal or suboptimal stream temperature has not unequivocally or universally been defined. The use of a CDF permits readers to choose a reference or threshold value for a stream temperature or ecological indicator, and see what proportion of the sampled population is estimated to fall below or above the value for that measurement or indicator. Tabular summaries stratify the data according to a reference value defined by the data analyst, but the reader is unable to see how an interpretation could change if a different reference value was chosen (FHM, 1994). If needed, a tabular summary can be prepared for any particular reference value. Until such time as biologically meaningful thermal threshold values are widely accepted, the CDF graphical presentation is an effective means of disseminating information.

The examination of the cumulative distribution of temperatures across the region is an effective means of gaining an understanding of the thermal regimes across the region. Before this information is presented, a discussion of how to interpret a cumulative distribution function graph is appropriate.

How to Interpret a CDF

Each CDF is identified by the variable X (a measurement or indicator, on the horizontal axis) and by the subset of spatial entities (e.g., sites, streams, watersheds, etc.) in the population that the graph represents. For example, X could be the highest seven-day moving average of the daily mean stream temperature and the subset of the population could be those sites on Class I streams that fall within a FSP assessment area of interest. To find the estimated proportion of the population that falls below some reference value, say for example the MWAT threshold, use the following procedure (Figure 3.1).

1. Find the desired reference value (X) on the horizontal axis.
2. Draw a line perpendicular from the chosen X value to meet the solid line that is plotted on the CDF.
3. Draw a line from this intersection to the left to perpendicularly meet the vertical axis.
4. Read the estimated proportion where the line meets the vertical axis.
5. The proportion is the fraction of the population that is estimated to have a value of X that is less than the reference value.

In the example, a reference value of 18.3°C in step 1 leads to the interpretation that about 95% of the sites, streams, watersheds, or other unit of the population have an X value less than 18.3°C. Different reference values (in step 1) will yield different cumulative proportion estimates (in step 4). By experimenting with reference values, the reader can see how data interpretations change with changes in the reference value. For example, a different

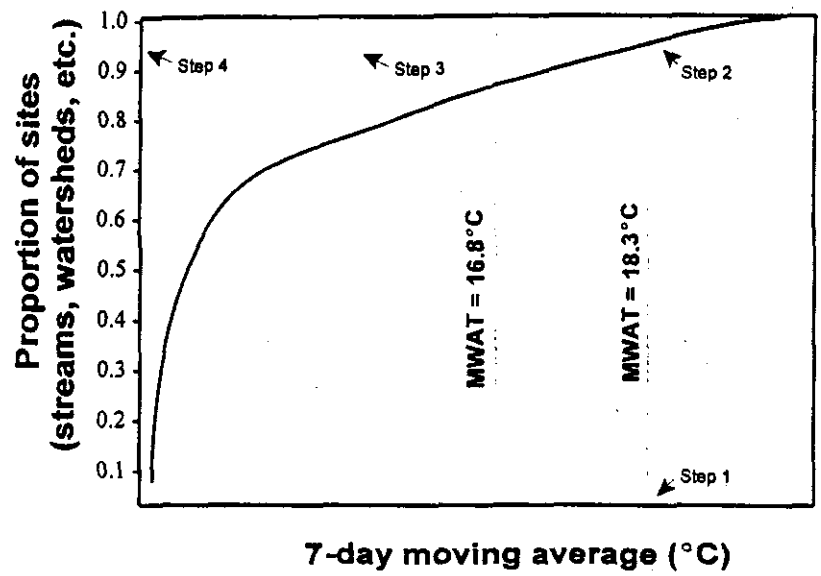

Figure 3.1. Hypothetical cumulative distribution function graph.

reference value of 16.8°C in step 1 leads to the interpretation that about 88% of the population is below the MWAT threshold.

There are some important considerations to keep in mind when using the above procedure. First, this graphical technique is suitable for obtaining **rough estimates**, but precise computation requires the use of the data base and appropriate algorithms. Algorithms were applied to the data base in this report to calculate the precise cumulative proportion at the reference value. Second, the CDF cannot be used (strictly) to get estimates of the proportion of the population **greater** than some value of X. Instead, a new chart of $1\text{-}f(X)$ must be prepared, again using the data base and appropriate algorithms. If the cumulative distribution function (CDF) were the true, continuous, cumulative distribution function of the population resource, it would be acceptable to take $1\text{-}f(X)$ as the probability of being larger than value X. But in survey sampling, one does not have the continuous population CDF. Instead, one has an approximation which has gaps and jumps that reflect the variability seen in the sample. A jump in the CDF may be due to large sample weights, or to a large number of sample values in that vicinity. In particular, an X value near one of these jumps becomes sensitive to the presentation of the CDF. Near one of these jumps in the CDF the estimate of the exceedance probability may not be well-estimated by one minus the estimated proportion less than or equal to X. For this reason, it is recommended that exceedance probabilities be calculated from the descending CDF (Diaz-Ramos et al., 1996).

In summary, the CDF technique is a flexible format for presenting a overview of data. It gives any reader or analyst the ability to chose their own threshold and determine what fraction of the population is estimated to be above or below that criterion. The CDF does not change the data in any way, it simply presents it in a non-tabular fashion. Despite the simplicity of the approach, some readers will never be comfortable with the CDF technique. For these readers, only the possibility of making one's own interpretation will be lost; it is always possible to

accept or reject the interpretations that other scientists will make when they assign thresholds and present the data in a tabular format.

Sidebar #2
Reference Values and CDFs

The reference values presented on the various CDF graphs in Appendix B are for reference purposes only. Until such time as agreed upon threshold or exposure values are developed for Northern California, reference values should be used as such, reference values.

CDFs of Seven-Day Moving Averages and Daily Maximum Stream Temperatures

The highest seven-day moving average of both the daily mean (XYA7DA) and the daily maximum (XYA7DX), and the highest daily maximum temperature (XY1DX) for each site for each year was used in cumulative distribution analyses. The highest seven-day moving averages were compared to two reference values of 16.8°C and 18.3°C. These two values have been commonly used to evaluate chronic thermal stress metrics such as seven-day moving averages (Armour, 1991; Becker and Genoway, 1979). The highest daily maximum temperature was compared to the upper lethal incipient temperature (26°C) for juvenile coho salmon and a two-degree safety margin temperature (24°C) (Coutant, 1972). The highest daily maximum temperature is an acute thermal stress metric and thus should be compared to an acute thermal threshold. CDF graphs for the three temperature metrics can be found in Appendix B. The highest seven-day moving average of the daily average is often referred to as the Maximum Weekly Average Temperature or MWAT. This value is compared to MWAT thresholds for various species and life stages to determine potential chronic exposure to elevated stream temperatures. Oregon, Washington, and Idaho have adopted the seven-day moving average of the daily maximum as the metric for evaluation of stream temperature in their states. There is debate in California as to whether the highest seven-day moving average of the daily mean or the seven-day moving average of the daily maximum should be used to assess potential chronic stress. Therefore, both metrics are presented in this report.

The precise cumulative proportion above and below two reference values, 16.8°C and 18.3°C, was calculated mathematically (not visually estimated from the graph) and are presented with their accompanying CDF graphs in Appendix B.

The CDF graphs and data tables are applicable to the year in which the data were gathered. It must be kept in mind that comparisons across years are not appropriate because different sites were sampled in each year (See Sidebar #1).

Chapter 4

REGIONAL TRENDS IN AIR TEMPERATURE

Introduction

Air temperature is known to have a significant influence on stream temperatures. In conjunction with solar radiation it is an important source of heat input into aquatic systems (Hostetler, 1991; Sullivan et al., 1990; Stoneman and Jones, 1996). Most stream temperature models based on the physics of heat transfer use air temperature as a driver to predict temporal change in stream temperature (Bartholow, 1989; Sullivan et al., 1990). The difference between air and water temperature determines the rate of energy exchange for several heat transfer processes included in the energy balance equations of these models. The location at which air temperature should be monitored varies depending on which energy balance equation requires the data. For example, the back radiation equation requires input of air temperature data collected well above the stream (sky temperature) (Adams and Sullivan, 1990). The convection equation considers air temperature collected just above the stream surface. The evaporation rate is often calculated using air temperature data collected at about two meters above the stream surface.

Local air temperature is an important parameter influencing the ***daily mean stream temperature*** at equilibrium (Edinger et al., 1968; Adams and Sullivan, 1990). The daily mean stream temperature under equilibrium conditions is generally near the daily mean air temperature (Adams and Sullivan, 1990). Unfortunately, not many stream temperature data contributors submitted local air temperature data collected near their stream temperature sites. To determine the effects of air temperatures on mean stream temperature, acquisition of ***local*** air temperatures is particularly important. If one uses remote or approximate air temperature data, then one can only hope for remote or approximate stream temperature predictions (Sullivan et al., 1990). Alternatively, if one wants to account for daily maximum stream temperatures, information on solar insolation is also necessary. The amount of solar heat input would most likely be obtained from estimates of effective canopy and topographic shading.

To understand how water temperatures vary regionally, an understanding of regional trends in air temperature is required. This chapter examines the variation in air temperatures across Northern California using data from National Oceanic and Atmospheric Administration (NOAA) weather stations and modeled air temperatures obtained from Oregon State University. We show that air temperature, an important variable in determining water temperature, varies greatly across the area of interest. Using air monitoring station data, air temperature was found to be strongly related to distance from coast (marine influence) for the Coastal Steppe Province and elevation (adiabatic influence) for the Sierran Steppe - Mixed Forest - Coniferous Forest Province. An advanced climate analysis procedure was used to estimate long-term air temperatures regimes across the ecoprovinces and basins of Northern California. Yearly air temperatures were compared to the 30-yr long-term averages for each ecoprovince. Finally, yearly average air temperature was used to estimate groundwater temperatures across the area of interest.

Air temperature discussed in this chapter is considered to be macroair temperature, and not stream-side air temperature (microair). Macroair temperature represents above-ground temperatures like those reported on the evening news.

Air Temperature Data Acquisition and Analysis

Air Monitoring Station Data

Air temperature data were downloaded from two Internet sources: Western Regional Climate Center (WRCC; web address: http://www.wrcc.dri.edu/climsum.html) and University of California Statewide Integrated Pest Management Project (UCIPM; web address: http://axp.ipm.ucdavis.edu/WEATHER/retrieveavgs.html). The downloaded data for all 25 WRCC air temperature data sets were from stations operated by NOAA. The downloaded data for the 47 UCIPM air temperature data sets were from three different sources: data providers were listed as automatic, touchtone, and climate stations. The automatic stations are part of the California Irrigation Management Information System (CIMIS) Network operated by California Department of Water Resources. The touchtone stations are volunteers that record observations daily and transmit them to the UCIPM computer. The climate stations are maintained by NOAA. There were 11 downloaded data sets for the automatic stations, 3 sets for touchtone stations, and 33 sets for climate stations. Although water temperature data from FSP data contributors were for years 1990 through 1998, air temperature data were acquired for the entire period of record at each air station. The historical air temperature data were later used in Chapter 11 to interpret historical trends in water temperature.

The air temperature data obtained from WRCC only included monthly averages for the minimum, maximum, and daily average. Daily data were not available. UCIPM provided only daily minimum and maximum air temperatures. Daily averages were not available. There are two commonly used methods for calculating daily average air temperatures. One method is the ***true average*** of the hourly (or some other sampling rate) readings for a 24-hour period. The other method is performed by adding the daily maximum and daily minimum air temperatures and dividing the sum by two, henceforth referred to as the ***maximum-minimum average***. The method used by WRCC in their monthly summary reports is that of the maximum-minimum averaging technique. Since we did not have the ability to calculate a ***true average*** for each month in the study period, the ***maximum-minimum average*** was calculated for each day, and subsequently the daily maximum, minimum, and maximum-minimum averages were averaged by month and year. If a particular site had more than five days with missing daily maximum and/or minimum values (and hence a missing value for the calculated daily max-min average), the monthly average was set to null. Application of this procedure was similar to the way in which water temperature summary statistics were calculated (see Chapter 3). Potential errors are introduced into monthly averaging procedures if partial monthly records are included. The criterion that FSP used for the number of records that were permitted to be missing in a monthly average air temperature, i.e., 85% data completeness criterion, is used by NOAA and the WRCC in their data summaries.

After thorough examination of the integrity of the data, e.g., completeness of the record, level of temporal aggregation across all sites, etc., 72 sites were found to exhibit sufficient consistency across the nine years of the stream temperature assessment period (1990 through 1998) allowing for their inclusion in the regional assessment. Figure 4.1 shows the location of the 72 sites used in the analyses.

PRISM Air Temperature Data

In addition to the data acquired from the aforementioned 72 sites, regional air temperature data were acquired from Oregon State University (OSU) Climate Analysis Service and the Oregon Climate Service at OSU. These data were developed using PRISM (Parameter-elevation Regressions on Independent Slopes Model). PRISM is a climate analysis system that uses point data, a digital elevation model (DEM), and other spatial datasets to generate gridded estimates of annual, monthly and

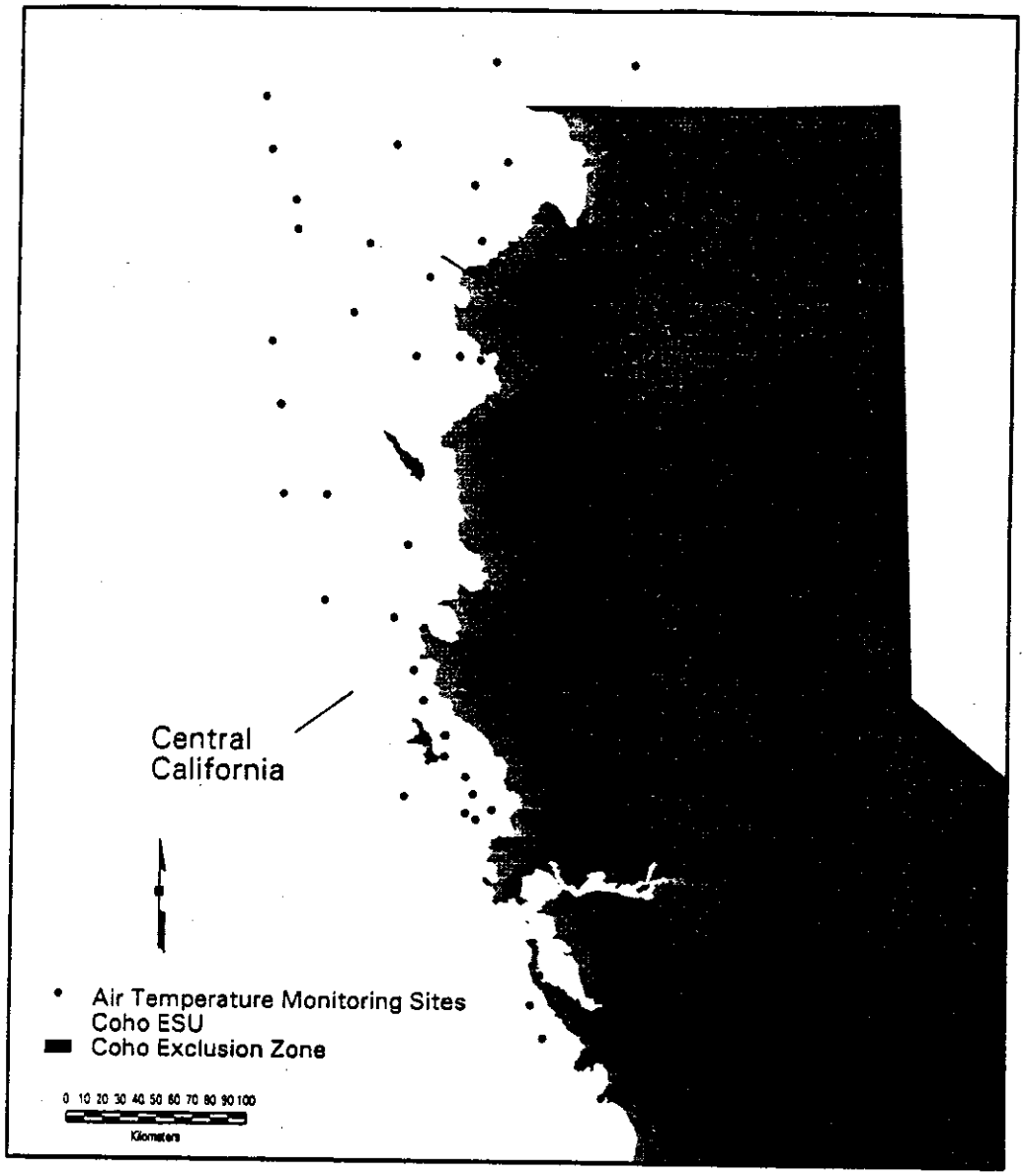

Figure 4.1. Location of air temperature monitoring sites used in the Forest Science Project's regional stream temperature assessment.

event-based climatic parameters (Daly et al., 1994). Originally developed in 1991 for precipitation estimation, PRISM has been generalized and applied successfully to temperature, snowfall, growing degree-days, and weather generator parameters, among others (Johnson et al., 1997, Taylor et al., 1997). It has been used extensively to map precipitation and minimum and maximum air temperature over the United States, Canada, and other countries (Kittel et al., 1997; Parzybok et al., 1997).

The acquired PRISM air temperature data has been reduced to 30-yr long-term monthly averages at 4-km grid resolution. The monthly averages for the maximum and minimum were available, from which the monthly average was calculated by adding the maximum and minimum and dividing by two. Most of the data from the 72 sites mentioned above were most likely utilized in PRISM model development.

The PRISM system determines climate at grid cells by calculating linear relationships between the climate element in question (e.g., air temperature) and elevation. The slope of these linear regression lines changes locally with elevation, as dictated by the available point climate data. With a separate regression function each grid cell estimate is determined using data from many nearby climate stations. Each station in the multiple regression is weighted based on five factors: distance, elevation, vertical layer, topographic facet, and coastal proximity. In short, the closer a given station is to a target grid cell in distance and elevation, and the more similar that station is in its climatology to the cell (given by the other three factors), the higher the weight the station will have on the final, predicted value for that grid cell. A technique within PRISM determines the lowest possible prediction error for the map as a whole (all cells). PRISM typically is configured to predict values approximately every 4 km horizontally.

PRISM has been compared to kriging, detrended kriging, and cokriging in the Willamette River Basin, Oregon (Daly et al., 1994). In a jackknife cross-validation exercise, PRISM exhibited lower overall bias and mean absolute error. PRISM was also applied to northern Oregon and to the entire western United States. Detrended kriging and cokriging could not be used in these regions because there was no overall relationship between elevation and precipitation. PRISM's cross-validation bias and absolute error in northern Oregon increased a small to moderate amount compared to those in the Willamette River Basin; errors in the western United States showed little further increase. PRISM has since been applied to the entire United States with excellent results, even in regions where orographic processes do not dominate precipitation patterns.

By relying on many localized, facet-specific air/elevation relationships rather than a single domain-wide relationship, PRISM continually adjusts its frame of reference to accommodate local and regional changes in orographic regime with minimal loss of predictive capability.

The PRISM data does not provide the temporal resolution needed for predicting stream temperatures. However, the spatial resolution was ideal for developing a regional picture of air temperature regimes across Northern California.

The following evaluation of how air temperature varies with elevation and distance from the coast relied on the finer temporal resolution of the data from the 72 air temperature sites.

Air Temperature as a Function of Elevation and Distance from Coast

A decrease in air temperature at higher elevations is well documented and known to be driven by adiabatic cooling processes. Adiabatic cooling deals with the cooling of parcels of air as they rise, or are forced upward, through the atmosphere. An example would be the cooling of an air parcel as it rises over a mountain range.

In Figure 4.2-A the monthly average air temperatures for all sites for which 1998 August monthly average values were available (66 sites) were plotted against elevation. The expected decrease in air temperature with increasing elevation was not discernable across the full range in elevation values (Figure 4.2-A). A slight negative slope (-0.0001) can be discerned from

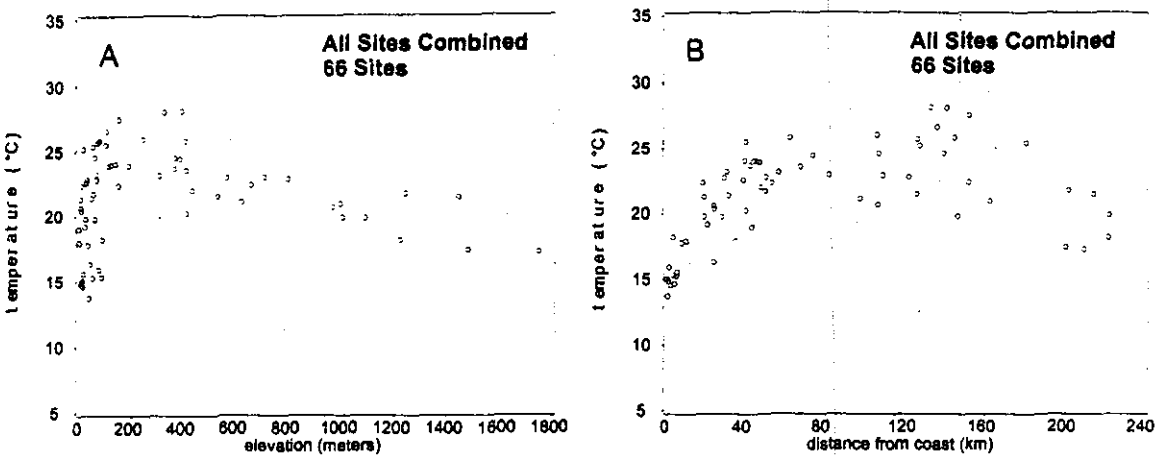

Figure 4.2. Relationship between August 1998 monthly average air temperature and elevation (A) and distance from the coast (B) for all sites combined (66 sites).

the graph. Air temperatures at the lower elevations were as low as or lower than air temperatures observed at elevations over 1000 meters (Figure 4.2-A). The relationship between monthly average air temperature and elevation is clearly not linear. The relationship was weak, as reflected by a low R^2 value of 0.0002.

Residents of Northern Coastal California are very familiar with the cooling effects of summertime oceanic air currents that tend to moderate temperatures during the summer months. For anyone who has driven from Arcata to Willow Creek or Weaverville on Route 299 in early August, they probably have experienced and appreciated the increasing air temperature while ascending in elevation, moving out of the affectionately termed 'fog zone' into the warmer, higher elevation areas. With this intuitive knowledge and first-hand experience of the warming trends in air temperature with increasing distance from the coast during the summer months, this relationship was examined in Figure 4.2-B.

Using 66 sites with August 1998 monthly average air temperatures in the analyses, a weak relationship (R^2 = 0.15) was observed (Figure 4.2-B). An overall positive slope of 0.02 was determined in the linear regression analysis. Visual inspection of Figure 4.2-B revealed that at the lower values for distance from the coast, air temperature increased with increasing distance from the coast. The increasing trend seems to level off at approximately 80 km (~50 mi) from the coast.

Given the apparent relationship between air temperature and both elevation and distance from coast that was discernable in Figures 4.2 and 4.3, these relationships were explored in greater depth in the following sections.

Monthly Average Air Temperature Versus Elevation

The air temperature sites were broken into two groups, sites at distances less than or equal 80 km from the coast and sites at distances greater than 80 km from the coast.

Figure 4.3-A presents the relationship between August 1998 monthly average air temperature versus elevation for sites at distances less than or equal to 80 km (~50 mi) from the coast. There was a slight improvement in the linear regression model fit to the data, with an R^2 value of 0.27, compared to an R^2 value of 0.0002 for all sites combined (Figure 4.2-A). A slope of +0.01 was observed.

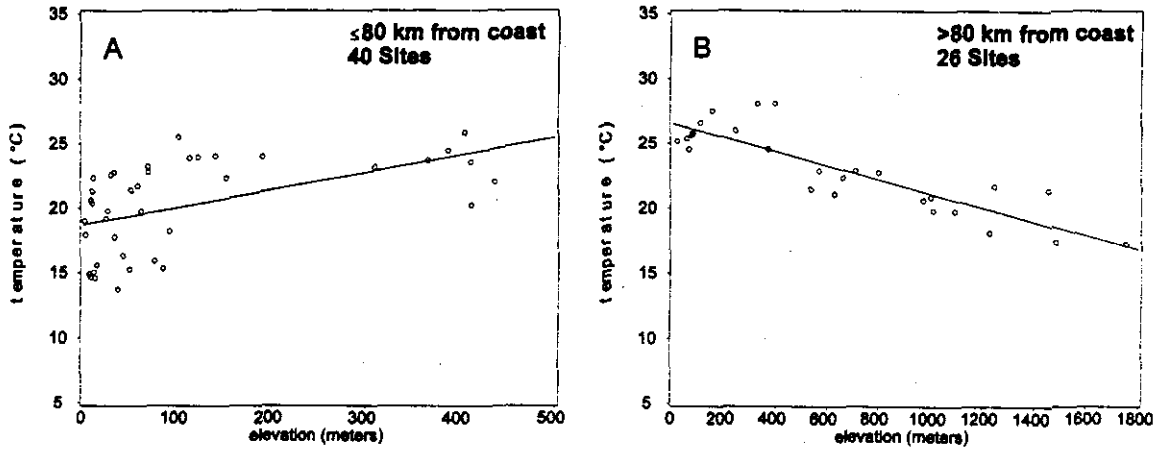

Figure 4.3. Relationship between August 1998 monthly average air temperature and elevation for 40 sites located ≤80 km (A) and 26 sites >80 km (B) from the coast.

Figure 4.3-B presents the same relationship for sites at distances >80 km (~50 mi) from the coast. The improvement in the linear regression model fit to the data was remarkable, with an R^2 value of 0.75 compared to an R^2 value of 0.0002 for all sites combined. A negative slope of -0.005 was found.

Monthly Average Air Temperature Versus Distance from Coast

Figure 4.2 illustrates the relationship between August 1998 monthly average air temperature versus distance from coast for all sites combined (66 sites). The R^2 value was 0.16 and the slope was +0.022. The relationship between August 1998 monthly average air temperature and distance from the coast was examined for the group of air temperature sites located at distances ≤80 km from the coast (Figure 4.4-A) and the group of sites located >80 km from the coast (Figure 4.4-B). For air temperature sites located >80 km (~50 mi) from the coast (Figure 4.4-B), the linear regression model relating August 1998 monthly average air temperature and distance from the coast was weak, with an R^2 value of 0.23 and a slope of -0.04. Air temperature sites located ≤80 km from the coast showed a great improvement in the linear regression model (Figure 4.4-A) with an R^2 value of 0.74 and a slope of 0.15.

There was a reversal in the importance of elevation and distance from the coast in explaining the variability in air temperature, depending upon the location of the air temperature site. For air temperature sites located at distances >80 km from the coast, elevation played a much greater role in explaining the variability in air temperature. Conversely, for air temperatures sites located ≤80 km from the coast, distance from the coast accounted for a large proportion of the variability in air temperature.

These changing relationships between air temperature with elevation and distance from coast should be borne in mind when attempting to model stream temperatures. Some researchers have used elevation as a surrogate for air temperature. We have demonstrated that surrogacy may or may not apply, depending on the location of the air or water temperature monitoring site with respect to distance from the coast. Relationships between air temperature versus distance from the coast and elevation vary seasonally as well. This seasonal variability is discussed later in the chapter.

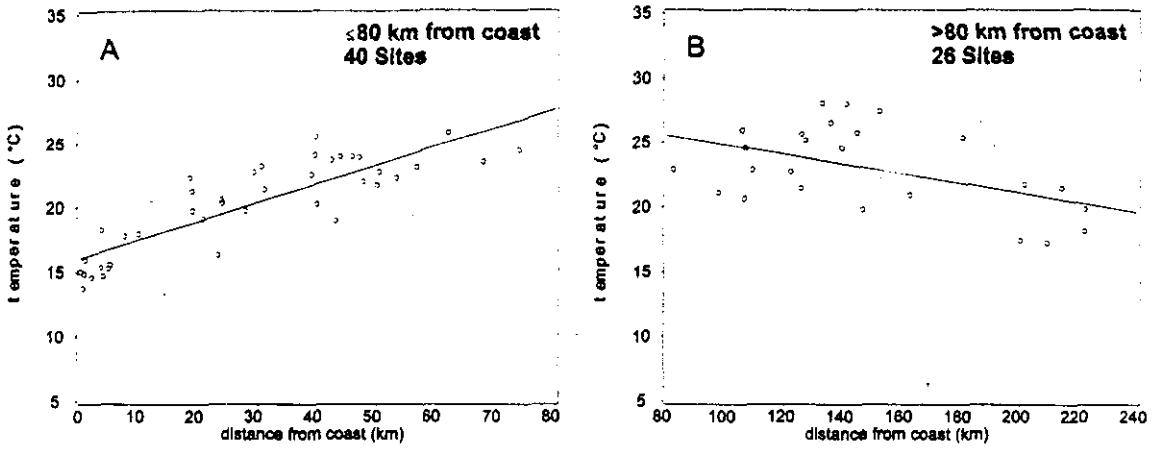

Figure 4.4. Relationship between August 1998 monthly average air temperature and distance from coast for 40 sites located ≤80 km (A) and 26 sites >80 km (B) from the coast.

Monthly Average Air Temperature by Ecoprovince

Although stratification of the air temperature data into distance-from-coast classes greatly improved the linear regression models, the stratification was somewhat arbitrary. The observed relationship between air temperature versus elevation and distance from the coast undoubtedly plays a role in the distribution of plant communities and ecosystems across the region. Using Bailey's ecophysiographic regions (USDA, 1997) to stratify air temperature data was the next logical step. The area of interest defined for the regional stream temperature assessment encompasses two major ecoprovinces, the California Coastal Steppe Province (263) (CSP) and the Sierran Steppe-Mixed Forest-Coniferous Forest Province (M261) (Figure 4.5). Within the California Sierran Steppe-Mixed Forest-Coniferous Forest Province (SSP), air temperature data were limited to five ecosections, the Klamath Mountains Section (M261A), the Northern California Coast Ranges Section (M261B), the Northern California Interior Coast Ranges Section (M261C), the Southern Cascades Section (M261D), and the Modoc Plateau (M261G). The four sections were aggregated together and represent those ecophysiographic areas for which both stream temperature and air temperature were used in the regional assessment.The relationship between elevation and distance from the coast is shown in Figure 4.6 for each ecoprovince. The highest elevation at which air temperature sites were located in the CSP was approximately 160 m (525 ft) at about 20 km from the coast, compared to about 1800 m (~5900 ft) in the SSP. The relationship between distance from the coast and elevation for the SSP was nearly linear. However, there were several low lying sites located a considerable distances from the coast (100 to 160 km).

Table 4.1 shows the air temperature versus distance-from-coast linear regression model fit to the air temperature sites in the CSP. The regression line fit to the data (Figure 4.7-A) had an R^2 value of 0.6925, a marked improvement over the all-sites-combined model ($R^2 = 0.1547$).

August 1998 monthly average air temperature versus elevation for each ecoprovince are compared to the ≤80 km and >80 km from the coast air temperature groups in Table 4.1. For the SSP the linear regression model was greatly improved over the all-sites-combined model, with an R^2 value of 0.6517.

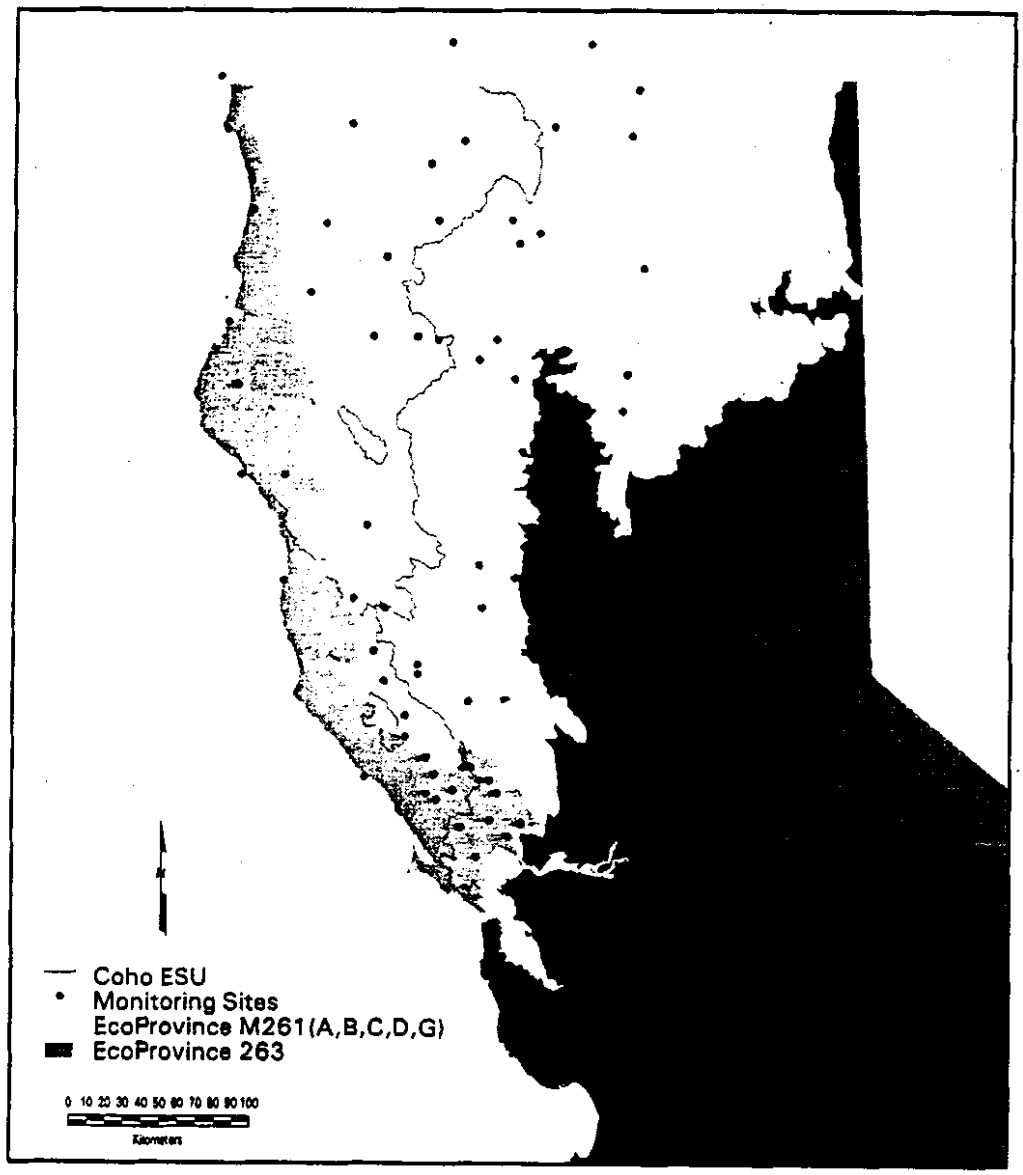

Figure 4.5. Distribution of air temperature monitoring sites in the Coastal Steppe, Mixed Forest and Redwood Forest Province (263) and the Sierran Steppe-Mixed Forest - Coniferous Forest Province (M261).

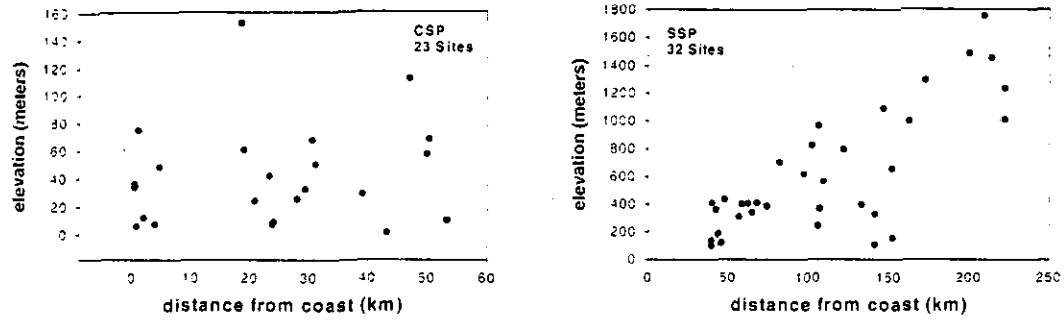

Figure 4.6. Relationship between distance from the coast and elevation for air temperature sites located in each ecoprovince.

Table 4.1. Linear Regression Models of August 1998 Monthly Average Air Temperature Versus Distance from Coast and Elevation by Air Temperature Site Groups.

Group	n	intercept	slope	R^2	F	pr (F)
			Air vs. Distance from Coast			
All Sites	66	21.3529	-0.0001	0.0002	0.0158	0.9004
≤80 km	40	18.7101	0.0134	0.2730	14.2703	0.0005
CSP[1]	22	17.9130	0.0350	0.1550	3.6685	0.0699
>80 km	26	26.5164	-0.0054	0.7531	73.2154	0.0001
SSP[2]	29	26.0759	-0.0052	0.6517	50.5287	0.0001
			Air vs. Elevation			
All Sites	66	19.6663	0.0216	0.1547	11.7129	0.0011
≤80 km	40	16.0482	0.1448	0.7378	106.9030	0.0001
CSP	22	15.5061	0.1583	0.6925	45.0362	0.0001
>80 km	26	28.5377	-0.0372	0.2325	7.2700	0.0126
SSP	29	25.2738	-0.0219	0.2128	7.3001	0.0118

[1]CSP = California Coastal Steppe Province
[2]SSP = Sierran Steppe-Mixed Forest-Coniferous Forest Province

This value is slightly less than the >80 km model, but has more of an ecological basis. The plot for the SSP (interior) air temperature versus elevation ecoprovincial model is shown in Figure 4.7-B.

There was a great improvement in the ecoprovincial linear regression models when coast distance was used as an independent variable. For the CSP, a strong R^2 value (0.6925) was found (Table 4.1, Figure 4.7-A). For the SSP, more of the variability in August 1998 monthly average air temperature was accounted for using elevation as the independent variable (Table 4.1, Figure 4.7-B).

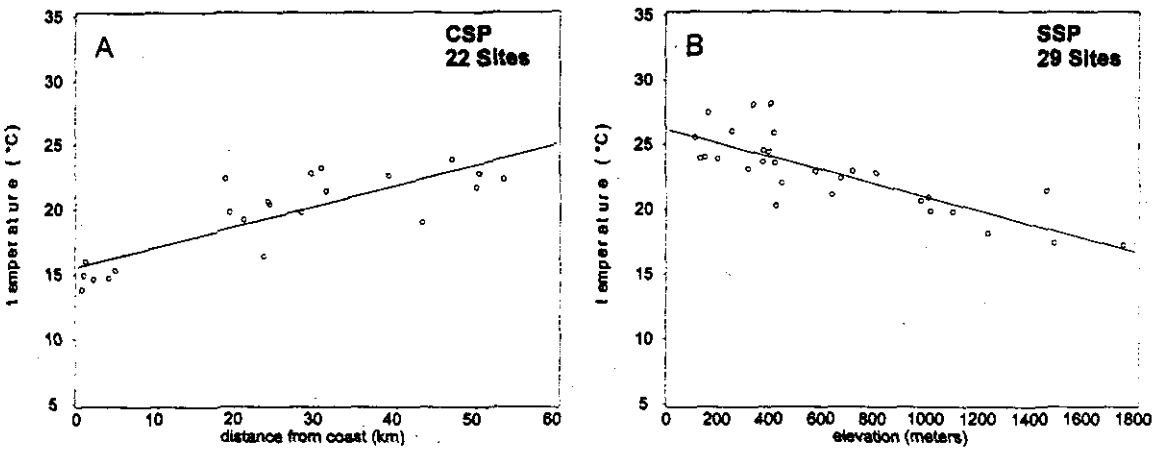

Figure 4.7. August 1998 monthly average air temperature versus distance from coast for 22 sites in the Coastal Steppe (A) and air temperature versus elevation for 29 sites in the Sierran Steppe-Mixed Forest-Coniferous Forest Province (B). Linear regression equations are presented in Table 4.1.

Seasonal Variation in Relationships

While it has been shown that elevation accounts for a large proportion of the variability in air temperatures for the SSP and distance from coast for the CSP, only August 1998 monthly average air temperature was used to develop these relationships. The relationship between air temperature and the two independent variables, elevation and distance from coast, changes seasonally. Linear regression analyses were performed on monthly average air temperatures for all months.

The winter months of December and January exhibited negative slopes for both air-versus-coast-distance and air-versus-elevation models for all air temperature site groups. The marine influence serves to make winter air temperatures warmer than those further inland and at higher elevations but cooler in the summer. This would account for the change in slope with season. The highest R^2 values were noted for the air-versus-elevation relationships for all sites combined, the >80 km-from-coast, and SSP groups. Moving into the warmer months, the slopes for the ≤80 km and CSP groups began to shift from negative to positive values for the air-elevation models. During the transition from winter to summer the R^2 values for these two groups steadily increased for the air-versus-coast distance relationships, and decreased for the air-versus-elevation relationships. The air-versus-elevation R^2 values for the >80 km and SSP groups remained high across all months and their accompanying slopes remained negative across all months.

These results clearly demonstrate the need to consider both the temporal and spatial relationships between air temperature versus elevation and distance from coast. If either elevation or distance from coast are to be used as surrogates for air temperature to predict water temperature, the geographic and seasonal variations in these relationships must be taken into account.

Ecoprovincial Differences in Air Temperature

The difference in the relationship between monthly average air temperature and distance from the coast, and monthly average air temperature and elevation has been demonstrated in the previous section. What has not been explored is the relative difference between air temperatures in the CSP and the SSP. Figure 4.5 shows the distribution of the 72 air temperature sites in these two ecoprovinces.

Figure 4.8 presents the August average and average maximum air temperatures for the CSP and SSP for 1990 through 1998. Only air temperature sites with August data for all nine years were used in the analyses. There were 22 sites in the SSP and 12 sites in the CSP with which to make comparisons across the nine years. The August averages were compared to the 30-yr long-term average derived for each site using the PRISM model. That is, at each of the 34 air monitoring site the 30-yr long-term average and average maximum for August was determined from the GIS data set developed from the PRISM model. PRISM data for air temperature sites in each ecoprovince were averaged to obtain the ecoprovincial long-term August average.

The CSP August average air temperatures were lower than SSP averages for all years. The cooling influence of marine air currents is responsible for the cooler air temperatures observed in the CSP compared to the SSP. The graph serves to illustrate that some years were warmer than the long-term average, and that these warmer years did not necessarily transcend ecoprovinces. For example, while 1996 exhibited above normal air temperature for the SSP, the CSP was about normal. Conversely, 1993 exhibited above normal air temperatures for the CSP, while SSP air temperatures were below normal. August was the month used in the comparison since this is the month when the highest water temperatures normally occur for most sites. Comparison of other ecoprovincial monthly average air temperatures (i.e., June, July, and September) to the long-term average for that month showed slightly different patterns.

The purpose of this comparison is to provide researchers with qualitative information on the year-to-year variability that is observed in each ecoprovince. If a group of water temperature sites was monitored across multiple years, this information could assist in determining whether trends in water temperature may be due to differences in air temperature across years.

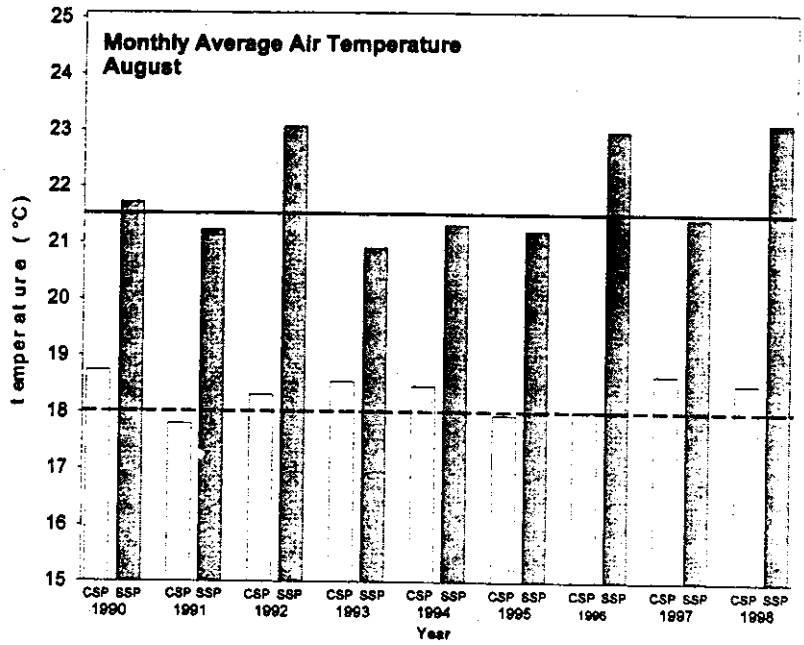

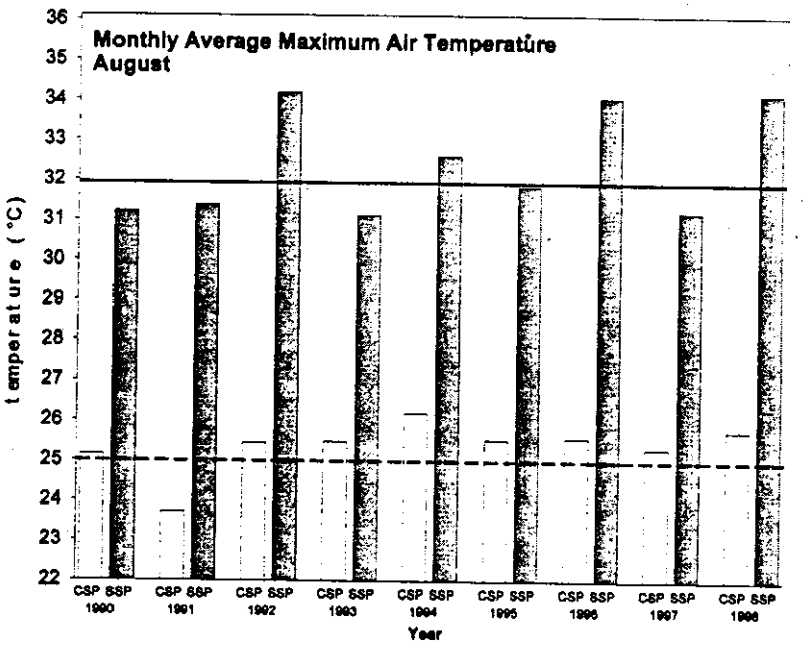

Figure 4.8. Comparison of ecoprovincial air temperatures for August 1990 - 1998. Ecoprovince CSP = California Coastal Steppe Province (12 coastal sites) and SSP = Sierran Steppe-Mixed Forest-Coniferous Forest Province (22 interior sites). Dashed and solid horizontal lines represent 30-yr long-term averages derived from the PRISM model for the coastal and interior ecoprovinces, respectively. PRISM monthly average calculated as max+min/2.

Air Temperature By Evolutionarily Significant Unit

Similar air temperature comparisons were performed by coho salmon evolutionarily significant units (ESU). There were 15 air temperature sites in the SONCC ESU with August air temperature for years 1990 through 1998 and 8 sites in the Central California ESU. The 30-year long-term averages derived by averaging the PRISM air temperature values at each of the 23 air temperature sites revealed that the ESU averages were very similar (Figure 4.9). We expected the SONCC ESU to exhibit higher long-term average temperatures than the CC ESU because of the greater inland areal extent of the SONCC ESU. The SONCC ESU transcends both the CSP and SSP ecoprovinces, whereas the CC ESU is mostly associated with the CSP ecoprovince. The more coastal distribution of sites in the SONCC ESU with complete August data for all nine years could account for the lower-than-expected 30-year long-term average. Weitkamp et al. (1995) reported that the average annual sunshine along the coast in the Central California ESU is higher than anywhere further north, averaging 2200-2800 hours per year, while the SONCC receives 2000-2200 hours per year of sunshine. If one only considers the coastal portion of the SONCC, the somewhat lower hours of sunshine may result in cooler air temperatures. However, we consider the SONCC as a whole (both the coastal and inland portions), and believe that, on average, it is most likely warmer than the CC ESU.

Both ESUs showed above normal August average air temperatures in 1990, 1992, 1996, 1997 and 1998 (Figure 4.9). Not unlike ecoprovincial trends in air temperature across years, August average air temperatures did not vary similarly in the two ESUs. In some years the CC ESU was above normal while the SONCC was below normal and in other years the opposite trend was observed.

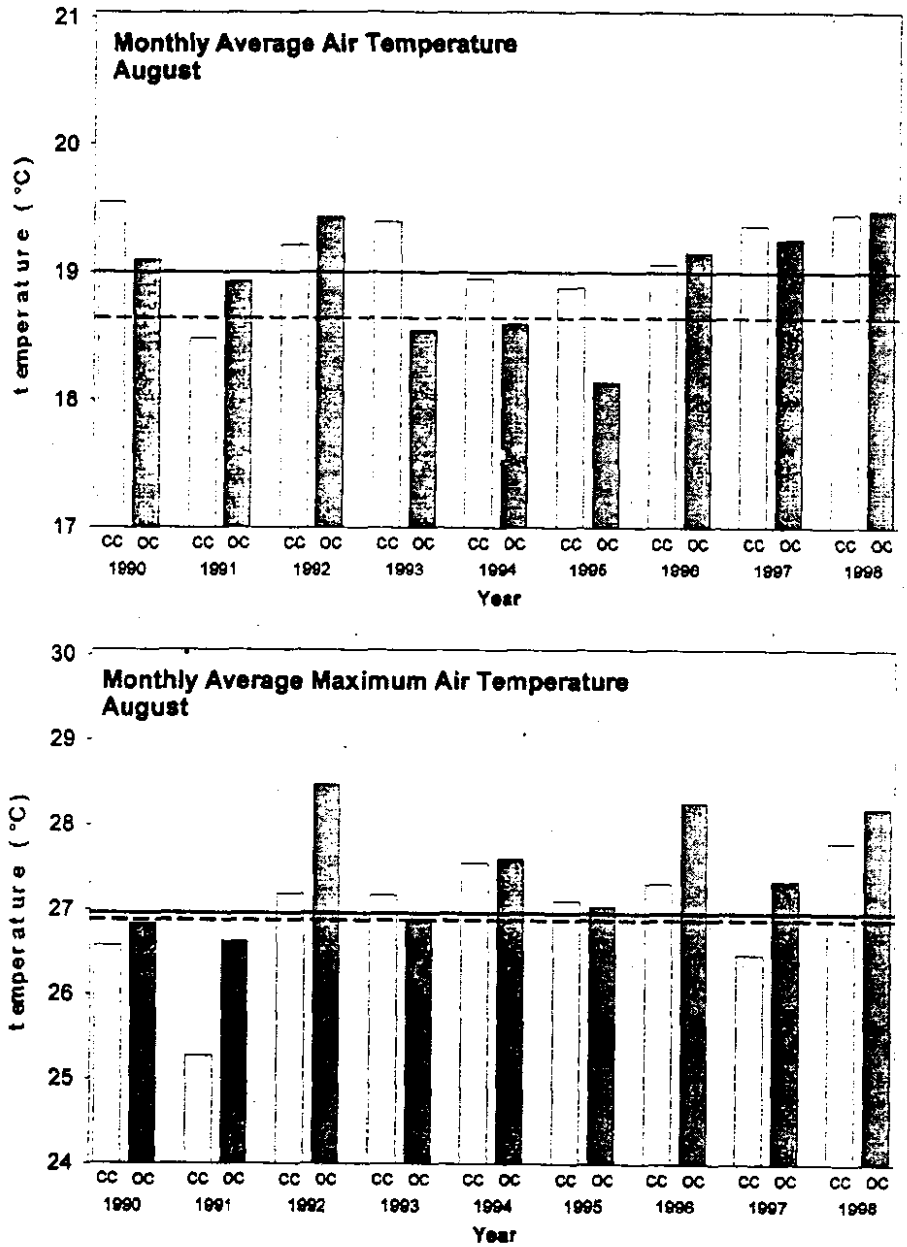

Figure 4.9. Comparison of ESU average air temperatures for August 1990 - 1998. CC = Central California ESU (8 sites) and OC = Southern Oregon Northern Coastal California ESU (15 interior sites). Dashed and solid horizontal lines represent 30-yr long-term averages derived from the PRISM model for the CC and SONCC ESUs, respectively. PRISM monthly average calculated as max+min/2.

Variation in Basin-Level Air Temperatures

Figure 4.8 serves to illustrate the variation in air temperatures between years and between ecoprovinces. The SSP exhibited higher air temperatures than the CSP. The CSP and SSP are comprised of hydrologic units (HUCs) that also possess unique air temperature regimes.

Figure 4.10 shows the hydrologic units (HUCs) that comprise the range of the coho salmon in Northern California. The inset table in Figure 4.10 lists the HUC ID number and the HUC name.

PRISM-derived 30-year averages for August are displayed with respect to the HUC boundaries in Figure 4.11. Figure 4.12 presents the 30-year average maximum August air temperature. The coastal zone is much cooler than the more interior portions of the region. The coastal HUCs with southeast-to-northwest orientations, like the Lower Eel, Mad-Redwood, and South Fork Eel, and combined Upper, Middle, and Lower Eel HUCs have large temperature gradients from the upper headwaters to the coast. Air temperature gradients can be as much as 5°C to 15°C from headwaters to coast.

HUC-level averages were calculated to develop a picture of how average temperatures vary across HUCs. Table 4.2 presents the HUC-level 30-year August average minimum, average, and maximum air temperatures and the standard deviation and range in temperatures within each HUC. The minima and maxima are the lowest and highest August average temperature values in the HUC in any given 4-km grid cell. Those HUCs with southeast-to-northwest orientations have higher average values due to the contribution of higher interior air temperatures to the average. HUCs that are predominately along the coast have lower average air temperatures. HUCs that are completely in the interior have higher averages than coastal HUCs.

At the time of writing of this report only 1961-1991 30-yr average PRISM data for each month were available for the regional stream temperature assessment. More recently it has been learned that monthly average PRISM air temperature data for individual years may be available but have not been acquired to date. With monthly average PRISM data for each year, more localized air temperature estimates will be possible. This will greatly improve the predictive power of air temperature in the statistical models presented in Chapter 10.

Zone of Coastal Influence

PRISM data sets were used to develop a relationship between the 30-year average maximum monthly air temperature (AVGMAX) and the inland extent of the coastal effect. The PRISM AVGMAX raster data sets were converted from a 4-km grid spacing to a 1-km cell size using a bilinear resampling technique (Arc/Info GRID). The first derivative (slope) was calculated for the July and August AVGMAX data. These grids represent the rate of change in air temperature over distance. The rate averaged 0.30 C°/km for both coho ESUs. The maximum rates of change for July and August were 1.60 C°/km and 1.66 C°/km respectively. Figure 4.13 illustrates the variability of this rate over the coho ESUs for the month of July. A high rate of change is evident, roughly paralleling the coast from 2.8 to 32 km inland. Using the rate-of-change grids, a linear feature representing the maximum rate of change was derived. The rate of temperature change along this line varies between 0.43 C°/km and 1.43 C°/km with a mean of 0.78 C°/km. This line is an approximation of the maximum inland extent of the coastal cooling effect and is hereafter referred to as the zone of coastal influence (ZCI). ZCI is also our best approximation of the fog zone. It has not been validated. The extent of inland fog varies daily, seasonally, and from year to year.

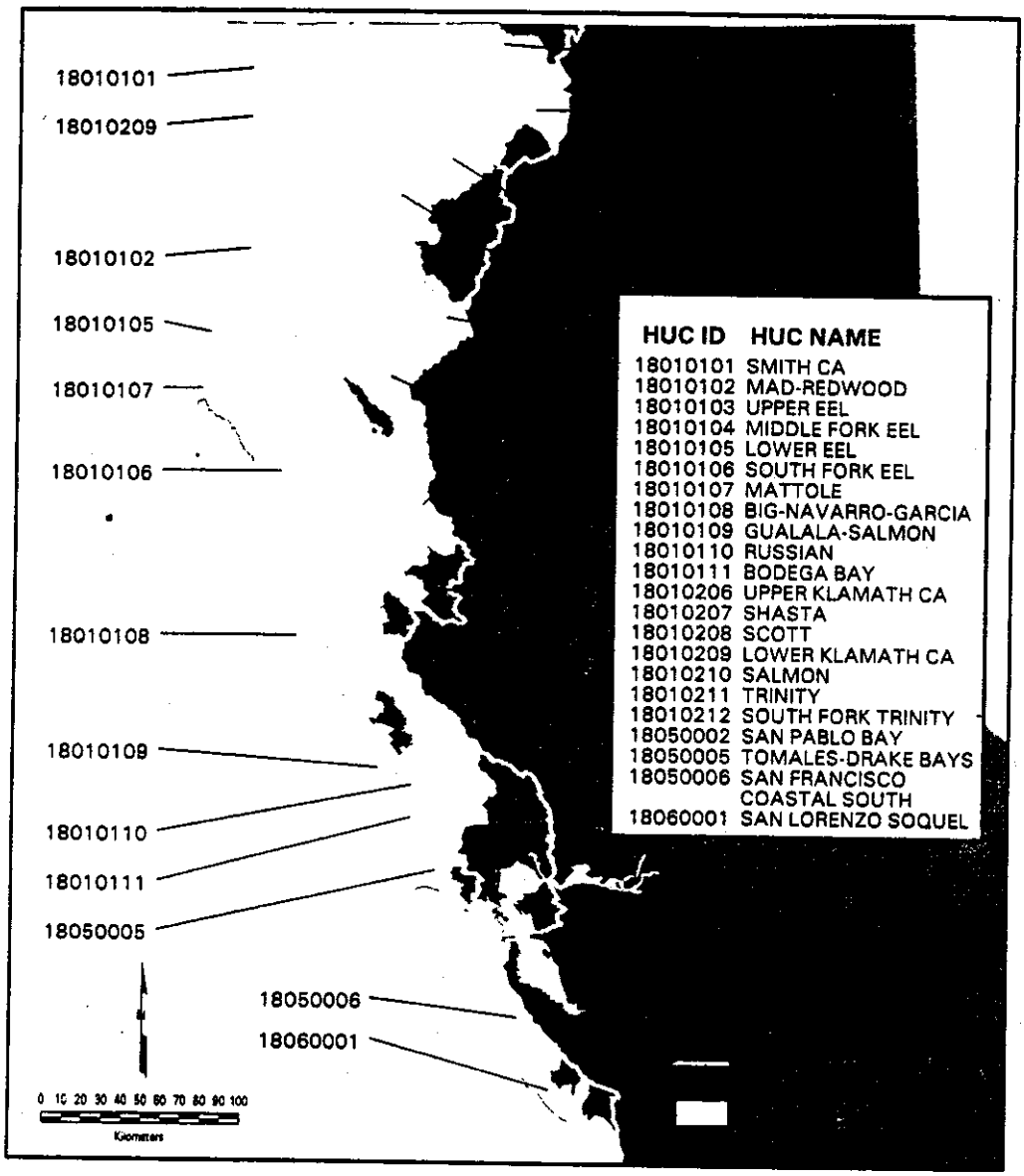

Figure 4.10. Hydrologic units that comprise the range of coho salmon in Northern California. The shaded area represents the coho ESU boundary.

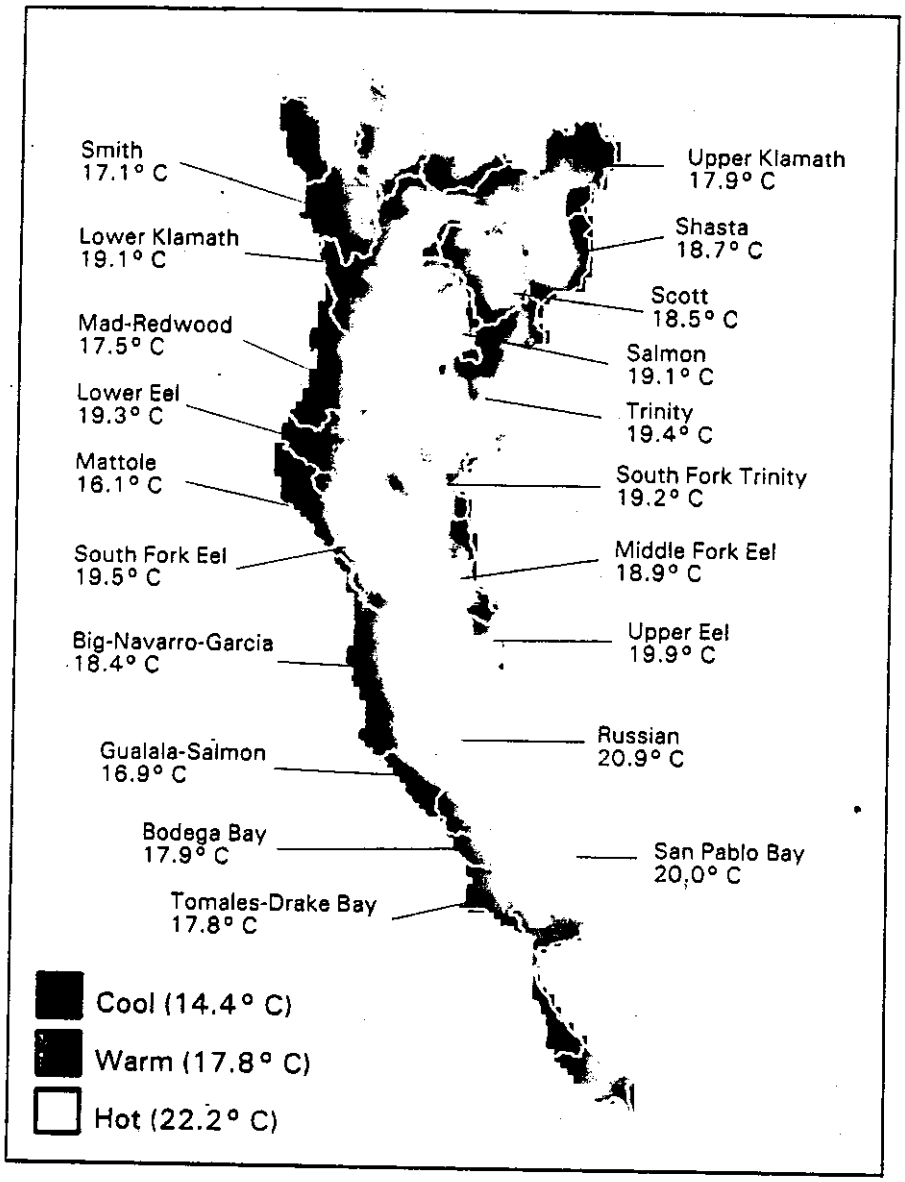

Figure 4.11. PRISM-derived August monthly average air temperatures across HUCs that comprise the range of the coho in Northern California.

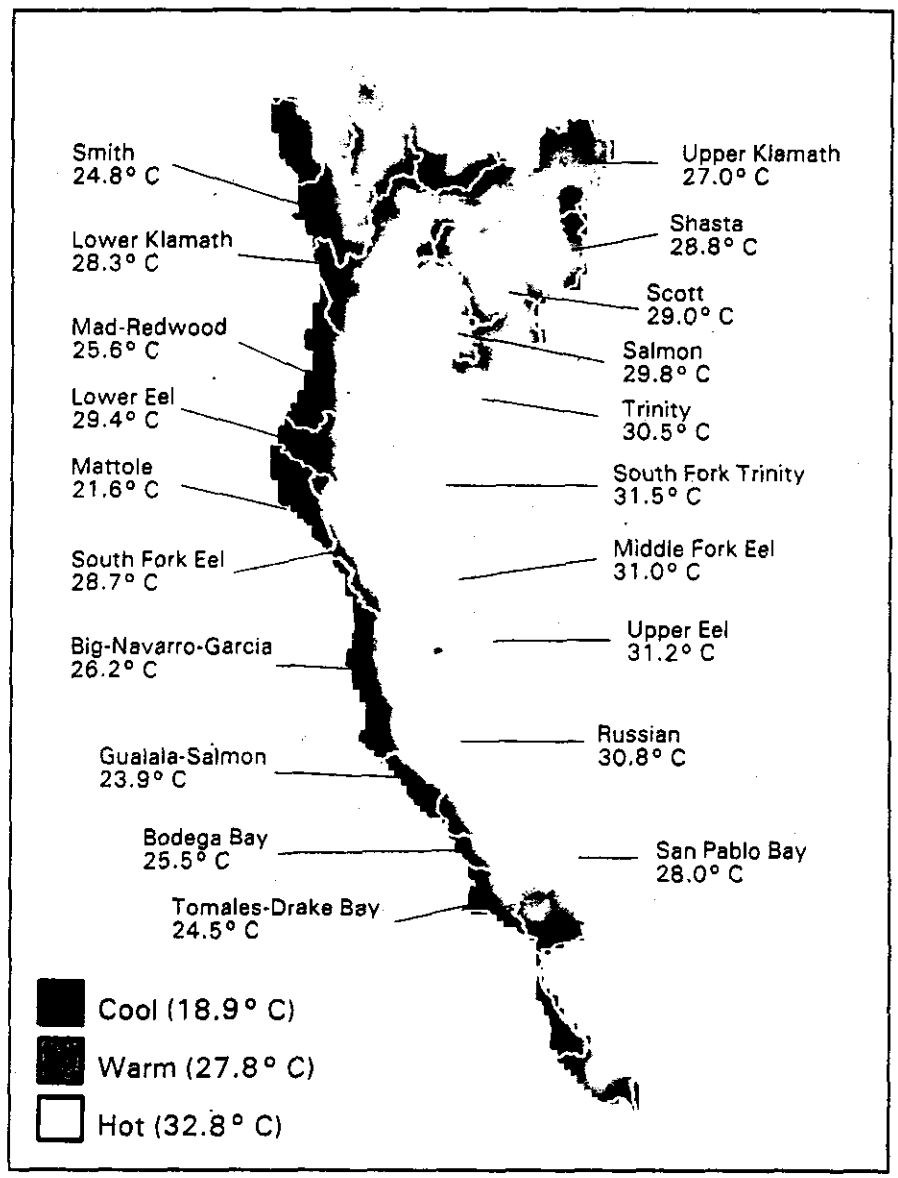

Figure 4.12. PRISM-derived August monthly average maximum air temperatures across HUCs that comprise the range of the coho in Northern California.

Table 4.2. PRISM 30-Year August Average Air Temperature Statistics for Hydrologic Units that Comprise the Range of the Coho Salmon in Northern California.

HUC Name	Minimum	Maximum	Range	Average	Std. Dev.
Smith	13.9	19.8	5.9	17.1	1.48
Mad-Redwood	14.5	20.4	5.9	17.5	1.94
Upper Eel	16.8	21.9	5.1	19.9	1.07
Middle Fork Eel	14.9	21.7	6.8	18.9	1.84
Lower Eel	14.7	21.6	6.9	19.3	1.68
South Fork Eel	15.9	21.5	5.6	19.5	1.27
Mattole	14.7	20.1	5.4	16.1	1.25
Big-Navarro-Garcia	14.6	22.1	7.5	18.4	2.16
Gualala-Salmon	13.6	21.2	7.6	16.9	2.45
Russian	14.8	22.7	7.8	20.9	1.45
Bodega Bay	15.3	19.9	4.6	17.9	1.35
Upper Klamath	13.1	21.1	8.1	17.9	1.89
Shasta	8.1	22.3	14.2	18.7	2.81
Scott	15.1	20.4	5.3	18.5	1.27
Lower Klamath	15.1	22.4	7.3	19.1	2.15
Salmon	15.5	21.9	6.4	19.1	1.67
Trinity	13.4	22.4	9.0	19.4	1.99
South Fork Trinity	15.1	22.4	7.3	19.2	1.34
San Pablo Bay	15.7	21.9	6.2	20.0	1.26
Tomales-Drake Bays	15.8	20.6	4.8	17.8	1.36
San Francisco Coastal South	15.0	17.9	2.9	16.1	0.76
San Lorenzo Soquel	15.8	20.1	4.3	18.1	1.08

NOTE: August Minimum, Maximum, Range, Average, and Standard Deviation are statistics based on the August average air temperature across all 4-km cells that comprise the HUC.

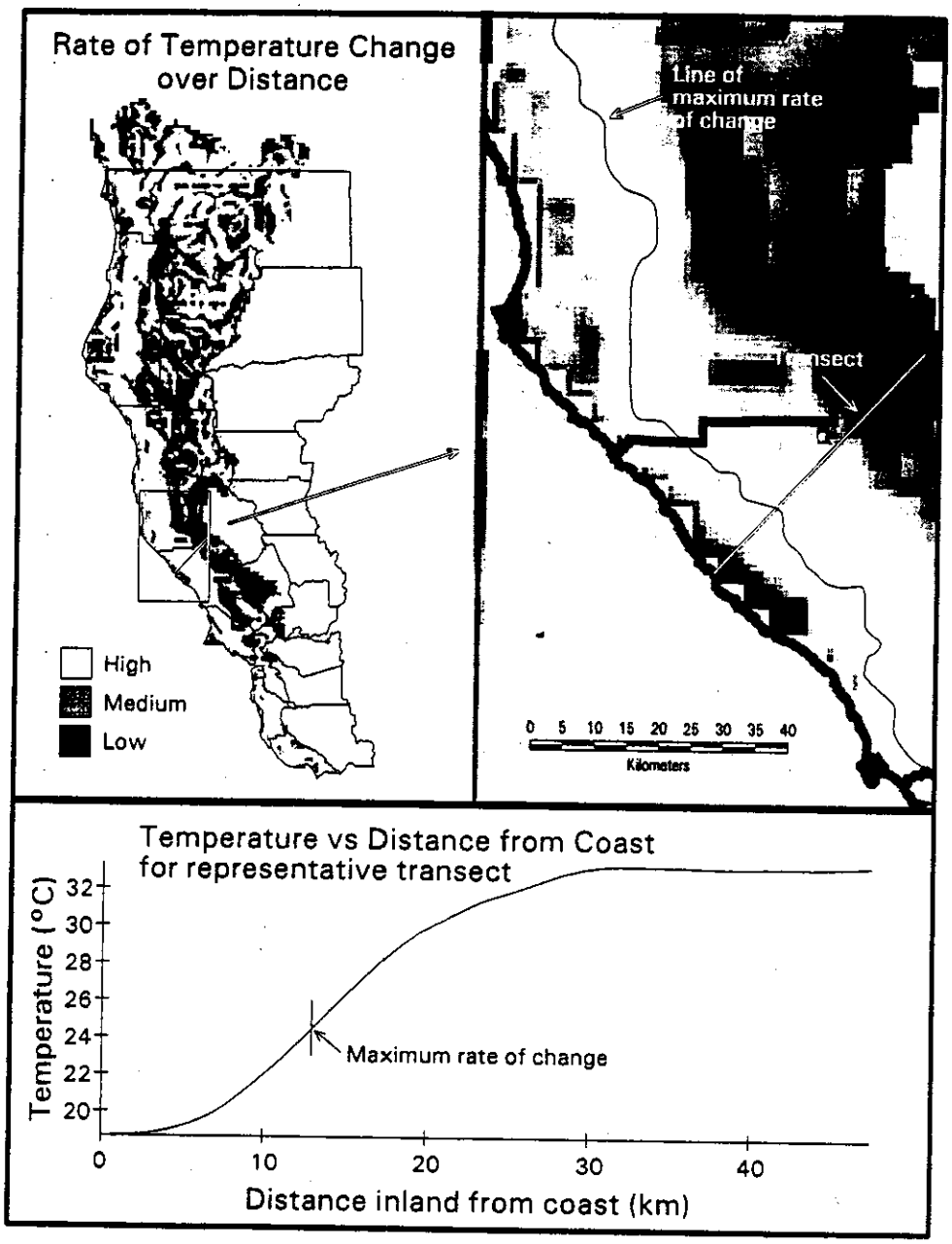

Figure 4.13. Derivation of the zone of coastal influence. Maximum rate of change determined using 30-yr PRISM August maximum average grid coverage across the range of coho salmon. Maximum rate of change is shown for a representative transect.

Mean Annual Air Temperature and Estimated Groundwater Temperature

Groundwater temperature is reportedly within ± 1°C to 3°C of mean annual air temperature (Collins, 1925; Sullivan et al., 1990). Using PRISM 30-yr air temperature data the mean annual air temperature was calculated within each 4-km grid cell. The resulting spatial display shown in Figure 4.14 presents the estimated groundwater temperature throughout the HUCs within the range of the coho salmon. HUC-level average groundwater temperatures are indicated. It is interesting to note that in some locations, the estimated groundwater temperature is within a few degrees of the Maximum Weekly Average Temperature (MWAT) threshold of 18.3°C that is often used as a target temperature for coho salmon streams. The Forest Science Project is acquiring and analyzing well-monitoring data from the U.S. Geological Survey and other sources to validate these groundwater temperature estimates.

If these groundwater estimates are accurate, then many headwater streams in the range of the coho salmon originate in areas of high air and groundwater temperature. Given the natural warming trend of streams in a longitudinal direction, very little downstream travel distance would be needed before stream temperatures exceed various chronic and acute thermal stress thresholds for juvenile coho salmon and other salmon species that have been developed in the laboratory and applied to field conditions.

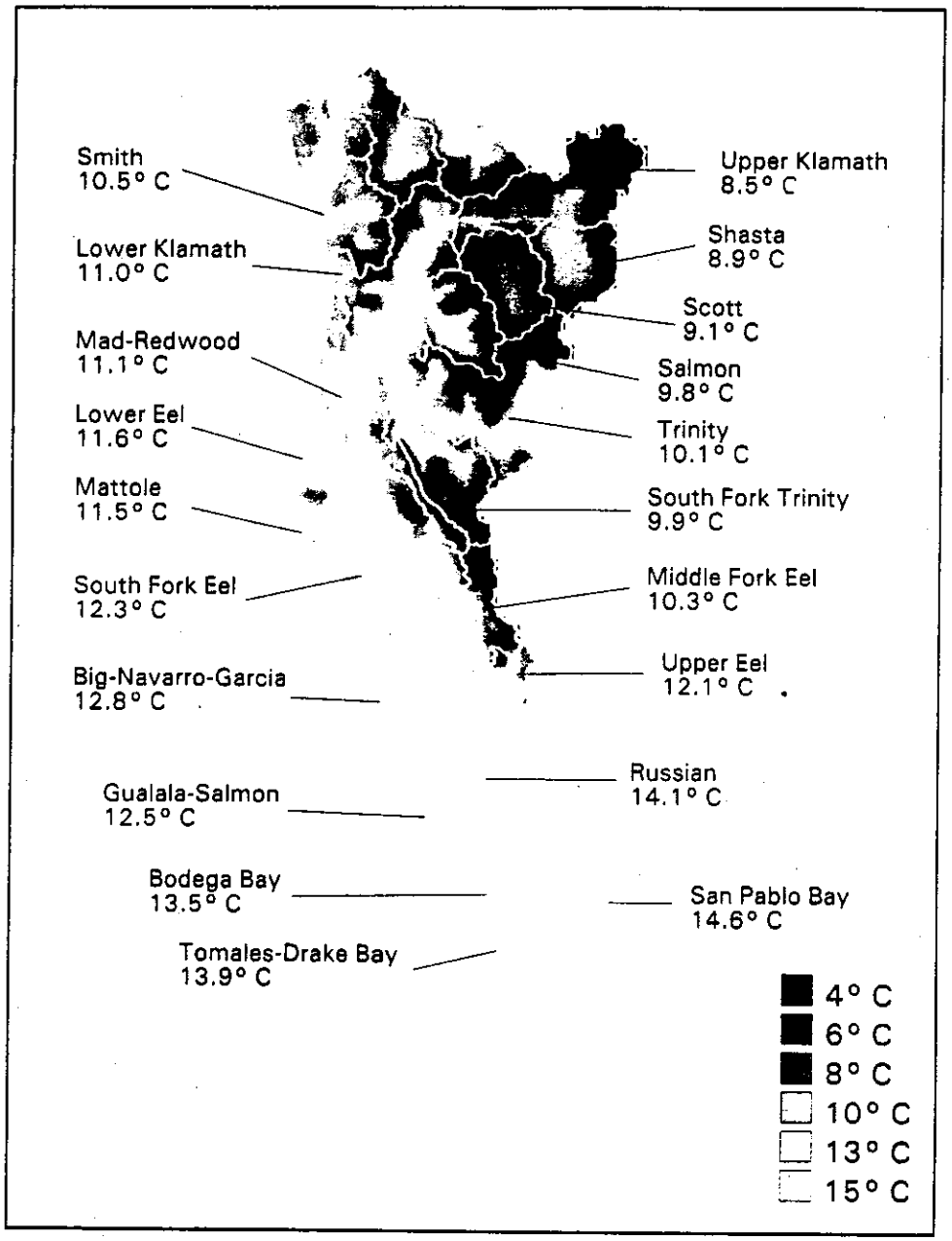

Figure 4.14. Groundwater temperature estimated from PRISM 30-yr mean annual air temperature in HUCs that comprise the range of the coho salmon in Northern California.

Summary

Air temperatures did not follow expected adiabatic cooling trends across the entire study area. Near the coast, air temperature was more a function of distance from the coast rather than elevation. Near the coast, summertime air temperatures increased with increasing elevation. Modelers should use caution when using elevation as a surrogate for air temperature. In the interior portion of the study area, air temperatures followed a more expected trend: decreasing air temperature with increasing elevation. The relationship between air temperature and the two independent variables, distance from the coast and elevation varied seasonally. During the winter months air temperatures in the coastal portion of the study area conformed more to the negative relationship with elevation.

The 1990-1998 CSP August average air temperatures were lower than SSP averages for all years. The cooling influence of marine air currents is most likely responsible for the cooler air temperatures observed in the CSP compared to the SSP. Some years were warmer than the long-term average. Warmer years did not necessarily coincide between ecoprovinces. For example, while 1992 exhibited above normal air temperature for the SSP, the CSP was below normal. Conversely, 1993 exhibited above normal air temperatures for the CSP, while SSP air temperatures were below normal.

Air temperatures exhibit appreciable gradients within and across the HUCs that comprise the range of the coho salmon in Northern California. Hydrologic units that are predominantly coastal have cooler air temperatures whereas those that have a somewhat southeasterly to northwesterly orientation show strong thermal gradients. Some HUCs are 10°C to 15°C warmer in the upper reaches than near the coast. Interior HUCs have warmer air temperatures throughout their drainage area, with cooler air temperatures at higher elevations.

The zone of coastal influence (ZCI) was derived from 30-yr long-term PRISM air temperature data by defining the steepest rate of change in air temperature along transects at increasing distances from the coast. The ZCI is an approximation of the fog zone, which intuitively would have a cooling influence on water temperatures due to its associated cooler air temperatures and solar energy interception.

Spatial trends in air temperature across the region must be understood in order to predict their influence on water temperatures. A useful air temperature database has been developed to characterize air temperature regimes across Northern California. In the next chapter we will explore the influence of these significant air temperature gradients on regional water temperatures. Acquisition of the monthly average PRISM air temperature data for individual water temperature years will greatly improve our understanding of the role air temperature plays in influencing water temperatures at large spatial scales.

Groundwater temperature was estimated from PRISM 30-yr mean annual air temperature. At some locations in the range of the coho salmon in Northern California, groundwater temperature is within a few degrees of a commonly applied MWAT threshold of 18.3°C. Some headwater streams may originate in areas with high air and groundwater temperature. Very little downstream travel distance would be needed before these streams would exceed various chronic and acute thermal stress thresholds. These exceedances could conceivably occur with natural longitudinal warming of streams.

Chapter 5

AIR AND WATER TEMPERATURE RELATIONSHIPS

Introduction

The previous chapter examined regional trends in air temperature throughout the range of coho salmon in Northern California. It was shown that air temperatures vary greatly across the region. This chapter examines whether air temperature measured at remote sites can be useful in explaining the variability in water temperature. Ideally, air temperature monitored at stream-side would provide the most representative information on the equilibrium temperature of a stream. However, very few sites in the regional assessment data set had air temperature collected at the stream temperature monitoring location. Due to the paucity of stream-side air temperature data we evaluated whether NOAA and other remote air temperature station data may have some explanatory power with respect to water temperature. These data are referred to as ***macroair*** temperature throughout this chapter.

At 23 water temperature sites, air temperature was monitored in close proximity to the water temperature sensor. These data will be referred to as ***microair*** temperatures. Analyses were performed on data from this limited number of sites, comparing trends in macroair versus microair temperatures, and air versus water temperatures.

Use of remote estimates of air temperature may result in inaccurate estimates of water temperature. This was observed by Sullivan and coworkers (1990) using data from six NOAA stations and is borne out in this report, using 72 remote air sites. In model sensitivity analyses, Bartholow (1989) and Sinokrot and Stefan (1994) ranked air temperature as the single most important parameter for predicting water temperature, followed by solar radiation. However, as Bartholow (1989) points out, many other factors, including humidity, wind speed, riparian canopy, as well as factors in combination with air temperature, contribute to equilibrium water temperatures. The variability of these conditions make trying to predict water temperatures from remote air temperatures difficult. Given the importance of air temperature in predicting water temperature at daily, seasonal, and yearly temporal scales, it is perplexing that more data contributors did not measure stream-side air temperature.

Various studies (Collins, 1925; Moore, 1967; Kothandaraman and Evans, 1972) indicate that mean water temperature is generally within a few degrees of mean air temperature measured at stream-side. Moore (1967) found that for Oregon streams air temperature was a reasonable index of water temperature, but, because of other factors affecting water temperature, some Oregon streams were warmer and some were cooler than air temperature. The correlation between air temperature and water temperature is largely a function of upstream riparian conditions along a thermal reach, and to other factors controlling water inflow into the channel. However, air temperature influences both mean and maximum water temperatures regardless of riparian cover or stream size (Sullivan et. al., 1990). As streams increase in size at points more distant from the watershed divide, riparian characteristics become less influential in controlling water temperature. Large streams, because of their width relative to flanking

vegetation, naturally have less shade (Essie, 1998). Water temperature becomes more a function of air temperature.

At some sites where air temperature was monitored near the stream, good correlation was found with remote air temperature. We found that microair correlated better with water temperature than did macroair at 10 water temperature sites where air temperature was monitored at stream-side.

At 154 FSP sites that were monitored across three consecutive years (1996-1998), year-to-year changes in air temperature were shown to have some influence on water temperatures. The level of influence was dependent upon the stream's size, as estimated by the distance from the watershed divide.

Determining Nearest Remote Air Station

For many aspects of stream temperature analysis, ambient air temperature data are needed. If air temperature is not recorded in the immediate vicinity of the stream temperature site, data from remote air stations must be used to estimate local air temperatures. However, as Sullivan et al. (1990) pointed out, if remote or approximated air temperature data are used in predicting stream temperatures, then one can only hope for remote or approximated predicted stream temperature values.

The simplest method of determining the nearest air site to a stream temperature site is to use a minimum straight-line distance. However, as noted in the previous chapter, *Regional Trends in Air Temperature*, distance from coast and elevation are important parameters for describing regional variability in air temperature regimes within the study area. As such, these parameters should also be included in the model to select the most appropriate air temperature site. Using four parameters (UTM X-coordinate, UTM Y-coordinate, elevation, and distance to coast), four-dimensional Euclidian distances were calculated between each stream site and each air site. Air temperature sites with the smallest Euclidian distance were matched with water temperature sites for analysis. Monthly mean stream temperatures for June through September 1998 at 546 sites and corresponding monthly mean air temperature data were used to examine the strength of the relationship. Figure 5.1-A shows the linear regression of monthly mean stream temperatures to mean air temperatures using the four-dimensional Euclidian distance criteria. The relationship was highly variable ($R^2 = 0.15$).

Because of the relatively low R^2 value for the four-dimensional model, additional parameters were added to the model in an attempt to improve the estimate. These additional parameters were long-term minimum and maximum air temperatures at each air station estimated from the PRISM data model. PRISM 30-year long-term monthly air temperature metrics for June through September (1961 - 1991) resulted in eight additional parameters being included in the model. Twelve-dimensional Euclidian distances were calculated between each stream site and each air site. Figure 5.1-B shows the regression of monthly mean stream temperatures to monthly mean air temperatures using the 12-dimensional Euclidian distance model. Although there was only a slight improvement in the R^2, it was felt that, based on best professional judgement and personal knowledge of the climate regimes in Northern California, the 12-parameter method appeared to provide more realistic matchings between air and water temperature sites. The most notable changes were in the coastal areas, where the four-dimensional model selected air sites that were closer to the water site yet were 20 to 50 km inland. The 12-dimensional model was more sensitive to coastal versus inland air temperature differences. Moreover, the 12-dimensional model was better at selecting air sites that were more representative of air temperature at the water site based on the PRISM 30-year long-term values for the water site. This often meant that for a coastal water site the model might select a coastal air site that was 84 km away as opposed to an inland site that was only 20 km away. The mean distance between air stations and stream temperature sites using the 12-dimensional Euclidian distance method was 25 km, with a range of 0.3 to 84 km.

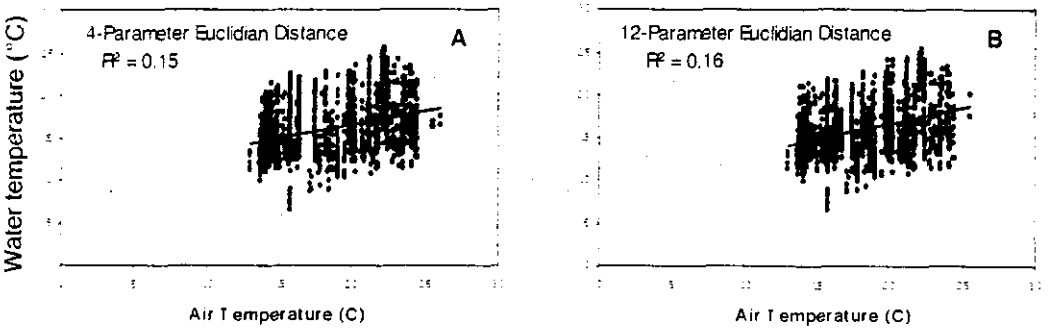

Figure 5.1. Comparison of linear regressions for monthly average air temperatures versus monthly average water temperatures using (A) four- and (B) 12-dimensional minimum Euclidian distance models. June, July, August, and September 1998 monthly averages are plotted for 546 water temperature sites.

Micro- and Macro-Air Temperature Relationships

To determine how well remote air temperature might predict local air temperature at a water temperature site, we acquired stream-side air temperature data. There were 40 water temperature sites where stream-side air temperature was monitored. Of these 40 sites, 23 sites had complete microair temperature data for comparison to data collected at macroair temperature sites selected using the 12-dimensional Euclidian distance model described above. Figure 5.2 shows comparisons between August monthly macro- and micro-air average and maximum temperature data. The monthly average microair temperature generally fell below the line of one-to-one correspondence (Figure 5.2-A), while the monthly maximum microair temperature was above this line (Figure 5.2-B). While there was an obvious positive correlation between average micro- and macro-air temperature ($R^2 = 0.1902$) and maximum micro- and macro-air temperature ($R^2 = 0.1790$), microair temperatures exhibited a 5-10°C range at certain macroair temperature values.

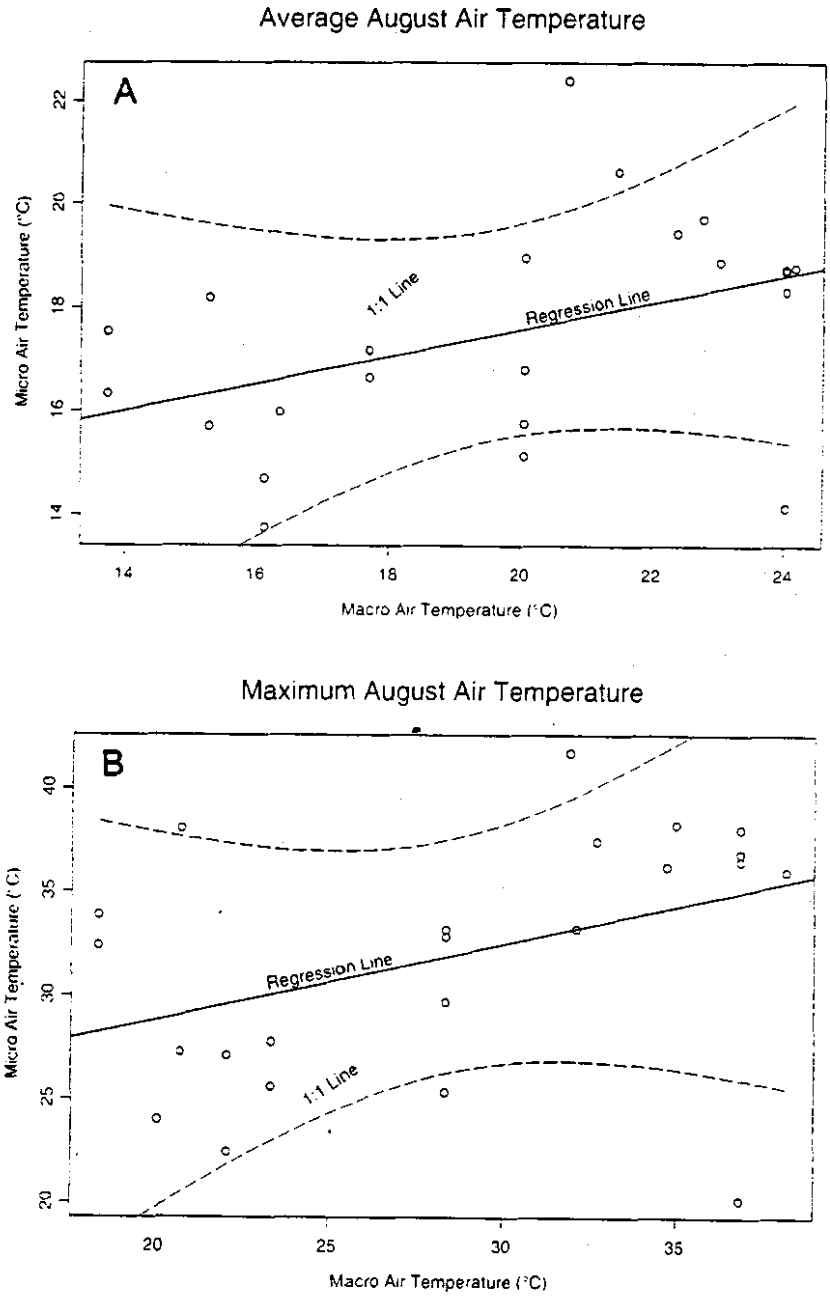

Figure 5.2. Comparison of August monthly average (A) and maximum (B) macro- versus micro-air temperature. Regression line and line of one-to-one correspondence is shown. Dashed lines represent 95% confidence bounds for predicting microair temperature from macroair temperature.

Comparison of Macroair and Stream Temperatures

Monthly average air temperature data from the nearest 12-dimensional Euclidian distance site was merged with its corresponding monthly average stream temperature at each site. Analyses were performed to explore the relationships between air-water temperatures across the entire study area, i.e., the two coho salmon ESUs in Northern California, and smaller spatial scales (e.g., ecoprovinces, HUCs, zone of coastal influence).

Figure 5.1 illustrates the rather poor correlation between macroair and water temperature exhibited for all 1998 sites in the study area. While a positive correlation was observed, the ability to predict water temperature from macroair temperature alone would not be of sufficient accuracy to be useful for most purposes. This is further evidenced by the poor correlations between macro- and micro-air temperatures at 23 sites shown in Figure 5.2. Stefan and Preud'homme (1993) found that as the time interval increased, better relationships between air and water temperature were realized at a given site. Relying on macroair temperature data, we are unfortunately limited to monthly averages at most sites. Going to the next time step, yearly averages, may provide better correlations at single sites, but then biological relevancy is lost. At a yearly temporal scale we are limited by not having stream temperature data spanning an entire 12-month period. Thus, we are limited to making macroair-water temperature comparisons of June, July, August, and September monthly averages. Using a larger temporal scale (e.g., yearly average) will not solve the problem that is inherent in this regional assessment, and that is spatial variability.

Figure 5.3 compares the monthly minima, means, and maxima for air-water temperature relationships for 1998 FSP sites for the months of June, July, August, and September. Figure 5.3-C is the same data as shown in Figure 5.1-B, but with a one-to-one line of correspondence drawn instead of the linear regression line. Monthly minimum water temperatures nearly always exceeded monthly minimum air temperatures (Figure 5.3-A), whereas for monthly maxima, the opposite was observed (5.3-B). The opposite minimum-maximum relationships can be related to the specific heat of water. Specific heat is the amount of energy required to raise a unit mass of a material 1 °C. The specific heat of water is ~1.0 calorie/gram/°C while air has a specific heat of ~0.24 calories/gram/°C, both at zero degrees Celsius and one atmosphere pressure. Thus, it takes about one fourth the energy to raise air temperature 1 °C than it does water. Water is slow to cool down and slow to heat up, much slower than air. While air temperatures can reach higher levels in the day and lower levels in the evening, water is in a constant state of disequilibrium. Water temperatures seek to come into equilibrium with air temperatures during the day, but insufficient time is available during daylight hours for the slower heating water to reach the maximum air temperature. After sundown, air temperatures decrease more rapidly than water temperatures. Given adequate time, water temperature would eventually equilibrate with minimum and maximum air temperatures. But water temperatures never have enough time to catch up. Sunrise comes and the process begins again. Moreover, streams are flowing bodies of water. The air temperature regime changes as water moves down through the watershed.

The above discussion focuses on minimum and maximum temperatures. Figure 5.3-C shows that average water temperatures frequently exceed average air temperatures. It must also be remembered that these are macroair temperatures, and may be 5 °C to 10 °C different than microair temperatures at stream-side (Figure 5.2). Also, given the spatial variability in air temperature regimes across Northern California as presented in Chapter 4, water temperature at one location may have come into equilibrium with much warmer air temperature at a more upstream location. This spatial lag could partially explain many instances of water temperature exceeding air temperature at certain locations. Additionally, average water temperature will be lower than average air temperature because water generally exhibits higher daily minima than air.

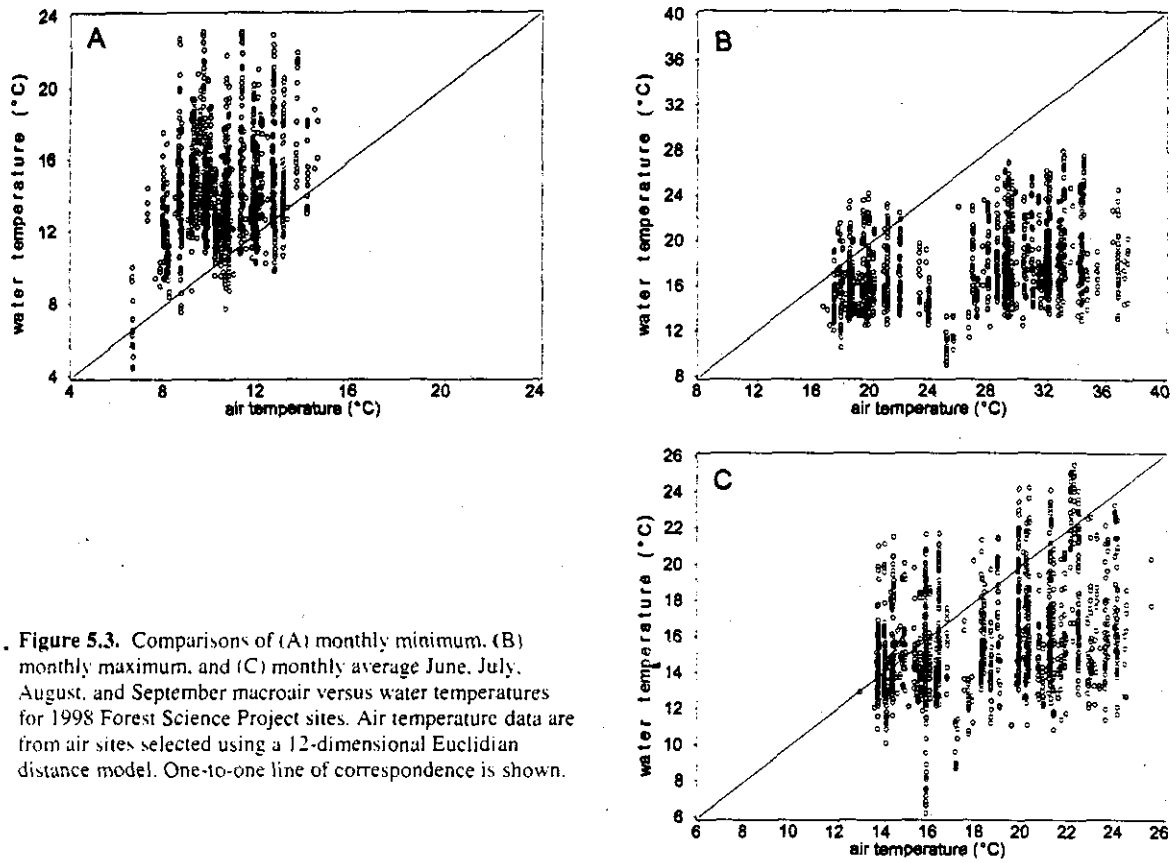

Figure 5.3. Comparisons of (A) monthly minimum, (B) monthly maximum, and (C) monthly average June, July, August, and September macroair versus water temperatures for 1998 Forest Science Project sites. Air temperature data are from air sites selected using a 12-dimensional Euclidian distance model. One-to-one line of correspondence is shown.

Ecoprovincial Comparisons

Water temperature sites and their matched 12-dimensional Euclidian macroair sites were grouped by CSP and SSP ecoprovinces. Figure 5.4 shows the relationship between the monthly average macroair and water temperature in each ecoprovince for all summer months combined. Figure 5.4-A shows that many monthly average water temperatures in the CSP exceeded monthly average macroair temperatures over most of the range in macroair temperature. At monthly average macroair temperatures as low as 14 °C, water temperatures over 21 °C were observed. Interestingly, at the highest air temperatures, the highest corresponding water temperatures were well below the line of one-to-one correspondence. The lower water temperatures observed at higher air temperatures may indicate that the macroair temperature may not adequately reflect localized climate conditions. Additionally, this seems to suggest that water temperatures may only reach some maximum value, and will not go much above this value, even with continually increasing air temperatures. The maximum equilibrium concept was also postulated by Sullivan et al. (1990). As discussed above, water temperature would eventually attain the same temperature as air, given sufficient equilibration time. However, the diurnal cycles in air temperature change at a faster rate than water. Another factor that may account for

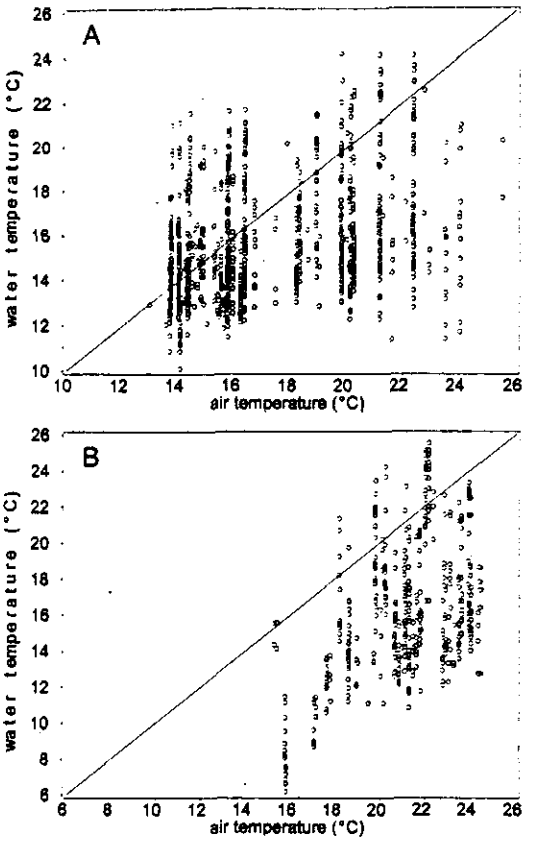

Figure 5.4. Relationship between 1998 monthly (June, July, Aug, Sept) average macroair and water temperatures for A) CSP and B) SSP ecoprovinces.

the observed maximum-equilibrium phenomenon is that other important meteorological variables co-vary with air temperature and solar radiation, such as humidity. As air temperature increases, humidity decreases, which, in turn, increases evaporation at the air-water interface. Increased evaporation tends to have a cooling influence on water temperature.

In the SSP, water temperatures exceeding the macroair temperature monthly averages were not observed until the air temperatures attained values over ~18°C (Figure 5.4-B). Generally, there appeared to be a more discernable increasing trend in water temperature with increasing air temperature in the SSP. Similar to the CSP, at the highest air temperatures, water temperatures fell below the line of one-to-one correspondence.

Water temperature tends to approach air temperature as water travels down through a watershed (Hynes, 1970; Sullivan et al., 1990). However, as presented in Chapter 4, interior air temperatures in Northern California are often 10°C to 15°C warmer than air temperatures near the coast, where most drainages find their eventual outlet. Next, we will examine how air-water temperature relationships vary by HUC and by watershed position within a HUC.

Air-Water Temperatures and Watershed Position

The difficulty in developing good predictions of water temperature from remote air temperature is illustrated in Figure 5.5 for the Lower Eel and Big-Navarro-Garcia HUCs. The plotted monthly average was calculated by averaging 1998 July and August averages. There were 60 sites in the Lower Eel HUC and 113 sites in the Big-Navarro-Garcia HUC. However, only five air sites in each HUC were matched with multiple water sites. For a given monthly average air temperature at a macroair site, the associated water temperatures ranged up to 15°C in some instances.

The variation in water-to-macroair temperature ratio (W:A_RATIO) with distance from the watershed divide was investigated in each hydrologic unit (HUC) comprising the range of the coho salmon in Northern California (Figure 5.6). Two HUCs were not included, the Salmon and Russian, due to insufficient data points. July and August monthly mean temperatures were averaged together to generate the plots in Figure 5.6.

All HUCs showed a general increase in the W:A_RATIO with increasing divide distance. More mainstem sites were over unity than tributary sites. The Scott and Upper Klamath did not exhibit any sites with W:A_RATIO values over unity. These two HUCs are among the warmest in terms of air

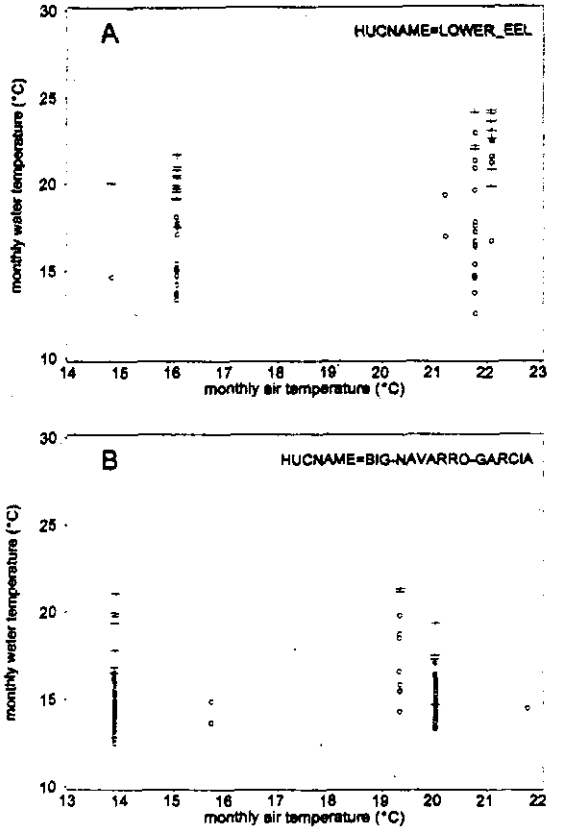

Figure 5.5. Monthly macroair versus water comparison for the (A) Lower Eel HUC and the (B) Big-Navarro-Garcia HUC. Monthly averages are the means of July and August monthly averages. Open circles are tributaries and crosses are mainstems.

temperature (see Table 4.2). Both HUCs lie entirely in the interior portions of the study area, far removed from the influence of cooler coastal air temperatures. In HUCs with tributaries originating in warm interior areas and draining towards the coast, more sites showed W:A_RATIO values greater than one. This suggests that water temperatures began to equilibrate with warmer inland air temperatures and upon arrival of these warmer waters in the zone of coastal influence, water temperatures exceeded the cooler coastal air temperatures.

Many HUCs began to exhibit W:A_RATIO values greater than one within a similar range in divide distances, roughly between 5 km to 10 km from the watershed divide. At distances less than about 10 km from the watershed divide shade plays a more important role in controlling stream temperatures than does air temperature (Sullivan et al., 1990). The divide distance at which the ratio becomes greater than one will also depend on the geographic position of the HUC, the air temperature regime of the drainage, the rate at which channels widen in the downstream direction (reduced effective shade as channels widen), depth and flow of the stream, and land use patterns throughout the HUC.

These results must be interpreted cautiously. A water:air ratio greater than one can result by water temperatures increasing, air temperatures decreasing, or both. The latter is the case for Northern Coastal California, where air temperatures are much cooler in the zone of coastal influence. The air temperature where the water originated and the air temperature where it arrives at the coast can be markedly different. The most likely reason for the poor correlations between macroair and water temperatures is the 12-dimensional Euclidian distance macoair site may not necessarily be the best approximation of the air temperature at the site where water temperature was measured (Figures 5.2 and 5.5).

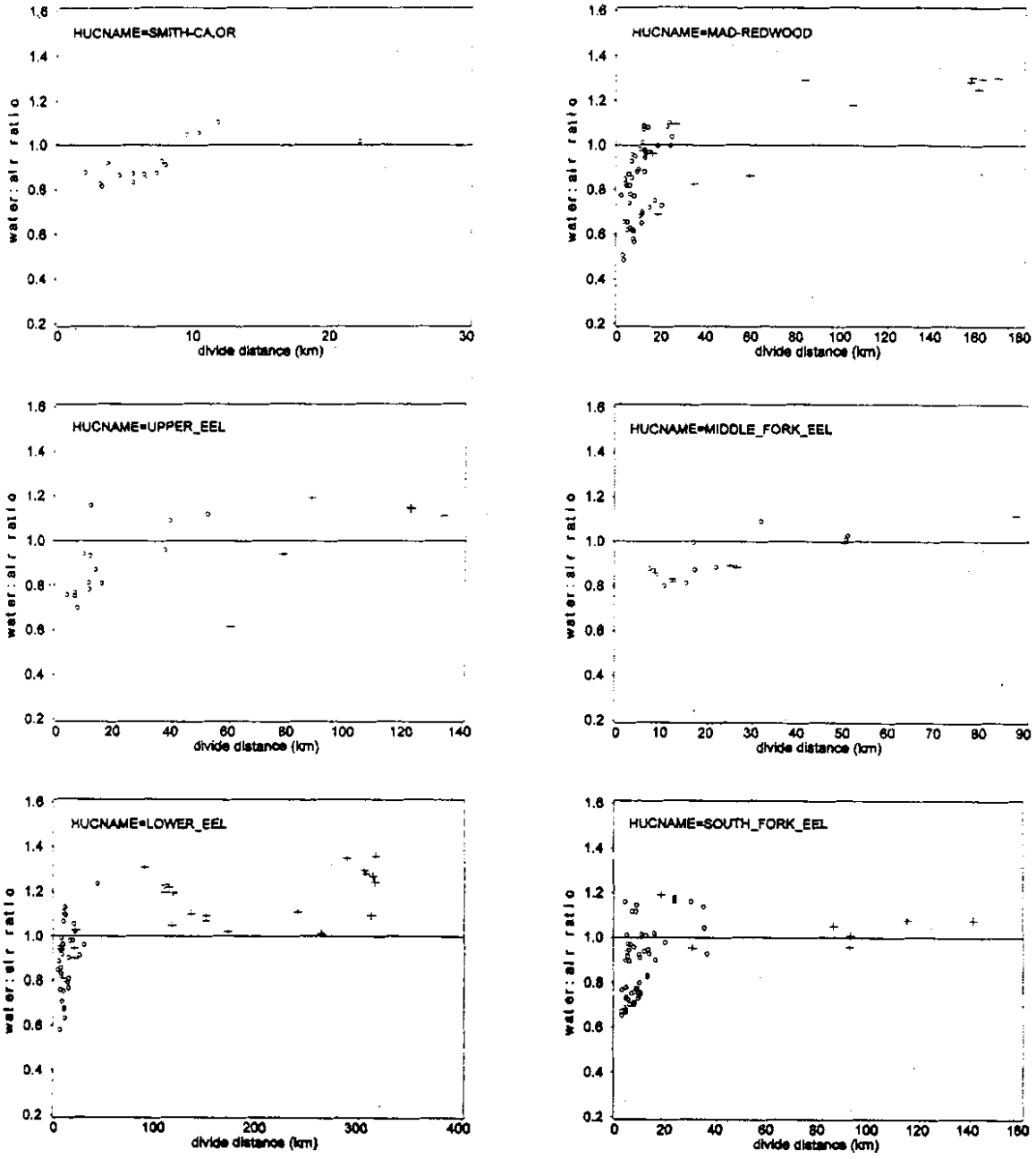

Figure 5.6. Change in water:air temperature ratio with distance from watershed divide by HUC. Macroair and water temperatures are monthly averages for July/August combined, 1998. Open circles are tributary sites and crosses are mainstems.

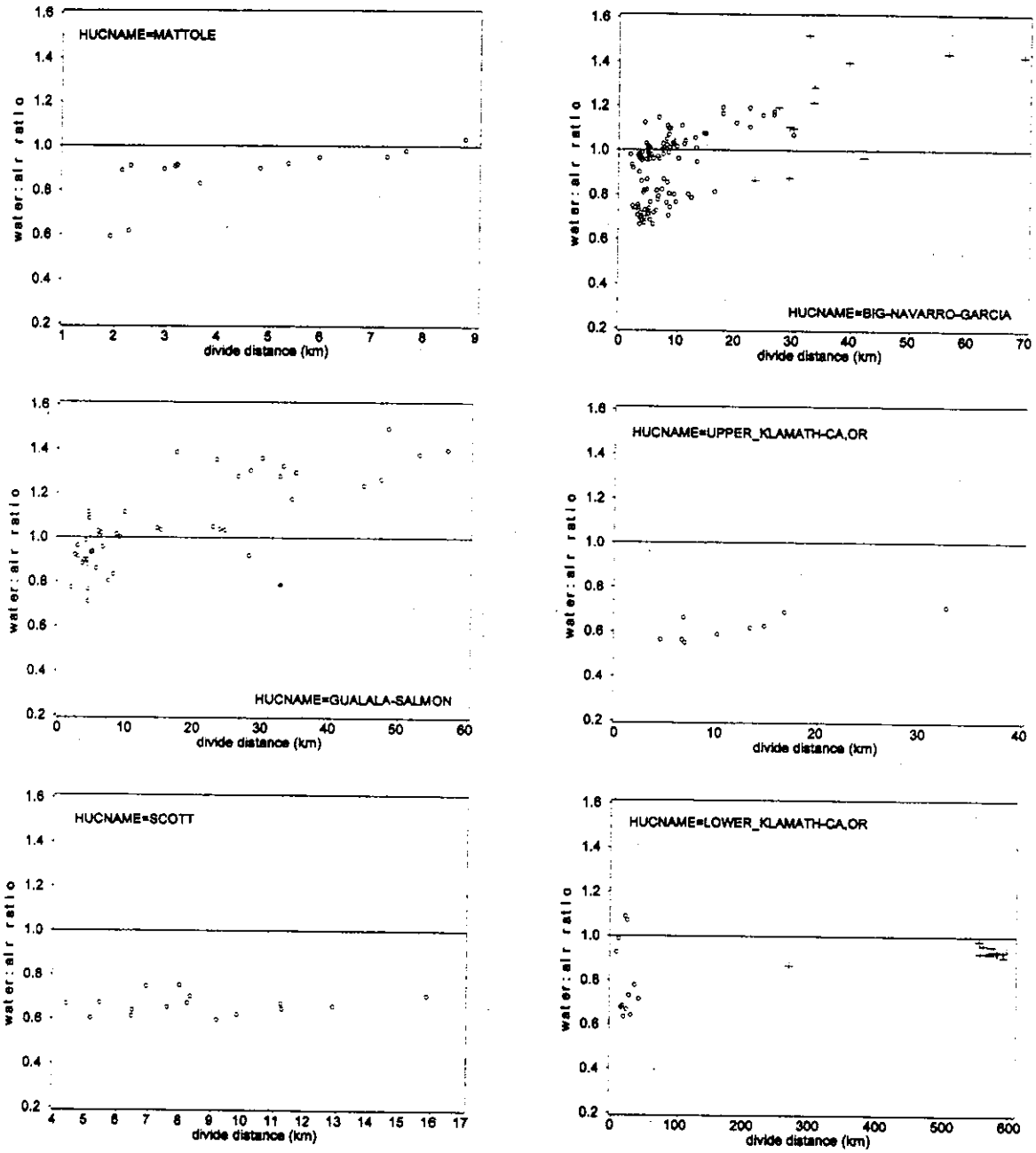

Figure 5.6. (continued)

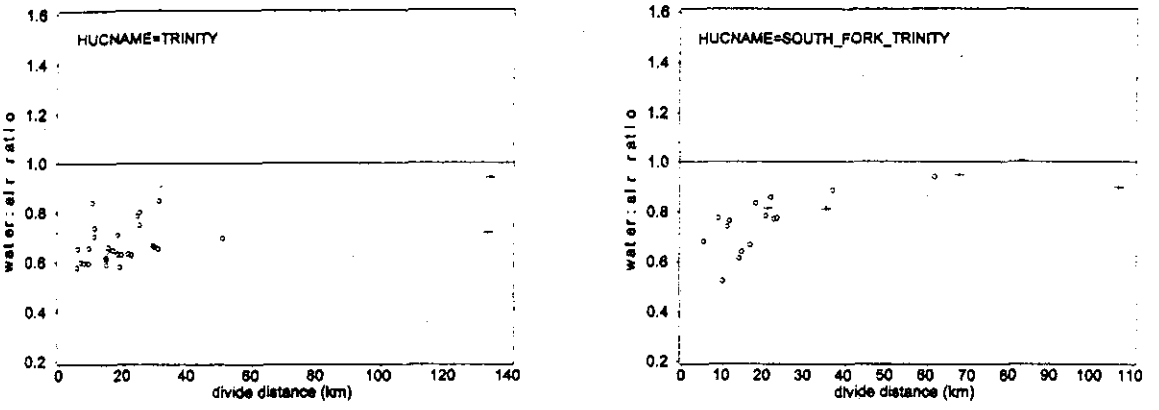

Figure 5.6. (continued)

PRISM Air Temperature and Watershed Position

The 30-year long-term average maximum air temperature from the PRISM data set was used to examine air temperature regimes in selected hydrologic units. Although year-to-year variations in air temperature cannot be discerned from the data, more representative air temperatures at each water site are obtained, given PRISM's 4-km grid resolution. Figure 5.7 presents the 30-year August average maximum air temperature at each Mad-Redwood HUC water site plotted by divide distance. Symbols denote whether the highest 1998 daily maximum temperature at either a tributary or mainstem site exceeded 26°C. Only one mainstem site exceeded 26°C at a divide distance of about 60 km. The August average maximum air temperature at the site was ~29°C (84°C). There was about a 7°C decrease in the August average air temperature at mainstem sites located 80 km or more from the watershed divide. The decrease in air temperature and concomitant lack of mainstem sites that exceeded 26°C is most likely due to cooling influence of the coastal zone.

The four HUCs that comprise the Eel River basin (Upper, Middle, Lower, and South Fork) are presented in Figure 5.8. August average maximum air temperatures at water sites in the four Eel River HUCs were markedly higher than in the Mad-Redwood HUC.

August average maximum air temperature ranged between 30°C to 34°C (86°F to 93°F) at all tributary and mainstem sites along the 140 km divide distance of the Upper Eel River HUC (Figure 5.8-A). All but one mainstem site exceeded 26°C. At divide distances less than 20 km, all but one tributary site were below 26°C. This site fell in the 0-24% canopy class.

In the Middle Fork Eel River HUC, August average maximum air temperatures at each stream temperature monitoring site showed a similar range as in the Upper Eel River HUC. At air temperatures above 32°C (90°F) both tributary and mainstem sites exhibited daily maximum stream temperatures over 26°C. (Figure 5.8-B). Three sites on the Middle Fork Eel River between 20 km and 50 km from the watershed divide had XY1DX values under 26°C. However, at a site further downstream (~90 km) air temperature increased by about 3°C and the highest daily maximum water temperature exceeded 26°C. This trend supports the concept that large rivers tend

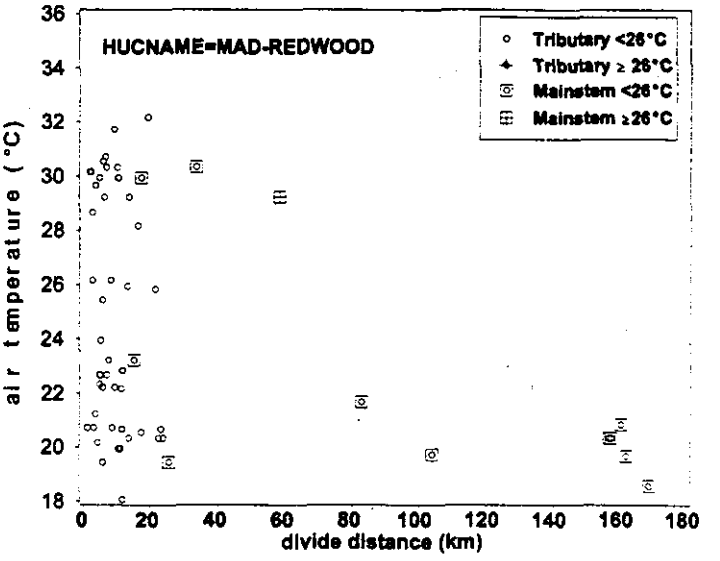

Figure 5.7. PRISM 30-year August average maximum air temperatures at each stream temperature monitoring site versus divide distance in the Mad-Redwood HUC. Open circles are tributary sites and squares are mainstem sites. Crosses indicate that the highest 1998 daily maximum temperature exceeded 26°C.

to come into equilibrium with air temperature (Sullivan et al., 1990). August average maximum air temperatures at sites on the mainstem Eel River in the Lower Eel HUC showed about a 14°C (25°F) decrease between 100 km and 320 km from the watershed divide (Figure 5.7-C). Despite the large decrease in air temperatures, mainstem sites continued to have XY1DX values over 26°C until sites at about 300 km from the watershed divide were reached. Mainstem water temperatures seem to have equilibrated to the higher interior air temperatures, imparting thermal inertia that requires considerable cooling from the zone of coastal influence before water temperatures begin to reequilibrate. The North Fork Eel River enters the Eel River in an area where August average maximum air temperatures are near 32°C (~90°C). Two sites on the North Fork Eel River had water temperatures that appear to be influenced by warm air temperatures in the interior portion of the HUC.

August average maximum air temperatures were lower at two water temperature sites on the South Fork Eel River at divide distances less than 40 km than sites further downstream (>80 km divide distance). Generally, it is believed that both air and water temperatures increase longitudinally. Exceptions to this commonly observed phenomenon have been shown for Northern Coastal California. The South Fork Eel River conforms to the norm, but for a different reason. The South Fork Eel River is oriented such that the upper reaches are located within the zone of coastal influence. The South Fork Eel River enters the main Eel River outside of the zone of coastal influence where air temperatures are higher. Thus, two mechanisms are working simultaneously to account for the longitudinal increase in air and water temperature.

In the four HUCs that comprise the Eel River Basin, the majority of tributary sites with XY1DX values exceeding 26°C were associated with warm August average maximum air temperatures.

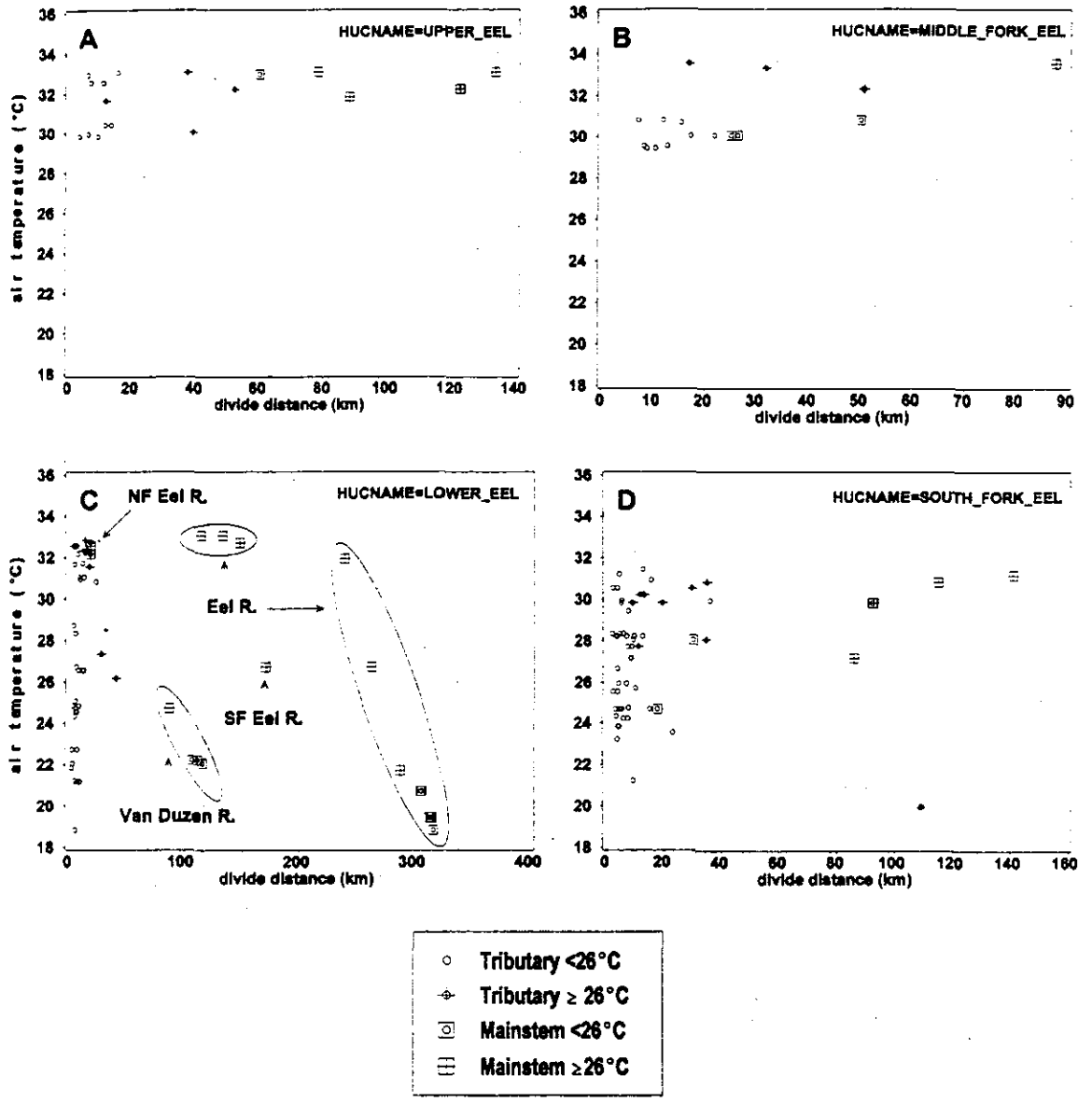

Figure 5.8. PRISM 30-year August average maximum air temperatures at each stream temperature monitoring site versus divide distance in Eel River HUCs. Open circles are tributary sites and squares are mainstem sites. Crosses indicate that the highest 1998 daily maximum stream temperature exceeded 26°C.

Water-Macroair Temperature Relationships and Canopy

Figure 5.9 presents a bar graph of the average W:A_RATIO by canopy class within each divide distance class. The graph illustrates that in the lowest canopy class (0 - 24%), the W:A_RATIO is closer to the 1:1 reference line in the lower divide distance classes (i.e., 1 and 2, representing 1 to 50 km) than at higher canopy class values. This trend suggests that in smaller headwater streams with little or no canopy, the water temperature may tend to exceed air temperatures more than in similar size streams with more developed canopy. The lack of sites at higher divide distances that had canopy values in the 50-74% and 75-100% classes indicates that streams may be becoming too wide for stream-side vegetation to provide adequate shading.

Air temperature is largely influenced by solar radiation (Miller and Thompson, 1975). The rate of heating and eventual maximum temperature is greater in the sun than in the shade for both air and water (Essig, 1998). Plots of PRISM air temperature versus divide distance similar to those shown in Figure 5.8 were used to focus on the possible effects of canopy on stream temperature at different air temperature regimes. Stream temperature sites that were located at distances less than 50 km from the watershed divide in the four HUCs that comprise the Eel River basin are presented in Figure 5.10. Sites that exhibited highest 1998 daily maximum stream temperatures over 26°C were generally located in areas of warmest air temperatures. Sites with less than 50% canopy were most frequently those with stream temperature excursions above 26°C. Some sites with canopy greater than or equal to 50% exhibited XY1DX values greater than 26°C. These sites were located predominantly in areas of high air temperatures and at greater distances from the watershed divide.

The relationship between canopy and divide distance is explored in greater detail in Chapter 9.

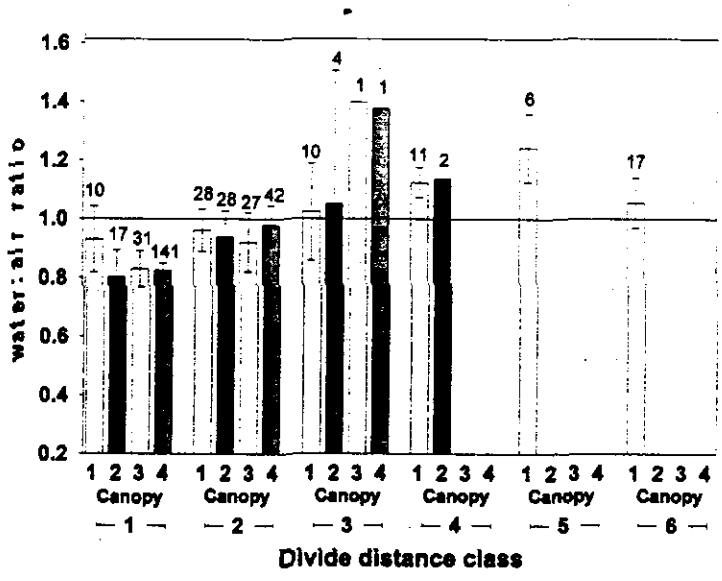

Figure 5.9. Change in water:air temperature ratio at four different canopy classes at six different divide distance classes. Based on the average of July and August monthly averages for 1998. Canopy classes: (1) 0-24%, (2) 25-49%, (3) = 50-74%, (4) = 75-100%. Divide distance classes: (1) 1 - 10 km, (2) 10 - 50 km, (3) 50 - 100 km, (4) 100 - 150 km, (5) 150 - 200 km, and (6) greater than 200 km. Error bars represent ± 1 standard deviations. Above each error bar is the number of sites in the class.

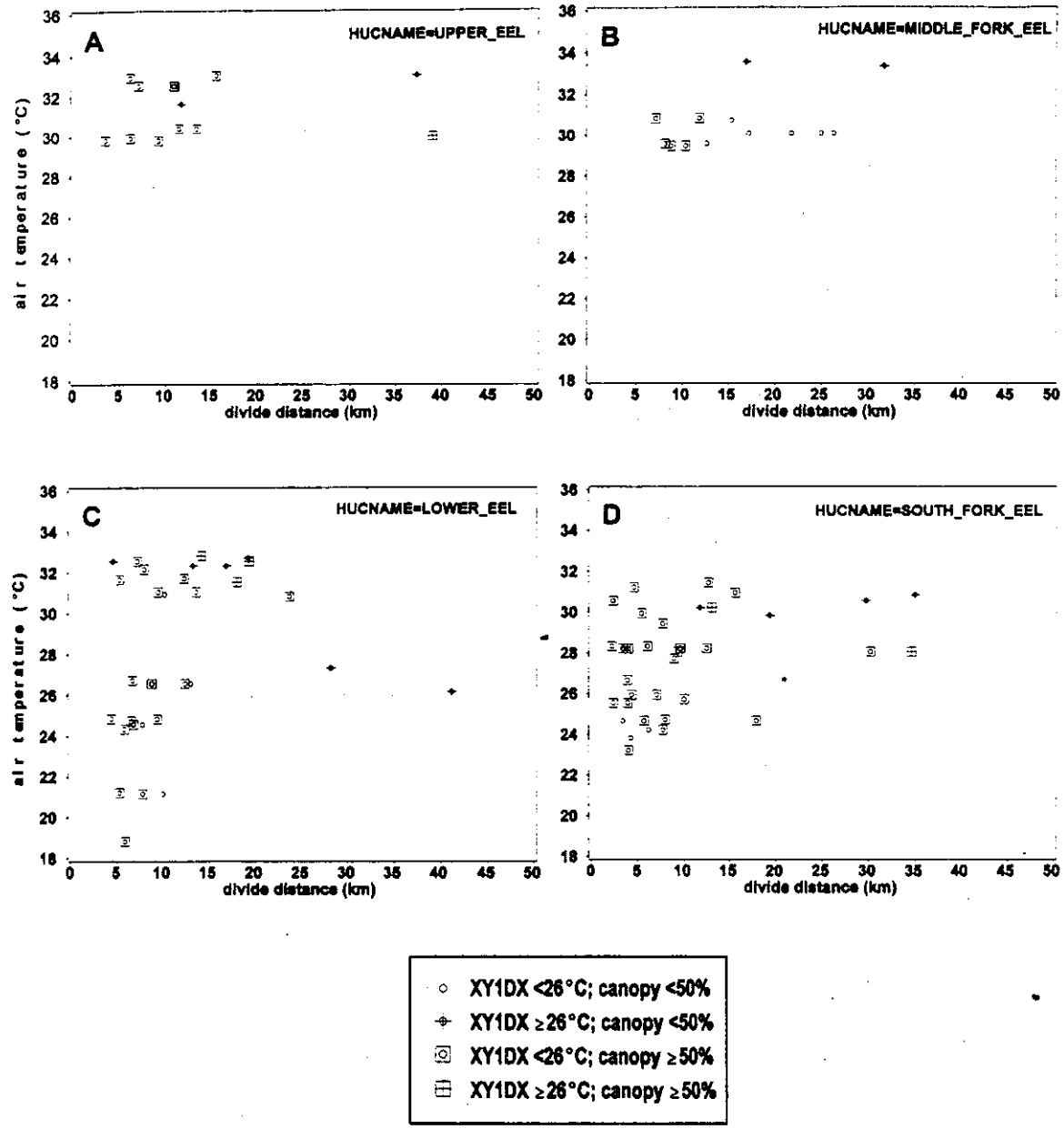

Figure 5.10. PRISM 30-year August average maximum air temperatures at stream temperature monitoring sites located less than 50 km from the watershed divide versus divide distance in Eel River HUCs. Open circles are stream temperature sites with highest 1998 daily maximum water temperature (XY1DX) less than 26°C and crosses are sites with XY1DX ≥26°C. Square indicates 1998 canopy ≥50%, no square indicates canopy <50%.

Water-Air Temperature Relationships and Flow

An important factor that we have not addressed is the influence of flow on the water-air relationship. In large systems the contribution of groundwater influx becomes proportionally less at increasing distances from the watershed divide. In fact, some systems may become losing streams (Kjelstrom, 1992; Donato, 1998). The water in these larger systems experiences exposure to atmospheric heating proportionate to its travel time from the source. As flow drops so does velocity, giving more time for water to approach thermal equilibrium with the overlying air (Essig, 1998). In many geographic locations larger systems at lower elevations will equilibrate with warmer air temperatures. In the case of Northern Coastal California, large systems have time to equilibrate with cooler maritime air temperatures. This was indeed the case in the Eel and Mad River systems (see Chapter 7).

Flow data were recorded at very few FSP stream temperature monitoring sites, fewer than air temperature measurements. In future updates to FSP's regional stream temperature assessment, it is hoped that more stream flow data will be available.

Water Temperature Versus Micro- and Macro-Air Temperature

Microclimate refers to the "layer of air from ground" or water level "to a height of two meters" (Geiger 1965, cited in Bartholow, 1989) and is represented by the microair temperature. Stream-side average air temperatures are, generally, less than ambient (remote) air temperatures, and large variability can be seen over relatively short distances (Troxler and Thackson, 1975). Many of the remote air sites in the present study were at lower elevations than the elevations at the water sites with which they were matched. Moreover, some of the air sites in our study were used for fire predictions and were located on south-facing slopes, which are warmer than other slope aspects. For regional-type assessments such as the current study, models developed from more readily available remote air temperature data proved to be poor in predicting water temperatures.

This section demonstrates the value of measuring microair temperatures in predicting the variability in stream temperatures. Ten water temperature sites out of 1090 had both micro and macro air temperatures available at daily intervals. One site in the Eel Basin had two microair temperatures recorded at the location: one at 0.15 m and another at 2 m above the water. The microair at 0.15 m was used for analyses unless otherwise noted. Most sites were located in the central and more northern portions of the region-wide study area, and all sites were within 40 km of the coast. Microair temperature was collected in close proximity to the water temperature sensor, all within 600 meters of the stream temperature monitoring site. The macroair site was determined using the 12-dimensional Euclidian distance method as described in the section *Determining Nearest Remote Air Station* in this chapter. Comparisons were made using the daily mean, daily minimum, and daily maximum temperatures during the period between July 21 through August 19. Data regarding habitat and canopy were available for only a few sites, thereby precluding their use in exploring associations between air-water temperature relationships and site-specific attributes.

To characterize relationships between water and air temperatures, regression analyses were performed on daily mean, daily minimum, and daily maximum water temperatures in combination with micro- and macro-air temperatures for all sites combined and for each site separately. A summary of results are presented in Table 5.1.

The strongest overall correlation for all sites combined was between daily mean water and daily mean microair temperatures ($R^2 = 0.61$). Daily maximum water versus daily maximum microair temperature also had a moderate overall relationship ($R^2 = 0.59$). Although these are only moderate relationships, it indicates that the variables tended to respond in somewhat similar manners (i.e., to similar meteorological influences). Relationships between daily air and water minimum temperatures for all sites combined showed much variability. Daily

Table 5.1. Linear Regression Models for Water Temperature versus Microair and Macroair Temperatures.

		Mean			Minimum			Maximum		
Stream	Relationship	intercept	slope	R^2	intercept	slope	R^2	intercept	slope	R^2
All Sites	water vs. microair	6.02	0.67	0.61	9.91	0.34	0.22	8.27	0.46	0.49
	water vs. macroair	11.21	0.34	0.22	16.21	0.07	0.00	11.43	0.30	0.31
Hall Creek	water vs. microair	14.37	0.06	0.15	14.35	0.07	0.30	15.87	-0.03	0.05
	water vs. macroair	14.05	0.08	0.26	14.09	0.08	0.43	14.78	0.03	0.04
Redwood Creek	water vs. microair	13.05	0.39	0.76	12.52	0.47	0.75	16.40	0.25	0.69
	water vs. macroair	12.00	0.35	0.77	13.16	0.40	0.74	14.85	0.25	0.71
Redwood Creek	water vs. microair	15.07	0.33	0.64	16.68	0.25	0.28	17.90	0.23	0.59
	water vs. macroair	14.41	0.28	0.73	16.39	0.26	0.60	16.40	0.22	0.52
Minor Creek	water vs. microair	11.54	0.30	0.69	10.70	0.39	0.68	13.06	0.21	0.71
	water vs. macroair	11.49	0.23	0.71	12.68	0.25	0.62	12.15	0.18	0.70
Minor Creek	water vs. microair	11.76	0.31	0.74	11.41	0.37	0.83	15.17	0.17	0.55
	water vs. macroair	10.93	0.27	0.73	11.04	0.35	0.73	14.48	0.17	0.52
Eel River	water vs. microair	18.63	0.20	0.23	14.55	0.45	0.46	23.70	0.07	0.01
	water vs. macroair	16.03	0.34	0.43	19.44	0.20	0.14	19.12	0.20	0.05
Rattlesnake Creek	water vs. microair	12.95	0.39	0.72	11.31	0.48	0.73	16.97	0.29	0.64
	water vs. macroair	16.18	0.22	0.34	12.61	0.45	0.44	20.12	0.16	0.37
Cedar Creek	water vs. microair	12.75	0.22	0.59	14.17	0.09	0.06	14.61	0.16	0.47
	water vs. macroair	12.94	0.16	0.48	11.03	0.33	0.44	13.80	0.15	0.59
Rock Creek	water vs. microair	7.38	0.53	0.81	7.60	0.58	0.83	11.14	0.29	0.58
	water vs. macroair	12.04	0.19	0.38	8.62	0.52	0.66	14.15	0.10	0.30
Sprowl Creek	water vs. microair	10.89	0.39	0.71	12.70	0.33	0.39	13.01	0.25	0.66
	water vs. macroair	13.64	0.22	0.50	13.78	0.26	0.22	14.85	0.16	0.64

minimum water temperature had a somewhat weak relationship to daily minimum microair temperatures ($R^2 = 0.22$), while the relationship between daily minimum water and daily minimum macroair temperatures was not significant.

Comparing R^2 values from Table 5.1 for individual sites gives a somewhat different impression than the all-sites-combined regressions. For instance, as previously noted, the combined-site relationship between daily mean water and microair temperatures was relatively weak. However, the strongest individual site relationships were seen with daily minimum water temperatures versus daily minimum microair temperatures for Minor Creek and Rock Creek ($R^2 = 0.83$).

Some general observations can be made. Daily mean water temperatures were better estimated than daily minimum or maximum water temperatures using microair data. At some sites, little difference was observed between R^2 for correlations between daily means of water-macroair versus water-microair.

Proximity of the remote air site to the stream-side air site did not seem to account for the degree of similarity in R^2 values. If daily extremes in water temperature are of interest, then microair stations should be used.

Variability in the relationship between water temperature and microair temperatures can be illustrated by using hourly data for two sites located in the Eel Basin (Figure 5.11). The first site was located on Rattlesnake Creek approximately 18.6 km from the coast (left graph). The second site was located on the Eel River near Nashmead Bar approximately 35.9 km from the coast (right graph). Water temperature regimes were similar for both sites during the period of study. The Rattlesnake Creek and Eel River sites had average water temperatures of 20.8°C and 23.5°C, respectively. For both sites, the mean water temperature was within 0.6°C of the mean microair temperature for the study period. The diurnal fluctuation in microair temperature at the Eel River site was much greater than at the Rattlesnake Creek site. However, the diurnal water temperature

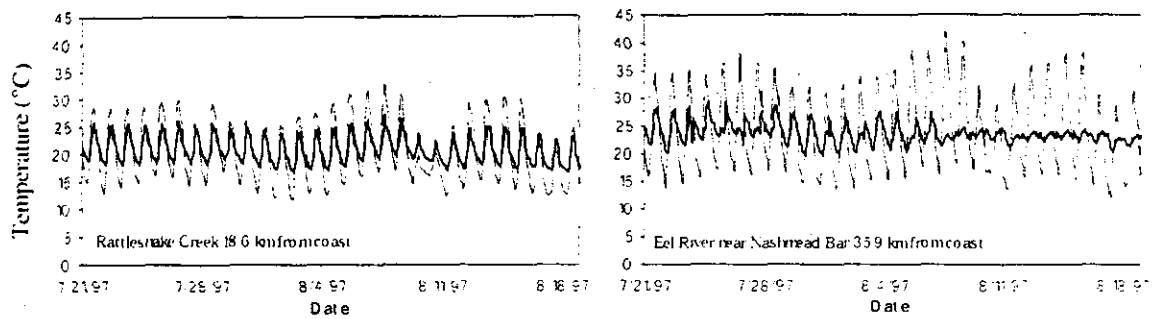

Figure 5.11. Hourly water and micro air temperatures for (A) Rattlesnake Creek and (B) the mainstem Eel River near Nashmead Bar in the Eel River Basin, for period of 21 July to 19 August 1997. Solid line is water temperature and dashed line is air temperature.

fluctuation in the mainstem Eel River was of an amplitude similar to the tributary site. This trend exemplifies the concept of thermal inertia of large mainstem systems. It should also be noted that the daily minimum air temperatures on the days when the highest daily maximum water temperatures occurred were near a commonly used MWAT threshold (i.e., 16.8°C). Essig (1998) reported that at some locations in Idaho water warms to above state temperature standards even without exposure to direct or indirect solar radiation. Daily minimum air temperatures at some sites are so warm that stream heating can occur throughout the evening. He reported that in some regions of Idaho July minimum air temperature, ~15°C, exceeds Idaho's salmonid spawning instantaneous maximum temperature (13°C).

Figure 5.11 helps to illustrate the value of having hourly observations to examine aspects of the air-water temperature relationship that are not readily apparent by looking at summary temperature metrics, such as daily mean and range or monthly averages. Unfortunately, hourly observations were not available for the macroair temperature data. Graphs of daily minimum, mean, and maximum water, microair, and macroair are presented in Appendix C for each of the 10 sites discussed above.

Distance Above Water Surface

At the Rock Creek site, two microair data sets were available, one collected at 0.15 m above the stream and the other at 2 m. Visual inspection of plots in Figure 5.12 shows that mean and maximum microair temperatures collected at 2 m above the water surface were consistently warmer than the microair temperature at 0.15 m, and minimum temperatures were consistently cooler. The 2-m microair trends more closely followed the macroair trends (Table 5.2). The 0.15-m microair trends more closely followed the water temperature trends (compare R^2 values for mean temperatures). This indicates that water is having a moderating influence on microair temperatures, the influence increasing with decreasing distance from the water surface. The effects of evaporative cooling are more apparent with decreasing distance above the water surface.

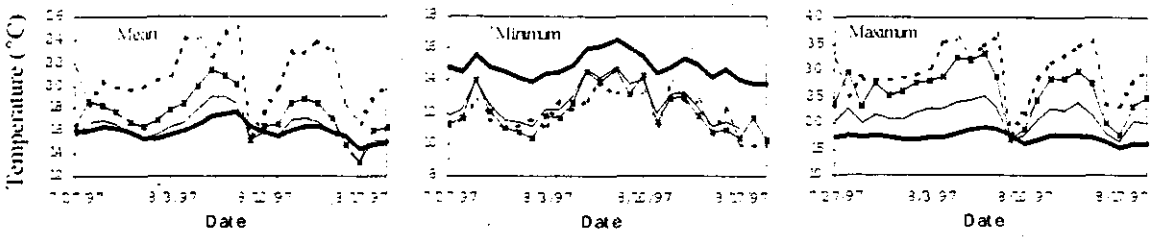

Figure 5.12. Daily mean (left), minimum (middle), and maximum (right) temperatures for water and microair sites located on Rock Creek, a tributary of the South Fork Eel River, and a macroair station located 17 km north. This site had two microair temperatures recorded at 0.15 m and 2 m above the water surface. Bold solid line = water temperature, dashed line = macroair, thin solid line = microair at 0.15 m, solid line with 'x' = microair at 2 m.

Table 5.2. Linear Regression Models Comparing Microair Temperatures Measured at 0.15 m and 2 m above the Water Surface to Water Temperature and Macroair Temperatures for a Site on Rock Creek.

	Mean			Minimum			Maximum		
Relationship	**intercept**	**slope**	**R^2**	**intercept**	**slope**	**R^2**	**intercept**	**slope**	**R^2**
water vs. micro air (0.15 m)	7.38	0.53	0.81	7.60	0.58	0.83	11.14	0.29	0.58
water vs. micro air (2 m)	9.78	0.36	0.71	8.83	0.50	0.82	13.28	0.15	0.54
micro air (0.15 m) vs. macro air	8.15	0.39	0.55	3.08	0.79	0.61	8.84	0.42	0.70
micro air (2 m) vs. macro air	5.57	0.57	0.62	1.27	0.91	0.61	3.93	0.74	0.67
micro air (0.15 m) vs. micro air (2 m)	3.84	0.71	0.97	2.14	0.86	0.99	7.16	0.54	0.98

Year-to-Year Variability in Water-Air Relationships

Stream temperature data from 154 sites were available that spanned three consecutive years (1996-1998). The data set was explored to determine whether year-to-year differences in air temperature had a noticeable effect on water temperatures in each year. Figure 5.13 shows the geographic distribution of the 154 sites.

Combined July-August average macroair temperatures were estimated at each of the 154 water temperature sites using the 12-dimensional Euclidian model. Figures 5.14-A and 5.14-B show that 1996 had the highest monthly maximum and the lowest monthly minimum average air temperature. Only 15 macroair temperature sites were matched with the 154 water temperature sites. Figure 5.5 illustrates the large source of variability introduced into the analyses by having a limited number of macroair stations available to match up with a multitude of water temperature sites.

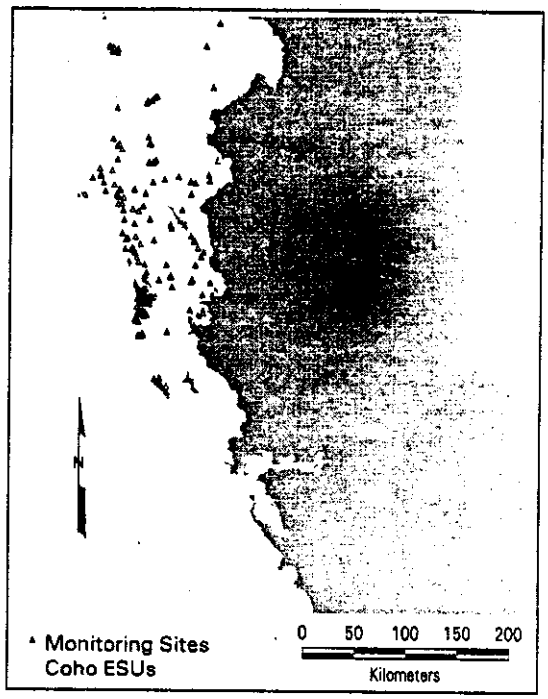

Figure 5.13. Geographic distribution of 154 sites where stream temperature was monitored across three consecutive years, 1996 through 1998. Sites had uninterrupted data for the time period between July 21 and August 19.

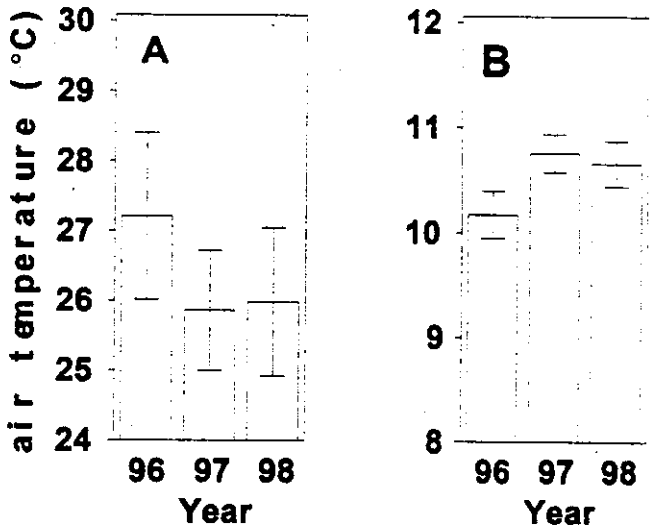

Figure 5.14. Average July-August monthly maximum (A) and minimum (B) macroair temperature associated with 154 stream temperature sites over three consecutive years (1996-1998). Error bars represent ± 2 standard deviations.

CDF graphs were produced for four stream temperature metrics. The cumulative distributions for XY1DX, XYA7DA, and XYA7DX were very similar for all three years (Figure 5.15-A through C). Inset bar graphs indicate that 1997 was a few tenths of a degree Celsius higher for average values of XY1DX, XYA7DA, and XYA7DX. These differences would be of little or no biological significance. There was a noticeable difference in the distribution of IY1DI values, with 1996 having lower daily minimum temperatures than either 1997 or 1998 (Figure 5.15-D). The inset bar graph in Figure 5.15-D also illustrates a lower daily minimum temperature in 1996.

While average air temperatures were generally warmer in 1996 based on macroair temperatures at 15 remote sites, stream temperature metrics dealing with daytime temperatures showed only slight differences across years. The 1996 July-August monthly minimum air temperature was significantly lower than 1997 and 1998, suggesting that 1996 may have had had more cloud-free days. Fewer cloudy days would result in higher daytime air temperatures and lower nighttime temperatures. Minimum water temperature seems to be more sensitive to year-to-year changes in minimum air temperature. The discrepancy between the year showing the highest air temperature (1996) and the year showing the highest water temperature suggests that the 15 remote air temperature sites may not be representative of conditions at the stream site. Using only a small number of remote air temperature sites, caution should be exercised when making broad generalizations about climatic conditions from one year to the next to explain trends in stream temperatures.

The total hours spent above 26°C was calculated for each site sampled over three consecutive years. Because of the strict temporal window imposed on the data, that is each site having complete uninterrupted data for the time period between July 21 and August 19, each site had equal total time. Thus, direct comparisons can be made between sites and between years of the total hours above 26°C, because all sites had equal total hours in their data sets. Figure 5.16 presents a CDF graph of the proportion of sites that spent less than x hours above 26°C. It is of interest to note that the y-axis begins at 0.8 at the x-axis zero origin. This means that 80% of the sites did not have any hours above 26°C. At an arbitrary reference value of 50 hours, between 88% and 91% of the sites had less than 50 hours over 26°C. This represents a difference of roughly 3% of the sites in the three-year period, which is about 4 or 5 sites. Essentially, there appears to be only a slight difference in the total hours spent above 26°C across the three years.

Using a threshold of 26°C may limit the ability to discern differences between years by focusing on sites that routinely exhibit high temperatures. The same cumulative distribution for sites that had less than x hours above 18°C was examined to see if there was a more discernable difference between years. The sum degrees over 18°C was also examined. Figure 5.17 shows that even at this lower threshold, very similar CDF curves were observed. See Chapter 7 for a more detailed discussion of the derivation of the sum degree temperature metric.

The similarity in stream temperatures at 154 sites monitored over three consecutive years is striking. At least at the 154 sites examined here, it appears that stream temperatures show very little year-to-year variability. This constancy has also been noted for streams in Idaho (Essig, 1998) and select streams throughout the United States (Vannote and Sweeney, 1980). With a large enough data set one could conceivably predict future stream temperatures from historical trends, and using a similar CDF approach, detect departures from expected temperatures regimes. Differences could be due to much larger changes in air temperatures, larger than those observed in the 1996-1998 period examined here. Changes may also be detectable as riparian vegetation develops as the result of natural regeneration or restoration efforts. Conversely, changes in the CDF curve for a watershed or sub-basin may be detected due to cumulative effects of channel aggradation from flooding, or watershed- or basin-wide cumulative effects from timber harvest, agriculture, urbanization, or all of the above.

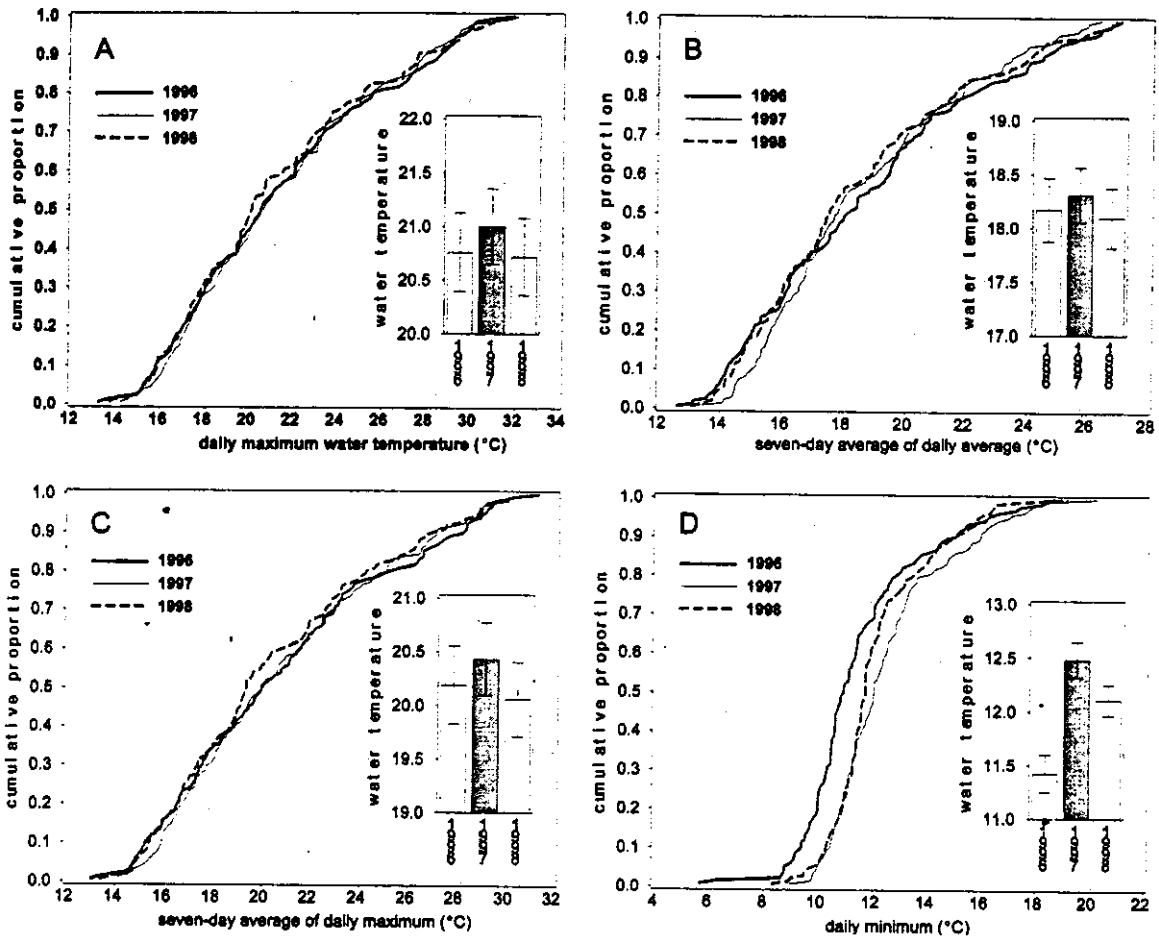

Figure 5.15. Cumulative distributions of temperature metrics (A) highest daily maximum (XY1DX), (B) highest seven-day moving average of the daily average (XYA7DA), (C) highest seven-day moving average of the daily maximum (XYA7DX), and (D) lowest daily minimum (IY1DI) for 154 sites that had stream temperatures measured during three consecutive years (1996 through 1998) and having continuous observations between July 21 and August 19. Inset bar graphs show the average stream temperature metrics for each year with ± 2 standard deviation error bars.

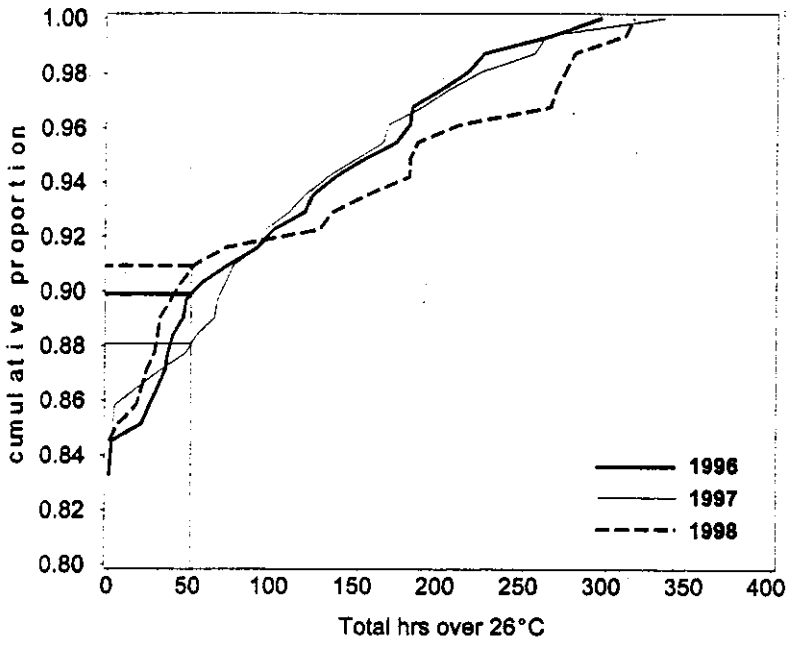

Figure 5.16. Cumulative distribution of proportion of sites that had less than x total hours over 26°C water temperature. Distribution based 154 sites that had stream temperatures measured during three consecutive years (1996 through 1998) and had continuous observations between July 21 and August 19.

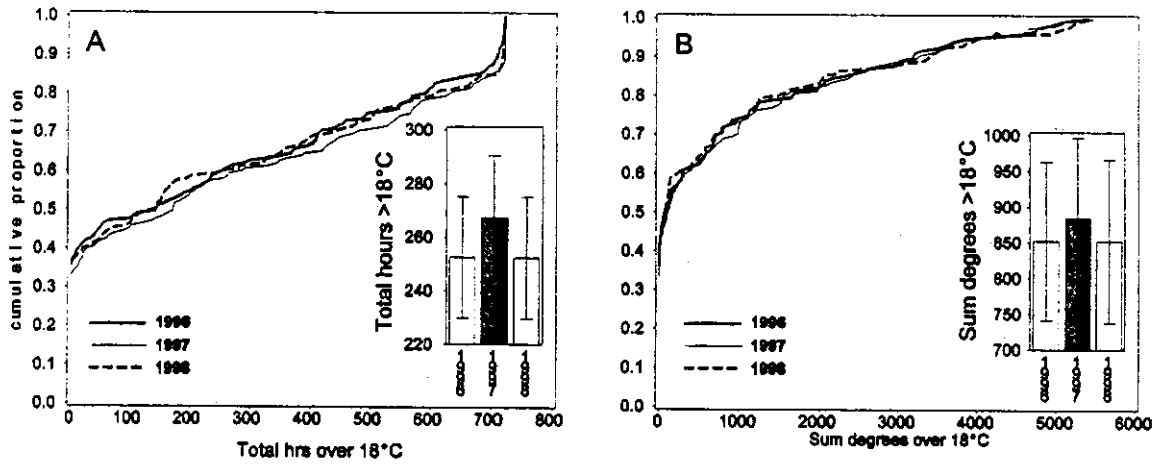

Figure 5.17. Cumulative distribution of proportion of sites that had (A) less than x total hours over 18°C water temperature and (B) less than x cumulative degrees over 18°C. Distribution based 154 sites that had stream temperatures measured during three consecutive years (1996 through 1998) and had continuous observations between July 21 and August 19. Inset bar graphs show the average stream temperature metrics for each year with ± 2 standard deviation error bars.

Temporal predictability is a very important aspect of a streams's thermal regime. Aquatic biota have developed a dependency on the temporal predictability of running waters (Vannote and Sweeney, 1980).

Larger streams respond to air temperature changes to a greater extent than smaller streams (Sullivan et al., 1990; Bartholow, 1989). To corroborate this finding the monthly average maximum water temperature (July and August combined) was calculated for sites at each divide distance class. The associated monthly average maximum air temperature (July and August combined) at each divide distance was also calculated from the nearest 12-dimensional Euclidian air site. Average monthly water and air temperatures were plotted versus divide distance class for each year (Figure 5.18). The warmest year for the 154 sites combined was 1996, followed by 1998, and 1997 being cooler. At divide distances up to approximately 100 km, average monthly maximum stream temperatures showed a nearly identical rate of increase. Air temperatures in 1996 were about 3°C higher than 1997 or 1998. However, the effects of higher 1996 air temperatures on stream temperatures did not manifest themselves until water arrived at sites located over 100 km from the watershed divide. The number of sites in the higher divide distance classes was smaller than in the 1 to 3 classes. However, the trend supports the concept that as stream systems become large, air temperature has more of an influence on water temperature than other site-specific attributes. The mainstem sites at higher distances from the watershed divide account for the slight differences in CDFs observed across the three years shown in Figures 5.15 - 5.17.

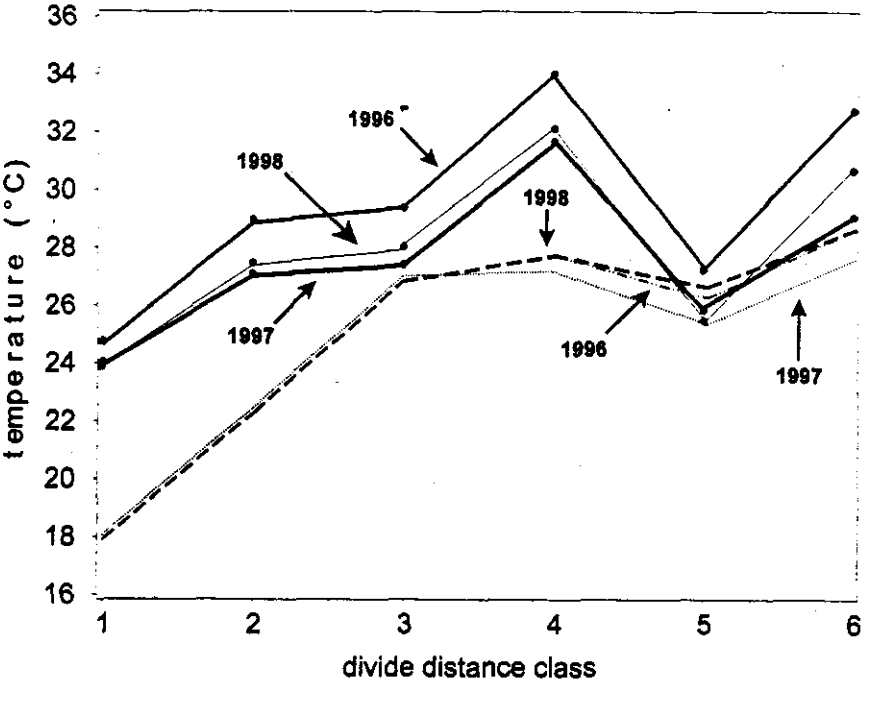

Figure 5.18. Change in monthly average maximum water (broken lines) and air temperatures (solid lines) at six different divide distance classes at 154 sites monitored in 1996, 1997, and 1998. Divide distance classes: (1) 1 - 10 km, (2) 10 - 50 km, (3) 50 - 100 km, (4) 100 - 150 km, (5) 150 - 200 km, and (6) greater than 200 km.

Summary

The success of describing air-water relationships may be somewhat dependent on the region being studied. Greater success in predicting water from air temperatures may be experienced in regions with relatively small air temperature gradients within the study area as opposed to regions with abrupt changes. As presented in Chapter 4, areal air temperature patterns observed in Northern California often exhibit large temperature gradients within relatively short distances (see Chapter 4, Figure 4.10 and 4.11). Air temperatures obtained from 12-dimensional Euclidian distance air stations were found to show some correlation with water temperatures at a regional scale. August monthly macroair versus microair temperature comparisons revealed that remote sites may not be very representative of stream-side air temperatures.

Monthly mean water temperatures in the SSP seemed to vary more closely with monthly mean macroair temperatures than water temperatures in the CSP.

The water-to-macroair temperature ratio increased with increasing distance from the watershed divide. The divide distance at which the ratio began to exceed unity varied by HUC, but generally fell between 6 km and 10 km. HUCs with tributaries that originate in the warm interior portions of the study area and drain into the zone of coastal influence exhibited greater numbers of sites with water-to-air ratios greater than one. HUCs that lie entirely within the interior portion of the study area exhibited fewer sites with water-to-air temperature ratios exceeding one. Water-to-air ratios can exceed one because water temperatures have increased, air temperatures have decreased, or both. Given the fact that water temperatures normally tend to increase in a longitudinal downstream direction and that air temperatures decrease in the zone of coastal influence, in coastal HUCs of Northern Coastal California the exceedance of one in water-to-air ratio is most likely due the simultaneous increase in water temperature and decrease in air temperature in the downstream direction.

Microair temperatures generally showed greater correlations with water temperature than remote macroair temperatures, and correlations were greatest for daily maximum and daily minimum water temperatures. Moore (1967) noted that air temperature affects water temperature through the advection of heat from air to water or vise versa, but not to the degree that might seem to be indicated by the correlation between the two. The close correlation is caused largely by the fact that solar radiation affects both water and air temperature. Some sites in the present study showed little difference between microair and macroair relationships with water temperature. Local environmental conditions probably play a role in the similarities in micro- and macro-air temperatures and water temperatures at some sites. To model water temperatures at hourly, daily, or weekly time steps, the data suggests that microair temperature data are needed.

At a subset of sites where stream temperature was monitored for three consecutive years, very small year-to-year variability was observed. While 15 macroair temperature sites associated with 154 water site indicated that 1996 was relatively warmer than 1997 or 1998, stream temperatures showed very little difference in any of the daytime temperature metrics examined. The 1996 daily minimum stream temperature was lower than 1997 or 1998. July-August monthly average minimum macroair temperatures were also significantly lower than the subsequent two years. Lower nighttime and higher daytime temperatures in 1996 suggest that there may have been more cloud-free days. Cumulative distributions of the total hours spent above 26°C indicated that about 80% of the sites did not exceed this threshold in any of the three years. In a comparison of air and stream temperatures at increasing distances from the watershed divide, larger systems seemed to respond more to year-to-year variations in air temperature than smaller systems. This agrees with other research findings from other geographic areas (Bartholow, 1989; Sullivan et al., 1990).

The discrepancy between the year showing the highest air temperature (1996) and the year showing the highest water temperature suggests that the 15

remote air temperature sites may not be representative of conditions at the stream site. Caution should be exercised when making broad generalizations about climatic conditions from one year to the next to explain trends in stream temperatures.

Chapter 6

GEOGRAPHIC POSITION AND STREAM TEMPERATURES

Introduction

California's climate and ecosystems are varied. Within the state's borders lie glaciers and deserts. The state spans ten degrees of latitude from 42°N at its border with Oregon to 32°N at its border with Mexico. Landsberg (1958) reported that average annual air temperature decreases about 0.8°C (1.5°C) for each degree increase in latitude in the middle latitudes (40° to 50°N). Within the study area of the present assessment, i.e., the California portion of the Southern Oregon Northern Coastal California and the Central California evolutionarily significant units, about five degrees of latitude are covered, from 42°N at the Oregon-California border to about 37°N near San Francisco, CA.

This chapter examines the influence of broad-scale geographic position on stream temperatures. These factors include distance from the coast, ecoprovince, zone of coastal influence, north-south distribution (latitude), and elevation. Do local site factors completely control water temperatures or can some regional scale patterns be observed? The environmental variable that exerts its influence across all of these geographic factors is predominantly air temperature. Similar patterns that were observed for air temperature variability across the region are expected to be seen for variability in water temperature. However, local site-specific factors also influence water temperature, such as canopy, flow, gradient, and topographic shading. These other factors will confound the response of water temperatures to purely geographic phenomena.

Four different stream temperature metrics were explored for their variation with geographic position. The highest daily maximum (XY1DX) for the year, the highest seven-day moving average of both the daily average (XYA7DA) and maximum (XYA7DX) for the year, and the lowest daily minimum for the year were examined for 520 sites monitored in 1998. These sites had uninterrupted data for the time period July 21 to August 19, 1998.

We found that some trends in stream temperature are discernable at broad regional scales. However, given the large variability in the relationships, site-specific factors appear to play an important role. Geographic position may serve as a surrogate for macroair temperature in any given year. However, by using geographic position as a surrogate for air temperature, one loses the ability to explain year-to-year changes in water temperature that may be due to changes in air temperature.

Distance from Coast and Stream Temperatures

The distance from the coast was calculated for each site using a GIS. This distance was calculated as the nearest direct line from the stream temperature monitoring site to the coast. Figure 6.1-A shows the number of sites in each 10-km coast-distance class. The distribution revealed that a larger proportion of sites were near the coast, with 80% of the sites being within 40 km of the coast. The SONCC ESU has a maximum distance from the coast of 165 km and a

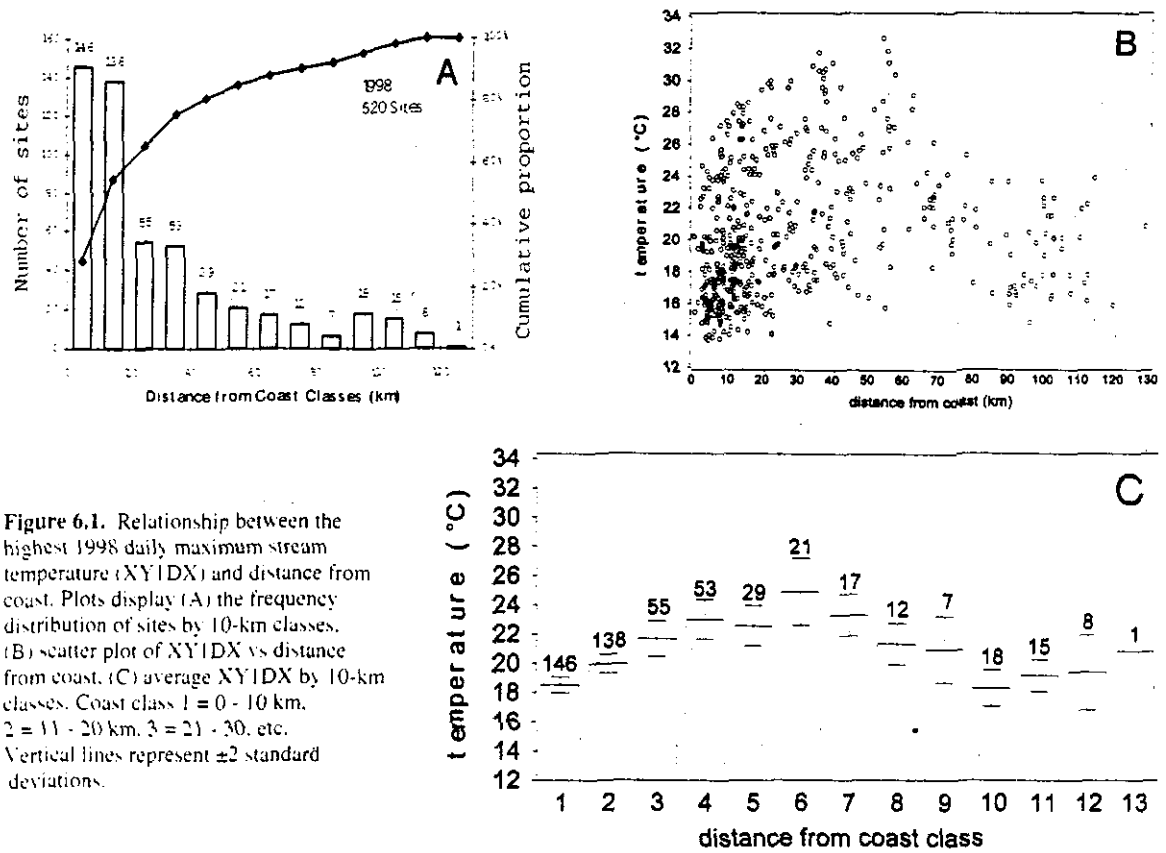

Figure 6.1. Relationship between the highest 1998 daily maximum stream temperature (XY1DX) and distance from coast. Plots display (A) the frequency distribution of sites by 10-km classes, (B) scatter plot of XY1DX vs distance from coast, (C) average XY1DX by 10-km classes. Coast class 1 = 0 - 10 km, 2 = 11 - 20 km, 3 = 21 - 30, etc. Vertical lines represent ±2 standard deviations.

minimum of 52 km. The Central California ESU has a maximum coast distance of 56 km and a minimum of 0.4 km.

Daily Maximum and Distance from the Coast

Figure 6.1-B is a scatter plot of the highest daily maximum temperature versus distance from the coast.

There is considerable scatter in the data. However, there appears to be an increasing trend in XY1DX values up to about 50 to 60 km from the coast and then a decreasing trend as distance from the coast continues to increase. Although the trend is not as clearly defined as that observed for air temperature (see Figure 4.2), a weak trend is apparent in the data. The trend becomes more apparent when XY1DX values are grouped by coast-distance classes of 10-km increments (Figure 6.1-C). The highest class average for XY1DX was in class 6, that is 50 to 60 km from the coast.

Figure 6.1 includes stream temperature measured at all sites in 1998 that had continuous data between July 21 and August 19. These sites included tributaries and mainstem rivers. Mainstem rivers that drain to the coast and large inland rivers (e.g., Klamath River) may have influenced the observed trend in XY1DX with coast distance. Without bankfull width or stream order to group streams together, it is difficult to compare streams of similar size. Watershed area was used as a surrogate to group streams of similar size.

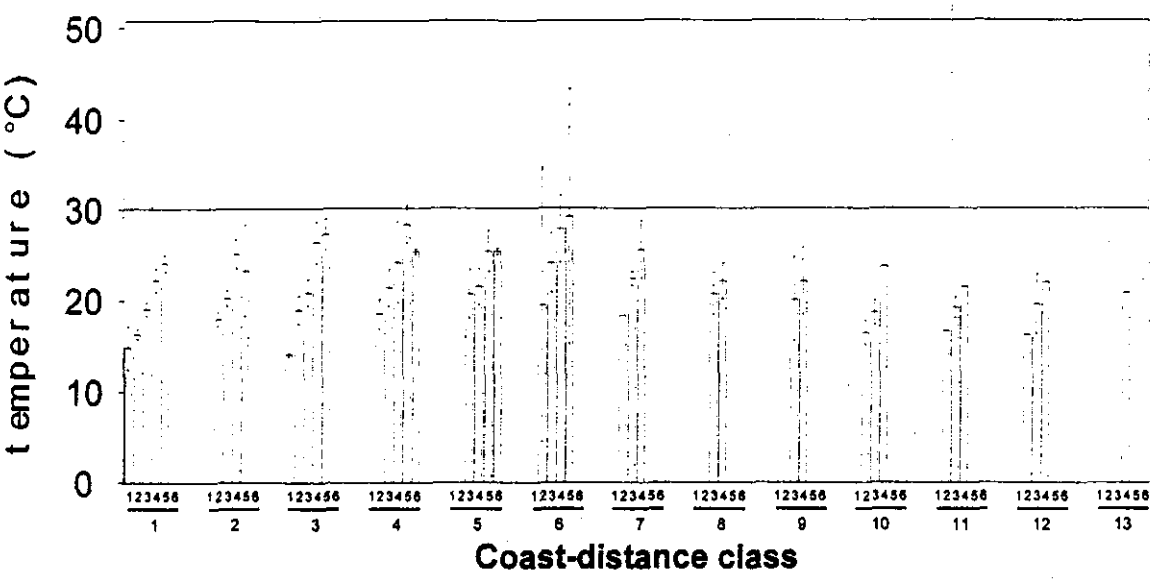

Figure 6.2. Variation in the highest 1998 daily maximum stream temperature (XY1DX) by watershed area (1-6) and coast distance class (1-13). Watershed area classes: 1 = 0 - 100 ha, 2 = 101 - 1000 ha, 3 = 1001 - 10,000 ha, 4 = 10,001 - 100,000 ha, 5 = 100,001 - 1,000,000 ha, 6 = >1,000,000 ha. Coast-distance classes: 1 = 0 - 10 km, 2 = 11 - 20 km, 3 = 21 - 30, etc. Horizontal reference line drawn at 30°C for visual comparison across classes.

Figure 6.2 (above) shows the change in 1998 XY1DX values with watershed area at different coast-distance classes. Two sites dropped out of the analyses because they lacked watershed area values. The average XY1DX values in the same coast-distance classes were greater in larger watershed area classes. This supports other documented studies that reported an increase in stream temperature with increasing watershed area and distance from the watershed divide (Allan, 1995; Sullivan et al., 1990). The greatest increase in XY1DX with watershed area was observed in coast-distance class 3 (i.e., 21 - 30 km from the coast). In coast-distance class 3, the cooling influence of ocean currents on air temperature is waning, but also elevation is increasing. See Chapter 4 for a discussion on the variation in air temperature with distance from the coast and elevation. Streams in coast-distance class 3 may be at the transition between being inside and outside of the zone of coastal influence. The relationship between stream temperature and watershed position is explored in greater depth in Chapter 7.

The distribution of the highest 1998 seven-day moving average of the daily average (XYA7DA) and highest seven-day moving average of the daily maximum (XYA7DX) showed similar patterns.

Daily Minimum Temperature and Distance from Coast

The distribution of the lowest 1998 daily minimum (IY1DI) measured at each site was plotted against coast distance (Figure 6.3). There was clearly a decrease in IY1DI values at greater distances from the coast. The moderating influence of coastal air temperatures on water temperatures can account for the higher IY1DI values nearer to the coast. Proximity to the coast has a moderating effect on extremes in stream temperature, i.e., both lower daily maxima and higher daily minima.

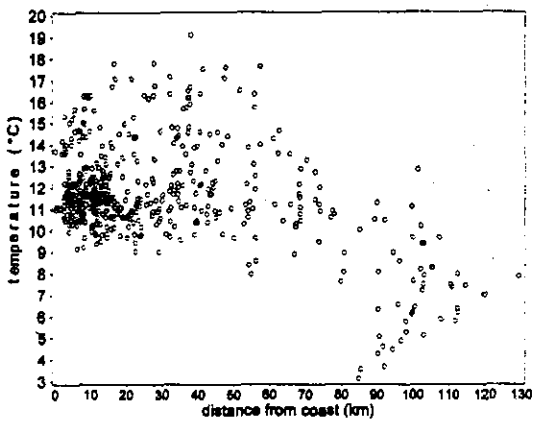

Figure 6.3. Variation in lowest 1998 daily minimum stream temperature (IY1DI) as a function of distance from coast.

UTM X-Coordinate (Longitude) and Stream Temperatures

UTM x-coordinate (a surrogate for longitude or easting) serves as a crude surrogate for distance from coast. Longitude does not follow the curves in the coastline. Therefore, it would be less precise and redundant to examine the variation in stream temperature with x-coordinate. There appears to be a west-to-east trend in water temperature based on the above distance-from-coast analyses. We suspect that this trend is largely a function of air temperature. However, there is considerably more scatter in water temperatures with coast distance than was observed with air temperatures. Obviously, there are more factors influencing water temperatures than simply macro-scale air temperatures. Local channel and riparian conditions and micro-scale air temperatures also play a role in the observed scatter seen in the data.

Ecoprovincial Stream Temperatures and Distance from the Coast

The data were stratified by ecoprovince and the relationship between the four temperature metrics and coast distance were examined. The three metrics show a general increase with increasing distance from the coast in the CSP and a decrease with increasing distance from the coast in the SSP (Figure 6.4). The series of graphs in Figure 6.4 reveals that there is overlap between the two ecoprovinces between ~15 km and 55 km from the coast. The CSP extends inland up to about 55 km in some locations, and the SSP comes within about 20 km of the coast in some locations.

UTM Y-Coordinate (Latitude) and Stream Temperatures

It is generally believed that air temperature increases in a north-to-south direction. This large scale geographic phenomenon operates at a global scale, and may manifest itself more regionally as a north-to-south stream temperature pattern within the range of the coho salmon in Northern California.

The distribution of sites with respect to UTM y-coordinate classes is shown in Figure 6.5-A. The majority of sites (438) were located between UTM y-coordinates 4,300,000 and 4,600,000 (43 and 46 in Figure 6.5-A). A UTM y-coordinate of 4,300,000 equates with a latitude of approximately 37°N and a UTM y-coordinate of 4,600,000 equates with a latitude of approximately 42°N.

The four previous temperature metrics (XY1DX, XYA7DA, XYA7DX, and IY1DI) were evaluated for possible dependancy on the UTM y-coordinate value, explained above as a surrogate for latitude. Figure 6.5-B shows the change in XY1DX values with UTM y-coordinate. Y-coordinate values increase in a northerly direction. A left-to-right unit change on the graph (e.g., 42 to 43) represents a change of 100 km northward. For reference in Figure 6.5-B, the Oregon-California border is at about 46.5 and San Francisco is near 41. The distribution of XY1DX values is quite scattered. However, there does appear to be a greater number of sites with higher XY1DX values at more southerly locations. A similar pattern was observed for XYA7DA and XYA7DX (graphs not shown). In the more interior ecoprovince (SSP), the decrease in stream temperature with increasing latitude appears more

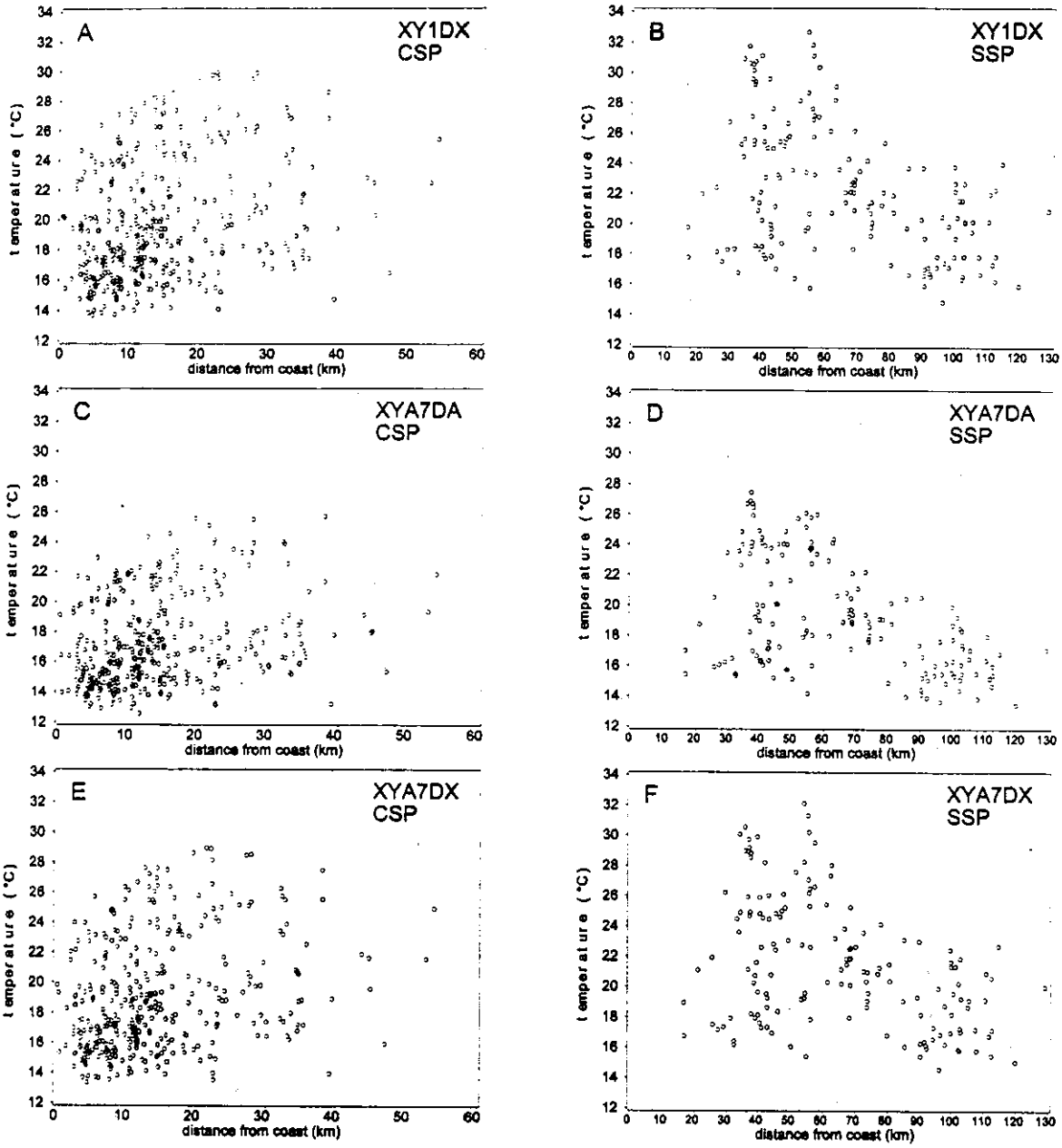

Figure 6.4. Comparison of 1998 temperature metrics versus distance from coast by ecoprovince. (A) XY1DX - CSP, (B) XY1DX - SSP, (C) XYA7DA - CSP, (D) XYA7DA - SSP, (E) XYA7DX - CSP, and (F) XYA7DX - SSP.

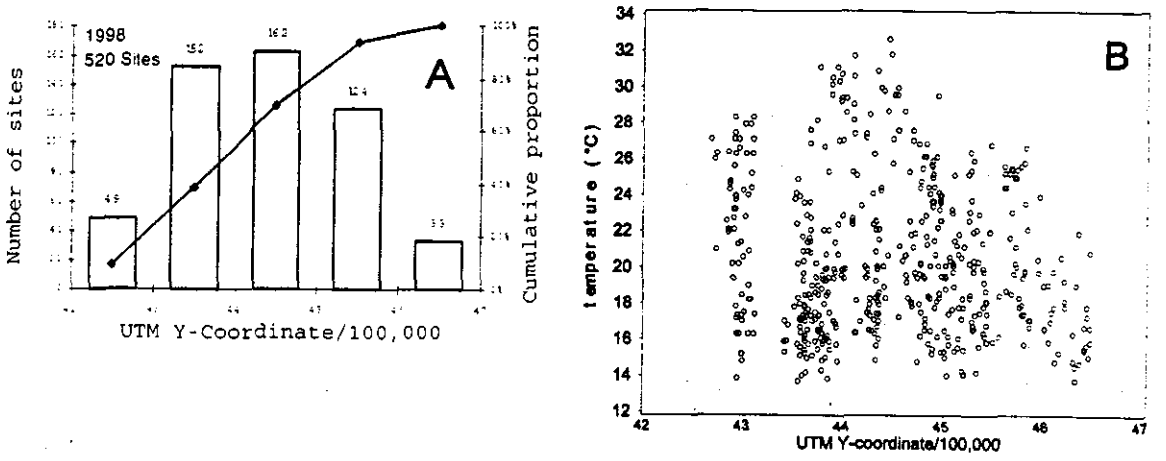

Figure 6.5. Variation in 1998 XY1DX values with Y-coordinate. (A) Frequency distribution of number of sites by UTM Y-coordinate class. (B) Scatterplot of XY1DX versus UTM Y-coordinate. Left-to-right on the graph is a south-to-north direction. X-axis values are UTM Y-coordinates divided by 100,000. San Francisco, CA is at approximately 41 and the Oregon-California border is at approximately 46.5.

defined, whereas the coastal ecoprovince (CSP) displays considerable scatter (Figure 6.6). The CSP ranges from 0 km from the coast to ~55 km inland while the SSP ranges from ~20 km to nearly 130 km inland.

Using the same coast distance classes as presented in Figure 6.1-C, the variation in XY1DX values with Y-coordinate was examined. This analysis essentially aggregates temperature sites into 13 north-south transects paralleling the coast, each transect being 10 km in width. The variation in XY1DX along each transect in a south-to-north direction by UTM y-coordinate classes is presented in Figure 6.7. Not all y-coordinate classes were represented, therefore south-to-north trends were not well defined. However, there does appear to be a general decreasing trend in XY1DX from y-coordinate classes 1 to 5. Whether there is more of a south-to-north cooling trend along the coast than inland cannot be determined from the data due to an under representation of sites in coast-distance classes in each of the five y-coordinate groupings.

Zone of Coastal Influence and Stream Temperatures

Using 30-yr long-term average PRISM air temperature data the ZCI was determined by calculating the steepest rate of change in air temperature for August. August is the month when the majority of highest XY1DX, XYA7DA, and XYA7DX values occur for most sites throughout the range of coho salmon in Northern California. The ZCI is our best approximation of the inland extent of the *fog zone*. See Chapter 4 for a more detailed explanation of how the ZCI was developed.

Figure 6.8-A shows the average XY1DX class values for sites combined (518) with ZCI values of zero or one. Sites with ZCI = 0 were outside the approximated zone of coastal influence and those with ZCI = 1 were considered inside the ZCI. The average XY1DX value for the ZCI = 0 group was 21.7°C and 18.7°C for the ZCI = 1 group. The two groups were significantly different ($p < 0.0001$)

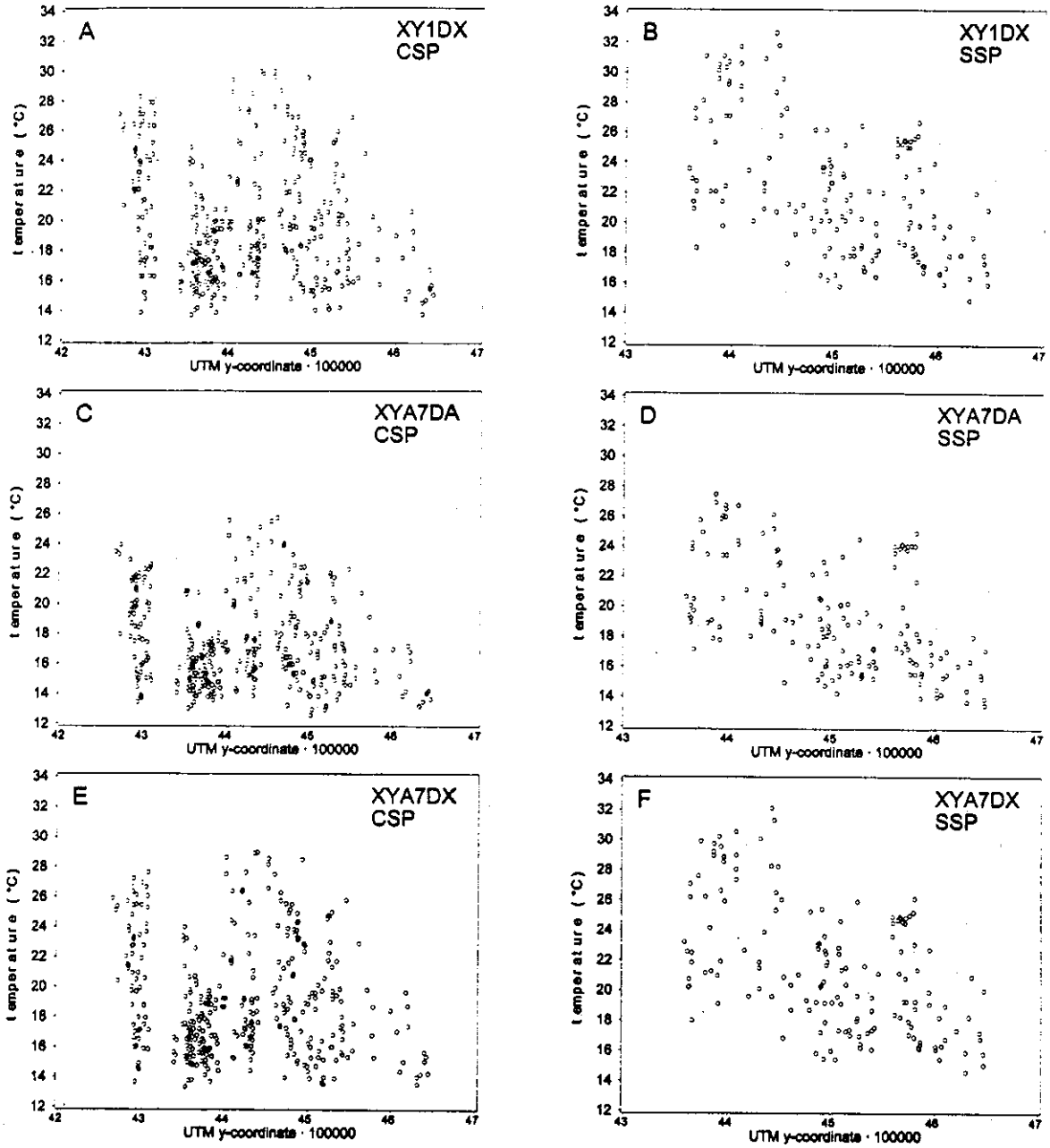

Figure 6.6. Comparison of 1998 temperature metrics versus UTM y-coordinate (northing) by ecoprovince. A) XY1DX - CSP, B) XY1DX - SSP, C) XYA7DA - CSP, D) XYA7DA - SSP, E) XYA7DX - CSP, and F) XYA7DX - SSP.

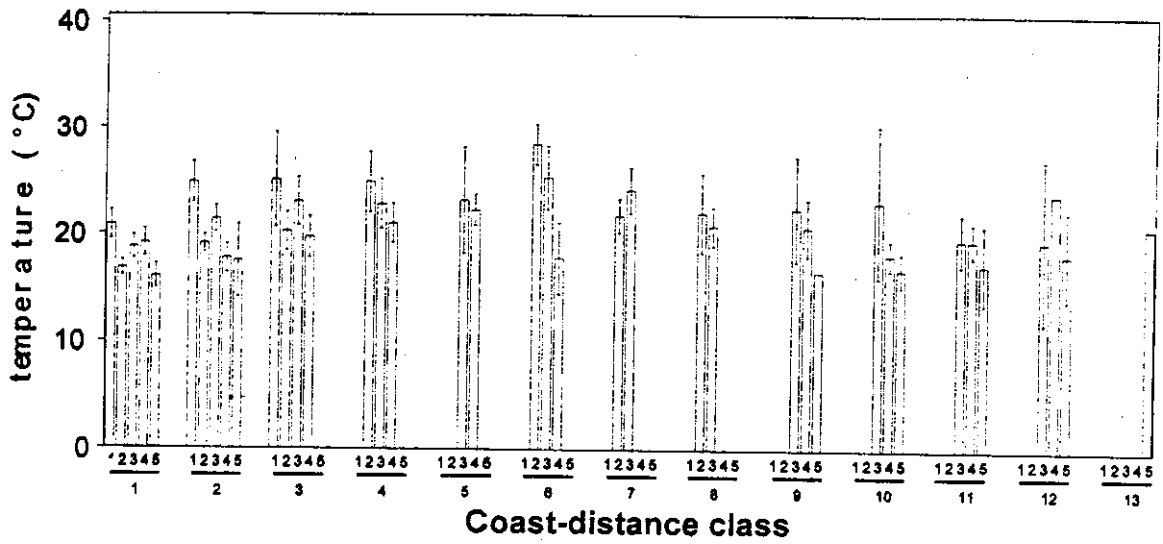

Figure 6.7. Average XY1DX values by UTM y-coordinate (latitude) and distance-from-coast classes. UTM y-coordinates divided by 100,000. Y-coordinate classes are 1 = 42-43, 2 = 43-44, 3 = 44-45, 4 = 45-46, 5 = >46. Coast-distance classes (1 - 13) as defined in Figure 6.2 caption.

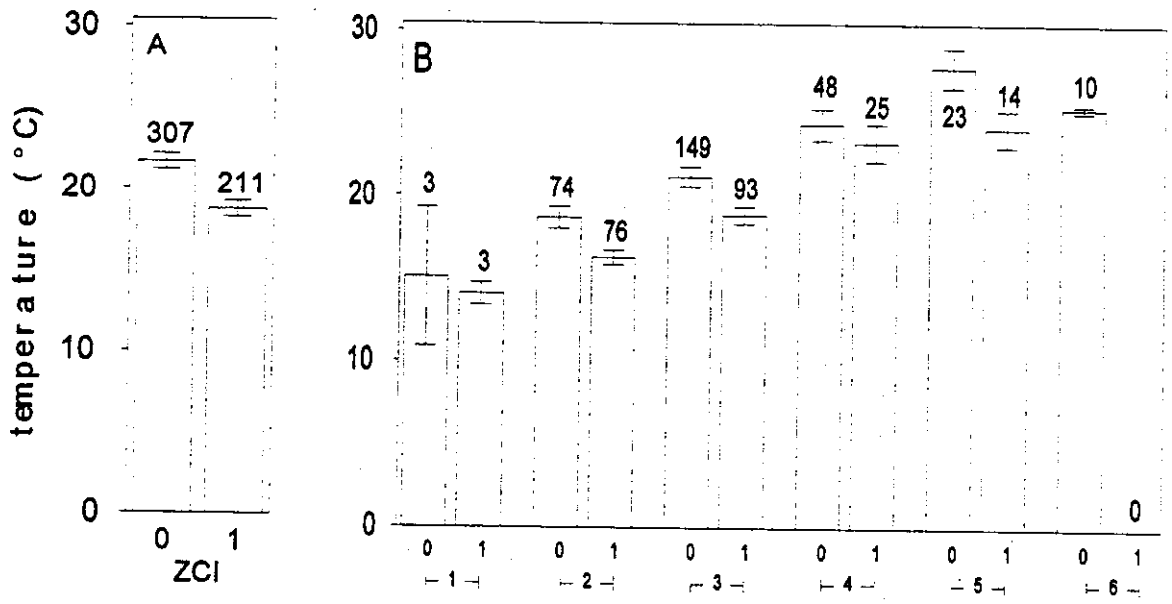

Figure 6.8. Average XY1DX for sites within and outside of the zone of coastal influence (ZCI) for (A) all sites combined and (B) by watershed area class. ZCI = 0 outside, ZCI = 1 inside. Watershed area classes 1 - 6 as defined in Figure 6.2 caption. Error bars represent ± 2 standard deviations. Number of sites shown above error bar.

based on analysis of variance results using PROC GLM (SAS, 1985). Streams of similar size were grouped together using watershed area as a surrogate for stream size. Figure 6.8-B shows that for all watershed area size classes (watershed area class 6 had no sites inside the ZCI) the average XY1DX for sites outside the ZCI was approximately 1°C to 2°C higher than the average for sites inside the ZCI. Analysis of variance showed that both ZCI and watershed area classes were significantly different ($p < 0.0001$), however the interaction term was not.

Elevation and Stream Temperature

Elevation is expected to have an influence on stream temperature in that air temperature is believed to decrease with increasing elevation. Air temperature, in turn, influences water temperature. A decrease in air temperature at higher elevations is well documented and known to be driven by adiabatic cooling processes. Adiabatic cooling deals with the cooling of parcels of air as they rise, or are forced upward, through the atmosphere. An example would be the cooling of an air parcel as it rises over a mountain range. A reasonable hypothesis is that streams at higher elevations should have cooler water temperatures.

This hypothesis may prove false, however, based on the discussion in Chapter 4, where it was demonstrated that air temperature variation is more a function of distance from the coast rather than elevation in areas under the influence of maritime air currents. In the more interior areas, air temperature was shown to have the more traditional inverse relationship with elevation. Does water temperature vary with elevation as does air temperature?

Daily Maximum and Elevation

It is instructive to examine the distribution of elevation values for stream temperature monitoring sites. Sites were grouped into elevation classes. The number of sites in each elevation class and the cumulative proportion are shown in Figure 6.9-A. The distribution of water temperature sites is dominated by sites at elevations less than 400 m (~1300 ft). Approximately 80% (~416 sites) of the 520 sites monitored in 1998 had elevations below 400 m.

Figure 6.9-B shows the relationship between elevation and the highest 1998 daily maximum stream temperature (XY1DX). There was not a clear relationship between the two variables. Generally, elevations between 200 and 600 m exhibited some of the highest XY1DX values (~32°C). At elevations greater than 600 m, XY1DX values were usually below ~26°C. All XY1DX values were greater than 13°C across all elevations. Examination of plots of XYA7DA and XYA7DX revealed similar patterns. These graphs are not shown for sake of brevity.

Daily Minimum and Elevation

There was more of a discernable trend in the lowest 1998 daily minimum stream temperature (IY1DI) and elevation (Figure 6.10). The lowest 1998 IY1DI observed between July 21 and August 19 was about 3°C, at around 1300 m (~4300 ft). The highest IY1DI was about 19°C at ~50 m elevation (Figure 6.10-A). The decreasing trend in IY1DI is shown by elevation class in Figure 6.10-B. The same data were stratified by ecoprovince in Figure 6.11. There was a much greater range in daily minimum temperatures in the SSP than in the CSP. Maritime air temperature probably moderates daily minimum water temperature in the CSP. At higher elevations of the CSP, which are more inland, much cooler evening air temperatures are attained, resulting in lower daily minimum water temperatures. Some sites at higher elevations in the SSP may also be more influenced by snowmelt and colder groundwater inflow.

Daily minima occur in the late evening and early morning hours after sundown and prior to sunrise. In the absence of incoming solar radiation, the daily minimum water temperature attained at a site is more a function of air temperature. The daily maximum temperature reached at a site will also play a role in what daily minimum can be reached. Radiative heat from the substrate can continue to contribute heat input after sundown. Sites that reach high daily maxima may not have sufficient time to come into equilibrium with late evening and early morning air temperatures before the sun rises and the heating cycle begins again.

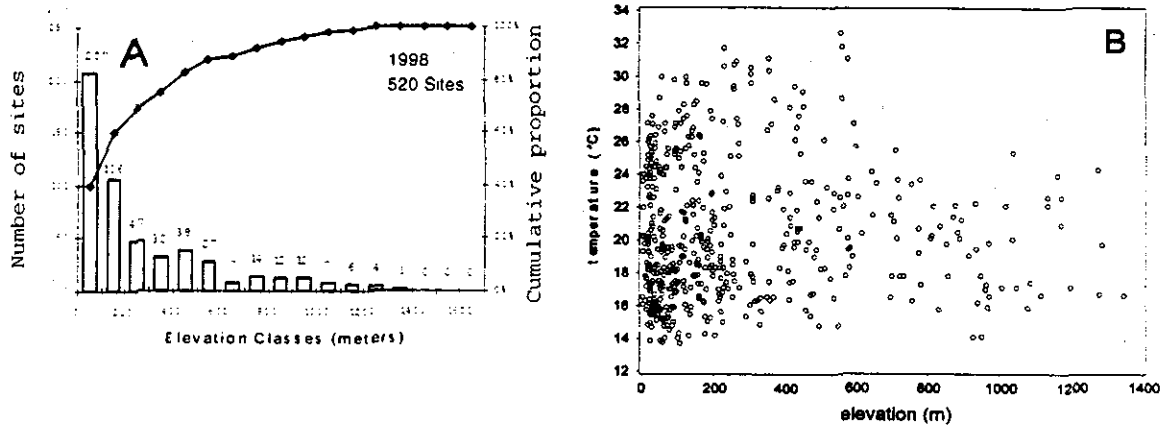

Figure 6.9. Relationship between the highest 1998 daily maximum water temperature (XY1DX) and elevation. Plots display (A) the frequency distribution of sites by elevation classes and (B) scatter plot of XY1DX vs elevation.

As pointed out in Figure 6.6. there is overlap in sites within the CSP and SSP between about 20 km and 55 km from the coast. Thus. stratification of water temperature sites by ecoprovince may not adequately characterize the sites that are influenced by coastal air temperatures. Sites were stratified by ZCI and average IY1DI values were plotted by elevation class. Figure 6.12 shows that there is a large decrease in IY1DI values with increasing elevation for the sites outside the ZCI. Not all elevation classes were represented by sites inside the ZCI. Only elevation classes 1 through 3 were found inside the ZCI. A less distinctive decrease in IY1DI was noted with increasing elevation for sites inside the ZCI.

Summary

Stream temperatures across Northern California appear to vary with geographic position. The variation in water temperature with respect to distance from the coast. UTM y-coordinate (latitude). ecoprovince. zone of coastal influence. and elevation was large for the highest 1998 values of the daily maximum (XY1DX) and the seven-day moving average of the daily average (XYA7DA) and daily maximum (XYA7DX) stream temperatures. These three temperature metrics are indicative of day time stream temperatures. a time when solar radiation may be more influential in controlling air and water temperature. Large variation in day-time temperature metrics suggests that local site-specific factors may play a greater role in controlling stream temperatures through their influence on both local microair temperatures and direct and diffuse solar radiation.

Variation in daily minimum temperature in relation to various geographic position factors was not as great. with much clearer trends discernable. Geographic position factors are largely surrogates for macroair temperature. Since the daily minimum stream temperature. in this case the lowest 1998 daily minimum observed at each site (IY1DI). occurs at the time when solar radiation is absent. the reduced scatter in IY1DI values suggests that air temperature may be asserting more influence on this stream temperature metric than on those metrics that have more of a solar heating and daily maximum air temperature component. While air temperature is

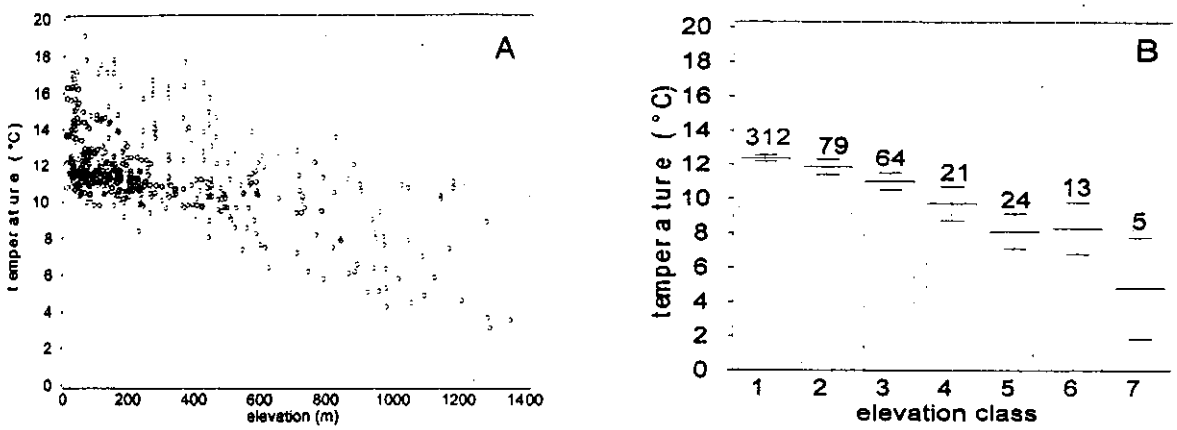

Figure 6.10. Relationship between the lowest 1998 daily minimum water temperature (IY1DI) and elevation. (A) scatterplot of IY1DI versus elevation. (B) average IY1DI by elevation class. Error bars are ± 2 standard deviations. Number of sites shown above error bar. Elevation class 1 = 0 - 200 m, 2 = 201 - 400 m, 3 = 401 - 600 m, 4 = 601 - 800 m, 5 = 801 - 1000 m, 6 = 1001 - 1200 m, 7 = >1200 m.

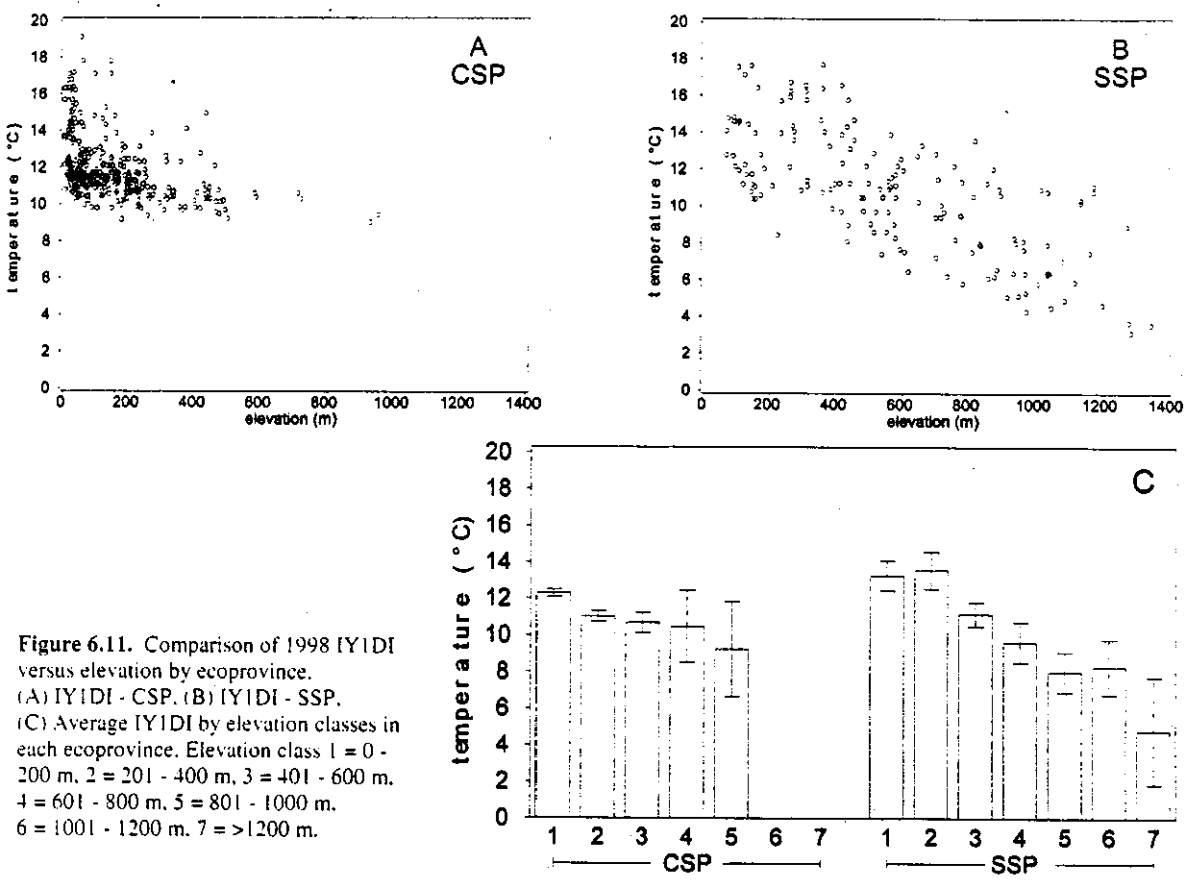

Figure 6.11. Comparison of 1998 IY1DI versus elevation by ecoprovince. (A) IY1DI - CSP. (B) IY1DI - SSP. (C) Average IY1DI by elevation classes in each ecoprovince. Elevation class 1 = 0 - 200 m, 2 = 201 - 400 m, 3 = 401 - 600 m, 4 = 601 - 800 m, 5 = 801 - 1000 m, 6 = 1001 - 1200 m, 7 = >1200 m.

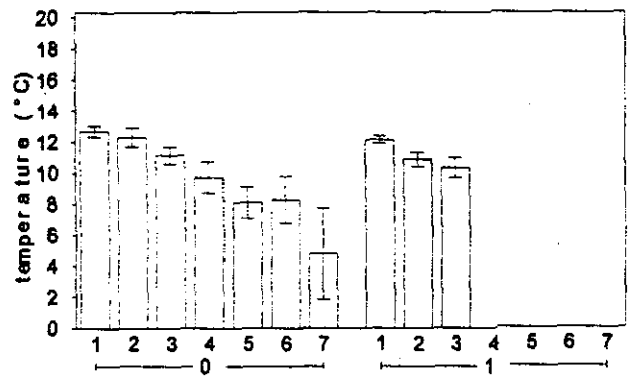

Figure 6.12. Average IY1DI values by elevation class for sites outside (group 0) and inside (group 1) the ZCI. Elevation classes as defined in Figure 6.10 caption.

known to influence water temperatures, the large variation observed for XY1DX, XYA7DA, and XYA7DX suggests that other factors are important in explaining the observed variability across the region. These factors include canopy closure, watershed area, distance from the watershed divide, flow, gradient, and channel orientation. These factors are explored in greater depth in the following chapters.

Chapter 7

WATERSHED POSITION AND STREAM TEMPERATURE

Introduction

Water temperature has a tendency to increase with increasing distance from the watershed divide and with increasing drainage area (Allan, 1995; Sullivan et al., 1990). Water temperature near the source is the coolest, usually close to groundwater temperature. Groundwater temperature is usually within =[-3 °C of mean annual air temperature (Collins, 1925; Allan, 1995; Sullivan et al., 1990). Seasonal temperature variation in springs and some headwater streams is slight. For example, a spring source in northern Colorado remained between 8 °C and 10 °C over the year, despite much greater annual variation in air temperature at this site (Ward and Dutford, 1979).

Because long rivers originate at higher elevations with generally cool climates and flow into warmer lowlands, a longitudinal temperature increase is the norm. Longitudinal temperature increase has been observed in streams throughout the world. In Central African streams that originate from ice water on mountains over 4000 m in elevation, the temperature increases from near freezing to the high twenties (Celsius) over their length (Hynes, 1970). Several European researchers have shown that summertime stream temperatures increase in a downstream direction in such a way that the rise is more or less proportional to the logarithm of the distance from the watershed divide (Schmitz and Volkert, 1959, Schmitz, 1961, and Eckel, 1953 as cited in Hynes, 1970). The logarithmic relationship has also been observed in streams in United States (Vannote and Sweeney, 1979; Sullivan et al., 1991; Allan, 1995). Even in the tropics stream temperatures increase in a downstream direction until they reach equilibrium with the air temperature. For instance, the Marowijne River in Surinam rises 22 °C and reaches 31 °C at its mouth (Geijskes, 1942 as cited in Hynes, 1970).

This simple picture of stream temperature change over downstream distance can be altered by local conditions. Riparian shading can vary along the length of a stream course due to natural or human-induced causes. Air temperature regimes can change from the headwaters to the mouth, not always in an increasing manner, as shown in Chapter 4. In Northern Coastal California air temperatures may decrease by as much as 15 °C by the time a parcel of water reaches the ocean after its journey from the headwaters, due to oceanic control on air temperatures near the coast.

In this chapter we report that stream temperature was highly dependent upon watershed position, both in terms of watershed area and distance from the watershed divide. Each of the eighteen hydrologic units (HUC) that comprise the range of the coho salmon showed an increase in stream temperature with an increase in watershed area and distance from the watershed divide. The rate of downstream increase in stream temperature appeared to vary with HUC location, i.e., whether the HUC was completely coastal, partly coastal and partly interior, or completely interior. The mainstems of the Eel and Mad Rivers showed decreased water temperatures at their greatest distances from the watershed divide, most likely due to the cooling influence of marine air currents. Using Brown's mixing equation we demonstrated that tributaries can have a cooling or

warming influence on mainstem or receiving water temperatures, but that this influence was transient. The recipient of the cooler or warmer tributary water appeared to re-equilibrate with climatic and local riparian downstream conditions. Streams originating entirely inside the zone of coastal influence exhibited cooler temperatures than streams of similar size that originated outside the zone of coastal influence (ZCI). Streams that originated outside the ZCI showed a decrease in water temperature upon entry into the ZCI.

Watershed Area and Bankfull Width

Watershed area is a useful variable for grouping streams of similar size together, especially when bankfull width is not available for all sites. Watershed area was derived in GIS for all 1090 sites in the regional assessment area of interest. If watershed area could be used as a surrogate for bankfull width, a larger number of sites could be used in the analyses.

Figure 7.1-A shows the relationship between log watershed area versus log bankfull width for the Upper Salmon River of Idaho (FISRWG, 1998). A similar plot is shown in Figure 7.1-B for 177 Forest Science Project sites monitored in 1998 that had non-null values for bankfull width. While the relationship may not be adequate for prediction purposes, it is deemed adequate for grouping streams of approximately the same size based on their watershed area.

Sullivan et al. (1990) used watershed area as a surrogate for stream flow. Watershed area calculated for FSP sites will be used in this chapter to derive relative stream-flow ratios for use in Brown's mixing equation (Brown, 1972).

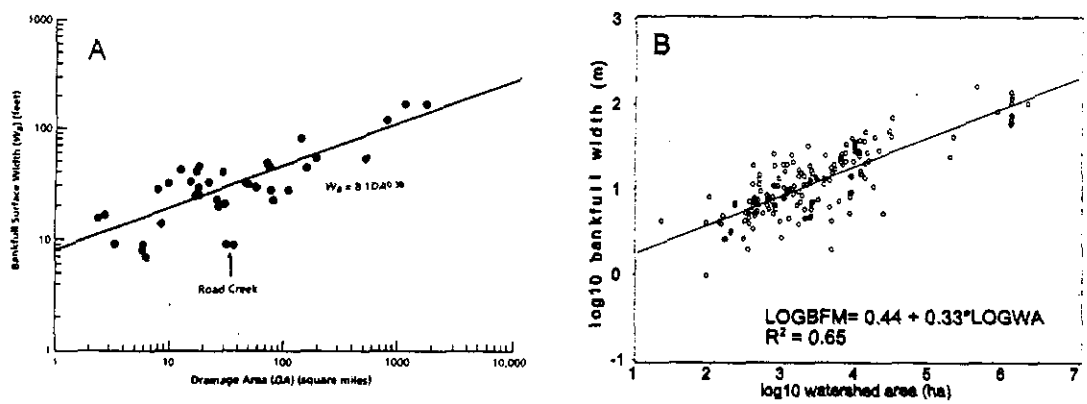

Figure 7.1. Relationship between watershed area and bankfull width. (A) Bankfull surface width versus drainage area - Upper Salmon River, Idaho. Taken from FISRWG, 1998. (B) Bankfull width (LOGBFM) versus watershed area (LOGWA) for 1998 Forest Science Project stream temperature monitoring sites (177 sites).

Distribution of Watershed Area and Distance from Watershed Divide Values

A characterization of the watershed position of stream temperature monitoring sites used in the regional stream temperature assessment was performed by examination of the frequency distribution of values for watershed area and distance from the watershed divide. Such an examination of frequency distributions showed whether most sites were closer to the headwaters or if more were located near the mouths. Since many cooperators did not provide the Forest Science Project with bankfull width values for each site, watershed area and distance from the watershed divide were the two most important variables that allowed us to aggregate sites by relative stream size. Both these variables were derived in GIS, based on point locations. Positional accuracy was thus critical for estimating these two variables (see Chapter 2).

Watershed Area Values

Watershed areas were calculated for all sites for years 1990 through 1998. The year with the most complete data set was 1998, so analyses will focus on data collected in that year. Figure 7.2-A shows the frequency distribution of watershed areas for stream temperature monitoring sites in 1998. The mean watershed area for 1998 sites was 58.299 ha with a median of 2404 ha and mode of 85 ha. The minimum was 21 ha and the maximum was 2,007,819 ha

Distance from Watershed Divide Values

Figure 7.2-B shows the frequency distribution of distance from watershed divide values for sites monitored in 1998. The mean divide distance for 1998 sites was 32 km, with a minimum of 1.3 km and a maximum of 331 km. The median was 9.9 km and the mode was 4.8 km.

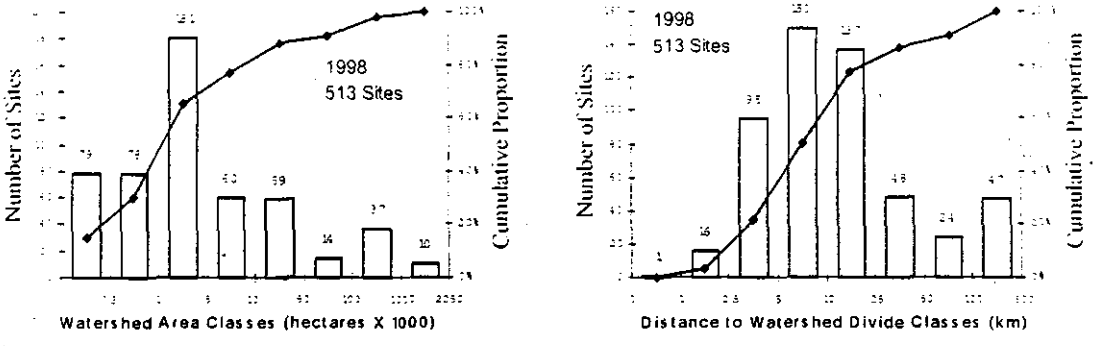

Figure 7.2. Frequency distribution of stream temperature monitoring sites by (A) watershed area classes and (B) distance from watershed divide classes. Plotted line is the cumulative proportion. Sites are those with complete data from July 21 to August 19.

Relationship Between Watershed Area and Distance From the Watershed Divide

One would expect a significant relationship between watershed area and distance from the watershed divide. Figure 7.3 shows that the two variables are highly correlated, with an R^2 value of 0.97 for the log transformed data. The relationship is based on 1087 unique site locations monitored in 1990 through 1998. If a point is located further down in the drainage it is expected that the area draining into the point will be greater. Distance from the watershed divide and watershed area can be easily calculated in a GIS, given a high-quality digital elevation model. Divide distance may be easier to acquire from topographic map. The equation in Figure 7.3 can be used to estimate the watershed area if distance from the watershed divide is known.

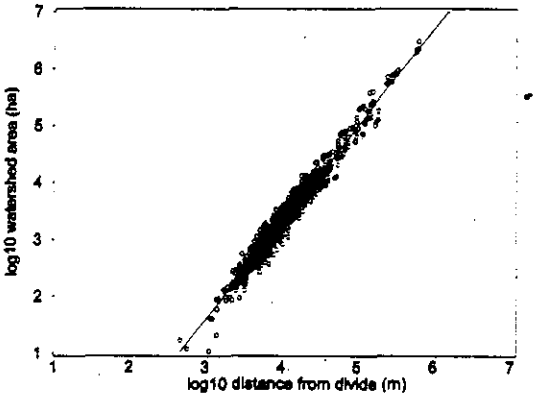

Figure 7.3. Relationship between watershed area and distance from the watershed divide. Linear regression line fit to the data has the equation: $\log_{10}$(watershed area) = 1.693*$\log_{10}$(divide distance) - 3.4135. R^2 = 0.97, based on all sites and all years, 1087 sites.

Watershed Area and Stream Temperature Across the Region

The relationship between watershed area and five stream temperature metrics was investigated. The five metrics were: the highest daily maximum (XY1DX), the highest seven-day moving average of the daily average (XYA7DA), the highest seven-day moving average of the daily maximum (XYA7DX), the lowest daily minimum (IY1DI), and the average diurnal fluctuation.

Daily Maximum and Watershed Area

Figure 7.4-A shows the relationship between $\log_{10}$ watershed area and the highest daily maximum water temperature (XY1DX) for sites monitored in 1998. For the purposes of graphical presentation, watershed area was grouped into six classes: (1) 0 - 100 ha, (2) 101 - 1000 ha, (3) 1001 - 10,000 ha, (4) 10,001 - 100,000 ha, (5) 100,001 - 1,000,000 ha, and (6) greater than 1,000,001 ha (Figure 7.4-B). Each bar represents the average of the XY1DX for each watershed area class. The error bars represent ± 2 standard deviations.

There was an increase in XY1DX temperature with increasing watershed area. The average XY1DX ranged from 14.6°C for watershed areas between 0 and 100 ha to 26.4°C for watershed areas between 100,001 and 1,000,000 ha. It is interesting to note that the XY1DX in the greater-than-one-million-hectare class showed about a one degree Celsius decrease compared to the previous class. The water temperature decrease in the largest watershed area class is possibly due these sites being predominantly located on mainstem rivers near the coast. The decrease in the XY1DX temperature is most likely be due to the cooling effects of coastal air temperatures. Sites were poststratified by ecoprovince and are presented in Figure 7.5.

Figures 7.5-A and 7.5-B show that both ecoprovinces exhibited a slight decrease in the highest daily maximum temperature at the highest watershed area values. However, the CSP bar graph (Figure 7.5-C) does not reveal the decrease due to the grouping by watershed area classes. The sites showing the decrease in the highest daily maximum temperature for the CSP were just shy of one million hectares (~980,000 ha), and were grouped in watershed area class 5. Class 5 contained sites with watershed areas as low as 100,001 ha, thus the class average was not responsive to the minority of sites close to one

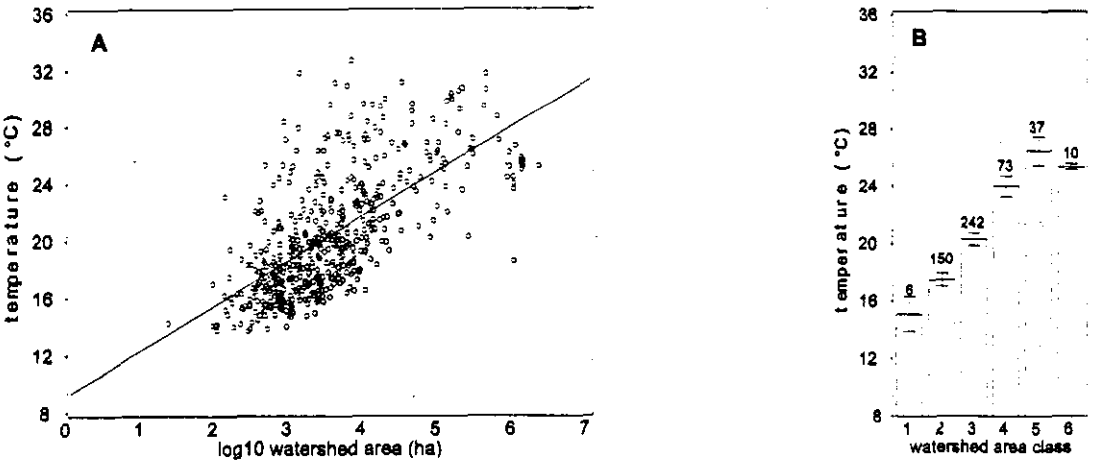

Figure 7.4, Relationship between the highest 1998 daily maximum stream temperature (XY1DX) and log watershed area (logwa). Scatter plot (A) with linear regression equation: XY1DX = 9.344683 + 3.13764*logwa, R^2 = 0.452726. Bar chart (B) with watershed area classes: (1) 0 - 100 ha, (2) 101 - 1000 ha, (3) 1001 - 10,000 ha, (4) 10,001 - 100,000 ha, (5) 100,001 - 1,000,000 ha, and (6) greater than 1,000,000 ha. Error bars represent ± 2 standard deviations. Above each error bar is the number of sites in the class.

million hectares. Sites on the lower Eel River in the CSP represent the points in Figure 7.5-A exhibiting a decrease in temperature. Sites in the SSP that showed a decrease in temperature at over one million hectares were on the Klamath River (Figure 7.5-B). The sites on the Klamath River are approximately 80 km from the coast, placing them in the SSP. Air temperatures are nearly 15°C warmer in this area compared to coastal areas. What could account for the decrease in water temperature at large watershed areas in a warm interior portion of the SSP? Significant regulation of flow on the Klamath River began in 1962 when Iron Gate Dam went into operation (Blodgett, 1970). Water temperatures in the Klamath River may be influenced by dam releases from the impounded reservoir.

The distribution of XY1DX values in the CSP (Figure 7.5-A) are more closely clustered than SSP values (Figure 7.5-B). Also, the linear regression line is shifted down and has a lower y-intercept, indicating that, in general, the CSP XY1DX values are lower than the SSP values at similar watershed areas. The difference in water temperatures between the two ecoprovinces is supported by previous discussions of the differences in air temperature regimes in the two ecoprovinces (see Chapter 4). The cooler air temperatures along the coast seem to have a moderating influence on the daily maximum temperatures.

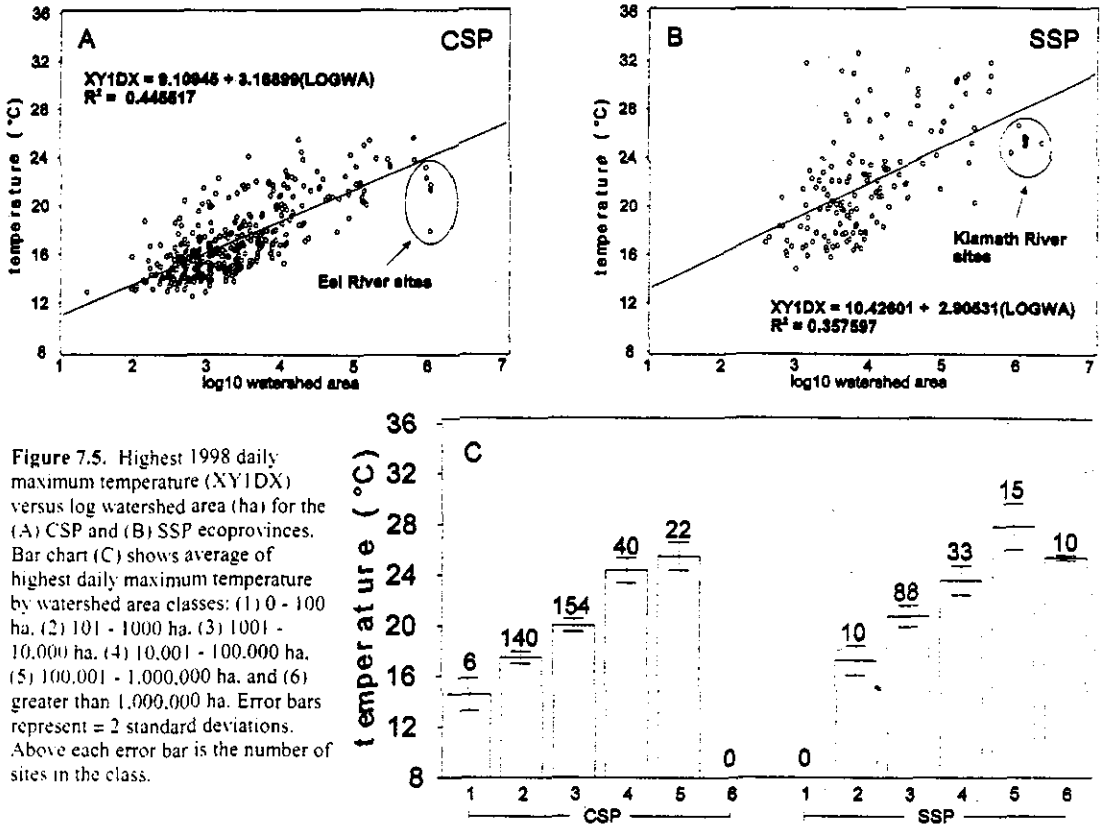

Figure 7.5. Highest 1998 daily maximum temperature (XY1DX) versus log watershed area (ha) for the (A) CSP and (B) SSP ecoprovinces. Bar chart (C) shows average of highest daily maximum temperature by watershed area classes: (1) 0 - 100 ha, (2) 101 - 1000 ha, (3) 1001 - 10,000 ha, (4) 10,001 - 100,000 ha, (5) 100,001 - 1,000,000 ha, and (6) greater than 1,000,000 ha. Error bars represent ± 2 standard deviations. Above each error bar is the number of sites in the class.

Seven-Day Moving Averages and Watershed Area

The relationship between the highest 1998 seven-day moving average of the daily average (XYA7DA) and the highest seven-day moving average of the daily maximum (XYA7DX) versus $\log_{10}$ watershed area was investigated. The relationships were found to be similar to those observed for the XY1DX plots. For sake of brevity, graphs are shown in Appendix D and only linear regression equations are presented in Table 7.1.

The R^2 values for the XYA7DA-watershed area relationships were slightly higher than those observed for XYA7DX. Sullivan et al. (1990) believed that mean daily water temperatures were more responsive to air temperatures than the daily maxima, the latter they postulated were more a function of solar radiation. This is supported by results of micro- and macroair temperature analyses presented in Chapter 5. Sullivan et al. (1990) found that the average water temperatures approached an equilibrium temperature that was close to the average air temperature for the basin. The slightly better correlation between XYA7DA (the average of the daily averages) and $\log_{10}$ watershed area, rather the XYA7DX (the average of the daily maxima), would seem to reflect the greater association between average water temperature and air temperatures. The decrease in water temperature metrics (XY1DX, XYA7DA, and XYA7DX) at the highest watershed areas, i.e., nearest the coast, seems to further support the postulate that water temperatures tend to come into equilibrium with cooler coastal air temperatures at increasing watershed areas.

Table 7.1. Linear Regression Equations for Relationship between 1998 XYA7DA[1] and XYA7DX[2] versus Log_{10} Watershed Area, Combined and by Ecoprovince.

Variable	Ecoprovince	No. of Sites	Slope	Intercept	R^2
XYA7DA	combined	518	2.81392	7.87853	0.58539
XYA7DX	combined	518	3.06196	8.92433	0.46575
XYA7DA	CSP	362	2.62661	8.44315	0.559684
XYA7DA	SSP	156	3.07022	6.99033	0.537656
XYA7DX	CSP	362	3.05958	8.83760	0.45668
XYA7DX	SSP	156	2.87608	9.89085	0.366816

[1]XYA7DA = seven-day moving average of the daily average.
[2]XYA7DX = seven-day moving average of the daily maximum.

Daily Minimum and Watershed Area

The relationship between watershed position, as expressed in terms of watershed area, and the lowest 1998 daily minimum stream temperature (IY1DI) showed an increasing trend with increasing watershed area (Figure 7.6). The average IY1DI in the lowest watershed area class was 10.4°C, with a range from 9.0°C to 13.0°C.

There was a large scatter in IY1DI values at watershed areas less than approximately 31,600 ha (log_{10} watershed area = 4.5) (Figure 7.6-A). The average IY1DI for watershed classes 2 and 3 was about 11°C, with ranges of 4.9°C to 14.4°C for class 2 and 3.1°C to 15.2°C for class 3, respectively (Figure 7.6-B).

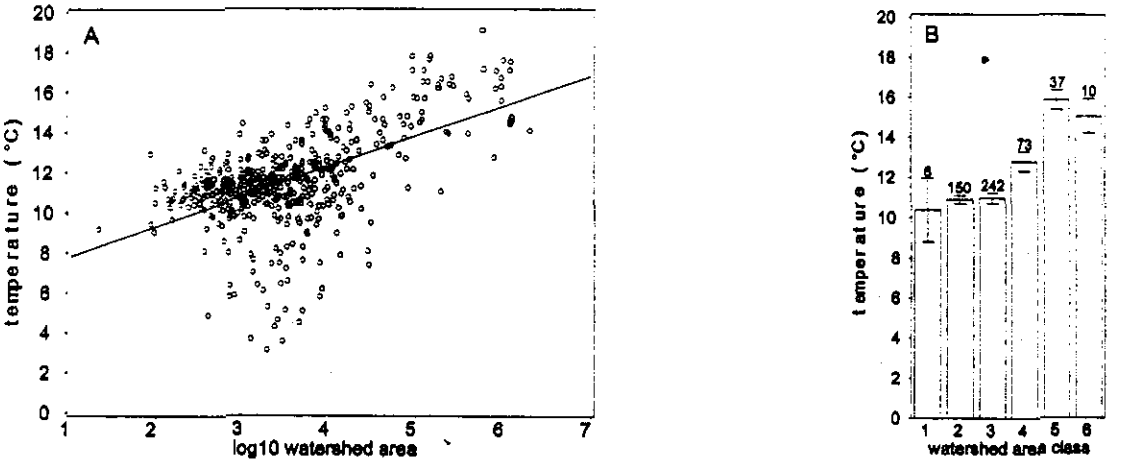

Figure 7.6. Relationship between the lowest 1998 daily minimum stream temperature (IY1DI) and log watershed area (ha) (LOGWA). Scatter plot (A) with linear regression equation: IY1DI = 6.324127 + 1.499672*LOGWA, R^2 = 0.331635. Bar chart (B) with watershed area classes: (1) 0 - 100 ha, (2) 101 - 1000 ha, (3) 1001 - 10,000 ha, (4) 10,001 - 100,000 ha, (5) 100,001 - 1,000,000 ha, and (6) greater than 1,000,000 ha. Error bars represent ± 2 standard deviations. Number of sites in each class is shown above error bar.

Sites were poststratified by ecoprovince and the IY1DI versus log watershed area relationship was examined. Figures 7.7-A and 7.7-B reveal the source of scatter noted in Figure 7.6-A. The CSP showed a much tighter distribution of IY1DI values with $\log_{10}$ watershed area (Figure 7.7-A) whereas the SSP displayed much greater scatter (Figure 7.7-B). The moderating influence of coastal air currents on stream temperatures are believed to play a role in the reduced scatter of the lowest daily minimum temperatures at various positions in watersheds of Northern Coastal California.

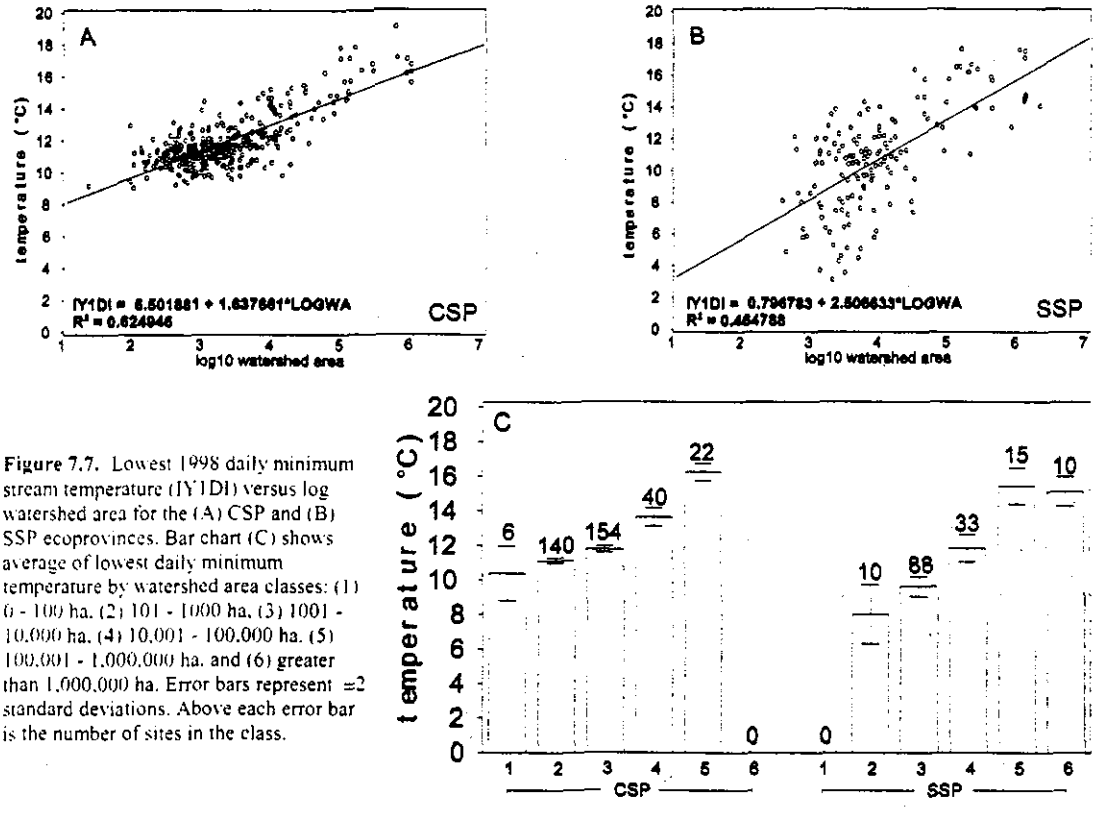

Figure 7.7. Lowest 1998 daily minimum stream temperature (IY1DI) versus log watershed area for the (A) CSP and (B) SSP ecoprovinces. Bar chart (C) shows average of lowest daily minimum temperature by watershed area classes: (1) 0 - 100 ha, (2) 101 - 1000 ha, (3) 1001 - 10,000 ha, (4) 10,001 - 100,000 ha, (5) 100,001 - 1,000,000 ha, and (6) greater than 1,000,000 ha. Error bars represent ±2 standard deviations. Above each error bar is the number of sites in the class.

Diurnal Fluctuation and Watershed Area

Diurnal fluctuation was calculated for each site and each day by subtracting the daily minimum stream temperature from the daily maximum. The average diurnal fluctuation was calculated using the PROC MEANS procedure in SAS (SAS, 1985). The restricted temporal window (July 21 to August 19) was imposed upon the 1998 daily stream temperature to calculate the average diurnal fluctuation for each day. Sites with complete records within this window were used in the calculations.

Figure 7.8-A shows the variation in diurnal fluctuation with $\log_{10}$ watershed area. Great variability was observed in the diurnal fluctuation, with the lowest values near 0°C and the highest near 13°C. The general trend showed an increase in the diurnal fluctuation in the middle range of the watershed areas, followed by a decrease at the highest watershed areas. The relationship between diurnal fluctuation and $\log_{10}$ watershed area is not linear. The bell-shaped distribution in diurnal fluctuation becomes more apparent in the bar chart presented in Figure 7.8-B. Small tributaries near the headwaters have less variable stream temperatures because of groundwater influence and shading. Large rivers exhibit less diel temperature fluctuation because of their greater volume and thermal inertia (Allan, 1995). Vannote and Sweeney (1980) showed the relationship between maximum daily temperature range and stream order for streams in temperate climates (Figure 7.9). Our findings seem to coincide with those of Vannote and Sweeney (1980) rather than those of Sullivan et al. (1990) who hypothesized a continual decrease in diurnal temperature fluctuation with increasing distance from the watershed divide based on a smaller sample size.

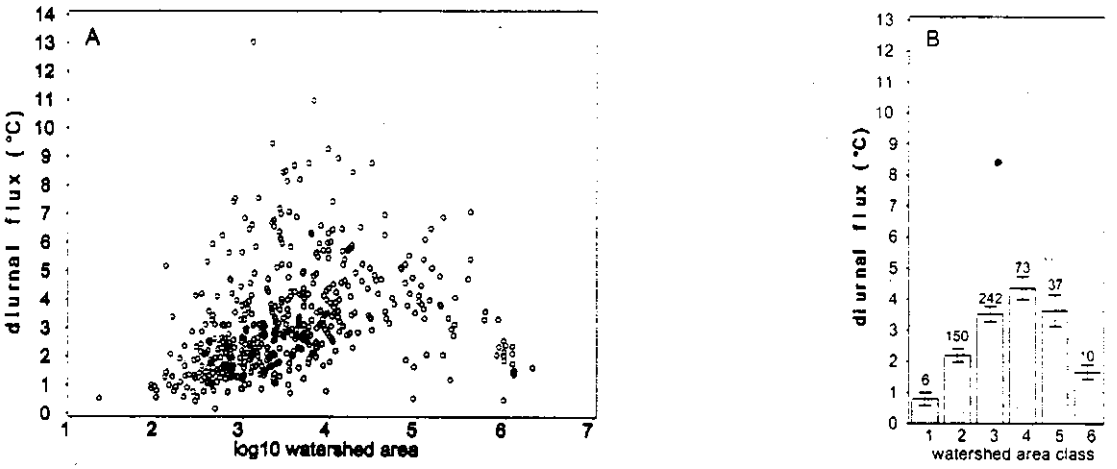

Figure 7.8. Relationship between the 1998 average diurnal stream temperature fluctuation (AFLUX) and log watershed area (LOGWA). Scatter plot (A) and bar chart (B) with watershed area classes: (1) 0 - 100 ha, (2) 101 - 1000 ha, (3) 1001 - 10,000 ha, (4) 10,001 - 100,000 ha, (5) 100,001 - 1,000,000 ha, and (6) greater than 1,000,000 ha. Error bars represent = 2 standard deviations. Above each error bar is the number of sites in the class.

Sites were grouped by ecoprovince to discern differences in diurnal fluctuations between the two subregions. Figures 7.10-A and 7.10-B show the variation in diurnal temperature fluctuation with $\log_{10}$ watershed area for each ecoprovince, CSP and SSP, respectively. The linear regression line is shown on the graph to demonstrate that the relationship is clearly not linear. The shape in Figure 7.10-C is similar to Figure 7.9.

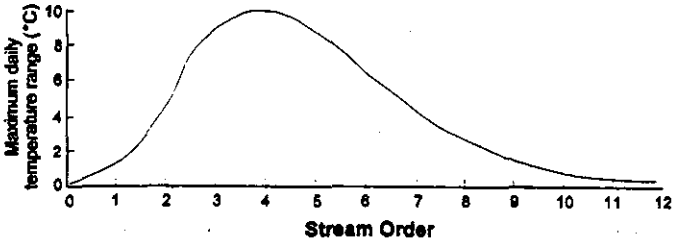

Figure 7.9. Maximum daily temperature range in relation to stream order in temperate streams. (From Vannote and Sweeney, 1980.)

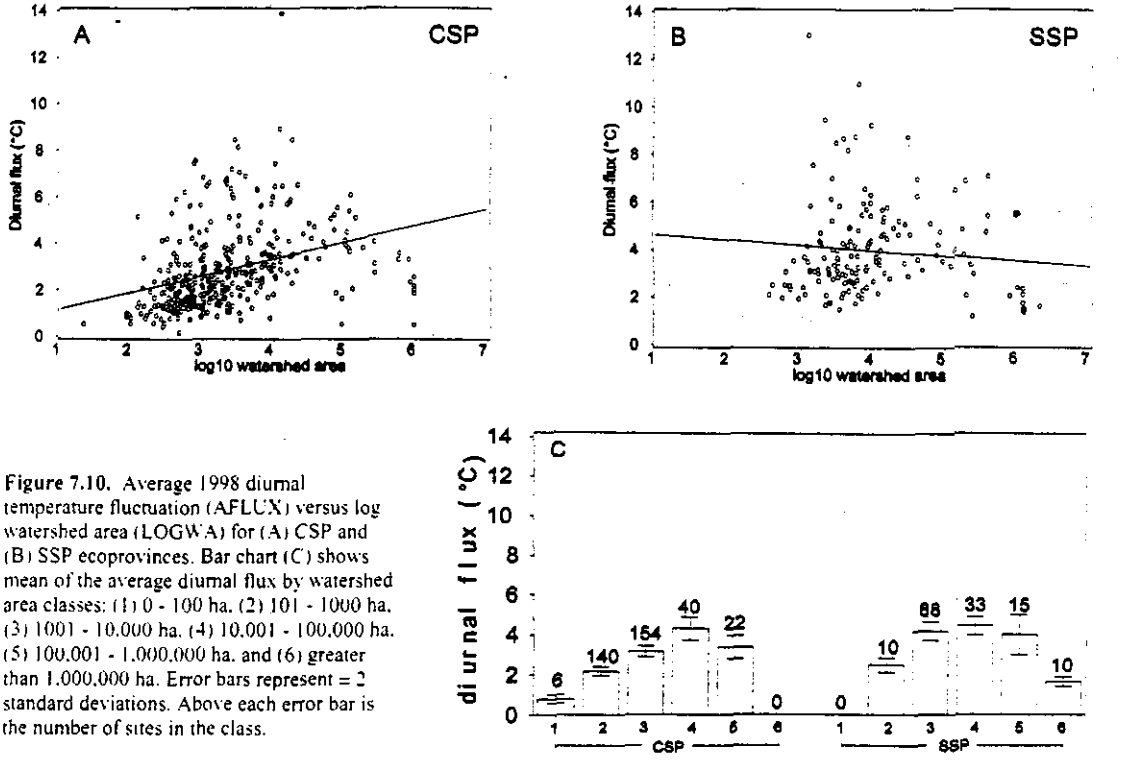

Figure 7.10. Average 1998 diurnal temperature fluctuation (AFLUX) versus log watershed area (LOGWA) for (A) CSP and (B) SSP ecoprovinces. Bar chart (C) shows mean of the average diurnal flux by watershed area classes: (1) 0 - 100 ha. (2) 101 - 1000 ha. (3) 1001 - 10,000 ha. (4) 10,001 - 100,000 ha. (5) 100,001 - 1,000,000 ha. and (6) greater than 1,000,000 ha. Error bars represent = 2 standard deviations. Above each error bar is the number of sites in the class.

The ecoprovincial average diurnal fluctuations for each watershed area class were strikingly similar. Class 6 did not have sites represented in the CSP and class 1 had no sites in the SSP, so no comparisons could be made. Class 3 showed the largest difference between the CSP and SSP, with the former having a mean diurnal flux of 3.1 °C and the latter being 4.2 °C. Class 4 had mean diurnal fluxes of 4.3 °C and 4.5 °C for the CSP and SSP, respectively. The CSP class 5 had a mean diurnal flux of 3.4 °C and the SSP was 4.0 °C.

Distance from Watershed Divide and Stream Temperature Across the Region

The relationship between temperature and distance from the watershed divide was similar to that observed for watershed area. This similarity was expected given the strong correlation between watershed area and distance from the watershed divide shown in Figure 7.3.

Daily Maximum and Distance from Divide

Figure 7.11-A presents the relationship between the highest 1998 daily maximum stream temperature (XY1DX) and the $\log_{10}$ of the distance from the watershed divide. Divide distances were grouped into classes and XY1DX class averages were plotted in bar chart form (Figure 7.11-B). The XY1DX increased from the 18.2 °C in the 1000 to 10,000 m distance from divide class (class 1) to 27.3 °C in class 4. Class 5 and 6 divide distance sites exhibited about a 2 °C decrease from the class 4 average XY1DX.

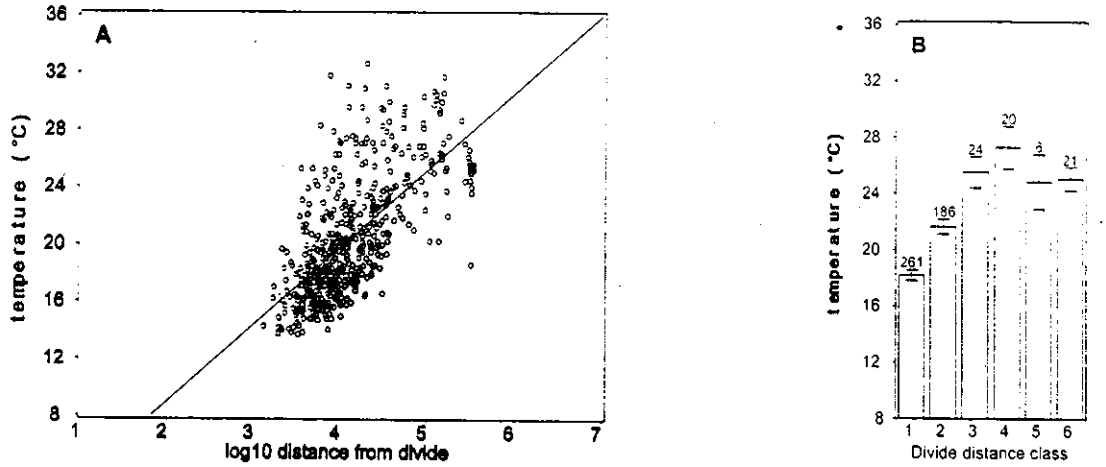

Figure 7.11. Relationship between the highest 1998 daily maximum stream temperature (XY1DX) and log distance from the watershed divide (logdivi). Scatter plot (A) with linear regression equation: XY1DX = -1.727626 + 5.396833*logdivi, R^2 = 0.441697. Bar chart (B) with divide distance classes: (1) 1000 - 10,000 m, (2) 10,001 - 50,000 m, (3) 50,001 - 100,000 m, (4) 100,001 - 150,000 m, (5) 150,001 - 200,000 m, and (6) greater than 200,000 m. Error bars represent = 2 standard deviations. Above each error bar is the number of sites in the class.

Similar to the watershed area relationships, 1998 stream temperature monitoring sites were separated into two ecoprovinces. The CSP and SSP XY1DX values showed a bell-shaped (normal) distribution. No sites fell into class 5 in the SSP. For equivalent divide distance classes the average XY1DX was about 1 °C higher in the SSP than in the CSP. The CSP XY1DX values (Figure 7.12-A) were more tightly clustered around the regression line than those for the SSP (Figure 7.12-B). The greater fit is expressed by the higher R^2 value for the CSP. The potential influence of air temperature is manifested in the distribution of the XY1DX values versus divide distance classes (Figure 7.11-C). Streams originating in the upper reaches of the watershed (class 1 divide distance) start out at approximately ground water temperature. As water moves down through the watershed, it tends to come into equilibrium with air temperature. The sites in the class 2 - 4 divide distances are exposed to warmer air temperatures in the SSP and the interior portions of the CSP. As SSP and CSP mainstems approach the coast and enter the ZC1, air temperatures decrease. Water temperature is coming into a new equilibrium with the lower air temperatures, as expressed by the decreasing XY1DX values in both the CSP and SSP for classes 5 and 6 divide distances (Figures 7.12-A and 7.12-B).

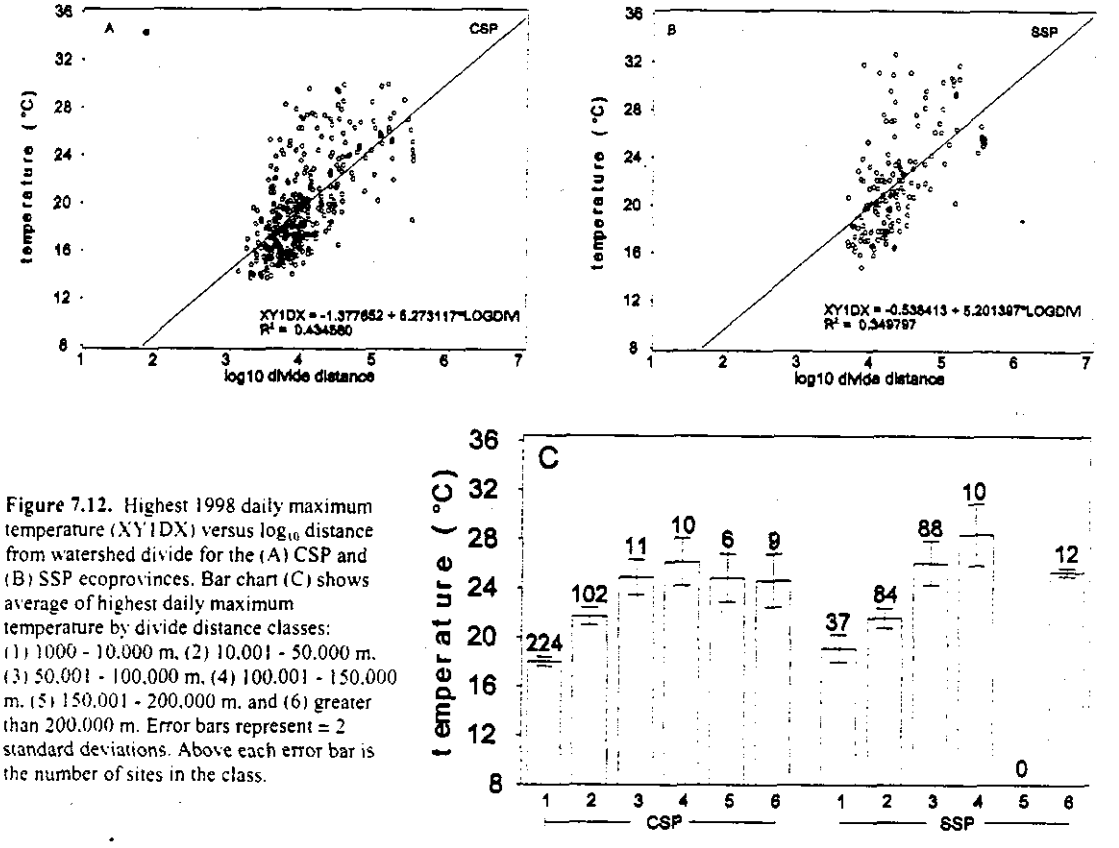

Figure 7.12. Highest 1998 daily maximum temperature (XY1DX) versus $\log_{10}$ distance from watershed divide for the (A) CSP and (B) SSP ecoprovinces. Bar chart (C) shows average of highest daily maximum temperature by divide distance classes: (1) 1000 - 10,000 m, (2) 10,001 - 50,000 m, (3) 50,001 - 100,000 m, (4) 100,001 - 150,000 m, (5) 150,001 - 200,000 m, and (6) greater than 200,000 m. Error bars represent = 2 standard deviations. Above each error bar is the number of sites in the class.

To illustrate the change in air temperature as water masses approach the coast, the August PRISM-derived monthly average maximum air temperature was determined for each stream temperature monitoring site based on its location (UTM X- and Y-coordinates). Figure 7.13 shows the air temperature at each stream temperature monitoring site as a function of distance from the coast. The graph does not provide information on year-to-year variation in air temperatures, but does show the spatial variation in the CSP. The 30-year August monthly average maximum air temperature increases by approximately 15°C from zero to 60 km (37 mi) from the coast.

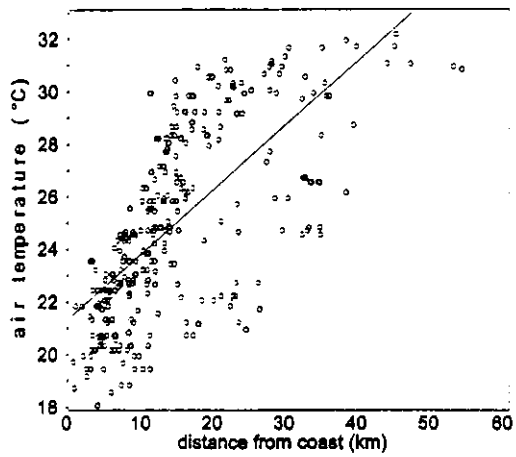

Figure 7.13. PRISM-derived air temperatures at each stream temperature monitoring site located in the CSP as a function of distance from the coast. Air temperature is the August 30-yr long-term monthly average maximum.

Seven-Day Moving Averages and Distance from Divide

Relationships between XYA7DA and XYA7DX versus distance from watershed divide are shown in Table 7.2. Similar to the watershed area relationships, the CSP sites showed a slightly higher R^2 value than the SSP sites for both temperature metrics with respect to distance from watershed divide.

Diurnal Fluctuation and Distance from Divide

The variation in diurnal stream temperature fluctuation in relation to distance from watershed divide was similar to that observed for watershed area (Figure 7.8). The distribution was not linear but suggestive of the bell-shaped curve shown in Figure 7.9. There was great variation in diurnal fluctuation values at any given divide distance, ranging from near zero to 13°C.

The CSP exhibited a smaller range in diurnal flux values than the SSP. The highest diurnal flux values were observed in the SSP at divide distances between 10 km and 30 km. The CSP had a greater proportion of sites with diurnal fluxes less than 2°C.

The scatter seen in the stream temperature values at different watershed areas and divide distances is not unexpected, given an understanding of the air temperature regimes experienced across basins in Northern California. Each basin has its own unique air temperature characteristics. Stratifying sites by ecoprovinces showed a slight reduction in the scatter. Examination of individual basins or HUCs shows an even greater reduction in the scatter. A much clearer picture emerges.

Watershed Position within Hydrologic Units

Spatial trends in water temperature were examined by USGS cataloging units (HUCs). Cataloging units are often referred to as fourth field watersheds, but more appropriately are geographic areas representing part or all of a surface drainage area, a combination of drainage areas, or a distinct hydrologic feature (Seaber et al., 1987). The term subbasin is suggested as a substitute for cataloging unit since this term has no common use or meaning and should be avoided (McCammon, 1994). Subbasins within the California coho salmon ESUs range from 40,000 ha to 533,000 ha with an average of 230,000 ha. For clarity the term

Table 7.2. Linear Regression Equations for Relationship between 1998 XYA7DA[1] and XYA7DX[2] versus Log_{10} Distance from Watershed Divide, Combined and by Ecoprovince.

Variable	Ecoprovince	No. of Sites	Slope	Intercept	R^2
XYA7DA	combined	518	4.85887	-2.12888	0.57558
XYA7DA	CSP	362	4.36730	-0.29115	0.55200
XYA7DA	SSP	156	5.57786	-4.94992	0.54158
XYA7DX	combined	518	5.26481	-1.87331	0.45409
XYA7DX	CSP	362	5.06076	-1.23044	0.44574
XYA7DX	SSP	156	5.16197	-1.01943	0.36062

[1]XYA7DA = 7-day moving average of the daily average.
[2]XYA7DX = 7-day moving average of the daily maximum.

HUC is used to refer to the USGS subbasin. See Figure 4.9 in Chapter 4 for a spatial display of the HUCs that comprise the range of the coho salmon in Northern California. Watershed position within each HUC, as represented by watershed area and distance from watershed divide, was assessed for each of the temperature metrics presented in the previous sections of this chapter. These analyses were limited to 1998, the most data-rich year.

Watershed Area and Stream Temperature in Hydrologic Units

Stream temperature monitoring sites were aggregated by HUC. The highest daily maximum, seven-day moving average of both the daily average and daily maximum, lowest daily minimum, and diurnal fluctuation were plotted versus log_{10} watershed area by HUC. These graphs can be found in Appendix D. The following discussion on the relationship between stream temperature and distance from the watershed divide also apply to graphs of temperature-watershed area relationships found in Appendix D.

Distance from Watershed Divide and Stream Temperature in Hydrologic Units

Although there is strong correlation between watershed area and distance from watershed divide (Figure 7.3), the relationship between the two can depend upon the hydrologic configuration of a drainage, e.g., whether it is dendritic or trellis (Figure 7.14).

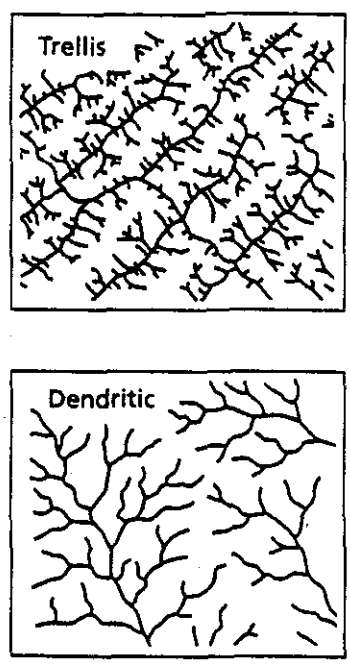

Figure 7.14. Two examples of watershed drainage patterns common in Northern California hydrologic units, dendritic and trellis. Patterns are determined by topography and geologic structure. Modified after FISRWG (1998).

In round types of HUCs a dendritic drainage pattern is common. In more elongated HUCs, a trellis drainage pattern is more the norm. In a dendritic type of HUC, for a unit increase in distance from divide,

the watershed area would be greater than for the same divide distance unit increase in a trellis HUC. Given these potential differences we felt it was not redundant to examine in greater detail the variation in each of the temperature metrics as a function of distance from watershed divide.

Daily Maximum and Distance from Watershed Divide by HUC

What is most striking is the consistent increase in the highest daily maximum (XY1DX) stream temperature with increasing watershed area and distance from the watershed divide in all HUCs (Figure 7.15). Even in HUCs with large numbers of data points, each point representing a different tributary, the increase was consistent. Both tributaries (open circles) and mainstems (crosses) showed an increase in XY1DX with increasing distance from the divide and watershed area. It was disappointing that few temperature records were available on mainstems at lower watershed areas divide distances. Most of the mainstem temperatures were measured far down in the drainage, often near the point where the river drains to the ocean.

The Klamath River sites located at the highest watershed areas appeared to have lower temperatures than other sites in Figure 7.5-B. However, looking at these sites in the context of their basin, they fall in alignment with the general increasing trend for the basin (Figure 7.15-L). The Lower Eel HUC (Figure 7.15-E) clearly shows a decrease in mainstem temperatures at the highest divide distances. This is most likely due to the cooling influence of air temperatures as the water nears the coast. Other mainstem rivers in the Lower Eel HUC exhibited decreases with increasing divide distance, namely the North Fork Eel and the Van Duzen River.

A similar decrease in water temperature at the highest divide distance was noted in the Mad-Redwood HUC (Figure 7.15-B). Both Mad River and Redwood Creek showed a decrease in XY1DX with increasing divide distance. Mad River XY1DX values decreased by about 4°C over a 10 km distance. Redwood Creek decreased by about 7°C over a 40 km distance. The decrease is quite striking, considering the thermal inertia of these systems. Again, the cooling influence of coastal air temperatures is believed to be responsible for the decrease in XY1DX at the higher divide distances. Two sites on the Little River showed an increase with increasing divide distance. However, no sites were located on the Little River near its outlet into the Pacific Ocean near Trinidad, CA to verify the cooling influence of coastal air temperature on water temperature in this river.

In the Big-Navarro-Garcia HUC (Figure 7.15-H) a cluster of mainstem sites are seen at the highest divide distances. These sites include the Big, Garcia, Ten Mile, and Noyo Rivers, all making up the major drainages in the HUC. Although too few sites were located in any one of the four rivers to clearly discern a similar cooling trend at the highest divide distance, the four sites on the Garcia River seem to exhibit this behavior. There was approximately a 5°C decrease in the XY1DX from the next-to-highest to highest divide distance. The trio of points in both lower parts of the Big and Noyo Rivers also seem to show a decrease in XY1DX values from the next-to-highest to highest divide distance, although not as large as that observed in the Garcia River. The clustering of the four rivers' sites into four distinct groups indicate that they may be integrating the thermal regimes within their respective basins, which includes differing air temperature regimes and land use patterns.

The reported upper lethal incipient temperature (ULIT) for juvenile coho salmon is 26°C (Brett, 1952). Subtracting a two-degree safety margin from the ULIT as recommended by Coutant (1972) gives us a potential reference value of 24°C to compare XY1DX values against. Comparing XY1DX values to the 24°C acute reference value shows that no tributary sites in the Mad-Redwood exceeded this value (Figure 7.15-B). It is not until greater distances from the watershed divide are reached on the mainstem Mad River and Redwood Creek do temperatures exceed 24°C.

In both the Upper Eel (Figure 7.15-C) and Middle Fork Eel (Figure 7.15-D) HUCs XY1DX values exceeded 24°C at divide distances less than those observed in the Mad-Redwood HUC. More tributary XY1DX values were observed above 24°C in the Upper and Middle Fork Eel HUCs. The divide

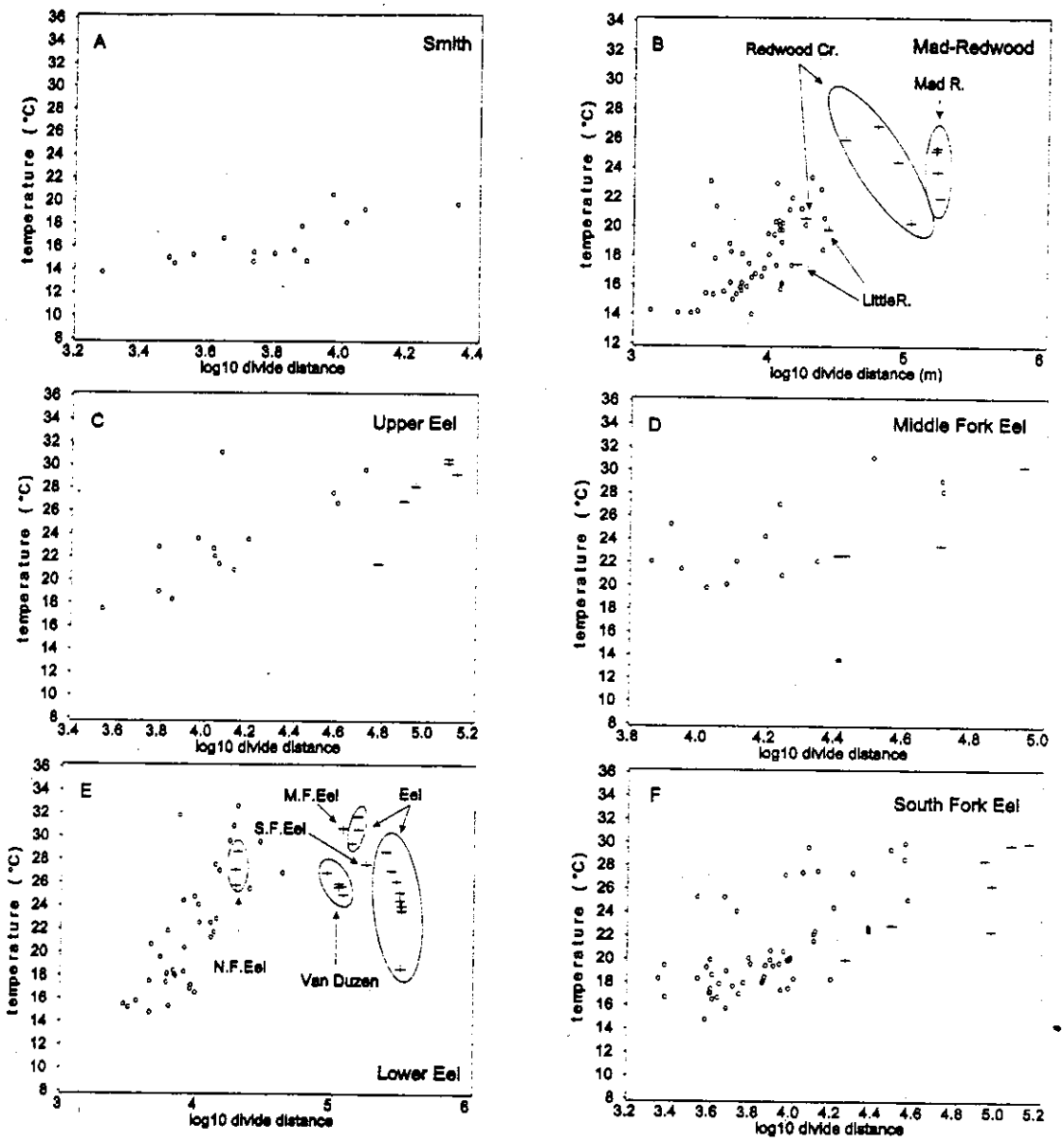

Figure 7.15. The 1998 highest daily maximum stream temperature (XY1DX) versus log $_{10}$ distance from watershed divide (meters) for HUCs comprising the range of the coho salmon in Northern California. Circles represent tributaries and crosses represent mainstems.

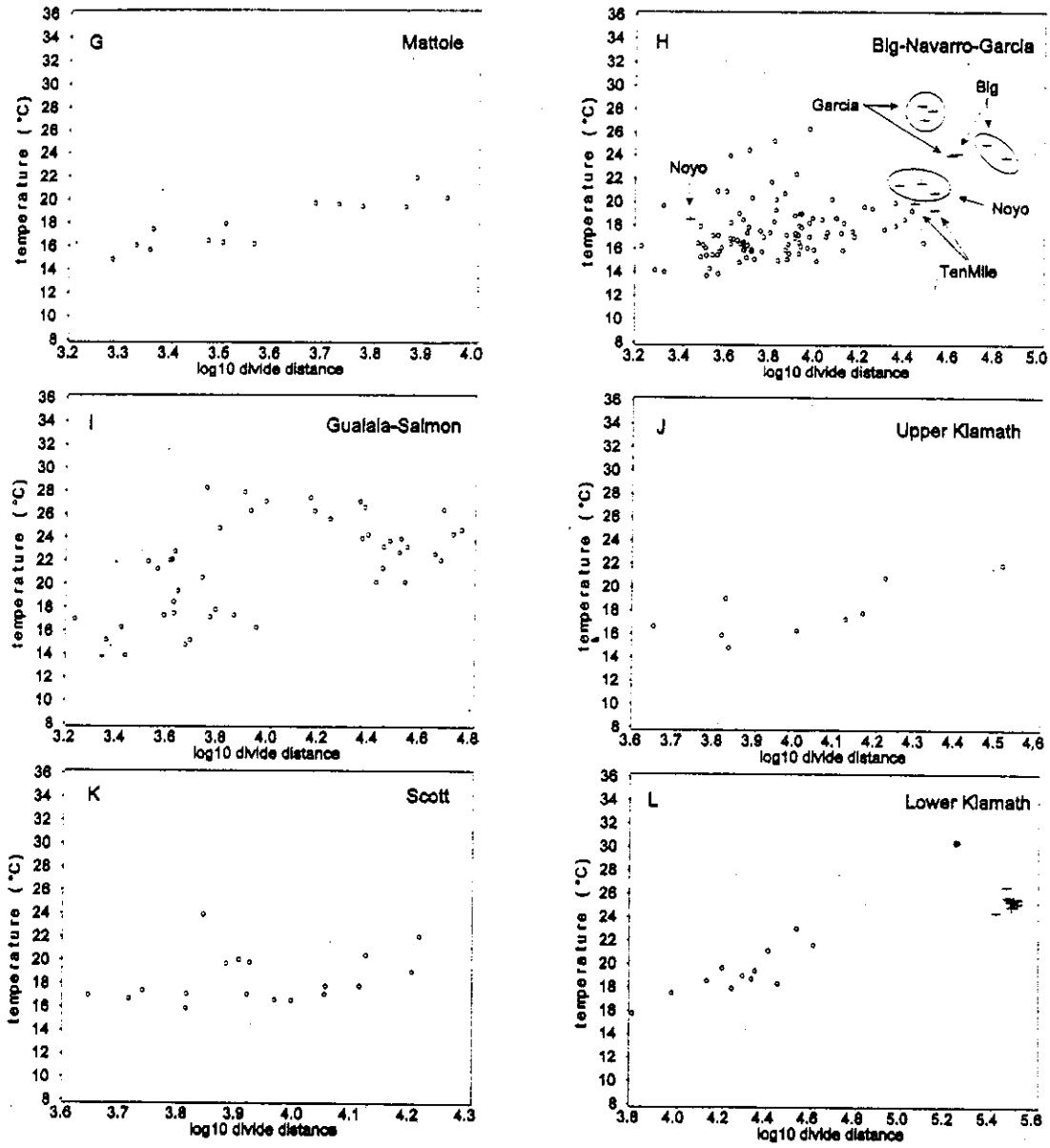

Figure 7.15. (continued)

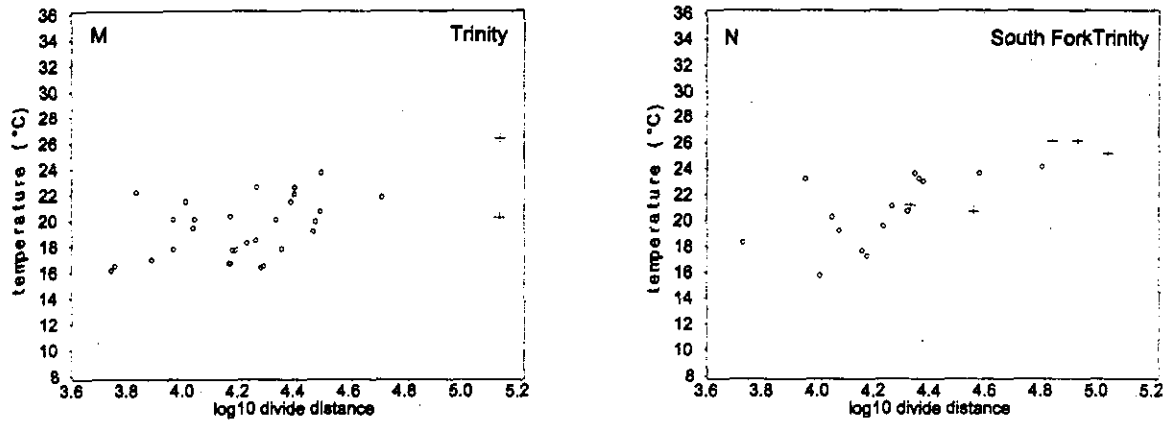

Figure 7.15. (continued)

distance at which XY1DX values begin to exceed 24°C in the Lower Eel HUC was approximately 10 km (Figure 7.15-E). Not all tributaries exceeded this reference value at 10 km or greater ($\log_{10} = 4$ for 10,000 m divide distance) from the watershed divide. The PRISM 30-year average air temperature in the three Eel HUCs are 1°C to 1.5°C higher than in the Mad-Redwood HUC (see Chapter 4, Table 4.2). The XY1DX values dropped in the Van Duzen River by about 2°C over an increase in divide distance of about 100 km. The mainstem Eel River exhibited a 14°C decrease in XY1DX over about a 150 km increase in divide distance. The mainstem Eel River drainage, from Lake Pillsbury to the ocean is examined in greater detail in a subsequent section.

Some HUCs had no sites or only one site with XY1DX values above 24°C (Smith, Mattole, Upper Klamath, Scott). The Smith and Mattole HUCs have the lowest August average air temperatures (based on 30-year PRISM average air temperatures, see Chapter 4, Table 4.3). The Scott HUC, a relatively warm HUC, had only one tributary site with a XY1DX value that exceeded 24°C (Figure 7.15-K) at a divide distance of about 8 km. The Gualala-Salmon is one of the coolest HUCs in terms of air temperature, yet had several tributary sites that had XY1DX values in excess of 24°C at divide distances between 5 km and 25 km. The majority of sites that exceeded 24°C in the Big-Navarro-Garcia HUC (Figure 7.15-H) were on the mainstems of the Garcia and Big Rivers at over 25 km from the watershed divide. The Lower Klamath HUC (Figure 7.15-L) had XY1DX values over 24°C in the mainstem Klamath at distances over 600 km from the watershed divide. In the Trinity and South Fork Trinity HUCs, sites that exceeded 24°C were mostly mainstem sites (Figures 7.15-M & N).

The upstream extent of XY1DX values exceeding 24°C seems to be greater in those HUCs with higher average air temperatures.

Seven-Day Moving Averages and Distance from the Watershed Divide by HUC

Seven-day moving average statistics are often compared to Maximum Weekly Average Temperature (MWAT) thresholds. MWAT thresholds have often been assumed to be protective of certain species and life stages (McCullough, 1999). MWAT can either be calculated as 1) the temperature halfway between the optimal growth temperature (OT) and the temperature at which there is zero net growth, or 2) a third of the difference between the UILT and the optimum temperature (Brungs and Jones, 1977; Ferraro et al., 1978; Armour, 1991). The second method is the one most commonly used in California and other states in the Pacific Northwest, primarily because the data are

more readily available to perform the calculation. Using the second method for calculating MWAT:

$$MWAT = OT + \frac{(UILT - OT)}{3}$$

and values for OT and UILT of 14.8°C and 26°C, respectively (Brett, 1952), a value of 18.3°C is calculated for an MWAT threshold.

Using 18.3°C as a reference value, XY7DA and XYA7DX values were assessed for each HUC in relation to distance from watershed divide. Figure 7.16 presents plots of the relationship between XYA7DA and divide distance by HUC.

The distribution of points on each graph was very similar to the plots of XY1DX versus $\log_{10}$ divide distance (Figure 7.15). Sites on the mainstem Mad River and Redwood Creek (Figure 7.16-B), as well as those on the North Fork Eel, Van Duzen, and Eel Rivers (Figure 7.16-E), showed the characteristic decrease in water temperature with increasing divide distance, suggestive of the cooling effects of coastal air temperatures. Again, the four rivers that comprise the Big-Navarro-Garcia HUC were clustered into four distinct groups (Figure 7.16-H).

The sites in the Smith HUC had no XYA7DA values over 18.3°C (Figure 7.16-A). The Smith HUC is the coolest HUC in terms of air temperature (see Chapter 4, Table 4.2). The Mad-Redwood HUC had several tributary and mainstem sites with XYA7DA values over 18.3°C, most of which occurred at divide distances greater than 10 km (Figure 7.16-B). The mainstems of Redwood Creek and Mad River showed the same decrease in XYA7DA values at the higher divide distances as did XY1DX. We postulate that the decrease is due to cooler air temperatures in the zone of coastal influence.

The four Eel River HUCs, i.e., Upper, Middle Fork, Lower, and South Fork, exhibited a preponderance of sites with XYA7DA values exceeding 18.3°C (Figures 7.16-C through F). In the Lower and South Fork Eel HUCs, some sites below 18.3°C were observed extending as far down from the watershed divide as 16 km. Although mainstem sites on the Eel River exhibited a decrease in XYA7DA with increasing divide distance, the only mainstem temperature that did not exceed 18.3°C was the last site on the Eel River just before it drains to the Pacific Ocean (Figure 7.16-E). Many of the tributaries in the four Eel River HUCs have their origins in very warm interior portions of the drainage. Air temperatures reach 100°C and higher during the summer months.

Very few of the sites in the four Eel River HUCs for which water temperature data were available were accompanied by canopy closure data. In the Upper Eel HUC, three sites with canopy closure values greater than 70% had XYA7DA values less than 18.3°C, while seven sites with canopy closure values greater than 70% had XYA7DA values greater than 18.3°C. In the Middle Fork Eel HUC two sites with canopy greater than 70% were below the reference while three were above. In the Lower Eel HUC, 12 sites with canopy greater than 70% had XYA7DA values less than 18.3°C and five were above the reference value. In the South Fork Eel HUC, 23 sites with canopy greater than 70% were below 18.3°C while six were above. Canopy will be discussed in greater detail in Chapter 9.

The Mattole HUC, a cool HUC with respect to air temperature, did not have any sites with XYA7DA values over 18.3°C (Figure 7.16-G). Also, the Scott (Figure 7.16-K) and Upper Klamath (Figure 7.16-J) HUCs had no sites with XYA7DA values over 18.3°C. In the Big-Navarro-Garcia HUC (Figure 7.16-H), three tributary sites had XYA7DA values that exceeded the reference value. The most upstream site on the Noyo River was below the reference value, while three Noyo River sites at the highest divide distances were slightly above the reference value. The XYA7DA values for sites at the highest values for divide distance in the Big and Garcia Rivers were all above 18.3°C. The two sites on Ten Mile River were below the reference value.

Examination of the relationship between XYA7DX and distance from the watershed divide for each HUC revealed a very similar distribution of data points as XYA7DA. Since XYA7DX is based on daily maxima rather than daily averages, values were

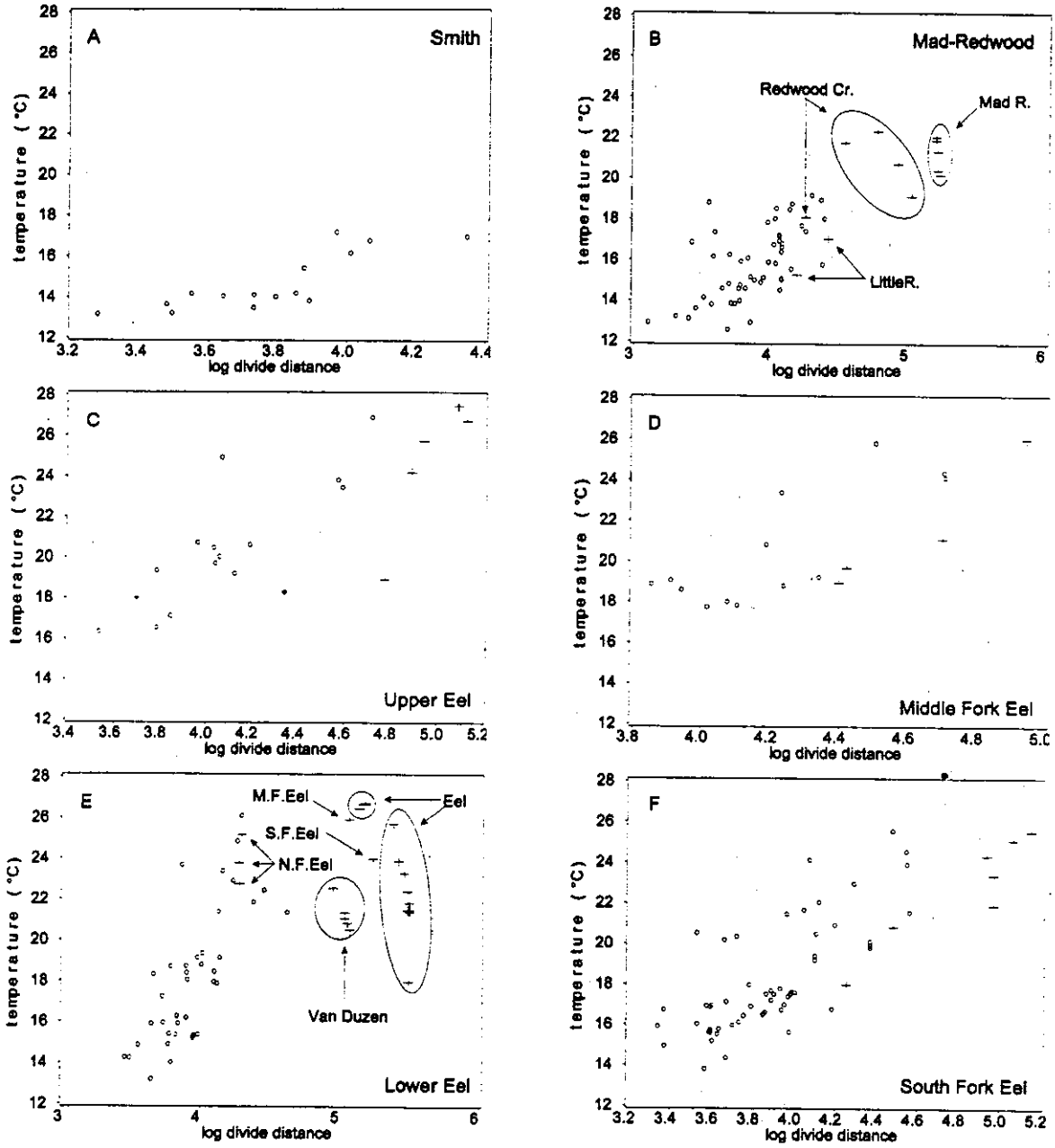

Figure 7.16. The highest 1998 seven-day moving average of the daily average stream temperature (XYA7DA1 versus $\log_{10}$ distance from watershed divide (meters) for HUCs comprising the range of the coho salmon in Northern California. Circles represent tributaries and crosses represent mainstems.

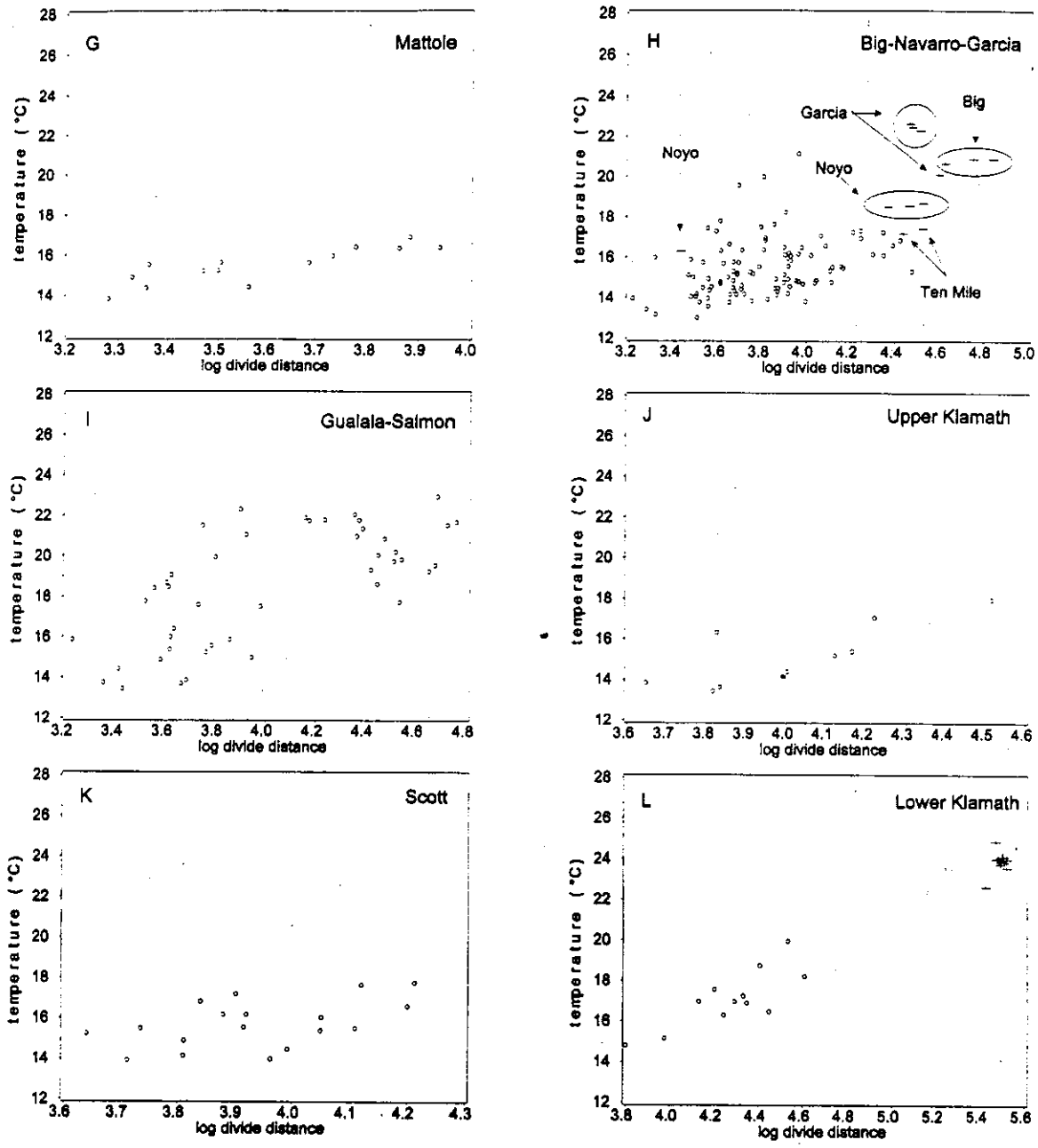

Figure 7.16. (continued)

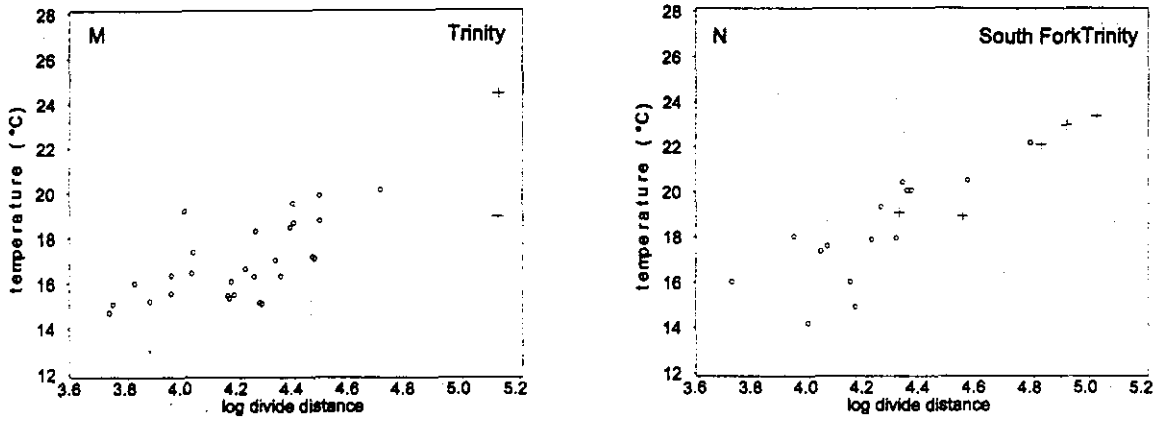

Figure 7.16. (continued)

higher and more sites exceeded the 18.3°C MWAT reference value. Even those HUCs that did not have any XYA7DA values above 18.3°C had XYA7DX values over the reference value. The distance from watershed divide where sites began to exceed 18.3°C decreased for XYA7DX values. Graphs of XYA7DX versus distance from the watershed divide can be found in Appendix D.

Sullivan et al. (1990) and Adams and Sullivan (1990) found that water temperatures seem to level off at some equilibrium temperature that is approximately equal to the average air temperature for the basin. It is not clear how or where average basin air temperatures were determined in their studies. A general trend was observed across HUCs in stream temperature metric values in that HUCs with higher monthly average air temperatures (Chapter 4, Table 4.2) attained higher stream temperatures. The Smith and Mattole HUCs exhibited lower XY1DX, XYA7DA, and XYA7DX values than other HUCs and are the coolest in terms of air temperature. The PRISM 30-year long-term average air temperatures for August in the Smith and Mattole HUCs are 17.1°C and 16.1°C, respectively (see Chapter 4, Table 4.2). Both the Smith and Mattole HUCs are largely coastal HUCs, with minimal area extending into the warmer interior sections of the region. Those coastal HUCs that are oriented with large areal portions in the interior and HUCs that are entirely inland generally have higher 30-year average air temperatures and exhibited higher stream temperatures.

The MWAT metric is an extrapolation of laboratory studies that may or may not be representative of actual field conditions. Some well-designed stream temperature monitoring studies that are coupled with fish presence/absence and/or abundance surveys are needed to validate both chronic and acute thermal stress thresholds. Essig (1998) found that state temperature criteria were exceeded at over 50% of the 98 Idaho stream locations where salmonid spawning was observed. At the same sites where exceedance of temperature criteria was noted, rearing was observed in the following year.

Diurnal Fluctuation and Distance from Watershed Divide by HUC

The diurnal fluctuation of stream temperature with respect to distance from the watershed divide was examined. Figure 7.17 shows that diurnal flux did not follow a linear trend with $\log_{10}$ divide distance (or watershed area - see graphs in Appendix D). HUCs that had sites representing a wide range in divide distances exhibited more of a bell-shaped distribution (see Figure 7.9) than HUCs that had sites at only lower or higher divide distances. Only a portion of the curve may be expressed in those HUCs that do not have sites along the entire continuum of divide distances. The lack of sites at higher values of

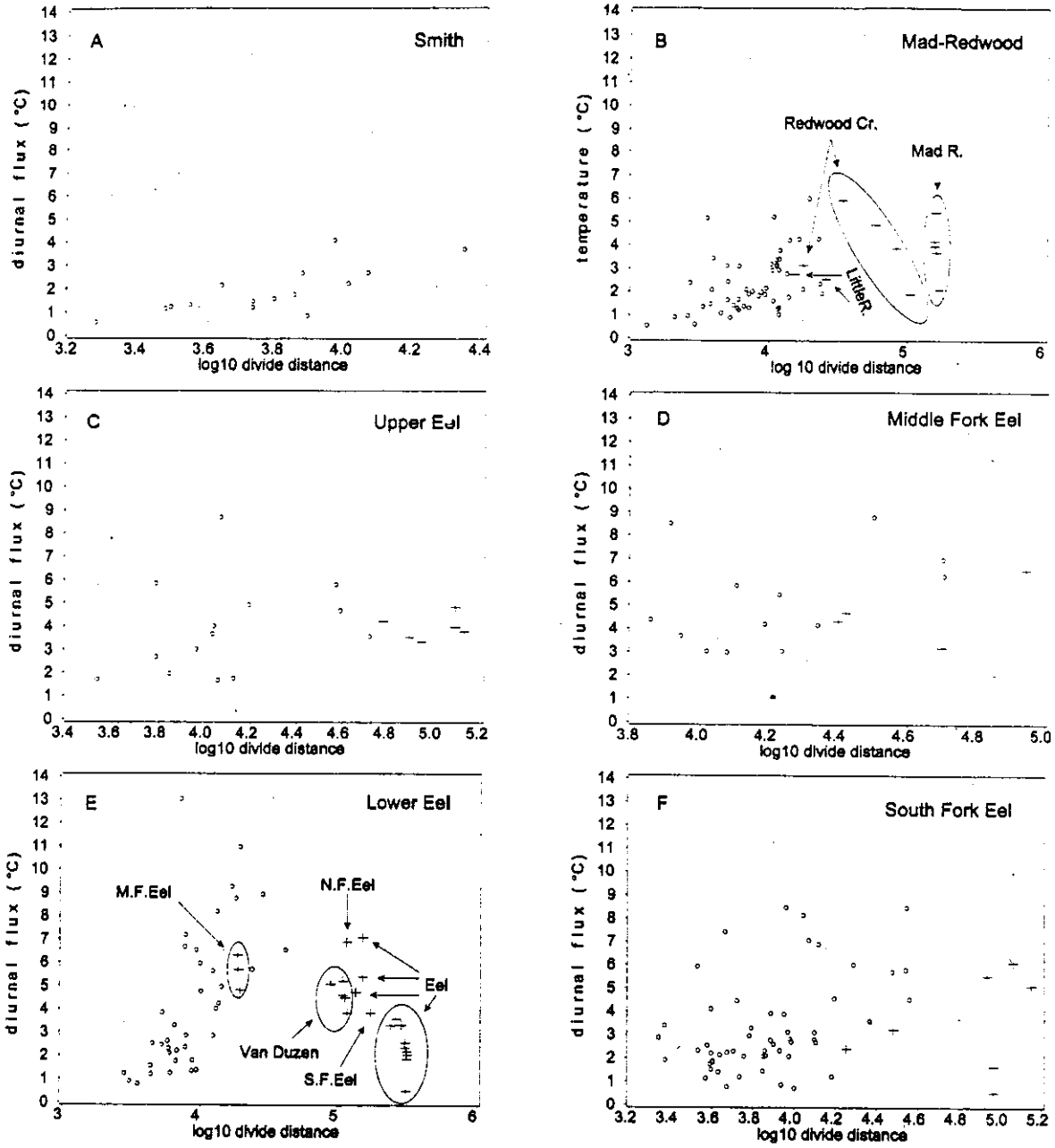

Figure 7.17. The average 1998 diurnal stream temperature fluctuation versus $\log_{10}$ distance from watershed divide (meters) for HUCs comprising the range of the coho salmon in Northern California. Circles represent tributaries and crosses represent mainstems.

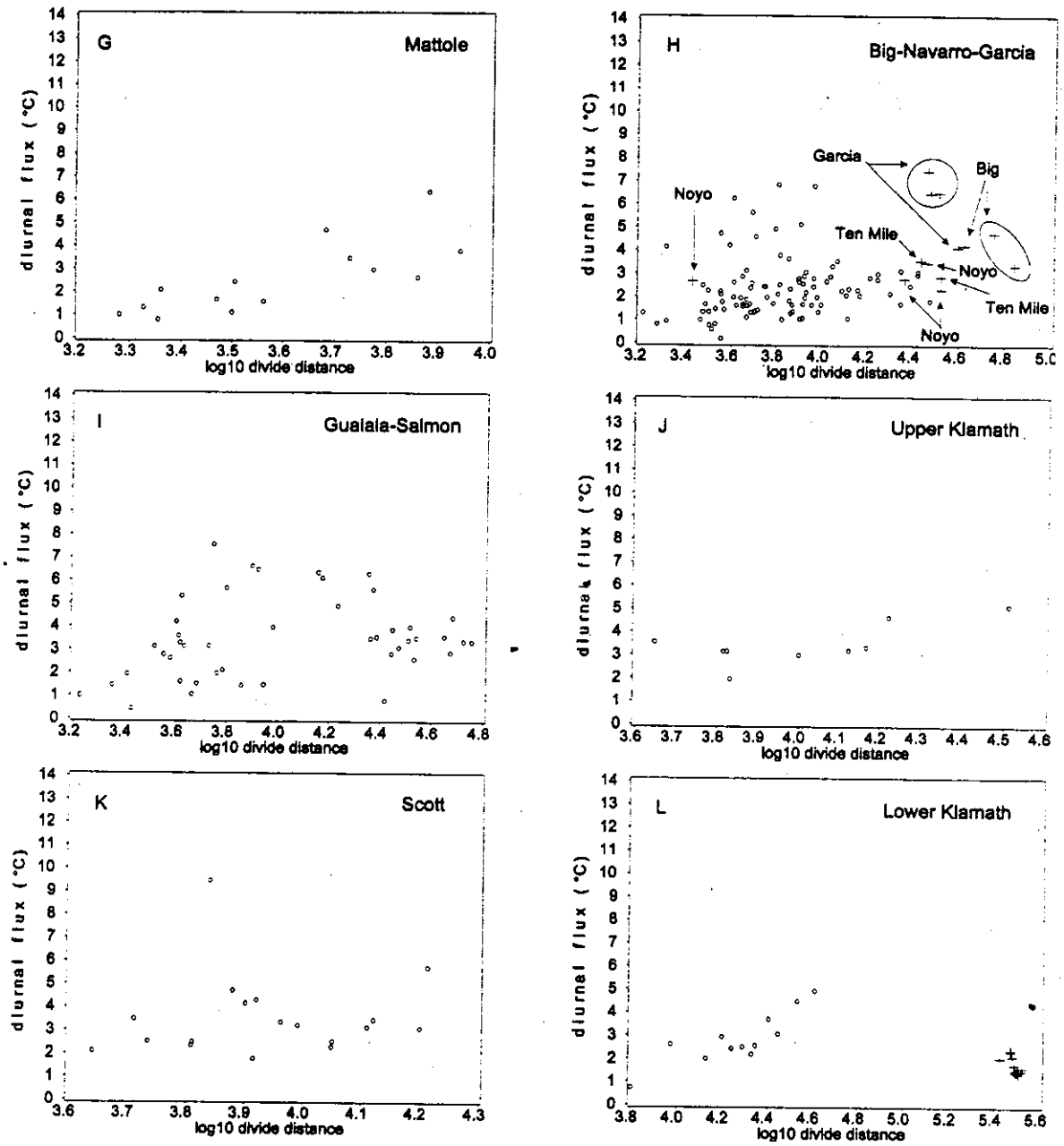

Figure 7.17. (continued)

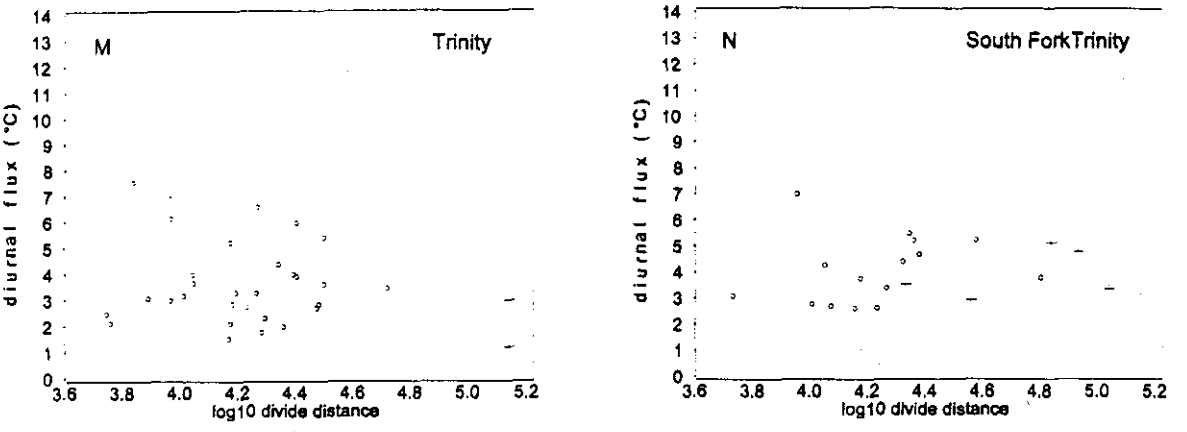

Figure 7.17. (continued)

watershed area may be because the HUC is smaller and simply does not have divide distances any higher than those observed or no sites were available at the greatest divide distances that exist in the HUC. It must also be borne in mind that some HUCs are not complete hydrologic units with respect to a mainstem river. For example, the mainstem Eel River is broken up into three HUCs, the Upper, Middle, and Lower.

Thus, the largest divide distance for the mainstem Eel River is not found until one examines the Lower Eel HUC. For HUCs with sites lacking at the lower divide distances, small order streams were not adequately sampled. Examination of only a portion of the curve may account for the observed decrease in diurnal fluctuation with increasing divide distance reported by Sullivan et al. (1990).

The Lower Eel HUC (Figure 7.17-E) exhibited the greatest diurnal fluctuation, with the highest being about 13°C at a watershed area of approximately 1300 ha and about 10 km from the divide. The decrease in mainstem diurnal fluctuation is most likely due to the arrival of mainstem water at the coast and the thermal inertia of the larger volume of water. Air temperatures near the coast are characterized by lower daily maxima and higher daily minima. The smaller diurnal fluctuation in air temperature is manifested in a smaller diurnal fluctuation in water temperature.

In general, HUCs with the highest PRISM 30-year average air temperatures showed the greatest diurnal fluctuations. Conversely, HUCs with the lowest air temperatures exhibited the lowest diurnal fluctuations. It must be considered, however, that not all tributaries or mainstems in every HUC are represented. Obviously, only data that were submitted to the FSP for this regional assessment can be included in the analyses.

Sum Degrees and Sum Degree Hours

While the previously presented stream temperature metrics reveal a great deal about the thermal behavior of sites with respect to their watershed position and other landscape and site-specific attributes, another set of metrics was developed to evaluate cumulative exposure to elevated temperatures. These elevated temperatures are transient in nature and are closer to the upper lethal incipient temperature. Temperatures near the upper lethal incipient temperature present acute thermal stress to coho salmon and other aquatic organisms.

Considering the highest daily maximum or highest seven-day moving average of both the daily average and daily maximum for a site sheds no light on whether the highest observed daily or weekly temperature was transient or persisted at or above the acute threshold for long periods (duration). Moreover, the highest daily and weekly metrics do

not provide any information on the magnitude of temperatures above an acute thermal stress value. That is, was the highest daily or weekly metric simply a blip on the radar screen while the remainder of temperatures were below, at, or barely above an acute threshold? Alternatively, were the temperatures elevated significantly above the acute threshold for long periods of time, e.g., several hours (consecutive or nonconsecutive) for many days at a time (consecutive or nonconsecutive)? Although we do not normally think of temperature in terms of concentration, it is useful to do so in this case. If we consider the magnitude of temperature as concentration then we could consider the dose to be concentration multiplied by time.

Sites used for these analyses had continuous, uninterrupted observations for a 30-day period in 1998, from July 21 through August 19. Figure 7.18 illustrates the concept of sum degrees and sum degree hours for seven hypothetical temperature observations. This illustration helps to demonstrate how sampling intervals (hourly or some other interval) were allocated into areas above the acute thermal reference value. Different sampling frequencies do not affect the calculation, since the area above the reference value is calculated geometrically and not arithmetically.

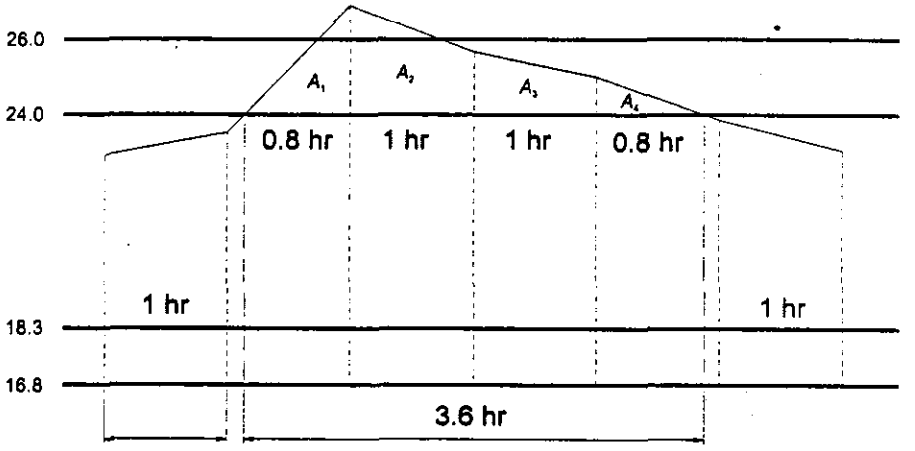

Figure 7.18. Graphical representation of seven hypothetical temperature observations with four acute thermal stress reference values (solid heavy lines). Short vertical dashed lines represent sampling intervals and long vertical dashed lines represent the total time (sum degree hours) above the 24 °C threshold. $\sum(A_1, A_2, A_3, A_4)$ represents the area under the curve above 24 °C (sum degrees).

To obtain better estimates of these metrics, relatively simple geometric calculations were performed. By considering the portion of each sampling interval above the threshold as an area (A_1, A_2, A_3, A_4), the sum of these areas represents the sum degrees above the threshold (shaded portion in Figure 7.25). The sum degree hours above the threshold (3.6 hr) was determined by summation of the total time spent above the threshold. Figure 7.18 may represent only one excursion of stream temperature above an acute reference value at a particular site. Such excursions may occur on more than one occasion, in which case the total hours and all the areas above the reference value are summed for the entire July 21 to August 19 sampling window to determine sum degree hours and sum degrees, respectively.

In this example, the 24°C reference value was exceeded in the second 1-hr sampling interval for eight-tenths of an hour as was the fifth 1-hr interval. Note that only a portion of the second and fifth 1-hour interval exceeded the temperature threshold (Figure 7.18). Allocating the entire 1-hr sampling interval as being above the threshold would tend to overestimate (or underestimate) the total amount of time spent (sum degree hours) above the threshold (3.6 hr), as well as give an imprecise estimate of sum degrees.

Sum degrees are comparable to degree days as a means of quantifying cumulative warmth in a season or year at a given location. It is a measure that takes into account both magnitude and duration of departure from a chosen threshold temperature. Degree days originated as a means to predict residential heating and cooling needs. They are also used in agriculture to predict an area's suitability for growing certain crops or the day of maturation of a crop in a given year (Trewartha, 1968). The degree day concept provides a single quantity that is better at characterizing the warmth at a given site than is annual average temperature (Essig, 1998). The metric has not been commonly applied to stream temperature monitoring and assessment.

Figure 7.19 shows the relationship between divide distance and sum degrees over 24°C (SUMDEG24) by HUC. For brevity, plots of watershed area versus SUMDEG24 are not shown. These plots were similar to those shown in Figure 7.19. A fixed range on the y-axis was not possible due to the large distribution in sum degree values. As expected, those sites that did not have daily maxima over 24°C obviously had zero values for SUMDEG24. HUCs with sites having all SUMDEG24 values of zero were the Smith, Mattole, Upper Klamath, and Scott.

In the Mad-Redwood HUC only the mainstem sites in the lower portions of Redwood Creek and Mad River exhibited SUMDEG24 values greater than zero. In the Eel HUCs (i.e., Upper, Middle, Lower, and South Fork), both tributary and mainstem sites were observed with SUMDEG24 values greater than zero. The Eel HUCs exhibited the highest SUMDEG24 values of all the HUCs in the range of the coho for which temperature data were available. The occurrence of high SUMDEG24 values was seen at sites within a few kilometers of the watershed divide.

One problem with the use of sum degrees is the lack of published reference or threshold values for determining what values for this metric can be considered to be potentially injurious to juvenile coho or other species and life stages. Inasmuch as the derivation of the sum degree metric has imbedded in it an acute thermal stress reference value (i.e., 24°C), it would stand to reason that any values greater than zero would suggest the potential for acute thermal stress. The metric does allow for relative comparisons between sites.

Hydrologic Unit Case Studies

Examination of stream temperature metrics with respect to watershed area and distance from the watershed divide revealed a great deal about the thermal regimes in each hydrologic unit. However, watershed area and divide distance do not always coincide with the relative position (topology) of tributary and mainstem sites. A tributary with a large watershed area or divide distance may enter the mainstem upstream from another tributary site with a

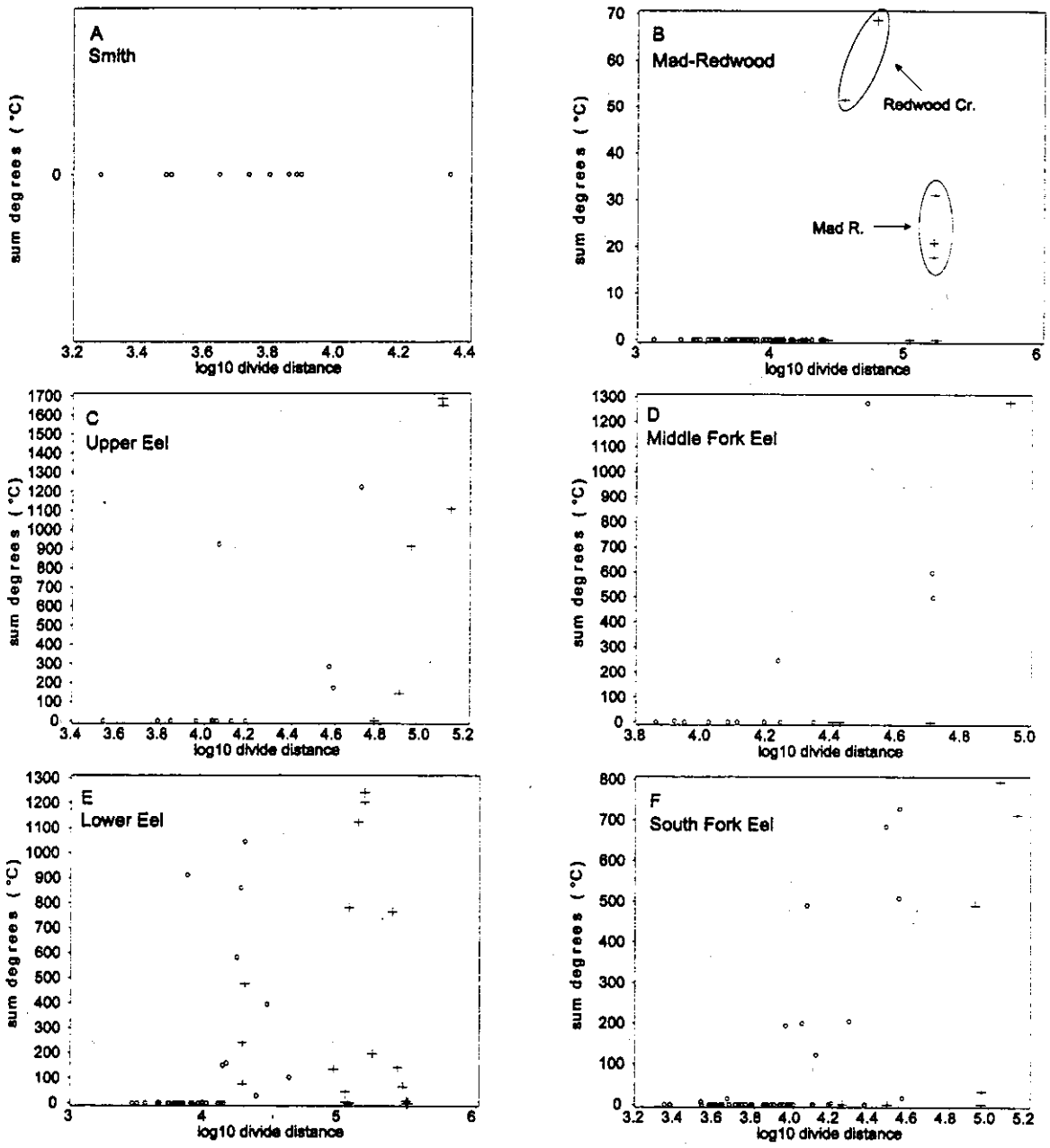

Figure 7.19. Sum degrees over 24°C versus $\log_{10}$ divide distance (meters) for HUCs that comprise the range of coho salmon in Northern California. Circles are tributary sites and crosses are mainstem sites.

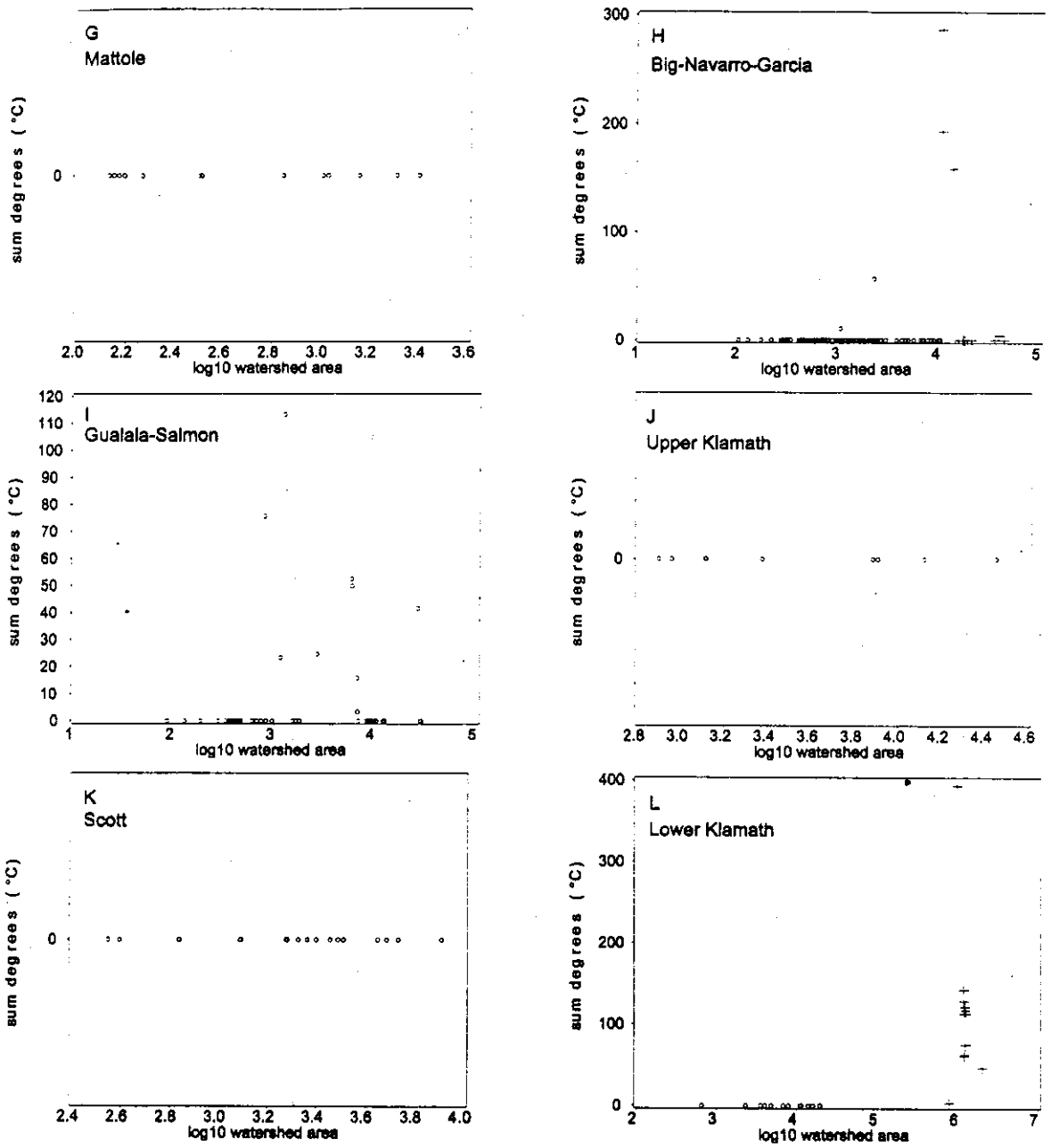

Figure 7.19. (continued)

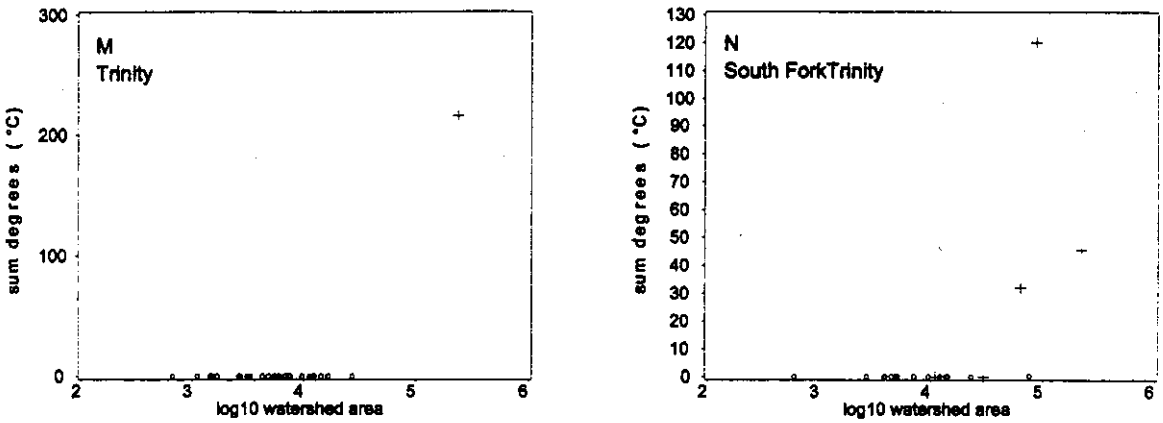

Figure 7.19. (continued)

smaller watershed area or divide distance. To develop a better understanding of stream hierarchical thermal regimes and the potential cumulative effects of tributary temperatures on mainstem temperatures, tree graphs and stream network diagrams were developed for three basins that had a relatively large number of sites on both tributaries and mainstems.

The daily maximum and diurnal fluctuation on the warmest day in 1997 and the sum degrees and total time above 24°C for day of year 201 to 230 were calculated for sites in the mainstem Eel River and Gualala River drainages. The same metrics were calculated for the warmest day in 1998 in the Ten Mile River drainage. While 1998 data were used in previous sections, 1997 had a better distribution of sites on both tributaries and the mainstems in the Eel and Gualala River drainages for the conduct of a hierarchical stream temperature assessment.

Mainstem Eel Drainage from Lake Pillsbury to the Pacific Ocean

There were 35 sites in the Eel River drainage located on the mainstem and on tributaries nearest the confluence with the mainstem from Lake Pillsbury to the Pacific Ocean. This represents a distance of approximately 320 km along the mainstem Eel River. All tributary monitoring sites nearest the mainstem confluence were within 6000 m of the mainstem, with most being less than 1000 m from the mainstem. The database was queried for the day in 1997 on which the most sites in the drainage had their highest daily maximum temperature, which was 08 August. The daily maximum temperature on 08 August 1997 was plotted against $\log_{10}$ watershed area and $\log_{10}$ distance from watershed divide (Figure 7.20). The distribution of daily maximum temperatures are not unlike those observed for the Upper, Middle, and Lower Eel HUCs in 1998 (Figures 7.16-C, D and E).

The characteristic increase in stream temperature with increasing watershed area and divide distance is evident in Figure 7.20. Similar to the 1998 XY1DX values for the Lower Eel HUC (Figure 7.15-E and 7.16-E), the 08 August 1997 daily maximum temperatures in the mainstem Eel River show a decrease at the highest watershed areas and divide distances.

The daily maximum and diurnal fluctuation are displayed on the tree graph shown in Figure 7.21. The daily maximum below Lake Pillsbury was 19.1°C (divide distance = 54 km) with a diurnal fluctuation of 1.6°C. The low diurnal fluctuation is most likely due to the stable temperature of hypolimnetic waters discharged from the bottom of the reservoir through Scott Dam. In about 16 km

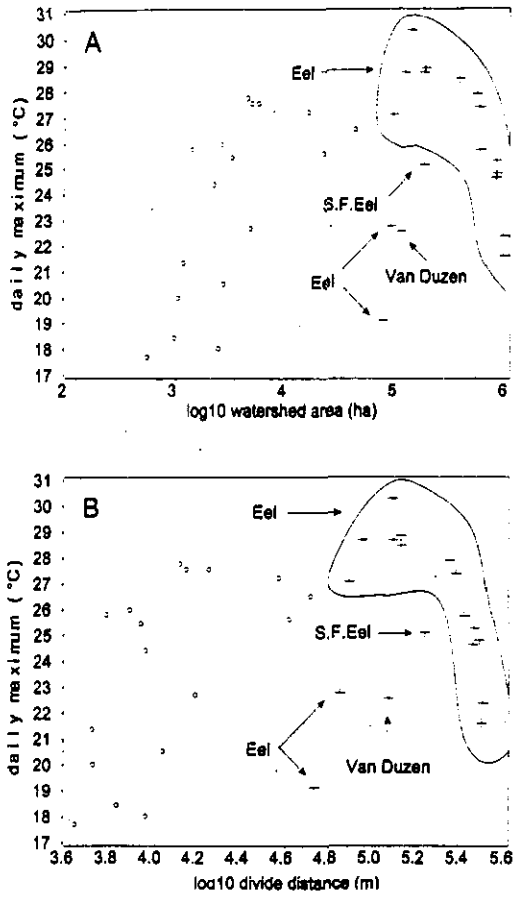

Figure 7.20. Daily maximum stream temperature measured on 08 August 1997 at 35 sites in the mainstem Eel River drainage from Lake Pillsbury to the Pacific Ocean. (A) Daily maximum versus log10 watershed area and (B) daily maximum versus log10 distance from the watershed divide. Circles are tributary sites and crosses are mainstem sites.

(divide distance = 75 km) the Eel River daily maximum increased by 3.6°C. Between mainstem divide distances of 54 km and 75 km three warmer tributaries enter the mainstem. Benmore (25.8°C), Soda (20.6°C), and Bucknell (22.7°C) Creeks (Figure 7.21). The entrance of three tributaries with warmer temperatures could partially contribute to the increase in Eel River temperatures 20 km below the dam.

Daily maximum air temperatures in this portion of the Eel River drainage are near 40°C in August. Water temperatures in the Eel could be coming into equilibrium with warmer air temperatures. Sullivan et al. (1990) state that tributaries had more of an observed cooling or warming effect on mainstem temperatures in the upper reaches of a basin. However, below Lake Pillsbury, the Eel River is already a rather sizable river. The 30-year mean August discharge below Scott Dam is 182 cfs (USGS, 1994). Tributaries would need to contribute a large proportion of the combined flow to alter the mainstem temperature. However, based on the watershed areas of the three tributaries (Benmore = 1360 ha, Soda = 2705 ha, Bucknell = 4710 ha) their total relative contribution to the flow of the Eel River (watershed area = 74,956 ha below the dam) is less than 10%. Caution should be exercised, considering that the Eel River flow is highly regulated. Watershed area may not be a very good surrogate under such regulated flow conditions.

The river continues to warm up to a divide distance of 88 km, where the daily maximum water temperature reached 28.6°C (Figure 7.21).

Outlet Creek is a large tributary that enters the Eel River at about 122 km from the mainstem watershed divide. Outlet Creek entered the mainstem with a daily maximum temperature of 26.5°C. The Eel River daily maximum temperature above the confluence with Outlook Creek was 30.2°C (Figure 7.21). A simple calculation on the expected cooling effects of Outlet Creek on the mainstem Eel River can be made by assuming that Outlet Creek is approximately 31% of the water volume and the mainstem is 69%, based on their respective watershed areas, 41,808 ha and 135,980 ha. Using a mixing equation developed by Brown et al. (1972):

$$\text{temperature} = (p_1 \times T_1) + (p_2 \times T_2) + \ldots (p_n \times T_n)$$

where p_n is the proportion of combined flow contributed by each of n streams and T_n = temperature of stream n, the predicted mainstem temperature below the confluence with Outlook Creek can be calculated as,

temperature = (0.31 x 26.5°C) + (0.69 x 30.2) = 29.1°C.

The predicted temperature was within 0.2°C of the observed temperature of 28.9°C. Thus, it appears that given sufficient flow (watershed area ratios being used as a surrogate for relative flow ratios), a cooling effect was realized. The downstream distance of the cooling influence cannot be ascertained from the distribution of sites in the Eel Drainage.

While fairly good agreement was noted for observed and predicted values using Brown's equation, this was for a single temperature metric (XY1DX) and represents the highest daily maximum temperature on a single day. We examined the predictive ability of the equation for a one-week time period to determine whether there was good agreement over several diurnal cycles. Figure 7.34 shows observed tributary, upstream, downstream temperatures and the predicted downstream temperature for Tomki Creek's confluence with the mainstem Eel River. The day of the highest daily maximum was bracketed by three days on either side to examine diurnal fluctuations in observed versus predicted temperatures over the course of a week. The observed and predicted downstream stream temperatures showed good overlap over the entire one week period. Other system confluences also showed good agreement between the observed and predicted downstream stream temperatures (see Appendix D).

The Middle Fork Eel River enters the main fork of the Eel River at about 130 km from the mainstem watershed divide (Figure 7.21). Unfortunately, no temperature sites were available on the Middle Fork that were close enough to the confluence with the Eel River to be representative of incoming water temperatures.

Reference to Figures 7.16-D and 7.16-E shows that the Middle Fork Eel had XY1DX values between 28°C and 30°C at sites with the highest divide distances. These sites were still 10 to 20 km from the confluence with the Eel River. However, given the stability of water temperatures in large mainstems, the Middle Fork temperatures may be quite close to the water temperature at its confluence with the mainstem Eel. Above the Middle Fork the mainstem Eel had a daily maximum of 28.9°C. Just below the confluence, the mainstem Eel daily maximum temperature was 28.5°C. It appears that the Middle Fork Eel was at a temperature very similar to the main Eel River. Very little change in the mainstem Eel temperature was observed below the confluence with the Middle Fork.

The remaining tributaries that enter the Eel River below the Middle Fork are small in watershed area and have daily maxima very close to mainstem daily maximum temperatures. Their influence on mainstem temperatures appears to be negligible. From the confluence with North Dobbyn Creek and continuing downstream, the daily maxima begin to decrease (Figure 7.21). The South Fork Eel River enters the main Eel River at ~262 km from the main Eel's watershed divide. The South Fork has about a third of the watershed area as the main Eel at this point. The two rivers have daily maxima within 0.7°C of each other.

At about 312 km from the watershed divide on the main Eel River the Van Duzen enters the Eel with a daily maximum of 22.6°C. The Van Duzen has a watershed area of 110,778 ha compared to the Eel River's watershed area of 814,997 ha. The Van Duzen was estimated to be about 13% of the flow of the mainstem Eel. Using Brown's equation the predicted Eel River temperature below the Van Duzen was 24.5°C, compared to an observed temperature of 21.6°C. Although Strongs Creek with its cooler water entered the Eel River about 5 km downstream from the Van Duzen, its watershed area was less than 1% of the Eel's. The decrease in Eel River temperatures, beginning at North Dobbyn Creek and continuing to the Pacific Ocean, are believed to be due to the influence of cooler coastal air temperatures.

While the predicted temperature of the Eel River below Outlet Creek was surprisingly close to the observed value, caution should be used in applying watershed area as a surrogate for flow in these types of calculations. This is especially prudent in systems that are strongly influenced by flow regulation, and

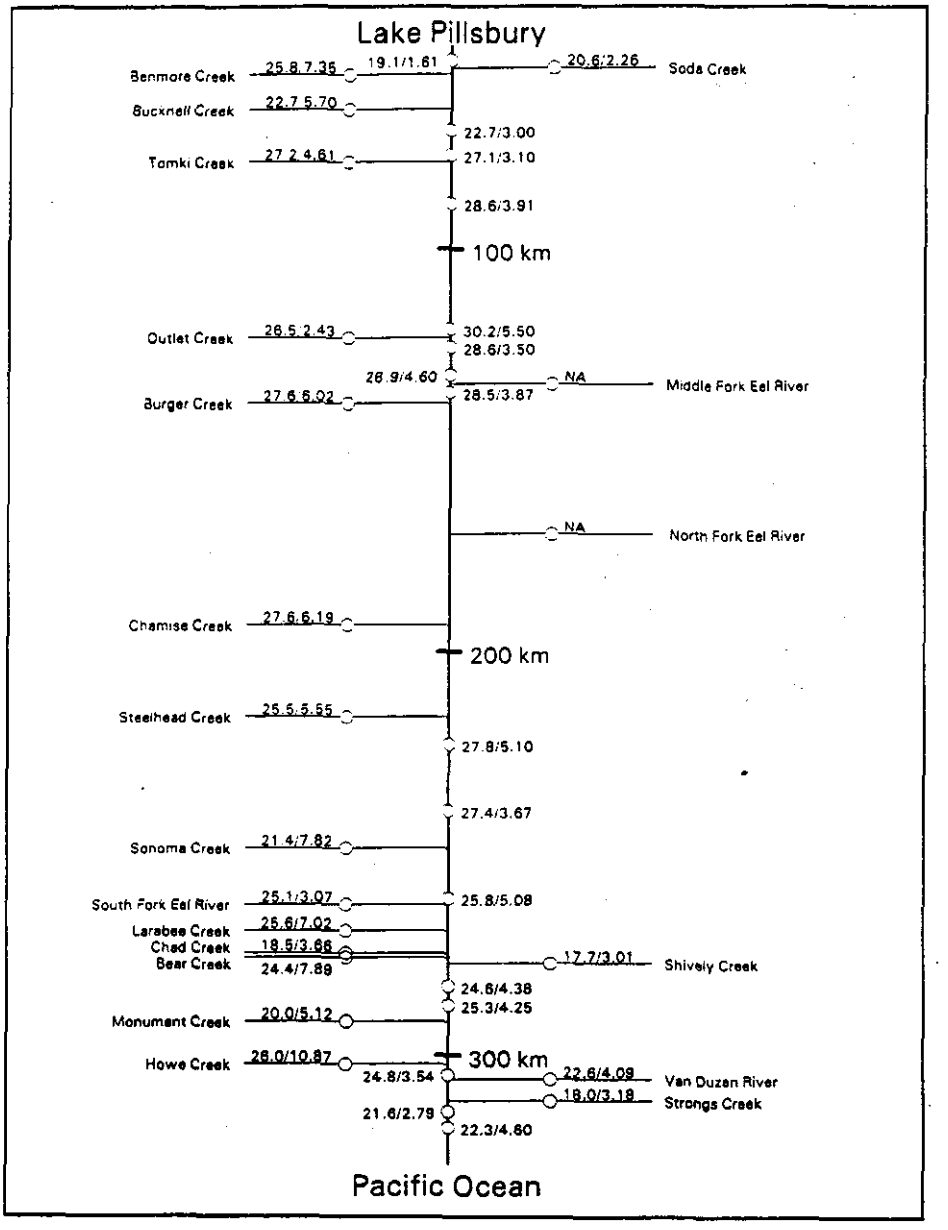

Figure 7.21. Tree graph of tributary and mainstem Eel River daily maximum stream temperatures (°C) (left number) and diurnal fluctuation (°C) (right number) measured on August 8, 1997. Monitoring sites and tributary confluence locations are to scale. Tributary monitoring site locations are not to scale. Divide distances are shown in 100-km increments. Tributary sites varied from 105 m to 5600 m from the mainstem.

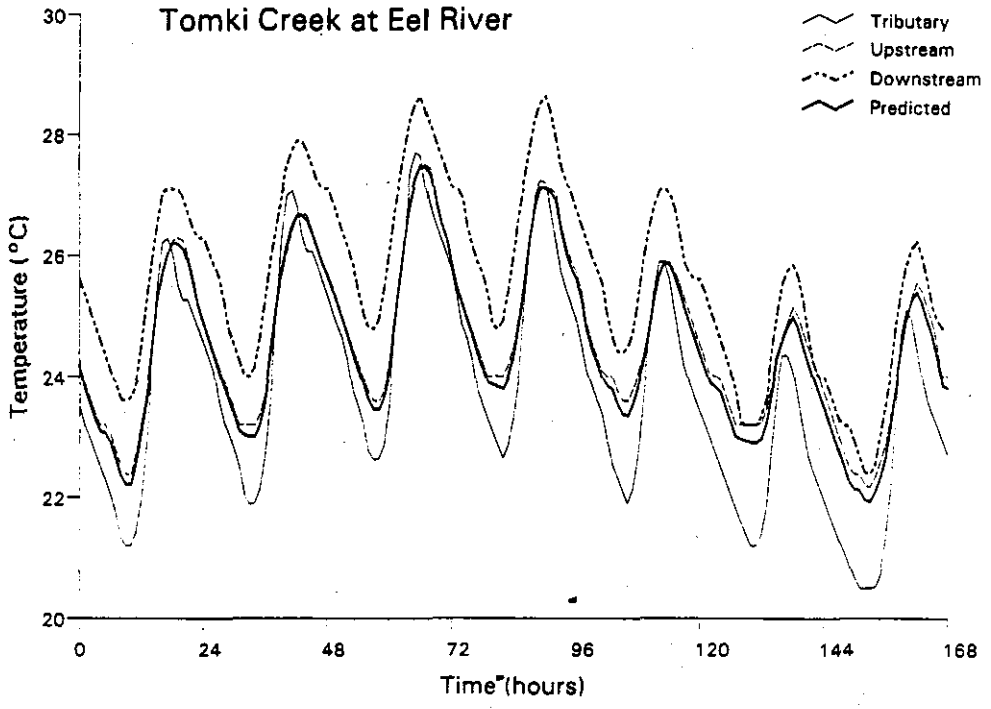

Figure 7.22. Diurnal trends in water temperatures for Tomki Creek, above the confluence on the Eel River, below the confluence on the Eel River, and the predicted (Brown's equation) temperature below the confluence. Temperatures were measured during the week of August 8, 1997.

reach very low summer baseflows, such as the Eel River system.

The diurnal fluctuations observed in the Eel River drainage appear to vary with the magnitude of the daily maximum and the watershed area of the tributary and mainstem. In general, the smaller the watershed area of a tributary, the higher the diurnal fluctuation. Canopy closure also plays a significant role in the level of daily maximum water temperature attained and the diel variation (Bartholow, 1989; Sullivan et al., 1990). Canopy effects on the highest daily maximum were presented in Chapter 5. Additional discussion is presented in Chapter 9.

Examination of the sum degrees over 24°C (SUMDEG24) and the total time spent above 24°C (SUMT24) provides some interesting insights and contrasts to the thermal regime that was developed previously for the Eel River drainage using the daily maximum temperature. Figure 7.23 shows the same tree graph with SUMDEG24 (number to left of slash) and SUMT24 (number to right of slash) values calculated for each site. The mainstem Eel River sites exhibited many of the highest SUMDEG24 values and corresponding SUMT24 values. Benmore and Larabee Creeks had comparable daily maxima (~26°C), however Benmore had a SUMDEG24 of 28°C for 45 total hours above 24°C, while Larabee had a SUMDEG24 value of 148°C for 135 total hours (Figure 7.23). The differences in SUMDEG24 and SUMT24 for these two streams that exhibited comparable daily maxima and seven-day moving averages illustrate the potential utility of these two acute thermal stress metrics.

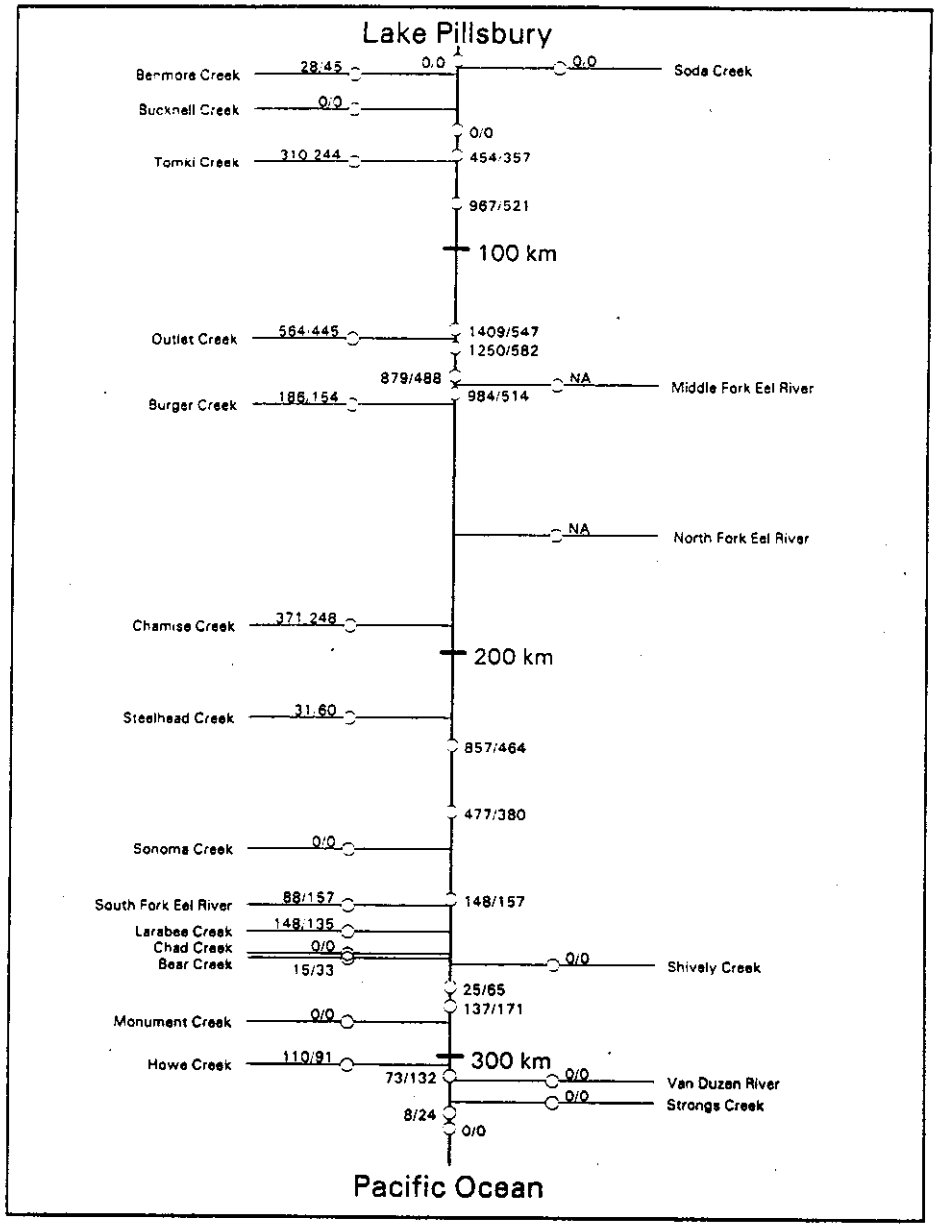

Figure 7.23. Tree graph of tributary and mainstem Eel River sum degrees (left number) and total time (hrs) (right number) over 24°C measured on August 8, 1997. Monitoring sites and tributary confluence locations are to scale. Divide distances are shown in 100-km increments. Tributary sites varied from 105 m to 5600 m from the mainstem.

Daily maxima for North Dobbyn Creek and the Eel River near its confluence were both 27.8°C. North Dobbyn exhibited a diurnal fluctuation 5°C greater than the Eel River. However, the SUMDEG24 value for the Eel River site was nearly four times greater than the North Dobbyn site and temperatures above 24°C lasted nearly 3 times longer (Figure 7.23).

Two sites on the main Eel River, one at approximately 89 km divide distance (i.e., the site below Tomki Creek) and the other site at 122 km divide distance (i.e., the site below Outlet Creek) had daily maxima of ~29°C (Figure 7.21). The SUMDEG24 for the upstream site was 967°C (SUMT24 = 547 hr) and the SUMDEG24 for the downstream site was 1250°C (SUMT24 = 582 hr) (Figure 7.23). In this case, the amount of time each site spent above 24°C was quite similar, however the downstream site had higher temperatures above 24°C than the upstream site, that is it had more cumulative warmth.

Gualala River Drainage

The year with the greatest number of sites on both receiving waters and tributaries in the Gualala River drainage was 1997. There were 39 sites available for analysis, 16 on tributaries and 23 on receiving waters. The warmest day for the majority of sites was found to be July 8, 1997. Daily maximum and diurnal fluctuations for this day were used to examine hierarchical stream temperature relationships. The 39 sites had continuous, uninterrupted temperature data between July 21 and August 19 for the calculation of the SUMDEG24 and SUMT24 acute thermal stress metrics.

Figure 7.24 depicts the hydrological distribution of daily maximum and diurnal fluctuation values in the Gualala River drainage. The shaded area on the graph is an estimate of the areal distribution of the (ZCI) for the month of July, based on PRISM 30-year average maximum air temperatures. Chapter 4 provides a more detailed description of the derivation of the ZCI.

In general, there was a decrease in daily maxima as water entered the ZCI. Beginning with the northernmost drainage, the North Fork of the Gualala River, a daily maximum of 25.9°C was observed outside of the ZCI (Figure 7.24). A warmer tributary enters the North Fork with a daily maximum of 27.1°C. The entrance of this warmer tributary did not seem to greatly influence the North Fork temperature, for the next daily maximum below the tributary was 25.2°C. About 2 km downstream another site on the North Fork recorded a daily maximum of 26.9°C, followed by a site another 2 km downstream with a daily maximum of 23.8°C. Below this point, a tributary (Dry Creek) enters the North Fork from the north. This tributary showed a decrease in daily maxima from 20.5°C to 16.1°C as it approached the ZCI (Figure 7.24). Other factors may contribute to the 4°C decrease in stream temperature over about a two kilometer distance, e.g., changes in riparian vegetation, habitat type where sensor was placed, etc.

The North Fork daily maximum dropped 2.4°C at the point where it entered the ZCI to a daily maximum of 21.1°C (Figure 7.24). We applied the Brown's equation to evaluate the predicted effect of the cooler Dry Creek tributary water on the North Fork temperature. The tributary site has a watershed area of 1677 ha and the site on the North Fork upstream of Dry Creek has a watershed area of 6840. Solving the equation below:

Predicted temperature = (0.245 x 16.1°C) + (0.755 x 23.8°C) = 21.9°C (observed = 21.1°C).

The upstream and downstream North Fork sites were about 2 km from the confluence with Dry Creek. The slightly cooler observed daily maximum value of 21.1°C compared to the predicted 21.9°C may be due to the onset of the ZCI or that the true discharge of Dry Creek was significantly larger or the North Fork's discharge was lower than predicted based on their respective watershed areas.

The generally accepted pattern is that of an increase in water temperature as water travels from headwaters to downstream reaches. The Little North Fork, which lies entirely within the ZCI, seems to exhibit this pattern, with temperature increasing with increasing distance from the watershed divide. The Little North Fork temperature increased about 4°C before merging with the North Fork (Figure 7.24). The South Fork had a daily maximum of 23.7°C at

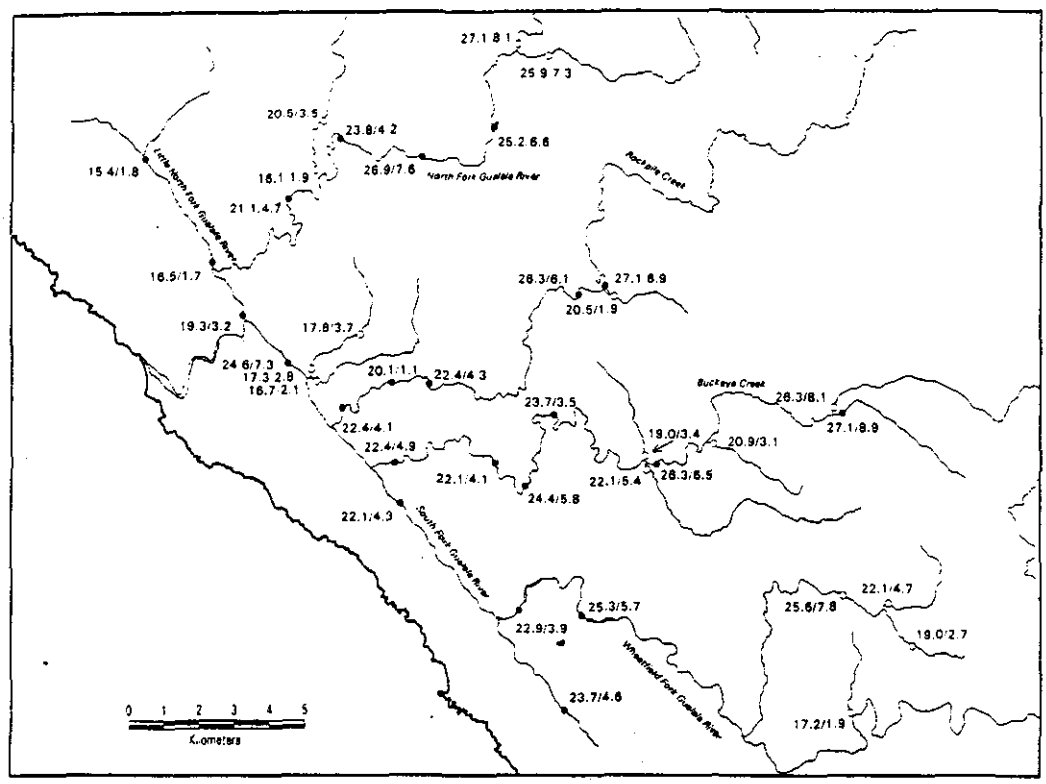

Figure 7.24. Stream network of tributaries and receiving waters in the Gualala River drainage showing the daily maximum stream temperatures (°C) (number on left side) and diurnal fluctuations (°C) (number on right side) on July 8, 1997. Receiving water (solid circles) and tributary (open circles) monitoring site locations are to scale. Shaded area represents an estimate of the areal distribution of the zone of coastal influence, our best approximation of the fog zone.

the most upstream site, with about a 1 °C decrease at a site 17 km downstream. The last site before its confluence with the North Fork had a daily maximum of 24.6 °C.

Rockpile Creek has a fairly large drainage area that feeds into the South Fork. Its most upstream site had a daily maximum of 27.1 °C. A small tributary (Horsethief Canyon) enters Rockpile Creek with a daily maximum of 20.5 °C, about 7 °C cooler than Rockpile Creek (Figure 7.24). The watershed area at the Horsethief Canyon site is 667 ha and the site just upstream on Rockpile Creek is 5917 ha. The ratio of the two watershed areas indicates that Horsethief Canyon contributes approximately 11% of the flow at its confluence with Rockpile Creek. The predicted downstream temperature was 26.3 °C, in complete agreement with the observed daily maximum temperature in Rockpile Creek.

Sites on both the South Fork and Little North Fork, both watercourses residing entirely within the zone of coastal influence, showed an increase in diurnal fluctuation with increasing distance from the watershed divide (Figure 7.24). Mainstems (North Fork, Rockpile, and Buckeye) that originate outside the zone of coastal influence (ZCI) and flow westerly

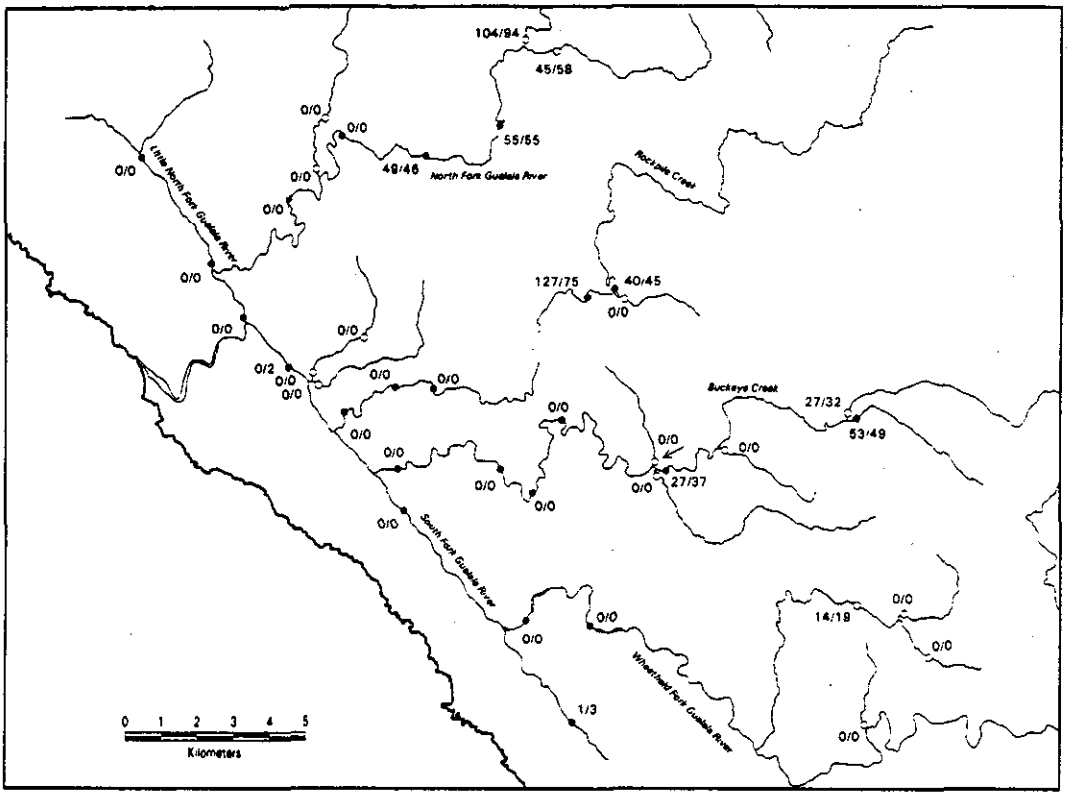

Figure 7.25. Stream network diagram of tributaries and receiving waters in the Gualala River drainage showing the sum degrees above 24°C (SUMDEG24) and the total time spent above 24°C (SUMT24). SUMDEG24 (number on left side) and SUMT24 (number on right side) were calculated from uninterrupted monitoring data collected between July 21 to August 19, 1997. Receiving water (solid circles) and tributary (open circles) monitoring site locations are to scale. Shaded area represents an estimate of the areal distribution of the zone of coastal influence, our best approximation of the fog zone.

into the ZCI exhibited a general decrease in diurnal fluctuation. The change in diurnal fluctuation coincided with the relative magnitude of the daily maximum stream temperature.

Sites outside of the ZCI were predominantly the ones that showed values greater than zero for SUMDEG24 and SUMT24 (Figure 7.25). Only two sites within the ZCI had greater than zero values for these two acute thermal stress metrics. The site with the highest values for SUMDEG24 and SUMT24 was on a tributary to the North Fork, with values of 113°C and 127 hr, respectively. A site within the ZCI on Wheatfield Fork had values of 42°C and 75 hr.

Ten Mile River Drainage

The warmest day in 1998 for the majority of sites in the Ten Mile River drainage was August 4th. Daily maxima and diurnal fluctuations for this day were used to evaluate the hierarchical thermal regimes in the drainage. There were 31 sites that had complete data for the time period July 21 to August 19. SUMDEG24 and SUMT24 were calculated for data in this 30-day window. There were 13 sites on tributaries and 18 on tributary receiving waters.

The three forks of Ten Mile River did not show significant decreases in daily maximum temperatures upon entering the ZCI (Figure 7.26). The North Fork Ten Mile River started with a daily maximum of 20.7°C at 7 km from the watershed divide. Five kilometers downstream on the North Fork, a sensor recorded a daily maximum of 18.3°C. Proceeding downstream approximately 5 km a daily maximum of 19.5°C was recorded. At 22.2 km from the watershed divide the daily maximum was 20.0°C. The last site on the North Fork had a daily maximum of 19.3°C. Thus, the North Fork realized only about a 1°C decrease upon entering the ZCI, even with two cooler tributaries entering the mainstem in the ZCI. The Little North Fork enters from the north and has a watershed area of 1990 ha. It had a daily maximum of 16.2°C (Figure 7.26). The watershed area of the North Fork site upstream from the Little North Fork has a watershed area of 7527 ha. The predicted temperature of the combined flows is 18.9°C, compared to an observed downstream daily maximum of 19.3°C. Thus, the lower water temperature of the Little North Fork seems to account for the decrease in the North Fork temperature.

The Middle Fork begins with a daily maximum of 16.4°C outside the ZCI and begins to increase in temperature as it flows towards the coast. The temperature remained near 19°C, except at one site at a divide distance near 22 km, where the daily maximum dropped about 3°C (Figure 7.26). The temperature stayed fairly constant through the ZCI despite the entrance of four cooler tributaries. The relative watershed areas of the tributaries compared to the mainstem Middle Fork would suggest that they would have a minor influence on the mainstem water temperature. There may be other warmer tributaries entering the Middle Fork for which no temperature data were available. There were no sites spatially situated in the Middle Fork to apply Brown's equation to determine tributary cooling effects.

The South Fork Ten Mile River started out with a daily maximum temperature similar to the Middle Fork, i.e., 16.5°C. Daily maxima increased in a downstream direction and remained between 18.5°C and 20.2°C until reaching about 30 km from the watershed divide, where the daily maximum was 16.5°C. A cool tributary entered the South Fork from the south at about 20 km from the watershed divide and its watershed area was 1019 ha. It had a daily maximum temperature of 15.9°C. The site upstream on the South Fork had a daily maximum of 19.5°C with a watershed area of 4817 ha. The predicted temperature after mixing was 18.7°C, compared to an observed temperature of 18.5°C at about 25 km from the divide.

The cooling influence of the ZCI did not appear to act on the forks of the Ten Mile River as significantly as that observed in the Eel River drainage. The Eel is a much longer system and resides for a longer distance, and hence a longer period of time, in the ZCI than the Ten Mile River system. There may have been insufficient time for water in the Ten Mile River drainage to come into equilibrium with cooler coastal air temperatures.

The diurnal fluctuation of water temperatures in the Ten Mile drainage were small in comparison to the Eel drainage network. The coolest tributaries with small watershed areas exhibited the lowest diurnal fluctuations, ranging from 0.6°C to 3.9°C. Diurnal fluctuations on the mainstems ranged from 1.4°C at the uppermost site on the South Fork to 4.2°C on the North Fork. We evaluated the application of the Brown's equation to diurnal fluctuations and found very good predictive capabilities. On the tributary of the South Fork discussed previously, the predicted diurnal fluctuation was 2.9°C compared to an observed fluctuation of 3.0°C. On the tributary entering the North Fork the predicted diurnal fluctuation was 3.5°C, in complete agreement with the observed value. Thus, cooler tributaries appear to not only decrease the receiving water temperature in an amount proportional to its flow, but also

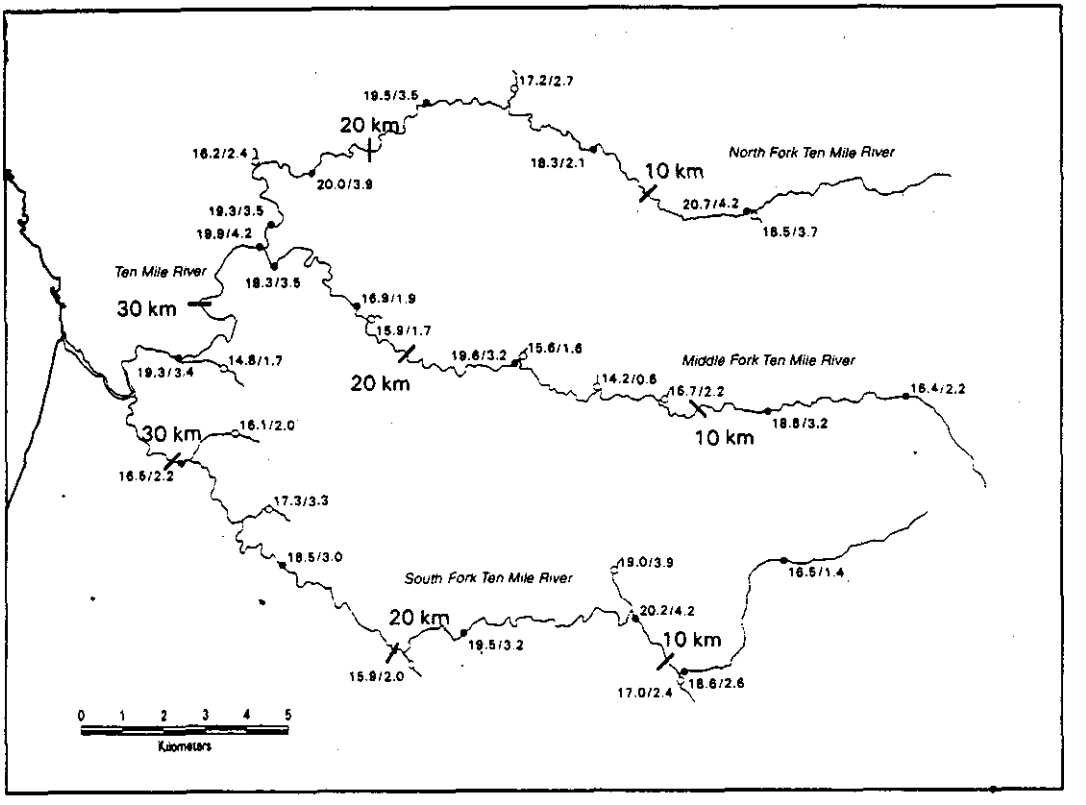

Figure 7.26. Stream network of tributaries and receiving waters in the Ten Mile River drainage showing the daily maximum stream temperatures (°C) (number on left side) and diurnal fluctuations (°C) (number on right side) on July 8, 1998. Receiving water (solid circles) and tributary (open circles) monitoring site locations are to scale. Shaded area represents an estimate of the areal distribution of the zone of coastal influence, our best approximation of the fog zone.

attenuate the diurnal fluctuation of the receiving water.

Examination of the daily maxima and diurnal fluctuations in the Ten Mile drainage revealed that water temperatures were fairly moderate compared to other HUCs. The SUMDEG24 and SUMT24 provide additional evidence that water temperatures were not greatly elevated, in that no values for either acute thermal stress metric had values greater than zero. Nearly half of the drainage network falls within the ZCI, which may partially account for the observed temperatures.

Potential Downstream Influence of Tributaries on Mainstem Temperatures

The downstream distance the cooling or warming influence of tributaries has on receiving waters has been a matter of speculation and debate for many years (Caldwell et al., 1991; Zwieniecki and Newton, 1999). To adequately address such a question, a sampling design needs to be developed specifically to address this issue. The data used in this regional assessment were not collected with any underlying sampling design specifically geared towards answering this question. However, Brown's equation can be used to make an initial examination of this issue with the available data. Many environmental factors will influence the distance a cooling or warming effect will linger downstream, e.g. canopy, depth, flow, gradient, air temperature, groundwater influx, fog zone.

The observed and predicted daily maximum temperatures below various tributaries in the three case study drainages are presented in Table 7.3. The analyses can provide information on the minimum distance receiving water temperatures may have water temperatures near the predicted value after mixing with a cooler or warmer tributary. However, the maximum distance cannot be determined with existing data.

At a distance 10 km below the confluence with Tomki Creek the Eel River exhibited a temperature about 1 °C warmer than the predicted value (Table 7.3). At some distance less than 10 km downstream of the confluence the mainstem temperature began to come into equilibrium with riparian and climatic conditions. Two tenths of a kilometer below Outlet Creek the Eel River was 0.4 °C below the predicted value. At 10.4 km downstream the Eel was at 28.5 °C, within 0.5 °C of the predicted value. The Eel River about 6 km below the confluence with the Van Duzen was about 3 °C cooler than predicted. The fog zone could account for this discrepancy between observed and predicted values. In the Gualala River drainage, receiving water temperatures were within ~1 °C of the predicted value at up to about 5 km downstream from the confluence with cooler tributary temperatures. In the Ten Mile drainage, receiving water temperatures were within 0.5 °C of the predicted at distances up to about 5 km downstream of the confluence.

These analyses seem to indicate that the extent of the influence of cooler tributaries on receiving water temperatures is at least partially dependent on the ratio of mixing volumes. The closer the ratio was to 1:1, the closer the observed values were to the predicted and the further downstream the agreement between observed and predicted was realized. That is, the greater the tributary's contribution to the mainstem flow, the greater and longer lasting is the influence of cooler tributary waters on mainstem temperatures. Zwieniecki and Newton (1999) found that slightly warmer stream temperatures within a clearcut area with a buffer zone returned to the predicted trend line temperature at a distance of 150 m. The streams they evaluated were much smaller in size than those examined in Table 7.3. Caldwell et al. (1991) examined Type 4 and 5 stream temperatures in Washington state, and their influence on Type 3 streams. Type 4 and 5 streams are defined by Washington state forest practice rules as small headwater streams that do not support significant fish populations. These would be similar to California's Class 2 and 3 streams. Washington's Type 1-3 streams include, by definition, all large streams and shorelines of the state. Any stream with a late-summer base flow of greater than 0.009 cms (0.3 cfs), and any stream that supports a significant fish population, is classified as Type 1, 2, or 3. The tributaries and receiving waters assessed in Table 7.3 are all Class 1 streams by California forest practice rules definition. Thus, direct comparisons may not be totally appropriate. Caldwell et al. (1991) found that small headwater streams of Type 4 did not have an influence on Type 1-3 streams if their confluence was more than about 7 km (4.5 mi) from the receiving water's distance from watershed divide. The authors used divide distance as a surrogate for stream size and drainage area.

Table 7.3. Comparison of Predicted and Observed Mainstem Temperatures below Tributaries in the Eel, Gualala, and Ten Mile River Drainages.

tributary/mainstem	mainstem:trib. flow ratio	upstream mainstem temp. (°C)	trib. temp. (°C)	predicted downstream mainstem temp. (°C)	observed downstream mainstem temp. (°C)	downstream distance from trib. (km)
Eel River Drainage						
Tomki/Eel	6:1	27.1	27.2	27.1	28.6	10.2
Outlet/Eel	3.2:1	30.2	26.5	29.0	28.6	0.2
					28.5	10.7
Van Duzen/Eel	7.7:1	24.8	22.6	24.5	21.6	5.9
Gualala River Drainage						
Horsethief/Rockpile	9:1	27.1	20.5	26.3	26.3	0.9
Dry/NF Gualala	4:1	23.8	16.1	21.9	21.1	1.1
Wheatfield/SF	2.4:1	23.7	22.9	23.2	22.1	4.6
Franchini-Grass-hopper/Buckeye	6.7:1	26.3	19.0/22.1	25.3	23.7	5.7
Ten Mile River Drainage						
Little Fork NF/NF	3.8:1	20.0	16.2	18.9	19.3	2.4
Church/SF	4.8:1	19.5	15.9	18.7	18.5	4.7

Note: All temperatures are daily maxima. Eel River drainage temperatures measured on August 16, 1997. Gualala River drainage temperatures measured on July 8, 1997, and Ten Mile drainage temperatures measured on August 4, 1998.

The results of a preliminary analysis of a small data set (Table 7.3) suggest that the distance from the divide at which a tributary may have an influence on the receiving stream's temperature is a function of the ratio of flows (or watershed areas being used as a surrogate for flow). The distance downstream the influence lasts is dependent upon the ratio, as well as the characteristics of the receiving water environment and climatic conditions.

Graphs of predicted and observed stream temperatures over a one-week period for each of the sites in Table 7.3 can be found in Appendix D.

Summary

At the ecoprovincial scale watershed position, as represented by watershed area and distance from the watershed divide, played an important role in explaining spatial trends in stream temperature. Stream temperature generally increased with increasing stream size (higher watershed area) and distance from the watershed divide. Stream temperature decreased at the highest divide distances at many mainstem sites. The decrease was attributed to the cooling influence of coastal air temperatures. At a given divide distance daily maximum and daily minimum stream temperatures in the Coastal Steppe Province were less variable than in the Sierran

Steppe Province. Just as the maritime climate tends to moderate air temperature in the CSP, it appears to have a similar effect on stream temperatures.

What is most striking is the consistent increase in the highest daily maximum (XY1DX) stream temperature with increasing distance from the watershed divide in all HUCs that comprise the range of the coho salmon in Northern California. Even in HUCs with large numbers of data points, each point representing a different tributary or mainstem, the increase was consistent. The site's location in the HUC played a large role in explaining stream temperature at any given location.

Stream temperatures in some HUCs showed steeper increases than others. As shown in Chapter 4 and 5 air temperature regimes vary greatly between and within HUCs. In coastal HUCs with large areal portions laying in the interior (e.g., Mad, the four Eel HUCs, and the Big-Navarro-Garcia) air temperature in the interior can be 10° to 15°C warmer than near the coast. Low order streams in these HUCs originate in areas of high air temperatures (~100°F). These coastal-interior oriented HUCs were predominantly the ones showing the steepest rate of stream temperature increase with increasing divide distance.

Coastal HUCs (e.g., Mattole, Smith) showed more moderate longitudinal increases in stream temperature. Streams in coastal-interior HUCs that lie completely within the zone of coastal influence also showed a moderate longitudinal increase in stream temperature. Streams that originate outside of the ZCI and flow into the ZCI often showed a decrease in water temperature.

Sum degree is comparable to degree days as a means of quantifying cumulative warmth in a season or year at a given location. It is a measure that takes into account both magnitude and duration of departure from a chosen threshold temperature. At some sites where traditional temperature metrics, such as the highest daily maximum or highest seven-day moving average, did not exceed acute or chronic thermal threshold values, sum degree was higher than at sites where traditional metrics did not exceed thresholds. While there is little documented use of sum degree or degree day in assessing thermal stress on aquatic biota, it is hoped that the use of this metric will increase. Development of sum degree thresholds is needed to lend biological relevance to this metric. Reanalysis of existing stream temperature data where fish presence/absence and/or abundance data were also collected, such as the work of Essig (1998) on streams in Idaho, would be useful for establishing sum degree thresholds.

Application of Brown's mixing equation revealed very good predictions in receiving water temperature change below the confluence with a warmer or cooler tributary. The closer the downstream mainstem site was to the confluence, the better the agreement between observed and predicted water temperature. With increasing distance below a confluence, the mainstem is probably beginning to adjust to new equilibrium conditions of air temperature, groundwater influx, canopy, and other riparian conditions. The downstream extent to which a tributary influences mainstem temperatures could not be determined from our meta-analysis. The downstream influence appears to be a function of discharge ratio (watershed area used as a surrogate for discharge).

While the predicted temperature of the Eel River below Outlet Creek was surprisingly close to the observed value, caution should be used in applying watershed area as a surrogate for flow in these types of calculations. This is especially prudent in systems that are strongly influenced by flow regulation, and reach very low summer baseflows, such as the Eel River system.

When establishing stream temperature goals for maintenance of certain beneficial uses, watershed position is an important consideration. A natural gradient in stream temperature occurs from the headwaters to the lower reaches. This natural gradient produces discrete zones with temperature regimes suitable for distinctly different fish communities and activities (Armour, 1991). Stream temperature standards should be developed with an understanding of the natural temperature regimes in HUCs throughout the range of the coho salmon in Northern California.

Chapter 8

INFLUENCE OF SITE-SPECIFIC ATTRIBUTES ON STREAM TEMPERATURES

Introduction

In Chapters 6 and 7, trends in stream temperatures observable at broad regional scales were investigated. An appreciation of the climatic regimes that are imposed upon streams across Northern California is useful to gain a better understanding of status and trends in water temperature at smaller spatial scales (e.g., watersheds, streams, reaches). Such an appreciation enables one to place watersheds and streams in the context of the "big picture."

This chapter zooms in to a finer spatial scale to examine the influence of various site-specific attributes on stream temperature. These attributes were unfortunately limiting in terms of sample size. For years prior to 1998, values for many site-specific attributes that required measurement in the field were missing for many sites. Therefore, temperature and site-specific attribute data for 1998 were primarily used in this chapter. The site-specific attributes examined in this chapter are channel orientation, gradient, habitat type, and bankfull width.

Channel orientation seems to have an influence, although not a significant influence, on daily maximum stream temperatures. The daily maximum temperature near the solar equinox was greater in the east-west (EW) channel orientation than the north-south (NS). While it was expected that a greater channel orientation signal would be apparent in the 0-24% canopy class, the greatest differences between EW and NS daily maximum temperature was observed in the intermediate canopy classes (25-49% and 50-74%). Observed trends may simply be an artifact of site location and lack of a sampling design specifically developed to address the channel orientation issue.

Stream temperatures generally decreased with increasing channel gradient. This is most likely because sites with higher gradients are generally closer to the headwaters. Riffle and run sites had average stream temperatures only slightly higher than shallow pool sites. Deep pool sites exhibited the highest average daily maximum stream temperatures. The geographic distribution of all habitat types was not uniform in 1998. A large number of deep pool sites were located in the southern portion of the SONCC ESU where air temperatures are warmer than the northern portion of the ESU. Additionally, most of the deep pool sites were located in large systems, such as the lower Eel River, where the stream is potentially too wide for stream-side vegetation to provide adequate canopy. Canopy closure was less than 20% in 36 out of the 41 deep pool sites. The disproportionate geographical distribution of deep pool sites and the low canopy associated with these sites could account for their higher daily maximum stream temperature average. Stream temperatures generally showed an increasing trend with increasing bankfull width. The sample size was too limited to draw definitive conclusions. As bankfull width increases, effective stream-side shading is reduced. Moreover, sites are usually at greater watershed areas and divide distances at higher bankfull widths.

Influence of Channel Orientation on Stream Temperatures

Streams with generally north-to-south or south-to-north flows have relatively shorter periods of direct overhead solar radiation than do east-to-west or west-to-east flowing streams (Sullivan et al., 1990). Arguments for both EW and NS having higher stream temperatures have been made. Given the east-to-west solar path and the solar zenith during the summer months, riparian vegetation along E-W or WE flowing streams might contribute greater shade than NS or SN flowing streams. Topographic relief, if higher than the solar zenith angle, could also provide shade in EW/WE streams. Direct sun would only intercept EW stream surfaces in the early morning and late afternoon, a time when solar heat energy is near a minimum. The alternative argument that EW streams may have higher stream temperatures is that NS oriented streams have relatively short periods of direct overhead solar radiation (Sullivan et al., 1990). Therefore, riparian shade might be less important on NS oriented streams than along EW oriented streams. Both are valid arguments, which leads to the formulation of the null hypothesis, that water temperatures in streams with NS or EW orientations are not significantly different.

The relationship between channel orientation and the highest seven-day moving average of the daily average (XYA7DA) and daily maximum (XYA7DX) and the highest daily maximum (XY1DX) was investigated. Channel orientation was derived in GIS for each site by measuring the downstream bearing of the channel over a distance of approximately 600 meters upstream from the temperature sensor location to the nearest degree. Six hundred meters is our best estimate of the length of a thermal reach that could be applied across all streams. This may be an overestimate or underestimate of the length of a thermal reach at some sites, depending on the size and flow of the particular stream.

Distribution of Channel Orientations

The distribution of channel orientations for sites monitored in 1998 is presented in Figure 8.1. Similar distribution graphs of channel orientation for data collected in 1990 through 1997 can be found in Appendix E. Orientations were grouped into 30-degree classes starting at 345°. Orientations from 345° to 15° (a thirty-degree class) are shown on the graph as a vertical bar between the x-axis origin at 345° and 15°. Orientations from 15° to 45° are represented by the vertical bar between 15° and 45°, and so forth for the other 30-degree classes. The cumulative proportion of sites in each channel orientation class is overlaid on the graph.

With an understanding of the hydrology and basin characteristics of Northern California it is not surprising to find that there were fewer streams in the 0° to 90° and 90° to 180° orientation classes (Figure 8.1). These classes represent streams that flow in a northeasterly to easterly or southeasterly to southerly direction. Many of the Northern California basins and watersheds within basins have northwesterly and southwesterly orientations. However, streams can meander or follow tortuous geologic formations over some portions of their total length in a NE, E, or SE direction.

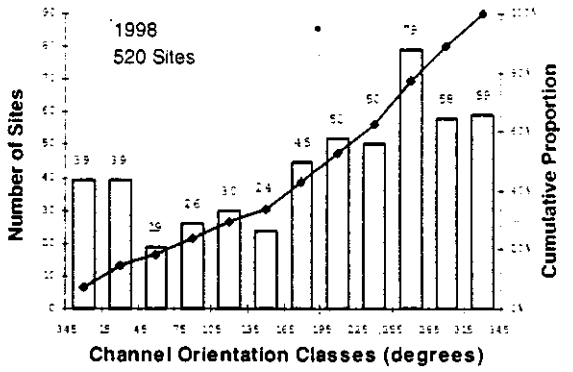

Figure 8.1. Distribution of stream temperature monitoring sites by channel orientation classes. Orientation was derived in GIS at a point ~600 meters upstream from the stream temperature monitoring site. Orientation is in a downstream direction.

Polar Plots of Stream Temperature

Figure 8.2 is a presentation of polar plots showing the highest daily maximum temperature (XY1DX) for each site by year, plotted with respect to channel

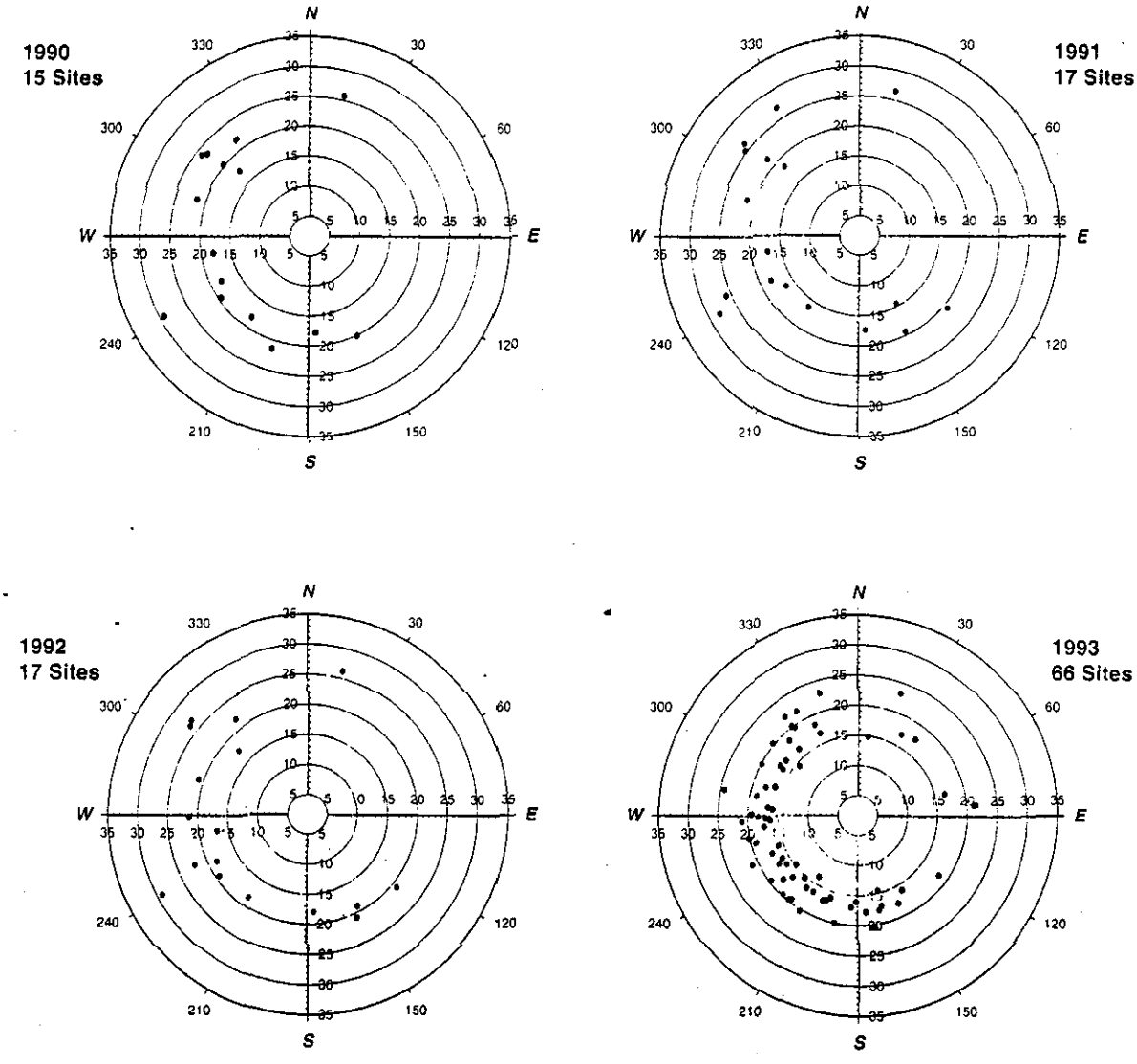

Figure 8.2. Highest daily maximum stream temperature (°C) with respect to channel orientation (degrees) for years 1990 - 1998. Orientation was derived in GIS over the reach ~600 meters upstream from the stream temperature monitoring location. Orientation was determined in a downstream direction along the 600-m reach.

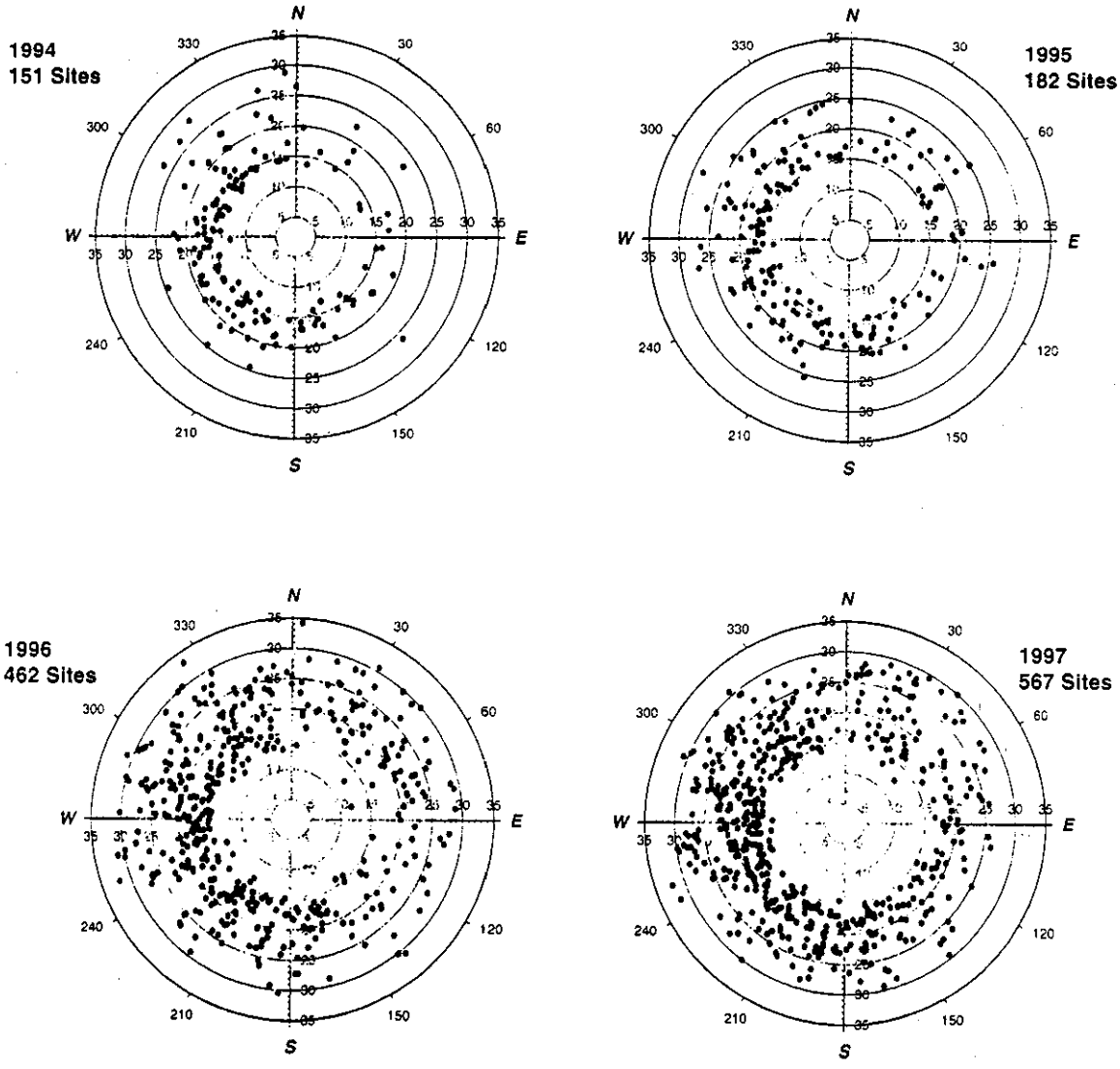

Figure 8.2. (continued)

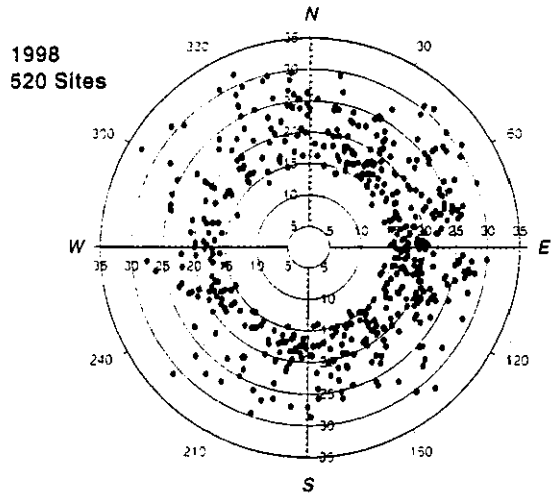

Figure 8.2. (continued)

orientation. The temporal window from July 21 to August 19 was imposed upon the data to ensure that the highest temperature values were indeed the "true" highest. Sites with no more than five missing daily records within the one-month temporal window were used in the analyses.

Visual examination of the polar plots in Figure 8.2 did not reveal any obvious trends. The polar plots can be visually misleading by virtue of the distribution of channel orientations. There were more data points in those sectors that had a greater occurrence of sites with a given channel orientation. Careful inspection of the polar plots does not indicate a preponderance of higher XY1DX values in any particular sector. Similar polar plots for the XYA7DA are presented in Appendix E.

Further graphical and statistical treatments of the data were performed and are presented in the following sections.

Graphical and Statistical Analyses by Orientation Classes

Channel orientations were grouped into two classes, north-south or south-north (NS) and east-west or west-east (EW):

NS

$330 \leq \text{orientation} \leq 30$

OR

$210 \geq \text{orientation} \geq 150$

EW

$120 \geq \text{orientation} \geq 60$

OR

$240 \leq \text{orientation} \leq 300$

A thirty-degree range on either side of the major compass points (N, S, E, and W) was chosen for orientation classes to remove orientations that fell between NS and EW (Figure 8.3).

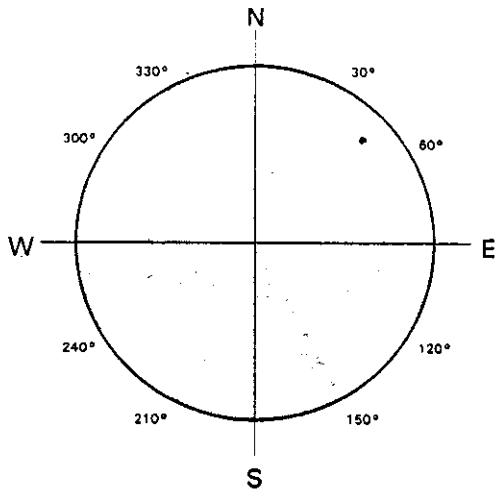

Figure 8.3. North-South and East-West channel orientation classes used to assess the influence of channel orientation on stream temperatures. Shaded area represents 30 degrees on either side of cardinal directions.

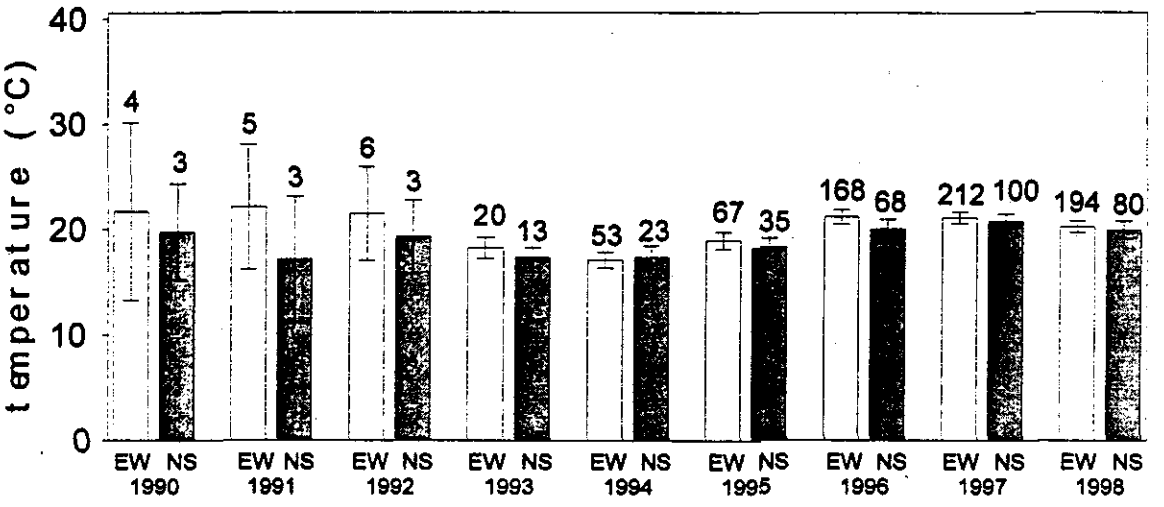

Figure 8.4. Average of the highest daily maximum stream temperature by orientation class and year. EW = streams with orientations flowing east-west or west-east; NS = streams with orientations flowing north-south or south-north. Error bars represent two standard deviations. Number of sites in each orientation class is shown above the error bars.

These borderline orientations would include channel orientations such as NNE, NSE, SSW, and NNW. These borderline orientations could possibly obscure any discernable trends in stream temperature with respect to channel orientation.

Figure 8.4 shows the class average XY1DX by orientation class and year. The error bars represent plus or minus two standard deviations. The EW group exhibited higher average temperatures compared to the NS group for each yearly comparison. The differences between EW and NS average temperatures lessened in 1997 and 1998, probably due to a greater sample size with greater representation of streams in each of the channel orientation classes. Error bars overlapped between orientation classes within each yearly comparison. No significant difference was discernable between the NS and EW orientation classes in any of the nine years as exhibited by the overlap in error bars. Comparisons should be made between orientation classes within a given year **only**, since different sites were monitored in each year.

An analysis of variance (ANOVA) was performed using the PROC GLM procedure in SAS (1985), the preferred procedure for unbalanced designs. Both *orientation class* and *year* were used as independent variables in the model, with an interaction term included (Table 8.1).

Table 8.1. ANOVA Results of Highest Daily Maximum Stream Temperature Versus Channel Orientation and Year and the Interaction Term.

Source	DF	Sum of Squares	Mean Square	F Value	Pr > F
Model	3	508.95415	169.65138	11.23	<0.0001
orientation class	1	14.1398854	14.1398854	0.94	0.3335
year	1	411.6886690	411.6886690	27.26	<0.0001
year*orientation class	1	14.0875693	14.0875693	0.93	0.3344

Results of ANOVA shown in Table 8.1 indicate that the model was significant, with a probability of <0.0001. However, the largest source of variability in XY1DX was explained by the *year* model term. Significant differences in the XY1DX across years was expected due to the different sites that were monitored across years. The *orientation class* and *year*orientation class* terms in the model were not significant. Similar statistics performed on the highest seven-day moving average of the daily average and the highest seven-day moving average of the daily maximum returned similar results. Also, scientific curiosity led to the examination of the lowest daily minimum temperature metric with respect to channel orientation. No significant relationship was found.

These findings are consistent with other researchers (Swift and Messer, 1971; Sullivan et al., 1990) who found that channel orientation did not account for differences in stream temperatures. Sullivan et al. (1990) found that in streams flowing easterly or westerly, there appeared to be a slightly lower maximum and mean stream temperature and diurnal fluctuation. Unfortunately, in the Timber, Fish, and Wildlife Study (Sullivan, 1990) there were relatively few streams that flowed EW or WE, and those that did were partially shaded, making comparisons tenuous. Although the relationship between channel orientation and stream temperature is not strong, some states' forest practice guidelines have in the past conditioned buffer-strip shade requirements based on channel orientation.

Channel Orientation and Canopy

The interaction between channel orientation and canopy was examined for streams in Northern California. The streams used in the examination of the influence of channel orientation on stream temperature consisted of a diversity of channel widths and canopy closure values. Sites with non-null canopy values were used to examine the relationship between stream temperature versus channel orientation and canopy. The year with the least number of null values for canopy was 1998. The same channel orientation classes (NS and EW) and canopy classes (0-24%, 25-49%, 50-74%, and 75-100%) were used to group stream temperature sites. At lower canopy classes, higher XY1DX values were observed. Within canopy classes there was no significant difference between average XY1DX values observed in each channel orientation class. Table 8.2 shows ANOVA results for the comparison. *Canopy class* was a significant model term explaining the variability in the highest daily maximum stream temperature. *Channel orientation* was not significant singly or in its interaction with the *canopy class* term.

The highest 1998 daily maximum temperature at each site usually occurred during the last two weeks in July and first two weeks in August. This was true for all years in our data set. The sun azimuth is lower during this time of year than near the time of the summer equinox. The influence of channel orientation and canopy on stream temperature may be more pronounced near the solar equinox. The daily maximum stream temperature observed at each site on June 26, 1998 and the highest 1998 daily maximum were compared. Not all sites with XY1DX values had stream temperature data for 26 June 1998. Therefore, to make valid comparisons, the same sites must be compared. Only XY1DX values for sites that had valid 26 June daily maxima were used in the comparison. Figure 8.5 indicates that there was a larger difference between EW and NS 26 June daily maxima in the two intermediate canopy groups

Table 8.2. ANOVA Results of Highest Daily Maximum Stream Temperature (XY1DX) Versus Channel Orientation and Canopy Classes and the Interaction Term.

Source	DF	Sum of Squares	Mean Square	F Value	Pr > F
Model	7	1133.584474	161.940693	16.28	<0.0001
orientation class	1	6.5332162	6.5332162	0.66	0.4186
canopy class	3	935.2782947	311.7594316	31.35	<0.0001
orientation*canopy	3	65.5386644	21.8462215	2.20	0.0898

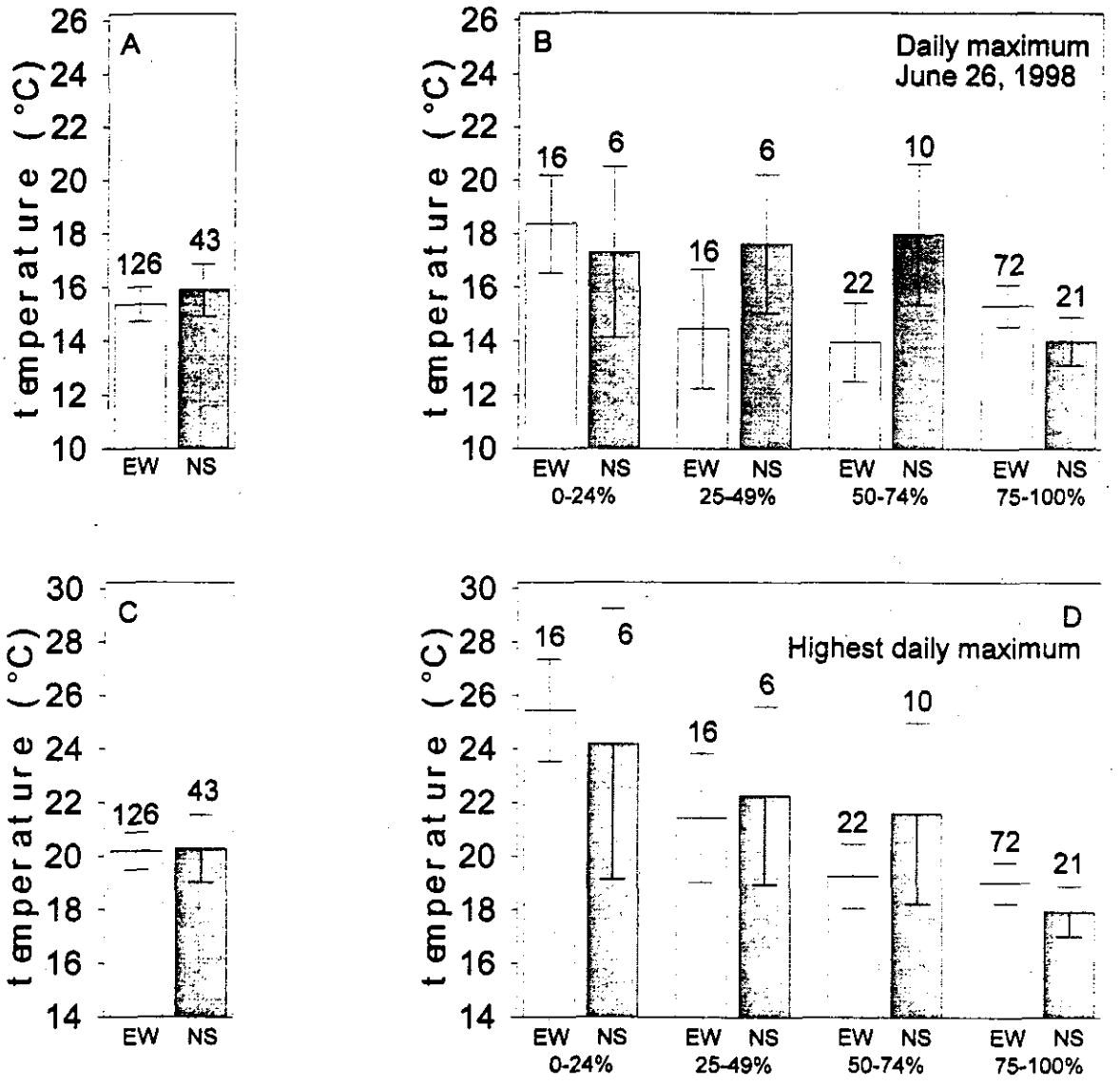

Figure 8.5. Comparison of the daily maximum stream temperature measured on 26 June 1998 and the highest 1998 daily maximum by orientation class and canopy class. (A) 26 June daily maximum by orientation class. (B) 26 June daily maximum by orientation class and canopy class. (C) highest 1998 daily maximum by orientation class, and (D) highest 1998 daily maximum by orientation class and canopy class. EW = streams with orientations flowing east-west or west-east; NS = streams with orientations flowing north-south or south-north. Number above error bar is the number of sites in the orientation class.

(Figure 8.5-B) compared to the XY1DX values that occur later in the year (Figure 8.5-D). While there seems to be a stronger channel orientation signal in the 26 June daily maximum stream temperatures, the reason the signal only appears in the 25-49% and 50-74% canopy classes is unclear. Topographic shading may account for the lower daily maxima observed in the NS orientation group at the lowest and highest canopy classes. Moreover, differences in canopy measurement procedures and varying channel lengths along which canopy was measured upstream from the stream temperature sensor may partially explain the results. A study specifically designed to address the channel orientation issue is warranted.

Streams with wide channels have a reduced shading effectiveness from stream-side vegetation because of the distance of the canopy from the stream. Streams with such wide channels would most likely show very little correlation between stream temperature and channel orientation. Out of 548 sites with 1998 stream temperature data, 365 had non-null canopy values. Of these 365 sites, 203 fell within one of the four orientation quadrants (Figure 8.3). Of these 203 sites used to assess the relationship between canopy and channel orientation, the five smallest watershed areas (21, 85, 93, 142, and 149 hectares) in the data set all had canopy values greater than 90%. Of the 203 sites, the five largest watershed areas had canopy values of 50, 0, 0, 1, and 0%. The 50% value may be anomalous. Some investigators placed temperature probes in side channels of lower mainstem rivers to characterize the extent of thermal refugia. Side-channel canopy values could potentially be higher than wider, mainstem channels.

To assess the interaction between canopy and channel orientation on water temperature in streams of similar size, an arbitrary watershed area of ≤18,000 ha was used to subset the 1998 data. Using the relationship between drainage area and bankfull width shown in Figure 8.6, a drainage area of approximately 18,000 hectares (~70 square miles) corresponds to a bankfull width of ~12 m (~40 ft). This watershed area and corresponding bankfull width would potentially be capable of providing riparian shade given adequate canopy retention. The distance where streams may become too wide for stream-side vegetation to provide adequate shading is empirically developed using FSP data in Chapter 9 - Canopy.

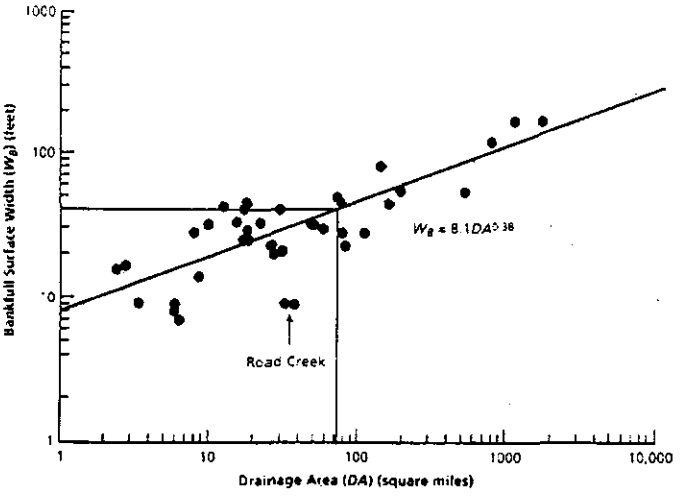

Figure 8.6. Bankfull surface width versus drainage area - Upper Salmon River, Idaho. Local variations in bankfull width may be significant. Road Creek widths are narrower because of lower precipitation. Taken from FISRWG (1998).

The relationship between XY1DX, channel orientation, and canopy class was examined for sites with watershed areas less than or equal to 18,000 ha. ANOVA revealed that no significant difference in XY1DX existed between channel orientation within each canopy class. However, there was a significant difference in XY1DX between canopy classes.

Sullivan et al. (1990) found that EW oriented streams had slightly lower diurnal fluctuations than NS oriented streams. This relationship was examined for the average diurnal fluctuation for the time period between July 21 and August 19, 1998, for 243 FSP sites. Diurnal fluctuation values (daily maximum - daily minimum) for 274 FSP sites and 243 FSP sites with watershed areas less than or equal to 18,000 ha (~70 sq mi) did not reveal any significant differences between channel orientation classes (Figure 8.7).

Canopy/channel orientation interaction and average 1998 diurnal stream temperature fluctuation was examined for FSP sites with watershed areas less than or equal to 18,000 ha. The results are presented in Figure 8.8. Similar to the comparison of XY1DX (Figure 8.5), there was no significant difference in the diurnal fluctuation between each channel orientation class within a given canopy class (Figure 8.8).

There appears to be a slightly higher diurnal fluctuation in the EW orientation group for the 0-24%, 25-49%, and 75-100% canopy classes, although the differences were not significantly different from the NS orientation group. Greater sample size is required in the lower canopy classes in each of the channel orientation classes to definitively determine whether a difference actually exists.

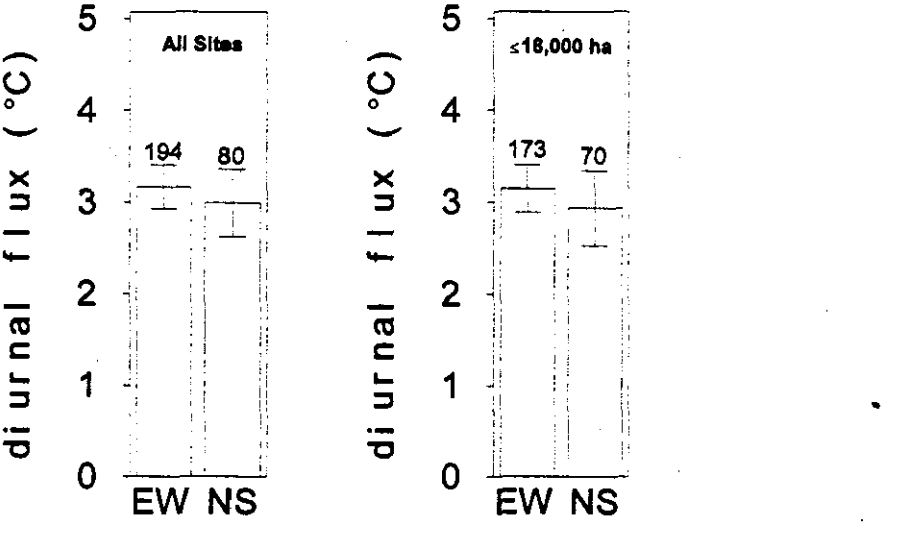

Figure 8.7. Comparison of average diurnal fluctuation by channel orientation class. Diurnal fluctuation averaged for July 21 through August 19, 1998. All sites (A) and sites with watershed area less than or equal to 18,000 ha (B).

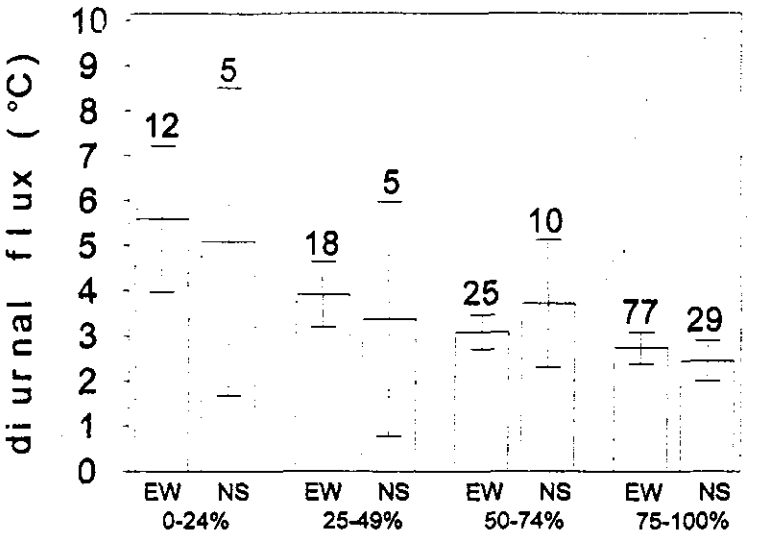

Figure 8.8. Average 1998 diurnal temperature fluctuation by orientation class and canopy class for 181 sites with watershed area less than or equal to 18,000 hectares (~70 sq. mi.). EW = streams with east-west or west-east orientations; NS = streams with north-south or south-north orientations. Error bars represent two standard deviations. Number of sites in each orientation class is shown above the error bars.

Influence of Channel Gradient on Stream Temperatures

Channel gradient is an important factor influencing stream temperature. Gradient may be correlated with other variables such as flow, bankfull width, elevation, distance from watershed divide, and channel type. While gradient is correlated with other variables, it may be more responsive to more localized channel characteristics that are not discernable with other independent variables. Gradient may serve as a surrogate for flow, and hence its significance and inclusion in the empirical models described in Chapter 10. Very few flow measurements were collected by FSP cooperators, too few to be used in a regional assessment.

Channel gradient is determined by measuring the change in vertical distance over a given horizontal distance. Gradient may be expressed in m/km, ft/mi, or percentages. Channel gradient was a GIS-derived variable in FSP's stream temperature assessment.

The average gradient along a 600-m reach upstream from the stream monitoring point was determined using an Avenue script macro program executed in Arc View. A 30-m digital elevation model was used with digital raster graph images of 1:24,000 USGS quadrangles. A more detailed description of the procedure can be found in Chapter 2 - Methods. The avenue script code can be found in Appendix A.

Figure 8.9 shows the distribution of channel gradients for streams where temperature was monitored in 1998. There were 60 sites with gradients of zero. There were 23 sites that had negative values due to their low gradients and the inability to determine these low gradient streams with existing digital elevation models. Gradients ranged from zero (including negative gradient values) to 24%, with about 80% of the sites having gradients between zero and 5%. Thus, a large majority of temperatures was measured at sites with gradients potentially suitable for coho salmon.

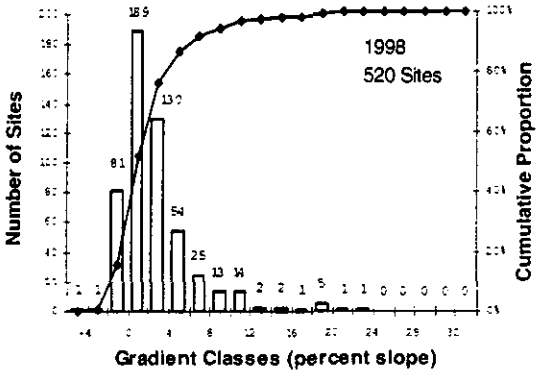

Figure 8.9. Distribution of 1998 stream temperature monitoring sites by channel gradient classes. Gradient was derived in GIS along a ~600-m reach upstream from the stream temperature monitoring site.

Variation in the highest 1998 daily maximum stream temperature (XY1DX) with channel gradient is presented in Figure 8.10. There was a decreasing trend in XY1DX with increasing gradient. This trend may have several underlying mechanisms. As gradient increases, the distance from the watershed divide and drainage area decreases. Stream temperatures are expected to be cooler closer to the headwaters. Streams become narrower at higher gradients, thereby making riparian vegetation more effective in providing shade.

The average XY1DX for all channel gradient classes (Figure 8.10-A) was less than 26°C, the upper lethal incipient threshold for juvenile coho salmon. Subtracting a two-degree safety margin from the upper lethal incipient threshold, as suggested by Coutant (1972), offers another reference temperature which to compare stream temperatures against. None of the channel-gradient-class XY1DX averages exceeded the safety-margin reference value (Figure 8.10-B). However, examination of the scatter plot shows that at many sites, both the 26°C and 24°C reference values were exceeded. At channel gradients greater than approximately 10%, temperatures did not exceed the lower reference value. However, channel gradients greater than 10% are probably too steep to serve as potentially suitable habitat for juvenile coho. Steelhead trout can be found in high-velocity/high-gradient streams (Barnhart, 1986).

Analysis of variance using the PROC GLM procedure in SAS (SAS, 1985) revealed that for 518 sites in 1998, channel gradient explained about 10% of the variability in XY1DX, XYA7DA, and XYA7DX. All three models had significant F values. Channel-gradient class averages for the three temperature metrics were significantly different at the 0.0001 level. Channel gradient was considered an important variable for inclusion in the empirical models presented in Chapter 10. The four gradient classes were used as categorical variables in the models.

Influence of Habitat Type on Stream Temperatures

While the Forest Science Project Stream Temperature Protocol (Appendix A) calls for placement of temperature sensors in well-mixed habitats, e.g., riffles and runs, many data contributors placed their sensors in pools. There was no overriding sampling design. Each organization had their own objectives for monitoring temperature, which often included characterization of the extent of cold water refugia.

Figure 8.11 presents the distribution of sites monitored in 1998 by habitat type. Out of 518 sites for which complete, uninterrupted temperature data were available between July 21 and August 19, 466 sites had non-null habitat type values. About 50% of the sites were in either riffles or runs. The remaining 50% were in shallow pools, medium-depth pools, or deep pools.

Figure 8.12 shows the average XY1DX for each habitat type. Riffle and run sites had average XY1DX values only slightly higher than SPOOL sites. DPOOL sites exhibited the highest average XY1DX. The geographic distribution of all habitat types was not uniform in 1998. A large number of DPOOL sites were located in the southern portion of the SONCC ESU where air temperatures are warmer than the northern portion of the ESU. Additionally, most of the DPOOL sites were located in large systems, such as the lower Eel River, where the

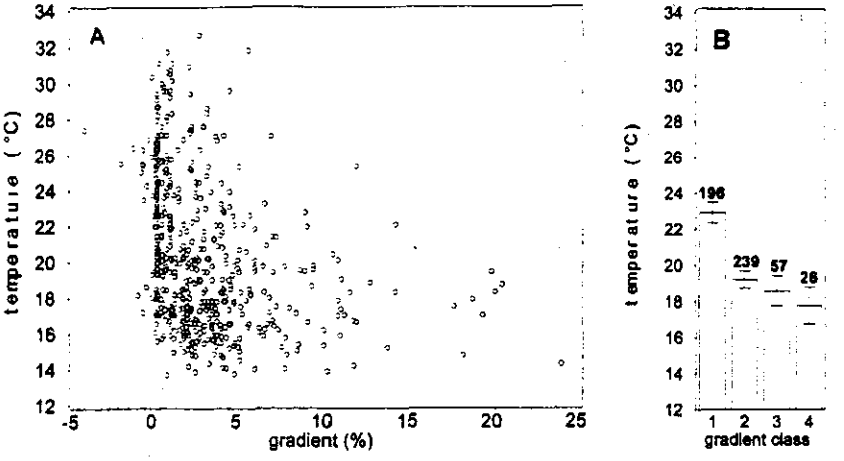

Figure 8.10. Variation in the highest 1998 daily maximum stream temperature (XY1DX) with channel gradient. Scatter plot (A) and bar chart (B). Gradient classes are 1 = <1%, 2 = 1% to <5%, 3 = 5% to <10%, and 4 = >10%. Gradient was derived in GIS along a ~600-m reach upstream from the stream temperature monitoring site.

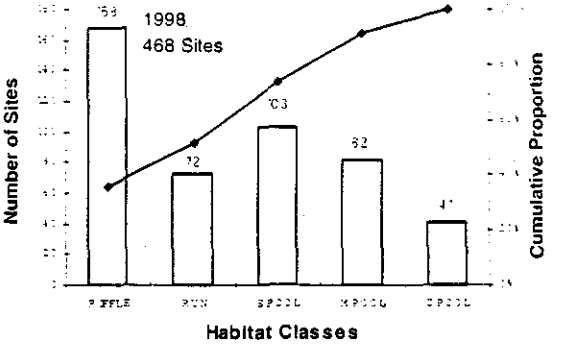

Figure 8.11. Distribution of 1998 stream temperature monitoring sites by habitat type. Plotted line is the cumulative proportion. SPOOL = shallow pool less than 2 ft in depth, MPOOL = medium-depth pool 2 to 4 ft in depth, DPOOL = deep pool greater than 4 ft in depth or pools suspected of maintaining thermal stratification.

stream is too wide for streamside vegetation to provide adequate canopy. Canopy closure was less than 20% in 36 out of the 41 DPOOL sites. The disproportionate geographical distribution of DPOOL sites and the low canopy associated with these sites could account for their higher XY1DX average.

Comparing temperatures in different habitat types across broad geographic areas may be inappropriate, as shown in Figure 8.12, unless the sites are placed in proper geographic context. In any given stream, deep pools are expected to be cooler than riffles or runs from the same stream. A misleading view of stream temperatures can result by having a preponderance of deep pools in a restricted (warmer) geographic area and in predominantly large stream systems. The habitat types used in this assessment are relative terms. A deep pool in a low-order stream may be similar, at least in terms of depth, to a riffle or run in a high-order stream.

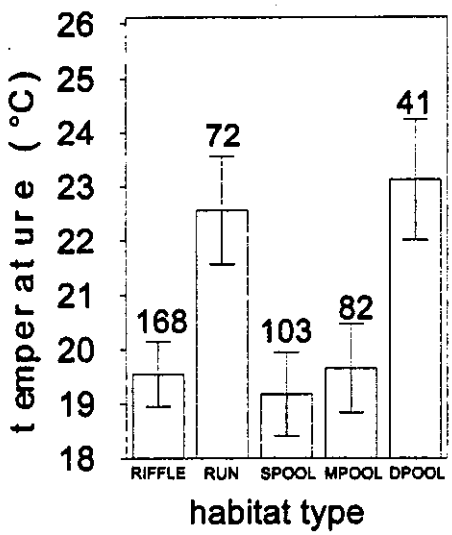

Figure 8.12. Average of the highest 1998 daily maximum stream temperature by habitat type. Habitat types are defined in Figure 8.11 caption. Error bars represent ±2 standard deviations. Number of sites in each habitat type are shown above error bar.

Influence of Bankfull Width on Stream Temperatures

The number of sites for which bankfull width was provided was somewhat limited. In 1998 there were 176 sites for which bankfull width was available. The frequency distribution of 1998 bankfull width values is shown in Figure 8.13-A. Approximately 90% of the sites had bankfull widths less than 32 m. This is the width at which canopy is estimated to become too wide for riparian vegetation to effectively shade streams (See Chapter 9). Figure 8.13-B shows a general increase in stream temperature with bankfull width. Bankfull width is correlated with divide distance and watershed area.

Bankfull width is an important variable in all of the process-based models compared by Sullivan et al. (1990). In empirical models developed by Sullivan et al. (1990) for 36 sites in Washington, bankfull width was highly significant in explaining the variability in stream temperature. In the present study, about 44% of the variability in the highest daily maximum stream temperature was predicted by $\log_{10}$ bankfull width. However, this was based on a small sample size. There is a strong correlation between bankfull width and discharge (Bartholow, 1989). All the heat flux processes in the SSTEMP model, and other process-based models, occur at the air-water or water-ground interface, both interfaces being functions of stream width. Bankfull width is negatively correlated with canopy closure. As streams widen, the ability of riparian vegetation to provide effective shading is diminished. The interplay between bankfull width and canopy is discussed in Chapter 9.

Interactions

The variables discussed in this chapter are strongly correlated with other stream characteristics, such as canopy, divide distance, watershed area, and elevation. Table 8.3 presents a Pearson correlation matrix for three site-specific attributes (channel orientation, channel gradient, and bankfull width) examined in this chapter, canopy (discussed in Chapter 9), and three watershed variables (divide distance, watershed area, and elevation).

The site-specific variables presented here may integrate a cadre of factors that influence stream temperature. However, many of the correlating variables are easier to estimate. Most of the correlating variables were derived in GIS. However, in predicting stream temperatures using variables that correlate well with certain site-specific attributes one loses some amount of site-specific information. In our study, we gain significant numbers of observations by using correlated variables rather than site-specific attributes. Table 8.3 shows the large decrease in sample size when bankfull width (176 sites) or canopy (376 sites) is used in a comparison. Using both bankfull width and canopy in a model would limit the sample size to 161 sites.

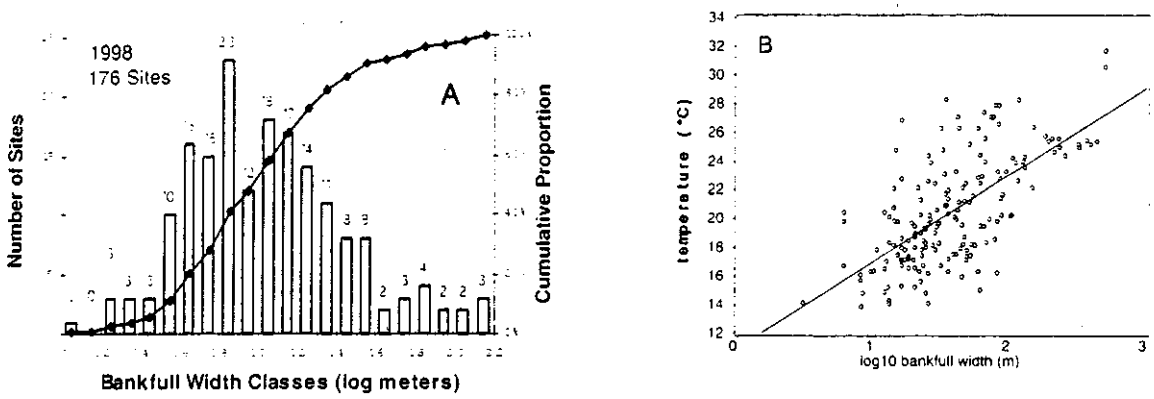

Figure 8.13. Frequency distribution (A) of 176 stream temperature monitoring sites measured in 1998 with non-null bankfull widths. Plotted line is the cumulative proportion. Plot B shows the highest daily maximum temperature versus $\log_{10}$ bankfull width in meters. Regression equation is: XY1DX = 10.9007 + 6.1034*LOGBF, R^2 = 0.4366.

Table 8.3. Pearson Correlation Coefficients for Various Site-Specific and Watershed-Level Attributes for 1998 Stream Temperature Data Set.

	canopy closure	channel gradient	$\log_{10}$ divide distance	$\log_{10}$ watershed area	elevation
$\log_{10}$ bankfull width	-0.6051 <0.0001 161	-0.40051 <0.0001 176	0.80727 <0.0001 176	0.80482 <0.0001 176	-0.23104 0.0020 176
canopy closure		0.30484 <0.0001 376	-0.68279 <0.0001 376	-0.69808 <0.0001 376	-0.05772 0.2643 376
channel gradient			-0.49288 <0.0001 518	-0.49659 <0.0001 518	0.25243 <0.0001 518
$\log_{10}$ divide distance				0.98683 <0.0001 518	-0.10064 <0.0220 518
$\log_{10}$ watershed area					-0.06548 0.1366 518

NOTE: Top number is Pearson correlation coefficient, middle number is probability of correlation due to random chance, and bottom number is number of sites.

Summary

Channel Orientation

Graphical and statistical evaluations of the relationship between XY1DX and channel orientation did not show any significant differences between channel orientation classes. Averages for XY1DX were slightly higher in the EW orientation class, although they were not significantly different from the NS orientation class.

Examination of canopy closure in relation to channel orientation did not show any significant differences between channel orientation class within each canopy class. That is, the interaction between canopy and channel orientation was not significant. However, there were significant differences in stream temperatures across canopy classes, with the lower canopy values showing higher average values for the highest daily maximum stream temperature. Other temperature metrics, i.e., XYA7DA and XYA7DX showed similar trends with respect to channel orientation and canopy closure. The influence of canopy of stream temperature is explored in depth in Chapter 9.

Diurnal fluctuation was compared at each channel orientation for all sites combined and sites with watershed area less than or equal to 18,000 ha. No significant differences were determined. The interactive effects of channel orientation and canopy on diurnal fluctuation was not significant. Similar to the XY1DX, diurnal fluctuation in each canopy closure class showed significant differences, with the lower canopy classes showing higher diurnal fluctuations.

Given all the other factors that have been shown to influence stream temperatures (e.g., canopy, air temperature), channel orientation appears to play a minor role. Due to a lack of significance in the interaction between canopy class and channel orientation, special canopy retention levels for certain channel orientations may not be warranted. Canopy was shown to be significant in influencing stream temperatures. The relationship between canopy and stream temperature is explored in greater depth in Chapter 9.

All sites in our regional stream temperature analysis contained non-missing values for channel orientation due to our ability to derive this attribute in GIS. Out of 548 sites with water temperature data available for regional analyses in 1998, 365 had non-null canopy values, and of these 203 fell in one of the four channel orientation quadrants (Figure 8.3). There was an even greater paucity of canopy data in years prior to 1998. These data voids are a great impediment to our ability to discern regional status and trends in stream temperatures and the factors that control them. A statistically valid sampling design coupled with canopy measurements collected using a consistent protocol is needed to better address the interaction between channel orientation, canopy, and stream temperature.

Channel Gradient

There was a decreasing trend in XY1DX with increasing gradient. This trend may have several underlying mechanisms. As gradient increases, the distance from the watershed divide and drainage area decreases. Stream temperatures are expected to be cooler closer to the headwaters. Streams become narrower at higher gradients, thereby making riparian vegetation more effective in providing shade.

None of the channel-gradient-class XY1DX averages exceeded the 24°C reference value (Figure 8.10-B). However, examination of the scatter plot shows that at many sites, both the 26°C and 24°C reference values were exceeded. At channel gradients greater than approximately 10%, temperatures did not exceed the lower reference value. However, channel gradients greater than 10% are probably too steep to serve as potentially suitable habitat for juvenile coho.

Analysis of variance using the PROC GLM procedure in SAS (SAS, 1985) revealed that for 518 sites in 1998, channel gradient explained about 10% of the variability in the XY1DX, XYA7DA, and XYA7DX temperature metrics. All three models had significant F values. Channel-gradient class averages for the three temperature metrics were significantly different at the 0.0001 level.

Habitat Type

Riffle and run sites had average XY1DX values only slightly higher than SPOOL sites. DPOOL sites exhibited the highest average XY1DX. Comparing temperatures in different habitat types across broad geographic areas may be inappropriate, unless the sites are placed in proper geographic context. In any given stream, deep pools are expected to be cooler than riffles or runs from the same stream. A misleading view of stream temperatures can result by having a preponderance of deep pools in a restricted (warmer) geographic area and in predominantly large stream systems. The habitat types used in this assessment are relative terms. A deep pool in a low-order stream may be similar, at least in terms of depth, to a riffle or run in a high-order stream.

Bankfull Width

Bankfull width is an important variable in many process-based models. In 1998 there were 176 sites for which bankfull width was available. Approximately 90% of the sites had bankfull widths less than 32 m. In the present study, about 44% of the variability in the highest daily maximum stream temperature was predicted by $\log_{10}$ bankfull width. Bankfull width is negatively correlated with canopy closure. As streams widen, the ability of riparian vegetation to provide effective shading is diminished. The interplay between bankfull width and canopy is discussed in Chapter 9.

Chapter 9

INFLUENCE OF CANOPY ON STREAM TEMPERATURES

Introduction

Canopy has been widely acknowledged as influencing stream temperature. Canopy, or some derivative thereof, is an input variable in many process-based stream temperature models. In Sullivan et al. (1990) canopy, in some form, was included in all but one of the six stream temperature models that were evaluated.

It has been shown that timber harvesting or road building that removes riparian vegetation (canopy) increases the water temperature of the adjacent stream. In Northern Coastal California, maximum stream temperature has been documented to increase by as much as 9.4°C (17°F) after complete removal of riparian vegetation (Kopperdahl et al., 1971). The report cites numerous other increases in northern coastal stream temperature after complete removal of riparian canopy. Increased solar radiation due to canopy removal was cited as the primary cause of increased stream temperature.

There is little debate today over the fact that complete removal of riparian vegetation can elevate stream temperatures. Scientific literature abounds documenting increased stream temperature with decreased canopy. The debate today is more over how much canopy must be retained to provide adequate stream protection. Changes made in the 1980's to California's Forest Practice Rules prohibit complete removal of streamside vegetation and require *"at least 50% of the overstory and 50% of the understory canopy covering the ground and adjacent waters shall be left in a well distributed multi-storied stand composed of a diversity of species similar to that found before the start of operations* (CDF, 1999).

What exactly is *canopy*? What may appear as a trivial question is actually quite complex. The canopy that influences stream temperature is more than just the riparian cover over the site where temperature is monitored. Water temperature at a site is a function of both the local site conditions and the temperature of the incoming upstream water. The theoretical upstream distance above a water temperature site where factors, such as air temperature and canopy, influence water temperature is known as a *thermal reach* (TFW, 1993). Once above the thermal reach, different canopy values or other changes in riparian conditions are not expected to affect stream temperature at the downstream terminus of a thermal reach. A study of 14 Oregon streams found that water that was slightly warmer in areas recently clearcut, with 8.6- to 30.5-m buffers along the stream, cooled to "trend line" temperatures, in most cases, within 150 m downstream (Zwieniecki and Newton, 1999). The decrease in canopy affected stream temperature for approximately 150 m. For those streams, the thermal reach may have been about 150 m. However, the larger the stream the slower it is to respond to changes in the physical environment. Thus, larger streams have longer thermal reaches. The length of a thermal reach varies from site to site and is difficult to determine. The notion of thermal reach may be useful from a conceptual standpoint, but may have little operational value because it cannot be measurably defined.

A ***thermal reach*** is a reach with similar (relatively homogenous) riparian and channel conditions for a sufficient distance to allow the stream to reach equilibrium with those conditions. The length of reach required to reach equilibrium will depend on stream size (especially water depth) and morphology (TFW, 1993). A deep, slow moving stream responds more slowly to heat inputs and requires a longer thermal reach, while a shallow, faster moving stream will generally respond faster to changing riparian conditions, indicating a shorter thermal reach. Generally, it takes about 300 meters (or 1000 feet) of similar riparian and channel conditions to establish equilibrium with those conditions in fish-bearing streams.

The canopy of interest is canopy cover over the entire thermal reach. Since the length of a thermal reach varies from site to site and is not clearly understood, it is entirely possible that the canopy that was measured in the field and submitted to the FSP was not the operative canopy that influences stream temperature.

Prior to a discussion on canopy closure and stream temperature relationships it should be pointed out that canopy closure is not the operative variable for assessing trends in stream temperature. In reality, effective shade is the variable that would best correlate with stream temperature. For example, in an east-west flowing stream found at Northern California latitudes the sun on August 1 would be north of the river at midday. If all the shade-producing vegetation was on the north side of the stream, than the effective shade may be near 100%, whereas canopy closure may be only 50%. In the case where shade-producing vegetation was found on both north and south banks, on August 1 the effective shade would still be near 100% and canopy closure may be also be near 100%. The relationship between effective shade and canopy closure should be borne in mind when interpreting the relationships between canopy closure and stream temperature discussed below.

Canopy Measurements

The canopy values submitted to the Forest Science Project for inclusion in the regional stream temperature assessment were collected using a diversity of methodologies. Some cooperators used concave spherical densiometers and measured canopy only at the location where the temperature sensor was deployed. Others, using the same device, measured canopy along a *thermal reach*, the reach length of which varied by cooperator, and submitted average canopy along the reach. The length of the thermal reach along which the canopy was measured was requested from each cooperator. However, often the thermal reach length value was null. Other times, the reported thermal reach length was tens of thousands of meters. Most likely the cooperator submitted the length of the entire tributary.

Some cooperators estimated canopy closure optically. A canopy closure computer-generated card (Figure 9.1) was provided to cooperators for use in 1998 in an attempt to increase the number of sites with non-null canopy values. The card served to calibrate the eye to different canopy levels. The card presented canopy closure in 10% increments, in three different crown geometries. The field person could visually match the canopy closure observed overhead to the nearest canopy closure image on the card. The card is an adaptation of one used by the National Forest Health Monitoring Program (Lewis and Conkling, 1994).

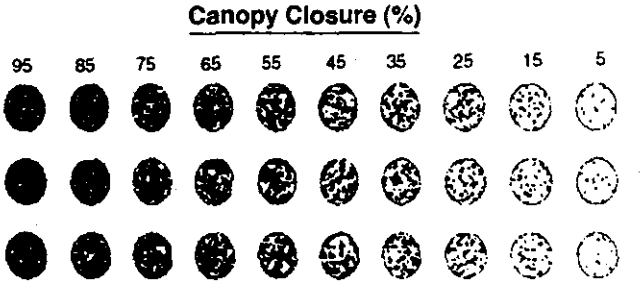

Figure 9.1. Example of computer-generated canopy closure card used by some FSP cooperators to estimate canopy closure at stream temperature monitoring sites.

Considering the different methodologies used to collect canopy data submitted to the FSP, large sources of variability exist. A FSP *Technical Note* can be found in Appendix B that compares different canopy measurement methodologies. The canopy data supplied by the cooperators may represent different attributes of canopy cover and geometry. This leads to two substantial concerns. First, a great amount of "noise" is introduced into fitted models when mixed canopy measurement systems are used. Second, different canopy measurement systems probably have their own characteristic canopy-temperature relationships. Thus, the parameters for any fitted model using canopy data may be a function of the diversity of different methods used to measure canopy. Analyses would be less ambiguous if the same protocol was used for measuring all canopy values at each stream temperature monitoring site.

Distribution of Canopy Data

Figure 9.2 shows the frequency distribution of canopy values in each year. Without a probability-based sampling design, the true distribution of canopy values cannot be determined. There were no canopy data submitted in conjunction with temperature data collected in 1993 and earlier. There were relatively few values submitted for 1994 through 1996. Figure 9.2 shows that the distributions of canopy closure values were not evenly distributed across all canopy bins. There were greater numbers of sites in the lowest (0 - 10%) and highest (90 - 100%) canopy bins than in the midrange of the distribution. It is unknown if the distribution was due to a bias in canopy estimation methods, a bias in site selection, or if the distribution reflects the "true" distribution in canopy values.

Figure 9.3 shows that the geographic distribution of canopy data in each year was not uniformly distributed. In 1995-1997, sites were clustered in the northern and southern portion of the study area. This pattern is particularly true for 1994 through 1996, making them inappropriate for regional analyses. In 1997, data were still somewhat patchy, while 1998 was much more geographically homogeneous. Thus, the focus of this chapter will be on 1998 canopy data.

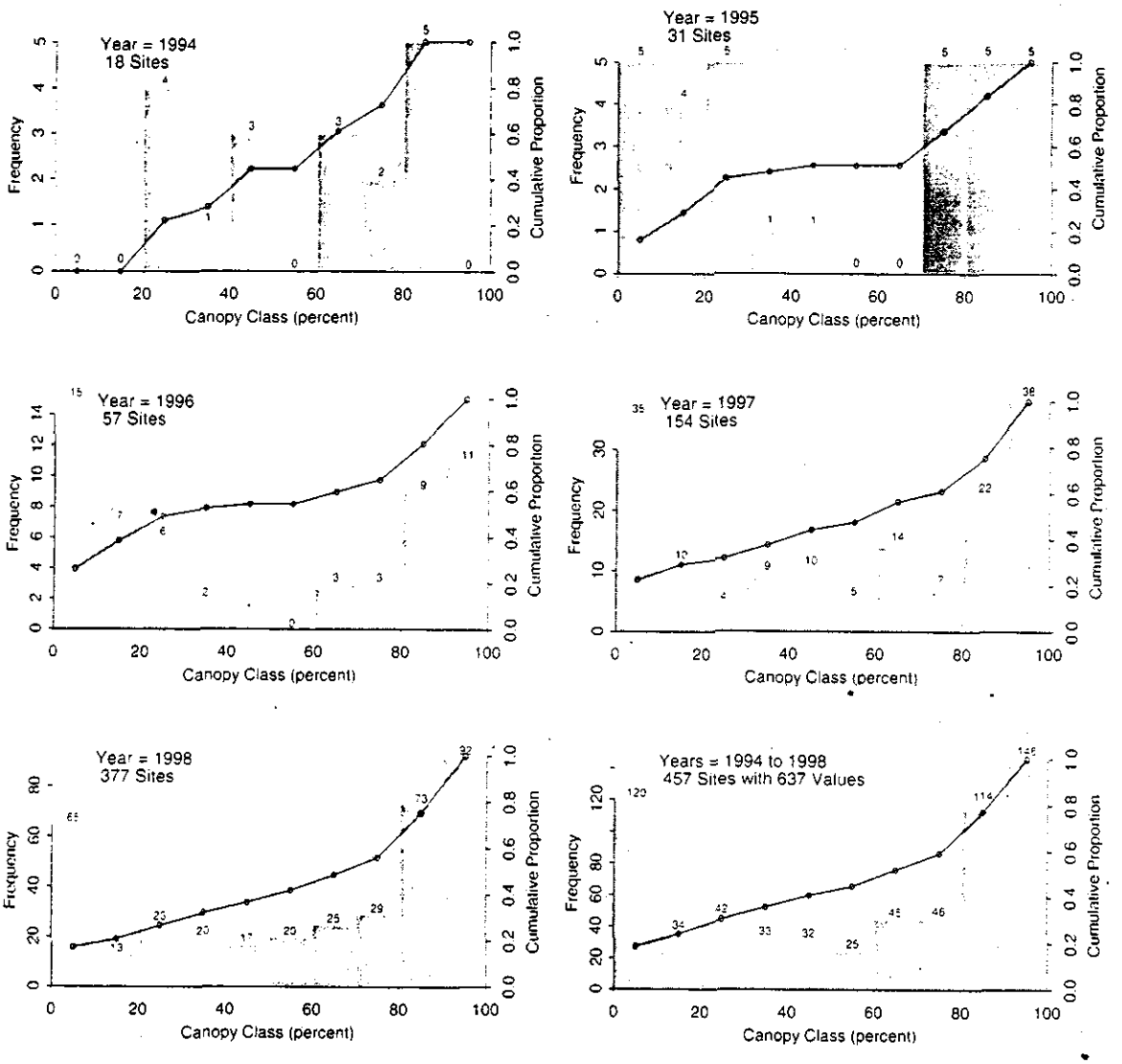

Figure 9.2. Frequency distribution of stream temperature monitoring sites by ten-percent canopy bins for 1994 through 1998 and all years combined. Plotted line is the cumulative proportion.

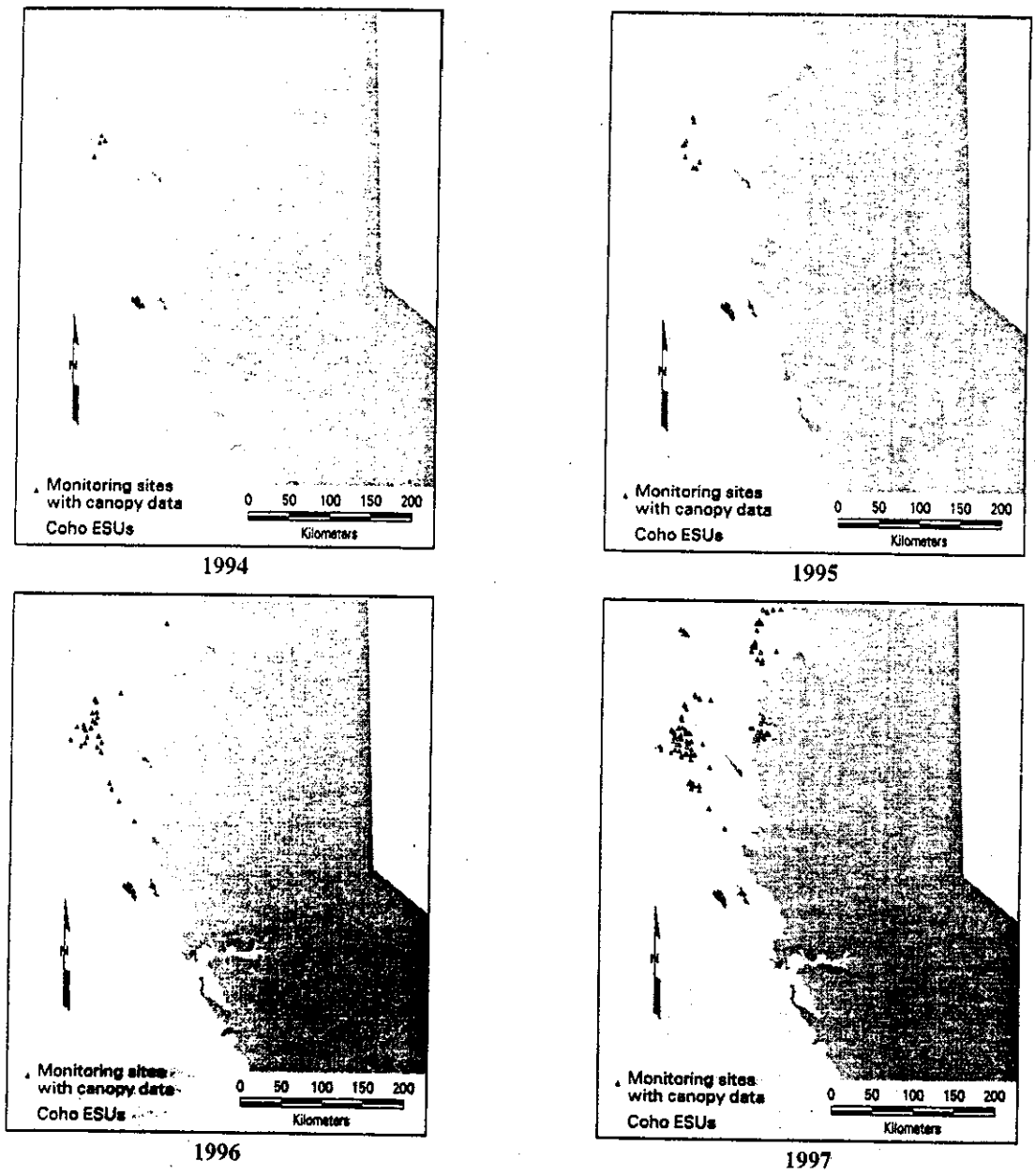

Figure 9.3. Geographic distribution of stream temperature monitoring sites with non-null canopy closure values for 1994 through 1998 and all years combined.

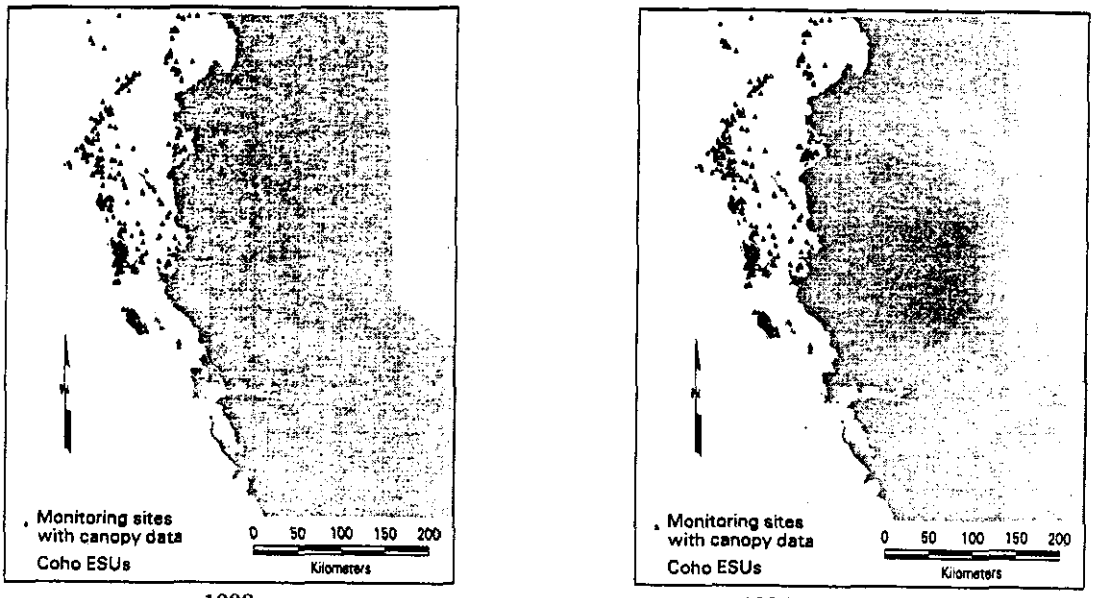

Figure 9.3. (continued)

Threshold Distance

Sullivan et al. (1990) developed the concept of *threshold distance*, that is the distance from the watershed divide at which streams become too wide for riparian vegetation to provide adequate shading. They found that streams seemed to reach an equilibrium temperature at approximately 40-50 km from the watershed divide. At this point, stream temperature was more a function of air temperature than canopy cover. This theoretical threshold distance is a function of channel width and riparian vegetation. Thus, the threshold distance will be different for different drainages and no single value should be applied to all streams. Moreover, as streams widen, the influence of topographic shading diminishes.

The threshold distance concept was explored empirically using data gathered on streams throughout Northern California. Figure 9.4 is a plot of canopy closure versus distance from watershed divide for all 1994-1998 sites with reported canopy closures. At a divide distance greater than 70 km, there were no reported canopy closure values greater than 30%, and most were 10% or less. This suggests that 70 km may be the approximate distance from the divide where streams become too wide for streamside vegetation to have an effect on shading. However, the data were from many basins. Moreover, canopy closure was measured and not effective shade. Thus, this distance is considered the theoretical maximum threshold distance. The threshold distance for some basins may be less than the 70 km. The lack of higher canopy values at distances greater than 70 km from the watershed divide may be a result of relatively few canopy closure measurements at greater distances from the divide and the lack of a sampling design. If a curve (curve b in Figure 9.4) is fit to the outer most points, representing the maximum canopy closure potential for a given distance from watershed divide, a threshold distance becomes much more difficult to define. The decision then becomes what is acceptable and what is realistically achievable. More importantly, the threshold distance is based on contemporary canopy levels along streams and rivers in Northern California and may not be representative of historical levels.

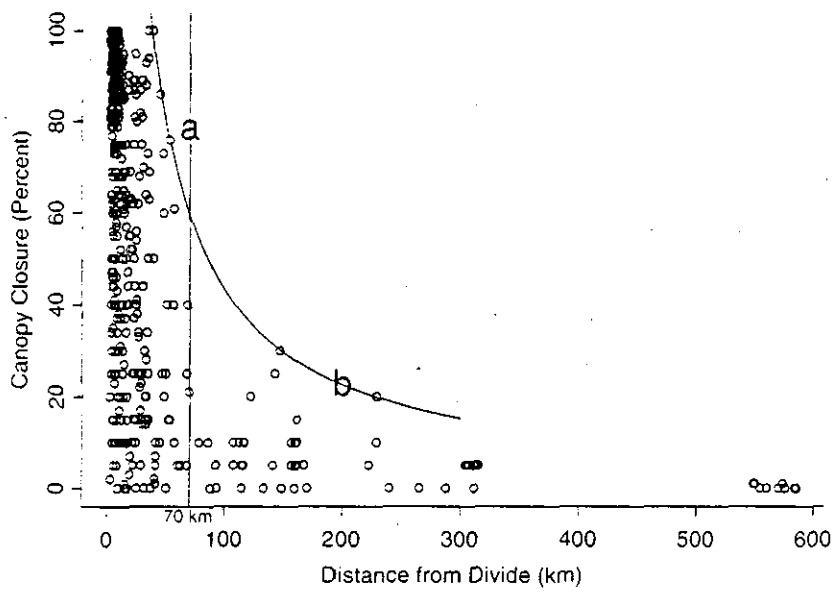

Figure 9.4. Relationship between canopy and distance from watershed divide. The vertical line (a) delineates the theoretical *threshold distance* (70 km) where the stream may be too wide for canopy to influence stream temperature. The curve (b) represents the maximum canopy closure potential a site has at a given distance from watershed divide. Using the points as the only clue to find the threshold distance, 70 km seems like a reasonable choice, but if the curve (b) is appropriate, then defining a threshold might not be recommendable.

Brown and Brazier (1972) found a decline in effectiveness of buffer widths and streamside vegetation with increasing stream size (Figure 9.5). Stream size would correspond to distance from the watershed divide. The shape of the curve in Figure 9.5 is strikingly similar to *curve b* shown in Figure 9.4.

Watershed area is another attribute that will influence channel widths. There may be a watershed area threshold value where channels become too wide to have a significant amount of shade provided by riparian canopy. Figure 9.6 is a plot of canopy closure versus the natural log of watershed area for all 1994-1998 sites with reported canopy closures.

With the exception of two Russian River sites, sites with watershed areas about 63,000 ha or larger had canopy closure values of less than 20%. The Russian River sites had vegetation growing within the bankfull channel and are an exception to this concept. The visually estimated value of 63,000 ha for a watershed area threshold value has similar problems as the distance from watershed divide threshold. This should be viewed as the maximum watershed area threshold. The threshold watershed area value in some basins may actually be less.

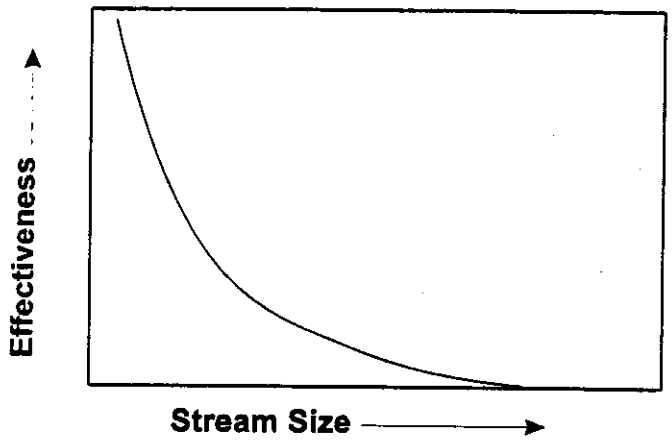

Figure 9.5. Decline in importance of buffer strips (effectiveness) for water temperature control with increasing stream size. Taken from Brown and Brazier (1972).

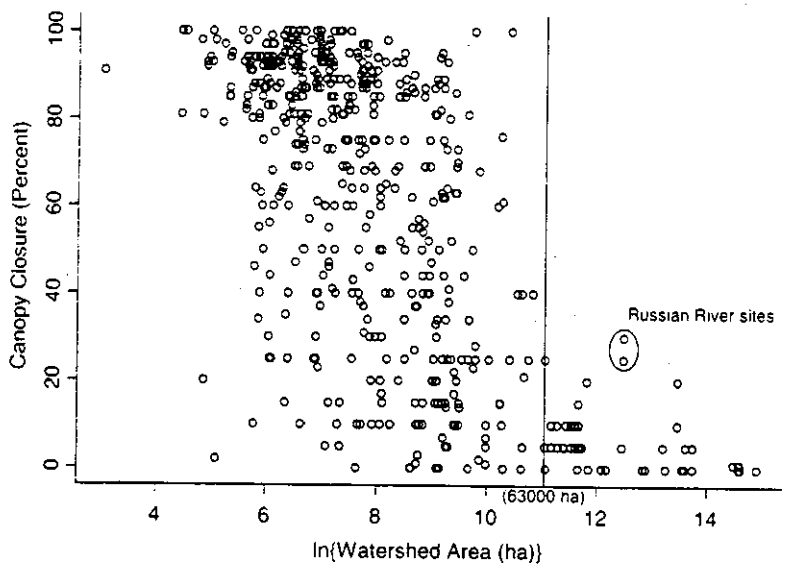

Figure 9.6. Relationship between percent canopy closure and the natural log of watershed area (ha). The vertical line delineates the theoretical *threshold distance* (63,000 ha) where the stream may be too wide for canopy to influence stream temperature. The Russian River sites had vegetation growing in the bankfull channel. Thus, those sites had higher canopy closure values than other large streams.

Watershed area not only provides information on the width of the channel, but also discharge. Flow and canopy interact to influence stream temperature through a simple equation developed by Brown (1969):

$$\Delta T = \frac{A(H_1)}{D}(C)$$

where ΔT is the predicted change in temperature in °F, A is the surface area of the section of stream exposed by riparian vegetation removal, H_1 is the net radiation absorbed by the stream in BTU/ft^2-min, D is the stream discharge in cubic feet per second, and C converts discharge to pounds of water per minute. ΔT is then expressed in BTU/pound of water, which is equivalent to °F.

From the two threshold criteria, stream sites that were small enough to be influenced by canopy closure could be identified. Stream sites that had a distance from watershed divide less the 70 km **and** that had a watershed area less than 63,000 ha were classified as the small-stream group. There were ten sites that had a distance from watershed divide less than 70 km (group minimum was ~52 km) and also had watershed areas greater than 63,000 ha. Additionally, there were two sites that had a distance from watershed divide greater than 70 km and had watershed areas less than 63,000 ha (group minimum was ~52,000 ha). These 12 sites have been classified as too large to have a significant level of canopy from streamside vegetation.

The approach described above is somewhat backwards. A better approach would be to start with the species composition and geometry of riparian vegetation and establish a relationship between maximum potential canopy closure and bankfull width for the existing riparian vegetation. However, the FSP database lacked riparian vegetation data for the stream temperature sites, thus such a relationship could not be established. Instead, the relationship between bankfull width and distance from watershed divide or watershed area was examined to discern if the selected thresholds were reasonable.

A linear regression of the natural log of bankfull width versus the natural log of the distance from watershed divide was fit using the S-PLUS function *lm*. Approximate 95% confidence bands to predict the natural log of bankfull widths for a given natural log of distance from watershed divide was estimated using the S-PLUS function *predict.lm* with the option *se.fit=T*:

$$\hat{b}_d \pm 2\sqrt{r^2 + s.e._d^2}$$

where $\hat{b}_d$ is the estimated natural log of bankfull width at a natural log of distance from watershed divide *d*, *r* is the residual scale from the *predict.lm* output; and $s.e._d$ is the estimated standard error for the average $\hat{b}_d$.

Points for the fitted lines were created by fitting $\hat{b}_d$ and the confidence bands to the vector $\vec{d}$, where $\vec{d}$ is an evenly spaced vector on the interval (0,7). These points were transformed to the original scale, by $e^{(x,y)}$, where *x* is an element of $\vec{d}$ and *y* is either $\hat{b}_d$ or a corresponding confidence value. Figure 9.7 is a scatter plot of bankfull width versus distance from watershed divide with lines drawn by connecting the points $e^{(x,y)}$, yielding the fitted relationship and the approximate 95% confidence bands for prediction.

The divide-distance-defined threshold of 70 km had a mean bankfull width of 32 m with a 95% confidence band for prediction of a particular bankfull width of 10 m to 100 m. However, there were only 14 points for divide-distance values greater than 70 km, compared to 162 points with distances less than or equal to 70 km. Of the larger divide distance points, 10 were from the mainstem Klamath River, two from the mainstem Eel River, and one each from the Salmon and Trinity Rivers. The two Eel River points have much wider bankfull widths than any of the other sites even though the distance from the watershed divide was less than either the Klamath

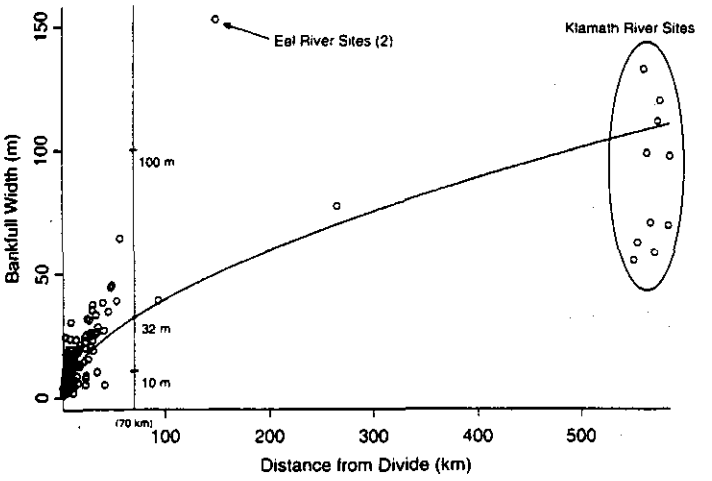

Figure 9.7. Relationship between percent bankfull width (m) and distance from watershed divide (km) with the fitted line (solid line) and the approximate 95% confidence bands for prediction (dotted line). The vertical line delineates the theoretical *threshold distance* (70 km) where the stream may be too wide for canopy to influence stream temperature. The average bankfull width at the threshold distance was 32 m with an approximate 95% confidence interval for predicting bankfull width from a given distance from watershed divide of (10 m, 100 m). The two Eel River sites with high bankfull widths were the only mainstem Eel River sites with reported bankfull widths. All of the points with large distance from watershed divide values were from the mainstem Klamath River.

River or Trinity River sites. The inability of the model to select a well-defined bankfull width given the selected divide-distance threshold is partly due to the large number of different basins used to fit the model. Thus, a single threshold is not a useful assessment tool across all basins. Still, the model indicates that most streams with bankfull widths of 100 m or more would be excluded from the canopy-affected divide-distance group. The intent of this exercise was to remove sites that may be too wide for shade-producing canopy to reach a significant level. It is possible that some sites with bankfull widths slightly greater than 10 m might be excluded, but the low confidence value is due to the high range in Klamath River bankfull widths at large distances from the watershed divide. More bankfull width data is required for each individual basin in order to better define threshold distances.

A model was fit for bankfull width versus watershed area using the same method as the model fit for bankfull width versus distance from the watershed divide. The watershed-area model produced similar results for estimating bankfull width as the divide-distance model. The bankfull width at the threshold watershed area (63,000 ha) had an average of 36 m (compare to 32 m for divide-distance model) and a 95% confidence band for prediction of bankfull width of 13 m to 99 m (Figure 9.8).

Canopy and Stream Temperature Relationships

Three 1998 stream temperature metrics were fit against the reported canopy closure values using the S-PLUS function *lm*. The three stream temperature metrics were (1) the maximum seven-day moving average of the daily average (XYA7DA), (2) the maximum seven-day moving average of the daily

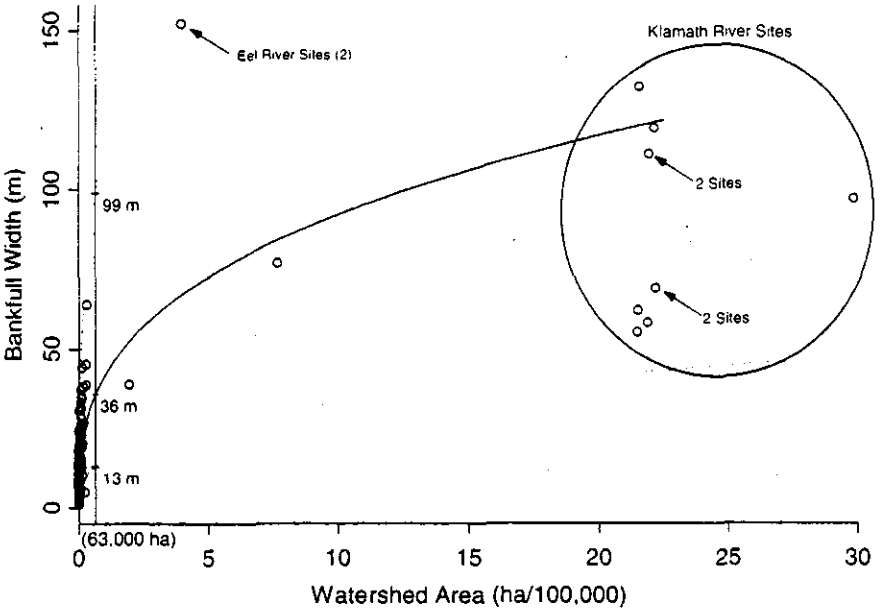

Figure 9.8. Relationship between percent bankfull width (m) and watershed area (ha) with the fitted line (solid line) and the approximate 95% confidence bands for prediction (dotted line). The vertical line delineates the theoretical *threshold distance* (63,000 ha) where the stream may be too wide for canopy to influence stream temperature. The average bankfull width at the threshold distance was 36 m with a approximate 95% confidence interval for predicting bankfull width from a given distance from watershed divide of (13 m, 99 m). The two Eel River sites with the high bankfull widths are the only mainstem Eel River sites with reported bankfull widths. All of the points with large watershed areas (>2,000,000 ha) are from the mainstem Klamath River.

maximum (XYA7DX), and (3) the highest daily maximum stream temperature (XY1DX). R^2 was small for all three regressions (0.232 to 0.286), but the fits were significant ($F = 100$ to 132 on $df = 1$ and 331, $p \approx 0$) with the average stream temperature for all metrics decreasing with increasing canopy closure. Approximate 95% confidence bands were also fit about the line. From the scatter plot (Figure 9.9) and the low R^2 values, it is apparent that there is a high variability in the temperature metrics for all levels of canopy closure. This is due partly to the myriad of other factors influencing stream temperature and partly to the error in measuring stream-temperature-influencing canopy. The confidence bands fit around the regression lines assumed that there was no error in the canopy values, thus the bands do not necessarily capture the true average. However, the true variability is probably lower than the reported data, thus the confidence bands about the relationship using "true" canopy values is probably much tighter.

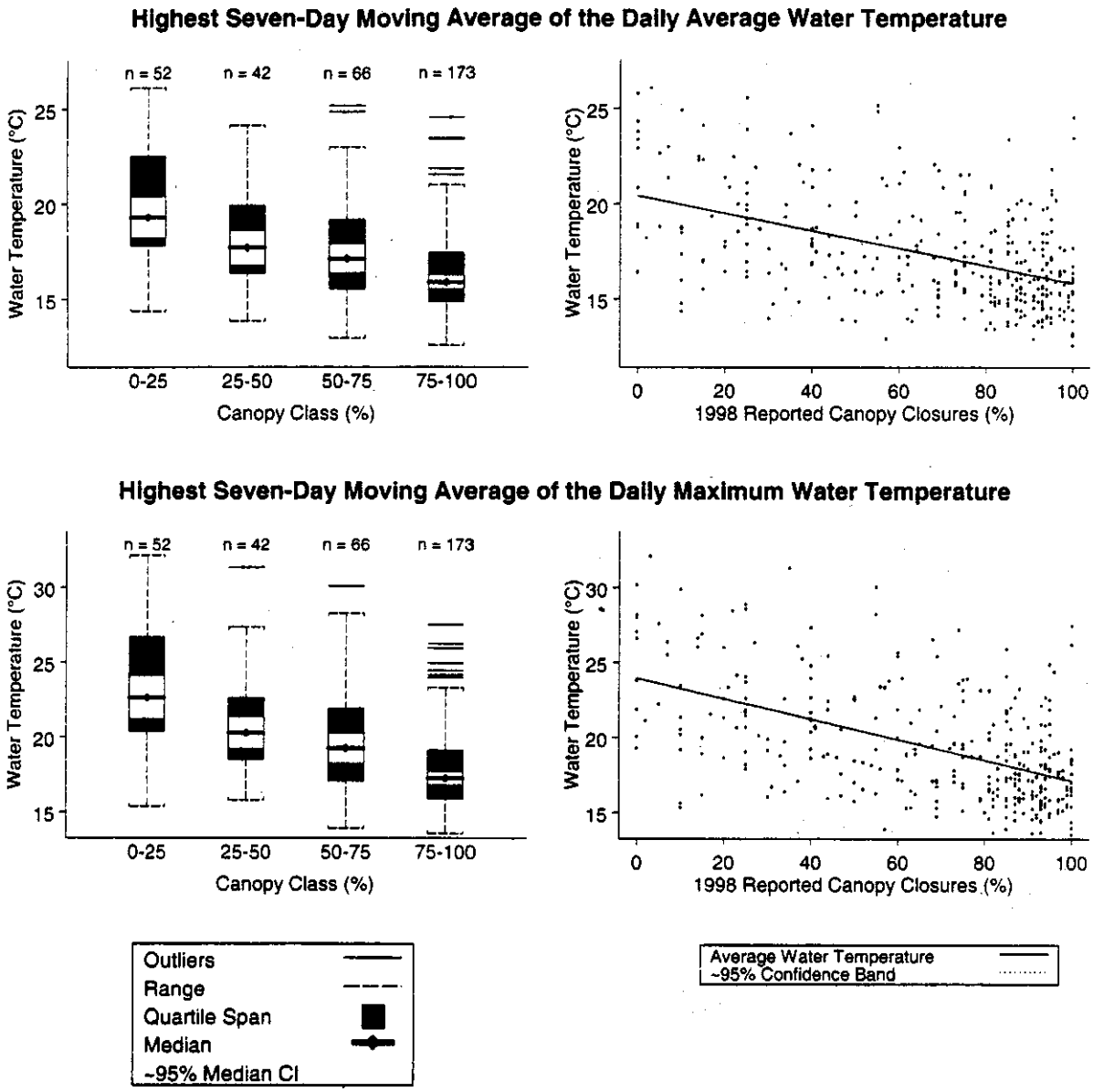

Figure 9.9. Box plot and scatter plot with fitted regression lines for three different stream temperature metrics against canopy. For box plots, canopy values were grouped into four canopy classes. Box plot outliers are defined as 1.5 times the inter-quartile range. The solid regression line is the average stream temperature metric for a given canopy closure, and the dotted lines are 95% confidence bounds for the average temperature values.

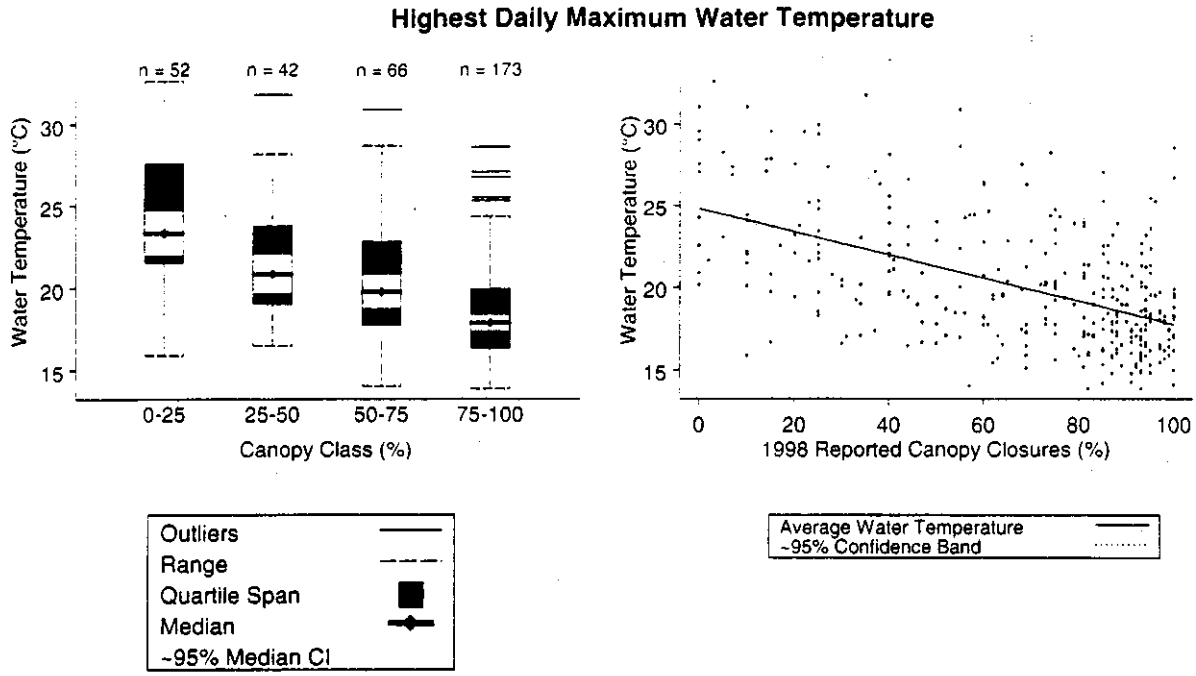

Figure 9.9. (continued)

Because of the uncertainty in the canopy data, the canopy values were combined into 25 percent ranged bins: the bin groups were 0 - 24%, 25 - 49%, 50 - 74%, and 75 - 100. Box plots were created for (1) the highest seven-day moving average of the daily average temperature, (2) the highest seven-day moving average of the daily maximum stream temperature, and (3) the highest daily maximum stream temperature by canopy class using the S-PLUS function *boxplot*. The median and the approximate 95% confidence band for the median of each canopy group was estimated with the *boxplot* function.

The medians for each group for all temperature metrics showed a decreasing trend with increasing canopy (Figure 9.9). The 95% confidence intervals about the medians for the 75 - 100% group did not overlap with and were lower than all other intervals for all temperature metrics (Table 9.1). Although the medians for the 50 - 74% group were lower than the 25 - 49% group, the median confidence intervals overlapped substantially and might not be different for all temperature metrics. The medians for the 50 - 74% group were higher than the 75 - 100% group but the median confidence interval overlapped a minimal amount for XYA7DA. The intervals about the other two metrics between the 50 - 74% and 75 - 100% groups did not overlap. The medians of the three temperature metrics for the 75 - 100% group were lower than the other canopy groups.

A Kruskal-Wallis rank sum test also revealed significant differences in each of the three temperature metrics at various canopy classes. A Welch Modified Two-Sample t-Test for Unequal Variances indicated that the three temperature metrics were significantly different at the $p = 0.01$ level except for the two middle canopy classes, i.e., 25 - 49% and 50 - 74%.

Table 9.1. Median Values and Approximate 95% Confidence Intervals about the Median by Canopy Group for Three Different 1998 Stream Temperature Metrics.

		Canopy Group			
Temperature Metric	**Statistic**	0 - 24%	25 - 49%	50 - 74%	75 - 100%
XYA7DA[1]	Upper CI[4]	20.30°C	18.56°C	17.82°C	16.20°C
	Median	19.29°C	17.70°C	17.12°C	15.89°C
	Lower CI	18.27°C	16.8°C	16.43°C	15.59°C
XYA7DX[2]	Upper CI	24.00°C	21.27°C	20.19°C	17.65°C
	Median	22.64°C	20.27°C	19.26°C	17.27°C
	Lower CI	21.28°C	19.28°C	18.32°C	16.88°C
XY1DX[3]	Upper CI	24.65°C	21.99°C	20.76°C	18.32°C
	Median	23.34°C	20.85°C	19.79°C	17.89°C
	Lower CI	22.03°C	19.71°C	18.82°C	17.46°C

[1]XYA7DA = Highest Seven-Day Moving Average of the Daily Average Temperature

[2]XYA7DX = Highest Seven-Day Moving Average of the Daily Maximum Stream Temperature

[3]XY1DX = Highest Daily Maximum Stream Temperature

[4]CI = approximate 95% confidence interval

NOTE: The highest canopy group of 75 - 100% had statistically lower medians than all other groups for all metrics; there was no overlap in confidence intervals. With the exception of a 0.29 °C overlap between median confidence intervals for the 0 - 25% and 25 - 49% groups, the lowest canopy group had statistically higher median stream temperatures than the other groups.

In Figure 9.9 box plots and scatter plots are displayed side by side. Displayed in this manner, it is clear that there was a trend in higher canopy values or classes resulting in lower stream temperatures, even though the correlation was not high. Much of the variability will be taken into account by other variables that will be explored in the stream temperature modeling chapter (Chapter 10).

Canopy and the Zone of Coastal Influence

The cooling influence of coastal air currents has been shown to influence water temperatures. Does canopy influence stream temperatures in streams inside or outside of the zone of coastal influence (ZCI)? Sites were stratified by whether they fell inside or outside of the ZCI. Sites were then grouped by canopy class. Figure 9.10 shows that there was a significant difference in the highest 1998 daily maximum stream temperature for the 0 - 24% canopy class, with sites outside of the ZCI (encoded as zero) being warmer than sites inside the ZCI. The mean for the 0-24% class outside the ZCI was above the 24°C acute thermal exposure threshold minus a 2°C safety margin (Coutant, 1972). In all canopy classes the mean XY1DX was higher for the ZCI-out group than the ZCI-in group, although not significantly different. Figure 9.10 illustrates that even within the cooler ZCI, stream temperatures decrease with increasing canopy. While air temperatures may be cooler in the ZCI, solar heating still occurs while skies are clear or overcast.

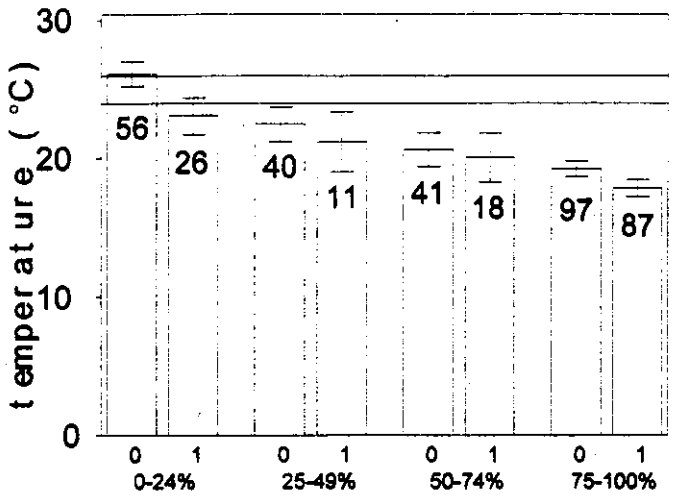

Figure 9.10. Highest 1998 daily maximum stream temperature for sites in four different canopy classes, grouped by whether the site was outside (0) or inside (1) the zone of coastal influence. Horizontal reference lines are drawn at 24°C and 26°C. Number of sites in each group are shown below error bars.

The highest daily maximum stream temperature for sites with canopy greater than or equal to 75% was plotted against $\log_{10}$ divide distance. Sites were stratified by whether they were inside or outside the zone of coastal influence (ZCI). Figure 9.11 shows plots for two HUCs that had adequate representation of sites with canopy ≥75% and sites inside and outside of the ZCI. These HUCs are Mad River - Redwood Creek and Big-Navarro-Garcia. Fully canopied sites inside and outside the ZCI both showed increases in stream temperature with increasing distance from the watershed divide. However, the sites inside the ZCI were 1°C to 2°C lower at similar divide distances than sites outside of the ZCI.

The rate of increase in stream temperature with increasing downstream distance was similar in both the ZCI-out and ZCI-in sites. The two linear regression lines in both HUCs were nearly parallel. Even with high canopy cover, sites inside the ZCI continued to increase in temperature, although the temperatures remained lower than the sites outside the ZCI.

The regression lines shown for the two HUCs (Figure 9.11) could be considered analogous to the "trend lines" developed for single streams in Oregon by Zwieniecki and Newton (1999), although at a much larger HUC scale. It is conceivable and highly desirable that HUC-level or watershed-level regression lines be developed for other drainages that could be used as assessment tools for determining what stream temperatures are achievable under fully canopied conditions. This would require a more integrated stream temperature monitoring program with a well thought out sampling design to provide adequate sample sizes at various divide distances. Additionally, more complete and consistent canopy measurements collected along a thermal reach would need to be part of such a monitoring program.

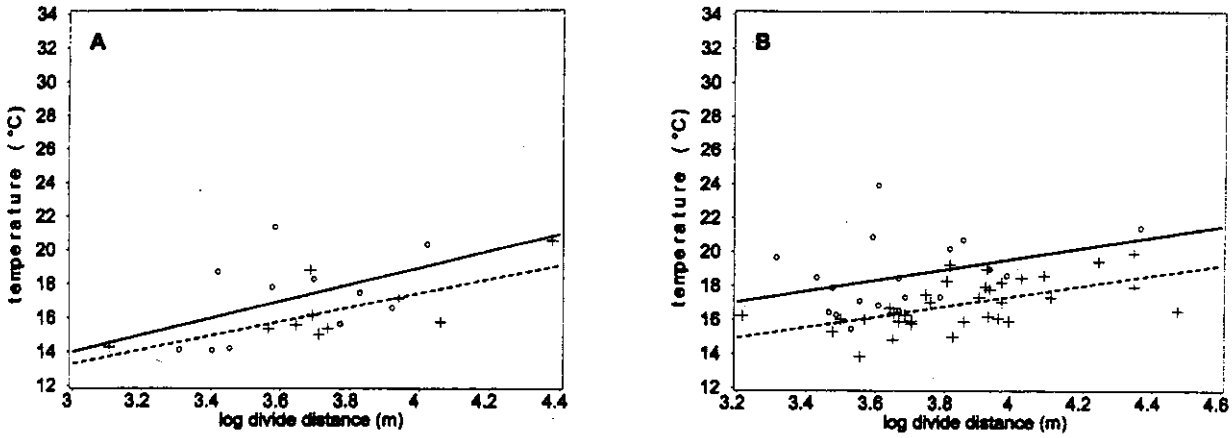

Figure 9.11. Variation in the highest 1999 daily maximum stream temperature with $\log_{10}$ distance from the watershed divide for sites with canopy values greater than or equal to 75%. Sites in the Mad River - Redwood Creek (A) and Big-Navarro-Garcia River (B) hydrologic units are presented. Linear regression lines were fit to sites outside (open circles) and inside (crosses) the zone of coastal influence. Solid lines and dashed lines represent linear regressions for sites outside and inside the ZCI, respectively.

Summary

Canopy values were not well distributed. There were more sites with canopy values in the 0% to 30% bin classes and in the 70% to 100% bin classes. Sites with canopy data were not evenly distributed geographically in 1994-1997. In 1998, sites were more evenly distributed across the study area, thus making 1998 more useful for regional analyses.

Plotting canopy data versus divide distance and watershed area, theoretical maximum thresholds of 70 km and 63,000 ha appear to be plausible for determination of the point where streams may become too wide for streamside vegetation to provide adequate shading. However, these thresholds may vary by basin. The authors do not imply that retention of stream-side vegetation is not important at divide distances greater than the theoretical maximum. We simply attempt to approximate the divide distance at which stream-side vegetation may no longer play a role in mediating stream temperature. There are other important reasons for maintaining stream-side vegetation, such as potential large wood input, sediment retention, and wildlife habitat.

There was a wide range in canopy values in streams at divide distances less than or equal to 70 km and watershed areas less than or equal to 63,000 ha. Despite the diversity of methodologies used to estimate canopy, three stream temperature metrics showed reasonably good response to varying canopy levels. Much of the 'noise" in the temperature-canopy relationship may be due to inconsistent protocols. The variability in stream temperatures due to other independent variables are taken into account in Chapter 10, Modeling.

Sites inside and outside the ZCI with canopy greater than or equal to 75% showed increasing stream temperatures with an increase in distance from the watershed divide. The ZCI-in sites were generally 1 °C to 2 °C cooler than ZCI-out sites, at similar divide distances. The rate of longitudinal temperature increase for ZCI-in and ZCI-out sites with full canopy were very similar (nearly parallel regression lines in Figure 9.11).

While streams that originate in the ZCI and remain within the ZCI along their length exhibit cooler temperatures than those outside the ZCI, it would still be advantageous to maintain adequate canopy. Even within the ZCI, if adequate canopy is not maintained on streams, solar radiation can counteract the cooling influence of coastal air temperatures. Maintaining adequate canopy will provide lower temperatures on both ZCI-in and ZCI-out streams. A goal should be to maximize the total length of low-gradient portions of streams that are potentially suitable for coho salmon by maintaining suitable temperatures in the lower reaches. While all streams tend to come into equilibrium with air temperature along their longitudinal profiles, the downstream distance at which streams approach this equilibrium can be extended by reducing solar heating by maintenance of adequate riparian canopy cover.

While the California Forest Practice Rules require a minimum of 50% canopy retention along Class I and II streams, a random survey of timber harvest plans found that canopy ranged from 74% to 79% (MSG, 1999). In the present study sites located at distances less than the divide-distance-derived and watershed-area-derived threshold distance had canopy values ranging from 0% to 100%. This points out a potential disparity in the way canopy is measured. For compliance purposes canopy is measured in the watercourse and lake protection zone (WLPZ) prior to and following timber harvest. Canopy in the present study was measured in the thalweg of the stream. The objectives and the aquatic resource of concern for why canopy is being assessed should drive the way (method) in which canopy is measured and where (location) it is measured.

To better discern threshold distances and stream temperature differences between canopy classes, a consistent protocol is needed for estimating canopy along thermal reaches above each temperature monitoring site. Additionally, estimates of bankfull width at all temperature monitoring sites would greatly facilitate development of more meaningful threshold distances in a more direct fashion rather than via the more circuitous method applied in this chapter.

Chapter 10

EMPIRICAL MODELING OF REGIONAL STREAM TEMPERATURES

Introduction

This chapter is a culmination of empirical meta-analyses of stream temperatures and various landscape-level and site-specific variables presented throughout previous chapters. It has been illustrated throughout this report that variation in stream temperature is not well explained by any single independent variable, particularly in regional analysis. Many factors influence the thermal regime of running waters. In this chapter, various models are developed that serve to show the interaction of various independent variables that operate at different spatial scales.

Process-Oriented Versus Empirical Models

Many factors act singly and interactively to influence stream temperatures. It is difficult to evaluate the effects of one variable in the absence of other factors. One of the values of process-based models, such as SSTEMP, SNTEMP, and TEMP86, is the ability to vary the factor of interest while keeping all other factors constant (Bartholow, 1989; Sullivan et al., 1990). Such models are better suited to exploration of system changes and alternative aquatic/riparian management scenarios, but at the cost of more intensive data collection, data entry, and manual calibration (Bartholow, 1989). Conversely, one of the advantages of empirical models is the ability to identify streams where temperatures are likely to be affected by climatic and land management constraints (Sullivan et al., 1990). Purely statistical models lend themselves well to temperature prediction when the stream geometry and hydrologic conditions are not expected to change dramatically and long periods of record are available (Bartholow, 1989). However, empirical models are only representative of the geographic location from which the data were collected. Extrapolation outside the area is tenuous.

Applying process-based models to large stream networks has not proven very successful in the past (Sullivan et al., 1990). Acquisition and management of auxiliary data sets to run many process-based stream temperature models at basin-wide scales has been overwhelming to all but the most well-staffed and well-funded organizations. More recent modeling efforts with greater reliance on remotely sensed data and GIS have shown some promise, such as the Hydrologic Simulation Program in Fortran (HSPF) (Bicknell et al., 1997; Chen et al.1998a, 1998b).

Empirical modeling was undertaken in the present study due to a number of constraints that prevented development of a new process-based model or use of an existing one. Intensive data requirements and a small staff were the major reasons for opting for development of empirical models. The level of complexity of empirical models can range from very complex to quite simple. Complex models are good for hypothesis testing, whereas simple models are good for forecasting. If the model is intended to determine uncertainty in risk assessment or to do decision analysis, the level of model complexity is less clear (Bartholow, 1989). The nature of this type of meta-analysis, that is, using data collected with multiple field protocols with varying levels of data quality, limits the analysis to hypothesis formulation. That is, models were developed to propose hypotheses that will then require testing with data collected using a probabilistic sampling design to

select sites that should be monitored using a consistent field protocol.

Hypothesis Formulation

Two of the major factors that control stream water temperature are air temperature and solar radiation. Higher air temperatures and higher solar radiation exposure result in higher water temperature. The position of a site within a watershed is also important in explaining the temperature profile for that location. Sites lower in a watershed tend to have greater water volume, wider channel width (resulting in less effective shade), and generally have had more time to equilibrate with air temperature. The wider the channel, the less effective is stream-side vegetation at shading a stream from solar radiation, and air temperature becomes a more important factor controlling stream temperature at site locations further down in the watershed (Sullivan et al., 1990). Larger volumes of water are slower to respond to changes in both air temperature and solar radiation exposure due to thermal inertia. Some data providers placed probes in pools and, given the possibility of thermal stratification, pools may be cooler than runs or riffles in the same general location. Thus, habitat type may be an important factor influencing water temperature at the sensor. Stream temperature at a particular location may be estimated as a function of air temperature, solar radiation exposure, watershed position, stream size, and habitat type.

Air Temperature

Data from few water temperature sites were submitted with corresponding air temperature data. As a consequence, air temperature data from 72 remote air temperature stations were matched up with each water site (see chapter 5). The remote air temperature station data were summarized by month, which was then matched with daily and weekly water temperature metrics. Daily maximum and seven-day moving average temperature metrics were focused on because of their common usage in assessing stream temperature regimes. With fewer remote air temperature sites available to match up with water sites, a single remote air temperature station may be matched up with many water sites. For example, one air site that had a 1998 July and August average maximum air temperature of 32.45°C was matched up with thirty-one 1998 water sites. The highest 1998 seven-day moving average of the daily maximum water temperature at these 31 sites ranged from 15.5°C to 25.4°C, with a mean of 20.3°C. Water sites were assigned air temperature metrics that were not necessarily well correlated with local air temperature at the water sites (see chapter 5). In an attempt to find better air temperature surrogates for each water site, monthly PRISM estimated air temperature values for the four-km grid cells that contained the water site (see Chapter 4) were evaluated. However, the PRISM data is a 30-year long-term average for each month. As a result, there is no difference in estimated air temperature at each location for different years. Additionally, similar to remote air station data, only monthly data where available.

Some locational information was explored as possible air temperature surrogates. Air temperature tends to cool in a northward direction. The UTM Y-coordinate (UTMY) at each water temperature site may function as a surrogate for the north-south air temperature gradient. Sites located at greater distances from the coast (COASTDIS), or further east, easting estimated by the UTM X-coordinate (UTMX), tend to have warmer air temperatures. Higher elevations, estimated by the UTM Z-coordinate (UTMZ), tend to have cooler air temperatures, excluding sites within the zone of coastal influence (ZCI). Air temperatures within the ZCI (FOG08 = 1) are cooler than air temperatures outside the ZCI (FOG08 = 0). Since the ZCI was derived from PRISM data, there are no between-year differences that can be modeled using purely locational information as surrogates for air temperature.

Direct Solar Insolation

Canopy closure was the only variable available that could be used as a surrogate for direct solar insolation, although channel orientation and topographical shading may also influence the amount of solar radiation reaching the stream. Topographic shading was not available for this regional assessment. Canopy data were collected with different protocols, some of which may not

adequately characterize the canopy closure for an entire thermal reach (see Chapter 9). Thus, there is substantial measurement error in the canopy closure estimates. Moreover, the canopy closure value may not be indicative of the effective shade provided at a given site. Out of 520 sites monitored in 1998, 376 sites had non-null values for canopy closure.

Watershed Position

The further the distance a water temperature site is from the watershed divide and the larger the watershed area above the site, the warmer the expected water temperature for the site. The further a water site is from the watershed divide, the greater is the travel time with the potential for longer exposure to both solar radiation and different air temperature regimes. The longitudinal increase in water temperature as water travels down the stream does not account for localized decreases in water temperature as streams enter areas with different riparian conditions or as they enter the zone of coastal influence. Generally, the larger the watershed area above a stream site the larger the stream. Watershed area was used as a surrogate for stream size. The relationship between distance from watershed divide (DIVIDIS) and watershed area (WAAREA) and several stream temperature metrics were found to be non-linear. The logs of both DIVIDIS (LOGDIVI) and WAAREA (LOGWA) linearized these relationships. Stream gradient measured along a 600-meter reach above the site was also modeled because gradient is highly correlated with watershed position. Stream sites closer to the headwaters tend to have steeper gradients than those lower in the watershed. However, the gradient was approximated in GIS using a 30-meter digital elevation model. Because of uncertainty in the error, gradient was classified into four categories: 1) flat = <1% slope, 2) sloped = 1% to <5%, 3) steep = 5% to <10%, and 4) very steep =>10%. The categorical form of gradient was used in model development.

Stream Size

Bankfull width and depth were requested for all stream temperature sites. However, only 158 bankfull widths and 58 bankfull depths were submitted with canopy and habitat values for the 520 water temperature data sets submitted for 1998. No sites had bankfull width or bankfull depth data for 1997. Bankfull depth and bankfull width were largely excluded from modeling because of the large number of sites with null values. WAAREA and DIVIDIS, and their logs, were considered fairly good surrogates for stream size (See Chapter 9).

Habitat Type

A number of sites for which stream temperature data were submitted were intended for studies to characterize the extent of thermal refugia. About 50% of the 1998 sites had temperature sensors placed in pools, with the other 50% placed in riffles or runs. An analysis of the data indicated that deep pools, medium pools, and shallow pools could be combined into one group (POOL) and that runs and riffles could be combined into another group (RIFFLE_RUN).

Minimum Data Requirements

In addition to the GIS-derived variables that were available for nearly all sites, a site also had to have a reported canopy value and habitat type to be used in model fitting. Inclusion of habitat type in the list of required variables resulted in the loss of nine 1998 sites and four 1997 sites from the data set, after sites with missing canopy values were removed. Table 10.1 shows the number of sites for the coastal and interior ecoprovince, and both ecoprovinces combined, after various data requirements were imposed on the data. Data from 1997 are included in the table because data from this year were used in 1998 model validation analyses.

Models

Three temperature metrics were fit to empirical models: (1) the highest seven-day moving average of the daily average (XYA7DA), (2) the highest seven-day moving average of the daily maximum (XYA7DX), and (3) the highest daily maximum stream temperature (XY1DX). Models for the three stream temperature metrics were developed for two geographic areas, the coastal ecoprovince and the interior ecoprovince, plus a model for both

Table 10.1. Number of Sites for 1997 and 1998 by Ecoprovince with Non-null Canopy and Habitat Type Data (Minimum Requirement to Be Included for Modeling) Provided with the Water Temperature Data, Followed by the Number of Sites with Non-null Bankfull Widths (BFWIDTH) and Bankfull Depths (BFDEPTH).

Year	Independent Variables Available	Ecoprovince		
		Coastal	**Interior**	**Combined**
1997	all GIS-derived variables, canopy, and habitat	100	48	148
1998	all GIS-derived variables, canopy, and habitat	255	110	365
1997	with BFWIDTH	0	0	0
1998	with BFWIDTH	121	37	158
1997	with BFDEPTH	0	0	0
1998	with BFDEPTH	28	30	58

ecoprovinces combined. A total of nine models were developed.

While the average of combined July-August monthly air temperatures were used to model daily and weekly water temperature metrics, we found there to be good correlation between the monthly water temperatures and the daily and weekly water temperature metrics. Sullivan et al. (1990) also noted an unexpectedly close agreement between their 30-day water temperature criterion and the more commonly applied one-day and seven-day temperature metrics found in Washington's water quality standards and forest practice rules.

It was expected that the best models would indicate that stream temperature was a function of air temperature, direct solar radiation, and a few physical stream characteristics. Canopy closure was used as a surrogate for incoming solar insolation, although channel orientation and topographic shading may also be influential in the amount of solar radiation reaching a stream. Physical characteristics such as channel gradient, bankfull width, bankfull depth, whether the stream is in or out of the ZCI, and if the stream is in or out of the California Coastal Steppe Ecological Subregion (i.e., coastal ecoprovince) may influence stream heating processes. Groundwater temperature is believed to be the initial temperature at which water enters the stream (Allan, 1995; Sullivan et al., 1990). Groundwater temperature, estimated from PRISM long-term air temperature data, was also investigated as a possible explanatory variable. Some data providers placed temperature probes in deep pools in an attempt to describe the extent of thermal refugia. Habitat type was investigated to determine whether this categorical variable had an effect. A lack of stream-side air temperature data collected near the water temperature site may have been the largest impediment to developing good stream-temperature prediction models.

Relatively few water temperature sites had corresponding air temperature data. This necessitated using a number of alternatives to estimate air temperature at the stream site. Other studies have found that remote air stations can serve as a reasonable index of near-stream air temperature (Moore, 1967; Sullivan et al. 1990.) However, these studies relate air temperature at one station in a single watershed. Air temperature at a single remote location may be highly correlated with air temperature at a site in a distant watershed. However, the regional modeling described in this study attempted to fit data over a large geographic area. Single remote air temperature stations were related to many water temperature stations. Many different remote air temperature stations were used across the landscape. The result was a poor relationship between remote air temperature and air temperature at the water site when the relationship was examined across all water sites at the regional scale.

Model Selection Methods

Since the data, as a whole, were collected without a central assessment question and numerous protocols were used for measuring stream temperature and

various site-specific attributes, serious model fitting assumptions are violated. Noting that the selected models are only ***working hypotheses***, the process of "data dredging" was utilized. "Data dredging" explores the data set without an *a priori* model, searching for a good fitting model. This procedure has a tendency to over fit the data where unrelated variables are included in selected models exclusively due to chance (Burnham and Anderson, 1998).

As previously stated, 1998 was the most data-rich year and was used for model fitting. There were several sites from 1997 that were suitable for model validation. The first step used a backward elimination stepwise approach with one forward step on the variables listed in Table 10.2.

Table 10.2. List of Variables Used to Start the *Backward Selection with One Forward Step* Modeling Procedure.

Variable	Description
ECO263	Used only in combined ecoprovince model, ECO263 = 1 if in the coastal ecoprovince, otherwise ECO263 = 0.
COASTDIS	Shortest distance from the site to the coast (km)
UTMX.10E4	UTMX coordinate divided by 10,000 (east-west position measurement)
UTMY.10E5	UTMY coordinate divided by 100,000 (north-south position measurement)
UTMZ	Elevation of the site (meters)
CANOPY	Reported Canopy Closure (percent)
MO.MAX3	Average of combined July and August average daily maximum for the nearest remote air station (12-dimensional Euclidian distance) (°C)
MO.MIN3	Average of combined July and August average daily minimum for the nearest remote air station (12-dimensional Euclidian distance) (°C)
MO.AVG3	Average of combined July and August average daily average for the nearest remote air station (12-dimensional Euclidian distance) (°C)
LOGDIVI	Log (base 10) of the GIS estimated distance from site to watershed divide (km)
LOGWA	Log (base 10) of the GIS estimated watershed area above site (hectares)
POOL	if HABITAT = shallow, medium, or deep pool, POOL = 1 if HABITAT = run or riffle, POOL = 0 if HABITAT not reported, POOL = missing value
GRAD2	Gradient Classification: flat = < 1% slope, sloped = 1% to <5%, steep = 5% to <10%, very steep = >10%
FOG08	if site is in the zone of coastal influence defined for August, then FOG08=1 if site is out of the zone of coastal influence defined for August, then FOG08=0
P.MO.MAX	Average of PMAX07 and PMAX08 (PRISM estimated July and August, respectively, maximum air temperatures for the area containing the site (°C)
BFWIDTH	Bankfull width (meters)
BFDEPTH	Bankfull depth (meters)
CANOPY.LOGDIVI	Interaction between CANOPY and LOGDIVI
CANOPY.LOGWA	Interaction between CANOPY and LOGWA
UTMX.UTMY	Interaction between UTMX and UTMY
UTMZ.COASTDIS	Interaction between UTMZ and COASTDIS
LOGDIVI.LOGWA	interaction between LOGDIVI and LOGWA

Preliminary Modeling

At the outset of modeling, there was considerable discussion as to what method was most appropriate: a classical approach using backward selection or the information theory method of Akaike's Information Criterion (AIC: Burnham and Anderson, 1998). While investigating which was more appropriate, a large number of models were developed and AIC scores compared. With the large number of competing models examined, it became obvious there was a high probability that the *best* model (i.e., the one with the lowest AIC score) may include variables by chance and not due to real relationships. Many models had similar AIC scores, and given the chance that some might be slightly better due to chance, it was not readily apparent which models were best. However, a number of variables were always in models with higher, less desirable, AIC scores. These variables (Table 10.3) were not considered in the backward elimination with one forward step procedure discussed below.

Backward Selection

With the assistance of S-PLUS programs, nine models were selected (for three temperature metrics and three geographical extents) using a backward selection approach with one forward step. The backward steps stopped when the probability for the smallest partial F statistic was less than $0.05/k$ where k is the number of variables at the start of the procedure. The partial F-statistic is the F-statistic for each variable as if that variable was the last one to enter the model (Stevens, 1986). The one forward step tested all the removed variables, one at a time, by adding them back into the model to see if the partial F statistic for any of the removed variables became significant ($p < 0.05/k$) by the removal of any of the other variables. Two variables were exceptions to the rules for removal, BFWIDTH and BFDEPTH. The data set that had non-missing values for BFWIDTH and BFDEPTH was small and the sites with non-null values were poorly distributed spatially. These data were provided by only a few organizations and were not representative of the region. Thus, BFWIDTH and BFDEPTH were the first two variables removed from the models.

Interactive terms were entered into the model during the automated S-PLUS process as separate variables. For example, the CANOPY-LOGDIVI interaction term was the product of the CANOPY and LOGDIVI terms. The newly created variable was called CAN.LOGDIV. The new variable was then used in model development. During the backwards procedure if a primary variable of a retained interactive term was dropped from the final model, a new backwards procedure was performed using the selected model and all the dropped primary terms. If the interactive term did not meet the partial F statistic threshold, it was omitted, favoring the primary terms.

Table 10.3. Variables Found to be Poor Predictors of Stream Temperature and Subsequently Removed from Model Development.

Variable	Description
WAAREA	GIS estimated watershed area above site (ha)
DIVIDIST	GIS estimated distance from site to watershed divide (km)
PMAX07	PRISM estimated July maximum air temperature (°C)
PMAX08	PRISM estimated August maximum air temperature (°C)
PMEAN.ANN.AIR	PRISM estimated mean annual air temperature (°C)
SINUOSITY	A measure of curvature along a 600-m reach above the water site
CAZMUTH	Channel orientation (north-south, east-west) along a 600-m reach above the water site
CANOPY.DIVIDIST	Interaction between canopy closure and DIVIDIST
CANOPY.WAAREA	Interaction between canopy closure and WAAREA
DIVIDIST.WAAREA	Interaction between DIVIDIST and WAAREA

Alternative Model Selection and Model Comparisons

Upon examination of the models suggested by the backward selection procedure, alternative models were proposed in an educated search for better air temperature surrogates. One alternative model for each primary model from the backward selection procedure was suggested. The Forest Science Project staff used knowledge gleaned from the analyses reported in preceding chapters, literature reviews, and preliminary model building processes to formulate alternative models. The two models constructed for each of the three 1998 temperature metrics, the backward selected S-PLUS model and its alternative, were compared to each other using their AIC scores. Finally, both models fit to 1998 data were cross validated using 1997 data.

The 1997 data used for model validation were separated into two groups: those that were at the same location as 1998 sites (matched sites) and those that were at different locations than 1998 sites (unmatched sites). A W-statistic, a residual-like statistic, similar to that used by Sullivan et al. (1990) was calculated and averaged for matched, unmatched, and all 1997 sites combined:

$$\overline{W}_{97\,j} = \frac{\sum(\hat{y}_{i_{97\,j},98} - y_{i_{97\,j}})}{n_{97\,j}}$$

where

j is the group (all, matched, or unmatched sites)

$\hat{y}_{i_{97\,j},98}$ is the temperature estimate for the i^{th} 1997 data point estimated by the curve fit to 1998 data;

$y_{i_{97\,j}}$ is the measured temperature metric for the i^{th} 1997 observation from group j; and

$n_{97\,j}$ is the number of observations for group j in 1997.

The average W-statistic is the average error for the fit of the validation data set. If the model fit with the 1998 is good, the average W-statistic for the 1997 estimates should be near zero.

The standard deviation for the W-statistic was calculated as:

$$St.Dev\left(W_{97\,j}\right) = \sqrt{\frac{\sum\left[(\hat{y}_{i_{97\,j},98} - y_{i_{97\,j}}) - \overline{W}_{97\,j}\right]^2}{n_{97\,j} - 1}}$$

Note that the above standard deviation is not suitable for constructing confidence intervals about the average W-statistic. To construct confidence intervals about the average W-statistic, the standard error is required, which can be estimated by 1) squaring the reported standard deviation, 2) multiplying by (n-1), 3) dividing by (n-k-1) where k is the number of covariates used in the model, and 4) taking the square root of the result.

Consistency for all groups was calculated as the proportion of estimates within 2°C of the observed temperature metric.

Results

Backward Selection

In all models, air temperature (or at least surrogates of air temperature), canopy closure, and the log of distance from watershed divide and/or watershed area all were important components influencing water temperature. Additionally, the models selected for the same geographic area in the backward selection procedure for XY1DX and XYA7DX selected the same set of variables, while XYA7DA selected a different subset of variables. Note that when referring to the *backward selection procedure* the one forward step is included in addition to the repeated procedure for removed dependent variables

(covariates) that were retained in interactive terms. For the combined coastal and interior ecoprovince XY1DX and XYA7DX models, the most important covariates selected by the backward selection procedure were ecoprovince, canopy closure, the log of distance from watershed divide, the log of watershed area, habitat type (factored as being in or not in a pool), in or out of the ZCI, UTMX, UTMY, and the interaction between the log watershed area and log distance from divide (Table 10.4).

The most important covariates in the XYA7DA model for the combined ecoprovince data set were elevation, canopy closure, the log of distance from watershed divide, the log of watershed area, in or out of the zone of coastal influence, shortest distance from the coast, UTMX, the canopy and log divide distance interaction, and the elevation and coast distance interaction (Table 10.5). For this model, however, the log of distance from watershed divide, and the shortest distance from the coast did not meet the partial *F* statistic threshold, but interaction terms containing those variables remained significant. The single terms were left in the model to assist in interpreting the role of those variables in influencing the highest seven-day moving average of the daily average stream temperature.

Table 10.4. Linear Regression Results for the Dependent Variables XY1DX and XYA7DX in the Combined Interior and Coastal Ecoprovince Data Sets.

	Dependent Variable							
	XY1DX				XYA7DX			
Independent Variable	**Value**	**Std. Error**	**t value**	**Pr(>|t|)**	**Value**	**Std. Error**	**t value**	**Pr(>|t|)**
(Intercept)	96.929	11.347	8.542	>0.0001	96.383	10.822	8.907	>0.0001
ECO263	-1.778	0.522	-3.406	0.0007	-1.952	0.498	-3.922	0.0001
CANOPY	-3.824	0.524	-7.298	>0.0001	-3.628	0.500	-7.260	>0.0001
LOGDIVI	6.246	1.683	3.711	0.0002	6.400	1.605	3.987	0.0001
LOGWA	4.895	1.163	4.207	>0.0001	4.431	1.110	3.994	0.0001
POOL	-1.051	0.267	-3.935	0.0001	-0.960	0.255	-3.772	0.0002
FOG08	-2.641	0.318	-8.296	>0.0001	-2.507	0.304	-8.257	>0.0001
UTMY.10E5	-1.890	0.183	-10.316	>0.0001	-1.895	0.175	-10.844	>0.0001
UTMX.10E4	-0.352	0.068	-5.158	>0.0001	-0.346	0.065	-5.325	>0.0001
LOGDIVI.LOGWA	-0.963	0.190	-5.065	>0.0001	-0.915	0.181	-5.045	>0.0001

Model Performance		
Statistic	**XY1DX**	**XYA7DX**
Multiple R^2	0.6816	0.6900
Sample size	365	365
Model F-stat	84.43	87.81
df - numerator	9	9
df - denominator	355	355
p(F)	>0.0001	>0.0001

Note: Provided in the upper portion of the table are the coefficient values with their standard error, t-statistic, and the probability that the coefficient value is not different from zero. Model statistics are shown in the lower portion of the table.

Table 10.5. Linear Regression Results for the Dependent Variable XYA7DA in the Combined Interior and Coastal Ecoprovince Data Sets.

	Dependent Variable			
	XYA7DA			
Independent Variable	**Value**	**Standard Error**	**t value**	**Pr(>|t|)**
(Intercept)	-2.319	2.877	-0.806	0.4207
UTMZ	0.005	0.001	6.693	>0.0001
CANOPY	-6.365	1.169	-5.448	>0.0001
LOGDIVI	2.860	1.029	2.780	0.0057
LOGWA	0.068	0.634	0.107	0.9145
FOG08	-1.576	0.257	-6.128	>0.0001
COAST.KM	-0.003	0.009	-0.291	0.7713
UTMX.10E4	0.235	0.046	5.141	>0.0001
CAN.LOGWA	1.179	0.312	3.777	0.0002
UTMZ.COASTKM	0.000	0.000	-7.384	>0.0001
	Model Performance			
Statistic	**XYA7DA**			
Multiple R^2	0.7448			
Sample size	374			
Model F-stat	118.1			
Degrees of freedom - numerator	9			
Degrees of freedom - denominator	364			
p(F)	>0.0001			

NOTE: Provided in the upper portion of the table are the coefficient values with their standard error, t-statistic, and the probability that the coefficient value is not different from zero. Model statistics are shown in the lower portion of the table.

For the XY1DX and XYA7DX interior ecoprovince models, canopy closure, the log of distance from watershed divide, UTMX, UTMY, and the interaction between UTMX and UTMY where all variables selected in the backward procedure (Table 10.6). The XYA7DA model for the interior ecoprovince used the same covariates as the other two models, with the addition of elevation and distance to the coast (Table 10.7).

The XY1DX and XYA7DX coastal ecoprovince models included the variables canopy, log divide distance, log watershed area, habitat type (POOL or RIFFLE_RUN), within or outside ZCI, UTMX, and the interaction between the log watershed area and log divide distance (Table 10.8). From the list of variables for XY1DX and XYA7DX coastal ecoprovince models, the XYA7DA coastal ecoprovince model removed the log of watershed area and the interaction between the logs of watershed area and divide distance, and replaced UTMX with UTMY (Table 10.9).

Table 10.6. Linear Regression Results for the Dependant Variables XY1DX and XYA7DX in the Interior Ecoprovince Data Set.

	Dependant Variable							
	XY1DX				XYA7DX			
Independent Variable	**Value**	**Std. Error**	**t value**	**Pr(>|t|)**	**Value**	**Std. Error**	**t value**	**Pr(>|t|)**
(Intercept)	1581.337	256.396	6.168	>0.0001	1492.37	252.380	5.913	>0.0001
CANOPY	-4.447	0.829	-5.364	>0.0001	-4.083	0.816	-5.003	>0.0001
LOGDIVI	2.348	0.542	4.334	>0.0001	2.389	0.533	4.482	>0.0001
UTMY.10E5	-34.342	5.655	-6.073	>0.0001	-32.385	5.567	-5.818	>0.0001
UTMX.10E4	-29.557	5.244	-5.637	>0.0001	-27.813	5.162	-5.388	>0.0001
UTMY10E5.UTMX10E4	0.647	0.116	5.596	>0.0001	0.608	0.114	5.343	>0.0001
	Model Performance							
Statistic	**XY1DX**				**XYA7DX**			
Multiple R^2	0.7530				0.7495			
sample size	112				112			
Model F-stat	64.61				63.43			
df - numerator	5				5			
df - denominator	106				106			
p(F)	>0.0001				>0.0001			

NOTE: Provided in the upper portion of the table are the coefficient values with their standard error, t-statistic, and the probability that the coefficient value is not different from zero. Model statistics are shown in the lower portion of the table.

Table 10.7. Linear Regression Results for the Dependant Variable XYA7DA in the Interior Ecoprovince Data Set.

	Dependant Variable			
	XYA7DA			
Independent Variable	**Value**	**Standard Error**	**t value**	**Pr(>|t|)**
(Intercept)	1055.258	157.941	6.681	>0.0001
UTMZ	-0.002	0.001	-3.140	0.0022
CANOPY	-2.484	0.532	-4.666	>0.0001
LOGDIVI	2.783	0.402	6.928	>0.0001
COAST.KM	-0.069	0.022	-3.169	0.0020
UTMY.10E5	-23.610	3.461	-6.822	>0.0001
UTMX.10E4	-20.044	3.211	-6.243	>0.0001
UTMY10E5.UTMX10E4	0.455	0.071	6.463	>0.0001
	Model Performance			
Statistic	**XYA7DA**			
Multiple R^2	0.8731			
sample size	112			
Model F-statistic	102.2			
degrees of freedom - numerator	7			
degrees of freedom - denominator	104			
p(F)	>0.0001			

Note: Provided in the upper portion of the table are the coefficient values with their standard error, t-statistic, and the probability that the coefficient value is not different from zero. Model statistics are shown in the lower portion of the table.

Table 10.8. Linear Regression Results for the Dependant Variables XY1DX and XYA7DX in the Coastal Ecoprovince Data Set.

	Dependant Variable							
	XY1DX				XYA7DX			
Independent Variable	Value	Std. Error	t value	Pr(>|t|)	Value	Std. Error	t value	Pr(>|t|)
(Intercept)	-16.836	5.494	-3.065	0.0024	-18.598	5.174	-3.595	0.0004
CANOPY	-4.108	0.608	-6.753	>0.0001	-3.988	0.573	-6.962	>0.0001
LOGDIVI	7.424	1.934	3.839	0.0002	7.619	1.821	4.183	>0.0001
LOGWA	4.965	1.373	3.616	0.0004	4.659	1.293	3.603	0.0004
POOL	-1.278	0.287	-4.451	>0.0001	-1.206	0.270	-4.461	>0.0001
FOG08	-1.949	0.306	-6.378	>0.0001	-1.774	0.288	-6.164	>0.0001
UTMX.10E4	0.232	0.065	3.551	0.0005	0.252	0.062	4.097	0.0001
LOGDIVI.LOGWA	-1.095	0.253	-4.335	>0.0001	-1.080	0.238	-4.542	>0.0001

Model Performance		
Statistic	XY1DX	XYA7DX
Multiple R^2	0.6819	0.6917
sample size	255	255
Model F-stat	75.64	79.18
df - numerator	7	7
df - denominator	247	247
p(F)	>0.0001	>0.0001

Note: Provided in the upper portion of the table are the coefficient values with their standard error, t-statistic, and the probability that the coefficient value is not different from zero. Model statistics are shown in the lower portion of the table.

Table 10.9. Linear Regression Results for the Dependant Variable XYA7DA in the Coastal Ecoprovince Data Set.

	Dependant Variable			
	XYA7DA			
Independent Variable	Value	Std. Error	t value	Pr(>|t|)
(Intercept)	34.399	4.854	7.086	>0.0001
CANOPY	-1.909	0.388	-4.918	>0.0001
LOGDIVI	3.769	0.239	15.765	>0.0001
POOL	-0.881	0.187	-4.703	>0.0001
FOG08	-1.712	0.185	-9.259	>0.0001
UTMY.10E5	-0.669	0.109	-6.118	>0.0001

Model Performance	
Statistic	XYA7DA
Multiple R^2	0.7588
sample size	255
Model F-stat	156.7
degrees of freedom - numerator	5
degrees of freedom - denominator	249
p(F)	>0.0001

Note: Provided in the upper portion of the table are the coefficient values with their standard error, t-statistic, and the probability that the coefficient value is not different from zero. Model statistics are shown in the bottom portion the table.

Alternative Model Selection and Model Comparisons

Combined Ecoprovinces

Most of the suggested alternative models contained various air temperature metrics. Backward selection XY1DX and XYA7DX models for combined ecoprovinces contained the covariates ecoprovince, canopy closure, the log of distance from watershed divide, the log of watershed area, habitat type, in or out of the zone of coastal influence, UTMX, UTMY, and the interaction between the logs of watershed area and distance from divide. The alternative models used the PRISM estimated 30-year August average maximum air temperature (PMAX08) in place of UTMY and UTMX and removed the interaction term between the log of divide distance and the log of watershed area.

The alternative model was compared to the primary model (the model selected by the backward selection procedure) for XY1DX and XYA7DX (Table 10.10). For both stream temperature metrics the primary model had better AIC scores and higher R^2 values for the 1998 data. Generally, the mean W-statistic for all 1997 sites favored the alternative model (Table 10.10).

For XY1DX, the mean W-statistic for the 1997 matched and unmatched groups favored the primary model, but the statistics for the groupings in the alternative models had opposite signs resulting in an average W-statistic that favored the alternate model. Consistency values, that is the proportion of sites that had estimates within 2°C of the observed value, for the 1997 all-sites-combined validation comparisons favored the alternative XY1DX and XYA7DX models.

For the combined ecoprovince XYA7DA model, a similar change in variables was made in the alternative model. Air temperature surrogate variables (distance from coast, UTMX, elevation, and the elevation and coast distance interaction) were replaced with the same PRISM estimated 30-year August average maximum air temperature metric (PMAX08). The results of model comparisons were more complicated than previous comparisons. While the AIC score and the 1998 R^2 still favored the primary model, the 1997 W-statistics mostly favored the primary model as well. An exception was noted for the unmatched 1997 sites, with slightly lower mean W-statistics and higher consistency values for the alternative model.

Interior Ecoprovince

For the interior ecoprovince XY1DX, XYA7DX, and XYA7DA models, P.MO.MAX replaced UTMX, UTMY, and the UTMX-UTMY interaction as the air temperature surrogate for the alternative models (Table 10.11). Additionally, all alternative models used the canopy closure - log divide distance interaction term, which was not selected for any of the primary models. For all model comparisons, the primary model out performed the alternative model (Table 10.11). Though mixed, the W-statistics mostly favored the primary models. Still, the AIC score and R^2 values showed that the primary models were much better, but the cross validation statistics using the 1997 data indicated that the primary models were only marginally better.

Coastal Ecoprovince

The alternative models for XY1DX and XYA7DX in the coastal ecoprovince used PMAX08 and distance from coast as air temperature surrogates in place of UTMX used by the primary models (Table 10.12). The AIC score and the R^2 values were better for the primary model. However, the alternative models generally fit the 1997 data better (Table 10.12). The only exception was the W-statistics for the primary XY1DX models were slightly better than those for the alternative models. The alternative model for XYA7DA in the coastal ecoprovince similarly used PMAX08 and distance from coast as air temperature surrogates in place of UTMY (Table 10.12). Like the other models, the AIC and R^2 values were better for the primary XYA7DA model, while the 1997 data were better fit by the alternative model as indicated by lower W-statistics.

Table 10.10. Comparison of Combined-Ecoprovince Models Produced in the Backward Selection Procedure (Primary Columns) and an Alternative Model for XY1DX, XYA7DX, and XYA7DA.

	Dependent Variable Model					
	XY1DX		XYA7DX		XYA7DA	
Independent Variable	**Primary**	**Alternative**	**Primary**	**Alternative**	**Primary**	**Alternative**
(Intercept)	96.929	5.259	96.383	3.733	-2.319	1.629
COASTDIS	0	0	0	0	-0.003	0
UTMX.10E4	-0.352	0	-0.346	0	0.235	0
UTMY.10E5	-1.890	0	-1.895	0	0	0
UTMZ	0	0	0	0	0.005	0
CANOPY	-3.824	-4.148	-3.628	-3.958	-6.365	-4.914
LOGDIVI	6.246	2.674	6.400	3.060	2.860	4.069
LOGWA	4.895	0.348	4.431	0.071	0.068	-0.604
POOL	-1.051	-0.386	-0.960	-0.295	0	0
FOG08	-2.641	-1.252	-2.507	-1.107	-1.576	-0.687
PMAX08	0	0.191	0	0.195	0	0.125
ECO263	-1.778	1.785	-1.952	1.616	0	0
CANOPY.LOGWA	0	0	0	0	1.179	0.870
UTMZ.COASTDIS	0	0	0	0	-9.3E-5	0
LOGDIVI.LOGWA	-0.963	0	-0.915	0	0	0
Statistic	**Model Performance**					
AIC	645.1271	756.1424	610.5244	729.2842	380.6189	492.7467
R^2_{98}	0.6816	0.5636	0.6900	0.5661	0.7518	0.6570
$Consistency_{98}$	0.6274	0.5699	0.6685	0.5726	0.8137	0.7096
n_{98}	365	365	365	365	365	365
$W_{97\text{-}ALL}$	0.2562	-0.0839	0.3514	0.0102	0.4804	-0.1589
St Dev.($W_{97\text{-}ALL}$)	2.2872	2.1141	2.1664	2.0401	1.4148	1.5248
$Consistency_{97\text{-}ALL}$	0.6486	0.6892	0.6757	0.6959	0.8514	0.8378
$n_{97\text{-}ALL}$	148	148	148	148	148	148
$W_{97\text{-}match}$	0.1706	-0.3562	0.2639	-0.2610	0.4404	-0.3678
St Dev.($W_{97\text{-}match}$)	2.0492	1.8879	1.9163	1.8021	1.1871	1.4175
$Consistency_{97\text{-}match}$	0.6701	0.7010	0.7010	0.7216	0.9072	0.8454
$n_{97\text{-}match}$	97	97	97	97	97	97
$W_{97\text{-}unmatch}$	0.4190	0.4339	0.5180	0.5262	0.5564	0.2383
St Dev.($W_{97\text{-}unmatch}$)	2.6975	2.4248	2.5892	2.3635	1.7806	1.6529
$Consistency_{97\text{-}unmatch}$	0.6078	0.6667	0.6275	0.6471	0.7451	0.8235
$n_{97\text{-}unmatch}$	51	51	51	51	51	51

Note: Column values are coefficients for independent variable. A zero value indicates the variable was not used in that model. *The lower portion of the table presents comparative model performance statistics. Comparisons should only be made between* primary and alternative models within the same dependent variable. Lower AIC values indicate a *better* model. R^2 values are reported for the 1998 sample. 1997 data are grouped as: (1) all sites combined (ALL), (2) 1997 sites at the same location as 1998 sites (match), and (3) 1997 sites at different locations than 1998 sites (unmatch). W-statistic is the average error for the validation data set. Consistency is the proportion of sites with estimates within 2°C of the observed value.

Table 10.11. Comparison of Interior Ecoprovince Models Produced in the Backward Selection Procedure (Primary Columns) and an Alternative Suggestion for XY1DX, XYA7DX, and XYA7DA.

	Dependent Variable Model					
	XY1DX		XYA7DX		XYA7DA	
Independent Variable	**Primary**	**Alternative**	**Primary**	**Alternative**	**Primary**	**Alternative**
(Intercept)	1581.337	1.327	1492.37	-0.471	1055.258	-1.235
COASTDIS	0	0	0	0	-0.069	-0.052
UTMX.10E4	-29.557	0	-27.812	0	-20.044	0
UTMY.10E5	-34.342	0	-32.384	0	-23.610	0
UTMZ	0	0	0	0	-0.002	0.002
CANOPY	-4.447	-22.082	-4.083	-21.683	-2.484	-12.570
LOGDIVI	2.347	1.021	2.389	1.071	2.783	2.226
P.MO.MAX	0	0.592	0	0.615	0	0.461
CANOPY.LOGDIVI	0	4.279	0	4.272	0	2.627
UTMX.UTMY	0.647	0	0.608	0	0.455	0
Statistic	**Model Performance**					
AIC	190.5035	273.4447	187.1549	266.5003	84.5871	181.6462
R^2_{98}	0.7533	0.4661	0.7497	0.4756	0.8722	0.6854
$Consistency_{98}$	0.700	0.4909	0.7182	0.4909	0.9091	0.6545
n_{98}	110	110	110	110	110	110
$W_{97\text{-}ALL}$	0.287	-0.5936	0.3008	-0.5832	0.6218	0.5293
St Dev.($W_{97\text{-}ALL}$)	2.0027	2.3263	1.8848	2.2817	1.2864	1.6245
$Consistency_{97\text{-}ALL}$	0.687	0.6875	0.7500	0.6875	0.8542	0.8125
$n_{97\text{-}ALL}$	48	48	48	48	48	48
$W_{97\text{-}match}$	0.661	-0.7013	0.6548	-0.6981	0.6901	0.4242
St Dev.($W_{97\text{-}match}$)	1.8045	1.8077	1.6967	1.7212	1.0958	1.3717
$Consistency_{97\text{-}match}$	0.666	0.7222	0.7222	0.7222	0.8889	0.8333
$n_{97\text{-}match}$	36	36	36	36	36	36
$W_{97\text{-}unmatch}$	-	-0.2703	-0.7612	-0.2385	0.4168	0.8444
St Dev.($W_{97\text{-}unmatch}$)	2.2219	3.5458	2.0924	3.5560	1.7857	2.2680
$Consistency_{97\text{-}unmatch}$	0.750	0.5833	0.8333	0.5833	0.7500	0.7500
$n_{97\text{-}unmatch}$	12	12	12	12	12	12

Note: Column values are coefficients for independent variables. A zero value indicates the variable was not used in that model. The lower portion of the table presents comparative model performance statistics. Comparisons should only be made between primary and alternative models within the same dependent variable. Lower AIC values indicate a *better* model. R^2 values are reported for the 1998 sample. 1997 data are grouped as: (1) all sites combined (ALL), (2) 1997 sites at the same location as 1998 sites (match), and (3) 1997 sites at different locations than 1998 sites (unmatch). W-statistic is the average error for the validation data set. Consistency is the proportion of sites with estimates within 2°C of the observed value.

Table 10.12. Comparison of Coastal Ecoprovince Models Produced using the Backward Selection Procedure (Primary Columns) and an Alternative Model for XY1DX, XYA7DX, and XYA7DA.

	Dependent Variable Model					
	XY1DX		XYA7DX		XYA7DA	
Independent Variable	Primary	Alternative	Primary	Alternative	Primary	Alternative
(Intercept)	-16.836	-12.316	-18.598	-13.370	34.399	2.006
COASTDIS	0	-0.005	0	-0.011	0	-0.022
UTMX.10E4	0.232	0	0.252	0	0	0
UTMY.10E5	0	0	0	0	-0.669	0
CANOPY	-4.108	-4.228	-3.988	-4.109	-1.909	-2.070
LOGDIVI	7.424	8.937	7.619	9.189	3.769	3.739
LOGWA	4.965	5.097	4.659	4.883	0	0
POOL	-1.278	-1.138	-1.206	-1.055	-0.880	-0.630
FOG08	-1.949	-2.023	-1.774	-1.947	-1.712	-1.354
PMAX08	0	0.060	0	0.060	0	0.127
LOGDIVI.LOGWA	-1.095	-1.254	-1.080	-1.257	0	0
Statistic	**Model Performance**					
AIC	411.9348	425.9549	381.3281	399.2745	188.8292	219.4279
R^2_{98}	0.6819	0.6665	0.6917	0.6719	0.7588	0.7302
$Consistency_{98}$	0.686	0.6745	0.7059	0.7176	0.8745	0.8353
n_{98}	255	255	255	255	255	255
$W_{97\text{-}ALL}$	0.112	-0.1144	0.2664	0.0164	0.1746	0.0822
St Dev.($W_{97\text{-}ALL}$)	2.1272	2.0059	1.9826	1.8862	1.2710	1.1874
$Consistency_{97\text{-}ALL}$	0.760	0.7200	0.7700	0.7600	0.9100	0.9100
$n_{97\text{-}ALL}$	100	100	100	100	100	100
$W_{97\text{-}match}$	0.017	-0.1852	0.1931	-0.0333	0.1304	0.0492
St Dev.($W_{97\text{-}match}$)	1.8971	1.7928	1.7276	1.6391	1.0448	1.0393
$Consistency_{97\text{-}match}$	0.819	0.7869	0.8361	0.8197	0.9344	0.9344
$n_{97\text{-}match}$	61	61	61	61	61	61
$W_{97\text{-}unmatch}$	0.259	-0.0038	0.3811	0.0942	0.2436	0.1338
St Dev.($W_{97\text{-}unmatch}$)	2.4637	2.3209	2.3463	2.2397	1.5739	1.4010
$Consistency_{97\text{-}unmatch}$	0.666	0.6154	0.6667	0.6667	0.8718	0.8718
$n_{97\text{-}unmatch}$	39	39	39	39	39	39

Note: Column values are coefficients on independent variable. A zero value indicates the variable was not used in that model. The lower portion of the table presents comparative model performance statistics. Comparisons should only be made between *primary and alternative models within the same dependent variable*. Lower AIC values indicate a *better* model. R^2 values are reported for the 1998 sample. 1997 data are grouped as: (1) all sites combined (ALL), (2) 1997 sites at the same location as 1998 sites (match), and (3) 1997 sites at different locations than 1998 sites (unmatch). W-statistic is the average error for the validation data set. Consistency is the proportion of sites with estimates within 2°C of the observed value.

Discussion

All of the models indicate that canopy closure, air temperature, and watershed position have important influences on stream temperature. However, there are other variables not adequately investigated that may be important factors in stream temperature but were not addressed because of data gaps: bankfull depth, bankfull width, and basin to name a few.

Additionally, the lack of air temperature data at the stream site made it necessary to investigate the effects of air temperature through the use of surrogates. Air temperature probably plays a greater role in influencing water temperature than these models seem to indicate. Likewise, canopy closure data were collected with a variety of methods with different levels of accuracy; which leads to a similar problem with the canopy data as seen with the air data. *With the error introduced into the canopy* values by the collection methods, canopy should also have a much greater influence on water temperature than the models indicate.

Cross validation results indicated some possible model over fitting. Although model statistics indicated that all the primary models performed much better, mixed results from model validation procedures suggest the possibility that the some selected covariates in the primary models may fit the data well due to chance. Observed coefficients for some of the covariates may not be indicative of real relationships between dependent and independent variables.

Similarity Between XY1DX and XYA7DX

XY1DX, the highest maximum stream temperature for the year, and XYA7DX, the highest seven-day moving average of the daily maximum stream temperature, both measures of daily maxima, had similar models for all three geographic areas (Tables 10.4, 10.6, and 10.8). Both dependent variables used the same list of covariates in the same ecoprovince models. Although not identical, the coefficients for the coincident covariates in each model were similar and always of the same sign. An increase in the value of a covariate that results in an increase in water temperature for one dependant variable resulted in an increase in water temperature for the other dependant variable as well. In contrast, XYA7DA is the highest seven-day moving average of the daily average stream temperature, which is a measure of daily average and not daily maximum. XYA7DA models had a different list of covariates compared to the XY1DX and XYA7DX models for all geographic areas.

The similarities are not surprising given the relationships that exist between the dependant variables. The fit of XY1DX versus XYA7DX had an R^2 values of 0.995, while the R^2 of XYA7DA versus XY1DX and XYA7DX were still high, at 0.922 and 0.934, respectively. There was sufficient difference in the variation of each of the three temperature metrics to result in the selection of a different set of variables. Sullivan et al. (1990) believe that average water temperature may be more a function of average air temperature, whereas temperature metrics dealing with daily maxima are more related to solar heat input. Differences in the set of covariates chosen for the daily maxima type stream temperature metrics and the daily average metrics may be indicative of different heating processes.

Air Temperature

All selected models used surrogates for air temperature. Unfortunately, for the primary models, these surrogates were always related to geographic or topographic position. Latitude, longitude, distance from coast, ecoprovince, and zone of coastal influence all were selected covariates in the models. Not one air temperature metric went into any primary model. Remote air temperature data may work better than the surrogates listed above when modeling temperature for basins. If all the sites are within an ecoprovince with a small range in latitude and longitude, the other covariates might not be as significant (given a smaller range in values) and the remote air station might provided the better relationship. Without having a direct estimate of air temperature in the model, it is difficult to see the relationship between water temperature and air temperature. In chapter 5, a positive correlation between water temperature and air temperature was established.

The interior ecoprovince models (Table 10.6 and 10.7) illustrate the challenge in interpreting the effect of air temperature on water temperature. The further east the site (increasing UTMX) the cooler the water temperature. It is expected that moving eastward would result in an increase in air temperature. However, in the interior-ecoprovince portion of the coho salmon range there is a relationship between UTMX (easting) and elevation. Generally, at stream temperature sites within the interior ecoprovince, elevation increases in a west-to-east direction. Additionally, in the interior ecoprovince, there is a negative correlation between elevation and air temperature (adiabatic cooling). Thus, the further east a site is located, the cooler the air temperature. To further confound the analysis, elevation also entered the XYA7DA interior ecoprovince model as well. Potentially, there is an interactive relationship between elevation and UTMX.

Ecoprovince and the zone of coastal influence are examples of similar air temperature surrogates that entered the models. For the combined ecoprovince models, ecoprovince was factored as in or out (1 or 0) of the coastal ecoprovince. At the same time, the sites were factored as in or out of the zone of coastal influence. Although not the same, the zone of coastal influence is close to the same geographic area as the coastal ecoprovince. There were no sites that were in the interior ecoprovince and the zone of coastal influence, although the zone of coastal influence does enter the interior ecoprovince. Conversely, there were coastal ecoprovince sites that were out of the zone of coastal influence. For the XY1DX and XYA7DX models, both ecoprovince and zone of coastal influence were important factors. XY1DX and XYA7DX estimates were cooler in the coastal ecoprovince and in the zone of coastal influence. The XYA7DA model did not select ecoprovince as a factor, but the zone of coastal influence was significant with sites in the ZCI being cooler. Moreover, in the coastal ecoprovince models, all three dependent variables selected the zone of coastal influence as a significant factor.

Lack of time-step correspondence between air and water temperature metrics was a potential reason for mediocre water temperature prediction capabilities. Models were fit to stream temperature data on daily or weekly statistics. The weekly data were seven-day moving averages. While both the daily maximum and the seven-day moving averages change from day to day, the highest daily maximum and highest seven-day moving average for the year was used in model development. Most XY1DX, XYA7DX, and XYA7DA values occurred in late July and early August (see March 1998 FSP Technical Note in Appendix A).

Air temperatures used in model development were calendar monthly averages. Most of the air temperature data used in modeling were available only as monthly summaries. The time scales for air and water temperature metrics used in modeling were obviously mismatched. However, we were interested in modeling stream temperature metrics that are in common usage in California and the Pacific Northwest. Sullivan et al. (1990) found unexpectedly good agreement between the commonly used temperature metrics and monthly water temperatures.

Since the highest daily maxima and seven-day moving averages occur predominantly in July and August we chose to use the combined July-August average air temperature in model development. During preliminary modeling exercises, AIC scores almost always favored the combined July and August average maximum air temperature metric over the single July or August values. Thus, for the backward selection procedures, only the July and August average maximum air temperature metric was used. However, the relationship between PMAX08 (an August maximum air temperature metric) and P.MO.MAX (a July and August average maximum air temperature metric) was very high ($R^2 = 0.999$ for linear fit). Thus, there was little difference if PMAX08 or P.MO.MAX was used in the models.

Solar Radiation Exposure

Canopy closure was the single most important variable investigated with respect to solar radiation exposure, although ecoprovince and ZCI also play a role in the amount of solar radiation reaching the stream surface. The coastal ecoprovince and the ZCI generally will have more solar radiation filtered out by fog and clouds than areas outside of the ZCI and in the interior ecoprovince.

Every fitted model included canopy as a covariate, and in every model, there was an inverse relationship between canopy closure and water temperature. However, without a sound sampling design and without canopy data collected using consistent protocols that measure effective shade, the level of analysis required to answer questions like, "how much canopy needs to be retained to keep the water at *x* degrees under condition *y*?" cannot reliably be answered. Given the caveat that this modeling effort was exploratory in nature and that numbers presented lack any level of confidence, the primary XYA7DA interior ecoprovince model suggests that there was a positive interaction between canopy and the log of the watershed area. This poses an interesting conundrum that warrants further investigation. Just how do watershed area and canopy closure interact. Below, the terms that involve canopy were put into an inequality that indicates that there is a cooling effect on stream temperature:

$$1.2(CANOPY * LOGWA) - 6.4(CANOPY) < 0$$

The above statement is true only when:

$$LOGWA < \frac{6.4(CANOPY)}{1.2(CANOPY)}$$

or, canceling *CANOPY*, when *LOGWA* is less than 5.33 or about 215,000 ha. Once the log of watershed area exceeds 215,000 ha, canopy has a warming effect on stream temperature. This, however, should not be surprising since sites in our region-wide study area did not exhibit canopy levels above 30% at watershed areas greater than about 63,000 ha (see Chapter 9). With increasing watershed area and divide distance canopy is expected to decrease due to channel widening, rendering adjacent stream-side vegetation ineffective at providing shade to stream surfaces. Concomitantly, there is generally a longitudinal warming in stream temperature with increasing distance from the watershed divide and increasing watershed area.

Watershed Position

Watershed position, as expressed as either the log of distance from the watershed divide, the log of watershed area, or both, entered every model. In all cases, as the watershed area or distance from divide increased, there was an increase in steam temperature. However, the models for XY1DX and XYA7DX in the coastal and the combined ecoprovinces included an interactive term between log watershed area and log distance from divide that had a negative coefficient. Analyses similar to that for the canopy closure log watershed area interaction might reveal situations where certain combinations of watershed area and distance from divide might have a cooling effect. Such a phenomenon is not unreasonable since it was shown earlier that warm rivers flowing out of warm interior portions of watersheds exhibited a cooling down upon entering the zone of coastal influence.

Habitat Type

FSP had requested that temperature probes be placed in riffles were the water is well mixed. However, a number of temperature probes were placed in pools, some of which were designed to characterize the extent of cool thermal refugia. Since many pool probes were intentionally placed to measure water that is cooler than that found in the well-mixed riffles, habitat type was used as a factor for consideration in the models. The habitat type factor grouped shallow pools, medium pools, and deep pools together in one group and runs and riffles into the other. Habitat type was found to be a significant factor in the coastal and combined ecoprovince models, where, as expected, pools were cooler than runs and riffles. The result that habitat types were not significant in the interior but were on the coast might not be a real response, but may be due to differences in sampling methods. The probes that were known to be placed in pools for describing cool thermal refugia were all in the coastal ecoprovince. Thus, it was expected that these sites would be cooler. For pool sites in the interior ecoprovince, the purpose for placement in pool habitat was largely unknown. Additionally, fewer probes were placed in pools in the interior, making comparisons difficult. There was over 50% pool placement of probes in the coastal

ecoprovince and only about 30% pool placement in the interior.

The placement of temperature probes into pools adds additional unnecessary complexity to an already complex relationship. The relationship between water temperature and the covariates that control water temperature is difficult to model. Collecting data in pools as well brings into the model a relationship between the mixed water of the riffles and water that may or may not stratify in pools. If water temperatures were measured only in well- mixed riffles, then the water temperature models would have less variability, making interpretation much easier and more reliable.

Stream size

As stated in the watershed position section, there was a relationship between watershed area and distance from watershed divide with respect to stream temperature. Stream size is also related to watershed area and distance from divide, thus those variables might serve a surrogacy role for stream size in the model.

Bankfull width and bankfull depth were left in the backward selection procedure only to illustrate their possible importance. In preliminary modeling exercises, when either or both covariates entered the model a good AIC score with a high R^2 value was observed. However, model improvement may be because of the relatively small geographic area represented by sites with non-null bankfull data. Whether the good fits were due to an actual relationship between water temperature versus bankfull width and depth or whether due to the limited number of basins entered into the models is unknown. However, given the significance of bankfull width in several physical-based temperature models (Bartholow, 1989; Sullivan et al., 1990), it is believed that the observed importance of this variable in the present study is real and not an artifact of limited areal extent. In the future, bankfull width and bankfull depth should be recorded and investigated for the potential effects on stream temperature.

Basin

During preliminary model exploration, BASIN was one of the most important covariates. However, many basins had no stream temperature sites, others had a few, and some basins dominated the data set. One of the fitted models indicated that the Smith River basin was the hottest basin, when factoring out other effects in the model. The Smith River basin had only four stream temperature sites, making more in-depth investigation of such a small number of sites feasible. All four sites had high canopy values, were close to the coast, were located in the northern portion of the study area, and were close to the watershed divide. All of these factors would result in an lower estimated water temperature without taking basin into account. These four sites were all small coastal streams. None were mainstem or interior ecoprovince sites. These points were not representative of the Smith River basin as a whole. Given this problem and the large number of basins without any sites, BASIN was dropped from the analysis.

This underscores the effects of a lack of sampling design on the error structure of the data and the resulting models.

Summary

Researchers have had a great deal of success modeling stream temperature at basin and smaller scales. However, if the desire is to model stream temperature at a coho salmon ESU scale, many complications not seen at the smaller scale arise. Namely, remote air data coupled with surrogates, such as elevation, may work well for developing a basin-scale model, but at a regional scale, a better estimate of the local air temperature is required. Additionally, these analyses were confounded by the fact that there was no sampling design in place. Basins rich in data, like the Eel River, were over represented as compared to a basin like the Smith River, where only four sites were found. Without a sampling design to guide placement of stream temperature sensors it is difficult to know exactly what geographic area these models describe.

All the fitted models indicated that air temperature, solar radiation, and watershed position were important covariates. Positional covariates entered all the models. While these were viewed as air temperature surrogates, this underscores the fact that location is an important factor in stream temperature profiles. For example, two sites that appear to be identical with respect to habitat, riparian condition, shading, watershed area, and flow rate, but are in different basins will more than likely have different temperature profiles. Stream temperature "target" values that may be easily achieved in some areas might be impossible in others.

Although models were presented and statements made as to what independent variables influence water temperature, the lack of a sampling design makes in-depth analyses tenuous. Questions regarding each covariate's contribution to explaining variation in stream temperature requires data collected with a sampling design suited for developing explanatory models. Such a design would require a sampling frame, constructed from a well-defined sampling universe. Then, a random probability sample of some type must be drawn from the sampling frame. Finally, air temperature, canopy, and stream-size data collection, and stream temperature sensor placement must all adhere to consistent protocols and all collected values must be submitted. Note, the explanatory model would not work well to predict stream temperatures. The explanatory model will require local air temperatures and good canopy data that will be expensive to collect at a large scale. If a predictive model is desired, then a higher sampling rate applied over a smaller spatial scale, without collection of local air temperature, would be more cost effective. Nonetheless, a sampling design with a random probability sample is still required.

Chapter 11

HISTORICAL PERSPECTIVES

Introduction

The advent of digital continuous monitoring devices for stream temperature is a quite recent event. Continuous thermographs have been available since 1951 (Blodgett, 1970). There are reports dating back fifty years or more that contain synoptic hand-held thermometer temperature data reported for select stream and river locations across Northern California. Comparison of a single stream temperature datum point recorded at some arbitrary time of day at some arbitrary location on a stream in the past to more recent continuously monitored stream temperature data is difficult. It may lead to erroneous conclusions or no conclusions at all.

Matching up the location of the historical data or datum to more recent data can often be laborious detective work, attempting to identify the location of a crime scene for a crime committed several decades ago. Usually the location information is very sketchy. Locations may be referenced to some landmark (bridge, road, pool) that no longer exists or to a stream or confluence whose name has changed.

Recent FSP data contributor sites up to 2000 m from the historical site location were used in comparisons. However, for status assessment and regional trend analyses of FSP sites presented in Chapters 3 - 9, ten meters was the largest distance separating two sites that were considered to be the same site across multiple years. There was only one historical site that was approximately 10 m from a contemporary FSP site. If the more stringent standard for defining a unique site location was used for the historical comparisons, there would be only one historical comparison. Thus, some concessions were made in order to increase the number of matched sites for historical comparison purposes. Many of the historical sites were located on mainstem rivers, which are believed to have less longitudinal temperature variability over long (thousands of meters) distances. Less longitudinal variability allows comparisons of historical and contemporary sites that are not collocated.

Most of the historical data comes from larger streams where air temperature is most likely the major factor influencing water temperature. Thus, this analysis does little to address any stream temperature changes that have occurred since the 1950's in smaller streams, where most coho salmon rearing takes place and where land management practices may have a greater influence on thermal regimes and the extent of potentially suitable habitat. This historical analysis is on a site-by-site basis and not a regional assessment of trends in stream temperatures across the range of coho salmon in Northern California.

We found that stream temperatures at many sites have been fairly similar over two or more decades. Much of the variability that was observed could be attributable to year-to-year changes in air temperatures. On smaller streams, changes from historical stream temperature levels may be related to changes in certain site factors. However, no historical site attribute data, and in some cases no contemporary site attribute data, were available for which to relate changes in water temperature.

Sources of Historical Stream Temperature Information

Various reports from the Bureau of Fish Conservation, California Division of Fish and Game can be found in the government documents section of the library. Many of these reports contain max-min or single grab sample water temperatures, often accompanied by synoptic air temperatures measured at approximately the same time and place.

The U.S. Environmental Protection Agency (EPA) maintains a database of water quality information. The database, known as STORET, is a computerized data base utility maintained by the EPA for the STOrage and RETrieval of chemical, physical, and biological data pertaining to the quality of the waterways within and contiguous to the United States. A data request for all stream temperature data available in STORET for the HUCs comprising the range of the coho salmon in Northern California was submitted to the U.S. EPA. The data were received within two days of the request. The stream temperature monitoring point locations were displayed in GIS and compared to FSP's point coverage. It was found that 1996-1997 data from a large federally funded water temperature monitoring study in the Eel River Basin were submitted to the U.S. EPA for inclusion in STORET with their original site coordinates. On average, these points were 993 m from their true locations with a maximum of 63 km (See Chapter 2, Spatial Accuracy Assessment). This raises some concerns as to the spatial accuracy of other stream temperature data found in STORET. The quality of data in STORET, both for the numeric values of the parameter of interest and for the spatial location where the parameter was measured, is entirely up to the discretion of the data contributor. Also, the received data set had data from hand held thermometers, digital continuous monitoring devices, and thermographs, with no indication of which collection method was used for the site. Many sites had only one record, listed with a date; it was unknown whether these particular points were grab samples or daily maxima. Because of the uncertainty surrounding these data, STORET data were not used in historical comparisons.

The USGS has recorded water temperature at many of their stream gaging stations. The sites are located primarily on mainstem tributaries, usually fourth order or greater. A very good source of temperature data that was used in this chapter was a stream temperature summary report prepared by Blodgett (1970) who summarized USGS water temperature data in tabular format. Both periodic and continuous temperature data were reported. The data for some locations date back to the early 1950's. USGS has also published water temperature data in annual ***Water Resources Data for California*** reports (USGS, 1975, 1976, 1977, 1978, 1979, 1980). One of the impediments in using USGS stream temperature data as an assessment tool for historical status and trends is that the locations of gaging stations are mostly on large, mainstem portions of Northern California rivers. Water temperatures in these large, wide-channeled watercourses will be more a function of air temperature, as was discussed in Chapter 5. The effects of flow control on water temperature of many Northern California rivers was noted by Blodgett (1970) throughout his report.

The Pacific Gas and Electric Company (PG&E) of California conducted a water monitoring program in association with the Potter Valley Project (PG&E, 1996). Water temperature was monitored at 16 locations from 1980 through 1995. The Forest Science Project acquired these data in already summarized format: daily minimum, average, and maximum values. The Forest Science Project located six FSP sites that were within an estimated 1100 m of PG&E sites for comparisons. However, the exact location of the PG&E sites remains unknown and the true distances between the FSP site and the PG&E site may actually be less than or greater than 1100 m.

Summary of Administrative Reports

1951 Inland Fisheries Administrative Report

Stream temperature data collected in 1950 were found for a site located on the Eel River at Fernbridge, CA (Murphy and DeWitt, 1951). Data were reportedly collected with a thermograph of unknown make and model. Daily maxima and minima were reported for June through September, 1950. A Forest Science Project data contributor

deployed a continuous stream temperature sensor near Fernbridge in 1997. Data collection began on July 23, 1997 and ended on September 30, 1997. A comparison of the 1950 and 1997 daily maxima and minima for this location is shown in Figure 11.1. The daily maxima in August ranged from 18.3° to 22.2°C in 1950 and from 19.4° to 22.4°C in 1997. The August daily minima ranged from 17.2° to 21.1°C in 1950 and from 19.0° to 20.9°C in 1997.

There was no information in the Murphy and DeWitt (1951) report on the exact placement of the thermograph, e.g., whether it was placed in a pool or riffle, whether the sensor was shaded from direct sunlight, or whether the sensor was placed in the thalweg. The drainage area at this location is approximately two million acres. Such a large drainage area value would suggest that the Eel River at this location is quite wide with little or no stream-side shading. This hypothesis is supported by first-hand knowledge of the Eel River at this location and by the canopy closure value reported to the Forest Science Project at the Fernbridge site in 1997 (5%).

Monthly average air temperatures were obtained for a NOAA weather station located in Scotia, CA, approximately 17 km (~11 mi) from Fernbridge. The monthly average maxima and minima air temperatures are shown in Figure 11.2. Examination of monthly average air temperatures for the months of July, August, and September revealed that in 1997 these months were warmer than in 1950. Warmer air temperatures may account for the higher daily maxima and minima water temperatures observed in 1997 compared to 1950.

From the same report prepared by Murphy and DeWitt (1951) air and water temperature data were presented for various locations on the Eel River and at the mouth of the Van Duzen River at its confluence with the Eel River. Table 11.1 presents these data as they appeared in the 1951 report. There was no information in regards to canopy closure, flow rates, or other site-specific attributes.

Water temperature exceeded air temperature in most instances. On June 25, 1950, the weather was noted to be clear and warm. The water temperature in the Van Duzen River exceeded the air temperature at 6:00 PM by 7.2°C (13°F) on this particular day in 1950. Water at these locations originated in more interior portions of the basin, where air temperatures can be much warmer than more coastal areas (see Chapter 4). On July 8 and August 20, 1950, both days reported as clear and warm, the water temperature was 23.3°C around 1 pm. This may represent the maximum equilibrium stream temperature at this location on the Van Duzen River. On August 8, 1997 the daily maximum stream temperature was 22.6°C near the same location (see Figure 7.21). The stream temperatures recorded 47 years apart are quite similar, suggesting that this temperature value may be near the equilibrium temperature for this location on the Van Duzen.

Table 11.1 is a good example of the lack of locational information found with most historical temperature data. With better site location information more recent FSP stream temperatures could quite possibly have been collected at a site in close proximity to the 1950 sites. Not all locational information in historical sources is undetailed, as can be seen in the next Administrative Report by Blea (1938).

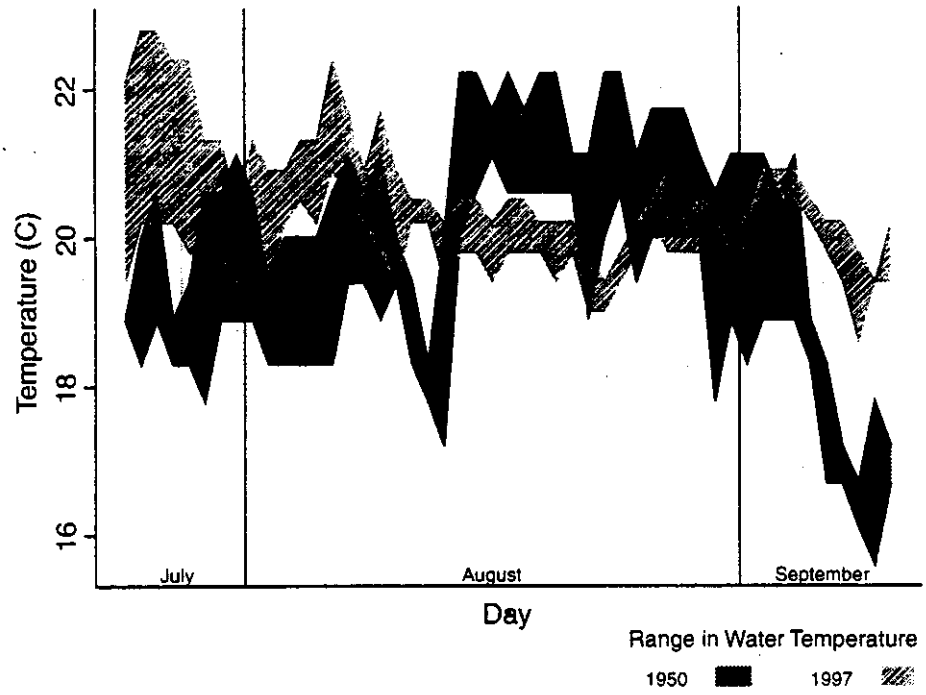

Figure 11.1. Comparison of daily maxima and minima Eel River water temperatures (°C) measured at Fernbridge, CA in 1950 and 1997 from mid-July through mid-September.

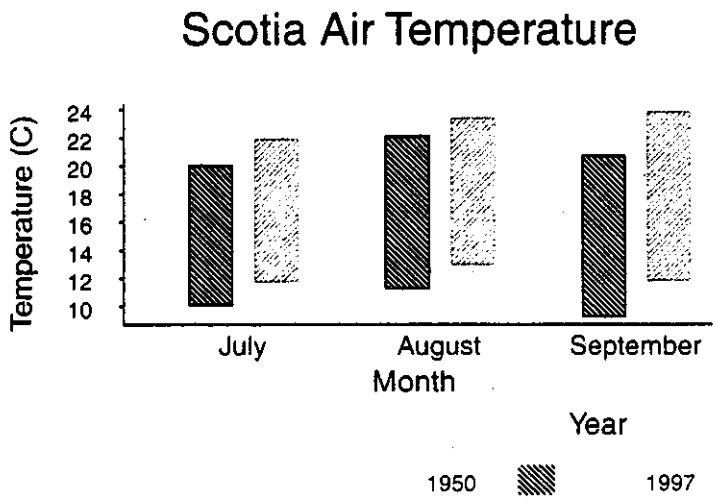

Figure 11.2. Comparison of air temperature for July, August, and September at Scotia, CA in 1950 and 1997. The tops of the bars indicate the average monthly maxima, while the bottoms represent average monthly minima.

Table 11.1. Hand-held Air and Water Temperatures Collected at Various Times and Locations During the Summer of 1950 in the Lower Eel Basin (Taken from Murphy and DeWitt, 1951).

Date	Time	Place	Temperature (°C) Air	Water	Remarks
June 10	9:35 AM	Eel River VD	16.1	17.2	Cloudy, cool
" "	9:45 AM	Van Duzen R.	16.1	16.1	" "
" "	11:45 AM	Weott Bay	13.3	15.0	In backwater of Bay
" "	12:05 PM	Salt R. Bridge	13.3	14.4	Flow 100 g.p.m. (rough)
" "	12:45 PM	Singley Pool	13.3	20.6	Water clear, green
June 11	11:30 AM	Van Duzen R.	16.7	15.0	Cloudy, mild
" "	1:30 PM	Singley Pool	14.4	16.7	Cloudy, cool
June 12	10:00 AM	Singley Pool	12.2	16.1	Cloudy, cool
" "	4:00 PM	Van Duzen R.	13.9	15.6	Cloudy, cool, water not too clear
" "	5:00 PM	Singley Pool	12.2	15.0	Cloudy, cool
June 13	6:20 PM	Van Duzen R.	12.2	13.9	Cloudy, cool, water muddy
June 17	10:00 AM	Van Duzen R.	14.4	14.4	Cloudy, warm
" "	11:30 AM	Fernbridge	13.3	15.6	Cloudy, warm
June 19	9:00 AM	Van Duzen R.	13.9	13.9	Cloudy, mild
June 20	4:15 PM	Van Duzen R.	14.4	15.6	Cloudy, cool, windy
" "	5:00 PM	Fernbridge	13.9	17.2	" " "
June 22	2:30 PM	Van Duzen R.	14.4	17.8	Partly cloudy, cool
June 24	10:40 AM	Van Duzen R.	15.6	16.7	Partly cloudy, mild
June 25	6:00 PM	Van Duzen R.	13.9	21.1	Clear, mild
June 28	10:20 AM	Van Duzen R.	18.9	19.4	Clear, warm
" "	2:30 PM	Dungan Pool	18.3	20.6	" "
June 29	10:30 AM	Van Duzen R.	15.6	18.9	" "
July 2	1:00 PM	Van Duzen R.	20.0	21.7	" "
July 3	11:30 AM	Dungan Pool	18.3	18.9	" "
" "	12:30 PM	Van Duzen R.	15.6	20.0	" "
July 8	1:00 PM	Van Duzen R.	21.7	23.3	" "
July 9	9:30 AM	Van Duzen R.	12.8	16.7	Cloudy, cool, misty
July 15	12:00 PM	Van Duzen R.	18.3	22.2	Clear, warm
July 23	10:30 AM	Van Duzen R.	15.6	17.8	Cloudy, mild
July 29	10:00 AM	Van Duzen R.	15.6	18.3	Clear, warm
July 31	12:00 PM	Van Duzen R.	19.4	22.8	" "
Aug. 5	3:30 PM	Dungan Pool	18.3	19.4	Clear, warm, breezy
Aug. 6	2:00 PM	Van Duzen R.	18.3	22.2	" " "
Aug. 20	1:30 PM	Van Duzen R.	18.9	23.3	" " "

1938 Inland Fisheries Administrative Report

In 1938 large steelhead trout mortality was reported on the South and Middle Forks of the Eel River. J.H. Blea of the California Division Fish and Game, Inland Fisheries Branch investigated the problem. He prepared a detailed report that appeared in the Administrative Records of the Inland Fisheries Branch in 1938 (Blea, 1938). Blea collected several air and water temperature readings with a hand-held thermometer at numerous locations in the South Fork and Middle Fork Eel Rivers and in various tributaries. Most of the tributary water temperatures were collected near the confluence with the river. At some tributary locations he also recorded the water temperature of the mainstem above and/or below the tributary. Blea also made observations of the number of steelhead trout and any mortalities or obvious signs of a diseased condition.

Upon arriving at the scene Blea learned that three weeks prior to 21 July 1938 the weather had been hot, and became even hotter over the next three days. Air temperatures in Garberville reached 44°C (112°F). He described both the South Fork and Middle Forks of the Eel River in the area of his investigation as:

> *. . . unusually exposed to the sun for distances of seventy-five miles or more. The broad river beds offer no shade to the relatively small flow of water which moves slowly along, alternately through large pools and wide, shallow riffles.*

Blea stated that despite the heavy winter rainfall the rivers were low because there had not been the usual spring rains. Blodgett (1970) states that flow regulation of the Eel River began in December of 1921, the time at which the Scott Dam went into operation. Construction of the Cape Horn Dam in 1908 may also have influenced flow regimes on the Eel River in 1938. Blea speculated that water temperatures had probably reached 80°F to 85°F (27° to 29°C) throughout much of the area where fish exhibited a high incidence of "disease". "These temperatures are very near the lethal limit for trout and this factor coupled with the consequently low oxygen content apparently reduced resistance of the fish to the diseases."

The Blea report is about the only historical report, other than USGS reports, that could be uncovered that had adequate location information for both tributary and mainstem sites that enabled us to compare more recent FSP water temperature data. Table 11.2 is a summary of air and water temperature measurements taken by Blea at various locations on the South and Middle Forks of the Eel River and tributaries entering the mainstems. More contemporary recordings of water and air temperature are included in the table for historical comparison purposes. Hourly air temperature recordings were not available for the nearest NOAA air station located at Richardson Grove State Park, therefore monthly averages are presented in Table 11.2.

On the Middle Fork of the Eel River at Fort Seward the water temperature reported by Blea was 23.9°C (75°F) at 9:30 am on 27 July 1938 (Table 11.2). A Forest Science Project site located near the same location (~1500 m upstream), as best as can be determined from the 1938 site location description, was found to have a water temperature of 24.4°C (75.9°F) at 9:47 am on 27 July 1997. It is highly unlikely that the 17-minute difference in the time of day the two readings were taken might account for the 0.5°C (0.9°F) difference in the water temperatures. A comparison of present-day water temperatures to synoptic grab sample water temperatures can be considered qualitative at best. Nevertheless, the similarity is striking.

Dean Creek is a tributary to the South Fork Eel and exhibited a water temperature of 19.4°C at 8:00 am on 31 July 1938 (Table 11.2). On the same day in 1996 at about the same time of day, the water temperature was 22.0°C. The July monthly average air temperatures indicated that July 1996 was warmer than July 1938. However, the monthly average air temperature for July 1997 was the same as 1996, but the water temperature was lower than the 1938 value.

Table 11.2. Hand-Held Air and Water Temperatures Collected at Various Times and Locations During the Summer of 1938 in the South Fork and Mainstem Eel River and Various Tributaries (Blea, 1938) in Comparison to More Contemporary Forest Science Project Data.

date	time	location	Water and Air Temperature (°C)														Dist (m)	Dir
			1938		1993		1994		1995		1996		1997		1998			
			H20	Air	H20	Air	H20	Air	H20	Air	H20	Air	H20	Air	H20	Air		
South Fork Eel River and Tributaries																		
7/31	8:00 AM	Dean Cr.	19.4	20.9							22.0	21.9	19.0	21.9			312	UP
7/26	8:30 AM	Redwood Cr.	18.3	20.9							21.1	21.9					1922	UP
7/28	8:30 AM	Sprowl Cr. at mouth	17.2	20.9							17.7	21.9	16.5	21.9			153	UP
7/25	10:30 AM	Six mi. above Benbow Dam	23.9	20.9											23.8	19.7	1463	UP
7/30	9:00 AM	Indian Cr. @ SF Eel	17.2	20.9									18.7	21.9			46	UP
7/30	12:00 PM	Indian Cr. two miles from Eel	19.4	20.9	19.0	19.6	21.1	20.1	20.4	21.3	21.7	21.9					747	UP
8/01	2:00 PM	Indian Cr. @ SF Eel	23.9	20.0									21.7	23.4			46	UP
7/25	1:00 PM	Red Mountain Cr. @ SF Eel	20.0	20.9							23.5	21.9	24.6	21.9	24.0	19.7	101	UP
7/31	6:30 PM	Rattlesnake Cr. @ SF Eel	23.3	20.9							26.1	21.9	25.2	21.9	23.2	19.7	164	UP
7/31	6:30 PM	SF Eel above Rattlesnake Cr.	23.9	20.9							26.7	21.9	26.0	21.9			351	UP
8/01	5:30 PM	Elder Cr. @ SF Eel	16.7	20.0							19.0	21.6	17.7	23.4	18.0	20.9	132	UP
8/01	5:30 PM	SF Eel above Elder Cr.	21.1	20.0									19.9	23.4	20.2	20.9	99	UP
8/01	5:00 PM	Dutch Charlie Cr. @ SF Eel	15.6	20.0							19.3	21.6	18.6	23.4			310	UP
8/01	4:00 PM	Redwood Cr. @ SF Eel	16.1	20.0							16.1	21.6					10	UP
Mainstem Eel River and Tributaries																		
7/26	1:00 PM	SF Eel @ Mainstem Eel	21.1	20.9							23.7	21.9	23.9	21.9	25.1	19.7	261	UP
7/29	12:00 PM	S. Dobbyn Cr. @ road xing	21.1	20.9									20.8	21.9	20.3	19.7	69	UP
7/27	9:30 AM	Eel @ Ft. Seward	23.9	20.9									24.8	21.9			1464	UP
7/27	9:30 AM	Eel @ Fort Seward	27.0	20.9									24.8	21.9			1160	UP
7/30	5:30 PM	MF Eel near Dos Rios	26.7	20.9							28.5	21.9	27.0	21.9	25.3	19.7	187	UP
7/30	5:30 PM	Eel @ Mf Eel near Dos Rios	25	20.9											24.3	19.7	37	UP
Other Points																		
7/26	3:00 PM	Little Van Duzen @ road xing	21.7	20.9							25.4	21.9	24.5	21.9	24.4	19.7	65	DN
7/29	1:30 PM	Larabee Cr. @ road xing (road fr Blocksburg to Bridgeville)	21.1	20.9							21.8	21.9	17.6	21.9	20.0	19.7	26	DN

NOTE: All air temperature data are monthly averages recorded at a NOAA station in Richardson Grove State Park. Distance up (UP) or downstream (DN) from FSP site is shown in last two columns.

Redwood Creek exhibited a water temperature of 18.3°C at 8:30 am on 26 July 1938. On the same day and time in 1996 the water temperature was 21.1°C at a FSP site located about 1900 m upstream from the Blea 1938 site. The monthly average air temperatures for July and August 1996 indicate it was a warmer year than 1938, which may partly account for the higher water temperatures observed in 1996.

Sprowl Creek at its confluence with the South Fork Eel showed very similar water temperatures at nearly a 60-year sampling interval. In fact, in 1997, while air temperatures were higher than 1938's, water temperature in Sprowl Creek was lower.

Out of the 21 comparisons of historical and contemporary water temperatures presented in Table 11.2, eight showed relatively little change, 10 showed an increase, and three showed a decrease in water temperature. It is difficult to determine whether some of the observed increases were due to differences in climate, riparian conditions, flow, or all the above. The observed decrease in water temperature at Indian Creek was in the presence of monthly average air temperatures about 3°C higher in 1997 compared to 1938.

Potter Valley Project

A stream temperature monitoring study was performed in conjunction with the Potter Valley Project by Pacific Gas and Electric (PG&E) of California (PG&E, 1996). Daily water temperature summary statistics (i.e., daily minimum, average, and maximum) were obtained from PG&E. Data were collected at various locations along the mainstem Eel River above Pillsbury Lake to Fort Seward, CA. Two tributaries were also monitored, Tomki Creek which enters the mainstem below the Cape Horn Dam and Outlet Creek which enters the mainstem upstream from Dos Rios, CA. Figure 11.3 shows the approximate location of the monitoring sites. Water temperature data were collected from 1980 to 1995, although all locations did not have all years for their data records. Some stations had continuous data spanning the entire year, while others ended in early July for most years.

The only site location information provided with the PG&E data was an 8 by 10 inch map with a mark for each site labeled with a location name (e.g. Eel River Below Scott Dam). The marks covered nearly 1 km of stream. The sites were placed into a GIS coverage by visual estimation of the marks' center on the map and placed on the blue-line stream using a digital raster graph topographic map in ArcView. The spatial accuracy of this method was poor. After placement, it became apparent that two PG&E sites were at the same location as two USGS sites (Eel River Below Scott Dam and Eel River Above Van Arsdale Reservoir). These two sites had differences between the estimated PG&E location and the USGS location of approximately 270 m and 1270 m, respectively. Table 11.3 shows the estimated distance from the PG&E site to the corresponding USGS and FSP sites. Since the location of the PG&E sites were rather imprecise, these distances are presented to demonstrate that the sites are probably in the general vicinity of each other, with the caveat that comparisons may not be entirely appropriate, particularly for the two tributary sites. Longitudinal variability in water temperatures for larger mainstem rivers is considered to be much smaller than tributaries. Thus, some leeway is afforded in terms of spatial accuracy.

The PG&E, USGS, and FSP sites listed in Table 11.3 were combined on a single chart to develop a historical view of stream temperatures at each location. Monthly average water temperatures were calculated from the continuous data for FSP sites and from daily averages for the PG&E data. USGS data are reported as monthly average values in the Blodgett report (1970) and the various USGS ***Water Resources Data for California*** reports. If a month was missing more than five days of data, the average was not presented on the graph. Each bar on the chart represents monthly averages for June, July, August, or September. The vertical lines represent the range in daily minimum and maximum temperatures for each month.

Data charts are presented in a downstream direction, with the most upstream site presented first and tributaries to mainstems presented last. Typically, the hottest two months of each year were presented in

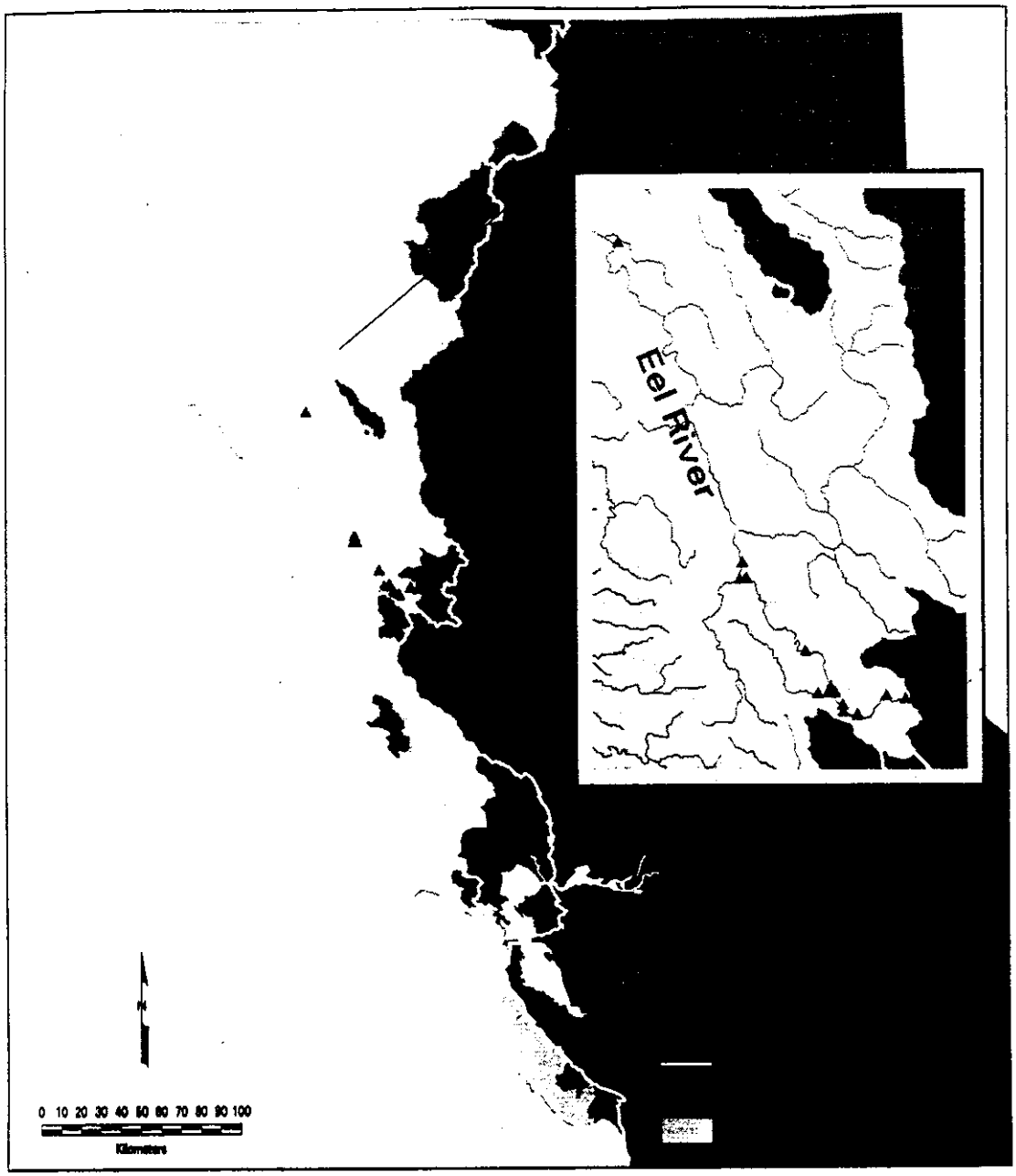

Figure 11.3. Location of PG&E Potter Valley Project stream temperature monitoring sites.

Table 11.3. The Estimated Distance from the PG&E Site to the Corresponding USGS and FSP Sites.

Site Location	Distance to FSP Site (m)	Distance to USGS Site (m)
Eel River Below Scott Dam	+350	+270
Eel River Above Van Arsdale Reservoir	-1030	-1270
Eel River Near Dos Rios	-620	-530
Eel River at Fort Seward	+720	0
Tomki Creek Near Eel River	-730	N/A
Outlet Creek Near Longvale	-620	N/A

NOTE: Positive values are upstream of the PG&E site, while negative numbers are downstream. The location of the PG&E sites are imprecise, thus the distances listed are only approximations to illustrate that the compared sites are probably in the same general vicinity.

the bar charts, i.e., July and August. More than one month may be shown on the graph because of the large number of months in various years with missing values for one or more months. Presenting multiple months increases the likelihood that a historical comparison can be made for at least one of the months across multiple years. The site below Scott Dam showed its highest stream temperatures in September; thus August and September were presented for the below-Scott-Dam site. Many PG&E sites did not have August data and some did not have July data. June data were presented for any site that did not have August data.

Figure 11.4 shows the monthly average water temperatures for the site situated below Scott Dam near Potter Valley, CA. Eel River water temperatures below Scott Dam do not seem to have changed appreciably over the last 33 years, with 1995 being one of the coldest years on record. Most years for this site show an increase in water temperature from June through September, which sets this site apart from almost all of the 1090 sites examined in the FSP regional assessment. Water temperatures at most other sites were hottest in July and August, while June and September were cooler. The steady increase from June through September is evident in the data collected by three different organizations over a 33-year time span, with 1977 being the only year on record where August had a higher monthly average than September. It would suffice to say that this trend is real, and not an artifact. The observed trend in water temperatures at this site is elaborated upon later in this chapter (USGS Continuous Data).

Figure 11.5 shows historical water temperature trends on the Eel River above Van Arsdale Reservoir, near Potter Valley, CA. The watershed area at this location was about 75,000 ha (290 sq mi) and the distance from the watershed divide was about 55 km (30 mi). Temperatures show the locally normal pattern for years where all four months of data were available, hottest in July and August. The temperatures varied between 16°C and 20°C for most months and most years. Water temperatures in 1992 and 1993 were some of the lowest July monthly averages for the 12 records spanning over 34 years. The August 1997 monthly average was the only one to exceed 20°C, however, most years did not have August data.

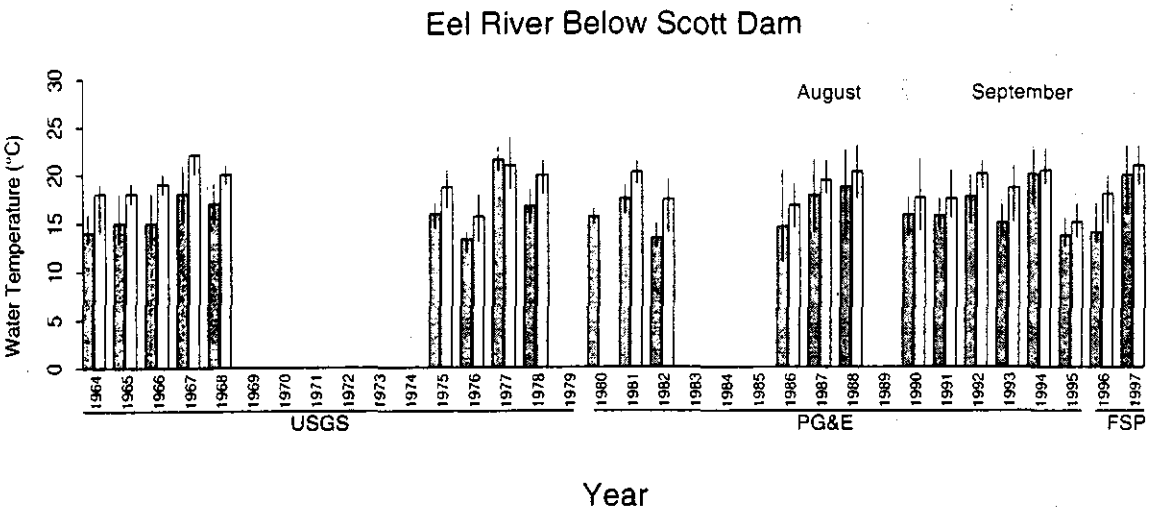

Figure 11.4. Comparison of historical USGS and PG&E monthly average stream temperature data with more recent Forest *Science Project data during* August and September. The site was located on the Eel River below Scott Dam, near Potter Valley, CA. Vertical lines represent the range in daily minimum and maximum temperatures for each month.

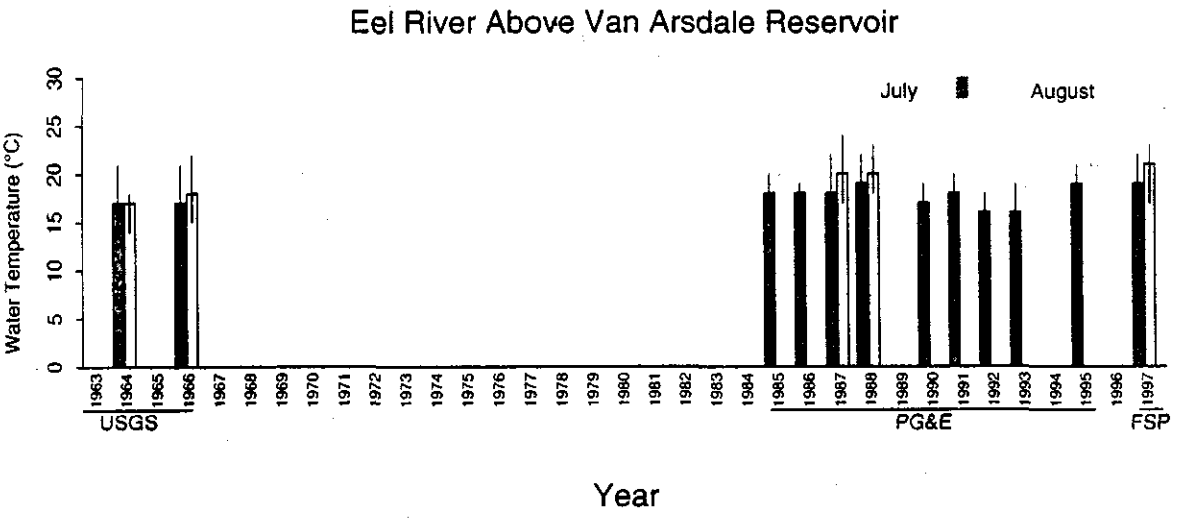

Figure 11.5. Comparison of historical USGS and PG&E monthly average stream temperature data with more recent Forest Science Project data during July and August. The site was located on the Eel River above Van Arsdale Reservoir. Vertical lines represent the range in daily minimum and maximum temperatures for each month.

Figure 11.6 presents a comparison of water temperatures at a site located on the Eel River near Dos Rios, CA. The watershed area at this location was about 136,000 ha (525 sq mi) and the distance from the watershed divide was 120 km (75 mi). The Eel River is quite wide near Dos Rios, with riparian vegetation too far from much of the stream to provide any appreciable shading. Most years of data collected for the PG&E site had data for only June and only three years of August data. The only year when August monthly average temperature (26°C) was higher than the July monthly average temperature (25°C) was 1966. June replaced August for the comparison since doing so greatly increased the number of years that could be examined. July monthly average water temperatures were near or above 25°C for most years in the long-term record. June 1993 was the lowest monthly average in the record, at about 18°C.

Figure 11.7 shows long-term monthly average water temperatures at a location on the Eel River at Fort Seward, CA. The watershed area at this location was about 544,000 ha (2100 sq mi) and the distance from the watershed divide was 225 km (140 mi). The channel is quite wide and aggraded at this location. The stream is mostly unshaded with vegetation offering minimal shading on the outside edges of bends. The canopy closure value submitted by a FSP cooperator in 1998 was 5%. The PG&E sites had enough data for only the month of June, thus June is the only month with data presented. No obvious increase in temperature can be detected.

Figure 11.8 presents a comparison of historical and more recent water temperatures at a site on Outlet Creek near Longvale, CA. The watershed area was 41,800 ha (160 sq mi) and the distance from divide was 50 km (30 mi). Unfortunately, only June monthly averages were available for the USGS and PG&E portions of the record. Thus, we are somewhat limited in our ability to discern any trends over time. Again, no obvious increase in temperature can be detected. June 1968 monthly average water temperature was slightly below 20°C. In 1985 the June monthly average was about 24°C, and in 1996 through 1998 was about 22°C.

Figure 11.9 compares monthly average temperatures on Tomki Creek near the Eel River over a 16-year period. The watershed area at this location was 15,800 ha (60 sq mi) and the distance from watershed divide was 35 km (25 mi). There was a gradual increase in monthly average temperatures from 1982 to 1988, followed by a return to 1982 levels in the 1990's. No data were available in 1990. In 1991, temperatures again reached levels seen in 1989. Water temperatures in 1996-1998 were at levels similar to those in 1986. The monthly average water temperatures fluctuated between 17°C and 25°C over the 16-year time period. There was no discernable increasing or decreasing trend.

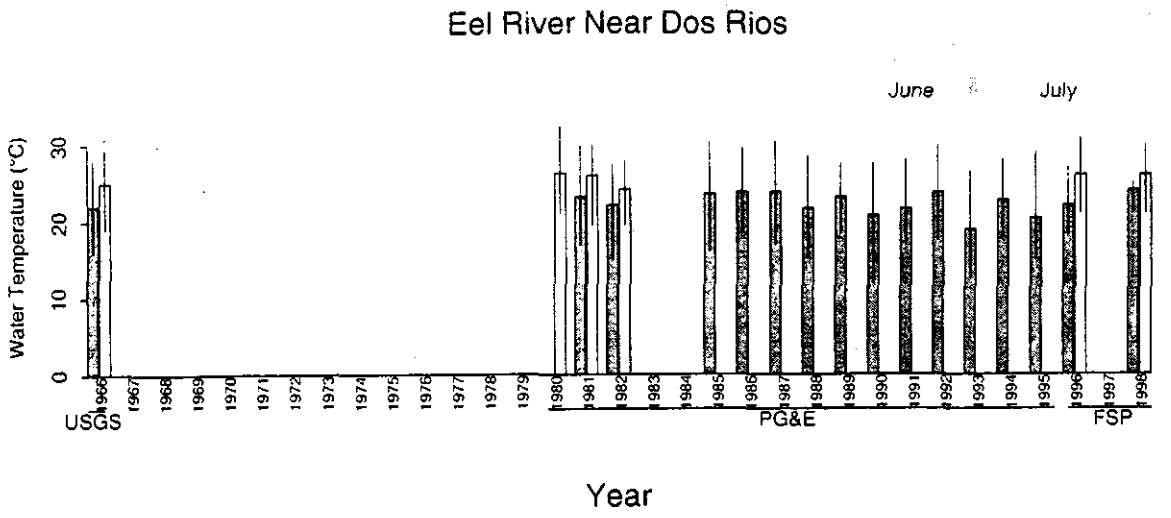

Figure 11.6. Comparison of historical USGS and PG&E monthly average stream temperature data with more recent Forest Science Project data during June and July. Location is on the Eel River near Dos Rios, CA. Vertical lines represent the range in daily minimum and maximum temperatures for each month.

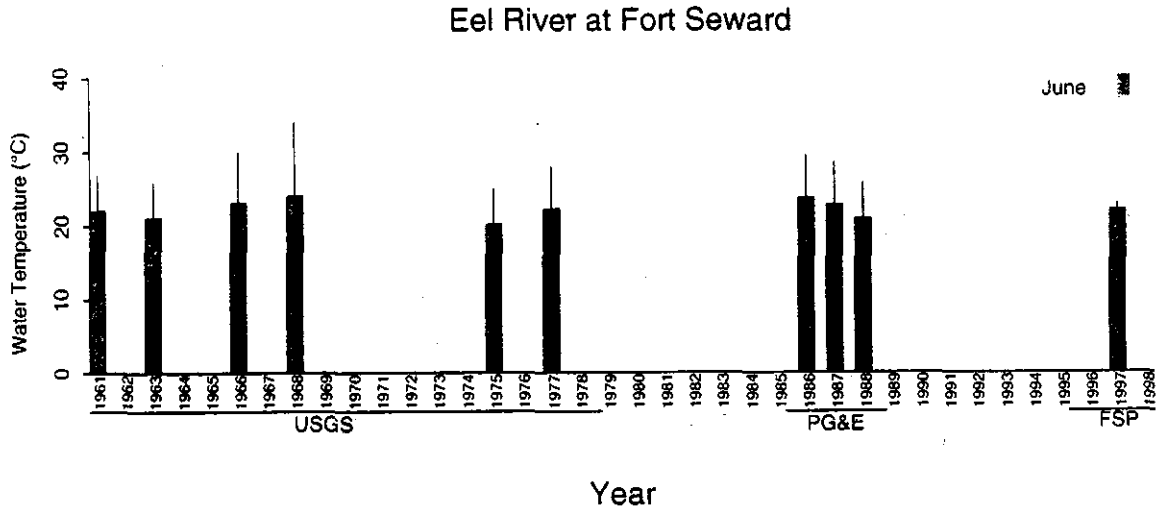

Figure 11.7. Comparison of historical USGS and PG&E monthly average stream temperature data with more recent Forest Science Project data during the month of June on the Eel River at Fort Seward, CA. Vertical lines represent the range in daily minimum and maximum temperatures for each month.

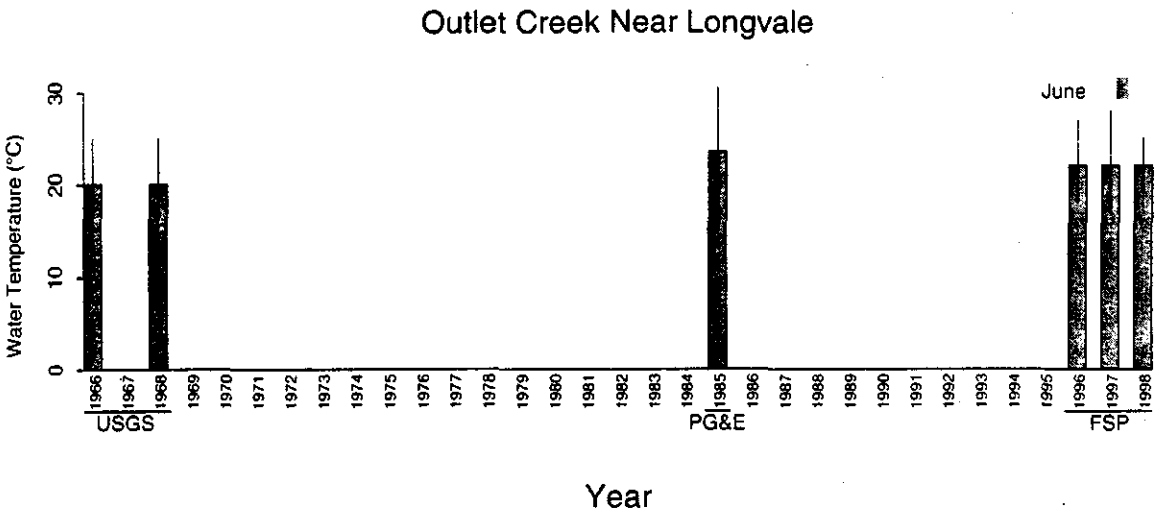

Figure 11.8. Comparison of historical USGS and PG&E monthly average stream temperature data with more recent Forest Science Project data during June for the site at Outlet Creek near the Longvale, CA. Vertical lines represent the range in temperatures for each month.

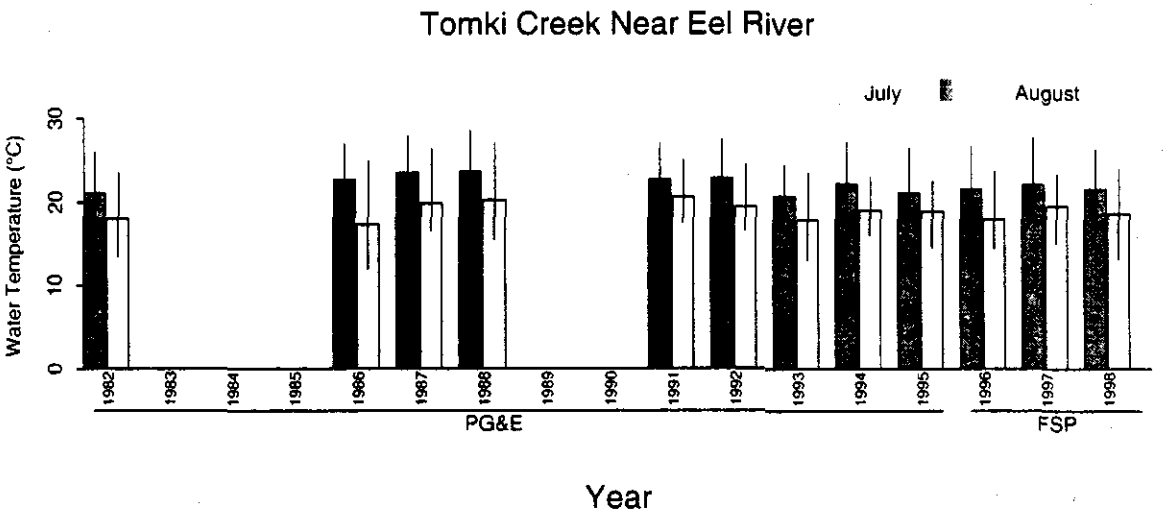

Figure 11.9. Comparison of historical PG&E monthly average stream temperature data with more recent Forest Science Project data during July and August at Tomki Creek near the Eel River. Vertical lines represent the range in temperatures for each month.

United States Geological Survey Gaging Stations - The Blodgett Report

A summary of stream temperature data collected from 1950 through 1969 at various locations throughout Northern California was prepared by Blodgett (1970). Stream temperatures were measured at USGS gaging stations using continuous sensors, hand-held thermometers, or both. Published in the report are temperature data obtained systematically either once or twice per day or by thermograph. Some periodic temperature observations (those obtained infrequently), as well as most of the thermograph and periodic records collected by other agencies, were also published in the report and do not appear in any other compilation. Latitude and longitude were reported for each station to the nearest second. Coordinates were entered into a GIS database. Generally, there were noticeable discrepancies in the location placement; sites usually did not fall on a blue-line stream on a USGS topographic map. If the coordinate-based placement of a USGS monitoring site was near a monumented USGS symbol on a DRG, the coordinates for the site were changed to place the site in the center of the stream adjacent to the USGS monitoring site marked on the DRG. There still is some error in the location placement of the USGS sites, but the placement of the USGS sites is without doubt closer to their true location than the PG&E sites. USGS sites that did not fall near the named stream indicated for that site were not used in the analysis. However, this lack of coordinate placement and stream name matching seldom occurred with USGS sites. In general, the location information contained in the Blodgett (1970) and other USGS reports was superlative. Figure 11.10 shows a map of USGS stream temperature monitoring locations found in the Blodgett report, with a dark triangle denoting those sites with matching FSP sites.

Figure 11.11 illustrates the location of continuous temperature sensors at USGS gaging stations circa 1970. There may be a concern as to the representativeness of water temperature measurements collected at gaging stations. Jones (1965) examined the relationship between the average water temperature of the stream and the temperature collected at the thermograph probe. Results showed that for 24 gaging stations with temperature monitors on streams in California compared to 180 temperature transects (cross sections surveyed with hand-held thermometers at different flow conditions) there were only 11 instances when the sensor reading differed from the average stream temperature by more than 1 °F (0.556 °C).

The USGS defines three stream temperature categories: true stream temperature (TST), temperature near the sensor (TNS), and the temperature recorded (TRC) (Stevens et al., 1975). The TST is defined as an instantaneous measurement obtained with a calibrated, full-immersion thermometer held in a shaded location in the stream's main flow away from the influence of tributaries or groundwater influx. The actual water temperature around the sensor (TRC) reflects its location in the channel cross section and may be quite different from TST. The TRC is the temperature value that is actually recorded and is a function of how well the thermometer or sensor is calibrated. If the device is calibrated correctly then TRC and TNS should be equal. The differences between TST and TNS remain, and will vary with each stream as well as diurnally and seasonally (Stevens et al., 1975). Moore (1967) as cited in Essig (1998) found about a 2 °C difference in temperature across the Middle Fork of the Willamette River near Dexter, OR. He noted that in all instances the difference between TST and TNS could be accounted for by "one or two observations of comparatively high temperatures near the bank where the flow is extremely sluggish." As Essig (1998) points out, this is the location where many stream temperature probes are placed, especially in wide streams, due to logistical and safety reasons. The differences between TST and TNS are simply not known in most cases. This holds true not only for historical data, but for all contemporary stream monitoring activities as well. Given the unknown differences between TST and TNS great caution should be applied when interpreting any stream temperature data, particularly in a regulatory context (Essig, 1998). In this chapter, and in preceding chapters, stream temperatures are used in a relative sense, to explore historical trends and associations between temperature and various landscape-level and site-specific attributes.

Figure 11.10. Location of USGS sites that were compared to more recent FSP stream temperature monitoring sites. Dark triangles (46 sites) represent USGS-FSP comparisons. Lighter triangles represent USGS sites with historical data available but no matching FSP site.

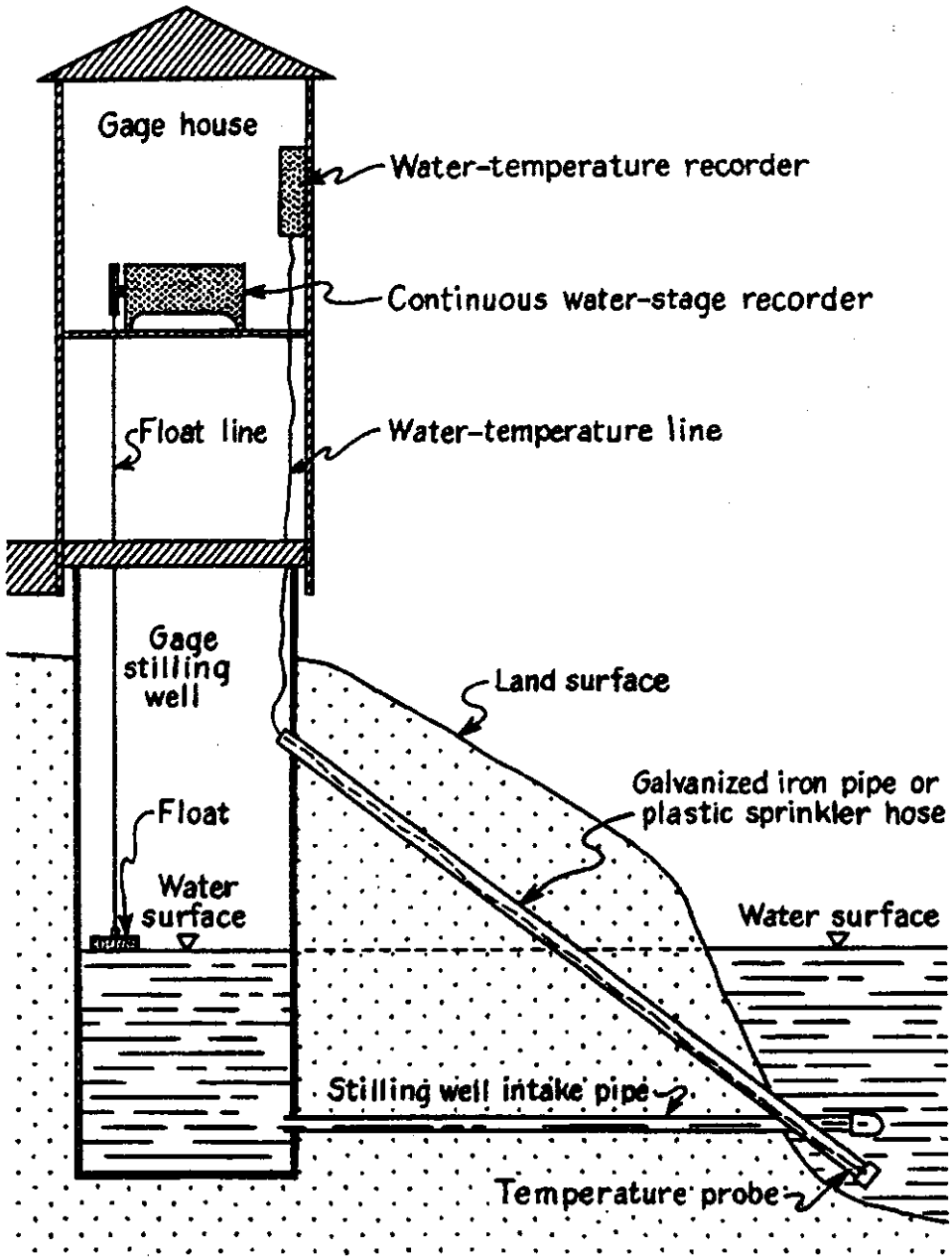

Figure 11.11. Diagram of typical USGS gaging station where both stage and water temperature are recorded. Taken from Blodgett (1970).

USGS Periodic Data

Periodic water temperature data were collected on an irregular basis and less frequently than continuous data. Periodic observations were obtained by holding a thermometer in the stream and reading it while the bulb was immersed. Periodic data were reported as the maximum value and date of occurrence of the maximum value at each site. Periodic data were only used in historical comparisons when no continuous temperature data were available. Below is an example of the way in which periodic data for maximum temperature were reported in the Blodgett report (1970) and other USGS reports.

EXTREMES. – PERIODIC DATA:
MAXIMUM = 29 DEG. C,
JULY 23, 1958, JULY 10, 1968

In this example, the values shown on the bar chart for this site would be 29°C for 1958 and 1968. The annual highest daily maximum temperature from the corresponding FSP site was graphed for each year that the FSP site was monitored. The periodic maximum, however, is a biased estimate for the maximum temperature for the period of record. A total of 12 July temperatures and 12 August temperatures (the hottest months of the year) were measured from 1958 through 1968. Even if the temperatures recorded were the maximum temperatures for the days of record, the true maximum temperature reached from 1958 through 1968 probably was not captured. Thus, the true maximum temperature for any periodic record could possibly be greater than the listed maximum value.

Additionally, the way in which the maximum temperature for the period of record was reported does not provide temperature values for years that did not have the highest value. That is, if periodic data were collected for years 1958 through 1968, only the maximum over this entire 11-year period was reported. If 1959 had the highest value out of all years, for example, 24°C, only the 1959 value would be shown in the data summary. If all other years had 23°C, their values were not reported.

The comparisons made in this section are on a site-by-site basis. They are not necessarily reflective of the larger ESU regional analysis. Any historical periodic data that had a nearby FSP site were included in the analysis. A discussion of site-specific attributes (e.g., canopy closure) was included to offer possible insight into historical stream temperature patterns. Canopy data were considered if such data existed for an FSP site and if watershed area or divide distance indicated the stream was not too wide for stream-side vegetation to provide shade.

Air temperature data were acquired for each date the daily maximum water temperature was reported. The "nearest" air temperature site, located using the 12-dimensional Euclidian distance algorithm described in Chapter 5, was compared to the water temperature site.

Sites are grouped by the USGS basin names as they appeared in the Blodgett (1970) report.

Summary of USGS Periodic Data

Trends in stream temperature varied from historic to contemporary times. There were a total of eight sites that appeared to have lower maximum stream temperatures in the 1990's than in the historic periodic record. Three of the eight sites had temperatures that were sightly less (~1°-2°C) than past temperatures and probably have similar temperature patterns today as they did historically. Those sites were:

(1) Little River near Crannell;
(2) Sugar Creek near Callahan in the Klamath River Basin; and
(3) Shackleford Creek near Mugginsville in the Klamath Basin.

Five of the eight sites had a 4°C or greater decrease in stream temperature for more recent stream temperatures compared to historic records. The sites that were cooler in more recent times were:

(1) Jacoby Creek near Freshwater
(2) Etna Creek near Etna in the Klamath Basin
(3) Big Creek near Hayfork in the Klamath Basin
(4) Albion River near Comtche
(5) South Fork Big River near Comtche

These sites all have relatively small watershed areas. The Little River site had the largest at 10,500 ha. Channel width at this watershed area size could still allow for stream-side vegetation to have an influence on stream temperature. Additionally, it is quite possible that the observed changes in water temperature from past to present times may be due to differences in the locations of the sites. The largest difference between contemporary and historic site placement was Etna Creek, where the FSP site was over 2 km upstream from the USGS site. It is also likely that an increase in canopy closure for some of these sites may have contributed to the cooling of more recent stream temperatures.

There was a total of four sites that showed little change in maximum stream temperatures from the historic record. With one exception, the maximum temperatures measured in the 1990's were within one degree of the periodic historic record. Those sites were:

(1) North Fork Mad River near Korbel
(2) Bluff Creek near Weitchpec
(3) Pudding Creek near Fort Bragg
(4) East Branch of South Fork Eel River near Garberville

Pudding Creek had two years of maximum temperatures that where 2°C greater than the historic record. However, the FSP site was ~1.3 km downstream of the USGS site. Moreover, the FSP site's watershed area was only 3681 ha, indicative of a relatively small stream. In such a small stream the downstream distance of the FSP site from the USGS site is more than adequate to explain the 2°C increase, due to natural longitudinal warming trends.

There were four sites that indicated stream temperature increases in more contemporary times. All four sites had at least a 4°C increase in water temperature for more recent years compared to the historical record. The sites were:

(1) Redwood Creek near Blue Lake
(2) South Fork Trinity River at Forest Glen in the Klamath Basin
(3) Mill Creek below Alder Creek near Covelo in the Eel River Basin
(4) Hulls Creek near Covelo in the Eel River Basin

The South Fork Trinity River site at Forest Glen has a relatively large watershed area (54,000 ha) and divide distance (50 km) compared to the other sites in the historical periodic record. The water temperature at this site should not be as susceptible to changes in canopy since the channel is quite wide. Yet, there was a large jump in stream temperature maxima from 1993 (20°C) to 1994 (27°C). Mill Creek and Hulls Creek both had smaller watershed areas and reductions in canopy could be responsible for increased stream temperature. All sites that exhibited an increase in maximum stream temperature lacked canopy data.

Periodic Data By Basin

Differences in air temperature can also account for a large proportion of the historical variability in stream temperatures at some sites. The influence of air temperature and other environmental factors on historical trends in stream temperature will be explored in more depth in the following section.

Mad River Basin

At a site located on the North Fork of the Mad River near Korbel, CA the periodic maximum water temperature in 1959 was 22°C, with a maximum air temperature on that day of 17.8°C (Figure 11.12). Nearly forty years later, at a FSP site located about 1700 m downstream from the USGS site, the highest daily maximum water temperature was 23°C, with an average daily maximum air temperature of 18.9°C. The air temperature value is the daily maximum air temperature for the date on which the maximum water temperature was reported. The 1998 site had a slightly higher water temperature than the periodic record, but the air temperature was slightly higher as well. The FSP site further downstream from the USGS site had a watershed area of 10,850 ha. The canopy closure value for the site was reported to be 5% in 1998. Given the distance traveled from the upstream USGS site to the downstream FSP site, the higher air temperature on the more contemporary date, and the open canopy, it is expected that the FSP site would be warmer than the USGS site.

Little River Basin (Humboldt County)

One USGS site in the Little River Basin (Humboldt County) was suitable for historical water temperature comparison. On the Little River near Crannell, CA the periodic maximum water temperature was reported to be 22°C in 1959 (Figure 11.13). The daily maximum air temperature was 14.4°C on the day of occurrence of the highest periodic maximum water temperature in 1959. In 1998 the highest daily maximum water temperature observed at a site located 110 m downstream from the USGS site was 20°C, with a daily maximum air temperature of 19.4°C. In spite of the much warmer air temperature in 1998, the 1998 maximum water temperature record was cooler. These sites were close enough together and the watershed area large enough (10,500 ha) that differences in temperature due to differences in site location should be minimal. No canopy data were available for this site.

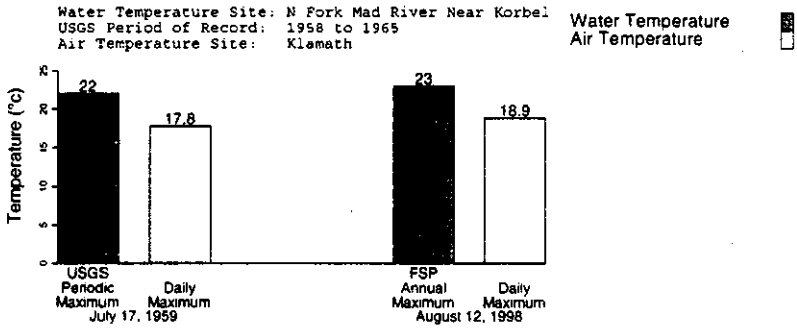

Figure 11.12. Comparison of yearly maximum stream temperatures at a historical USGS site and a more recent FSP site located on the North Fork of the Mad River near Korbel, CA in the Mad River Basin. The FSP site was located 1700 m downstream from the USGS site.

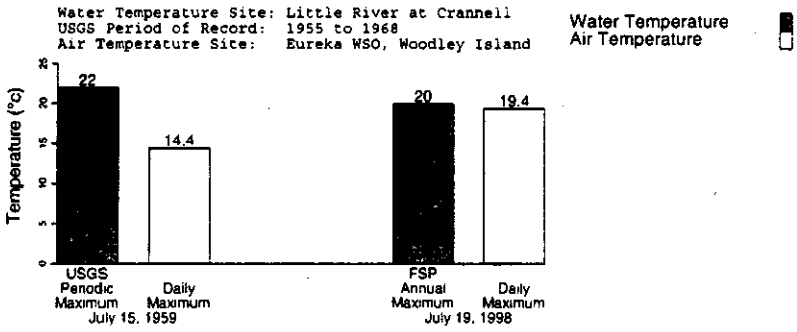

Figure 11.13. Comparison of yearly maximum stream temperatures at a historical USGS site and a more recent Forest Science Project site located in the Little River near Crannell, CA. The FSP site was located 110 m downstream from the USGS site.

Redwood Creek Basin

One Redwood Creek Basin USGS site was suitable for historical comparison. The USGS references this site as Redwood Creek near Blue Lake, CA. After placement of the site on a DRG, a better reference would be Redwood Creek near Highway 299 bridge. In 1953 and 1958 the periodic maximum water temperature at the Redwood Creek USGS site was 22°C (Figure 11.14). The daily maximum air temperature matched with the corresponding maximum periodic water temperature was 35.6°C in 1953 and 37.8°C in 1958. In 1997 and 1998, at a FSP site located about 30 m upstream from the USGS site, the highest daily maximum stream temperatures were 27°C and 26°C, respectively. The daily maximum air temperature was 40°C in 1997 and 38.3°C in 1998. The annual maximum temperatures measured in Redwood Creek near Highway 299 were higher than those measured for the periodic record. There were only four July records and two August records in the eight year historical periodic record. The probability is low that the true maximum water temperature for the historical period of record was captured.

Jacoby Creek Basin

One USGS site in the Jacoby Creek Basin in Humboldt County was suitable for historical water temperature comparison. The periodic maximum water temperature at a USGS site located on Jacoby Creek near Freshwater, CA was reported to be 21°C in 1959, with a corresponding daily maximum air temperature of 13.9°C (Figure 11.15). The proximity of this site to the coast is reflected by the low air temperature value. In 1994, a FSP cooperator deployed a sensor approximately 1060 m downstream from the USGS site. The highest daily maximum water temperature in 1994 was 15°C, with a daily maximum air temperature of 16.7°C on the day the highest water temperature occurred. The site was located close to the headwaters, with a watershed area of 1760 ha and distance from the watershed divide of 15 km. The 6°C decrease in the maximum water temperature in 1994 may be related to increased canopy along the upstream reaches of the stream. The FSP data contributor did not provide canopy information for this site.

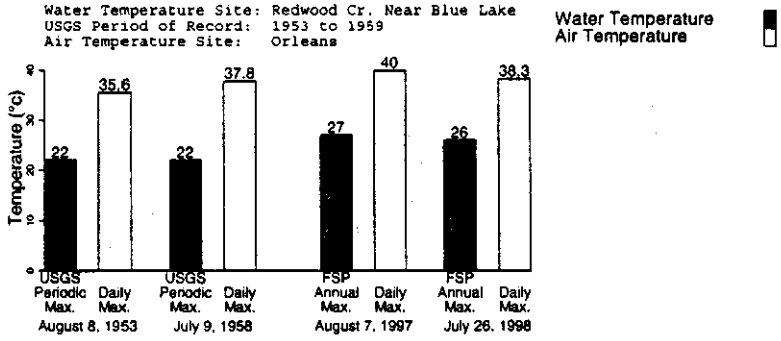

Figure 11.14. Comparison of yearly maximum stream temperatures at a historical USGS site and a more recent Forest Science Project site located in Redwood Creek near Blue Lake. The FSP site was located 30 m upstream from the USGS site.

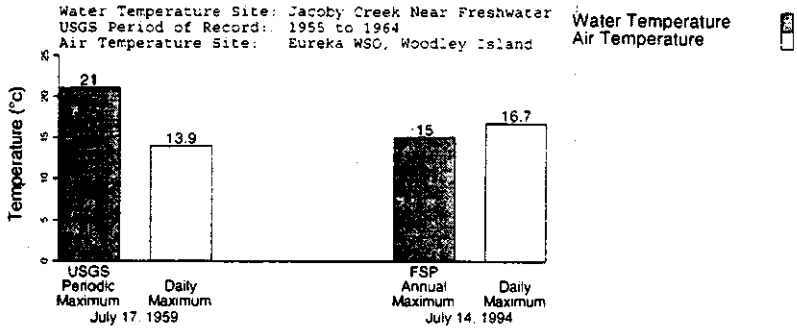

Figure 11.15. Comparison of maximum stream temperatures at a historical USGS site and a more recent FSP site on Jacoby Creek near Freshwater, CA. The FSP site was located 1060 m downstream from USGS site.

Klamath River Basin

Six periodic USGS sites in the Klamath Basin had FSP sites in relatively close proximity for historical water temperature comparison purposes. Comparisons of historical USGS water temperature data to more recent FSP data are shown in Figure 11.16.

The periodic maximum water temperatures reported for Sugar Creek near Callahan, CA for 1958 and 1959 were both 20°C, with maximum air temperatures of 38.9°C and 33.3°C, respectively (Figure 11.16-A). In 1998 the daily maximum air temperature was about the same as 1958, however, the highest daily maximum water temperature at a FSP site located 30 m upstream from the USGS site was 18°C. The water temperature was cooler in 1998 than the historic periodic maximum. The watershed area for this site was small (3065 ha) and had a reported canopy value of 5% in 1998. The decrease in maximum stream temperature may be due to an increase in canopy closure upstream from the water site.

Etna Creek near Etna, CA had a reported periodic maximum water temperature of 21°C in 1959. The daily maximum air temperature on the same day in 1959 was 33.3°C (Figure 11.16-B). In 1998 the highest daily maximum temperature observed at a FSP site located 2200 m upstream from the USGS site was 17°C, with a daily maximum air temperature on that day of 37.8°C. The 1998 water temperature was considerably lower than the historic periodic maximum. The relatively large decline in temperature at this site may be due to an increase in canopy or to a difference in site location. The site's watershed area was small (4450 ha) and had a listed canopy closure of 5% in 1998. At this size of a watershed, changes in canopy can have a significant effect. However, the FSP site was 2200 m upstream from the USGS site and the FSP site was only 11 km from the watershed divide. The extra distance from the FSP site to the USGS site is sufficient for significant increases in water temperature.

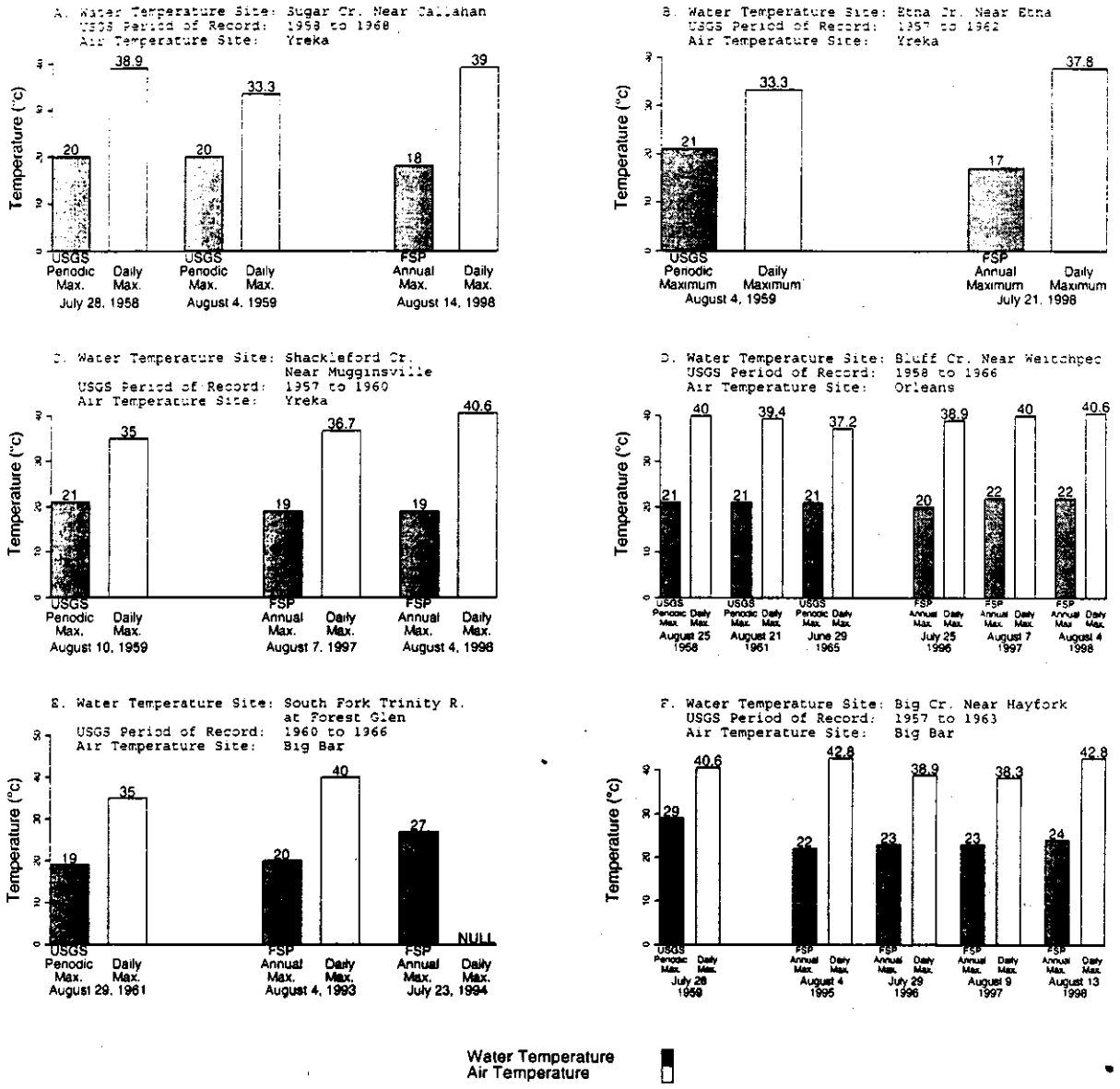

Figure 11.16. Comparison of maximum stream temperatures at historical periodic USGS sites and more recent continuous FSP sites located in the Klamath River Basin. The nearby FSP site was located A) 30 m upstream, B) 2200 m upstream, C) 1320 m upstream, D) 1420 m downstream, E) 740 m downstream, and F) 110 m downstream from the USGS site.

Shackleford Creek near Mugginsville, CA had a reported periodic maximum water temperature of 21°C in 1959, with a daily maximum air temperature of 35.0°C (Figure 11.16-C). The nearby FSP stream temperature monitoring site was located about 1320 m upstream from the USGS site. In 1997 and 1998, the highest daily maximum temperature in both years was 19°C. The maximum air temperatures were 36.7°C and 40.6°C, respectively. The more recent water temperatures were cooler than the historic periodic maximum. The Shackleford site also had a small watershed area (4800 ha) and stream temperatures at the site may be significantly influenced by canopy closure. Additionally, 1320 m downstream distance in a stream of this size is sufficient to account for the observed 2°C increase in water temperature at the historic site over the contemporary upstream temperatures.

Bluff Creek near Weitchpec, CA had reported periodic maximum water temperatures in 1958, 1961, and 1965 that were 21°C (Figure 11.16-D). The respective maximum air temperature was 40.0°C, 39.4°C, and 37.2°C on the day of occurrence for each of the periodic maximum water temperatures. A FSP site located approximately 1420 m downstream from the USGS site collected data for three consecutive years, 1996, 1997, and 1998. The highest daily maximum temperature was 20°C in 1996 and 22°C in 1997 and 1998. The average daily maximum air temperatures on the days the highest daily maximum water temperatures occurred were 38.9°C, 40.0°C, and 40.6°C, respectively. The stability in water temperature across the years is remarkable, with only a two-degree range. The site had a reported canopy value of less than 5% in 1998. The low canopy value may be due in part to the site's watershed position, being approximately 40 km from the watershed divide and having a drainage area of about 19,000 ha. The channel at this location may be too wide for canopy to provide much shade.

At a location on the South Fork of the Trinity River at Forest Glen, CA the reported periodic maximum water temperature for 1961 was 19°C, with a corresponding daily maximum air temperature of 35.0°C (Figure 11.16-E). At a FSP site located 740 m downstream from the USGS site, the highest 1993 daily maximum water temperature was 20°C, with a daily maximum air temperature of 40.0°C (104°F). In the following year, the highest daily maximum water temperature increased by 7°C. Unfortunately, no air temperature data were available on that day in 1994. The watershed area at this location was roughly 54,000 ha with a distance from the watershed divide of about 50 km. Although the water temperature in 1993 was similar to the historic periodic maximum, the 1994 water temperature was much warmer. On inspection of the records, 1994 was much hotter than 1993 for most of the summer. The 1994 record did not start until July 19, missing a significant portion of the summer. No reasonable explanation for the increase in temperature could be reached.

A USGS gaging station located on Big Creek near Hayfork, CA had a reported periodic maximum water temperature of 29°C in 1959 (Figure 11.16-F). This particular site is located in a very warm area. The daily maximum air temperatures in 1959 and in 1995 through 1998 were consistently near 40°C (104°F) on the days the highest maximum water temperatures were observed. A FSP site was located 110 m downstream from the USGS site. Despite the high air temperatures in 1995 through 1998 the highest daily maximum water temperature in these years was about 6°C lower than the periodic maximum water temperature reported in 1959. The watershed area at this location was about 7050 ha and the distance from the watershed divide was 22 km. The stream corridor is most likely capable of supporting shade-producing riparian vegetation. The decrease in daily maximum water temperatures may be due, in part, to increased shading upstream from this section of Big Creek. Unfortunately no canopy data were reported for this location.

Albion River Basin

Comparison of maximum water temperature was possible at one site located on the Albion River near Comtche, CA. A FSP site was located 1070 m upstream from the USGS site in 1996 and 1997. The periodic maximum water temperature reported in 1967 was 20°C, with a corresponding daily maximum air temperature of 34.4°C (Figure 11.17). In 1996 the highest daily maximum water temperature was 18°C, with a corresponding daily maximum air temperature of 38.3°C. In 1997 the air temperature was about 12°C lower than in 1996, with a 1°C decrease in the highest daily maximum water temperature. This site is located near the headwaters of the Albion River. The drainage area is 3530 ha (13 sq mi) and the distance from the watershed divide is 9 km (~6 mi). Water temperatures at this location are probably more responsive to changes in incoming solar radiation than to changes in air temperature, although these two sources of heat input are obviously related. Water temperatures at distances close to the headwaters are believed to be similar to groundwater temperatures (Sullivan et al., 1990). Sullivan et al. (1990) found that primary heat input into small headwater streams is via direct solar radiation input. Unfortunately, no canopy data were provided by the FSP data contributor. The maximum water temperatures in 1996 and 1997 were slightly cooler than the maximum historical periodic record. The FSP site, however, is 1.1 km upstream of the USGS site; the difference in temperature may be due to the difference in site location.

Big River Basin

There was one site in the Big River Basin that was suitable for historical comparisons. A USGS site located on the South Fork Big River near Comtche, CA had a reported periodic maximum water temperature of 26°C in 1961, with an daily maximum air temperature of 40.0°C (Figure 11.18). In 1997 the highest daily maximum water temperature at a FSP site located 490 m upstream from the USGS site was 22°C, with a corresponding daily maximum air temperature of 40.6°C. The watershed area (4289 ha) and distance from the watershed divide (14 km) indicate that the site was located near the headwaters. Despite similar daily maximum air temperatures in the two years, the daily maximum water temperature was 4°C lower in 1997 than in 1961. No canopy data were provided by the FSP data contributor, so no conclusions can be drawn. However, we cannot rule out the possibility that an increase in canopy in 1997 may be partly responsible for the lower daily maximum water temperature. Although this site has a small drainage area and the FSP site is upstream of the USGS site, the approximately 500 m is probably not enough distance to account for an increase in water temperature of 4°C.

Pudding Creek Basin

In the Pudding Creek Basin in Mendocino County, one site was suitable for historical water temperature comparisons. On Pudding Creek near Fort Bragg, CA the reported 1965 periodic maximum water temperature was 16°C, with a daily maximum air temperature of 37.2°C on the day the periodic maximum occurred (Figure 11.19). At a FSP site located 1320 m downstream from the USGS site the highest daily maximum water temperature for 1993 through 1998 varied by no more than 2°C from the 1965 periodic maximum water temperature. The daily maximum air temperatures in 1993-1998 ranged from 29 to 37°C. The site on Pudding Creek was located close to the headwaters, with a watershed area of 3681 ha and distance from watershed divide of 15 km. At such a watershed position water temperatures would be expected to be below air temperature. Air temperature has little effect near the headwaters, where direct solar radiation and groundwater temperature have greater influence on stream temperature (Sullivan et al., 1990). The FSP site is further downstream from the USGS site, which could account for the small increase in stream temperature experienced by the more recent records.

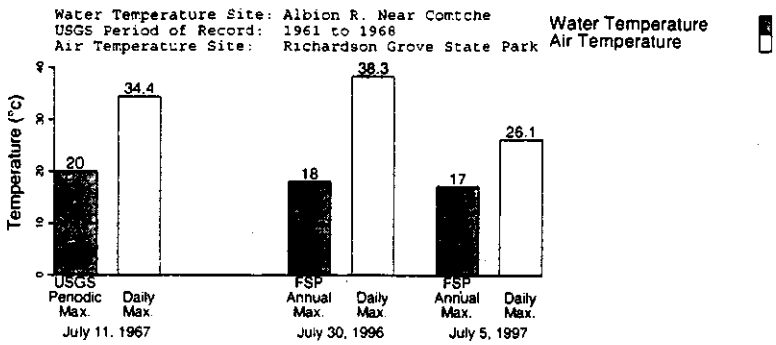

Figure 11.17. Comparison of maximum stream temperatures at historical USGS sites and more recent Forest Science Project sites located in the Albion River Basin. Nearest FSP site was located 1070 m upstream from the USGS site.

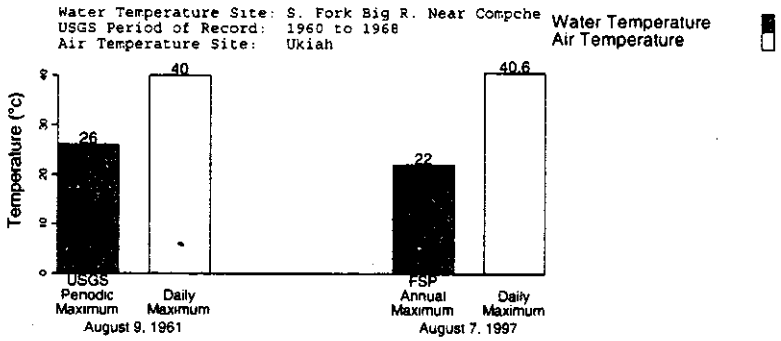

Figure 11.18. Comparison of maximum stream temperatures at a historical USGS periodic site and a more recent Forest Science Project site located on the South Fork of the Big River near Comtche, CA. The FSP site was located 490 m upstream from the USGS site.

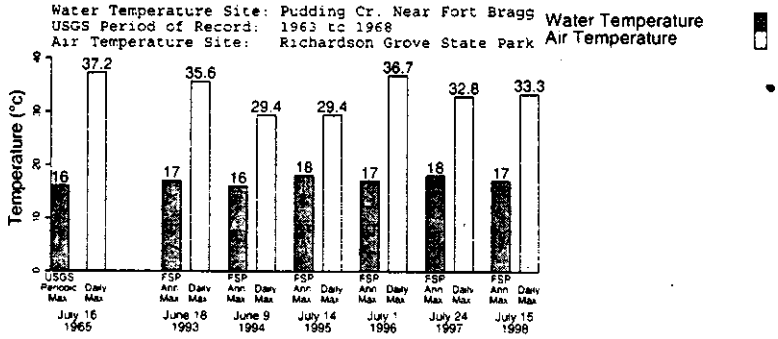

Figure 11.19. Comparison of maximum stream temperatures at a historical USGS site and a more recent Forest Science Project site located on Pudding Creek near Fort Bragg. CA. The nearest FSP site was located 1320 m downstream from the USGS site.

Eel River Basin

There were three USGS sites in the Eel River Basin with periodic water temperature data suitable for comparison to more recent FSP water temperature data acquisitions. Comparisons are shown in Figure 11.20.

A USGS site located on Mill Creek below Alder Creek near Covelo, CA had a reported periodic maximum water temperature of 24°C in 1965, with a corresponding daily maximum air temperature of 31.1°C (Figure 11.20-A). A FSP site was located 1330 m downstream from the USGS site monitored water temperature in 1996. The highest daily maximum water temperature was 31°C in 1996, a 7°C increase above the 1965 periodic maximum water temperature. However, the maximum air temperature was 8°C higher in 1996. The watershed area at the Mill Creek site was 4493 ha and the distance from the watershed divide was 14 km. Channel width at this watershed position should be capable of providing riparian shade. While the site is located fairly close to the headwaters, the water temperature at the site may have responded to the higher air temperature in 1996. If the site lacked stream-side vegetation, increased solar radiation could be responsible for the elevated daily maximum water temperature observed in 1996. No canopy data were provided by the FSP data contributor. It must also be kept in mind that with only a total of 12 periodic records taken for four years, the periodic maximum temperature is probably not the maximum daily water temperature for the periodic record period. Also, the 1330 m downstream location of the FSP site may contribute to higher stream temperatures than occurred at the USGS site.

On Hulls Creek near Covelo, CA the reported periodic maximum temperature in 1961 was 17°C, with a daily maximum air temperature of 30.6°C on the day the periodic maximum water temperature occurred (Figure 11.20-B). At approximately 470 m downstream from the USGS site, an FSP site measured a highest daily maximum water temperature of 28°C in 1996. The corresponding daily maximum air temperature was 38.3°C. Similar to the Mill Creek site, the water temperature increased with a substantial increase in air temperature. Also similar to the Mill Creek site, only 18 periodic records were taken over four years; thus, the periodic maximum temperature may not be the true maximum daily water temperature for the periodic record period. The watershed area at the Hulls Creek site was 6840 ha and the distance from the watershed divide was 17 km. The downstream distance of 470 m for the FSP site is not of sufficient distance to account for an 11°C difference between the stream temperature records. The channel width at this watershed position is most likely capable of providing stream side shade, although no canopy information was provided by the FSP data contributor.

A USGS site located on the East Branch of the South Fork of the Eel River near Garberville, CA had a reported periodic maximum water temperature of 28°C in 1967 (Figure 11.20-C). The daily maximum air temperature on that day was 27.2°C. At about 880 m downstream from the USGS site a FSP site had a highest daily maximum temperature of 29°C in 1996. The air temperature maximum for the day of the highest daily maximum water temperature was 11°C higher in 1996 than it was in 1967. The watershed area at this site was 1169 ha and the distance from the watershed divide was 5 km. The channel width at this watershed position should be narrow enough to allow stream side vegetation, if present, to provide shade. The periodic historical maximum is similar to the maximum stream temperature seen in 1996.

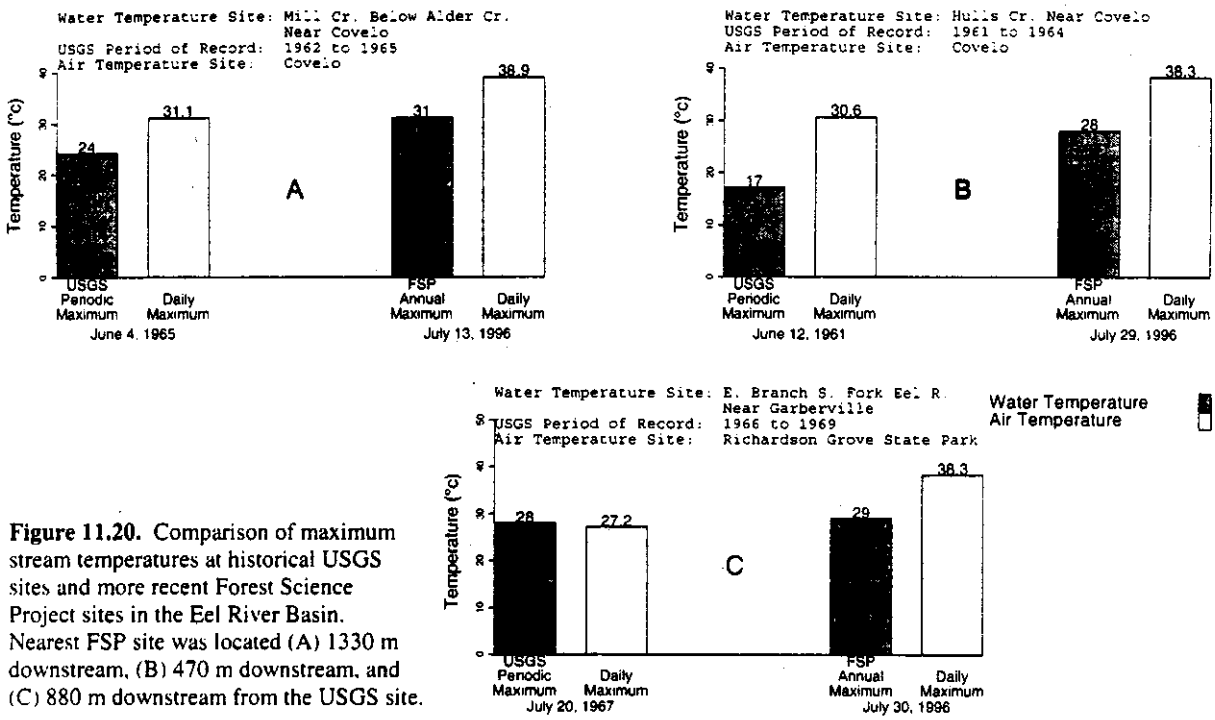

Figure 11.20. Comparison of maximum stream temperatures at historical USGS sites and more recent Forest Science Project sites in the Eel River Basin. Nearest FSP site was located (A) 1330 m downstream, (B) 470 m downstream, and (C) 880 m downstream from the USGS site.

Summary of USGS Continuous Data

Water temperature data from USGS gaging stations (Blodgett, 1970) equipped with continuous monitors were scanned from the hardcopy report using a flatbed scanner. The images were converted to characters using optical character recognition software. The data were verified against the hardcopy report. Corrections were made where necessary. The continuous data were entered into a Microsoft Access database for comparison to more recent FSP stream temperature data. The USGS continuous data were reported as monthly minima, means, and maxima. The stream temperature data from FSP sites located in close proximity to USGS continuous monitoring sites were aggregated to monthly minima, means, and maxima for direct comparisons to the USGS data.

Historical data comparisons were grouped by basin names as they appeared in the USGS report (Blodgett, 1970) and by sites that shared the same air temperature site. Basins are presented with the northernmost basin first. Each site is represented in a bar chart with the height of the bar indicating the monthly average temperature and vertical lines representing the range in temperatures for each month. July and August are usually the hottest months for the year and are the only months presented in the figures, with exceptions where noted.

Klamath River Basin

Four USGS sites with continuous monitoring data were located in the proximity of FSP sites in the Klamath River Basin. Figures 11.21, 11.22, and 11.23 show the temporal trends in water and air temperature at the four sites. The bars represent the monthly average water and air temperature value and the vertical lines represent the range in the monthly minimum and maximum temperature values.

A USGS site located on the Salmon River at Somes Bar had continuous water temperature data for 1966, 1968 and 1975 through 1978 (Figure 11.21-A). A FSP site was located about 70 m downstream from the USGS site. August 1966 was the warmest month in the 32-yr record, having both the highest monthly maximum (30.0 °C) and highest monthly average (22°C). The monthly average water temperature for more recent data (1997 and 1998) was slightly warmer (21.0°C) than most other years. However, it should be noted that the July and August monthly minima in 1997 and 1998 were higher, while the monthly maxima were quite similar to earlier years. Higher monthly minima would account for the higher monthly averages. August 1966 and 1977 monthly average air temperatures measured in Orleans at a distance of 9.8 km from the water monitoring location were the warmest August averages for the record. Summarily, there was not a noticeable change in stream temperature in the Salmon River at Somes Bar over the 32-year record.

The watershed area at the Salmon River site was 194,255 ha (~750 sq mi) and the distance from the watershed divide was approximately 93 km (~58 mi). The channel width at this watershed position was probably quite wide. The canopy value of zero at this site provided by an FSP data contributor provides additional evidence that the stream may be too wide for riparian vegetation to provide shading. Thus, localized changes in the vegetation will have little effect on stream temperature.

A USGS site was located on the Klamath River at Orleans, CA. The river is wide at this location, with a watershed area of about one million ha (nearly 4000 sq mi) and a distance from watershed divide of 306 km (190 mi). The canopy reported in 1998 at a FSP site located 470 m downstream from the USGS site was zero. All July and August monthly average temperatures throughout the record remained between 20°C to 25°C (Figure 11.21-B). The air site, located in Orleans, was 0.4 km from the USGS site. The monthly average air temperatures in July and August were also in the 20 to 25°C range (Figure 11.21-C). There were no detectable trends in stream temperature as a function of time.

A USGS site was located on Hayfork Creek near Hyampom, CA. The watershed area is 99,932 ha (386 sq mi) and the distance from watershed divide was 85 km (53 mi) at this location on Hayfork Creek. No canopy values were reported in 1990-1992 or 1998 at a FSP site located 470 m downstream from the USGS site. July and August monthly averages ranged from 19 to 25°C (Figure 11.22, top). In 1961, the site experienced the warmest monthly average water temperatures (25°C and 24°C for July and August, respectively). Unfortunately, air temperature data (collected at Big Bar at a distance of 21.9 km) for August 1991 and 1992 and July 1990 were not available, so a complete picture of air temperature trends is not possible. For the months with available data, it appears that 1990-1992 were warmer than similar months in 1961-1967 (Figure 11.22, bottom). Temperatures do not appear to be changing through time at this site.

A USGS site was located on Blue Creek near Klamath, CA. Water temperatures in the 1960's were very similar to those observed in 1994 and 1995 at a FSP site located 1800 m downstream from the USGS site. Average monthly water temperatures ranged from 16°C to 18°C for all years (Figure 11.23, top). Air temperature (measured at Prairie Creek State Park near Orick, 13.7 km from the water temperature site) was moderate, due to the close proximity to the coast (Figure 11.23, bottom). Thus, Blue Creek water temperatures may be more moderated by cooler coastal air temperatures than more interior Klamath Basin sites. The watershed area at this site was 31,415 ha (121 sq mi) and the distance from the watershed divide was 39 km (24 mi). This is a small enough watershed that the stream temperature may be influenced by canopy; however, no canopy data for the site was reported.

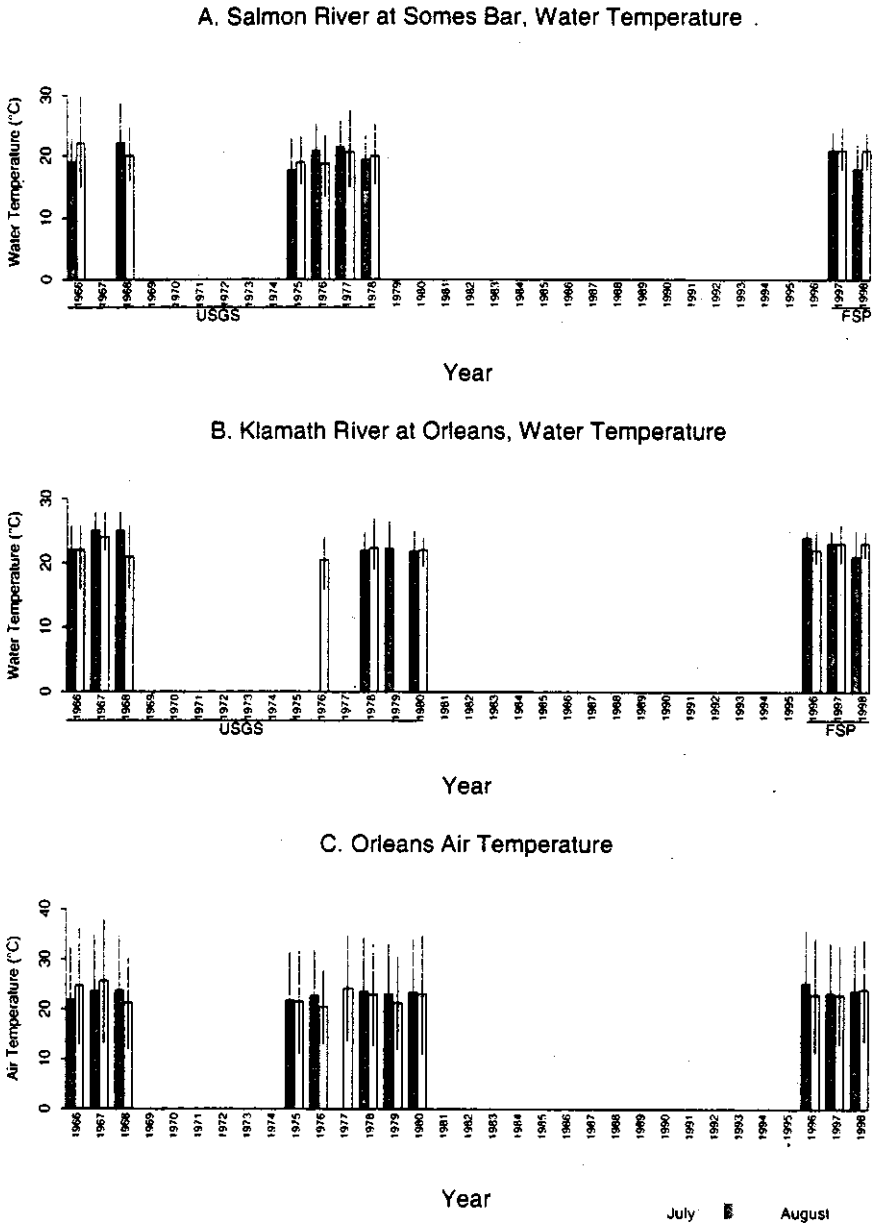

Figure 11.21. Comparison of historical USGS monthly average stream temperature and more recent FSP data for Klamath River Basin sites. Nearby FSP site on the Salmon River (A) was 70 m downstream from the USGS site and on the Klamath River (B) was 470 m downstream. NOAA air temperature site (C) in Orleans was 0.4 km from USGS site. Vertical lines represent the range in temperatures for each month.

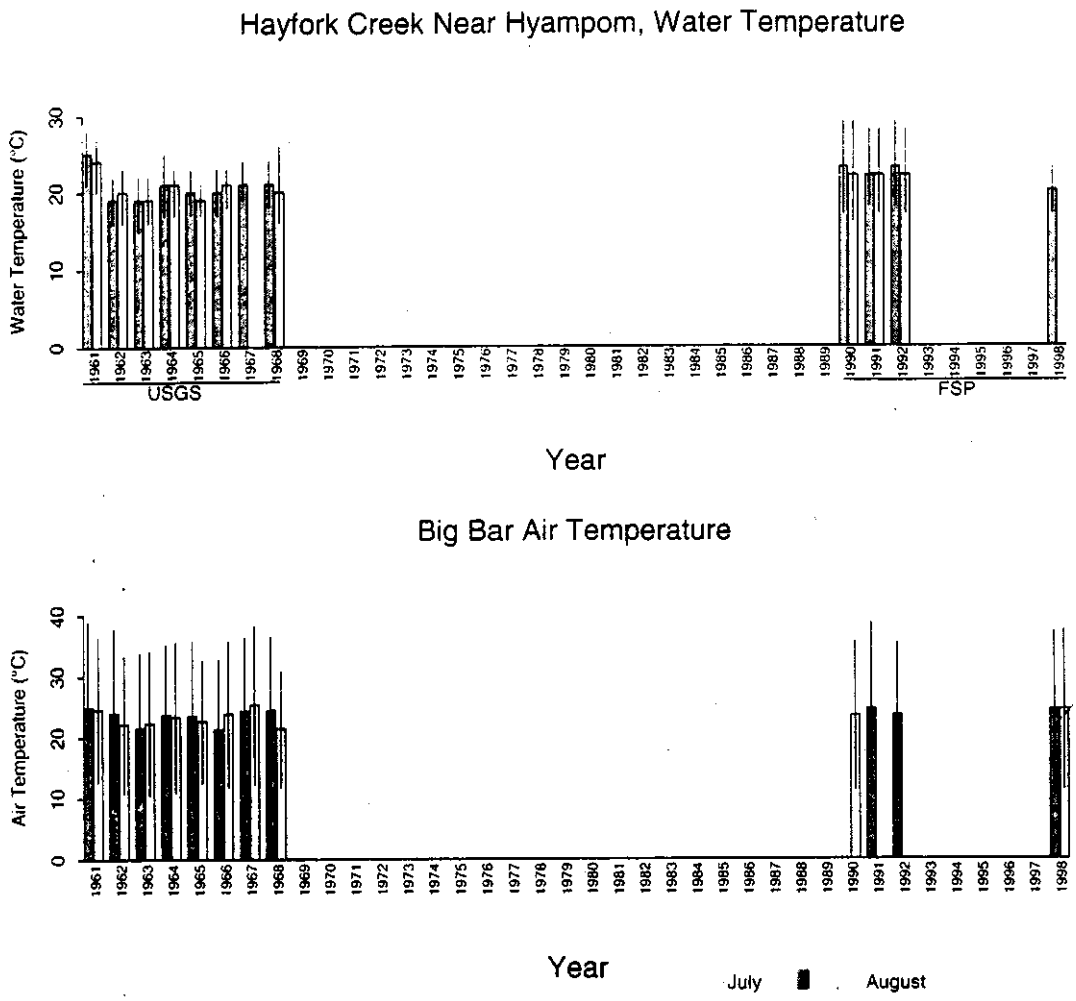

Figure 11.22. Comparison of historical USGS monthly average stream temperature data and more recent Forest Science Project data for two sites located in the Klamath River Basin. Nearest FSP site on Hayfork Creek (top) was 1500 m downstream from USGS site. Air temperature was measured at NOAA station at (bottom) Big Bar, CA. Vertical lines represent the range in temperatures for each month.

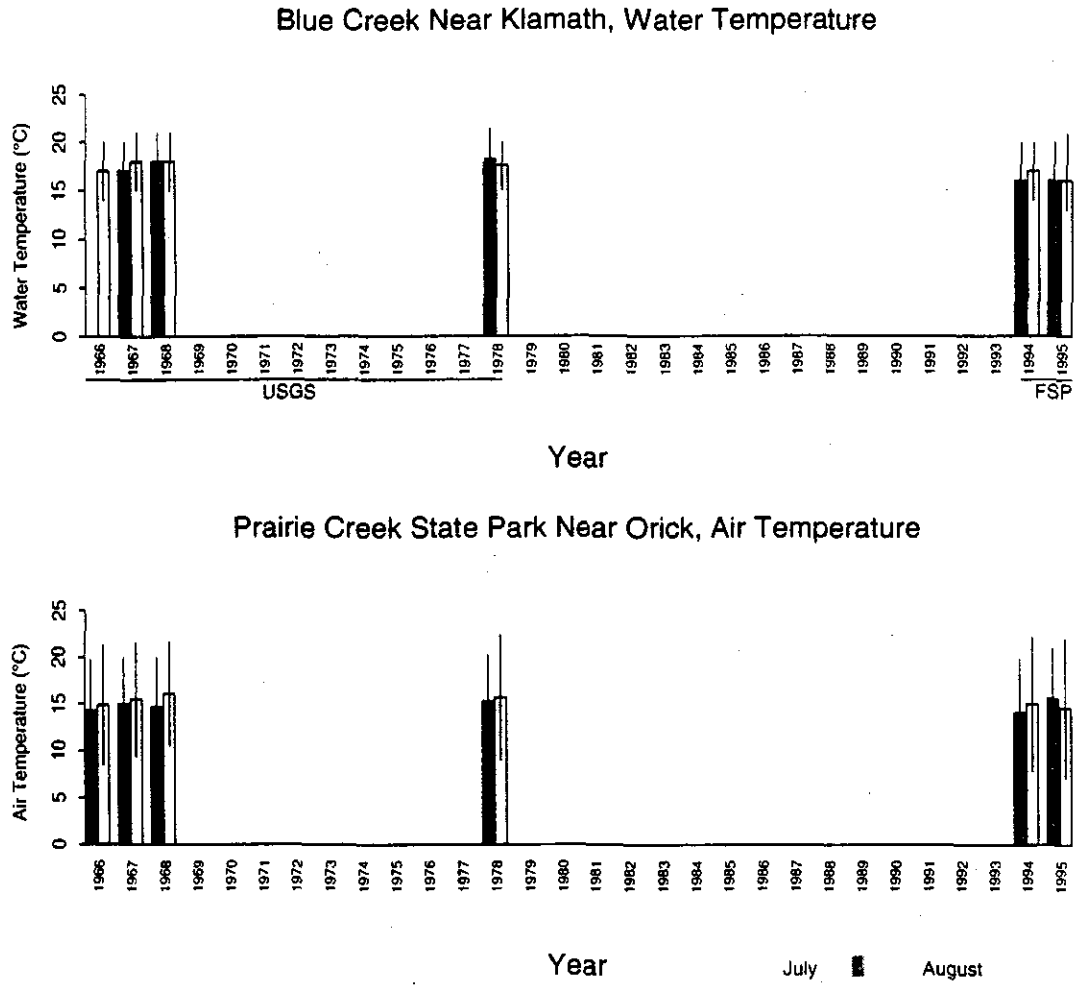

Figure 11.23. Comparison of historical USGS monthly average stream temperature data and more recent Forest Science Project data for a site located in the Klamath River Basin. Nearby FSP site on Blue Creek (top) was 1800 m downstream of the USGS site. Air temperature (bottom) was measured at NOAA station at Prairie Creek State Park near Orick, CA. Vertical lines represent the range in temperatures for each month.

Mad River Basin

In the Mad River Basin only one USGS site with continuous water temperature data was in close proximity to a more recent FSP site. This site was located on the Mad River near Arcata, CA. The nearest FSP site was located 1660 m downstream from the USGS site. The FSP site was operated only in 1998. The watershed area at this location on the Mad River was 125,504 ha (484 sq mi) and the distance from the watershed divide was 169 km (105 mi). The reported canopy cover at this site in 1998 was 5%. The monthly average water temperatures for July and August 1998 at the FSP site were 19°C and at the USGS site ranged from 18°C to 22°C. Figure 11.24 shows the monthly and yearly temporal trends in air temperature for the nearest air site located at the National Weather Service Office (WSO) on Woodley Island, Eureka, CA. Monthly water temperatures on the Mad River near Arcata do not seem to indicate either a warming or cooling trend over about the last 37 years.

Eel River Basin

There were twelve USGS continuous water temperature monitoring sites in the Eel River Basin that had more recent FSP sites in close proximity for historical comparison purposes. Sites are grouped together with their nearest air temperature station.

Figure 11.25 shows a comparison between three matched pairs of USGS and FSP sites in the Eel River Basin. A USGS site on the Eel River below Scott Dam exhibited monthly average water temperatures below 20°C for most months. Monthly average temperatures gradually increased from June to September. September proved to be the month with the highest monthly average water temperature for both the USGS and a FSP site located 80 m upstream.

Impoundment of a river alters the thermal regime, even in large rivers (Allan, 1995). If the flow through the reservoir is slow, the reservoir will undergo thermal stratification typical of lakes (Wetzel, 1983). During the summer, reservoir surface water will be warmer than is typical for river water, and deep water will be quite cool, often between 6°C and 10°C. A dam that releases surface water from its impoundment will usually increase the annual temperature range immediately downstream, whereas a deep release dam will lessen annual variation. Scott Dam is a deep release dam. The USGS and FSP sites were approximately 1000 m below the dam. If air temperature and solar radiation were the primary heat sources at this location, one would expect to see the highest monthly average water temperatures in July and August like the majority of other FSP sites. Another mechanism must be responsible for the continual increase in water temperature until the highest monthly average is attained in September. The delayed peak in water temperatures is most likely a result of the break up of the reservoir's thermocline as fall approaches, with warmer surface water mixing with deeper cool water. Also, the reservoir may be drawn down enough that warmer surface water is being released through the dam.

The watershed area at the below-Scott-Dam location was 74,956 ha (289 sq mi) and the distance from the watershed divide was 54 km (34 mi). No canopy data were submitted by FSP cooperators for this site, but given the site's watershed position, it is probably less than 5% and not affected by land management practices. While 1997 was one of the warmer years on record, it was not outside the range of the historical record and 1996 was more similar to earlier years (Figure 11.25-A). The August average water temperature ranged from 14°C to 22°C with maximum values ranging between 16°C and 23°C. Average August water temperature was 20°C in 1997 (over 1°C cooler than the 1977 record) and maximum August water temperature was 23°C in both 1977 and 1997. The September average water temperature ranged from 16°C to 22°C with maximum values ranging between 18°C and 24°C. Average September water temperature was 21°C in 1997 (almost the same as the 1977 record) and maximum September water temperature was 23°C in both 1967 and 1997(1°C cooler than the 1977 record). There was no discernible historical trend in water temperature at this site.

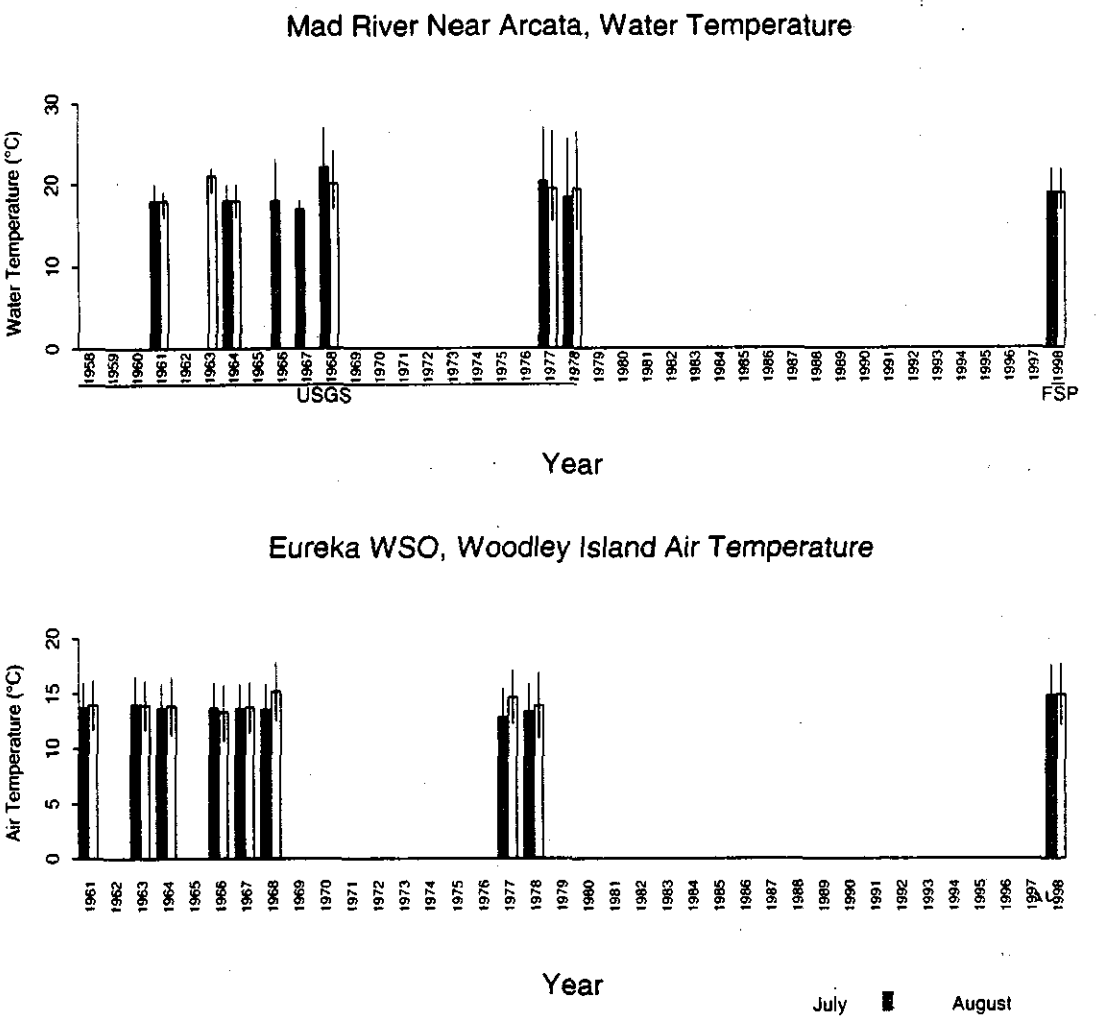

Figure 11.24. Comparison of (top) historical USGS monthly average stream temperature data in the Mad River near Arcata, CA and more recent Forest Science Project data for a site located 1660 m downstream from the USGS site, and (bottom) monthly average air temperature from nearest air site in Eureka, CA. Vertical lines represent the range in temperatures for each month.

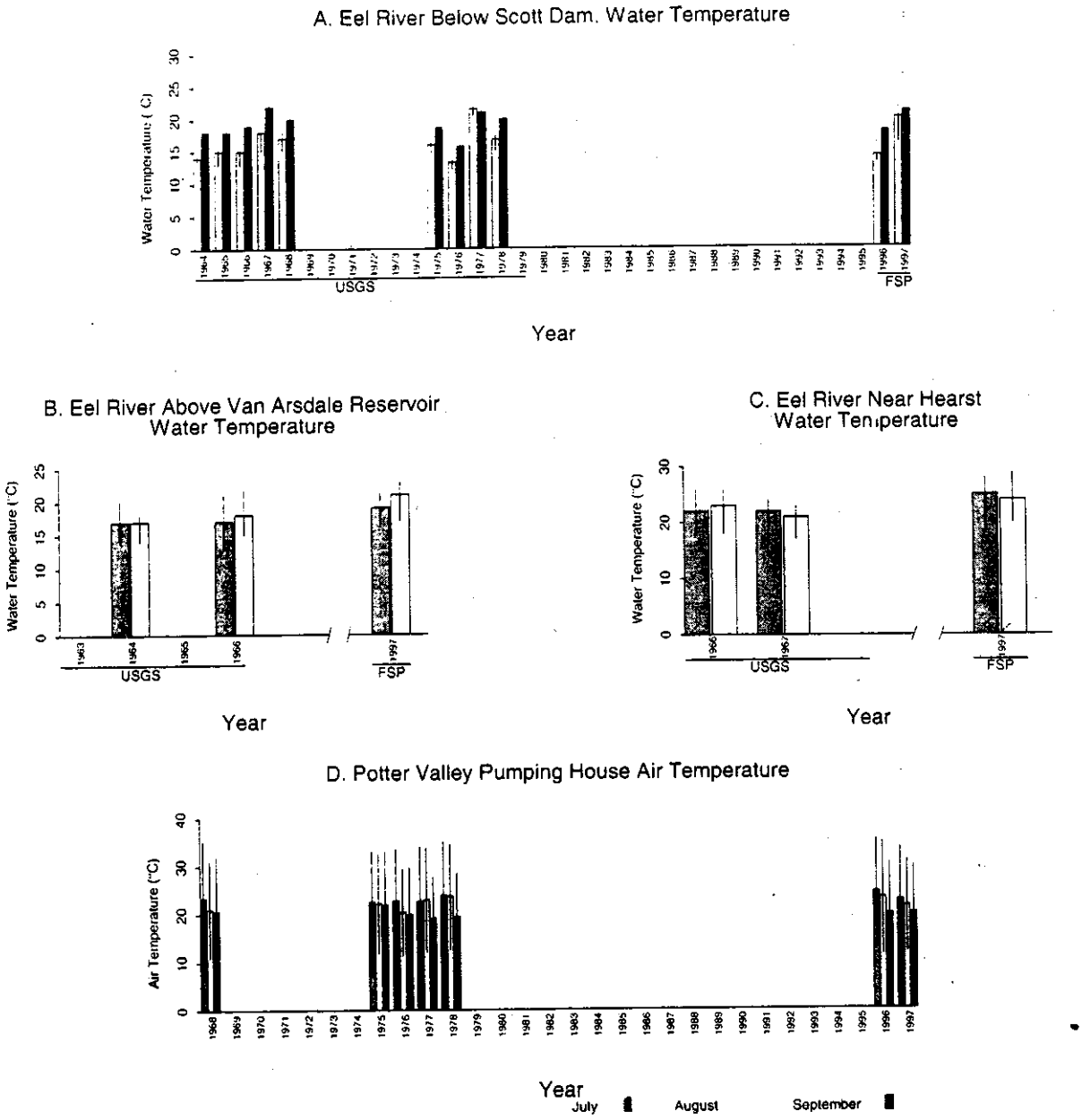

Figure 11.25. Comparison of historical USGS monthly average stream temperature data and more recent Forest Science Project data for a site located in the Eel River Basin. Nearby FSP sites were (A) 80 m upstream, (B) 240 m upstream, and (C) 350 m upstream from the USGS site. Air temperature (D) was measured at the Potter Valley Pumping House. Vertical lines represent the range in temperatures for each month.

A USGS site located above Van Arsdale Reservoir had a matching FSP site located 240 m upstream from the USGS site. The watershed area at this location was 89,343 ha (345 sq mi) and the distance from the watershed divide was 70 km (43 mi). No canopy data were submitted by FSP cooperators for this site, but given the site's watershed position, it is probably less than 5% and not affected by land management practices. Monthly average water temperatures were very stable in 1963, 1964, and 1966. Water temperatures varied between 16°C and 18°C (Figure 11.25-B). Monthly average water temperatures measured in 1997 at a FSP site located 240 m upstream from the USGS site were about 3°C higher than those in 1963, 1964, and 1966. Air temperatures measured at an air monitoring station at the Potter Valley Pumping House were incomplete. Only 1968 air temperature data were available, thus analysis with air temperature is not possible. Just as at the site below Scott Dam, this site had warmer water temperature in 1997 than in earlier years. Unlike the Scott Dam site, no data were available in the 1970's.

Three years of data are compared in Figure 11.25-C for a site located on the Eel River near Hearst, CA. The watershed area at this location was 118,897 ha (459 sq mi) and the distance from the watershed divide was 89 km (55 mi). No canopy data were submitted by FSP cooperators for this site, but given the site's watershed position, it is probably less than 5% and not affected by land management practices. The August monthly average water temperature in 1966 was higher than in 1967, while for July, both years were the same. Monthly average water temperatures in 1997, measured at a FSP site located 350 m upstream from the USGS site were higher than values in 1966 and 1967. Air temperatures in 1997 (Figure 11.25-D) did not appear to be warmer than other years. The data for the Hearst site was similar to the site above the Van Arsdale Reservoir. The site had recent data for only 1997, and, as seen at the site below Scott Dam, 1997 was the warmest year in the record.

Figures 11.26 and 11.27 show comparisons for six USGS and FSP matched site pairs that were within 20 km of Covelo, CA. All six matched water sites use the air temperature data collected at Covelo as an index for the air temperature.

A USGS water temperature site in the Eel River near Dos Rios in 1966 had FSP cooperator recorded stream temperature data 70 m downstream in 1996 and 1998. The USGS site was approximately 19.2 km from the Covelo air temperature site. The July 1966 average water temperature was 1°C cooler than both the July 1996 and 1998 records (Figure 11.26-A). The August 1966 average water temperature was 1°C warmer than August 1998 and 2°C warmer than August 1996. Monthly maximum temperatures were all between 29°C and 31°C. Monthly average air temperature was also quite similar, ranging from 21.7°C to 24.6°C. The records indicate that there was not a substantial difference at this site between the historical record and the two more recent records.

USGS and an FSP cooperator both collected one year of data at a site on the Middle Fork of the Eel River below Cable Creek. The FSP site, operated in 1998, was 300 m downstream of the USGS site, operated in 1959. The USGS site was 11.1 km from the Covelo air temperature site. The sites were similar between the two years with 1959 having a 1°C warmer July monthly average and a 1°C cooler August monthly average (Figure 11.26-B). The monthly maximum water temperatures were also similar to 1959, having a 3°C higher July maximum and a 3°C cooler August maximum. The air temperature was slightly higher in July 1959 compared to the other months, but both years of August air temperatures were similar. This site had a drainage area (~193,000 ha) strongly suggesting that canopy had little influence on stream temperature. In 1998, the FSP cooperator reported a canopy closure of 5%.

At a site in the Middle Fork of the Eel River above Black Butte River, USGS collected stream temperature data in 1959, 1966, and 1968. At a site 1400 m downstream, an FSP cooperator collected stream temperature data in 1996 and 1997. The USGS site was 16.3 km from the Covelo air temperature site. Average monthly stream temperatures for July and August ranged from 21°C to 23°C and the monthly maxima ranged from 26°C to 29°C (Figure 11.26-C) across all years in the record. With a 1400-meter difference between site

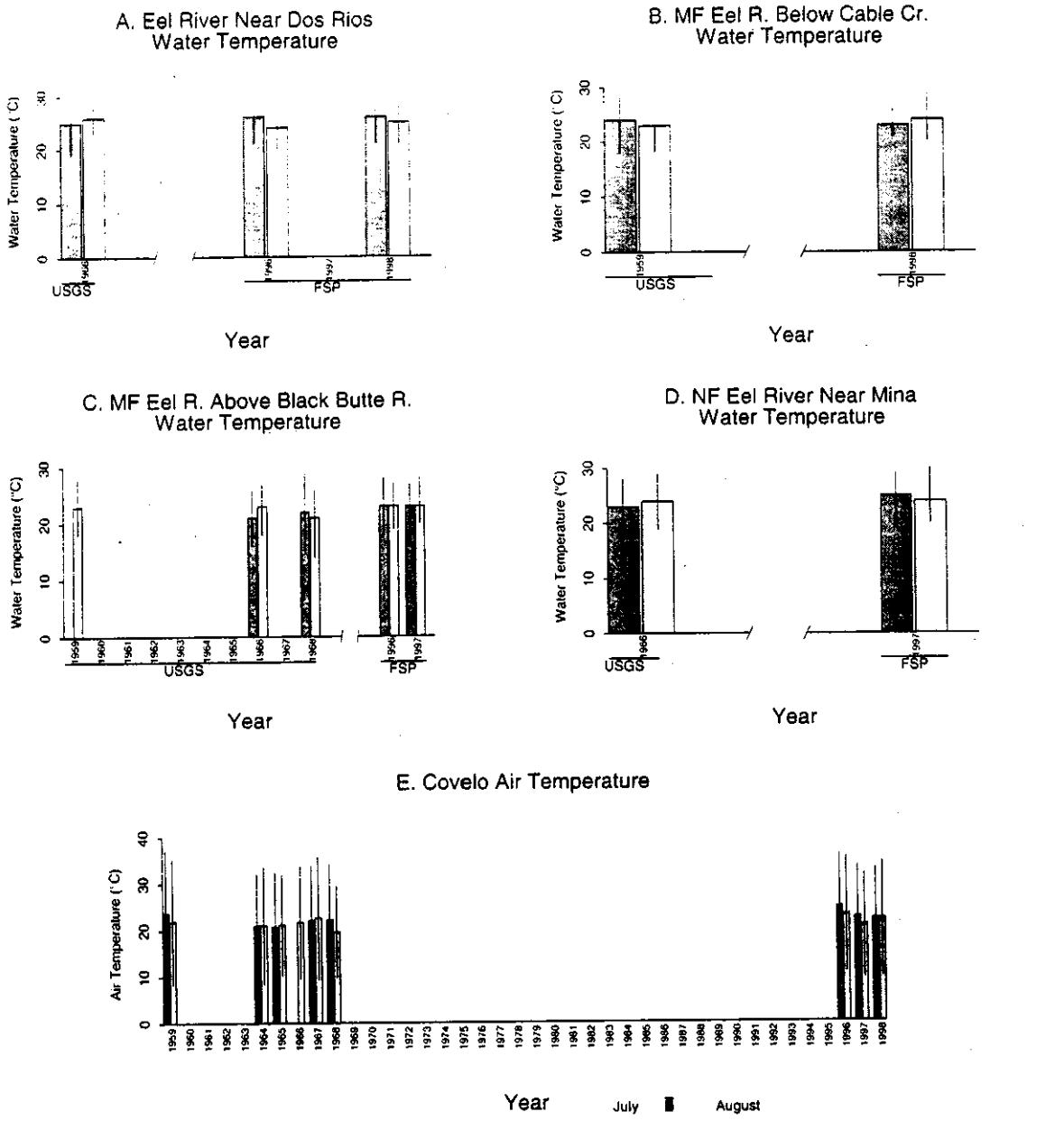

Figure 11.26. Comparison of historical USGS monthly average stream temperature data and more recent Forest Science Project data for four sites located in the Eel River Basin. Nearest FSP site was A) 70 m downstream, B) 300 m downstream, C) 1400 m downstream, and D) 360 m upstream from the USGS site. Air temperature (E) was measured at a NOAA site located in Covelo, CA. Vertical lines represent the range in temperatures for each month.

location, these differences may be due solely to location differences. Thus, there is no detectable difference in temperatures for this site.

The USGS collected water temperature data in the North Fork of the Eel River near Mina in 1959. A FSP cooperator recorded stream temperature 360 m upstream from the USGS site in 1998. The USGS site was 19.0 km from the Covelo air temperature site. The July monthly average water temperature for 1966 was 2°C cooler than the 1998 record (Figure 11.26-D). The August monthly average water temperature for both 1996 and 1998 was 24°C. The July and August monthly maxima for 1996 were 1°C cooler than those for 1998. There was not an air temperature record for July 1966, but August 1966 average air temperature was warmer than the 1998 record. A change in stream temperature at this site could not be perceived.

The USGS collected water temperature data in Black Butte River near Covelo from 1964 through 1968. An FSP cooperator collected water temperature data for 1996 through 1998 at a site 180 m downstream of the USGS site. The Covelo air temperature station was 15 km from the USGS site. For the 1996 through 1998 records, the July average stream temperature ranged from 22°C to 24°C, while the 1964 through 1968 July records ranged from 20°C to 25°C (Figure 11.27-A). For the 1996 through 1998 records, the August average stream temperature was 23°C for all three years, while the 1964 through 1968 August records ranged from 21°C to 25°C. Similarly, the monthly maximum temperatures for 1996 through 1998 also fell within the range of the 1964 through 1968 record.

At a site on the Middle Fork of the Eel River near Dos Rios, USGS collected water temperature data for thirteen separate nonconsecutive years from 1958 through 1980. A FSP cooperator collected data in 1998 at a site 610 m downstream from the USGS site. The USGS site was 10.7 km from the Covelo air temperature site. July average water temperature for the recorded years from 1958 through 1968 ranged from 23°C to 27°C and for 1976 through 1980 ranged from 23°C to 25°C (Figure 11.27-B). The 1998 July average stream temperature was 24°C. The earliest three years (1958, 1959, and 1961) had the warmest July water temperatures. For most years August was slightly (1°C to 2°C) cooler. August average water temperature for the years from 1958 through 1968 ranged from 24°C to 26°C and for 1976 through 1980 ranged from 23°C to 25°C. The 1998 July average stream temperature was 24°C. Again, the earliest three years had the warmest July water temperatures. The warmest water temperature records, 1958, 1959, and 1961, also had the warmest air temperatures. Canopy for this site was reported at 5% by a FSP data contributor for 1998. This site had a relatively large drainage area (193,000 ha), indicating that the channel is quite wide. Canopy probably has not played a role historically in influencing stream temperature at this site.

Figure 11.28 shows the comparison for a USGS site and a FSP matched site on the Eel River at Fort Seward. The sites use the air temperature data collected at Richardson's Grove State Park as an index for the air temperature at the water temperature sites. The FSP site on the Eel River at Fort Seward was 730 m upstream of the USGS site. July and August monthly average water temperatures for 1961 to 1964 were 22°C to 23°C, respectively. In 1966 and 1968, the July average water temperatures were 25°C and 26°C, respectively. The August 1966 average water temperature was 26°C. The July 1975, 1977, and 1997 average water temperatures were all close to 24°C. The August 1975, 1978, 1997, and 1998 average water temperatures were all approximately 24°C, while the August 1977 average was about 25°C. More recent data collected at the site indicated that there was no notable increase in stream temperature over time.

The USGS collected water temperature data in the Eel River at Fernbridge in 1957 and 1958. A FSP cooperator collected water temperature data at a site 230 m downstream. The matched pair uses the air temperature data collected about 16 km away at Scotia as an index for the air temperature. The July average water temperature for 1957, 1958, and 1997 and all four years for August was 20°C (Figure 11.29). The August 1998 average water temperature was 21°C. The maximum monthly stream temperature ranged from 22°C to 23°C, except for August 1998 which was 24°C. The water temperatures at this site were similar, while the air

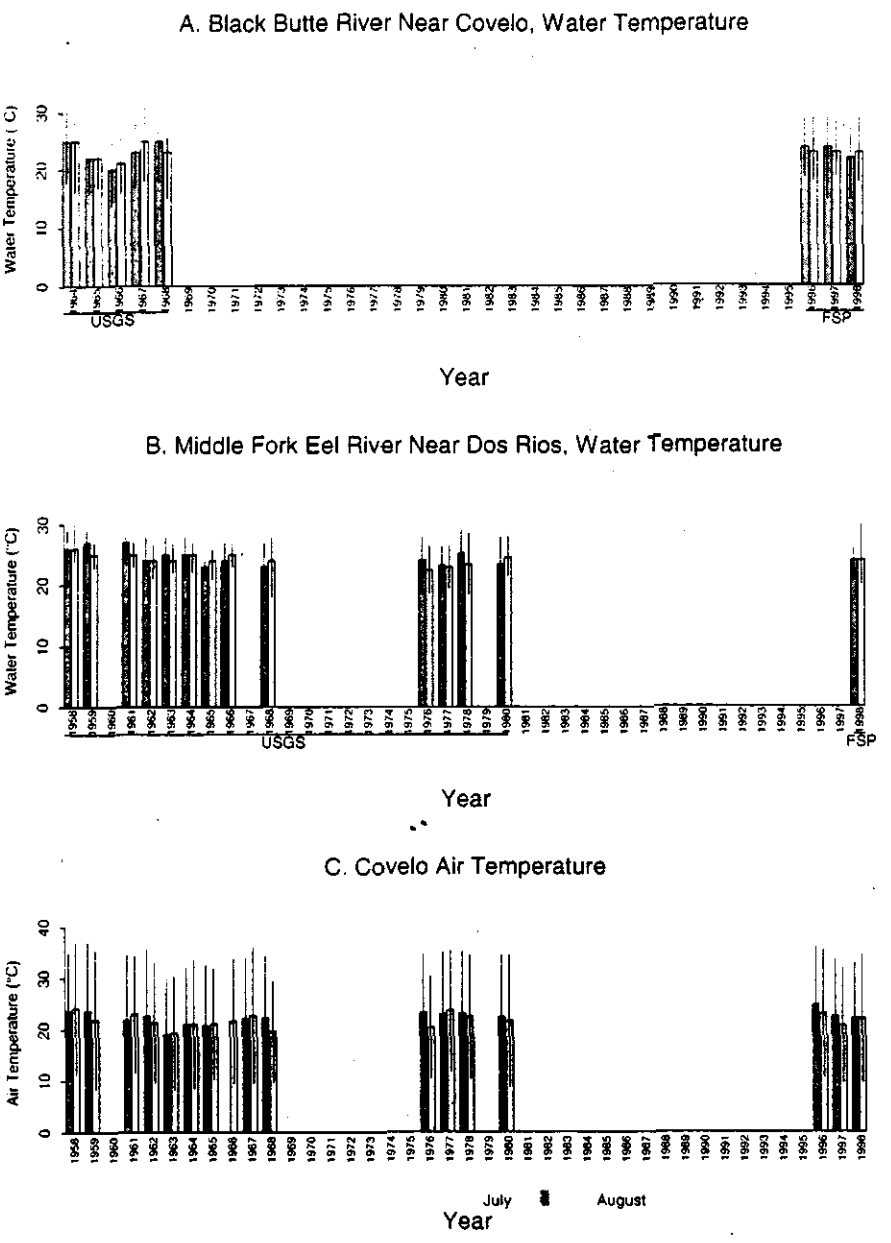

Figure 11.27. Comparison of historical USGS monthly average stream temperature data and more recent Forest Science Project data for two sites located in the Eel River Basin. Nearby FSP site was A) 180 m downstream, and B) 610 m downstream from the USGS site. Air temperature (C) was measured at a NOAA site located in Covelo, CA. Vertical lines represent the range in temperatures for each month.

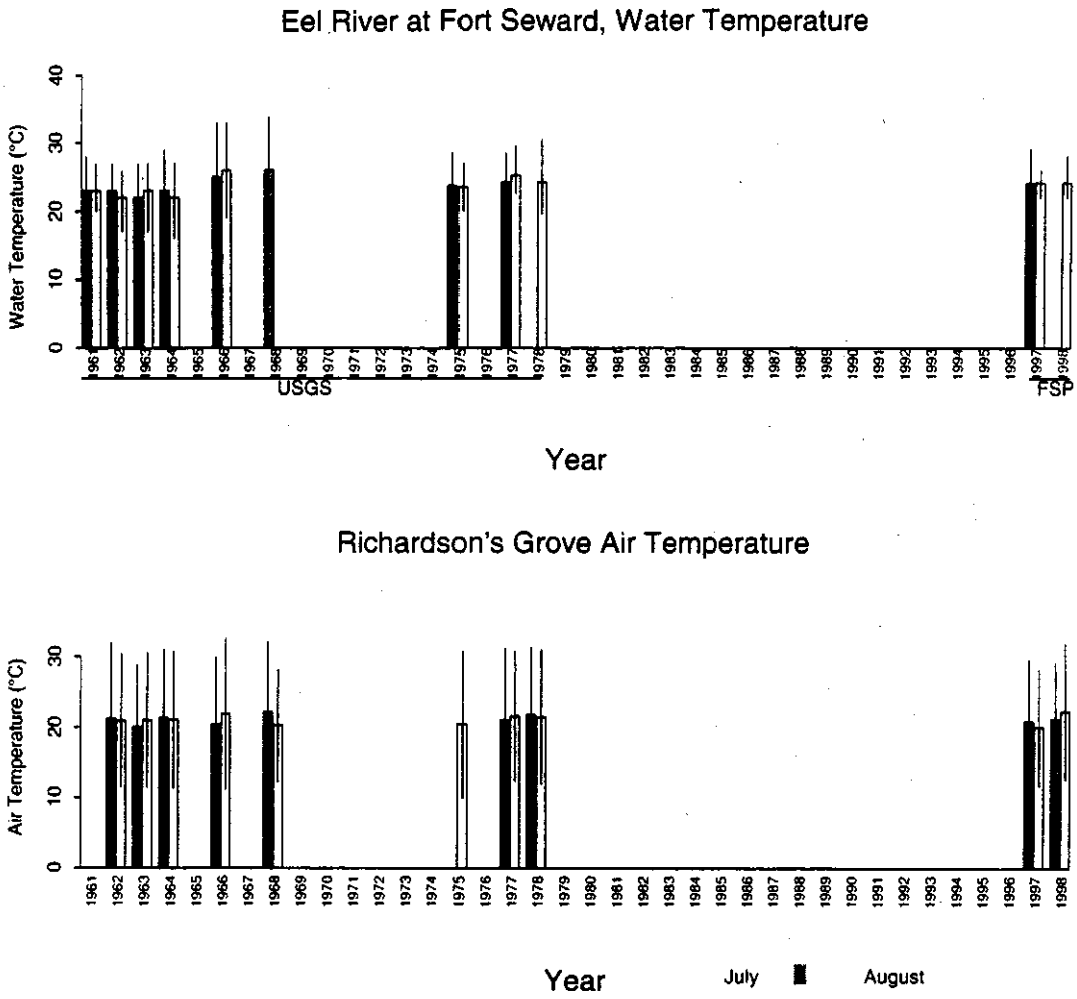

Figure 11.28. Comparison of historical USGS monthly average stream temperature data and more recent Forest Science Project data for a site located on the Eel River at Fork Seward (top). From the USGS site, the nearby FSP site was 730 m upstream. Air temperature (bottom) was measured at Richardson's Grove State Park. Vertical lines represent the range in temperatures for each month.

temperature was somewhat variable (a range for average monthly air temperature of 15.9°C to 17.7°C).

Water temperature data were collected by the USGS from 1961 to 1964 at the South Fork of the Van Duzen River near Bridgeville (South Fork of the Van Duzen is usually referred to as the Little Van Duzen River). A FSP cooperator collected water temperature data in 1996 through 1998 at a site 70 m downstream from the USGS site. However, the 1996 data has not been presented in the figure: the monthly maxima were much higher than the other monthly maxima, and the monthly minima were much lower than the other monthly minima. It is believed that the data provided in 1996 for this site either had a

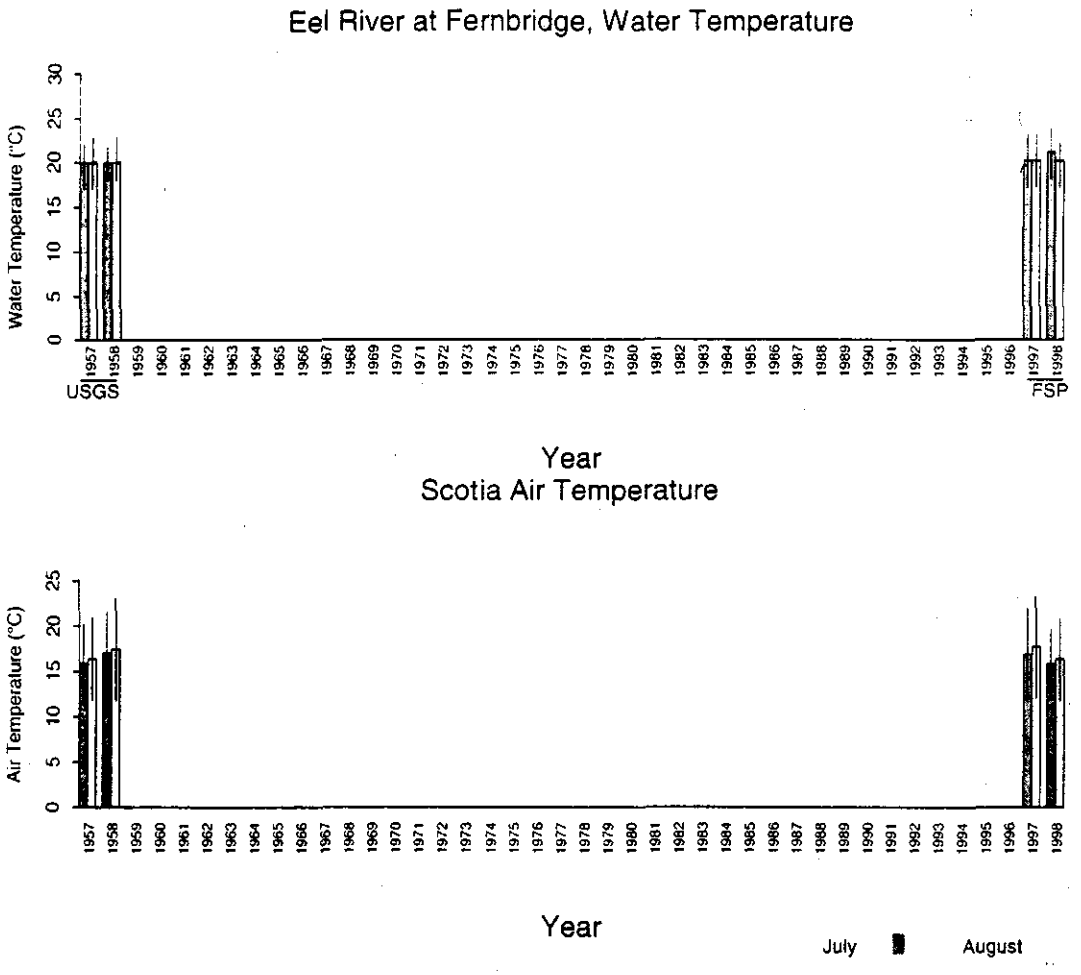

Figure 11.29. Comparison of historical USGS monthly average stream temperature data and more recent Forest Science Project data for a site located in the Eel River Basin(top). From the USGS site, the nearby FSP site was 230 m downstream. Air temperature (bottom) measured at a NOAA site located in Scotia, CA. Vertical lines represent the range in temperatures for each month.

dewatered temperature sensor and measured air temperature or came from another location. The USGS site was 69 km from the air temperature station at the Weaverville Ranger Station. The July 1961 to 1964 monthly average stream temperature ranged from 19°C to 21°C, while the 1997 and 1998 averages were both 20°C (Figure 11.30). The August 1961 to 1964 monthly average stream temperature ranged from 18°C to 21°C, while the 1997 and 1998 averages were both 19°C. The monthly average water temperature maxima for 1997 and 1998 also fell within the range of the 1961 to 1964 records. Monthly average air temperatures were also fairly consistent for the record, ranging from 19°C to 23°C. There does not seem to be much change in historical water temperatures at this site.

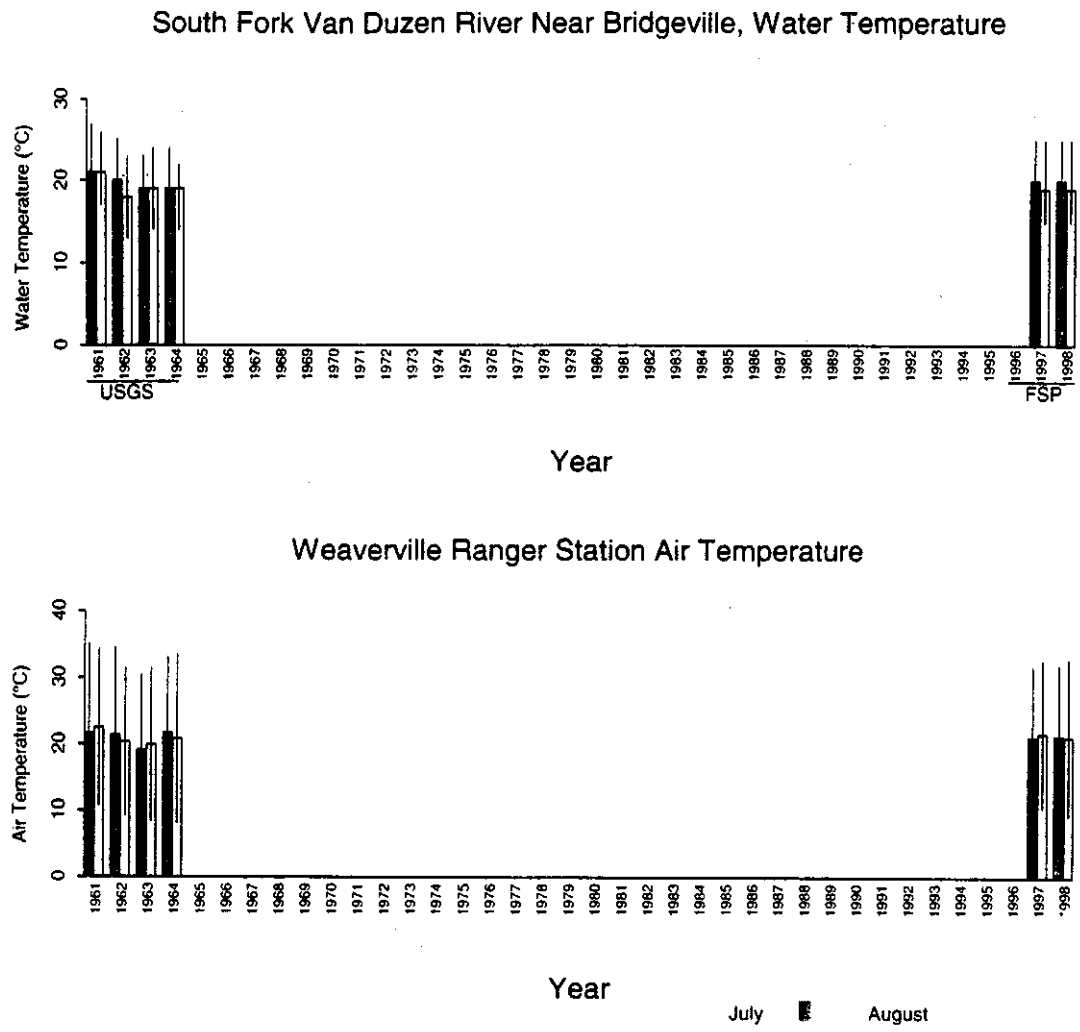

Figure 11.30. Comparison of historical USGS monthly average stream temperature data and more recent Forest Science Project data for a site located in the Little Van Duzen River (South Fork. Van Duzen River) of the Eel River Basin (top). From the USGS site, the nearby FSP site was 70 m downstream. Air temperature (bottom) measured at the Weaverville Ranger Station. Vertical lines represent the range in temperatures for each month.

Ten Mile River Basin

One USGS site was located in the Ten Mile River Basin that had a matching FSP site. The site was located on the Middle Fork of Ten Mile River near Fort Bragg, CA. USGS collected data from 1965 through 1968 while the FSP cooperator collected data from 1993 through 1998. The USGS site was 11 km from the air temperature station near Fort Bragg. The watershed area at this location was 8621 ha (33 sq mi) and the distance from the watershed divide was 26 km (16 mi). Canopy closure reported in 1998 was ~30%. All years of data were similar, with 1967 having the warmest monthly average water temperatures (Figure 11.31). The July monthly average water temperature ranged from 15°C to 18°C, and August monthly average water temperature ranged from 15°C to 17°C. There does not appear to be any trend in stream temperature at this site.

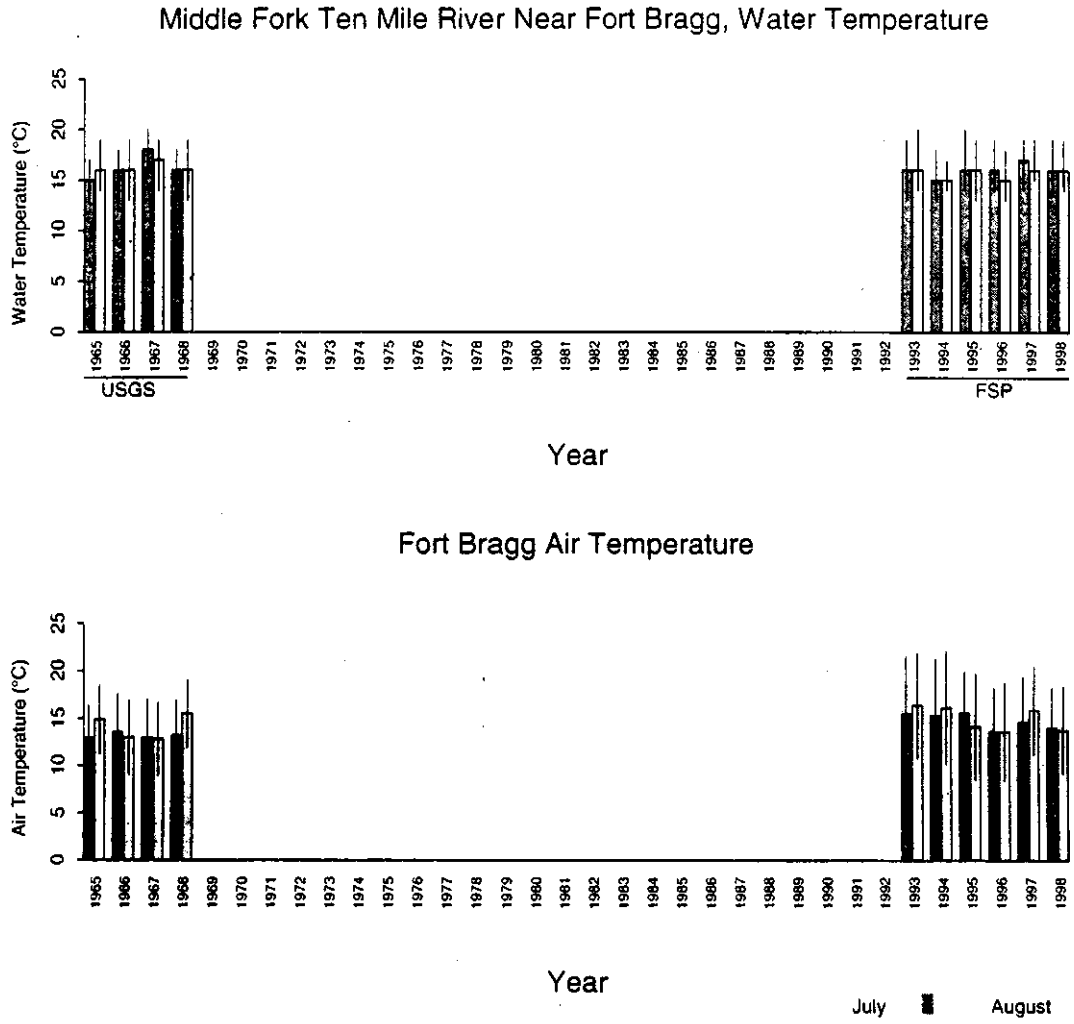

Figure 11.31. Comparison of historical USGS monthly average stream temperature data and more recent Forest Science Project data for a site located on the Middle Fork of Ten Mile River (top). Nearest FSP site is 1070 m downstream. Vertical lines represent the range in monthly minima and maxima. Air temperature (bottom) measured at a NOAA site located in Fort Bragg, CA.

Summary

Historical trends in water temperature appeared to be largely a function of air temperature. This relationship is probably due to the fact that most USGS stream temperature monitoring sites are located on large, mainstem rivers. Monthly average air and water temperatures from matched USGS-FSP sites were plotted in Figure 11.32. Air temperature sites were selected using a 12-dimensional Euclidian distance model. There is a definite positive correlation between historical air and water temperatures.

At some sites, contemporary water temperatures have shown appreciable increases or decreases from historical levels. Most of these sites were on tributaries, where local site factors may partially account for the observed trends. Large storm events that occurred in the historical record, such as the 1964 flood, may have left a legacy of altered riparian and channel conditions that could be related to some of the observed increases in contemporary stream temperatures from historical levels. Recovery of riparian vegetation from catastrophic natural disturbances and past timber harvesting practices are perhaps involved in the observed decrease in recent stream temperatures from levels seen in the 1950's and 1960's at some of the tributary sites.

The large database developed by the Forest Science Project and other organizations throughout the state should be maintained to serve as historical data for future stream temperature monitoring efforts. Purposive monitoring designs must be developed to capitalize on the existing network of stream temperature monitoring sites. More site-specific attribute data should be collected using consistent protocols so that trends in stream temperature can be interpreted more concisely. Site-specific data should also include local air temperature. These data are essential for gaging the effectiveness of current and future forest practice rules and other land management prescriptions.

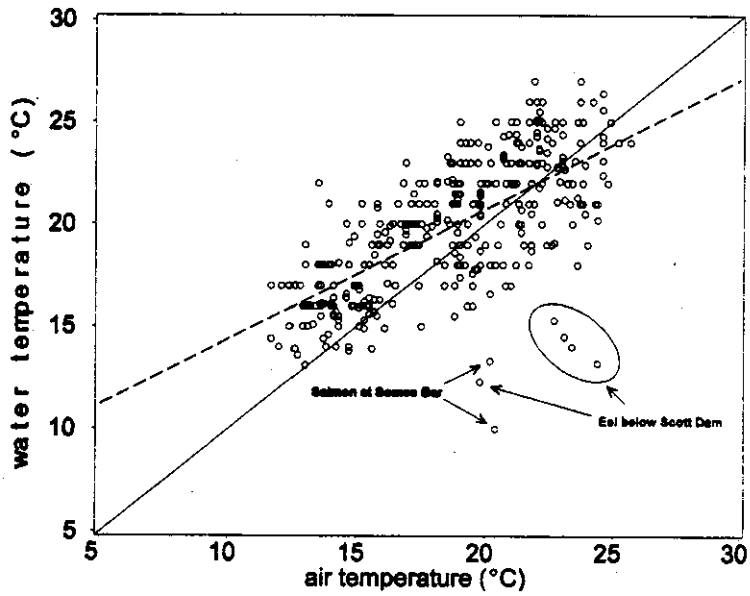

Figure 11.32. Monthly average air versus water temperature for all USGS - FSP matched sites for June, July, August, and September, wherever available. Regression equation (dashed line) is: water temperature = 7.995398 + 0.63657*(air temperature). R^2 = 0.4436. Solid line is one-to-one correspondence. Data spans 1957 through 1998. Two outlier sites are noted, the Eel River below Scott Dam and the Salmon River at Somes Bar.

Chapter 12

CONCLUSIONS AND RECOMMENDATIONS

The Forest Science Project's Regional Stream Temperature Assessment was an assessment using existing data, i.e., a meta analysis. As such, there was no sampling design in place to dictate (1) where stream temperature sensors should be located in the stream network, (2) what habitat type (e.g., pool versus riffle) sensors should be submerged, (3) what sampling frequency should be employed, or (4) what sampling window should be targeted. Each data contributor had their own objectives for stream temperature monitoring. These diverse objectives can be grouped into three broad categories:

- Pre- and post-timber harvest plan monitoring
- Thermal reach monitoring
- Characterization of thermal refugia

The data collected reflected a broad spectrum of climatic, hydrological, topographical, and ecophysiographical conditions. As a consequence, an array of sites reflecting a range of riparian conditions across the region allowed for post-stratification of variables by hierarchical spatial scales for statistical analyses. The area of interest (AOI) for the regional assessment was defined as the range of the coho salmon in Northern California, the largest spatial scale assessed.

Stream temperature data from over 1200 sites in Northern California were acquired, with 1090 sites meeting various physical, spatial; and temporal criteria defined for the regional assessment. An information management infrastructure was developed to process and analyze over six million stream temperature records and a myriad of other site-specific and geographic attributes. The most data-rich year was 1998, with more sites having both water temperature data and site-specific attribute data. It was the year that was used for most of the analyses presented in this report.

Methods (Chapter 2)

A large amount of stream temperature and ancillary data were acquired, processed, and synthesized for the regional assessment.

Conclusions

Considerable time and effort was invested in the development of stream temperature data processing procedures. Much of the process has been automated. However, detection of ambient air spikes and other anomalous readings still required manual inspection of each and every thermograph.

The salient features of stream temperature protocols developed by various state and federal organizations in Oregon, Washington, and California were combined to arrive at the peer-reviewed protocol found in Appendix A. Many organizations in California and the Pacific Northwest have adopted the Forest Science Project stream temperature protocol, in part or in its entirety.

Regional assessments of temperature sensor data in a geographic context require location information with a known level of spatial error. Moreover, the coordinate values of the sensors should be of the same or better quality than the base data used in the

spatial analyses. The importance of positional accuracy became more evident as our regional analyses progressed. The early determination that many of the coordinates provided by data contributors were kilometers from their true location and the initial results from these misplaced sensors convinced us that a successful regional study relies heavily on known probe placement. There seems to exist all too often a lack of appreciation of the importance of place in modern ecological research. The likely result is a misunderstanding of the relationships between location and response. For this reason all stream temperature probe coordinates were validated and in many cases upgraded by confirming the location with the person responsible for probe installation.

Once the precise location of each monitoring site was determined on the 1:24,000 base data, it was apparent that many sites were not associated with a blue line stream on the 1:100,000 hydrography layer developed from EPA Reach File 3 by Teale Data Center. This was due, in part, to the alignment differences between the layers of differing scale and also because many streams with temperature sensors were not illustrated on the 1:100,000 level data. At the time, this was the only readily available hydrography layer encompassing the region-wide study area. Recently, the 1:000,000 scale National Hydrography Dataset (NHD) has become widely available. This is a significantly enhanced river layer that includes many features necessary for network modeling. Unfortunately, the lack of resolution in 1:100,000 scale hydrography data required that we use many manual procedures to acquire the GIS attributes used in this assessment. Development of framework 1:24,000 scale hydrography is critical to future monitoring and research efforts. Cumulative watershed or basin assessment of stream temperature requires a channel-routed, topologically accurate stream network to enable one to model the transport of water masses in a GIS environment. While there are various 1:24,000 stream coverages available for select watersheds in California, a 1:24,000 seamless stream coverage does not exist for the region-wide study area. The USGS and EPA are taking the steps to begin development of the NHD at 1:24,000, but without support from data contributors outside their agencies this will be a long and arduous task. To this end the Forest Science Project recently completed a 1:24,000 stream coverage for the Van Duzen River sub-basin following protocols developed by the Interorganizational Resource Information Coordinating Council (IRICC) that supports the Northwest Forest Plan.

Digital Elevation Model (DEM) data of 30-meter resolution were compiled, edge-matched and validated for the entire study area. Watershed area, distance to divide, probe separation distance, and gradient were all calculated directly or indirectly from the underlying elevation model. Prior to compilation by FSP staff, no seamless elevation data existed for the study area. This data set required a substantial investment of time, but payed large dividends during analyses. Recently, the USGS announced the completion of the National Elevation Dataset (NED). A 30-meter raster dataset stored in the latitude-longitude coordinate system and tiled by 1 degree blocks. While not available throughout the study area, newly created 10-meter DEMs show promise in enhancing the ability to derive useful information for regional ecological assessments. On the horizon are Light Detection and Ranging (LIDAR) DEMs of 1 to 3-meter resolution having horizontal and vertical accuracies of 2 and 1.5 decimeters respectively. This product will give GIS analysts the ability to accurately map existing channels to the headwaters. Captured simultaneously and co-registered with ground elevation data are vegetation heights. From these data the riparian corridor including fine scale gradient, topographic shading, above-water channel morphology, and to some degree riparian vegetation characteristics can be evaluated.

Recommendations

Adherence to a standardized protocol to collect stream temperature data across the entire region would greatly facilitate regional assessments. Careful attention to positional accuracy is needed to topologically place stream temperatures in proper geographic and watershed context. A seamless, channel-routed 1:24:000 stream coverage should be developed to allow better modeling of temperature transport for cumulative effects assessment.

Although much was learned from this meta analysis, many relationships were blurred by the lack of a sampling design. In future work, clear and concise monitoring and assessment questions should be formulated and a sampling design constructed to address these questions.

Regional Trends in Air Temperature (Chapter 4)

Air temperature is considered to be one of the most important factors influencing stream temperatures. As such, it was important to develop a better understanding of air temperature regimes across the range of coho salmon in Northern California.

Conclusions

Northern California can be characterized as being climatically diverse, with cool coastal areas and warm interior regions. A widely accepted concept is that air temperature decreases with increasing elevation due to adiabatic cooling processes. In Northern Coastal California, air temperature was found to be more a function of distance from the coast. In the coastal areas, air temperature was actually found to increase with increasing elevation during the summer months. In fall and winter, air temperature trends follow normal adiabatic cooling patterns in both the coastal and interior portions of the study area. In the warmer interior portion of the AOI, summer air temperatures followed the more traditional adiabatic tendency. Stream temperature modelers should be cognizant of the inverse relationship between air temperature and elevation in the coastal area in the summer months. Elevation should not be used as a surrogate for air temperature until the inland extent of the maritime influence has been determined.

Using 30-year PRISM air temperature data HUC-level air temperature regimes were developed. In HUCs that are oriented such that a portion lies on the coast and a portion lies in the interior, air temperature gradients up to 15°C from the headwaters to the coast are realized. Headwater streams that originate in the warm interior portions of these HUCs may tend to attain higher temperatures at short distances from the watershed divide. Using PRISM data, the zone of coastal influence was delineated.

Recommendations

PRISM data should be acquired for individual years to provide better year-to-year discernment in air temperature trends at 4-km or finer spatial resolution (1- or 2-km). Acquisition of finer temporal and spatial air temperature data will improve our ability to model trends in water temperature.

Inasmuch as air temperature greatly influences stream temperature, air temperature regimes in Northern California should be taken into account when setting stream temperature target values.

Air-Water Temperature Relationships (Chapter 5)

The relationship between macro- (remote) air and micro- (local) air temperatures was examined in this chapter.

Conclusions

Some local, stream-side air temperature stations correlated better than others with remote air temperatures. After final matching of water temperature sites with nearest 12-dimensional Euclidian distance remote sites, the distance from the stream site did not seem to play a role in how well the matched remote air temperature coincided with stream-side air temperature. Microclimate most likely plays an important role in how well remote air temperature correlates with localized air temperature.

Stream temperature showed a slight to moderate relationship with remote air temperature. Having such a small number of remote air temperature sites to match up with a large number of stream temperature sites contributed to the large variability in the relationship. When using only a small number of remote air temperature sites, caution should be exercised when making broad generalizations about climatic conditions from one year to the next to explain trends in stream temperatures.

At ten sites where air temperature was monitored at stream-side, much better correlations between local air and water temperature were observed, as expected and documented in other studies.

Out of 1090 sites, there were 154 sites that were monitored over three consecutive years (1996 - 1998). Daytime stream temperature metrics (highest daily maximum, seven-day moving average of the daily average, and seven-day moving average of the daily maximum) showed very little change across the three-year period. Daily minimum stream temperature showed a significant difference, with lowest daily minima occurring in 1996, the year with the lowest daily minimum air temperatures.

Our ability to discern trends in stream temperatures with year-to-year variations in air temperature were hampered by the limited number of remote air temperature sites with which to match up with water temperature sites.

Recommendations

To determine the influence of air temperature on streams with varying levels of canopy and at various watershed positions, a sampling design is needed to specifically address this issue. More stream-side collection of air temperature is needed. A complete suite of site-specific attributes should be collected at each water temperature site, using consistent protocols.

More sensors should be kept in the same location for a greater number of consecutive years to improve trend detection capabilities. The location of trend-detection sensors should cover a range of watershed positions and riparians conditions. A well-defined sampling design coupled with a consistent stream temperature protocol should dictate sensor placement.

Geographic Position and Stream Temperatures (Chapter 6)

This chapter examined the influence of broad-scale geographic position on stream temperatures. These factors included distance from the coast, ecoprovince, zone of coastal influence, north-south distribution (latitude), and elevation. Do local site factors completely control water temperatures or can some regional scale patterns be observed? The environmental variable that exerts its influence across all of these geographic factors is predominantly air temperature.

Conclusions

All of the geographic independent variables examined can serve as surrogates for air temperature. However, as described in Chapter 5, for the data set that was available, stream temperatures correlated better with microair temperatures. Micro- and macro-air temperatures were found to not always correlate very well. While macroair temperatures will have an influence on microair temperature, site-specific factors will affect the degree of correlation between the two. Thus, geographic trends in water temperature will be obscured by localized effects on microair temperatures. This was manifested by the large variability seen in stream temperatures with various geographic position variables. The zone of coastal influence was perhaps the most useful geographic factor for explaining the variation in stream temperatures at the regional scale. ZCI was perhaps more effective than ecoprovince in explaining the variability in stream temperature. Separation of stream temperature sites by whether they fell inside or outside of the zone of coastal influence showed significant differences. For all sites combined, and at given divide distances, stream temperatures inside the ZCI were significantly cooler than those outside the ZCI.

Recommendations

In the formulation of stream temperature targets, whether narrative or numeric, ecoprovince and ZCI should be considered. The temperature that a stream can reasonably attain is dependent upon its location with respect to ecoprovince and ZCI. Air temperature may be the discriminating factor that operates at these two broad geographic delineations. The fog layer associated with the ZCI can decrease both air and water temperatures, by its attenuation of incoming solar radiation. The spatial extent of the ZCI varies daily, seasonally, and yearly. PRISM data

for individual years should be acquired to map the areal extent of the ZCI at different temporal resolutions.

Watershed Position and Stream Temperature (Chapter 7)

Water temperature has a tendency to increase with increasing distance from the watershed divide and with increasing drainage area. This simple picture of stream temperature change over downstream distance can be altered by local conditions. Riparian shading can vary along the length of a stream course due to natural or human-induced causes. Air temperature regimes can change from the headwaters to the mouth, not always in an increasing manner, as shown in Chapter 4. In Northern Coastal California air temperatures may decrease by as much as 15°C by the time a parcel of water reaches the ocean after its journey from the headwaters, due to oceanic control on air temperatures near the coast.

Conclusions

Stream temperature was highly dependent upon watershed position, both in terms of watershed area and distance from the watershed divide. Each of the eighteen hydrologic units (HUC) that comprise the range of the coho salmon showed an increase in stream temperature with an increase in watershed area and distance from the watershed divide. The rate of downstream increase in stream temperature appeared to vary with HUC location, i.e., whether the HUC was completely coastal, partly coastal and partly interior, or completely interior.

The traditional temperature metrics used to assess thermal impacts in streams (e.g., the highest seven-day moving average of the daily average or maximum, the highest daily maximum) may not adequately portray the thermal *dose* experienced by aquatic biota. Dose is determined by concentration multiplied by duration.

Stream network diagrams showed that streams can exhibit a decrease in stream temperature as the stream transitions from outside to inside the ZCI.

Recommendations

HUC location should be considered in setting realistically attainable stream temperature targets. When establishing stream temperature goals for maintenance of certain beneficial uses, watershed position within each HUC is an important consideration. A natural gradient in stream temperature occurs from the headwaters to the lower reaches. This natural gradient produces discrete zones with temperature regimes suitable for distinctly different fish communities and activities (Armour, 1991). Stream temperature standards should be developed with an understanding of the natural temperature regimes in HUCs throughout the range of the coho salmon in Northern California.

Using a sound sampling design, longitudinal stream temperature trend lines should be developed for each HUC. Sites with effective solar intercepting shade should be used to develop these trend lines. Stream temperatures at various sites in a HUC can be plotted and departures from the trend line can be assessed temporally and spatially.

Temperature metrics that embody the concept of dose, such as sum degrees or mean degree day, should be assessed with respect to their power in explaining presence/absence and abundance of salmonids. To develop linkages between these alternative thermal stress metrics and fish response, integrated temperature and fish monitoring is required. Too often fish surveys and temperature monitoring are conducted in different locations in a stream. Greater effort should be made to integrate all aspects of temperature and habitat characterization. Habitat typing data are often collected in stream reaches that are different from fish survey and temperature monitoring.

Site-Specific Attributes and Stream Temperature (Chapter 8)

The site-specific attributes examined in this chapter are channel orientation, gradient, habitat type, and bankfull width.

Conclusions

All sites in our regional stream temperature analysis contained non-missing values for channel orientation due to our ability to derive this attribute in GIS. Out of 548 sites with water temperature data available for regional analyses in 1998, only 365 of these were accompanied by canopy data. There was an even greater paucity of canopy data in years prior to 1998. These data voids are a great impediment to our ability to discern regional status and trends in stream temperatures and the factors that control them. A statistically valid sampling design coupled with canopy measurements collected using a consistent protocol is needed to better address the interaction between channel orientation, canopy, and stream temperature.

Comparing temperatures in different habitat types across broad geographic areas may be inappropriate, unless the sites are placed in proper geographic context. In any given stream, deep pools are expected to be cooler than riffles or runs from the same stream. A misleading view of stream temperatures can result by having a preponderance of deep pools in a restricted (warmer) geographic area and in predominantly large stream systems. The habitat types used in this assessment are relative terms. A deep pool in a low-order stream may be similar, at least in terms of depth, to a riffle or run in a high-order stream.

Bankfull width is an important variable in many process-based models. In 1998 there were 176 sites for which bankfull width was available.

The power of this regional assessment would have been greatly increased if more site-specific attribute data were collected at each stream temperature site. Bankfull width was available at very few sites, but was found to be highly significant in explaining trends in stream temperature. GIS-derived attributes (e.g., divide distance and watershed area) were used as surrogates for stream size, with fairly good success. However, localized variability in channel characteristics and flow rates can introduce errors in modeling the relationship between stream temperature and stream-size surrogates.

Recommendations

In future regional assessments a greater effort should be made to collect important site-specific attribute data that are known to be highly influential in controlling stream temperature. The use of consistent protocols and a sampling design developed to address well-articulated and agreed upon monitoring and assessment questions is critical.

Canopy (Chapter 9)

A diversity of methodologies were used by organizations who submitted canopy data to the Forest Science Project. Despite this diversity, some useful relationships were found in the data.

Conclusions

The amount of canopy appears to diminish with increasing distance from the watershed divide. A theoretical maximum divide distance was found to be approximately 70 km. At this distance, streams may potentially be too wide for stream-side vegetation to provide adequate stream shading. This distance is a theoretical maximum and will vary from watershed to watershed, HUC to HUC, and basin to basin. This distance may have also been influenced by past natural catastrophic events (e.g., the 1964 flood) and historical land management practices. For three temperature metrics commonly used to assess thermal regimes in streams, canopy was found to be highly correlated with stream temperature.

Recommendations

Development and adherence to a canopy measurement protocol that clearly relates to interception of incoming solar radiation is needed. Effective shade is the operative variable that influences stream temperature. Effective shade should be measured along a certain distance (thermal reach) upstream from the stream temperature monitoring device. Research should be undertaken to develop methods for estimating effective canopy cover using remote sensing imagery or hemispherical photography. Methods that require less subjectivity should be preferred.

Empirical Modeling (Chapter 10)

The chapter is a culmination of empirical meta-analyses of stream temperatures and various landscape-level and site-specific variables presented throughout previous chapters. It has been illustrated throughout this report that variation in stream temperature is not well explained by any single independent variable, particularly in regional analysis. Many factors influence the thermal regime of running waters. In this chapter, various models were developed that serve to show the interaction of various independent variables that operate at different spatial scales.

Conclusions

Geographic position played a major role in explaining variability in steam temperature at the regional scale. Geographic variables are believed to largely serve as surrogates for air temperature. None of the air temperature metrics based on data collected at remote air temperature sites were useful in explaining stream temperature variation. In alternative models where geographic variables such as UTMX and UTMY were excluded from the model, PRISM 30-year August average maximum air temperature was found to be somewhat useful in predicting stream temperature. However, using either geographic variables or PRISM 30-year long-term average air temperature, the ability to detect year-to-year changes in water temperature due to changing air temperatures is lost.

Researchers have had a great deal of success modeling stream temperature at basin and smaller scales. However, if the desire is to model stream temperature at a coho salmon ESU scale, many complications not seen at the smaller scale arise. Namely, remote air data coupled with surrogates, such as elevation, may work well for developing a basin-scale model, but at a regional scale, a better estimate of the local air temperature is required.

Canopy and habitat type were important site-specific attributes that helped explain variation in stream temperature. The logs of divide distance and watershed position were retained in backward elimination model development. These variables relate to watershed position and serve as surrogates for stream size (e.g., bankfull width).

Whether a site was in or out of the zone of coastal influence helped explain spatial trends in stream temperature. Inasmuch as ZCI was derived from 30-year long-term PRISM air temperature data, annual variability in the areal extent of the ZCI is not captured.

In the combined ecoprovince model, whether the site was located in the coastal or interior ecoprovince had some explanatory power in stream temperature. Differences in air temperature regimes probably account for the discriminatory power associated with ecoprovince.

All the fitted models indicated that air temperature, solar radiation, and watershed position were important covariates. Positional covariates entered all the models. While these were viewed as air temperature surrogates, this underscores the fact that location is an important factor in stream temperature profiles. For example, two sites that appear to be identical with respect to habitat, riparian condition, shading, watershed area, and flow rate, but are in different basins will more than likely have different temperature profiles. Stream temperature "target" values that may be easily achieved in some areas might be impossible in others.

Recommendations

The placement of temperature probes into pools added additional unnecessary complexity to an already complex relationship. If water temperatures were measured only in well- mixed riffles, then water temperature models would have less variability, making interpretation much easier and more reliable. We are, however, grateful that so many organizations were willing to provide data, regardless of habitat type. Without their generous contributions of both time and data, this assessment would not have been possible. In future regional assessments there should be greater adherence to the Forest Science Project's stream temperature protocol that stipulates placement of probes in well-mixed riffles.

In preliminary modeling exercises, when either or both bankfull width or depth covariates entered the model a good AIC score with a high R^2 value was observed. However, there was a paucity of data for these variables. Given the importance of stream size in many physical-based stream temperature models, greater effort should be made to measure these very important site-specific attributes.

Although models were presented and statements made as to what variables influence water temperature, the lack of a sampling design made in-depth analyses tenuous. Questions regarding each covariate's contribution to explaining variation in stream temperature requires data collected with a sampling design suited for developing explanatory models. Such a design would require a sampling frame, constructed from a well-defined sampling universe. Then, a random probability sample of some type must be drawn from the sampling frame. Finally, air temperature, canopy, and stream-size data collection, and stream temperature sensor placement must all adhere to consistent protocols and all collected values must be submitted.

Historical Perspectives (Chapter 11)

only the "historical" part

Most of the historical data came from larger streams where air temperature is most likely the major factor influencing water temperature. Thus, this analysis does little to address stream temperature changes that may have occurred since the 1950's in smaller streams, where most coho salmon rearing takes place and where land management practices may have a greater influence on thermal regimes and the extent of potentially suitable habitat. This historical analysis was on a site-by-site basis and not a regional assessment of trends in stream temperatures across the range of coho salmon in Northern California.

Conclusions

At some sites, contemporary water temperatures have shown appreciable increases or decreases from historical levels. Most of these sites were on tributaries, where local site factors may partially account for the observed trends. Large storm events that occurred in the historical record, such as the 1964 flood, may have left a legacy of altered riparian and channel conditions that could be related to some of the observed increases in contemporary stream temperatures from historical levels. Recovery of riparian vegetation from catastrophic natural disturbances and past timber harvesting practices are perhaps involved in the observed decrease in recent stream temperatures from levels seen in the 1950's and 1960's at some of the tributary sites.

An interesting commentary on the effects of the 1964 flood was noted in the USGS historical data in that many gaging stations did not have stream temperature data for 1965. Although the lack of data at many gaging stations following 1964 may have been a coincidence, it may more likely be a result of the widespread devastation that resulted from the flooding of many streams and rivers throughout Northern California.

Recommendations

The large database developed by the Forest Science Project and other organizations throughout the state should be maintained to serve as historical data for future stream temperature monitoring efforts. Purposive monitoring designs must be developed to capitalize on the existing network of stream temperature monitoring sites. More site-specific attribute data should be collected using consistent protocols so that trends in stream temperature can be interpreted more concisely. Site-specific data should also include local air temperature. These data are essential for gaging the effectiveness of current and future forest practice rules and other land management prescriptions.

A sad commentary is that as we worked through USGS water resource summary reports from the 1970's and 1980's, many gaging stations that had once gathered stream temperature data in the 1960's began to go offline in the following two decades. The loss of more and more gaging stations due to budgetary constraints will greatly hinder research in many ecological and physical science disciplines. It is hoped that the value of maintaining a network of strategically located gages throughout drainages in Northern California will be realized and that more stations will be brought back online.

REFERENCES

Adams, T.N. and K. Sullivan. 1990. *The Physics of Forest Stream Heating: A Simple Model.* Timber, Fish, and Wildlife Report No. TFW-WQ3-90-007, Washington Dept. Nat. Resources, Olympia, WA, 30 pp.

Allan, J.D. 1995. *Stream Ecology: Structure and Function of Running Waters.* Chapman & Hall, New York, NY, 377 pp.

Armour, C.L. 1991. *Guidance for Evaluating and Recommending Temperature Regimes to Protect Fish.* U.S. Fish and Wildlife Service, Biological Report 90(22), Fort Collins, CO, 13 pp.

Barnhart, R.A. 1986. *Species Profiles: Life Histories and Environmental Requirements of Coastal Fishes and Invertebrates (Pacific Southwest) -- Steelhead.* U.S. Fish and Wildlife Service Biological Report 82(11.60), U.S. Army Corp of Engineers, TR EL-82-4, 21 pp.

Bartholow, J.M. 1989. *Stream Temperature Investigations: Field and Analytic Methods.* Instream Flow Information Paper No. 13, U.S. Fish and Wildlife Service, Biological Report 89(17), Washington, DC, 139 pp.

Becker, C.D. and R.G. Genoway. 1979. Evaluation of the critical thermal maximum for determining thermal tolerance of freshwater fish. *Env. Biol. Fishes* 4:245-256.

Bicknell, B.R., J.C. Imhoff, J.L. Kittle, A.S. Donigan, Jr., and R.C. Johanson. 1997. *Hydrological Simulation Program - FORTRAN, User's Manual for Version II,* EPA/600/R-97/080. U.S. Environmental Protection Agency, National Exposure Research Laboratory.

Blea, J.H. 1938. *Mortality in Young Eel River Steelhead, July, 1938.* Bureau of Fish Conservation, California Division of Fish and Game, Inland Fisheries Branch, Administrative Report No. 38-10, August 6, 1938.

Blodgett, J.C. 1970. *Water Temperatures of California Streams North Coastal Subregion.* United States Geological Survey, Water Resources Division, Open File Report, Menlo Park, CA.

Brett, J.R. 1952. Temperature tolerance in young Pacific salmon, genus *Oncorhynchus. J. Fish. Res. Bd. Can.* 9:265-323.

Brown, G.W. 1969. Predicting temperatures of small streams. *Water Resour. Res.* 5(1):68-75.

Brown, G.W. 1972. *An Improved Temperature Prediction Model for Small Streams.* Water Resources Research Institute Paper No. WRRI-16, Oregon State University, Corvallis, OR, 20 pp.

Brown, G.W. and J.R. Brazier. 1972. *Controlling Thermal Pollution in Small Streams.* U.S. Environmental Protection Agency, Office of Research and Monitoring, Washington, DC, EPA-R2-72-083.

Brungs, W.A. and B.R. Jones. 1977. *Temperature Criteria for Freshwater Fish: Protocol and Procedures.* EPA-600/3-77-061. U.S. Environmental Protection Agency, Environmental Research Laboratory, Duluth, MN, 129 pp.

Burnham, K.P. and D.R. Anderson. 1998. *Model Selection and Inference: A Practical Information-Theoretic Approach.* Springer-Verlag. New York, NY. 353 pp.

Caldwell, J.E., K. Doughty, and K. Sullivan. 1991. *Evaluation of Downstream Temperature Effects of Type 4/5 Waters.* T/F/W Report No. WQ5-91-004, Timber, Fish, and Wildlife, Olympia Washington, 71 pp.

CDF (California Department of Forestry and Fire Protection). 1999. California forest practice rules. Title 14. *California Code of Regulations.* Chapters 4 and 4.5. Sacramento, CA

Chen, D.Y., S.C. McCutcheon, D.J. Norton, and W.L. Nutter. 1998a. Stream temperature simulation of forested riparian areas: I. Watershed-scale model development. *J. Env. Eng.* 4:304-315.

Chen, D.Y., S.C. McCutcheon, D.J. Norton, and W.L. Nutter. 1998b. Stream temperature simulation of forested riparian areas: II. Model application. *J. Env. Eng.* 4:316-328.

Collins, W.D. 1925. *Temperature of Water Available for Industrial Use in the United States.* In: U.S. Geological Survey, Water Supply Paper 520-F, Washington, DC, pp 97-104.

Coutant, C.C. 1972. Heat and Temperature. In: *Water Quality Criteria 1972.* Environmental Studies Board, National Academy of Sciences, Washington, DC, pp 151-170 & 410-419.

Daly, C., R.P. Neilson, and D.L. Phillips. 1994. A statistical-topographic model for mapping climatological precipitation over mountainous terrain. *J. Appl. Meteor.* 33:140-158.

Diaz-Ramos, S., D.L. Stephens, and A.R. Olson. 1996. *EMAP Statistical Methods Manual.* EPA/620/R-96/002. U.S. Environmental Protection Agency, Office of Research and Development, National Health and Environmental Effects Research Laboratory, Corvallis, OR.

Donato, M.M. 1998. *Surface Water/ground Water Relations in the Lemhi River Basin, East-central Idaho.* U.S. Geological Survey Water Res. Inv. Rep. 98-4185, Boise, ID, 28 pp.

Edinger, J.E., D.W. Duttweiler, and J.C. Geyer. 1968. The response of water temperatures to meteorological conditions. *Water Resources Research* 4(5):1137-1143.

Essig, D.A. 1998. *The Dilemma of Applying Uniform Temperature Criteria in a Diverse Environment: An Issue Analysis.* Idaho Division of Environmental Quality, November, 1998.

Everest, F.H., N.B. Armantrout, S.M. Keller, W.D. Parante, J.R. Sedell, T.E. Nickelson, J.M. Johnston, and G.N. Haugen. 1985. Salmonids. In: Brown, R. (ed.). *Management of Wildlife and Fish Habitats in Forests of Western Oregon and Washington.* Publication R6-F&WL-192-1985. U.S. Department of Agriculture, Forest Service, Pacific Northwest Region, pp 199-230.

Ferraro, F.A., Gaulke, A.E., and Loeffelman, C.M., 1978. Maximum weekly average temperature for 316(a) demonstrations, biological data in water pollution assessment: quantitative and statistical analyses. In: K.L. Dickson, John Cairns, Jr., and R.J. Livingston, Eds., American Society for Testing and Materials, *ASTM STP 652*, 1978, pp 125-136.

FHM. 1994. *Forest Health Monitoring 1991 Statistical Summary*. EPA/620/R-94/028. U.S. Environmental Protection Agency, Washington, D.C.

FISRWG. 1998. *Stream Corridor Restoration: Principals, Processes, and Practices*. Federal Interagency Stream Restoration Working Group, NTIS Number: PB98-158348INQ (ISBN-0-934213-59-3), Springfield, VA.

Hostetler, S.W. 1991. Analysis and modeling of long-term stream temperatures on the Steamboat Creek Basin, Oregon: Implications for land use and fish habitat. *Water Res. Bull.* 27(4):637-647.

Hynes, H.B.N. 1970. *The Ecology of Running Waters*, University of Toronto Press, Toronto, Ontario, Canada, 555 pp.

Johnson, G.L., Daly, C., G. Taylor, C. L. Hanson, and Y. Lu. 1997. GEM model temperature and precipitation parameter variability, and distribution using PRISM, Proceedings 10th Conf. on Applied Climatology, Reno, NV, Amer. Meteor. Soc., pp 210-214.

Jones, E.J. 1965. *Temperature of California Streams, Part 1. Evaluation of Thermograph Records.* U.S. Geol. Survey Open-File Report, 31 pp.

Kittel, T.G.F., et al. 1997. A gridded historical (1895-1993) bioclimate dataset for the conterminous United States, Proceedings 10th Conf. on Applied Climatology, Reno, NV, Amer. Meteor. Soc., pp 219-222.

Kjelstrom, L.C. 1992. *Stream Flow Gains and Losses in the Snake River and Ground Water Budgets for the Snake River Plain, Idaho and Eastern Oregon.* U.S. Geological Survey Open-File Report 90-172, Boise, ID, 71 pp.

Kopperdahl, F.R., J.W. Burns, and G.E. Smith. 1971. Water quality of some logged and unlogged California streams. *Inland Fisheries Administrative Report No. 71-12*, Sacramento, CA, pp 2-19.

Kothandaraman, V. and R.L. Evans. 1972. *Use of Air-Water Relationships for Predicting Water Temperature.* U.S. National Technical Info. Service PB-220-416, 14 pp.

Landsberg, H. 1958. *Physical Climatology, Second Edition*. Gray Printing Company, Inc., Du Bois, PA.

Lewis, T.E. and B.L. Conkling. 1994. *Forest Health Monitoring: Southeast Loblolly/Shortleaf Pine Demonstration Interim Report.* EPA/620/R-94/006, U.S. Environmental Protection Agency, Office of Research and Development, Washington, DC.

McCammon, B.P. 1994. Recommended watershed terminology. *Watershed Management Council Newsletter*, Fall, pp 12-14.

McCullough, D.A. 1999. *A Review and Synthesis of Effects of Alternations to the Water Temperature Regime on Freshwater Life Stages of Salmonids, with Special Reference to Chinook Salmon.* EPA/910-R-99-010, U.S. Environmental Protection Agency, Region 10, Seattle, WA, 279 pp.

Miller, A. and J.C. Thompson. 1975. *Elements of Meteorology, Second Edition*. Charles E. Merrill Publishing Co., Columbus, OH, 362 pp.

Moore, A.M. 1967. *Correlation and Analysis of Water-Temperature Data for Oregon Streams*, U.S. Geological Survey, Water Supply Paper 1819-K, U.S. Government Printing Office, Washington, DC, 53 pp.

MSG, 1999. *Hillslope Monitoring Program: Monitoring Results from 1996 through 1998.* Monitoring Study Group of the California State Board of Forestry and Fire Protection. Interim Report to the California State Board of Forestry and Fire Protection, Sacramento, CA.

Murphy, G.I. and J.W. DeWitt, Jr. 1951. *Notes on the fishes and fishery of the lower Eel River, Humboldt County, CA.* California Division of Fish and Game, Inland Fisheries Branch. Administrative Report No. 51-9.

Parzybok, T., W. Gibson, C. Daly, and G. Taylor. 1997. Quality assurance of climatological data for the VEMAP Project, Proceedings 10th Conf. on Applied Climatology, Reno, NV, Amer. Meteor. Soc., pp 215-216.

PG&E. 1996. *Potter Valley Project Monitoring Program: Effects of Operations on Upper Eel River Anadromous Salmonids.* Draft Final Report. FERC No. 77, Article 39. Prepared by Steiner Environmental Consulting for Pacific Gas and Electric Company, San Ramon, CA, September 1996.

SAS, 1985. *SAS/STAT Guide for Personal Computers, Version 6 Edition,* SAS Institute, Inc., Cary, NC, 378 pp.

Seaber, P., F.P. Kapinos, and G. Knapp. 1987. *Hydrologic Unit Maps.* U.S. Department of Interior, U.S. Geological Survey, Water Supply Paper No. 2294, 63 pp.

Sinokrot, B.A. and H.G. Stefan. 1994. Stream water-temperature sensitivity to weather and bed parameters. *J. Hydraulic Eng.* 120(6):722-735.

Spence, B.C., G.A. Lomnicky, R.M. Hughes, and R.P. Novitzki. 1996. *An Ecosystem Approach to Salmonid Conservation.* TR-4501-96-6057, Management Technology, Corvallis, OR.

Stefan, H.G. and E.B. Preud'homme. 1993. Stream temperature estimation from air temperature. *Wat. Res. Bull.* 29(1):27-45.

Stevens, H.H. Jr., J.F. Ficke, and G.F. Smoot. 1975. Water temperature-influential factors, field measurements, and data presentation. In: *Techniques of Water-Resources Investigations of the United States Geological Survey, Book 1. Chapter D1.* USGS, Arlington, VA, 65 pp.

Stevens, J. 1986. *Applied Multivariate Statistics for the Social Sciences.* Lawrence Erlbaum Associates, Inc., Hillsdale, NJ. 515 pp.

Stoneman, C.L. and M.L. Jones. 1996. A simple method to classify stream thermal stability with single observations of daily maximum water and air temperatures. *N. Am. J. Fish. Manag.* 16:728-737.

Sullivan, K., J. Tooley, K. Doughty, J.E. Caldwell, and P. Knudsen. 1990. *Evaluation of Prediction Models and Characterization of Stream Temperature Regimes in Washington,* Rep. No. TFW-WQ3-90-006, Washington Dept. Nat. Resources, Olympia, WA, 224 pp.

Swift, L.W. and J.B. Messer. 1971. Forest cuttings raise temperatures of small streams in the southern Appalachians. *J. Soil Water Cons.* 26(3):111-116.

Taylor, G., C. Daly, W. Gibson, and J. Sibul-Weisburg. 1997. Digital and map products produced using PRISM, Proceedings 10th Conf. on Applied Climatology, Reno, NV, Amer. Meteor. Soc., pp 217-218.

TFW, 1993. Stream Temperature Module. *1993 TFW Ambient Monitoring Manual,* Timber-Fish-Wildlife Ambient Monitoring Program, Northwest Indian Fisheries Commission, Olympia, WA.

Trewartha, G.T. 1968. *An Introduction to Climate, Fourth Edition.* McGraw-Hill Book Company, New York, NY, 408 pp.

Troxler, R.W., Jr. and E.L. Thackston. 1975. *Effect of Meteorological Variables on Temperature Changes in Flowing Streams.* EPA-660/3-75-002, U.S. Environmental Protection Agency, Washington, DC.

USDA, 1997. *Ecological Subregions of California: Section and Subsection Descriptions.* USDA Forest Service, R5-EM-TP-005, Pacific Southwest Region, San Francisco, CA.

USGS, 1975. *Water Resources Data for California, Water Year 1975, Volume 2. Pacific Slope Basins from Arroyo Grande to Oregon State Line except Central Valley.* U.S. Geological Survey Water-Data Report CA-75-2, USGS, Menlo Park, CA.

USGS, 1976. *Water Resources Data for California, Water Year 1976, Volume 2. Pacific Slope Basins from Arroyo Grande to Oregon State Line except Central Valley.* U.S. Geological Survey Water-Data Report CA-76-2, USGS, Menlo Park, CA.

USGS, 1977. *Water Resources Data for California, Water Year 1977, Volume 2. Pacific Slope Basins from Arroyo Grande to Oregon State Line except Central Valley.* U.S. Geological Survey Water-Data Report CA-77-2, USGS, Menlo Park, CA.

USGS, 1978. *Water Resources Data for California, Water Year 1978, Volume 2. Pacific Slope Basins from Arroyo Grande to Oregon State Line except Central Valley.* U.S. Geological Survey Water-Data Report CA-78-2, USGS, Menlo Park, CA.

USGS, 1979. *Water Resources Data for California, Water Year 1979, Volume 2. Pacific Slope Basins from Arroyo Grande to Oregon State Line except Central Valley.* U.S. Geological Survey Water-Data Report CA-79-2, USGS, Menlo Park, CA.

USGS, 1980. *Water Resources Data for California, Water Year 1980, Volume 2. Pacific Slope Basins from Arroyo Grande to Oregon State Line except Central Valley.* U.S. Geological Survey Water-Data Report CA-80-2, USGS, Menlo Park, CA.

USGS, 1994. *Water Resources Data for California, Water Year 1994, Volume 2. Pacific Slope Basins from Arroyo Grande to Oregon State Line except Central Valley.* U.S. Geological Survey Water-Data Report CA-80-2, USGS, Menlo Park, CA.

Vannote, R.L. and Sweeney, B.W. 1980. Geographic analysis of thermal equilibria: A conceptual model for evaluating the effect of natural and modified thermal regimes on aquatic insect communities. *Am. Nat.* 115:667-695.

Ward, J.V. and R.G. Dufford. 1979. Longitudinal and seasonal distribution of macroinvertebrates and epilithic algae in a Colorado springbrook-pond system. *Arch. Hydrobiol.* 86:284-321.

Weitkamp, L.A., T.C. Wainwright, G.J. Bryant, G.B. Milner, D.J. Teel, R.G. Kope, and R.S. Waples. 1995. *Status Review of Coho Salmon from Washington, Oregon, and California.* U.S. Dept. Commerce, NOAA Tech. Memo. NMFS-NWFSC-24, 258 pp.

Wetzel, R. 1983. *Limnology, 2nd Edition.* Saunders Publ., New York, NY.

Zwieniecki, M.A. and M. Newton. 1999. Influence of streamside cover and stream features on temperature trends in forested streams of western Oregon. *West. J. Appl. For.* 14(2):106-113.

APPENDIX A

Methods

AML Code

AML used to assign spatial attributes to stream temperature sensor sites.

```
/* Command name: ADDALLATTRIBUTES
/* Language: AML for ARC
/* Pathname: e:\boilerplate\amls\custom\..
/* Created: Joe Krieter Feb. 1998
/* Recoded: David W. Lamphear Dec. 1998
/* By:
/*    Forest Science Project
/*    Humboldt State University
/*    1 Harpst Street
/*    Arcata, CA
/*    Phone: 707-825-7350 ext 105
/*    Fax:  707-825-7350 ext 108
/*-------------------------------------------------------------------
/*
/* Purpose: ADDALLATTRIBUTES.AML used to assign Calwater codes, HUC
/*       codes, ecoregion, USGS quadrangle info, Distance to Coast,
/*       elevation, and TMDL information. Input is a DBASE file with
/*       SITE_ID, X_COORD, Y_COORD. Output is a DBASE file with all
/*       attributes including SITE_ID, X_COORD, and Y_COORD.
/*-------------------------------------------------------------------

&ARGS sites

&CALL Error_Check
&CALL Create_Point_Cov
&CALL Add_cpw_id
&CALL Add_huc_id
&CALL Add_eco_id
&CALL Add_Quadinfo
&CALL Dist_to_coast
&CALL Add_elev
&CALL Add_tmdl
&CALL Export_attributes
&CALL Cleanup
&CALL Exit
&RETURN
/*-----------------------------Error_Check Routine----------------------

&ROUTINE Error_Check

&SEVERITY &ERROR &ROUTINE Bailout
```

```
&IF [show program] ne 'ARC' &THEN
 &RETURN This aml must be run from ARC

&IF [null %sites%] &THEN
 &sv sites = [GETFILE *.dbf -file 'select input file' -none]

&IF [exists sitecov -cover] &THEN &DO
 &TYPE
 &TYPE Coverage sitecov already exists, please wait while it is killed.
 kill sitecov all
&END

&IF [exists allsites.in -info] &THEN &DO
 &TYPE
 &TYPE Info file allsites.in already exists, please wait while it is deleted.
 [delete allsites.in -info]
&END

&IF [exists sitecoord -file] &THEN &DO
 &TYPE
 &TYPE File sitecoord already exists, please wait while it is deleted.
 [delete sitecoord -file]
&END

&RETURN

/* ------------------------Routine Create_Point_Cov--------------------
&ROUTINE Create_Point_Cov

dbaseinfo %sites% allsites.in
tables
sel allsites.in
unload sitecoord site_id x_coord y_coord
q

/* Receives error message because there is no "end"
/* statement at the end of sitecoord

&SEVERITY &ERROR &IGNORE
generate sitecov
input sitecoord
points
q
&SEVERITY &ERROR &ROUTINE Bailout

build sitecov point

&describe sitecov
&IF %DSC$POINTS% gt 0 &THEN &DO
```

```
  &TYPE
  &TYPE
  &TYPE Sitecov has %DSC$POINTS% points.
  &TYPE
  &TYPE
&END
&ELSE &DO
  &TYPE Sitecov has no points, bailing out...
  &CALL Bailout
&END

additem sitecov.pat sitecov.pat site_id 4 5 b

tables
sel sitecov.pat
calc site_id = sitecov-id
q

joinitem sitecov.pat allsites.in sitecov.pat site_id site_id

&RETURN

/* -------------------------End of Create_Point_Cov---------------------

/* --------------------------Routine Add_cpw_id-----------------------

&ROUTINE Add_cpw_id

&IF [exists capwsadded -cover] &THEN &DO
  &TYPE
  &TYPE Coverage capwsadded already exists, please wait while it is killed.
  kill capwsadded all
&END

&TYPE Identity of sitecov with calif00capws underway...

identity sitecov e:\archives\lithosphere\watershed\nocal00capws capwsadded ~
point .001 join
kill sitecov all

&RETURN

/* --------------------------End of Add_cpw_id------------------------

/* --------------------------Routine Add_huc_id-----------------------

&ROUTINE Add_huc_id

&IF [exists mostadded -cover] &THEN &DO
```

```
 &TYPE
 &TYPE Coverage mostadded already exists, please wait while it is killed.
 kill mostadded all
&END

&TYPE Identity with calif00hucs underway...

identity capwsadded e:\archives\lithosphere\watershed\calif00hucs mostadded ~
point .001 join
kill capwsadded all

&RETURN

/* ----------End of Add_huc_id----------

/* ----------Routine Add_eco_id----------

&ROUTINE Add_eco_id

&IF [exists nalladded -cover] &THEN &DO
 &TYPE
 &TYPE Coverage nalladded already exists, please wait while it is killed.
 kill nalladded all
&END

&TYPE Identity with calif00ecoreg underway...

identity mostadded e:\archives\lithosphere\boundaries\calif00ecoreg nalladded ~
point .001 join
kill mostadded all

&RETURN

/* ----------End of Add_eco_id----------

/* ----------Routine Add_Quadinfo----------

&ROUTINE Add_Quadinfo

&IF [exists alladded -cover] &THEN &DO
 &TYPE
 &TYPE Coverage alladded already exists, please wait while it is killed.
 kill alladded all
&END

&TYPE Identity with quadsutm underway...

identity nalladded z:\misccovs\quadsutm alladded point .001 join
kill nalladded all
```

```
&RETURN

/* -------------------------End of Add_Quadinfo----------------------

/* -------------------------Routine Dist_to_coast--------------------

&ROUTINE Dist_to_coast

&IF [exists dist2coast -cover] &THEN &DO
  &TYPE
  &TYPE Coverage dist2coast already exists, please wait while it is killed.
 kill dist2coast all
&END

&SV coastcov = e:\archives\lithosphere\boundaries\calif00coast
near alladded %coastcov% line 100000000 dist2coast nolocation
build dist2coast point
kill alladded all

&RETURN

/* -------------------------End of Dist_to_coast---------------------

/* -------------------------Routine Add_elev-------------------------

&ROUTINE Add_elev

&IF [exists sitestuff -cover] &THEN &DO
  &TYPE
  &TYPE Coverage sitestuff already exists, please wait while it is killed.
 kill sitestuff all
&END


&SV elevlat = e:\archives\lithosphere\dem\calif30mmlat
latticespot %elevlat% dist2coast z_coord
build dist2coast point
rename dist2coast sitestuff

&RETURN

/* -------------------------End of Add_elev--------------------------

/* -------------------------Routine Add_tmdl-------------------------

&ROUTINE Add_tmdl

&IF [exists sitestuff2 -cover] &THEN &DO
  &TYPE
```

```
  &TYPE Coverage sitestuff2 already exists, please wait while it is killed.
 kill sitestuff2 all
&END
&SV tmdlcov = z:/tmdl/tmdlname


identity sitestuff %tmdlcov% sitestuff2 point .001 join
kill sitestuff all

&RETURN

/* ----------------------------End of Add_tmdl----------------------------

/* ----------------------Routine Export_attributes----------------------
&ROUTINE Export_attributes

tables
sel sitestuff2.pat
alter
idnum
cpw_id
~
~
~
~
pwsname
calname
~
~
~
huc
huc_id
~
~
~
mapname
toponame
~
~
~
distance
coast_distance
~
~
~
~
basin
tmdlname
~
```

```
~
~
~
q

pullitems sitestuff2.pat sitestuff2.out
site_id
x_coord
y_coord
z_coord
coast_distance
huc_id
cuname
rbuaspw
cpw_id
calname
subsection
toponame
tmdlname
cohoprov
steelprov
cutprov
chinprov
end

&IF [exists sitedata.dbf -file] &THEN &DO
 &TYPE
 &TYPE File sitedata.dbf already exists, please wait while it is deleted.
 [delete sitedata.dbf -file]
&END

&TYPE Creating output database file sitedata.dbf
infodbase sitestuff2.out sitedata.dbf

&RETURN

/* ----------End of Export_attributes----------

/* ----------Routine Cleanup----------

&ROUTINE Cleanup

/* Clean up coverages:

&IF [exists sitecov -cover] &THEN
  kill sitecov all

&IF [exists capwsadded -cover] &THEN
  kill capwsadded all
```

```
&IF [exists mostadded -cover] &THEN
  kill mostadded all

&IF [exists nalladded -cover] &THEN
  kill nalladded all

&IF [exists alladded -cover] &THEN
  kill alladded all

&IF [exists dist2coast -cover] &THEN
  kill dist2coast all

&IF [exists sitestuff -cover] &THEN
  kill sitestuff all

&IF [exists sitestuff2 -cover] &THEN
  kill sitestuff2 all

/* Clean up info:

&IF [exists allsites.in -info] &THEN
  [delete allsites.in -info]

/* Clean up files

&IF [exists sitecoord -file] &THEN
  [delete sitecoord -file]

&IF [exists covsite.dbf -file] &THEN
  [delete covsite.dbf -file]

&RETURN
/* ----------End of Cleanup----------

/* ----------Routine Exit----------
/*
&ROUTINE Exit
&SV close$stat [close -all]

&RETURN
/* ----------End of Exit----------

/* ----------Routine Bailout----------
&ROUTINE Bailout
&SEVERITY &ERROR &IGNORE
&CALL Exit
&RETURN; &RETURN &ERROR Bailing out of aaa.aml

/* ----------End of Bailout----------
```

Avenue Script

```
'-----------------------------------------------------------------
'Stream Channel Gradient and Azimuth, v.2c
'Written by Scott Webb, April 1999

'the script accepts a user input and uses that point to select a
'stream temperature site; next attribute values are returned from
'selected features database; these values are used to return a cell
'from an elevation grid; uses these values to calculate azimuth and
'gradient of stream channel between these points

'script call MinElev script
'-----------------------------------------------------------------

'set view info
currView = av.GetActiveDoc
aDisplay = currView.getdisplay

'unselects all themes
currTHMs = currview.getactivethemes
if (currTHMs.count > 0) then
  for each thm in currThms
    thm.setactive(false)
  end
end

'set theme info
elevThm = currView.findtheme("Calif0039lat")
elevGrid = elevThm.GetGrid
elevTab = elevGrid.getVTab
elevFld = elevTab.findfield("Value")

rchThm = currView.findtheme("Stream Reach")
rchTab = rchThm.getFTab
rchTab.SetEditable(true)
shpFld = rchTab.findfield("Shape")
idFld = rchTab.findfield("ID")
dateFld = rchTab.findfield("DateAdded")

rchtbl = av.getproject.finddoc("Attributes of Stream Reach")
rchVTAb = rchtbl.getvtab
```

```
 reachFld = siteTab.findfield("NewReach")
end

urlXFld = siteTab.findfield("URL_X")
if (urlXFld = nil) then
 field4 = field.make ("URL_X", #FIELD_LONG, 10, 0)
 fieldList = {field4}
 sitetab.addfields(fieldList)
 urlXFld = siteTab.findfield("URL_X")
end

urlYFld = siteTab.findfield("URL_Y")
if (urlYFld = nil) then
 field5 = field.make ("URL_Y", #FIELD_LONG, 10, 0)
 fieldList = {field5}
 sitetab.addfields(fieldList)
 urlYFld = siteTab.findfield("URL_Y")
end

urlZFld = siteTab.findfield("URL_Z")
if (urlZFld = nil) then
 field6 = field.make ("URL_Z", #FIELD_LONG, 10, 0)
 fieldList = {field6}
 sitetab.addfields(fieldList)
 urlZFld = siteTab.findfield("URL_Z")
end

lrlXFld = siteTab.findfield("LRL_X")
if (lrlXFld = nil) then
 field7 = field.make ("LRL_X", #FIELD_LONG, 10, 0)
 fieldList = {field7}
 sitetab.addfields(fieldList)
 lrlXFld = siteTab.findfield("LRL_X")
end

lrlYFld = siteTab.findfield("LRL_Y")
if (lrlYFld = nil) then
 field8 = field.make ("LRL_Y", #FIELD_LONG, 10, 0)
 fieldList = {field8}
 sitetab.addfields(fieldList)
 lrlYFld = siteTab.findfield("LRL_Y")
```

```
siteThm = currView.findtheme("sitecov.shp")
siteThm.setactive(true)

siteTab = siteThm.getFTab
siteTab.SetEditable(true)

currID_FLD = siteTab.findfield("SITE_ID")
xFld = siteTab.findfield("X_COORD")
yFld = siteTab.findfield("Y_COORD")
upgradeFld = siteTab.findfield("UPGRADE")

'check for field and creates it if it does not exist
gradFld = siteTab.findfield("NewGrad")
if (gradFLD = nil) then
 field1 = field.make ("NewGrad", #FIELD_FLOAT, 6, 4)
 fieldList = {field1}
 sitetab.addfields(fieldList)
 gradFld = siteTab.findfield("NewGrad")
end

azFld = siteTab.findfield("NewAzimuth")
if (azFld = nil) then
 field2 = field.make ("NewAzimuth", #FIELD_SHORT, 4, 0)
 fieldList = {field2}
 sitetab.addfields(fieldList)
 azFld = siteTab.findfield("NewAzimuth")
end

sinFld = siteTab.findfield("Sinuosity")
if (sinFld = nil) then
 field10 = field.make ("Sinuosity", #FIELD_FLOAT, 6, 3)
 fieldList = {field10}
 sitetab.addfields(fieldList)
 sinFld = siteTab.findfield("Sinuosity")
end

reachFld = siteTab.findfield("NewReach")
if (reachFld = nil) then
 field3 = field.make ("NewReach", #FIELD_FLOAT, 6, 2)
 fieldList = {field3}
 sitetab.addfields(fieldList)
```

```
end

lrlZFld = siteTab.findfield("LRL_Z")
if (lrlZFld = nil) then
  field9 = field.make ("LRL_Z", #FIELD_LONG, 10, 0)
  fieldList = {field9}
  sitetab.addfields(fieldList)
  lrlZFld = siteTab.findfield("LRL_Z")
end



'begin user input
userPt = currView.getdisplay.ReturnUserPoint

siteThm.selectbypoint (userPt, #VTAB_SELTYPE_NEW)

theBitmap = siteTab.getselection
selSite = theBitmap.getnextset (-1)
currID = siteTab.returnvaluestring(currID_FLD, selSite)
currX = siteTab.returnvaluenumber(xFld, selSite)
currY = siteTab.returnvaluenumber(yFld, selSite)


'checks if point is selected or if multiple points selected
if (theBitmap.count = 0) then
  msgbox.info ("No point selected. Please try again.", "Warning!")
  exit
elseif (theBitmap.count > 1) then
  msgbox.info ("More than one point selected. Please get help.", "Warning!")
  exit
else
  'its ok so do nothing
end

'uses measure tool
p = currView.ReturnUserPolyLine

startLinePt = point.make(currX, currY)
endLinePt = currView.getdisplay.getmouseloc
```

```
'checks direction of stream/user input

sLineZ = elevThm.ReturnValueString(elevFld.GetName, startLinePt)
 if ((sLineZ = nil) or (sLineZ = "")) then
  msgbox.info("Wrong elevation grid. Please change code IN BOTH SCRIPTS to correct
theme.","Warning")
  exit
 end

sLineZ = sLineZ.asnumber
eLineZ = elevThm.ReturnValueString(elevFld.GetName, endLinePt)
eLineZ = eLineZ.asnumber

if (eLineZ < sLineZ) then
 msgbox.info("Second point is below first point. Please go other direction!", "Warning")
 exit
end


'extract line segments coordinates from polyline
mp = p.asmultipoint
mptxt = mp.asstring
numsegs = mptxt.extract(1)
numsegs = numsegs.asnumber

'snap reach polyline to coords of site pt
p.Snap (startLinePt, 10)

'get coords pt2 of first seg
Pt2 = mptxt.extract(4)
txtlen = Pt2.count
txtmid = Pt2.indexof(",")
Pt2X = pt2.left(6)
Pt2Y = pt2.right(txtlen - txtmid - 1)

'get coords pt3 of last seg
Pt3 = mptxt.extract(numsegs - 1)
txtlen = Pt3.count
txtmid = Pt3.indexof(",")
Pt3X = pt3.left(6)
Pt3Y = pt3.right(txtlen - txtmid - 1)
```

```
'calc azimuth first seg
Zpt1 = pointZ.make(currx, curry, 0)
Zpt2 = pointZ.make(Pt2X.asnumber, Pt2Y.asnumber, 0)
vecSeg1 = vector.difference(Zpt1, Zpt2)
az1 = vecSeg1.getazimuth


Zpt3 = pointZ.make(Pt3X.asnumber, Pt3Y.asnumber, 0)
Zpt4 = pointZ.make(endLinePt.getx, endLinePt.gety, 0)
vecSeg2 = vector.difference(Zpt3, Zpt4)
az2 = vecSeg2.getazimuth - 180
if (az2 > 360) then
  az2 = az2 - 360
end


coords1 = list.make
 coords1.add(startLinePt)
 coords1.add(az1)
coords2 = list.make
 coords2.add(endLinePt)
 coords2.add(az2)

startPt = av.run( "MinElev", coords1)
startX = startPt.getX
startY = startPt.gety
startZ = elevThm.ReturnValueString(elevFld.GetName, startPt).asnumber

endPt = av.run( "MinElev", coords2)
endX = endPt.getX
endY = endPt.getY
endZ = elevThm.ReturnValueString(elevFld.GetName, endPt).asnumber

rchEndX = endLinePt.getx
rchEndY = endLinePt.getY

delta_x = (rchendX - currX)
delta_y = (rchendY - currY)
delta_z = (endZ - startZ)

'calc straight line distance between pts
```

```
distXY = ((delta_x^2) + (delta_y^2)).sqrt

'return length of rubberband line
reachLgth = p.returnlength


'calc percent gradient
grad = (delta_z/reachLgth)

'cal azimuth
ZptS = pointZ.make(currx, curry, 0)
ZptE = pointZ.make(rchEndx, rchEndy, 0)
vec1 = vector.difference(ZptS, ZptE)
azimuth = vec1.getazimuth


sinRatio = reachLgth/distXY

'write values to database
siteTab.SetValueNumber (upgradeFld, selSite, 2)
siteTab.SetValueNumber (gradFld, selSite, grad)
siteTab.SetValueNumber (azFld, selSite, azimuth)
siteTab.SetValueNumber (reachFld, selSite, reachLgth)
siteTab.SetValueNumber (lrlXFld, selSite, startX)
siteTab.SetValueNumber (lrlYFld, selSite, startY)
siteTab.SetValueNumber (lrlZFld, selSite, startZ)
siteTab.SetValueNumber (urlXFld, selSite, endX)
siteTab.SetValueNumber (urlYFld, selSite, endY)
siteTab.SetValueNumber (urlZFld, selSite, endZ)
siteTab.SetValueNumber (sinFld, selSite, sinRatio)



expr = "[ID] = " ++ currID          'creates logical expression for selection
rchBitmap = rchvTab.GetSelection                'creates variable for selection results
rchvTAB.Query(expr,rchBitmap,#VTAB_SELTYPE_NEW)
rchvtab.setselection (rchbitmap)
delRch = rchBitmap.getnextset (-1)

if (rchBitmap.count > 0) then
  'delete old reach before adding new reach
```

```
  rchvTAB.RemoveRecord (delRch)

end

currDate = Date.Now
currDate.setformat("MM/dd/yyyy")
currDate = currDate.asstring

'adds polyline as stream reach
newRch = rchTab.AddRecord
rchTab.SetValue(shpFLD,newRch, p)
rchTab.SetValue(idFLD,newRch,currID)
rchTab.SetValue(dateFLD,newRch,currDate)


currView.invalidate
msgbox.info ("All done. Go to next point!", "Thank You!")
```

```
'-----------------------------------------------------------------
'Stream Min Elevation, v.1
'Written by Scott Webb. April 1999

'the script accepts a point and searches surrounding cells for
'minimum elevation; returns point with min elev

'script called by Slope_and_Az script

'-----------------------------------------------------------------

currPt = SELF.get(0)
az = SELF.get(1)

'set view and theme info
currView = av.GetActiveDoc
aDisplay = currView.getdisplay

elevThm = currView.findtheme("Calif0039lat")
elevGrid = elevThm.GetGrid
elevTab = elevGrid.getVTab
elevFld = elevTab.findfield("Value")


startX = currpt.getx
startY = currpt.gety
startZ = elevThm.ReturnValueString(elevFld.GetName, currPt).asnumber

currX = startX
currY = startY
currZ = startZ

'finds min elevation from surrounding points, starts with B2
'A1  B1  C1
'A2  B2  C2
'A3  B3  C3

'calc A1
if ((az > 20) and (az < 250)) then
  A1X = startX - 30
  A1Y = startY + 30
```

```
  newPt = point.make(A1X, A1Y)
  A1Z = elevThm.ReturnValueString(elevFld.GetName, newPt).asnumber
  if (A1Z < startZ) then
    currX = A1X
    currY = A1Y
    currZ = A1Z
  end
end

'calc B1
if ((az > 70) and (az < 290)) then
  B1X = startX + 0
  B1Y = startY + 30
  newPt = point.make(B1X, B1Y)
  B1Z = elevThm.ReturnValueString(elevFld.GetName, newPt).asnumber
  if ((B1Z < startZ) AND (B1Z < currZ))then
    currX = B1X
    currY = B1Y
    currZ = B1Z
  end
end


'calc C1
if ((az > 110) and (az < 340)) then
  C1X = startX + 30
  C1Y = startY + 30
  newPt = point.make(C1X, C1Y)
  C1Z = elevThm.ReturnValueString(elevFld.GetName, newPt).asnumber
  if ((C1Z < startZ) AND (C1Z < currZ))then
    currX = C1X
    currY = C1Y
    currZ = C1Z
  end
end


'calc A2
if (((az > 340) and (az < 360)) or ((az >= 0) and (az < 200))) then
  A2X = startX - 30
  A2Y = startY + 0
```

```
  newPt = point.make(A2X, A2Y)
  A2Z = elevThm.ReturnValueString(elevFld.GetName, newPt).asnumber
  if ((A2Z < startZ) AND (A2Z < currZ))then
   currX = A2X
   currY = A2Y
   currZ = A2Z
  end
end

'started with B2

'calc C2
if (((az >= 0) and (az < 20)) or ((az > 160) and (az < 360))) then
  C2X = startX + 30
  C2Y = startY + 0
  newPt = point.make(C2X, C2Y)
  C2Z = elevThm.ReturnValueString(elevFld.GetName, newPt).asnumber
  if ((C2Z < startZ) AND (C2Z < currZ))then
   currX = C2X
   currY = C2Y
   currZ = C2Z
  end
end


'calc A3
if (((az > 290) and (az < 360)) or ((az >= 0) and (az < 160))) then
  A3X = startX - 30
  A3Y = startY - 30
  newPt = point.make(A3X, A3Y)
  A3Z = elevThm.ReturnValueString(elevFld.GetName, newPt).asnumber
  if ((A3Z < startZ) AND (A3Z < currZ))then
   currX = A3X
   currY = A3Y
   currZ = A3Z
  end
end


'calc B3
if (((az >= 0) and (az < 110)) or ((az > 250) and (az < 360))) then
```

```
  B3X = startX + 0
  B3Y = startY - 30
  newPt = point.make(B3X, B3Y)
  B3Z = elevThm.ReturnValueString(elevFld.GetName, newPt).asnumber
  if ((B3Z < startZ) AND (B3Z < currZ))then
    currX = B3X
    currY = B3Y
    currZ = B3Z
  end
end


'calc C3
if (((az > 200) and (az < 360)) or ((az >= 0) and (az < 70))) then
  C3X = startX + 30
  C3Y = startY - 30
  newPt = point.make(C3X, C3Y)
  C3Z = elevThm.ReturnValueString(elevFld.GetName, newPt).asnumber
  if ((C3Z < startZ) AND (C3Z < currZ))then
    currX = C3X
    currY = C3Y
    currZ = C3Z
  end
end

startX = currX
startY = currY

'msgbox.info(currX.asstring, "")
newPt = point.make(currX, currY)
```

Measurement Techniques

Monitoring Devices

A diversity of continuous sensor technology was used by the many parties that collected and submitted stream temperature data for inclusion in the assessment. Table A-1 shows the types of devices and the frequency of their use. Not all data contributors provided information on the type of monitoring device. The *unknown* category of device type represents the case where the data contributor did not provide the information. Based on the information received, the most commonly used device was the Hobo Temperature Data Logger, also known as the Hobo Temp™. Mention of trade names should not be construed as endorsement by the Forest Science Project or its cooperators.

Table A-1. Types of Monitoring Devices Used by Data Contributors.

Device Type[1]	1990	1991	1992	1993	1994	1995	1996	1997	1998	Total
HOBO				62	104	97	77	221	351	912
MENTOR	9	11	9	4	8	10	2	1	1	55
OSTOW	5	6	7	6	10	3	50	103	113	303
STOWTID									17	17
STOWXTI	1	1	1		6	1	2	4	2	18
UNKNOWN				4	43	85	371	300	64	867

[1]HOBO = Onset Hobo® Temp or Hobo® XT; MENTOR = Ryan Temp Mentor; OSTOW = Onset Optic StowAway® ; STOWTID = Onset StowAway® TidbiT®; STOWXTI = Onset StowAway® XTI

NOTE: Mention of trade names does not denote endorsement by the Forest Science Project or its cooperators.

Sampling Frequency

There was a broad range in sample frequencies used to collect stream temperatures (Table A-2). Frequencies ranged from 6.4 minutes to 206 minutes (~3.5 hours). Most of the monitoring devices were set to record stream temperatures at two-hour or more frequent intervals. Appendix A presents a Forest Science Project ***Technical Notes*** issue paper that discusses the effects of sampling frequency on the measurement of chronic and acute temperature statistics. It was found that as sampling intervals exceed 120 minute (2 hour) intervals, there was a significant decrease in the observed daily maximum temperature (Appendix A). The sampling frequency (from 6 minutes up to 2 hours) did not have a significant effect on the observed 7-day moving average.

Table A-2. Sampling Frequency Used at Each Site by Year (1990 - 1998).

Year	Freq. (min)	No. Sites
1990	60	18
	Total Sites	= 18
1991	60	17
	Total Sites	= 17
1992	60.	17
	Total Sites	= 17
1993	36	1
	48	2
	60	10
	72	62
	96	1
	Total Sites	= 76
1994	30	1
	36	1
	48	16
	60	23
	72	51
	96	6
	120	15
	144	55
	205.7	3
	Total Sites	= 171
1995	36	4
	48	18
	60	26
	72	18
	96	15
	120	15
	144	95
	180	4
	205.7	1
	Total Sites	= 196
1996	6.4	1
	10	1
	15	8
	24	24
	30	15
	36	19
	48	1
	60	24
	72	45
	96	200
	120	53
	144	111
	Total Sites	= 502
1997	6.4	1
	15	6
	24	26
	30	47
	36	29
	48	17
	60	31
	72	55
	96	223
	120	78
	144	116
	Total Sites	= 629
1998	6.4	1
	8	17
	16	2
	24	4
	30	32
	36	1
	48	3
	60	89
	72	38
	90	20
	96	256
	120	68
	144	17
	Total Sites	= 548

Calibration

In most cases, cooperators followed calibration procedures furnished by the manufacturer of the monitoring device or those specified in Fish, Farm, and Forest Communities Forum protocols (FFFC, 1996). If a device did not meet the accuracy and precision specifications for a particular device, the device was not deployed in the field. Table A-3 shows accuracy and precision specifications for the various devices listed in Table A-1.

Table A-3. Accuracy and Resolution of Various Continuous Temperature Monitoring Devices

Unit	Temperature Range (°C)	Accuracy Range (°C)	Resolution (°C)
Hobo® Temp	-20 to +70	0.6 to 1.3	0.4 to 0.9
Hobo® XT	-5 to +37	0.5 to 0.7	0.2 to 0.4
StowAway® XTI	-5 to +37	0.3 to 0.4	0.2 to 0.3
Optic StowAway®	-5 to +37	0.2 to 0.23	--
StowAway® TidbiT®	-5 to +37	0.2 to 0.23	--

Note: Accuracy and resolution are interpolated from graphs found in Onset Computer Corporation's product information. Resolution is the difference between temperature steps that the logger can record. Mention of trade names does not denote endorsement by the Forest Science Project or its cooperators.

Data Verification and Validation

The Forest Science Project received stream temperature data from a multitude of sources. These data were collected using several types of monitoring devices (Table A-1). The data were received in a variety of formats, including: *.dtf (direct downloads from the data loggers), *.xls (EXCEL™ worksheets), and *.txt (text files). The data were converted to a common format in preparation for data verification and validation. Data required verification and validation because in many cases the data files contained ambient air temperature spikes (most often occurring immediately prior to field deployment and immediately after retrieval from the stream), and any other anomalous data (such as unit malfunctions). A more detailed discussion is presented below. Data files that were intentionally and exclusively air temperatures were processed separately and maintained in a separate database.

Importing and Converting Data Files

The first step in the process of data verification was importing or converting data files into a common format. Data transfer format (DTF) files, the file format produced by the HOBO™ data-loggers, were converted into text files using Logbook™ 3.0.2 software (Onset Computer Corporation, Pocasset, MA). Microsoft EXCEL™ was used for data verification. A set of customized macros (EXCEL™ programs) was used to process and verify each data file. The macros processed the data in the following sequence:

- assign site identification (site ID) numbers,
- format the date/time and temperature fields,
- plot temperature vs. date on a line graph,
- remove spurious and anomalous data points,
- re-plot the temperature graph, showing the data points removed (shaded gray), and
- copy and save verified data to a comma-delimited text file.

All changes made to data files were recorded in a discrepancy log, which was sent to the data contributor for validation. This process is discussed below in greater detail. Only the validated data were imported into the database.

Data Verification

Each incoming data file was processed and verified. Verification of the data file insured that only **water** temperatures for a given site were included in the database. It was necessary to remove all temperatures that were not valid water temperatures. There were four basic types of errors and anomalies that were removed:

- Ambient air temperatures prior to gauge placement, and after gauge removal; (and also if the cooperator checked the unit at some point during mid-season)
- Sensor de-watering
- Unit Malfunctions
- Dead or dying batteries

In the verification process, all original data were retained. Temperature values were never changed, even if the observation appeared to be incorrect. Rather, data points that were verified and validated by the data contributor as anomalous were removed from the data set. Spurious or anomalous observations were deleted prior to import into the database. The original data with spurious and anomalous observations were retained in the Forest Science Project (FSP) archives for post-verification and chain-of-custody documentation.

Ambient Air Temperatures

Air temperature spikes were the most common types of errors that were encountered. To find where these errors occurred, (as with all other error types), time versus temperature graphs were generated in EXCEL™ for each site and visually inspected. Stream temperatures, in general, do not fluctuate by more than 10°C diurnally. However, daily fluctuations in air temperature by this amount and greater are common. Figure A-1 is an example of air temperature readings occurring in the middle of a data set.

Air temperature spikes prior to sensor placement and/or after sensor removal were also detected by visually inspecting the temperature graphs (Figure A-2). Most often the time of occurrence of ambient air spikes was identified by a rapid change in temperature, more rapid than generally occurs in water temperature data. This is typically several degrees Celsius in one or two hours.

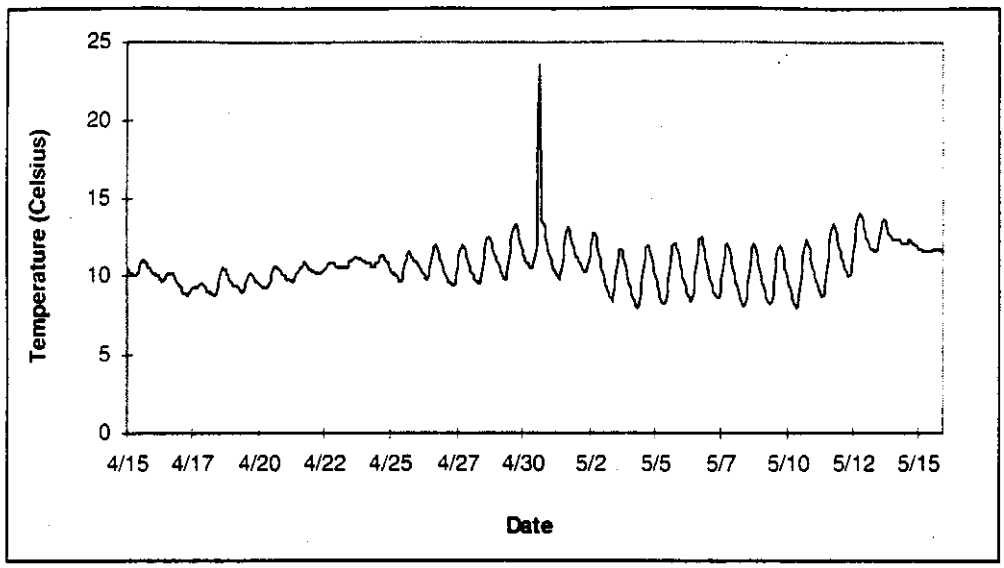

Figure A-1. Example thermograph with an ambient air spike. In this case, the device was removed from the water to determine its operating status.

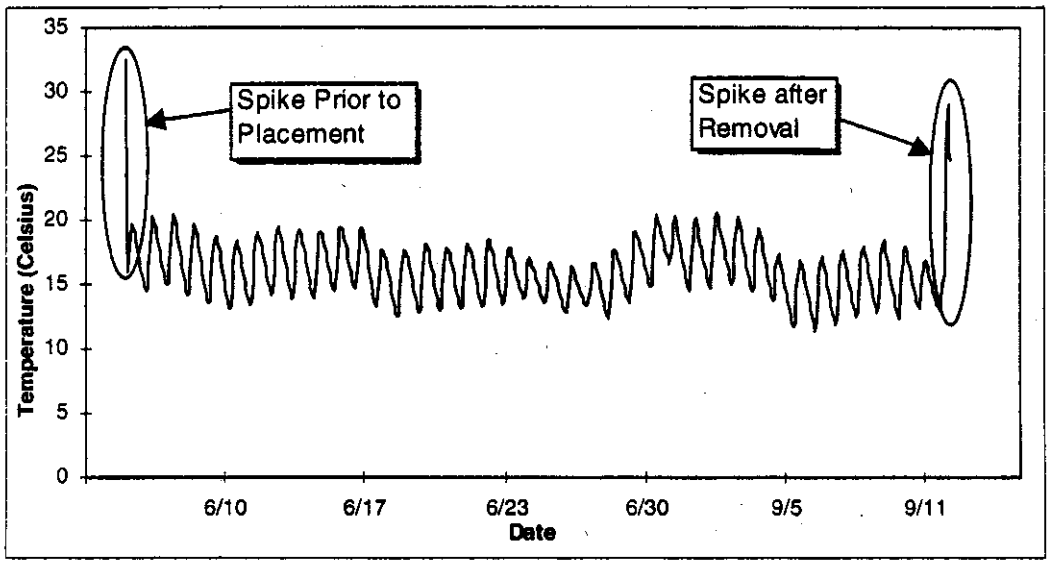

Figure A-2. Example thermograph with air temperature spikes occurring prior to gauge placement and after gauge removal. These anomalous air spikes were removed from the water temperature data set.

Sensor De-watering

This condition occurred when the water levels gradually dropped below the sensor as the summer progressed. The temperature sensor was gradually exposed to the air. On the temperature graph, these areas typically had diurnal temperature fluctuations greater than 15°C; often the daily maximum temperature was above 28°C (Figure A-3). In Figure A-3, note that during the hottest part of the summer, the diurnal temperature fluctuations were greatest; and that during the month of July, anomalous spikes appear in the daily maximum temperature. These are indicators of a sensor that will soon be de-watered.

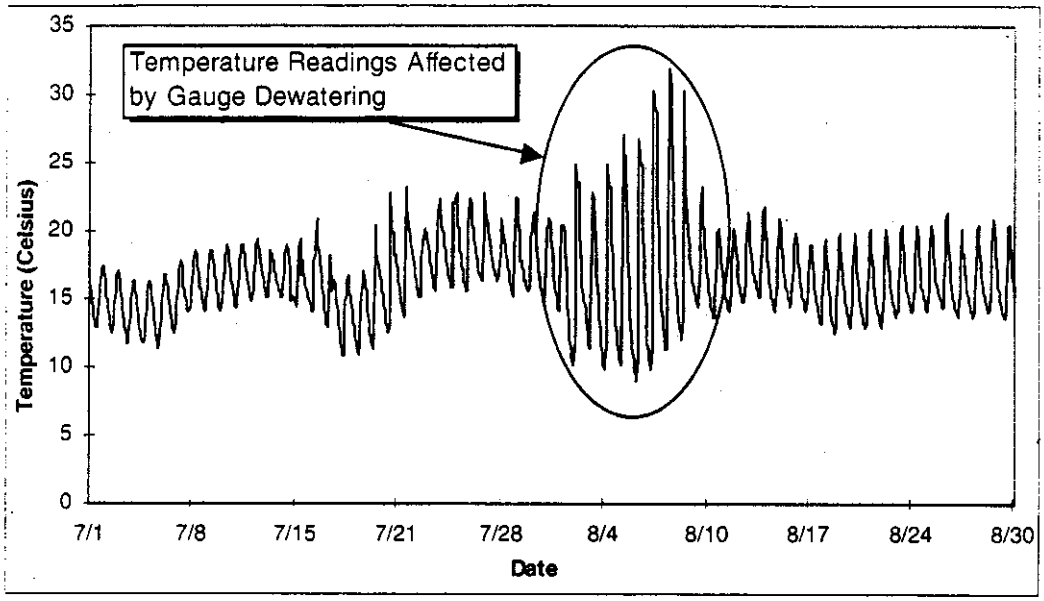

Figure A-3. Example thermograph where the sensing device was de-watered for about 10-days during the summer (August 1 to August 10).

Dead or Dying Batteries

When the charge on temperature sensing device batteries is waning, the unit will begin to record erroneous values. Typically there will be several consecutive readings (more than 5 in a row) that will be exactly the same down to the hundredths of a degree. These readings were removed from the data set. Typically, these thermographs displayed a 'stair-stepping' of values (many readings at the same value, then a sudden jump to another level of readings). Note that the diurnal temperature fluctuations gradually decayed (Figure A-4), until there was a flat line (i.e., no change in temperature value). Occasionally, there were sensors placed in deep pools that may have been influenced by significant summer-time, groundwater influx. These sites appeared as if a dying battery was the cause of the apparent anomalous readings (Figure A-5). The data were reported to the data contributor as possibly erroneous. However, the contributor confirmed that the data were valid, and represented a ground-water influenced, stratified deep pool.

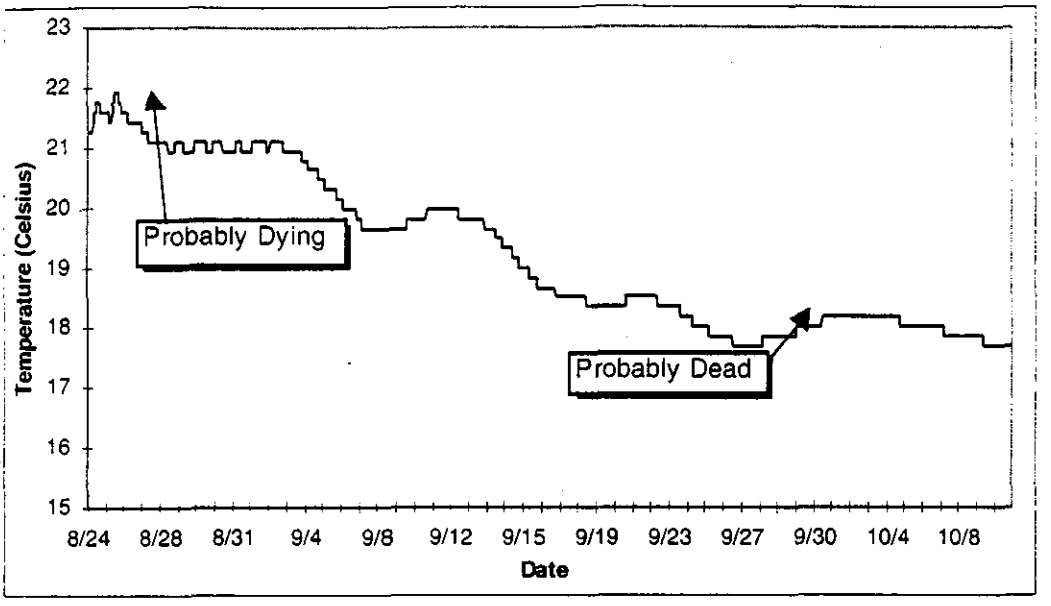

Figure A-4. Example thermograph where the sensing device had a dying battery.

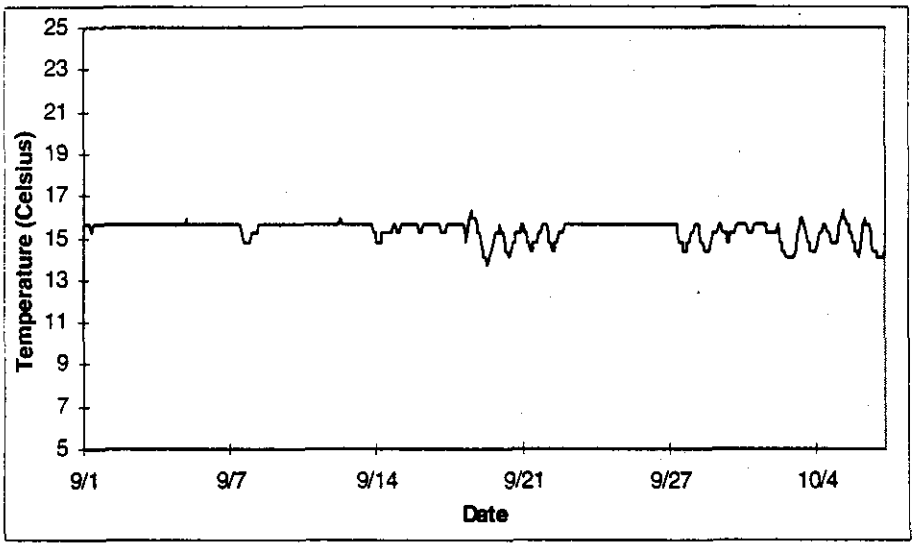

Figure A-5. Example thermograph that exhibits behavior similar to a dying battery, but is actually a deep, thermally-stratified pool, with groundwater as the primary source of water influx.

Unfortunately, many of the sensors used by data contributors do not have the capacity to determine battery charge prior to deployment in the field. The FSP has had an ongoing dialogue with engineers at one major manufacturer of

continuous temperature sensors about the lack of battery charge checking prior to deployment. Newer models that are now available on the market allow the user to check battery charge.

Unit Malfunctions

Unit malfunctions are difficult to detect and diagnose. This category of error can apply to any anomalous data sets that cannot be explained by any other error category. Typically, when this type of error occurred, the entire data set was discarded. However, before discarding the data, the data contributor was contacted to confirm a possible unit malfunction. Figure A-6 illustrates significant down-spikes at regular intervals. The readings were not actual water temperatures, but were unexplainable malfunctions with the sensor.

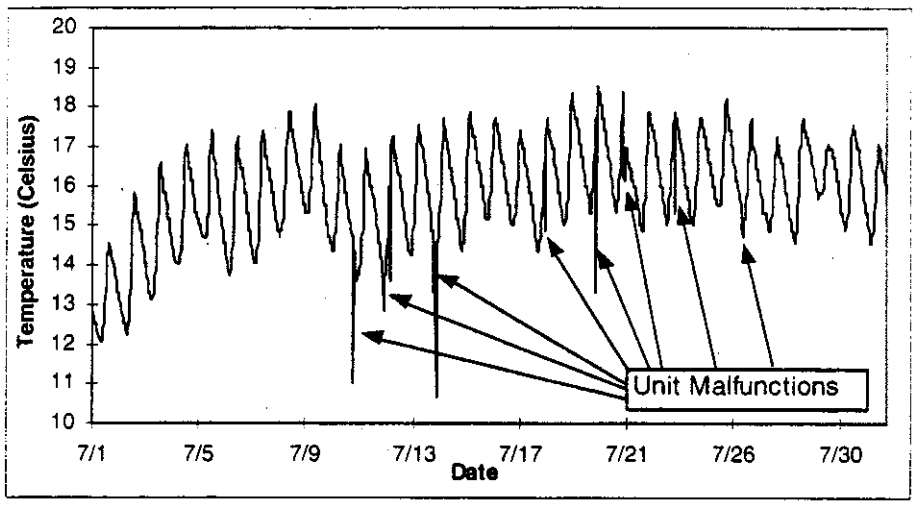

Figure A-6. Example thermograph where the sensing device was probably malfunctioning. In this case, the device recorded significant, instantaneous down-spikes that were not water temperatures.

In Figure A-7, the down-spike was clearly a unit malfunction. The abnormal fluctuations following the down-spike were problematic. The flattened tops and bottoms indicate either a unit malfunction or a dying battery. However, it is possible that this unit was placed in a deep pool with significant temperature stratification (diurnal temperature fluctuations are smaller than the resolution on the recording device; or the unit is strongly influenced by groundwater input). Where a unit malfunction is suspected, the data contributor was contacted to determine the most probable source of the problem, or if there was no problem with the device. If there was no confirmed problem with the device, but the thermograph indicated severe problems with the sensor, all anomalous readings were deleted with the permission of the data contributor.

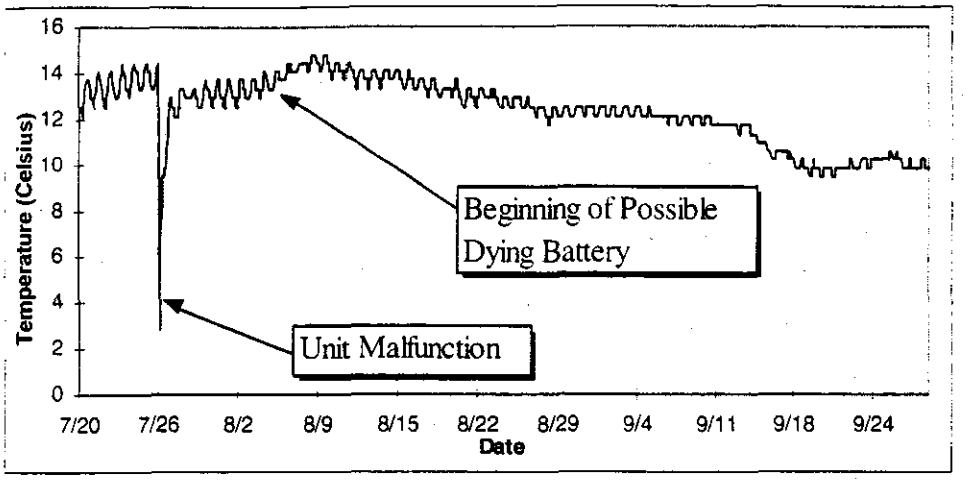

Figure A-7. Example thermograph with a significant unit malfunction, and indications of a dying battery (but probably associated with the unit malfunction).

General Rules for Data Removal

During the data verification and validation process the following guidelines were used when removing anomalous data. When conditions warranted, these guidelines were modified to retain as much data as possible.

1. Remove two (2) observations before and after the air temperature spike.
2. Remove 12 hours of observations before and after gauge [illegible]-watering spikes.
3. Remove two (2) days of observations before the point where a dying battery is indicated.
4. Remove two (2) observations before and after a single unit malfunction.
5. If there are several obvious malfunctions (e.g., Figure A-6), remove two (2) observations before the first error, two (2) observations after the last error, and all observations in between.

Discrepancy Logs

All changes made to temperature data files were recorded in a discrepancy log. This log was sent to the data contributor for validation of changes. The discrepancy log served as a chain-of-custody document for tracking and validating changes made to data files. For every changed file (even if only one datum point was removed), all changes were explicitly detailed in the discrepancy log. A discrepancy entry included the following:

- FSP site id number
- cooperator acronym (assigned by FSP)
- original file name (as assigned by the cooperator)
- the specific items affected (either by row numbers, or by date and time ranges)
- number of items affected
- the action taken
- the explanation/reason for the discrepancy
- and the name of the recorder who made the changes

As mentioned previously, no data point value was changed to a different value. If it was considered anomalous and confirmed as such by the data contributor, the data point was removed from the data base. The original values were retained in the raw data set.

Data Import

Prior to importing temperature data into the FSP database, all changes were confirmed with the data contributor. If there were no anomalies in a particular data file, the data were imported directly into the database. However, there were usually minor changes made to each data file. A list of all changes made was sent to the data contributor, who reviewed the changes. If all changes were correct, the data contributor signed the list, and the validated data were imported into the database. If the changes were incorrect, the appropriate changes were made to the data files as per the data contributor's instructions. A new list of changes was sent to the contributor for verification. This process was reiterated until final reconciliation of discrepancies was reached. Usually, no more than two iterations were necessary to resolve most data discrepancies.

Data Structure

Once the verification and validation process was completed, the stream temperature data and associated attributes were appended to Microsoft (MS) Access relational database tables for each data contributing organization and uploaded to ORACLE tables. Although the local databases were created using MS ACCESS and the regional database was maintained in ORACLE, both utilized the exact same table structure (Figure A-8).

It was necessary to use AML to assign appropriate California planning watershed, ecological subregion, and USGS cataloging (HUC) numbers to each stream temperature monitoring site. AML was also used to calculate site elevation and drainage area from DEMs. Other values such as the nearest straight line distance to the coast and distance from the watershed divide were derived using GIS AMLs (Appendix A). These values were appended to and maintained in the database.

Custom queries were created using structured query language (SQL). Summary tables and views were output to various software packages, including SAS, S-Plus, and Arc/Info for further analysis and display. Figure A-9 illustrates the flow of data and the general procedures used for incorporation of stream temperature and accompanying data into the database.

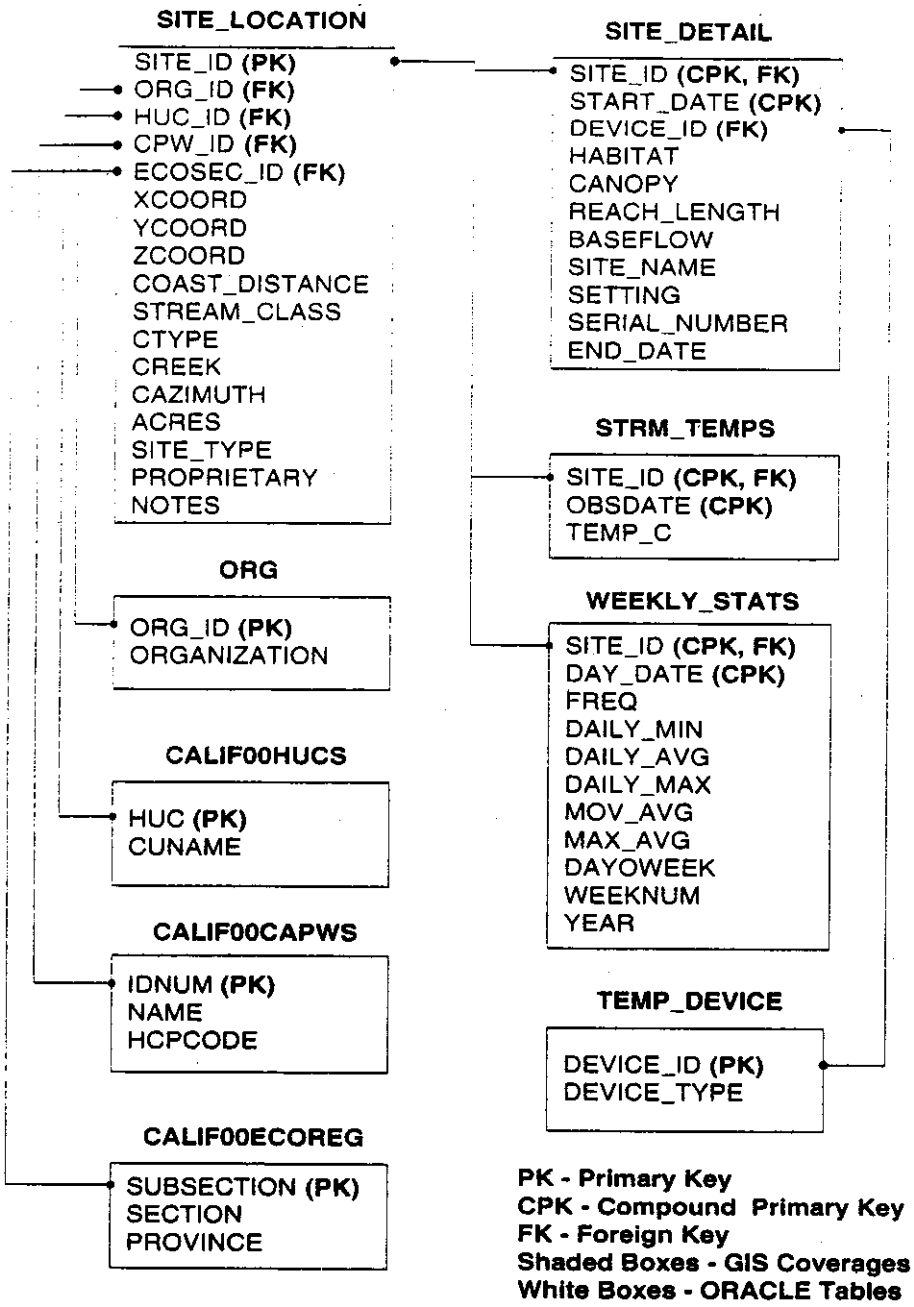

Figure A-8. A simplified stream temperature database diagram.

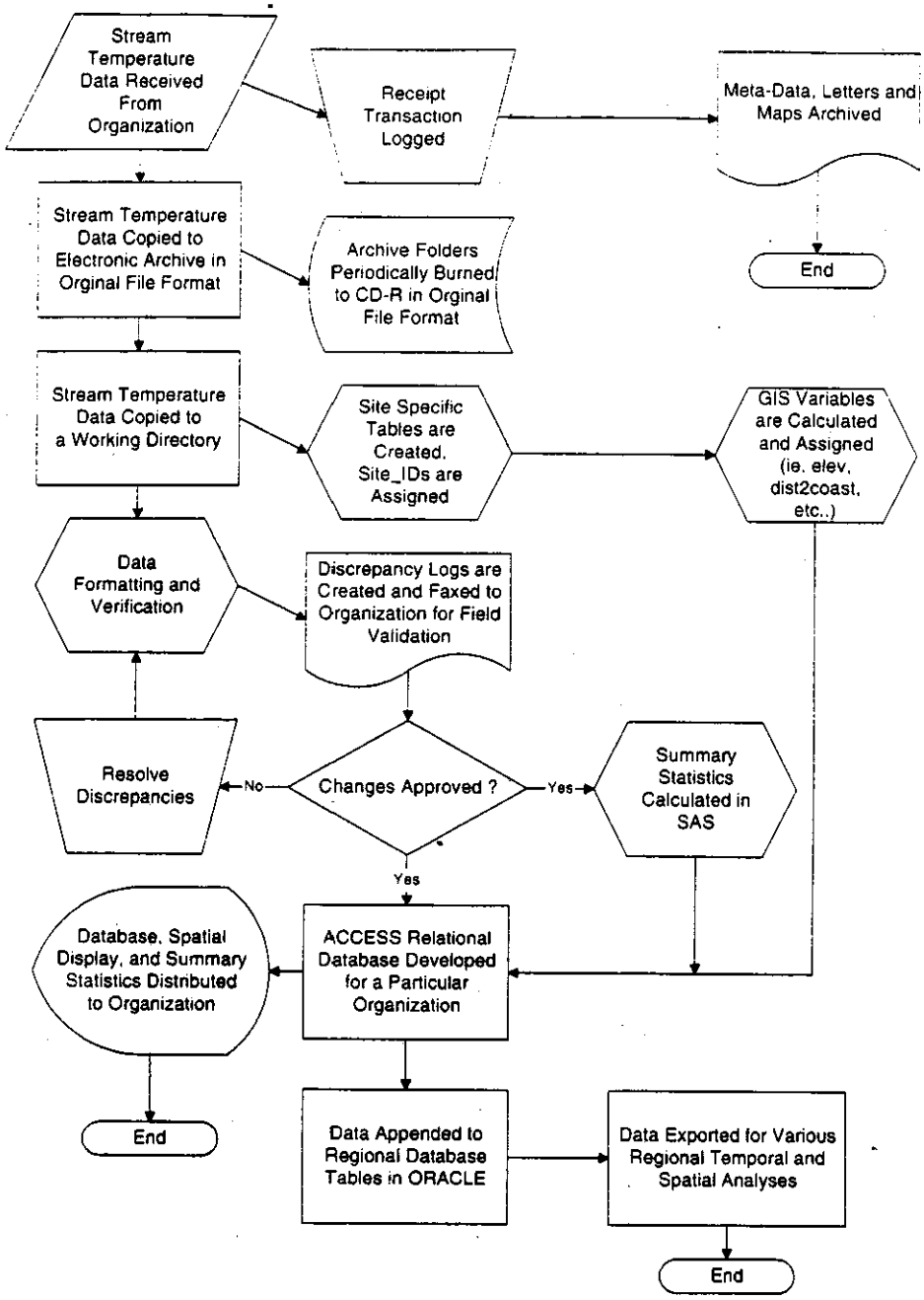

Figure A-9. Stream temperature data (I/O) flow diagram.

Forest Science Project
Stream Temperature Protocol

8075

Stream Temperature Protocol

Forest Science Project
Regional Stream Temperature Assessment

1 Overview

1.1 Background

Stream temperature is one of the most important environmental factors affecting aquatic ecosystems. The vast majority of aquatic organisms are poikilothermic -- their body temperatures and hence their metabolic demands are determined by temperature. Temperature has a significant effect on cold-water fish, both from a physiological and behavioral standpoint. Below is a brief list of the physiological and behavioral processes affected by temperature (Spence et al., 1996).

- Metabolism
- Food requirements, appetite, and digestion rates
- Growth rates
- Developmental rates of embryos and alevins
- Timing of life-history events, including adult migrations, fry emergence, and smoltification
- Competitor and predator-prey interactions
- Disease-host and parasite-host relationships

There has been a heightened awareness of the effects of increased stream temperatures on salmon, trout, and other aquatic/riparian species. Several regulatory measures have been promulgated to mitigate impacts of increased water temperatures on aquatic biota. Restoration activities have been initiated, conservation measures developed, and land use practices altered in an attempt to counteract a perceived but undocumented increase in stream temperatures throughout the state of California. One of the goals of the Forest Science Project's temperature monitoring protocol to obtain the consistent and representative data necessary to document thermal regimes in streams across Northern California.

With the onset of continuous temperature sensor technology, large volumes of stream temperature data are now being collected. Despite the wealth of knowledge regarding the effects of temperature on aquatic organisms, particularly fish, there seems to be a lack of a regional understanding of temperature regimes across Northern California. This protocol sets forth a sampling approach that will provide consistent data that can be used to address stream temperature issues at broad regional scales, i.e., watershed, basins, and regions.

1.2 Scope and Application

The field methods described in this protocol are for obtaining representative stream temperatures from perennial streams for regional monitoring. The field methods are specifically applicable for the deployment of continuous monitoring temperature sensors (e.g., Hobo Temps, Temp Mentors, Stowaways, etc.). Possible interferences in the accurate and precise measurement of stream temperature include: 1) exposure of the sensor to ambient air, 2) improper calibration procedures, including date and time settings, 3) improper placement of the sensor in the stream, 4) low battery, 5) inherent malfunctions in the sensor or data logger, and 6) vandalism.

1.3 Summary of Method

All continuous stream temperature monitoring sensors should be calibrated against a National Institute of Standards and Technology (NIST) traceable thermometer. Sensors not meeting precision and accuracy data quality objectives should not be used. Sensors should be placed in a well-mixed zone, e.g., at the end of a riffle or cascade. Monitoring location should represent average conditions — not pockets of cold water refugia or isolated hot spots. Location of sampling points should either avoid or account for confounding factors that influence stream temperatures such as:

- confluence of tributaries
- groundwater inflows
- channel morphology (particularly conditions that create isolated pools or segments)
- springs, wetlands, water withdrawals, effluent discharges, and other hydrologic factors
- beaver ponds and other impoundments

The sensor should be placed toward the thread or thalweg of the channel. Keep in mind that flow will decrease throughout the summer resulting in an exposed sensor. The thermistor portion of the device should not be in contact with the bottom substrate or other substrate that may serve as a heat sink (e.g., bridge abutment or boulder). Secure the sensor unit to the bottom of the channel with aircraft cable, surgical tubing, rebar, or diver's weights. The sensor should be set to record temperatures **at sampling intervals that should not exceed 1.6 hours (96 minutes)**.

2 Equipment and Supplies

2.1 Calibration and Standardization

Prior to deployment of sensors, calibration of each sensor must be performed. The following is a list of equipment and supplies for calibration:

- NIST traceable thermometer - resolution of 0.2°C or better, an accuracy of ±0.2°C or better.
- controlled-temperature water bath, or water-filled thermos or ice chest
- laboratory notebook
- ice

2.2 Field Measurements

There are several useful materials and pieces of equipment that should be taken to the field to install or service temperature sensors. These include:

- securing material such as zip ties, bailing wire, aircraft cable, surgical rubber tubing, locks, rebar, cinder blocks, large rocks with drilled holes, diver's weights

- surveyors marking tape or flagging
- sledge hammer (e.g., two-pound)
- wire cutters and/or pocket knife
- thermistor equipment items (silicone rings, submersible cases, silicone grease, silica packets)
- portable computer or interface for data downloading and launching
- backup batteries and thermistors
- timepiece/watch
- Rite in the Rain field book
- NIST-traceable auditing thermometer
- waders
- camera and film
- brush removal equipment (e.g., safety axe)
- maps and aerial photos
- spray paint
- metal stakes or spikes, rebar

3 Pre- and Post-Deployment Calibration and Standardization

1. A NIST-traceable thermometer must be used to test the accuracy and precision of the temperature sensors. The NIST-traceable thermometer should be calibrated annually, with at least two calibration points between 10°C (50°F) and 25°C (77°F). Calibrations should be performed using a thermally stable mass of water, such as a controlled-temperature water bath, or water-filled thermos or ice chest. The stable temperature of the insulated water mass allows direct comparison of the unit's readout with that of the NIST-traceable thermometer. Accuracy of the NIST-traceable thermometer must be within ±0.5°C.

2. Prior to use, all continuous monitoring devices should be calibrated at room temperature (~25°C, 77°F) and in an ice water bath to insure that they are operating within the accuracy over the manufacture's specified temperature range. Calibrate all continuous monitoring devices with a NIST-traceable laboratory thermometer at two temperatures, room temperature (i.e., ~77°F, 25°C) and near the freezing point of water as follows:

A. When calibrating and prior to deployment, set all units to the same current date and synchronize all devices using an accurate watch/clock that will be used to time the recording intervals of the reference thermometer. Call for the correct time.

B. Set the record interval of each thermograph to a short period, six to 30 seconds.

C. Record the date, sensor serial number, data logger serial number, and analyst's name in a laboratory notebook. Table 1 is an example of a format that can be used for data collection. The same sensor and same data logger should be deployed in the field as they were paired together during calibration.

D. Place the reference thermometer and the continuous monitoring devices in a five-gallon pail filled with about three gallons of water that has reached room temperature overnight or in a controlled-temperature water bath that has reached room temperature (~77°F, 25°C). Make sure the casings of all continuous monitoring devices are completely submerged. Stir the water, just prior to, and during the calibration period to prevent any thermal stratification.

E. After allowing 10 minutes for the continuous monitoring devices to stabilize, begin recording data for a 10-minute interval. Record the time, the reference thermometer temperature, and the continuous monitoring device temperatures measured at the predetermined sampling frequency (e.g., 6 second, 10 second) used during the 10-minute interval. After all readings are completed, calculate the difference between the reference thermometer and each of the continuous monitoring devices for each reading and calculate the mean difference. Record the data using a format similar to that shown in Table 1.

Table 1. Example of Calibration Data Collection Table

4/12/98	**Sensor Serial Number = 10043 Data logger S.N. = 2S256S**	**Analyst: Joe Celsius**	**Reference Thermometer No. 412**
Time (sec)	**NIST Thermometer Reading (°C)**	**Device Reading (°C)**	**Difference (°C)**
0	25.0	24.8	-0.2
10	25.1	25.0	-0.1
20	25.0	24.9	-0.1
30	25.2	25.0	-0.2
40	25.0	24.6	-0.4
50	25.1	24.9	-0.2
60	25.0	25.1	+0.1
Etc.		$\bar{x}$ = 24.9	Mean Diff. = -0.16
		S.D. = 0.16	

F. Any continuous monitoring devices not operating within their specified accuracy range should be thoroughly scrutinized. If a particular device returns readings that are outside of the manufacturer's accuracy limits, but is still precise, then a correction factor (addition and/or multiplication) can be applied to the data. Precision should be within 0.2 standard deviations (S.D.) of the mean. Acceptable precision should be observed over the range of temperatures that will be experienced in the field. The correction factor, when applied over the calibration range, should give temperature values that are within the accuracy limits of the device. If units are inaccurate and imprecise they should not be used.

G. Using the same water bath, add enough ice to nearly fill the bucket and bring the temperature down to nearly freezing. Stir the ice bath to achieve and maintain a constant water temperature. Place the reference thermometer and the continuous monitoring devices in the water bath or five gallon pail. Again, make sure that the casings are completely submerged.

H. Repeat steps 2B-D with ice water bath.

I. Also confirm that thermograph batteries have sufficient charges for the entire monitoring period (will the length of the upcoming field season fit into the life expectancy of the unit's lithium batteries?).

J. Calibration should also be repeated when sensors are retrieved at the end of the sampling season (post-deployment calibration). Repeat steps 2A-F.

4 Quality Assurance and Quality Control

4.1 Laboratory

Precision and accuracy should be 0.2 SD and ±0.5°C, respectively for each continuous monitoring device.

Monitoring equipment with detachable sensors must be marked in order to match the sensor with the data logger. This allows instrument and sensor to be calibrated and tested prior to deployment, and also makes malfunctions easier to diagnose and correct. A logbook must be kept that documents each unit's serial number, calibration date, test results, and the reference thermometer used (Table 1).

4.2 Field

In addition to laboratory quality control checks, temperature monitoring equipment should be audited during the field season. A field audit is a comparison between the field sensor and a hand-held NIST-traceable reference thermometer. The purpose of a field audit is to insure the accuracy of the data and provide an occasion for corrective action, if needed. A minimum of two field temperature audits should be taken during the sampling period — one after deployment when the instrument has reached thermal equilibrium with the environment, and ideally one prior to recovery of the device from the field. Reference thermometers used for field audits must meet the same specifications as those used for laboratory calibrations: accuracy of ±0.5°C, resolution of 0.1°C.

A field audit is performed as follows:

1. Place the reference thermometer in close proximity to the continuous monitoring device.

2. Record the reference thermometer temperature and the sensor temperature in a field notebook. A stable reading is usually obtained within 10 thermal response units or time constants. For example, a reference thermometer with a ten-second time constant should give a stable reading in 100 seconds.

> Response time (time constant) is the time required by a sensor to reach 63.2% of a step change in temperature under a specific set of conditions. Response time values should be provided by the manufacturer. Five time constants are required for the sensor to stabilize at 100% of the step change value. Ten time constants are recommended to insure that the reference thermometer has reached equilibrium with the stream temperature.

3. Most general purpose data loggers allow the user to connect a computer in the field and view "real-time" temperature data *without disrupting the data logger's* scheduled sampling schedule. This feature allows immediate comparison of the data logger's reading with the reference thermometer's reading. Real-time audit accuracy must be within ±1.0°C.

4. Conversely, most brands of miniature data loggers interrupt data collection when the unit is connected to a computer. With this type of unit, field audit data can only be applied by "post-processing", i.e., the stored data are downloaded and later compared to audit values. This does not permit on-site corrective action if the sensor is not within accuracy specifications. For this type of data logger, auditing times should be scheduled reasonably close to the data loggers download time. Otherwise, the sensor/data logger equipment may fail the audit criteria due to rapidly changing water temperatures. Post-processing audit accuracy must be within ±0.5°C .

5. Data loggers typically set date and time based on the set-up computer's clock. It is important that field personnel synchronize their watches to the computer clock's time. Prior to the field audit the computer clock should be set to the correct date and time by calling for the correct time.

5 Procedures

Water temperatures vary through time and space. The temporal and spatial aspects of deploying stream temperature monitoring devices is discussed in the following sections.

5.1 Temporal Considerations of Sensor Deployment

5.1.1 Sampling Window

Launch sensors to capture the hottest period of the field season, which will vary with watershed location. Coastal streams in Humboldt and Del Norte Counties require deployment at least during July, August, and September; whereas Mendocino County and more inland streams may require longer recording periods (June-October) (FFFC, 1996). For consistency **it is recommended that the sampling window**

be from June 1 to October 1. This sampling window will ensure that the highest temperatures during the summer will be captured in the data set (see FSP March Technical Note in Appendix A).

5.1.2 Sampling Frequency

The time interval between successive temperature readings can be adjusted from every few seconds, to every few hours, to every few days, for most continuous monitoring devices. Table 2 shows some of the typical sampling frequencies and the number of days the device can be left in the field prior to data downloading. In most monitoring activities, the primary objective is to determine the highest temperatures attained during the year. Thus, one of the deciding factors in setting the sampling frequency on a device will be to ensure that the daily maximum temperature is not missed.

Table 2. Typical Sampling Frequencies and Storage Capacity of a Hobo® Data Logger Used for Stream Temperature Monitoring

2K Memory / 1800 Meas.	8K Memory / 7944 Meas.	32K Memory / 32,520 Meas.	Sample Frequency
37.5 days	165 days	677 days	30 min
45 days	198 days	813 days	36 min
60 days	264 days	1084 days	48 min
75 days	331 days	1355 days	1 Hr
90 days	397 days	1626 days	1.2 Hr
120 days	529 days	2165 days	1.6 Hr
150 days	662 days	2710 days	2 Hr
180 days	799 days	3270 days	2.4 Hr
240 days	1050 days	4300 days	3.2 Hr
360 days	1590 days	6540 days	4.8 Hr

Note: BoxCar and LogBook software's launch menu allows the user to choose from 42 intervals ranging from 0.5 seconds to 4.8 hours. The table shows the most likely settings that may be used for stream temperature monitoring. Mention of trade names does not denote endorsement by the Fish, Farm, and Forests Community Forum, the Forest Science Project, or any of their cooperators.

The sampling frequency will depend on the monitoring question and the statistic to be calculated from the data. If the 7-day moving average of the daily average is to be calculated then a less frequent sampling frequency can be used (e.g., 1.2, 1.6, 2.0 hr) (FSP, 1998). However, if the 7-day moving average of the daily maximum is to calculated, then the daily maximum temperature should be captured. If monitoring data is collected infrequently, the daily maximum temperature is likely to be missed. The sensor should be set to record temperatures **at least every 1.6 hours (96 minutes)**.

The more frequent the monitoring, the more precisely the duration of daily maximum temperature can be characterized. The disadvantage of frequent data collection is reduced number of days of data storage and increased number of data points to be analyzed. Some agencies and other groups have found that an 80-minute sampling interval still captures the daily maximum stream temperatures for sites (OCSRI, 1996). If a less frequent sampling interval is desired, then a pilot study must be performed with monitoring at 30-minute intervals over a one to two week period during the hottest time of the year to determine how rapidly stream temperatures change. Pilot study information can provide information on the time interval most appropriate for capturing the daily maximum.

Selection of appropriate sites for monitoring is dependent upon the purpose and monitoring questions being asked. There are two scales of consideration for the appropriate monitoring site: selection of a sample point or location in the stream which provides representative data and the broader strategy of selecting sites that can provide useful information to answer the questions being asked.

5.1.3Data Downloading

It is preferable to have the data cover the entire monitoring without interruptions. However, if data must be downloaded during the monitoring period due to insufficient data logger memory, record the date and time the sensor was removed from the stream and the date and time when it was returned to the stream. Some models may allow for downloading of data without interruption or removal of the sensor from the stream. Be sure to return the sensor to the same approximate location and depth after downloading. During a field visit for data downloading or auditing, record in the field notebook whether the sensor was exposed to the air due to low flow, discontinued flow, or vandalism. This information will be valuable for verification and validation of the data in the office.

5.1.4 Mid-Season Field Audit/Calibration Check

If data downloading is performed in mid-season, an opportunity for a mid-season field audit and calibration check presents itself. See Section 4.2 for mid-season field audit and calibration procedures.

5.2 Spatial Considerations of Sensor Deployment

5.2.1 Stream Sample Point Location

The simplest and most specific scale is a sampling point on a stream. Here, the focus is on sample collection methods that will reduce variability and maximize representativeness.

Monitoring must record daily maxima at locations which represent average conditions - - not pockets of cold water refugia or isolated hot spots. Measurements should be made using a sampling protocol appropriate to indicate impact to beneficial uses (OCSRI, 1996). Thus, location of sampling locations should be done in a manner that is representative of the waterbody or stream segment of interest. In order to collect representative temperature data, sampling site selection must minimize the influence of confounding factors, unless the factor is a variable of interest. Some confounding factors include:

- confluence of tributaries
- groundwater inflows
- channel morphology (particularly conditions that create isolated pools or segments)
- springs, wetlands, water withdrawals, effluent discharges, and other hydrologic factors
- beaver ponds and other impoundments

5.2.2 Site Installation

1. All sensors should be placed in the thalweg of riffles to insure a complete mixing of the water and to maintain sufficient water depth for the duration of the sampling window. Alternatively, if riffles are too shallow place the sensor in a pool or glide that exhibits well-mixed conditions. **DO NOT** place the sensor in a deep pool that may stratify during the summer, unless this is the objective of your study. This measure insures that sensors are not selectively placed in cooler areas such as stratified pools, springs, or seeps or in warm, stagnant locations (hot spots) that would misrepresent a stream reach's temperature signature. A hand-held thermometer can be used to document sufficient mixing by making frequent measurements horizontally and vertically across

the stream cross section. If stream temperatures are relatively homogenous (±1-2°C) throughout the cross section during summer low-flow conditions, then sufficient mixing exists.

2. Monitoring devices should be installed such that the temperature sensor is completely submerged, but not in contact with the bottom. Place the sensor near the bottom of the stream by attaching it to a rock, large piece of woody debris, or a stake. Use zip ties, surgical tubing, or aircraft cable to attach the sensor to the bottom substrate. Rebar or diver's weights can be used if no suitable fastening substrate is available. For non-wadeable streams, the sensor should be placed one meter below the surface, but not in contact with a large thermal mass, such as a bridge abutment or boulder (ODF, 1994). If the monitoring site is not in a heavily visited area, mark the location of the sensor by attaching flagging marked with the gauge number or site ID number to nearby vegetation.

   Precautions against vandalism, theft, and accidental disturbance should be considered when installing equipment. In areas frequented by the public, it is advisable to secure or camouflage equipment. Visible tethers are not recommended because they attract attention. When equipment cannot be protected from disturbance, an alternative monitoring site should be considered. For external data loggers that are not waterproof, place them above the mean high water line to prevent loss during a freshet. Some data loggers must be housed in a waterproof metal or plastic box that should be locked and chained to a tree. Data logger boxes and cables should be covered with rocks, moss, and wood to hide equipment from passers by.

3. Install the sensor in a shaded location; shade can be provided by canopy cover or some other feature such as large woody debris. If no shaded locations are available, then it may be necessary to construct a shade cover for the sensor (e.g., using a section of large diameter plastic pipe.) The intention for this measure is to avoid direct solar warming of the sensor. The intent **is not** to suggest that sensors should be placed only in shaded thermal reaches.

4. Sensors should be located at the downstream end of a thermal reach, so as to characterize the entire thermal reach, as opposed to local conditions. Protocols for characterizing thermal refugia can be found in FFFC (1996).

5. The number of thermograph units deployed will vary with 1) drainage area of the watershed, 2) numbers and sizes of inflow tributaries or other transitions in riparian condition, 3) changes in elevation, and 4) proximity to coastal fog zone. In all circumstances, a continuous monitoring device should be located as far downstream as surface water flows during the summer. In watersheds with multiple sensors locate them in a lower/upper or lower/middle/upper distribution.

> A ***thermal reach*** is a reach with similar (relatively homogenous) riparian and channel conditions for a sufficient distance to allow the stream to reach equilibrium with those conditions. The length of reach required to reach equilibrium will depend on stream size (especially water depth) and morphology (TFW, 1993). A deep, slow moving stream responds more slowly to heat inputs and requires a longer thermal reach, while a shallow, faster moving stream will generally respond faster to changing riparian conditions, indicating a shorter thermal reach. Generally, it takes about 300 meters (or 1000 feet) of similar riparian and channel conditions to establish equilibrium with those conditions in fish-bearing streams.

6. Mark all monitoring site locations on a USGS 1:24,000 topographic map, aerial photo, or GIS map. Clearly show the location of the site with respect to other tributaries entering the stream, e.g.,

above or below the confluence. Record measured distance to a uniquely distinguishable map feature (i.e., road crossing, specific tributary, etc.) Draw a diagram of the monitoring area. Include details such as: harvest unit boundaries, sensor location and thermal reach length, tributaries with summer flow, description of riparian stand characteristics for each bank, areas where portions of the stream flow become subsurface, beaver pond complexes, roads near the stream, other disturbances to the channel or riparian vegetation (heavy grazing, gold dredging, gravel mining, water withdrawals).

7. Record the serial number of each sensor/data logger combination at each monitoring site. Make an effort to deploy the same sensor/data logger combination at the same site each year.

8. Once a sensor/data logger combination has been deployed at a site, **DO NOT** move the equipment to another location. Adjustments in sensor location may be necessary if the initial location ran dry, and the sensor must be moved to the active, flowing channel. This will necessitate a unique site_id for spatial statistical analysis. Make notes of such relocations in the field notebook.

9. If sensors are used to collect long-term baseline or trend data in specific watersheds, establish fixed-location monitoring stations so that data sets will be comparable.

5.3 Site-Specific Data Collection

Other site-specific data should be collected at the time of sensor deployment or retrieval. These additional attributes will greatly assist in post-stratification and interpretation of status and trends in stream temperatures.

5.3.1 Length of Thermal Reach or Stream Segment

The thermal reach extends 300-600 meters above the site, depending on stream size (TFW, 1993). With a hip chain or measuring tape, measure the length of thermal reach or stream segment (in feet). If the stream has more than one channel, measure along the channel that carries most of the summer flow.

5.3.2 Canopy Closure

Use a spherical densiometer at evenly spaced intervals to determine average canopy closure for the thermal reach above the monitoring site. Take canopy closure measurements at 50-meter intervals along the thermal reach. If the percent canopy cover varies by more than 20% between measurements, then take additional measurements at 25-meter intervals to more accurately determine the average percent canopy closure for the reach. In order to save time, it may be advantageous to determine canopy closure at 25-meter intervals from the start, thus avoiding the need to back-track in cases where the variability exceeds 20%. In addition to calculating the average canopy closure, keep a record in a field notebook of the percent canopy closure at each sampling interval and note the locations on a map or sketch of the reach to document how the shade level varies through the reach. At each 25- or 50-meter interval, stand in the center of the channel and measure canopy closure four times: facing upstream, downstream, right bank, and left bank. Average these four values to obtain canopy closure for the location.

5.3.3 Elevation

Determine the elevation at the midpoint of the thermal reach from a USGS topographic map, or altimeter and record on data sheet to nearest feet.

5.3.4 Average Bankfull Width and Depth

The width and depth of a channel reflect the discharge and sediment load the channel receives, and must convey, from its drainage area. Channels are formed during peak flow events, and channel dimensions typically reflect hydraulic conditions during bankfull (channel-forming) flows.

Bankfull width and depth refer to the width and average depth at bankfull flow. These dimensions are related to discharge at the channel-forming flow, and can be used to characterize the relative size of the stream channel. This characterization will be useful for later post-stratification and assessment of stream temperature data. In addition, the ratio of bankfull width to depth (width:depth ratio) of a stream channel provides information on channel morphology. Width:depth ratio is related to bankfull discharge, sediment load, and resistance to bank erosion (Richards, 1982). For example, channels with large amounts of bedload and sandy, cohesionless banks are typically wide and shallow, while channels with suspended sediment loads and silty erosion-resistant banks are usually deep and narrow. Changes in width:depth ratio indicate morphologic adjustments in response to alteration of one of the controlling factors (Schumm, 1977).

Refer to TFW Ambient Monitoring Manual (1993) for step-by-step procedures for estimating bankfull width and depth.

5.3.5 Average Wetted Width

Measure the wetted channel width at the location where the sensor is placed. This measurement should be collected at the time of deployment and at the time of retrieval. Change in wetted width over the field season will provide information on the change in flow during the monitoring period. Follow the method outlined in Flosi (1998). Figure 3 shows a comparison of wetted width and bankfull channel width dimensions.

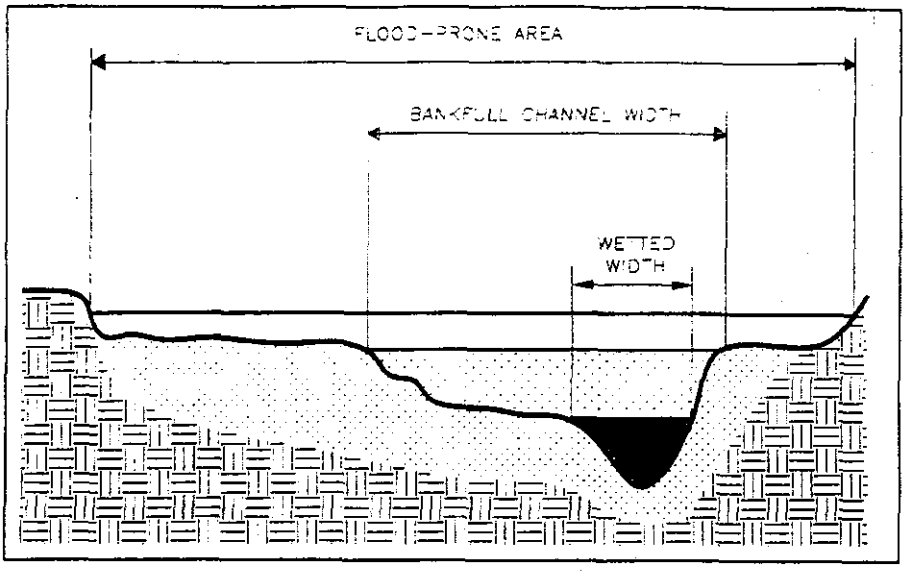

Figure 3. Comparison of wetted width and bankfull width dimensions. Taken from Flosi et al., (1998).

5.3.6 Habitat Type

Record the habitat type in which the sensor was placed. Use the following codes for the habitat types:

riffle Shallow reaches with swiftly flowing, turbulent water
run Relatively uniform flowing reaches with little surface agitation
spool Shallow pools less than 2 feet in depth with good flow (no thermal strata)
mpool Mid-sized pools 2 to 4 feet in depth with good flow (no thermal strata)
dpool Deep pools greater than 4 feet in depth or pools suspected of maintaining thermal strata (possible thermal strata)

5.3.7 Stream Class

Record the stream classification as defined by the California Forest Practice Rules.

1 - ***Class I Watercourse:*** Domestic supplies, including springs, on site and/or within 100 feet downstream of the operations area and/or 2) Fish always or seasonally present onsite, includes habitat to sustain fish migration and spawning.

2 - ***Class II Watercourse:*** a) Fish always or seasonally present offsite within 1000 feet downstream and/or 2) Aquatic habitat for nonfish aquatic species. 3) Excludes Class III waters that are tributary to Class I waters.

3 - *Class III Watercourse:* No aquatic life present, watercourse showing evidence of being capable of sediment transport to Class I and II waters under normal high water flow conditions after completion of timber operations.

4 - *Class IV Watercourse:* Man-made watercourses, usually downstream, established domestic, agricultural, hydroelectric supply or other beneficial use.

For Class I watercourses make a concerted effort to collect fish presence/absence and/or abundance data in the same thermal reaches or stream segments where stream temperature data is being gathered. Conduct fish surveys during the period when stream temperatures are highest (July-August).

6 Data Field Form

To assist in the collection and organization the site-specific information described in Sections 5.3.1 through 5.3.7 a field data form has been developed by the Forest Science Project. The form can be found in Appendix A. Please reduce and photocopy the form onto Write-in-the-Rain paper for data collection activities. Please use a No. 2 pencil.

7 Calculations

It is recommended that only data that meets quality control requirements be used for statistical analyses. Data are considered valid if the instrument's pre- and post-deployment calibration checks are within ±0.5°C of the NIST-traceable reference thermometer, as described in Section 4, and the data are bracketed by field audits which meet the ±1.0°C accuracy criterion (Section 4).

7.1 Maximum Weekly Average Temperature (MWAT)

The seven-day moving average of the daily average and the daily maximum can be calculated with most spreadsheet, database, and statistical software. The seven-day moving average of the daily average is simply the sum of seven consecutive daily average temperatures divided by seven. For consistency, it is recommended that the first day's daily average can be used as the first seven-day moving average, the second day's moving average would be the average of day one and day two daily averages, etc. The seven-day moving average of the daily maximum is the sum of seven consecutive daily maximum temperatures divided by seven.

After all the seven-day moving averages have been calculated, the highest of all the moving averages is referred to as the Maximum Weekly Average Temperature (MWAT) for a given site. Different agencies and groups are comparing either the seven-day moving average of the daily average or the seven-day moving average of the daily maximum to various MWAT criteria. The MWAT threshold can be calculated using the following equation:

$$MWAT = OT + \frac{(UILT - OT)}{3} \qquad (2)$$

where

OT = a reported optimal temperature for the particular life stage or function, and
UUILT = the upper temperature that tolerance does not increase with increasing acclimation temperature.

If the OT is not known, Armour (1991) recommended using the midpoint of a preferred range. The MWAT is interpreted as the upper temperature limit that should not be exceeded during a one-week period in order to prevent chronic lethal effects.

Thus, according to Armour, the MWAT is the threshold against which weekly temperatures are compared. The weekly temperatures are not MWATs.

8 Acknowledgments

This protocol is based on several existing stream temperature protocols. We would like to acknowledge the states of Oregon and Washington for providing stream temperature monitoring protocols for review and incorporation of sections into the FSP protocol. We would like to thank the Forest Science Project cooperators for their review and helpful comments of this protocol. Also, many insightful suggestions were provided by various reviewers from various state and federal agency personnel in California, Oregon, and Washington.

9 References

FFFC, 1996. Aquatic Field Protocols Adopted by the Fish, Farm, and Forest Communities (FFFC) Technical Committee, Compiled by Ross Taylor.

Flosi, G., S. Downie, J. Hopelain, M. Bird, R. Coey, and B. Collins. 1998. *California Salmonid Stream Habitat Restoration Manual*, State of California, The Resources Agency, California Department of Fish and Game, Inland Fisheries Division, Sacramento, CA.

FSP, 1998. Stream temperature sampling frequencies explored. *Forest Science Project Technical Notes.* Forest Science Project, Humboldt State University Foundation, Arcata, CA, April, 1998, 4 pp.

OCSRI, 1996. Stream Temperature Protocol. *Oregon Coastal Salmon Restoration Initiative*, Salem, OR.

ODF, 1994. Water temperature monitoring protocol. *Forest Stream Cooperative Monitoring*, Oregon Department of Forestry, Forest Practices Section, Salem, OR, 20 pp.

Richards, K. 1982. *Rivers: Form and Process in Alluvial Channels.* Methuen. New York, NY.

Schumm, S.A. 1977. *The Fluvial System.* Wiley-Interscience, New York, NY.

Spence, B.C., G.A. Lomnicky, R.M. Hughes, and R.P. Novitzki. 1996. *An Ecosystem Approach to Salmonid Conservation.* TR-4501-96-6057, Management Technology, Corvallis, OR.

TFW, 1993. Stream Temperature Module. *1993 TFW Ambient Monitoring Manual*, Timber-Fish-Wildlife Ambient Monitoring Program, Northwest Indian Fisheries Commission, Olympia, WA.

FSP Stream Temperature Field Data Form

Site_ID:	**File Name:**
Stream Name:	
X Coordinate:	**Y Coordinate:**
Projection (UTM Zone 10 NAD 27 preferred):	
Basin Name:	**USGS Quadrangle:**
Describe Placement:	
Surveyor:	**Organization:**
Device ID (serial #):	**Device Type:**
Calibration Date:	**Mid-Season Calibration Date:**
Date Launched:	**Date Retrieved:**
Depth Launched (ft.):	**Depth Retrieved (ft.):**
Wetted Width Launched (ft.):	**Wetted Width Retrieved (ft.):**
Bankfull Width (ft.):	**Diagram or Photo** (optional)
Bankfull Depth (ft.):	
Reach Length (ft.):	
Mean Canopy Closure (%):	
Avg. Gradient (%)[♦]:	
Avg. Channel Aspect (degrees)[♦]:	
Habitat Type*:	
Channel Type (Flosi et al., 1998):	
Stream Class (I, II, etc.):	
Elevation (ft.)[♦]:	
Drainage Area (acres)[♦]:	
Comments:	

*Habitat Types:

riffle	*shallow reaches with swiftly flowing, turbulent water*
run	relatively uniform flowing reaches with little surface agitation
spool	shallow pools less than 2 feet in depth with good water flow (no thermal strata)
mpool	mid-sized pool 2 to 4 feet in depth with good water flow (no thermal strata)
dpool	deep pools greater than 4 feet in depth or pools suspect of maintaining thermal strata (possible thermal strata)

[♦]OPTIONAL: This is a FSP GIS-derived variable. Supplying a value will assist with FSP accuracy assessment.

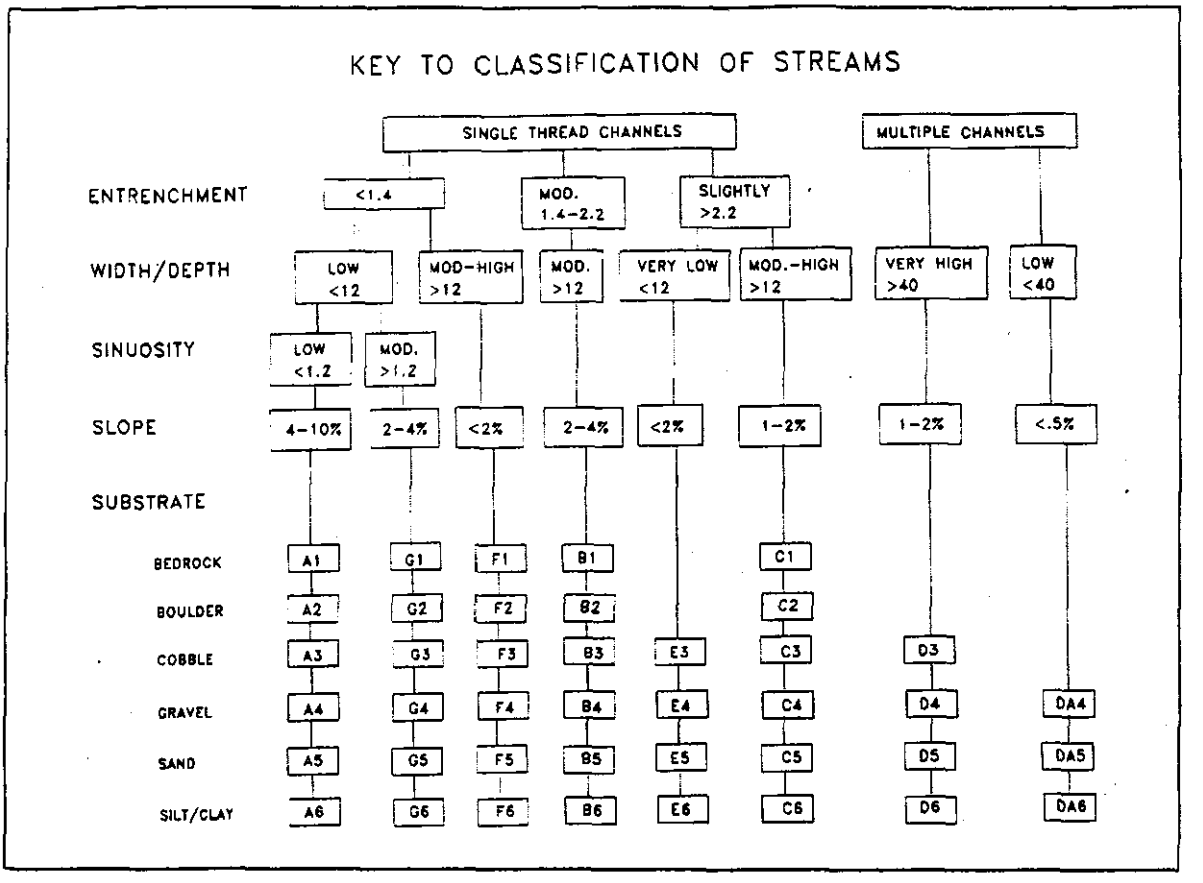

Figure A1. Channel type descriptions. Taken from Flosi et al. (1998).

Photocopy the Channel Type description on this page to the back of the Field Data Form.

Data Submission to Forest Science Project

The following attributes and their descriptions are useful to those that would like to submit their stream temperature data to the Forest Science Project for verification and validation and inclusion in stream temperature assessments. Refer to Section 7.2 *in the FSP Stream Temperature Protocol for more details.*

Fields	Attributes
SITEID	FSP Site ID (leave blank if you do not know what your FSP id numbers are. These are assigned by the FSP for all new sites.)
SITE	Specific monitoring site descriptor as assigned by the cooperator.
CSNAME	**Cooperators Site Name** as assigned by the cooperator.
FILENAME	*Data file name as assigned by the cooperator.*
SURVEYOR	Name of field personnel responsible for monitoring device deployment.
ORGID	Cooperator identification code as assigned by FSP.
UTMX	UTM Easting, Zone 10, NAD 27 (horizontal datum).
UTMY	UTM Northing, Zone 10, NAD 27 (vertical datum).
UTMZ	UTM Elevation, NGVD29 (vertical datum). **Optional.** This is FSP GIS derived.
ELEV	**Elevation** of monitoring station in feet from USGS 7.5 min quadrangle.
CAZIMUTH	Average **aspect** channel aspect of thermal reach in degrees from true north. **Optional.** This is FSP GIS derived.
ACRES	**Acres** of watershed contributing stream flow to the monitoring station (if available). Optional. This is FSP GIS derived.
BASIN	Major drainage basin that monitoring device is located within e.g. N. F. Eel, S. F. Eel, S. F. Trinity, etc. Optional. This is FSP GIS Derived.
WAAREA	Watershed area above monitoring station in hectares. **Optional.** This is FSP GIS derived.
HUCID	USGS fourth-field eight-digit hyrologic unit code. **Optional.** This is FSP GIS derived.
HUCNAME	Forth field hydrologic basin name as recorded by USGS. HUC ArcInfo coverage (available from the FSP-FTP site).**Optional.** This is FSP GIS derived.
CALWAID	California Planning Watersheds identification number. **Optional.** This is FSP GIS derived.
RBUASPW	California Planning Watersheds unique hierarchical identification number. **Optional.** This is FSP GIS derived.
CALNAME	Watershed name as recorded by CDF in the California Planning Watersheds ArcInfo coverage (available from the FSP-FTP site). **Optional.** This is FSP GIS derived.

STRMNAME Stream name as recorded by USGS on 7.5 min. quadrangle.

SITETYPE Data type collected by cooperator.

water - water temperature monitoring
air - air temperature monitoring.
humidity - humidity temperature monitoring.

DATE Date of record (mm/dd/yy)

TIME Time of record (hh:mm:ss)

TEMPC Water temperature in Celsius.

STRCLASS Stream classification as defined by the California Forest Practice Rules.
1 - Class I Watercourse
2 - Class II Watercourse
3 - Class III Watercourse
4 - Class IV Watercourse

HABITAT Habitat classification

riffle - Shallow reaches with swiftly flowing, turbulent water
run - Relatively uniform flowing reaches with little surface agitation
spool - Shallow pools less than 2 feet in depth (no thermal strata)
mpool - Mid-sized pools 2 to 4 feet in depth (no thermal strata)
dpool - Deep pools greater that 4 feet in depth (possible thermal strata)

CHANTYPE **Channel Type** from Flosi et al. 1998 (see Appendix A)

DEVICE Make and model of temperature recording device

hobo - Onset HOBO Temperature Data Logger
hoboxt - Onset HOBO XT Temperature Data Logger
stowxti - Onset stowaway XTI Temperature Data Logger
ostow - Onset Optic stowaway Temperature Logger
stowtid - Onset stowaway tidbit Temperature Data Logger
stowawaytxt - Onset stowaway tidbit XT Temp Data Logger
omnidata - Omnidata Temperature Data Logger
mentor - Ryan Temperature Mentor
other - hourly finger method, etc.

DEVICEID Serial number of the monitoring device.

SETTING	Device set to collect temperature data instantaneously or using some method of integration (averaging between readings). **instant** - set to collect instantaneous readings (most common). **integrated** - set to average between readings. **multimax** - set to collect max between readings.
CALDATE	**Calibration Date** Date of device calibration.
CANOPY	**Avg. Canopy Closure** Average canopy closure in percent for the thermal reach or stream segment above the stream monitoring station.
CCMETHOD	Methodology used for canopy cover estimation. **optical** - single optical estimate taken at site. **sdens** - single spherical densiometer measurement taken at site. **mdens** - multiple spherical densiometer measurement taken along thermal reach.. **none** - no measurements take.
TRLENGTH	**Reach Length** Length of thermal reach upstream of the site measured in feet.
CLENGTH	**Reach Length** Length of the stream segment in meters for which canopy closure was estimated.
BASEFLOW	Average summer baseflow (cfs) at monitoring site.
LWWIDTH	**Wetted Width Launched** Width of the wetted channel (feet) at sensor deployment.
RWWIDTH	**Wetted Width Retrieved** Width of the wetted channel (feet) at sensor retrieval.
BFWIDTH	**Bank Full Width** Width of the channel (feet) at bankfull flow.
BFDEPTH	**Bank Full depth** Depth of the channel (feet) at bankfull flow.
LDEPTH	**Depth Launched** Depth from water surface to monitoring device (feet) at launch.
RDEPTH	**Depth Retrieved** Depth from water surface to monitoring device (feet) at retrieval.
LDATE	**Launch Date** Date and time of monitoring device launch.
RDATE	**Retrieval Date** Date and time of monitoring device retrieval.
COMMENTS	Comments on site location and placement. To include reference distance from site to well defined 7.5 min quadrangle map location i.e. tributary confluence, road crossing, etc.

is an example of relational tables produced in EXCEL developed to prepare stream temperature data for submission to the Forest Science Project. This method duce data processing time, reduce transcription errors, and provide consistency. Please call (707) 826-3273 if you need assistance.

ıs.xls

x	y	elev (ft)	acres	huc name	huc	cal name	calwater	creek	site	str class	habitat	device	reading	canopy (%)	length (ft)	aspect (deg)	bankfull (ft)
401115	4497845	2200	21450	LOWER_EEL	18010105	Palmer	111.110220	My River	**humpty**	1	riffle	hobo	instant	80	500	20	620
400720	4497070	1520	126308	LOWER_EEL	18010105	Palmer	111.110220	Lucky River	Lucky Star	1	run	hoboxt	integral	75	100	80	380
414315	4526670	800	12753	MAD-REDWOOD	18010102	Powers Creek	109.100100	Whatever Stream	**dumpty**	1	spool	stowxti	instant	50	500	320	420
414480	4525720	832	638932	MAD-REDWOOD	18010102	Powers Creek	109.100100	Blue River	site4	1	mpool	ostow	instant	75	1000	270	500
402500	4492200	200	37428	LOWER_EEL	18010105	Newberg	111.110200	Red River	site5	2	dpool	stowtid	instant	90	1200	120	1000
402575	4496535	2582	4394	LOWER_EEL	18010105	Alton	111.110210	Green River	site6	3	riffle	stowtidx	integrat	95	600	270	200
416620	4528740	1263	486531	MAD-REDWOOD	18010102	Powers Creek	109.100100	Yellow River	site7	4	run	omnidata	instant	90	400	90	120

Due to space limitations not all site-specific variables are shown in the table. Refer to the attributes in the previous sections for a complete listing.

.xls

	date	time	temp_c
	8/9/96	16:33:00	16.3
	8/9/96	18:09:00	16.3
	8/9/96	19:45:00	15.9
	8/9/96	21:21:00	15.6
	8/9/96	22:57:00	15.2
	8/10/96	0:33:00	14.8

y.xls

	date	time	temp_c
3	8/9/96	11:28:58	14.8
3	8/9/96	13:04:58	16.3
3	8/9/96	14:40:58	17.8
3	8/9/96	16:16:58	18.6
3	8/9/96	17:52:58	17.8
3	8/9/96	19:28:58	17.1
3	8/9/96	21:04:58	16.3

Forest Science Project Technical Notes

Vol. I No. 1 Forestry Building, Humboldt State University, Arcata, CA 95521 March 1998

FSP Technical Notes

A Publication of the Forest Science Project

Dedicated to the acquisition, compilation, dissemination, and application of knowledge about managed ecological resources in Northern California.

Sampling Window for Stream Temperatures

2.1 Million Stream Temperatures Processed

The Forest Science Project has acquired and is in the process of verifying and validating stream temperature data from approximately 800 sites in Northern California. The data have been submitted to the FSP from both private and public entities. The data span five years. The table shows the number of sites for each year in which temperature data were collected.

Number of Stream Temperature Monitoring Sites (1993-1997)

Year	No. Sites
1993	76
1994	171
1995	196
1996	500
1997	627

Data were gathered using various brands and models of continuous temperature sensors. Data are stored in an ORACLE database and are georeferenced. The map shown below illustrates the location of these sites across the region. There are approximately 2.1 million temperature observations spanning the five-year period and the over 800 sites.

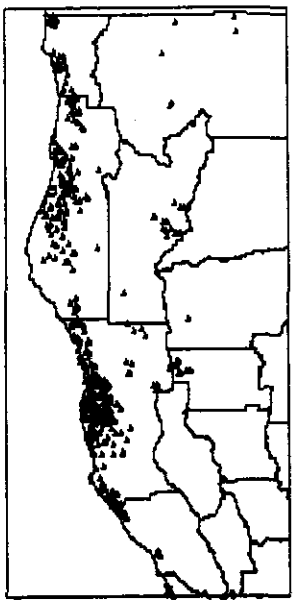

Distribution of Stream Temperature Monitoring Sites in FSP Database

The large database and its geographic extent provides an excellent opportunity to begin to explore large scale (regional) stream temperature issues.

When Should I Put Out My Hobo?

One monitoring question that can be answered with this large regional database is: ***What is the best time for deploying a continuous recording temperature probe in order to capture the highest temperatures of the year?***

Using the Statistical Analysis System (SAS), 7-day moving average values for the daily minimum, average, and maximum were calculated and plotted in the graph below. The plotted weekly statistics are the averages across all sites for each year. For the sake of clarity, only the weeks beginning on a Sunday were plotted.

The highest stream temperatures are expected in the summer, when air temperatures are the highest. Across all years and sites the peak stream temperatures occurred between the last week in July and the second week in August.

Given the time period when the highest stream temperatures occur, a reasonable sampling window could be defined from June 1 to October 1. This is about 120 days. If an instantaneous reading were collected every 1.6 hours, a data logger with 2K of memory could record data without the need for a field person to remove the sensor and download the data. Increasing

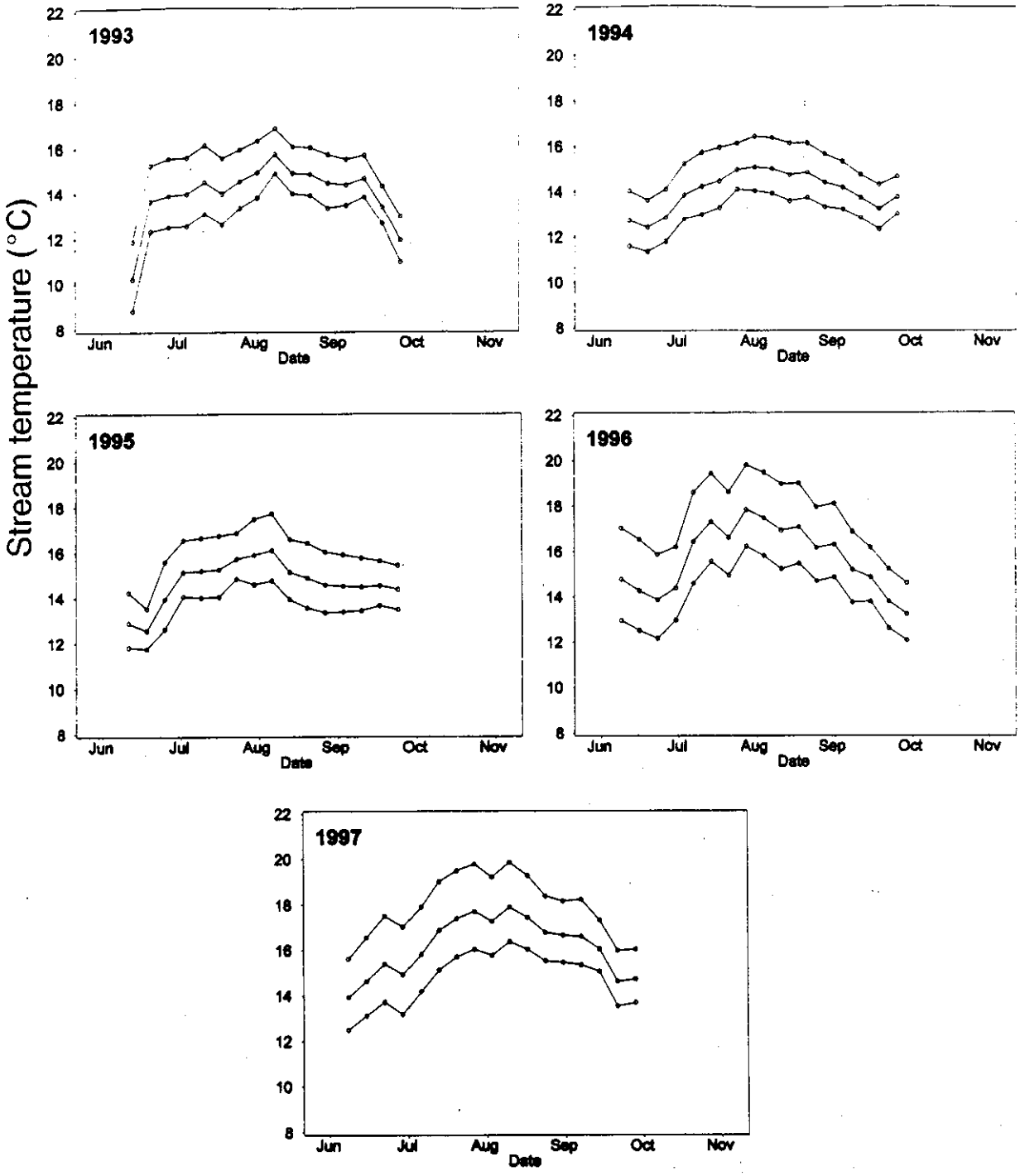

Yearly Plots of the Seven-Day Moving Average of the Daily Minimum, Average, and Maximum Stream Temperatures.

Only moving averages for Sunday are plotted for sake of graphical clarity.

Typical sampling frequencies and storage capacity of a Hobo® data logger used for stream temperature monitoring

2K Memory / 1800 Meas.	8K Memory / 7944 Meas.	32K Memory / 32,520 Meas.	Sample Frequency
37.5 days	165 days	677 days	30 min
45 days	198 days	813 days	36 min
60 days	264 days	1084 days	48 min
75 days	331 days	1355 days	1 Hr
90 days	397 days	1626 days	1.2 Hr
120 days	529 days	2165 days	1.6 Hr
150 days	662 days	2710 days	2 Hr
180 days	799 days	3270 days	2.4 Hr
240 days	1050 days	4300 days	3.2 Hr
360 days	1590 days	6540 days	4.8 Hr

Note: BoxCar and LogBook software's launch menu allows the user to choose from 42 intervals ranging from 0.5 seconds to 4.8 hours. The table shows the most likely settings that may be used for stream temperature monitoring. Mention of trade names does not denote endorsement by the Forest Science Project.

the memory of the data logger will allow the unit to be left in the field longer. The sampling frequency may vary depending on data management resources and first-hand knowledge about the rate of change in stream temperatures at a given site.

A data set was received from a FSP cooperator that had the sampling frequency set to record an instantaneous reading every 6 minutes. Using SAS, the data set was subsampled at increasing time intervals, which would simulate having instantaneous readings taken by the data logger at less frequent sampling frequencies. The influence of increasing sampling frequency on the 7-day moving average is shown in the table below. Changes on the order of a few hundredths of a degree Celsius were noted. It is unlikely that this difference is of biological significance or greater than the measurement error of the monitoring device.

Sampling frequencies between one and two hours can most likely be used with no discernable *influence on 7-day moving average* stream temperatures. The savings in terms of data processing time and the amount of computer resources for data storage are obvious to anyone who has had to process a large amount of stream temperature data.

In our next ***FSP Technical Note*** we will examine the influence of sampling frequency on our ability to capture the daily maximum and the length of time of excursions into acute thermal stress zones.

For additional information please contact the Forest Science Project at (707) 825-7350.

Influence of Sampling Frequency on 7-Day Moving Average Stream Temperature (°C)

	Sampling Frequency (minutes)							
Date	**6**	**12**	**18**	**24**	**30**	**60**	**110**	**120**
1-Jun-97	14.55	14.55	14.58	14.58	14.58	14.64	14.79	14.65
8-Jun-97	11.68	11.68	11.68	11.67	11.67	11.67	11.68	11.69
15-Jun-97	13.79	13.79	13.79	13.79	13.79	13.80	13.80	13.79
22-Jun-97	14.10	14.10	14.10	14.11	14.11	14.1	14.09	14.1
29-Jun-97	12.51	12.51	12.51	12.50	12.50	12.50	12.50	12.53
6-Jul-97	14.16	14.16	14.15	14.16	14.16	14.15	14.11	14.16
13-Jul-97	16.51	16.51	16.52	16.51	16.51	16.52	16.51	16.53
20-Jul-97	17.35	17.35	17.35	17.36	17.36	17.35	17.34	17.33

Vol. I No. 2 Forestry Building, Humboldt State University, Arcata, CA 95521 April 1998

http://www.humboldt.edu/~fsp/
e-mail: fsp@axe.humboldt.edu

FSP Technical Notes

A Publication of the Forest Science Project

Dedicated to the acquisition, compilation, dissemination, and application of knowledge about managed ecological resources in Northern California.

Stream Temperature Sampling Frequencies Explored

In the Last Issue

In the March issue of FSP Technical Notes we examined the effects of sampling frequency on the 7-day moving average. We found that for sampling frequencies up to two hours, there was no discernable influence on the 7-day moving average. The 7-day moving averages varied by a few hundredths of a degree Celsius for each of the sampling frequencies (6, 18, 24, 30, 60, 72, 96, and 120 minutes). This is most likely of no biological significance and within the measurement error of the monitoring device. We have continued our exploration of a stream temperature data set collected on Paralyse Creek, a third-order stream in the South Fork Eel River drainage basin. Data were collected at six-minute intervals.

How Often Should I Take a Reading?

The next logical question is: ***What effect does sampling frequency have on our ability to capture the daily maximum temperature?*** There have been various recommendations put forth in different stream temperature protocols, but none of these recommendations have been based on a statistically rigorous experiment. The Paralyse Creek data set provides an excellent opportunity to determine the effect of sampling frequency on the daily maximum temperature experienced at a given site. Paralyse Creek may be considered a worst case scenario. During July, the diurnal fluctuation in this stream was on the order of about 15°C within a 8-hour period or about 2°C/hour (Figure 1). This rate of change is dramatic and provides sharp peaks in the thermograph that may be missed at greater sampling intervals.

Experimental Design to Answer the Question

The 6-minute data set was considered the ***control*** treatment

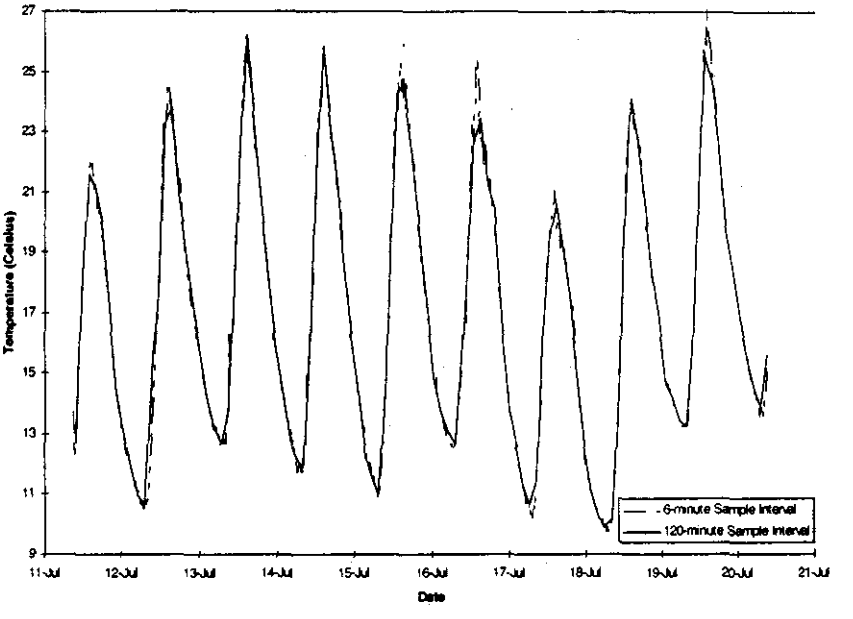

Figure 1. Diurnal fluctuations in Paralyse Creek during July 1997. The 6-minute and 120-minute sampling frequencies are plotted.

against which all other sampling frequencies were compared. Not only was sampling frequency a consideration in this experiment, but also the start time of the data logger. This is a random variable that introduces error into the measurement system. There is no *a priori way of knowing at what time* the daily peak will occur. Field crews cannot activate the data logger so that an instantaneous reading is taken at just the right time to coincide with the daily peak. The randomness in this variable must be introduced into the experiment in addition to different sampling frequencies

Start Time

Considering that a field crew activates a data logger in the office or in the field at the the time of deployment during normal work hours, we have defined the start-time window from 8 am to 5 pm. We truncated the data in the beginning of the data set so that the first observation was approximately 8 am on 31 May 1997 (actually it was 8:02 am). With 6-minute sampling intervals between 8 am and 5 pm there were 85 possible start times. Using a random number generator we obtained 20 random start times. Each start time was incremented at each of the 20 random *start times. The 8:02 am start time* was the zero-incremented start time. This procedure produced 21 data sets with 21 different start times (Table 1).

Table 1. Experimental Design.

Days	Start Times	Sampling Frequencies
51	21	8
May 31 through July 21	8:02 am, 20 random starts	6, 18, 30, 42, 60, 72, 96, and 120 minutes

Sampling Frequency

Eight different sampling frequencies were used to subsample each of the 21 start-time data sets. Using the PROC MEANS procedure in the Statistical Analysis System (SAS) daily maxima were calculated at each of the eight sampling frequencies for each of the 21 start-time data sets. The time period in each data set was from 31 May 1997 to 20 July 1997. Thus, 51 daily maxima were calculated for each sampling frequency and each start time, yielding 8568 daily maximum observations (51 x 21 x 8).

Results of ANOVA

An analysis of variance (ANOVA) was performed on the data using sampling frequency and start time as the main-effects variables. The means across all start times for each sampling frequency were compared for each day in the ANOVA. The results of the ANOVA are shown in Table 2. There was a significant effect from the sampling frequency term in the ANOVA.

Figure 2 illustrates the change in means of the daily maxima for each of the eight sampling frequencies. At increasing sampling frequencies the daily maximum that is observed decreases.

To determine at what point significant differences occurred between the 6-minute and each of the other seven sampling frequencies, four multi-comparison methods were employed, Fisher's LSD, Student Newman-Keuls (SNK), Scheffe's, and Tukey-Kramer.

Each multi-comparison test revealed that there was a significant difference between the 6-minute (control) sampling frequency and the 96- and 120-minute sampling frequencies. In the Fisher's LSD and Scheffe's tests, the 72- and 60-minute sampling frequencies also revealed a significant difference from the 6-minute sampling frequency. The results indicate that somewhere around the 60-minute sampling frequency the daily maximum that is captured starts to diverge from the 6-minute interval, in a decreasing direction.

Table 3 shows the groupings of the sampling frequency means for each of the four multi-comparison tests.

What Does it All Mean?

There is a significant difference between the 6-minute sampling interval and sampling intervals over 60 minutes. However, one must consider the magnitude of these differences. As shown in Figure 2, these mean differences are within a few tenths of a degree. We must keep in mind the measurement error of the sensor and we must also consider whether these differences are of biological significance. A statistical difference does not always directly translate into a biological significance.

The duration of time spent above some acute thermal stress threshold can have a direct biological effect on salmonids. We calculated the proportion of the total time spent above a hypothetical threshold value of 22°C for each of the eight sampling frequencies across the 21 start times. Table 4 shows that there was very little change in the proportion of time spent above 22°C for each of the sampling frequencies. The proportion of the total time above 22°C varies by a few tenths of an hour at each of the sampling frequencies.

Table 2. Results of Analysis of Variance (ANOVA) of Start Time and Sampling Frequency.

source term	degrees of freedom	sum of squares	mean square	F-ratio	probability level
A (sampling frequency)	7	343.5583	49.07975	3.53	0.000866*
B (start time)	20	5.299744	0.2649872	0.02	1.000000
A*B interaction	140	28.06271	0.2004479	0.01	1.000000
S	8400	116820.5	13.90721		
Total (adjusted)	8567	117197.5			
Total	8568				

*Term significant at alpha = 0.05

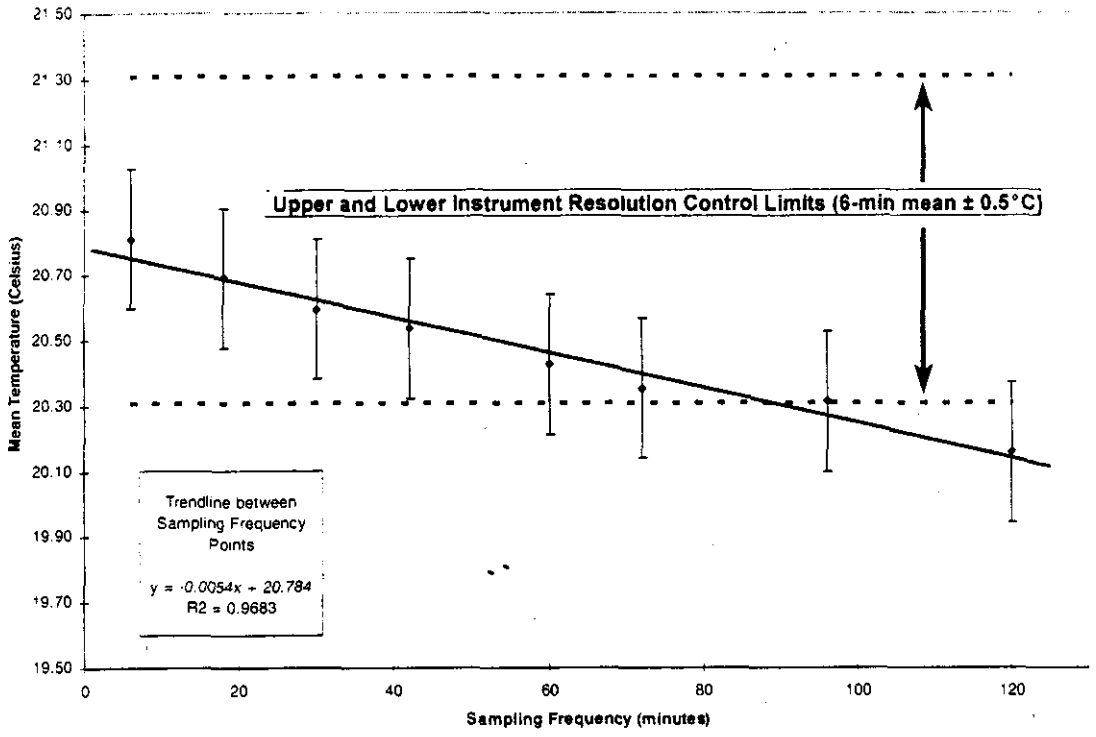

Figure 2. Plot of Sampling Frequency vs. Mean of Daily Maxima with ±1 standard deviation error bars.
Note: Upper and lower instrument resolution control limits are estimated from Onset literature at approximately the temperature range observed in this study.

Table 3. Results of Multi-Comparison Tests of Sampling Frequency Means.

	Sampling Frequency (minutes)							
Test	**6**	**18**	**30**	**42**	**60**	**72**	**96**	**120**
Fisher's LSD	———			———				
SNK	———			———		———		
Scheffe's	———			———				
Tukey-Kramer	———			———		———		

Note: Sampling frequency means connected by the same line are not significantly different at alpha = 0.05.

Table 4. Proportion of Total Time Above 22°C at Each Sampling Frequency.

	Sampling Frequency (minutes)							
	6	18	30	42	60	72	96	120
Average Proportion of Total Time (%)	6.24	6.22	6.23	6.22	6.21	6.16	6.35	6.23

The biological relevance of a variation of a few tenths of an hour exposure to temperatures above an acute thermal stress threshold at the eight sampling frequencies examined here is questionable.

We will provide this data set to anyone that would like to explore other sampling frequency issues or to anyone that would like to corroborate our findings.

These analyses were performed on one stream. These data were readily available and the 6-minute sampling frequency of the data set made it an ideal candidate for such a study. We would like to perform analyses on other data sets from streams that experience diurnal fluctuations greater than 2°C/hour. However, from examining stream temperature data from over 900 sites, we feel confident that this rate of change is extraordinary. Futhermore, we have not found a data set from any other stream where the sampling interval was as short as that for Paralyse Creek.

If you would like to discuss these issues please do not hesitate to call Tim Lewis at (707) 825-7350 or send an e-mail to the address shown on Page 1.

Vol. III No. 41 Harpst Street, Humboldt State University, Arcata, CA 95521 April 2000

http://www.humboldt.edu/~fsp/
e-mail: fsp@axe.humboldt.edu

FSP Technical Notes

A Publication of the Forest Science Project

Dedicated to the acquisition, compilation, dissemination, and application of knowledge about managed ecological resources in Northern California.

A Fish-Eye View of Riparian Canopy

Stream Temperature and Canopy

Incoming solar radiation is an important source of heat input into streams and rivers. Canopy retention in riparian corridors has been considered an important land management treatment for mitigating solar-induced stream heating. There are other riparian characteristics that are intermingled with the desire to maintain "good" canopy cover over streams, such as large wood recruitment, sediment retention, streambank stabilization, instream and riparian habitat availability, and aesthetics.

Riparian canopy measurement is often part of habitat characterization to prioritize stream protection efforts [1]. The underlying rationale behind collecting riparian canopy closure data is related to the general concern over increasing stream temperature. Canopy closure, however, is simply the proportion of an area, given a particular view angle (zenith), blocked by the vertical projection of vegetation crowns onto the ground or water surface [2]. Direct solar radiation cannot be calculated from common spherical densiometer measurement techniques.

There are numerous methods for estimating canopy. Each method measures different aspects of canopy. Canopy is measured in various locations, some adjacent to the channel and some directly in the channel. Where you measure canopy depends on what question you are trying to answer.

We were interested in how canopy influences stream temperature. Thus, measuring canopy from the middle of the stream seems intuitive.

Methods

Spherical densiometers are commonly used to measure riparian canopy in Northern California. Although several published journal articles have noted that these instruments may be subject to high observer bias and unpredictable variances [3, 4, 5], they remain the tool of choice because of a lack of other cost effective measurement devices. Optical estimates of canopy have been used in some monitoring programs [6]. Hemispherical (fisheye) canopy photography can be used to accurately determine canopy geometry and potential light penetration [7]. However, this type of canopy analysis requires specialized camera equipment and software.

The greatest differences among canopy closure measurement techniques involve the instrument's angle of view. Those instruments with wide angles of view generally increase the likelihood of detecting patchiness and spaces in canopy [3]. When measuring canopy closure, an appropriate and consistent angle of view should be used to assure analytical consistency.

Comparison of Methods

The Forest Science Project initiated a study in late Spring of 1998 that was designed to compare the variability in two commonly used methods of canopy measurement, i.e., optical assessment versus spherical densiometer. Assessing what is the best method for quantifying the amount of canopy closure along streams, with mitigation of solar-induced stream heating as the primary consideration, requires an understanding of the variability in both the natural system and the measurement system. The long-term objective of our on-going study is to determine the most appropriate canopy method for assessing effective solar-radiation-intercepting shade over a stream. Stream temperature at any given location is a function of environmental conditions and effective shade upstream for some given distance, this distance often referred to as a thermal reach. An ancillary objective of our study was to determine the optimal sampling frequency for collecting densiometer and optical canopy

closure estimates along a thermal reach, using hemispherical photography canopy closure estimates as the "true" value.

Study Sites

Four stream reaches were selected in various Northern California locations for riparian canopy analysis: Deadwood Creek (DC), Canyon Creek (CC), Grahm Gulch (GG), and Bear Creek (BC). All were in Humboldt County, except DC which was in Trinity County. The site selections were based on professional knowledge of each site's vegetation and channel size, personnel resources, landowner permission, and accessibility. Sites were also selected because of the existence of stream temperature data in the Forest Science Project database. The downstream sampling point was located at the point where a temperature sensor was located the previous year (1997). However, GG site was misidentified as having a stream temperature sensor when, in fact, it did not. Rather, an arbitrary starting point on GG was chosen about 500 meters upstream from the confluence with Freshwater Creek.

Sites were sampled after leaf out in Northern California in mid-May through early June of 1998. An attempt was made to select stream reaches demonstrating a broad range of canopy conditions. Three broad vegetation types were sampled: one site in predominantly deciduous (DC), two sites in mixed deciduous/conifer (BC and GG), and one site in predominantly conifer (CC).

Study Design

Hemispherical photos, densiometer measurements, and optical estimates were taken systematically along each stream reach (Figure 1).

A reach length of 360 meters was used, starting with the downstream plot at a known stream temperature monitoring site. Dominant overstory and understory vegetation, average bankfull width, channel gradient, channel type, and weather conditions were also recorded.

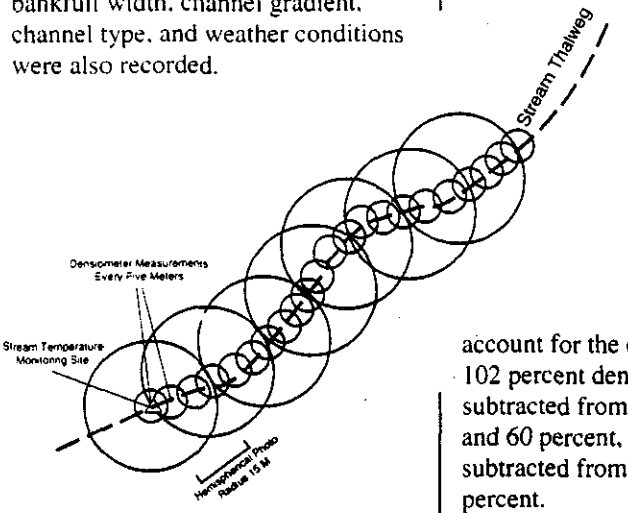

Figure 1. Systematic sampling schematic *(not to scale) for hemispherical* photography and densiometer riparian canopy measurements, June 1998.

Densiometer measurements were recorded every five meters upstream from the temperature monitoring site at each of the four stream reaches. Consistent with other organizations currently collecting these types of data in Northern California, our staff used a modified technique developed by Strickler in 1959 [8]. Densiometers were mechanically modified such that only a wedge-shaped area showing 17 observation points could be used. Holding the densiometer in hand, four observations were made over each plot center, rotating 90 degrees between observations. The modified technique minimizes bias due to point duplication [8]. All measurements were taken at breast height (4.5 ft.).

Percent canopy closure was calculated from the densiometer observations by adding all canopy covered points at each of the four directions then multiplying by 1.5 percent. A correction was applied to account for the complete coverage of 102 percent density. One percent was subtracted from averages between 30 and 60 percent, and two percent was subtracted from averages over 66 percent.

At each densiometer measurement location an optical canopy estimate was recorded. A canopy closure computer-generated card (Figure 2) was used to obtain an ocular estimate of riparian canopy.

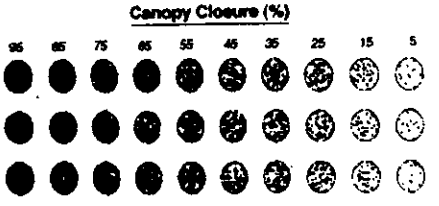

Figure 2. Example of computer-generated card used to estimate canopy closure at four stream sites.

The card served to calibrate the eye to different canopy levels. The card presented canopy closure in 10% increments, in three different crown geometries. The field person visually matched the canopy closure observed overhead to the nearest canopy

closure image on the card. The card is an adaptation of one used by the National Forest Health Monitoring Program [6].

Every fifteen meters upstream from the temperature monitoring site hemispherical photos were taken at breast height (4.5 ft).

Hemispherical Photography

Sam Chan at the USDA Forest Service's Pacific Northwest Forest Sciences Laboratory in Corvallis, OR provided invaluable assistance in the conduct of this study. A photo-graphic system for collecting fish-eye photos was provided by Dr. Chan as well as the use of his laboratory for processing the images. Equipment included the following: Canon AE-1 camera, Canon 7.5-mm fisheye lens (F 5.6 - F16), Sekonic Auto-Lumi light meter (I-158), Kodak Tmax 100 black and white film, tripod with leveling bubble, and a compass.

Black and white negatives were scanned and images processed using CANOPY [7], a software program for estimating direct and diffuse sunlight. It is a DOS-based program. However, a newer version for Windows is now available, called HemiView.

The solar path across the stream is known because each photo is taken with magnetic north at the top of the image. Thus, CANOPY can calculate diffuse and direct sunlight for anytime of the day and time of the year. After leaf out and prior to onset of senescence is our temporal window of interest.

Hemispherical photos provide a permanent archive of the geometry of sky visibility and obstruction. The images can be stored as negatives or transparencies, and/or as digital images. We chose both, permanent archival of TIF images on CD-ROM and cataloguing of negatives. Since images are permanently archived reanalysis can be performed at a later time. Moreover, images collected in future years can be directly compared to historical canopy geometries in a quantitative manner.

Variability: It's Out There

There was considerable variability in the densiometer and optical estimates of riparian canopy cover compared to the fisheye canopy values. Figure 3 shows the canopy cover measured at each 15-meter sampling interval along DC and CC.

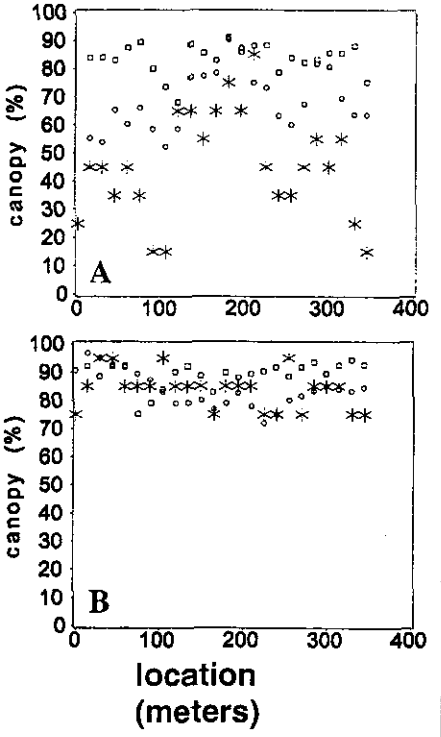

Figure 3. Variability in canopy cover on (A) Deadwood and (B) Canyon Creeks as measured by three different methods: square = fisheye, circle = densiometer, star = optical.

GG and BC showed variability similar to that seen in DC. Uncorrected indirect (diffuse) canopy from the CANOPY program was compared to the two other methods. The software-derived form of canopy is considered to be more similar to densiometer and optical estimates.

The fisheye canopy values were less variable than the other two methods. It is unclear why the three methods were better correlated at the CC site than at the other three sites. Canopy geometry and orientation and differences in field of view are believed to be involved in whether there is good agreement or large disagreement in the three canopy methods. The fisheye method takes into account the sun's path over the stream, and adjusts the amount of incoming solar radiation by the time of day, time of year, and latitude. The other two methods do not have such capabilities. Figure 4 shows a fish-eye photo taken at the 30-m interval on DC.

Figure 4. Fish-eye photo taken at 30-m interval on Deadwood Creek.

The optical and densiometer readings were about 45% and 55% shading respectively, whereas the estimated uncorrected diffuse shading estimate from the CANOPY program was about 85%. The photo is oriented with north at the top and east to the right.

While there appears to be a large sky view, the opening is oriented such that the trajectory of the sun would only allow direct solar heat input during a narrow temporal window. Thus, we believe the fish-eye canopy estimate provides a more realistic indication of the effective shade capable of intercepting direct solar radiation given the orientation and geometry of the riparian canopy.

Another source of variability contributing to the total variability in the measurement system is within- and between-observer variability. Figure 5 compares the optical canopy estimates for observer #1 and observer #2. Both measured canopy at the same locations in DC. Values tend to come into better agreement at the higher canopy values, but at the middle and lower range, 50% to 100% variability was observed.

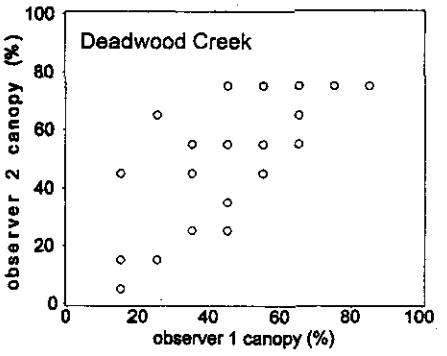

Figure 5. Between-observer variability at Deadwood Creek using canopy card.

Future research will deal with inputting various canopy estimates derived using different protocols into stream temperature prediction models. Model validation of observed versus predicted stream temperature using different canopy estimates will be a good test of which method provides canopy information that best accounts for solar radiation interception.

If your organization is interested in learning more about how to measure canopy please contact the Forest Science Project at **707-825-7350**.

References

[1] Flosi et al. 1997. *California Salmonid Stream Habitat Restoration Manual, Third Edition.*

[2] Vora, R.S. 1988. *Great Basin Naturalist* 48(2): 224-227.

[3] Bunnell, F.L., and Vales, D.J. 1989. *Can. J. For. Res.* 20: 101-107.

[4] Cook, J.G., et al., 1995. *Wildlife Soc. Bull.* 23(4): 711-171.

[5] Nuttle, T. 1997. *Wildlife Soc. Bull.* 25(3):610-611.

[6] Lewis, T.E. and B. Conkling. 1994. *Forest Health Monit.* EPA/620/R-94/006.

[7] Rich, P.M. 1989. *A Manual for Analysis of Hemispherical Canopy Photography.* Las Alamos National Laboratory, 77 pp.

[8] Strickler, G.S. 1959. *Use of the Densiometer to Estimate Density of Forest Canopy on Permanent Sample Plots.* USDA. Forest Service Res. Note 180, 5 pp.

APPENDIX B

Summary of the Statistical Attributes of Regional Stream Temperatures

Hourly Summary Statistics
Years 1990 - 1998

---------- YEAR = 1990 ----------

Variable: TEMP_C (TEMPC)

Moments

N	43920	Sum Weights	43920
Mean	15.263796	Sum Observations	670385.92
Std Deviation	3.51413212	Variance	12.3491245
Skewness	0.54598239	Kurtosis	0.18252409
Uncorrected SS	10774995.1	Corrected SS	542361.201
Coeff Variation	23.0226617	Std Error Mean	0.01676822

Basic Statistical Measures

Location		Variability	
Mean	15.26380	Std Deviation	3.51413
Median	14.78000	Variance	12.34912
Mode	14.39000	Range	22.78000
		Interquartile Range	4.67000

Quantiles

Quantile	Estimate
100% Max	29.28
99%	24.72
95%	21.61
90%	20.11
75% Q3	17.39
50% Median	14.78
25% Q1	12.72
10%	11.11
5%	10.28
1%	8.50
0% Min	6.50

Extreme Observations

Lowest			Highest		
Value	DATE	Obs	Value	DATE	Obs
6.50	06/01/1990	32900	29.00	08/06/1990	3288
6.50	06/03/1990	6421	29.00	07/15/1990	37710
6.50	06/03/1990	6420	29.22	08/09/1990	3342
6.50	06/01/1990	6380	29.22	07/15/1990	32327
6.61	06/03/1990	19157	29.28	07/15/1990	2908

---------- YEAR = 1991 ----------

Variable: TEMP_C (TEMPC)

Moments

N	49982	Sum Weights	49982
Mean	15.7395398	Sum Observations	786693.68
Std Deviation	3.50514798	Variance	12.2860623
Skewness	0.58674062	Kurtosis	0.00469558
Uncorrected SS	12996266.2	Corrected SS	614069.681
Coeff Variation	22.2696979	Std Error Mean	0.01567832

Basic Statistical Measures

Location		Variability	
Mean	15.73954	Std Deviation	3.50515
Median	15.22000	Variance	12.28606
Mode	15.28000	Range	21.39000
		Interquartile Range	4.61000

Quantiles

Quantile	Estimate
100% Max	28.11
99%	24.89
95%	22.39
90%	20.72
75% Q3	17.89
50% Median	15.22
25% Q1	13.28
10%	11.72
5%	10.78
1%	9.11
0% Min	6.72

Extreme Observations

----------Lowest----------			----------Highest----------		
Value	DATE	Obs	Value	DATE	Obs
6.72	06/20/1991	37750	27.61	08/12/1991	37552
6.72	06/20/1991	9066	27.72	08/11/1991	7861
6.89	06/20/1991	9067	27.89	08/11/1991	43900
7.11	06/20/1991	9065	28.11	08/12/1991	7876
7.22	06/20/1991	44162	28.11	08/12/1991	7877

---------- YEAR = 1992 ----------

Variable: TEMP_C (TEMPC)

Moments

N	49776	Sum Weights	49776
Mean	15.9403333	Sum Observations	793446.03
Std Deviation	3.40594725	Variance	11.6004767
Skewness	0.64209888	Kurtosis	0.30093062
Uncorrected SS	13225207.9	Corrected SS	577413.728
Coeff Variation	21.3668509	Std Error Mean	0.01526609

Basic Statistical Measures

Location		Variability	
Mean	15.94033	Std Deviation	3.40595
Median	15.39000	Variance	11.60048
Mode	14.72000	Range	22.72000
		Interquartile Range	4.50000

Quantiles

Quantile	Estimate
100% Max	29.11
99%	25.28
95%	22.39
90%	20.61
75% Q3	18.00
50% Median	15.39
25% Q1	13.50
10%	12.11
5%	11.28
1%	9.39
0% Min	6.39

Extreme Observations

Lowest			Highest		
Value	DATE	Obs	Value	DATE	Obs
6.39	09/01/1992	22858	29.00	07/28/1992	5254
7.11	06/14/1992	6611	29.00	07/30/1992	5293
7.11	06/13/1992	6604	29.11	07/16/1992	5048
7.22	06/14/1992	6613	29.11	07/29/1992	5274
7.22	06/14/1992	6612	29.11	07/30/1992	43163

---------- YEAR = 1993 ----------

Variable: TEMP_C (TEMPC)

Moments

N	148410	Sum Weights	148410
Mean	14.126924	Sum Observations	2096576.79
Std Deviation	2.11742237	Variance	4.48347751
Skewness	0.51801596	Kurtosis	1.27138827
Uncorrected SS	30283569.4	Corrected SS	665388.414
Coeff Variation	14.9885593	Std Error Mean	0.00549637

Basic Statistical Measures

Location		Variability	
Mean	14.12692	Std Deviation	2.11742
Median	13.89000	Variance	4.48348
Mode	13.89000	Range	18.04000
		Interquartile Range	2.33000

Quantiles

Quantile	Estimate
100% Max	24.32
99%	20.28
95%	18.00
90%	16.78
75% Q3	15.15
50% Median	13.89
25% Q1	12.82
10%	11.72
5%	10.93
1%	9.22
0% Min	6.28

Extreme Observations

----------Lowest----------			----------Highest----------		
Value	DATE	Obs	Value	DATE	Obs
6.28	06/05/1993	146930	23.77	08/02/1993	141831
6.28	06/03/1993	146923	23.96	08/01/1993	80806
6.28	06/03/1993	123848	23.96	08/02/1993	80822
6.39	06/05/1993	109214	24.13	08/01/1993	80804
6.39	06/05/1993	109213	24.32	08/01/1993	80805

---------- YEAR = 1994 ----------

Variable: TEMP_C (TEMPC)

Moments

N	278277	Sum Weights	278277
Mean	14.2265028	Sum Observations	3958908.53
Std Deviation	2.46447573	Variance	6.07364061
Skewness	1.27484567	Kurtosis	2.18433885
Uncorrected SS	58011571.8	Corrected SS	1690148.41
Coeff Variation	17.323131	Std Error Mean	0.00467182

Basic Statistical Measures

Location		Variability	
Mean	14.22650	Std Deviation	2.46448
Median	13.71000	Variance	6.07364
Mode	14.02000	Range	20.75000
		Interquartile Range	2.69000

Quantiles

Quantile	Estimate
100% Max	28.86
99%	22.39
95%	19.11
90%	17.61
75% Q3	15.30
50% Median	13.71
25% Q1	12.61
10%	11.69
5%	11.27
1%	10.28
0% Min	8.11

Extreme Observations

----------Lowest----------			----------Highest----------		
Value	DATE	Obs	Value	DATE	Obs
8.11	09/13/1994	226583	28.31	07/23/1994	265464
8.11	06/07/1994	165040	28.49	07/19/1994	265448
8.11	06/07/1994	165039	28.49	07/22/1994	265460
8.11	09/13/1994	159238	28.68	07/19/1994	147805
8.11	09/13/1994	159236	28.86	07/22/1994	147854

---------- YEAR = 1995 ----------

Variable: TEMP_C (TEMPC)

Moments

N	301484	Sum Weights	301484
Mean	14.6348509	Sum Observations	4412173.4
Std Deviation	2.45412936	Variance	6.02275093
Skewness	0.79105646	Kurtosis	1.38444559
Uncorrected SS	66387257	Corrected SS	1815757.02
Coeff Variation	16.7690766	Std Error Mean	0.00446957

Basic Statistical Measures

Location		Variability	
Mean	14.63485	Std Deviation	2.45413
Median	14.30000	Variance	6.02275
Mode	14.80000	Range	23.04000
		Interquartile Range	2.70000

Quantiles

Quantile	Estimate
100% Max	28.38
99%	22.09
95%	19.32
90%	17.90
75% Q3	15.80
50% Median	14.30
25% Q1	13.10
10%	12.00
5%	11.11
1%	9.50
0% Min	5.34

Extreme Observations

Lowest			Highest		
Value	DATE	Obs	Value	DATE	Obs
5.34	06/20/1995	221778	27.65	08/05/1995	294677
5.34	06/20/1995	221777	27.83	08/04/1995	192860
5.34	06/19/1995	221768	28.19	08/04/1995	248683
5.48	06/19/1995	221767	28.38	08/04/1995	192858
5.80	06/20/1995	221776	28.38	08/04/1995	192859

---------- YEAR = 1996 ----------

Variable: TEMP_C (TEMPC)

Moments

N	930534	Sum Weights	930534
Mean	16.2080775	Sum Observations	15082167.2
Std Deviation	3.52098233	Variance	12.3973166
Skewness	0.74364826	Kurtosis	0.23520079
Uncorrected SS	255989047	Corrected SS	11536112.2
Coeff Variation	21.7236272	Std Error Mean	0.00365004

Basic Statistical Measures

Location		Variability	
Mean	16.20808	Std Deviation	3.52098
Median	15.57000	Variance	12.39732
Mode	14.80000	Range	29.29000
		Interquartile Range	4.73000

Quantiles

Quantile	Estimate
100% Max	34.18
99%	25.76
95%	22.88
90%	21.35
75% Q3	18.30
50% Median	15.57
25% Q1	13.57
10%	12.25
5%	11.54
1%	10.31
0% Min	4.89

Extreme Observations

----------Lowest----------			----------Highest----------		
Value	DATE	Obs	Value	DATE	Obs
4.89	09/16/1996	608303	33.16	08/13/1996	704760
5.11	09/16/1996	608302	33.58	09/01/1996	262530
5.28	09/16/1996	608304	33.58	08/24/1996	820836
5.28	09/16/1996	608301	33.77	08/24/1996	262458
5.28	09/05/1996	608111	34.18	08/29/1996	262506

---------- YEAR = 1997 ----------

Variable: TEMP_C (TEMPC)

Moments

N	1223699	Sum Weights	1223699
Mean	16.4836544	Sum Observations	20171031.4
Std Deviation	3.31064147	Variance	10.9603469
Skewness	0.70835186	Kurtosis	0.31154281
Uncorrected SS	345904466	Corrected SS	13412154.6
Coeff Variation	20.0843902	Std Error Mean	0.00299278

Basic Statistical Measures

Location		Variability	
Mean	16.48365	Std Deviation	3.31064
Median	15.81000	Variance	10.96035
Mode	14.80000	Range	28.24000
		Interquartile Range	4.23000

Quantiles

Quantile	Estimate
100% Max	32.52
99%	25.34
95%	22.89
90%	21.38
75% Q3	18.40
50% Median	15.81
25% Q1	14.17
10%	12.92
5%	12.16
1%	10.24
0% Min	4.28

Extreme Observations

Lowest			Highest		
Value	DATE	Obs	Value	DATE	Obs
4.28	06/22/1997	1.06E6	31.47	08/07/1997	1.19E6
4.28	06/22/1997	1.06E6	31.68	08/07/1997	720880
4.28	06/22/1997	616823	31.68	08/07/1997	724866
4.28	06/22/1997	616820	32.06	08/08/1997	724878
4.28	06/22/1997	616819	32.52	07/28/1997	489829

---------- YEAR = 1998 ----------

Variable: TEMP_C (TEMPC)

Moments

N	1327892	Sum Weights	1327892
Mean	15.4922418	Sum Observations	20572023.9
Std Deviation	3.30583099	Variance	10.9285185
Skewness	0.98801436	Kurtosis	1.22242058
Uncorrected SS	333218650	Corrected SS	14511881.4
Coeff Variation	21.3386225	Std Error Mean	0.00286879

Basic Statistical Measures

Location		Variability	
Mean	15.49224	Std Deviation	3.30583
Median	14.67000	Variance	10.92852
Mode	14.80000	Range	29.50000
		Interquartile Range	3.80000

Quantiles

Quantile	Estimate
100% Max	32.64
99%	25.38
95%	22.27
90%	20.24
75% Q3	17.09
50% Median	14.67
25% Q1	13.29
10%	12.22
5%	11.57
1%	9.61
0% Min	3.14

Extreme Observations

Lowest			Highest		
Value	DATE	Obs	Value	DATE	Obs
3.14	06/02/1998	754038	32.06	07/26/1998	589203
3.14	06/02/1998	754037	32.06	09/02/1998	589619
3.53	06/08/1998	1.15E6	32.26	07/27/1998	589212
3.53	06/07/1998	1.15E6	32.45	07/25/1998	1.25E6
3.53	06/06/1998	1.15E6	32.64	07/26/1998	1.25E6

Daily and Weekly Summary Statistics
Years 1990 - 1998

Daily Summary Statistics
Years 1990 - 1998

Table B-1. Abbreviated Summary Statistics for 1990 Daily Temperature Metrics in °C.

No. Sites	No. Obs.	Daily Metric	Lowest	Avg.	Highest	Range	Variance	SD	Mode	Median
		minimum	6.5	13.9	23.2	16.7	10.1	3.2	14.4	13.7
15	1830	mean	7.5	15.3	25.8	18.2	11.1	3.3	13.1	14.9
		maximum	8.5	16.9	29.3	20.8	13.9	3.7	17.1	16.5

Table B-2. Abbreviated Summary Statistics for 1991 Daily Temperature Metrics in °C.

No. Sites	No. Obs.	Daily Metric	Lowest	Avg.	Highest	Range	Variance	SD	Mode	Median
		minimum	6.7	14.1	22.1	15.4	8.4	2.9	12.8	13.7
18	2079	mean	8.8	15.7	24.8	16.1	10.6	3.3	14.7	15.2
		maximum	9.2	17.6	28.1	18.9	15.2	3.9	16.2	16.6

Table B-3. Abbreviated Summary Statistics for 1992 Daily Temperature Metrics in °C.

No. Sites	No. Obs.	Daily Metric	Lowest	Avg.	Highest	Range	Variance	SD	Mode	Median
		minimum	6.4	14.3	22.8	16.4	7.4	2.7	13.6	13.9
17	2074	mean	7.8	15.9	25.0	17.2	9.9	3.2	13.8	15.5
		maximum	8.6	17.8	29.1	20.5	14.4	3.8	15.3	17.1

Table B-4. Abbreviated Summary Statistics for 1993 Daily Temperature Metrics in °C.

No. Sites	No. Obs.	Daily Metric	Lowest	Avg.	Highest	Range	Variance	SD	Mode	Median
		min	6.3	13.1	21.4	15.2	3.2	1.8	13.0	13.0
76	7109	mean	7.0	14.1	22.8	15.8	3.6	1.9	14.0	14.0
		max	7.8	15.4	24.3	16.5	5.0	2.2	15.0	15.2

Table B-5. Abbreviated Summary Statistics for 1994 Daily Temperature Metrics in °C.

No. Sites	No. Obs.	Daily Metric	Lowest	Avg.	Highest	Range	Variance	SD	Mode	Median
		minimum	8.1	13.1	23.9	15.8	3.4	1.8	12.5	12.8
171	16739	mean	8.9	14.1	26.0	17.1	4.5	2.1	13.1	13.6
		maximum	9.4	15.4	28.9	19.5	7.3	2.7	14.5	14.7

Table B-6. Abbreviated Summary Statistics for 1995 Daily Temperature Metrics in °C.

No. Sites	No. Obs.	Daily Metric	Lowest	Avg.	Highest	Range	Variance	SD	Mode	Median
		minimum	5.3	13.7	23.1	17.8	3.6	1.9	13.6	13.5
196	19694	mean	7.2	14.8	24.2	17.0	5.0	2.2	14.1	14.4
		maximum	7.7	16.1	28.4	20.7	8.2	2.9	14.8	15.5

Table B-7. Abbreviated Summary Statistics for 1996 Daily Temperature Metrics in °C.

No. Sites	No. Obs.	Daily Metric	Lowest	Avg.	Highest	Range	Variance	SD	Mode	Median
		minimum	4.9	14.4	25.8	20.9	7.4	2.7	13.4	13.9
502	48242	mean	7.7	15.9	27.9	20.2	10.0	3.2	13.7	15.3
		maximum	8.0	17.8	34.2	26.2	16.1	4.0	14.8	17.0

Table B-8. Abbreviated Summary Statistics for 1997 Daily Temperature Metrics in °C.

No. Sites	No. Obs.	Daily Metric	Lowest	Avg.	Highest	Range	Variance	SD	Mode	Median
		minimum	4.3	15.0	25.2	20.9	7.0	2.6	14.8	14.5
629	59712	mean	7.6	16.4	27.3	19.7	8.8	3.0	14.4	15.9
		maximum	8.8	18.2	32.1	23.3	14.0	3.7	14.8	17.5

Table B-9. Abbreviated Summary Statistics for 1998 Daily Temperature Metrics in °C.

No. Sites	No. Obs.	Daily Metric	Lowest	Avg.	Highest	Range	Variance	SD	Mode	Median
		minimum	3.1	14.5	26.5	23.4	8.3	2.9	14.8	14.0
548	54396	mean	4.5	15.9	27.9	23.4	10.4	3.2	13.9	15.2
		maximum	5.8	17.5	32.6	26.8	15.2	3.9	14.8	16.7

Weekly Summary Statistics
Years 1990 - 1998

Table B-10. Abbreviated Summary Statistics for 1990 Seven-Day Moving Average Stream Temperature Metrics in °C.

No. Sites	No. Obs.	Seven-Day Metric	Lowest	Avg.	Highest	Range	Variance	SD	Mode	Median
		minimum	7.3	14.0	22.8	15.5	9.4	3.1	13.9	13.8
15	1830	mean	8.6	15.4	25.0	16.4	10.4	3.2	17.8	15.1
		maximum	9.9	17.1	28.8	18.9	12.9	3.6	13.7	16.7

Table B-11. Abbreviated Summary Statistics for 1991 Seven-Day Moving Average Stream Temperature Metrics in °C.

No. Sites	No. Obs.	Seven-Day Metric	Lowest	Avg.	Highest	Range	Variance	SD	Mode	Median
		minimum	8.2	14.2	21.5	13.3	7.8	2.8	13.0	13.8
18	2079	mean	9.3	15.9	23.8	14.5	10.0	3.2	13.9	15.2
		maximum	10.1	17.8	27.3	17.1	14.4	3.8	16.3	16.8

Table B-12. Abbreviated Summary Statistics for 1992 Seven-Day Moving Average Stream Temperature Metrics in °C.

No. Sites	No. Obs.	Seven-Day Metric	Lowest	Avg.	Highest	Range	Variance	SD	Mode	Median
		minimum	8.0	14.4	21.9	13.9	6.9	2.6	12.8	14.0
17	2074	mean	9.2	16.0	24.6	15.4	9.5	3.1	12.6	15.5
		maximum	10.0	17.9	28.8	18.8	13.7	3.7	15.3	17.2

Table B-13. Abbreviated Summary Statistics for 1993 Seven-Day Moving Average Stream Temperature Metrics in °C.

No. Sites	No. Obs.	Seven-Day Metric	Lowest	Avg.	Highest	Range	Variance	SD	Mode	Median
		minimum	6.8	13.1	20.3	13.6	2.9	1.7	12.8	13.1
76	7109	mean	7.8	14.2	21.5	13.7	3.3	1.8	13.7	14.0
		maximum	8.9	15.5	23.2	14.3	4.5	2.1	14.9	15.2

Table B-14. Abbreviated Summary Statistics for 1994 Seven-Day Moving Average Stream Temperature Metrics in °C.

No. Sites	No. Obs.	Seven-Day Metric	Lowest	Avg.	Highest	Range	Variance	SD	Mode	Median
		minimum	8.9	13.1	22.7	13.8	3.1	1.8	12.5	12.8
171	16739	mean	9.6	14.2	25.3	15.8	4.4	2.1	13.2	13.6
		maximum	10.3	15.4	28.1	17.9	7.0	2.7	13.9	14.7

Table B-15. Abbreviated Summary Statistics for 1995 Seven-Day Moving Average Stream Temperature Metrics in °C.

No. Sites	No. Obs.	Seven-Day Metric	Lowest	Avg.	Highest	Range	Variance	SD	Mode	Median
		minimum	6.1	13.7	22.1	16.1	3.3	1.8	12.9	13.5
196	19694	mean	8.0	14.8	23.5	15.5	4.7	2.2	14.2	14.5
		maximum	8.8	16.2	26.4	17.6	7.6	2.8	14.3	15.6

Table B-16. Abbreviated Summary Statistics for 1996 Seven-Day Moving Average Stream Temperature Metrics in °C.

No. Sites	No. Obs.	Seven-Day Metric	Lowest	Avg.	Highest	Range	Variance	SD	Mode	Median
		minimum	7.2	14.4	25.3	18.1	6.9	2.6	12.7	14.0
502	48242	mean	8.1	16.0	27.4	19.3	9.6	3.1	13.8	15.4
		maximum	8.6	17.8	32.7	24.0	15.6	3.9	14.5	17.2

Table B-17. Abbreviated Summary Statistics for 1997 Seven-Day Moving Average Stream Temperature Metrics in °C.

No. Sites	No. Obs.	Seven-Day Metric	Lowest	Avg.	Highest	Range	Variance	SD	Mode	Median
		minimum	6.5	15.0	24.2	17.7	6.7	2.6	13.5	14.6
629	59712	mean	8.7	16.5	26.6	18.0	8.5	2.9	14.4	15.9
		maximum	9.5	18.3	31.0	21.5	13.5	3.7	15.4	17.6

Table B-18. Abbreviated Summary Statistics for 1998 Seven-Day Moving Average Stream Temperature Metrics.

No. Sites	No. Obs.	Seven-Day Metric	Lowest	Avg.	Highest	Range	Variance	SD	Mode	Median
		minimum	3.5	14.6	26.0	22.5	8.0	2.8	13.0	14.1
548	54396	mean	4.7	16.0	27.5	22.7	10.1	3.2	14.1	15.3
		maximum	6.9	17.6	32.1	25.2	14.6	3.8	15.8	16.8

CDF Analyses

XYA7DA, XYA7DX, and XY1DX

Highest Seven-Day Moving Average of the Daily Maximum (XYA7DA)

Table B-19. Mathematically Determined Cumulative Proportions for XYA7DA Above and Below Two Reference Temperature Values (16.8°C and 18.3°C) for 1990.

Year	Total Number of Sites[1]	Reference Value	Cumulative Proportion
1990	15	≤16.8	0.42138
		≥16.8	0.64528
		≤18.3	0.53509
		≥18.3	0.53158

[1]Total number of sites used in analyses after CDF filter procedure applied.

Table B-20. Mathematically Determined Cumulative Proportions for XYA7DA Above and Below Two Reference Temperature Values (16.8°C and 18.3°C) for 1991.

Year	Total Number of Sites[1]	Reference Value	Cumulative Proportion
1991	17	≤16.8	0.46229
		≥16.8	0.59653
		≤18.3	0.65789
		≥18.3	0.40093

[1]Total number of sites used in analyses after CDF filter procedure applied.

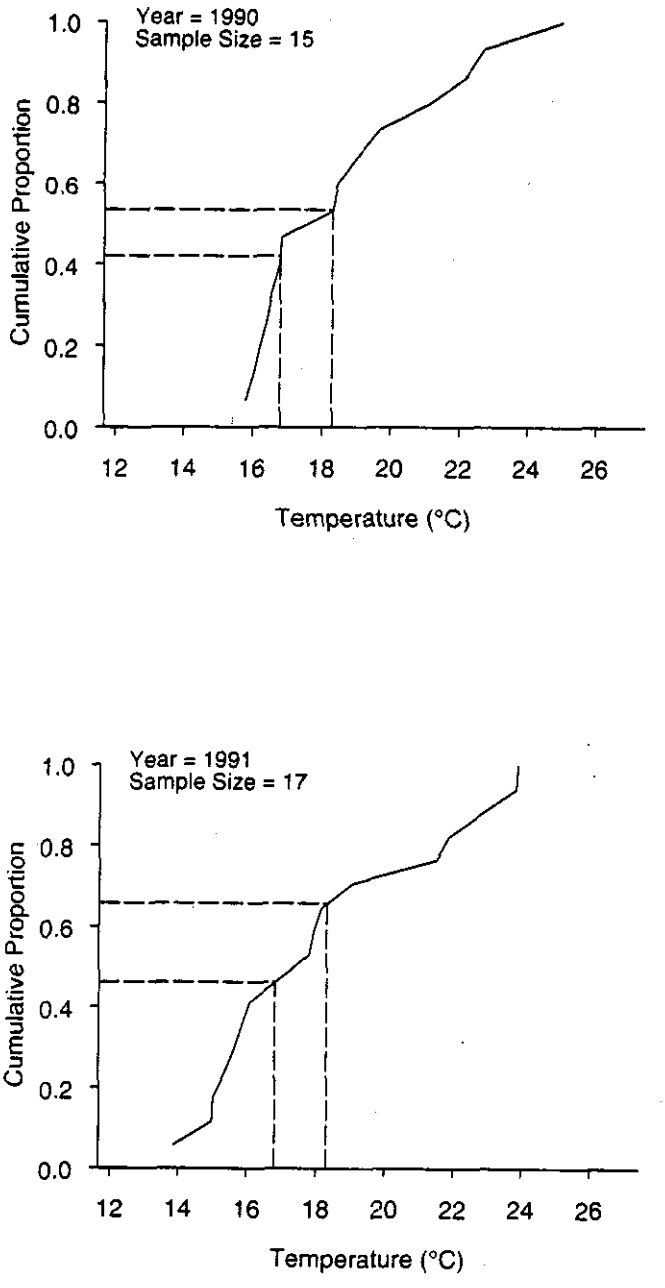

Figure B-1. 1990 and 1991 cumulative distribution of the highest 7-day moving average of the daily mean (XYA7DA) stream temperature. Vertical reference lines are drawn at 16.8°C and 18.3°C. Curves are based on 15 and 17 sites, respectively.

Table B-21. Mathematically Determined Cumulative Proportions for XYA7DA Above and Below Two Reference Temperature Values (16.8°C and 18.3°C) for 1992.

Year	Total Number of Sites[1]	Reference Value	Cumulative Proportion
1992	17	≤16.8	0.32699
		≥16.8	0.73184
		≤18.3	0.53611
		≥18.3	0.52271

[1]Total number of sites used in analyses after CDF filter procedure applied.

Table B-22. Mathematically Determined Cumulative Proportions for XYA7DA Above and Below Two Reference Temperature Values (16.8°C and 18.3°C) for 1993.

Year	Total Number of Sites[1]	Reference Value	Cumulative Proportion
1993	66	≤16.8	0.56591
		≥16.8	0.43856
		≤18.3	0.85902
		≥18.3	0.14545

[1]Total number of sites used in analyses after CDF filter procedure applied.

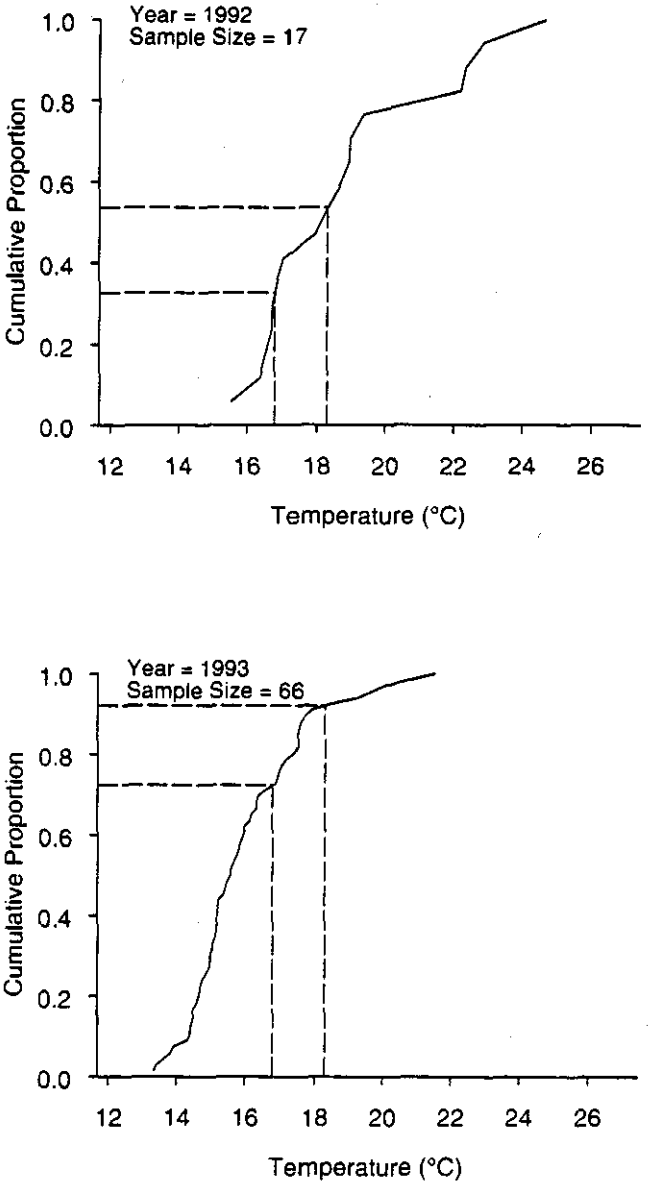

Figure B-2. 1992 and 1993 cumulative distribution of the highest 7-day moving average of the daily mean (XYA7DA) stream temperature. Vertical reference lines are drawn at 16.8°C and 18.3°C. Curves are based on 17 and 66 sites, respectively.

Table B-23. Mathematically Determined Cumulative Proportions for XYA7DA Above and Below Two Reference Temperature Values (16.8°C and 18.3°C) for 1994.

Year	Total Number of Sites[1]	Reference Value	Cumulative Proportion
1994	151	≤16.8	0.72667
		≥16.8	0.27678
		≤18.3	0.84705
		≥18.3	0.15940

[1]Total number of sites used in analyses after CDF filter procedure applied.

Table B-24. Mathematically Determined Cumulative Proportions for XYA7DA Above and Below Two Reference Temperature Values (16.8°C and 18.3°C) for 1995.

Year	Total Number of Sites[1]	Reference Value	Cumulative Proportion
1995	182	≤16.8	0.64670
		≥16.8	0.36096
		≤18.3	0.81629
		≥18.3	0.19137

[1]Total number of sites used in analyses after CDF filter procedure applied.

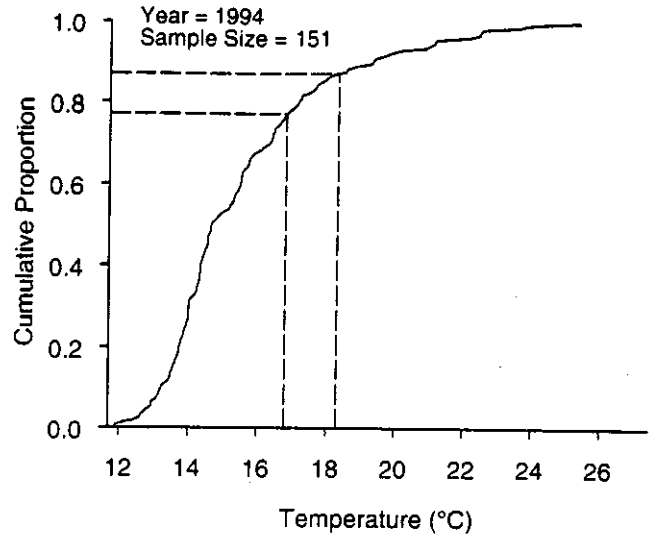

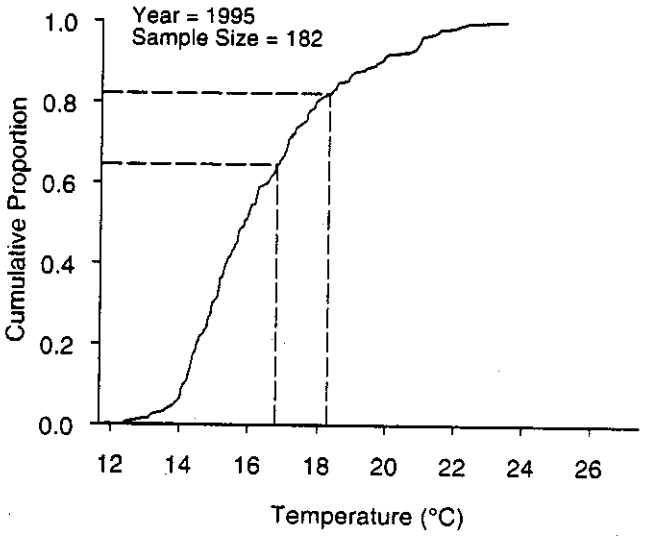

Figure B-3. 1994 and 1995 cumulative distribution of the highest 7-day moving average of the daily mean (XYA7DA) stream temperature. Vertical reference lines are drawn at 16.8°C and 18.3°C. Curves are based on 17 and 66 sites, respectively.

Table B-25. Mathematically Determined Cumulative Proportions for XYA7DA Above and Below Two Reference Temperature Values (16.8°C and 18.3°C) for 1996.

Year	Total Number of Sites[1]	Reference Value	Cumulative Proportion
1996	460	≤16.8	0.34837
		≥16.8	0.65374
		≤18.3	0.50265
		≥18.3	0.49985

[1]Total number of sites used in analyses after CDF filter procedure applied.

Table B-26. Mathematically Determined Cumulative Proportions for XYA7DA Above and Below Two Reference Temperature Values (16.8°C and 18.3°C) for 1997.

Year	Total Number of Sites[1]	Reference Value	Cumulative Proportion
1997	565	≤16.8	0.38858
		≥16.8	0.61336
		≤18.3	0.58241
		≥18.3	0.41953

[1]Total number of sites used in analyses after CDF filter procedure applied.

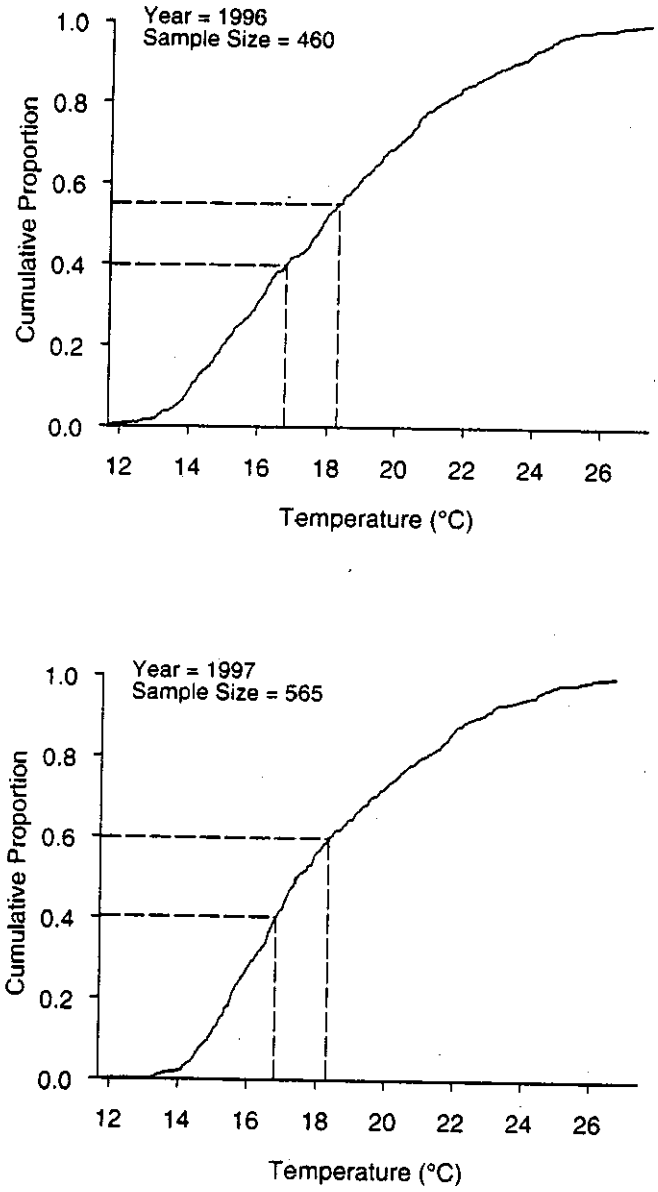

Figure B-4. 1996 and 1997 cumulative distribution of the highest 7-day moving average of the daily mean (XYA7DA) stream temperature. Vertical reference lines are drawn at 16.8°C and 18.3°C. Curves are based on 17 and 66 sites, respectively.

Table B-27. Mathematically Determined Cumulative Proportions for XYA7DA Above and Below Two Reference Temperature Values (16.8°C and 18.3°C) for 1998.

Year	Total Number of Sites[1]	Reference Value	Cumulative Proportion
1998	520	≤ 16.8	0.45982
		≥ 16.8	0.54230
		≤ 18.3	0.62824
		≥ 18.3	0.37374

[1]Total number of sites used in analyses after CDF filter procedure applied.

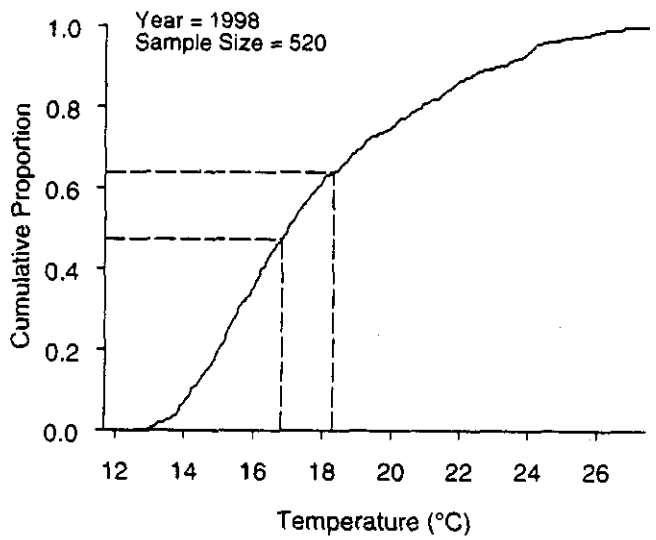

Figure B-5. 1998 cumulative distribution of the highest 7-day moving average of the daily mean (XYA7DA) stream temperature. Vertical reference lines are drawn at 16.8°C and 18.3°C. Curve is based on 520 sites.

Highest Seven-Day Moving Average of the Daily Maximum (XYA7DX)

Table B-28. Mathematically Determined Cumulative Proportions for the XYA7DX Above and Below Two Reference Temperature Values (16.8°C and 18.3°C) for 1990.

Year	Total Number of Sites[1]	Reference Value	Cumulative Proportion
1990	15	≤16.8	< 0.10
		≥16.8	> 0.90
		≤18.3	0.36193
		≥18.3	0.70474

[1]Total number of sites used in analyses after CDF filter procedure applied.

Table B-29. Mathematically Determined Cumulative Proportions for theXYA7DX Above and Below Two Reference Temperature Values (16.8°C and 18.3°C) for 1991.

Year	Total Number of Sites[1]	Reference Value	Cumulative Proportion
1991	17	≤16.8	0.23192
		≥16.8	0.82690
		≤18.3	0.36193
		≥18.3	0.63529

[1]Total number of sites used in analyses after CDF filter procedure applied.

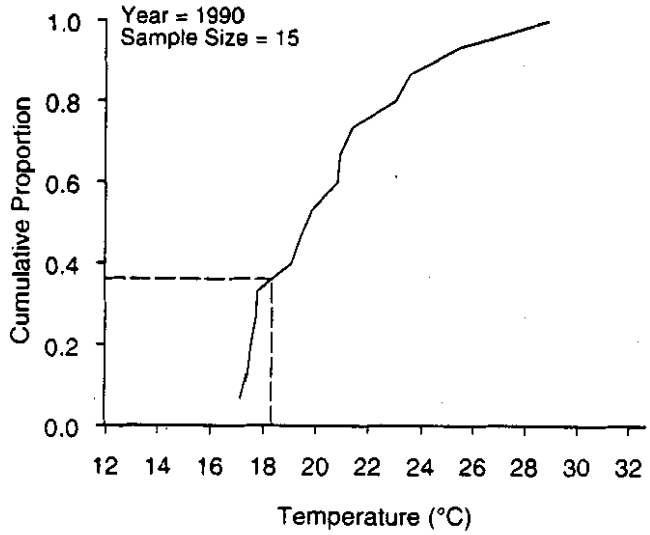

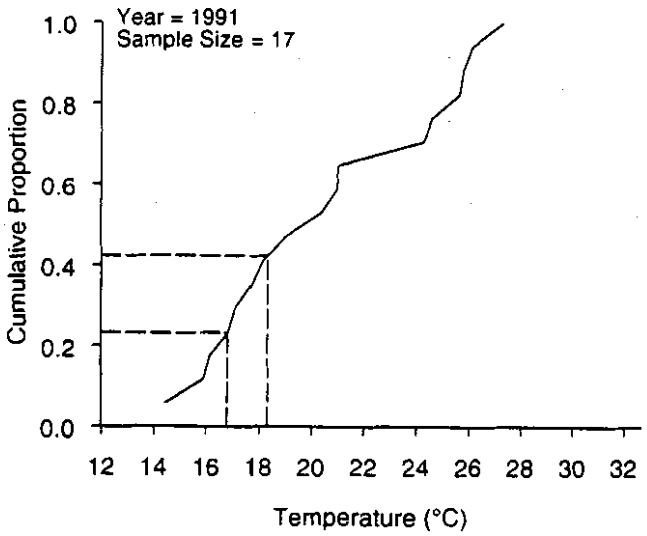

Figure B-6. 1990 and 1991 cumulative distribution of the highest seven-day moving average of the daily maximum (XYA7DX) stream temperature. Vertical reference lines are drawn at 16.8°C and 18.3°C. Curves are based on 15 and 17 sites, respectively.

Table B-30. Mathematically Determined Cumulative Proportions for the XYA7DX Above and Below Two Reference Temperature Values (16.8°C and 18.3°C) for 1992.

Year	Total Number of Sites[1]	Reference Value	Cumulative Proportion
1992	17	≤16.8	< 0.10
		≥16.8	>0.90
		≤18.3	0.31348
		≥18.3	0.74535

[1]Total number of sites used in analyses after CDF-filter procedure applied.

Table B-31. Mathematically Determined Cumulative Proportions for the XYA7DX Above and Below Two Reference Temperature Values (16.8°C and 18.3°C) for 1993.

Year	Total Number of Sites[1]	Reference Value	Cumulative Proportion
1993	66	≤16.8	0.32863
		≥16.8	0.67584
		≤18.3	0.55936
		≥18.3	0.44512

[1]Total number of sites used in analyses after CDF-filter procedure applied.

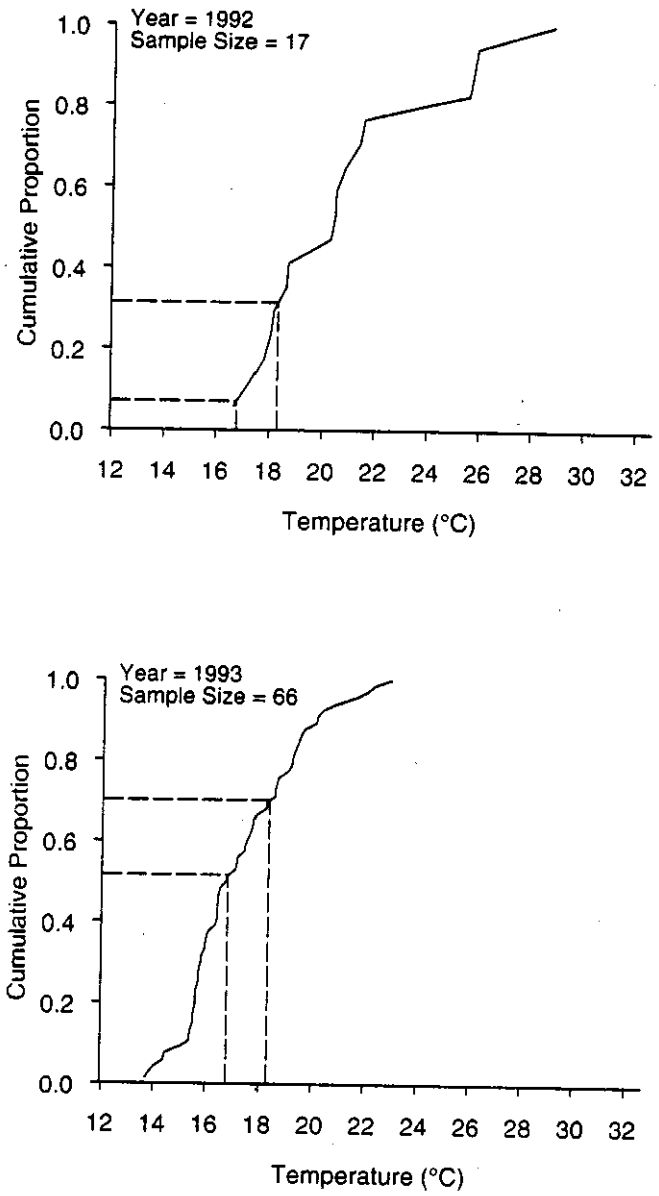

Figure B-7. 1992 and 1993 cumulative distribution of the highest seven-day moving average of the highest seven-day moving average of the daily maximum (XYA7DX) stream temperature. Vertical reference lines are drawn at 16.8°C and 18.3°C. Curves are based on 17 and 66 sites, respectively.

Table B-32. Mathematically Determined Cumulative Proportions for the XYA7DX Above and Below Two Reference Temperature Values (16.8°C and 18.3°C) for 1994.

Year	Total Number of Sites[1]	Reference Value	Cumulative Proportion
1994	151	≤ 16.8	0.55694
		≥ 16.8	0.44962
		≤ 18.3	0.69166
		≥ 18.3	0.31404

[1]Total number of sites used in analyses after CDF-filter procedure applied.

Table B-33. Mathematically Determined Cumulative Proportions for the XYA7DX Above and Below Two Reference Temperature Values (16.8°C and 18.3°C) for 1995.

Year	Total Number of Sites[1]	Reference Value	Cumulative Proportion
1995	182	≤ 16.8	0.41863
		≥ 16.8	0.58903
		≤ 18.3	0.58388
		≥ 18.3	0.42378

[1]Total number of sites used in analyses after CDF-filter procedure applied.

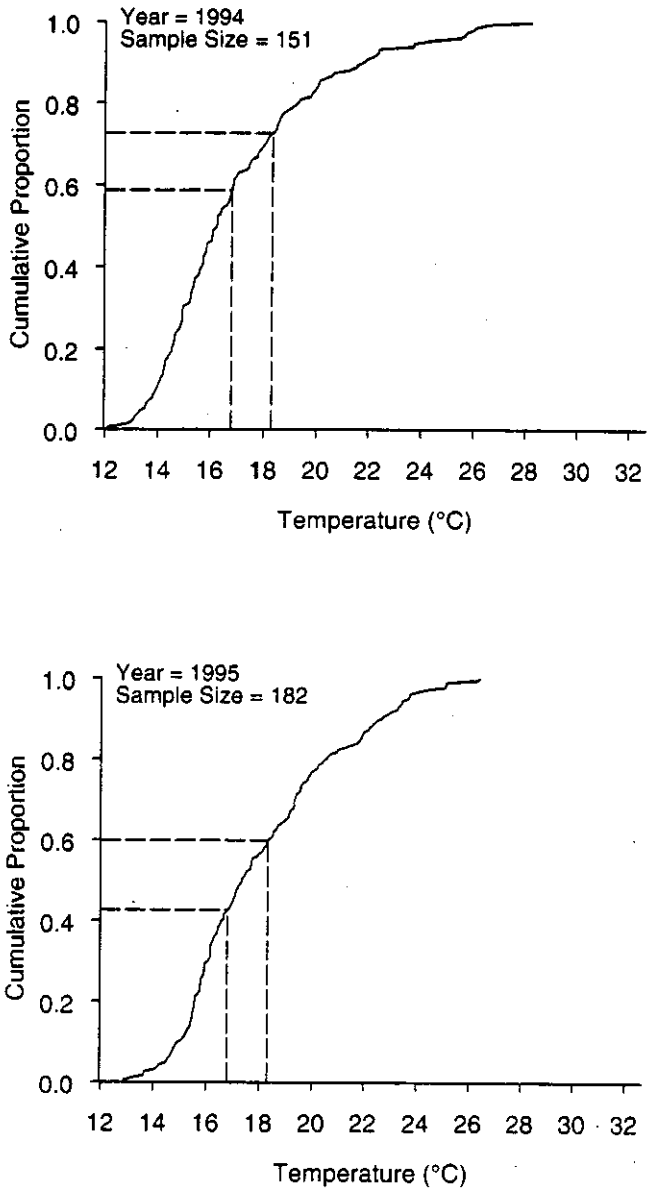

Figure B-8. 1994 and 1995 cumulative distribution of the highest seven-day moving average of the daily maximum (XYA7DX) stream temperature. Vertical reference lines are drawn at 16.8°C and 18.3°C. Curves are based on 151 and 182 sites, respectively.

Table B-34. Mathematically Determined Cumulative Proportions for the Highest Seven-Day Moving Average of the Daily Maximum Above and Below Two Reference Temperature Values (16.8°C and 18.3°C) for 1996.

Year	Total Number of Sites[1]	Reference Value	Cumulative Proportion
1996	460	≤16.8	0.22290
		≥16.8	0.77863
		≤18.3	0.32964
		≥18.3	0.67189

[1]Total number of sites used in analyses after CDF-filter procedure applied.

Table B-35. Mathematically Determined Cumulative Proportions for the Highest Seven-Day Moving Average of the Daily Maximum Above and Below Two Reference Temperature Values (16.8°C and 18.3°C) for 1997.

Year	Total Number of Sites[1]	Reference Value	Cumulative Proportion
1997	565	≤16.8	0.21962
		≥16.8	0.78174
		≤18.3	0.35456
		≥18.3	0.64860

[1]Total number of sites used in analyses after CDF-filter procedure applied.

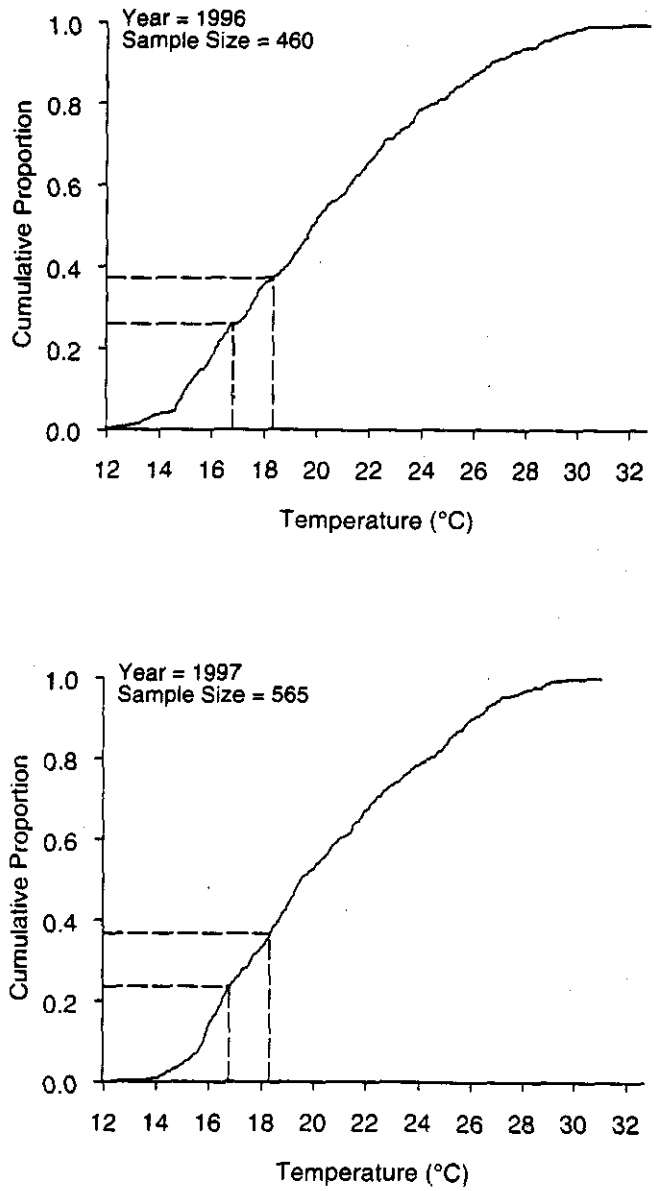

Figure B-9. 1996 and 1997 cumulative distribution of the highest seven-day moving average of the daily maximum (XYA7DX) stream temperature. Vertical reference lines are drawn at 16.8 °C and 18.3 °C. Curves are based on 460 and 565 sites, respectively.

Table B-36. Mathematically Determined Cumulative Proportions for the Highest Seven-Day Moving Average of the Daily Maximum Above and Below Two Reference Temperature Values (16.8°C and 18.3°C) for 1998.

Year	Total Number of Sites[1]	Reference Value	Cumulative Proportion
1998	520	≤ 16.8	0.27484
		≥ 16.8	0.72728
		≤ 18.3	0.42918
		≥ 18.3	0.57294

[1]Total number of sites used in analyses after CDF-filter procedure applied.

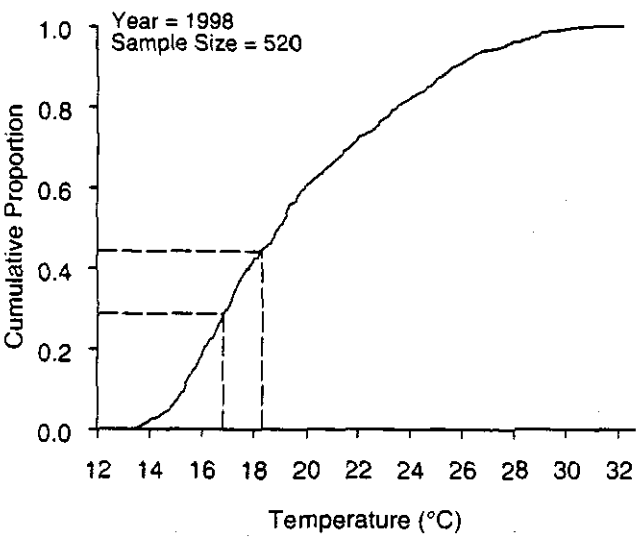

Figure B-10. 1998 cumulative distribution of the highest seven-day moving average of the daily maximum (XYA7DX) stream temperature. Vertical reference lines are drawn at 16.8°C and 18.3°C. Curve is based on 520 sites.

Highest Daily Maximum (XY1DX)

Table B-37. Mathematically Determined Cumulative Proportions for the XY1DX Above and Below Two Reference Temperature Values (24°C and 26°C) for 1990.

Year	Total Number of Sites[1]	Reference Value	Cumulative Proportion
1990	15	≤24.0	> 0.90
		≥24.0	0.20000
		≤26.0	> 0.90
		≥26.0	0.12914

[1]Total number of sites used in analyses after CDF-filter procedure applied.

Table B-38. Mathematically Determined Cumulative Proportions for the XY1DX Above and Below Two Reference Temperature Values (24°C and 26°C) for 1991.

Year	Total Number of Sites[1]	Reference Value	Cumulative Proportion
1991	17	≤24.0	0.68596
		≥24.0	0.37286
		≤26.0	0.79412
		≥26.0	0.26471

[1]Total number of sites used in analyses after CDF-filter procedure applied.

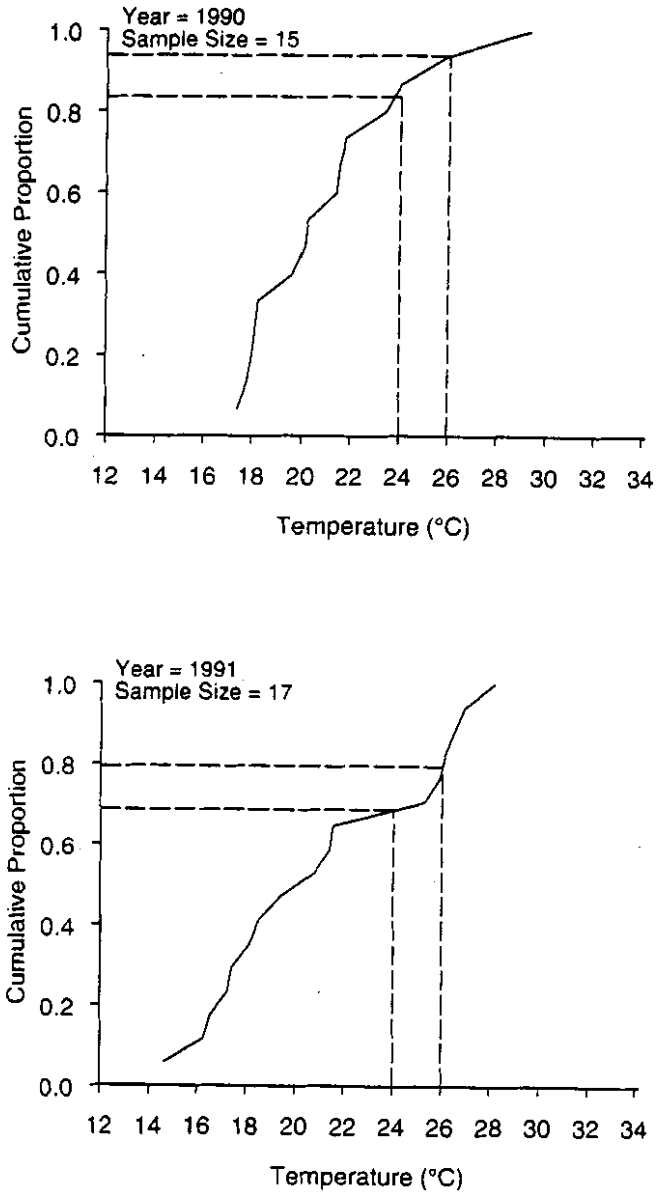

Figure B-11. 1990 and 1991 cumulative distribution of the highest daily maximum (XY1DX) stream temperature. Vertical reference lines are drawn at 24°C and 26°C. Curves are based on 15 and 17 sites, respectively.

Table B-39. Mathematically Determined Cumulative Proportions for the XY1DX Above and Below Two Reference Temperature Values (24°C and 26°C) for 1992.

Year	Total Number of Sites[1]	Reference Value	Cumulative Proportion
1992	17	≤24.0	0.79176
		≥24.0	0.26707
		≤26.0	0.82038
		≥26.0	0.23844

[1]Total number of sites used in analyses after CDF-filter procedure applied.

Table B-40. Mathematically Determined Cumulative Proportions for the XY1DX Above and Below Two Reference Temperature Values (24°C and 26°C) for 1993.

Year	Total Number of Sites[1]	Reference Value	Cumulative Proportion
1993	66	≤24.0	> 0.90
		≥24.0	< 0.10
		≤26.0	> 0.90
		≥26.0	< 0.10

[1]Total number of sites used in analyses after CDF-filter procedure applied.

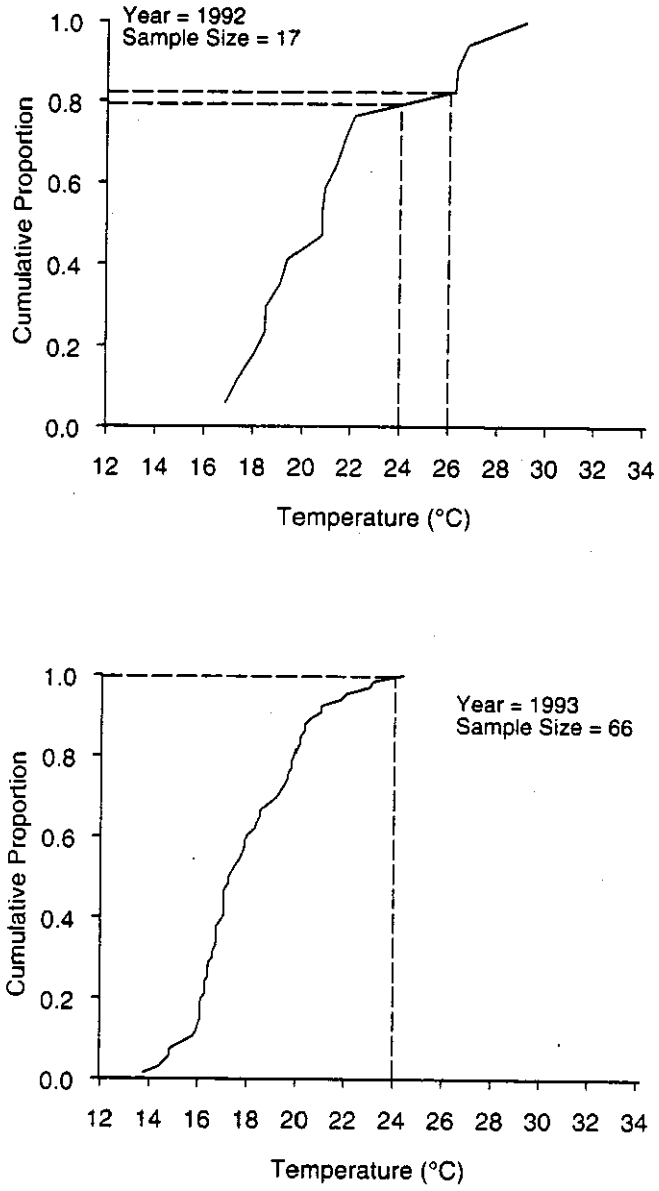

Figure B-12. 1992 and 1993 cumulative distribution of the highest daily maximum (XY1DX) stream temperature. Vertical reference lines are drawn at 24°C and 26°C. Curves are based on 17 and 66 sites, respectively.

Table B-41. Mathematically Determined Cumulative Proportions for the XY1DX Above and Below Two Reference Temperature Values (24°C and 26°C) for 1994.

Year	Total Number of Sites[1]	Reference Value	Cumulative Proportion
1994	151	≤24.0	> 0.90
		≥24.0	< 0.10
		≤26.0	> 0.90
		≥26.0	< 0.10

[1]Total number of sites used in analyses after CDF-filter procedure applied.

Table B-42. Mathematically Determined Cumulative Proportions for the XY1DX Above and Below Two Reference Temperature Values (24°C and 26°C) for 1995.

Year	Total Number of Sites[1]	Reference Value	Cumulative Proportion
1995	182	≤24.0	> 0.90
		≥24.0	< 0.10
		≤26.0	> 0.90
		≥26.0	< 0.10

[1]Total number of sites used in analyses after CDF-filter procedure applied.

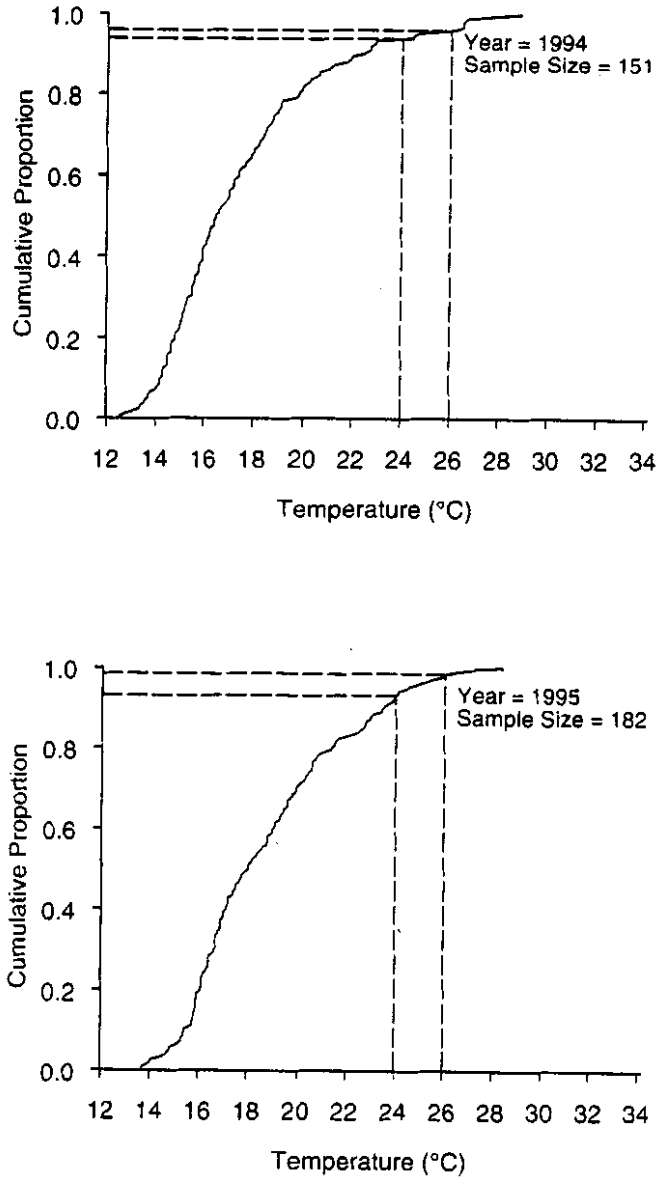

Figure B-13. 1994 and 1995 cumulative distribution of highest daily maximum (XY1DX) stream temperature. Vertical reference lines are drawn at 24°C and 26°C. Curves are based on 151 and 182 sites, respectively.

Table B-43. Mathematically Determined Cumulative Proportions for the XY1DX Above and Below Two Reference Temperature Values (24°C and 26°C) for 1996.

Year	Total Number of Sites[1]	Reference Value	Cumulative Proportion
1996	462	≤24.0	0.70623
		≥24.0	0.29732
		≤26.0	0.82577
		≥26.0	0.17672

[1]Total number of sites used in analyses after CDF-filter procedure applied.

Table B-44. Mathematically Determined Cumulative Proportions for the XY1DX Above and Below Two Reference Temperature Values (24°C and 26°C) for 1997.

Year	Total Number of Sites[1]	Reference Value	Cumulative Proportion
1997	566	≤24.0	0.74263
		≥24.0	0.25873
		≤26.0	0.84707
		≥26.0	0.15683

[1]Total number of sites used in analyses after CDF-filter procedure applied.

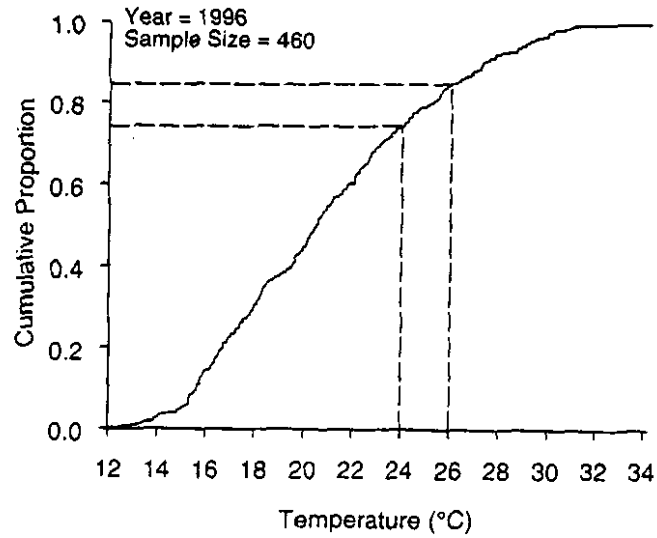

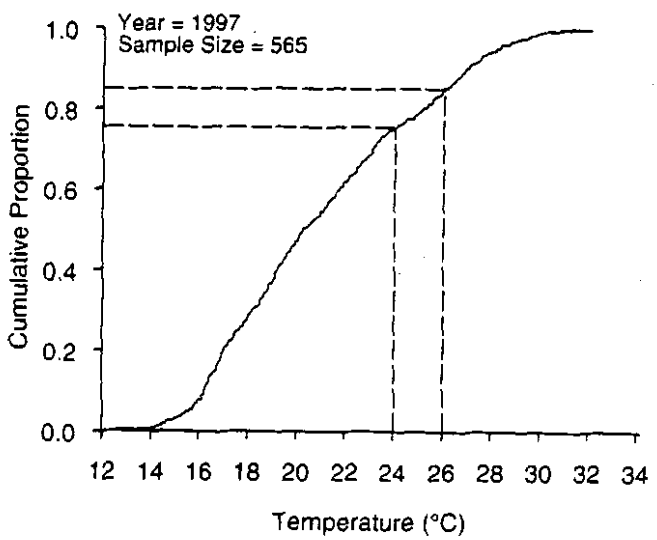

Figure B-14. 1996 and 1997 cumulative distribution of the highest daily maximum (XY1DX) stream temperature. Vertical reference lines are drawn at 24°C and 26°C. Curves are based on 460 and 565 sites, respectively.

Table B-45. Mathematically Determined Cumulative Proportions for the XY1DX Above and Below Two Reference Temperature Values (24°C and 26°C) for 1998.

Year	Total Number of Sites[1]	Reference Value	Cumulative Proportion
1998	15	≤24.0	0.77841
		≥24.0	0.22732
		≤26.0	0.87171
		≥26.0	0.12978

[1]Total number of sites used in analyses after CDF-filter procedure applied.

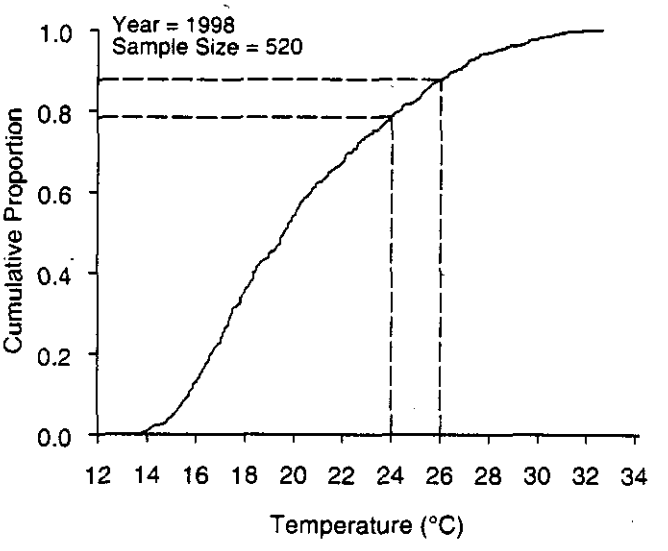

Figure B-15. 1998 cumulative distribution of the highest daily maximum (XY1DX) stream temperature. Vertical reference lines are drawn at 24°C and 26°C. Curve is based on 520 sites, respectively.

APPENDIX C

Air and Water Temperature Relationships

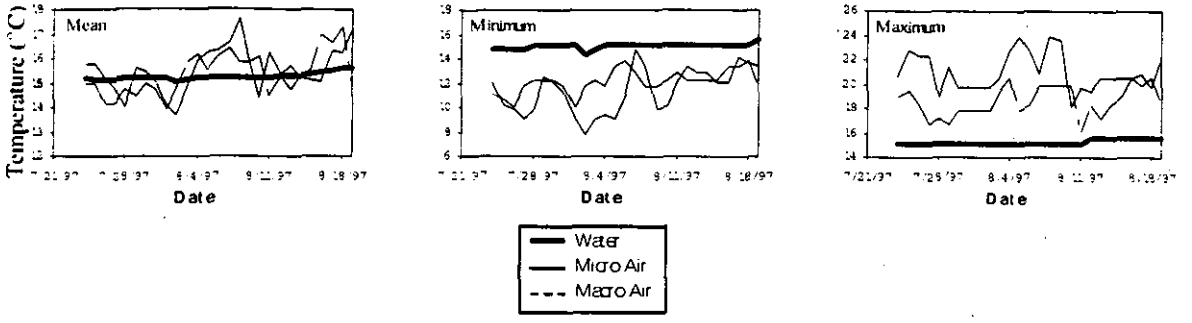

Figure C-1. Daily mean (left), minimum (middle), and maximum (right) temperatures for water and microair sites located on Hall Creek and at a macroair station located 17 km to the southwest.

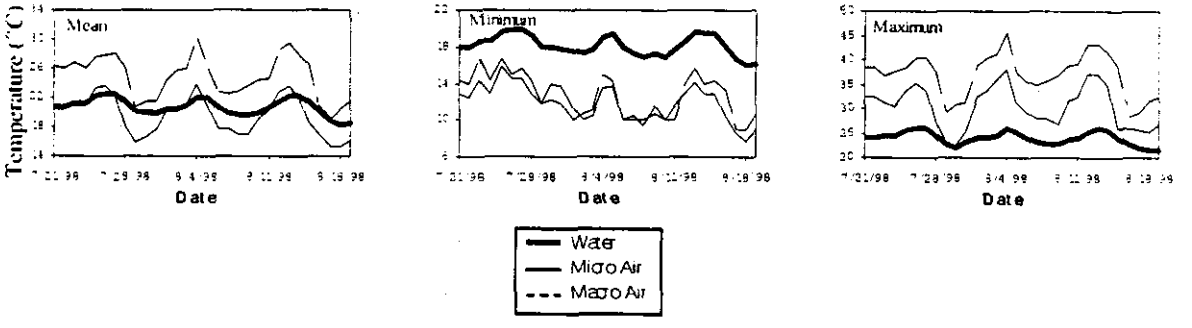

Figure C-2. Daily mean (left), minimum (middle), and maximum (right) temperatures for water and microair sites located on Redwood Creek above Lupton Creek and a macroair station located 16 km to east.

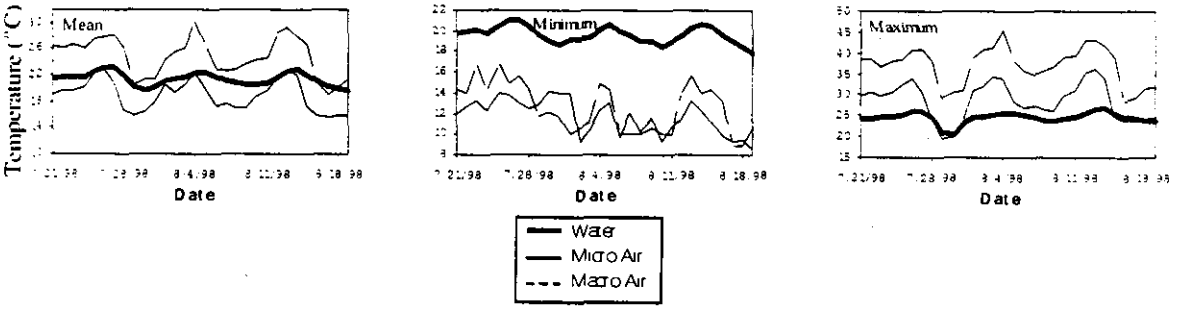

Figure C-3. Daily mean (left), minimum (middle), and maximum (right) temperatures for water and microair sites located on Redwood Creek above Lacks Creek and a macroair station located 24 km to southeast.

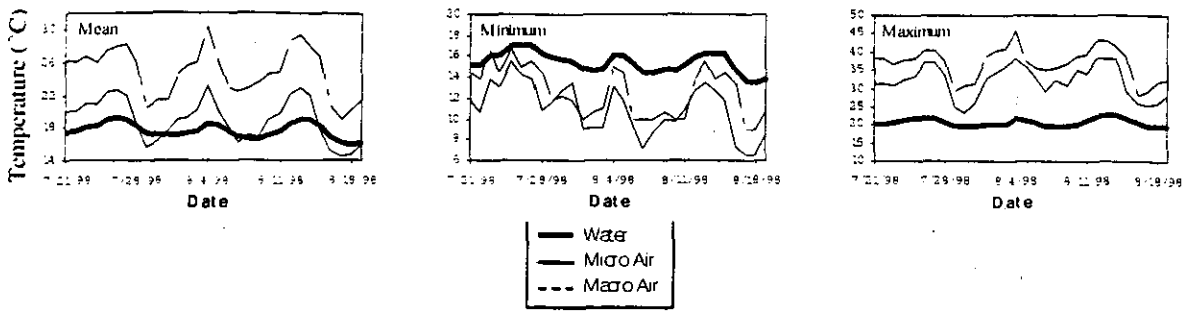

Figure C-4. Daily mean (left), minimum (middle), and maximum (right) temperatures for water and microair sites located on Minor Creek and a macroair station located 17 km to east.

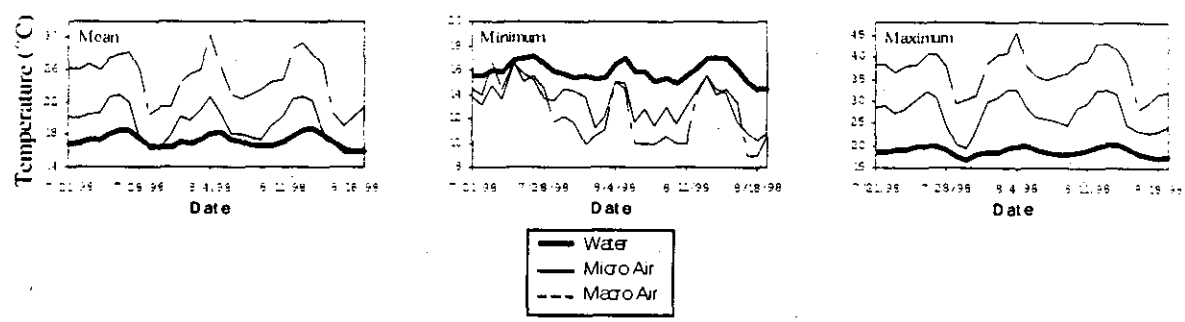

Figure C-5. Daily mean (left), minimum (middle), and maximum (right) temperatures for water and microair sites located on Minor Creek, a tributary to Redwood Creek, and a macroair station located 17 km to east.

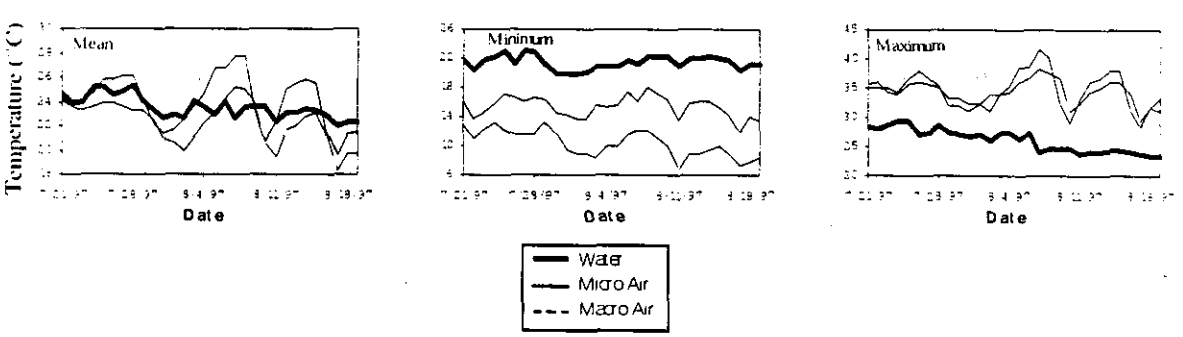

Figure C-6. Daily mean (left), minimum (middle), and maximum (right) temperatures for water and micro- air sites located on Eel River below Corbet Creek and a macroair station located 15 km to the southeast.

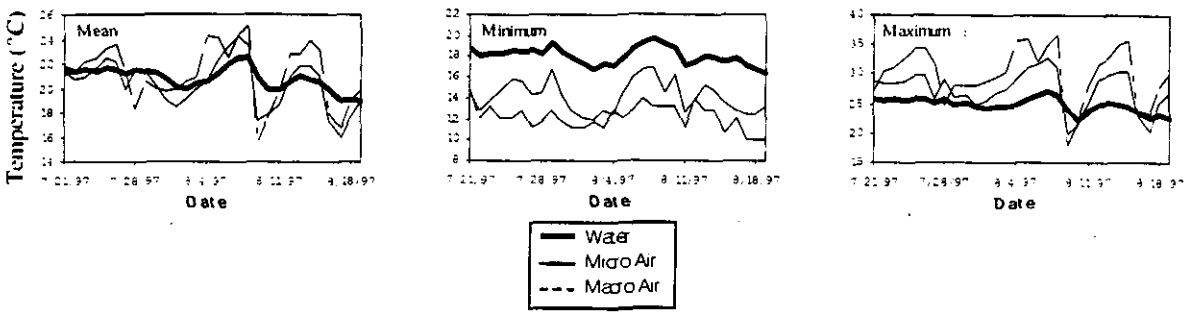

Figure C-7. Daily mean (left), minimum (middle), and maximum (right) temperatures for water and micro- air sites located on Rattlesnake Creek, a tributary of the South Fork Eel River, and a macro- air station located 26 km to northeast.

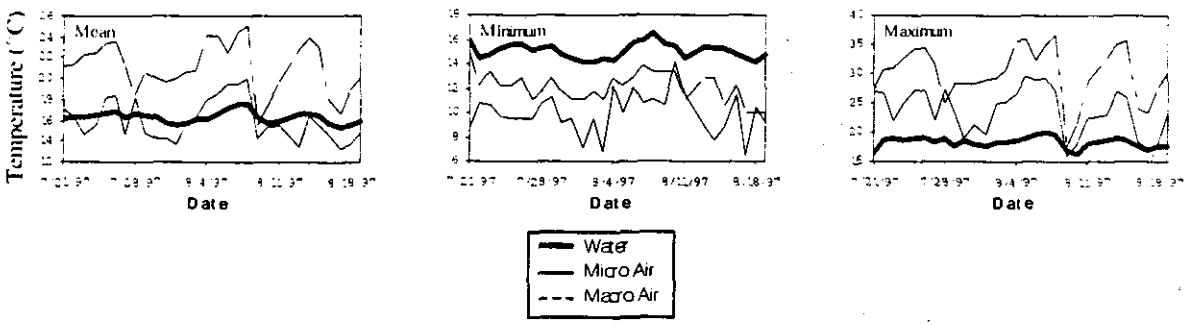

Figure C-8. Daily mean (left), minimum (middle), and maximum (right) temperatures for water and micro- air sites located on Cedar Creek, a tributary of the South Fork Eel River, and a macro air station located 18 km to northeast.

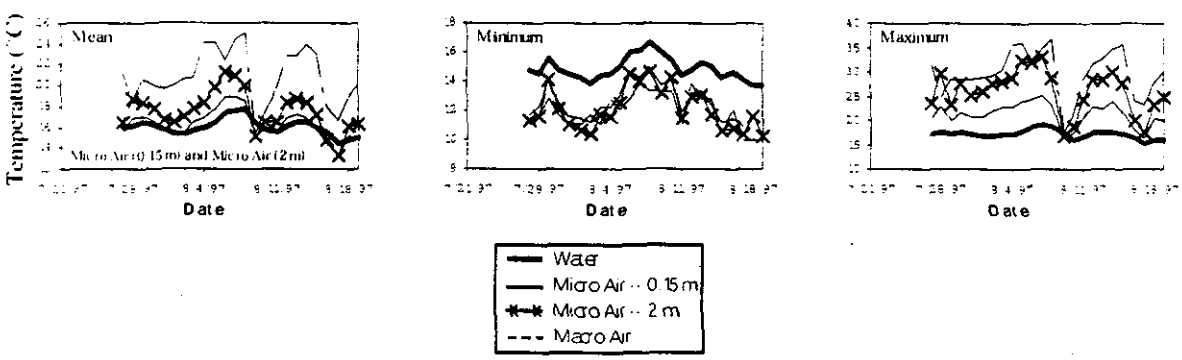

Figure C-9. Daily mean (left), minimum (middle), and maximum (right) temperatures for water and micro- air sites located on Rock Creek, a tributary of the South Fork Eel River, and a macroair station located 17 km to north. Note that this site had two microair temperatures recorded at this location.

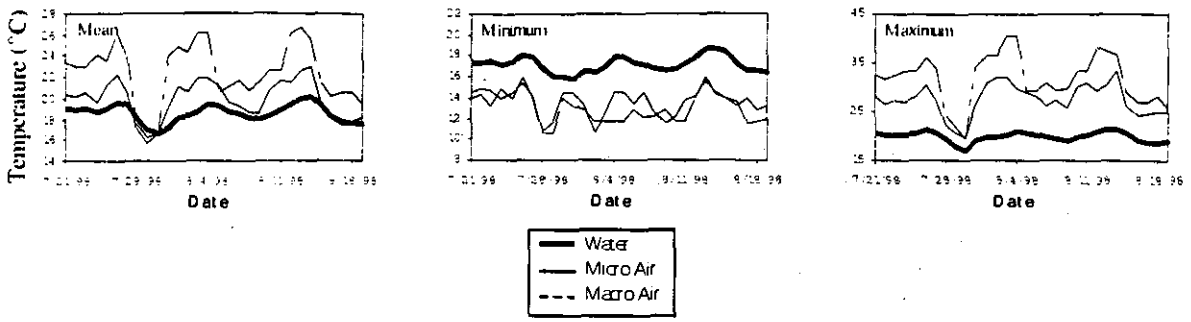

Figure C-10. Daily mean (left), minimum (middle), and maximum (right) temperatures for water and micro- air sites located on Sprowl Creek, a tributary of the South Fork Eel River, and a macro air station located 6 km to southeast.

APPENDIX D

Stream Temperature and Watershed Position

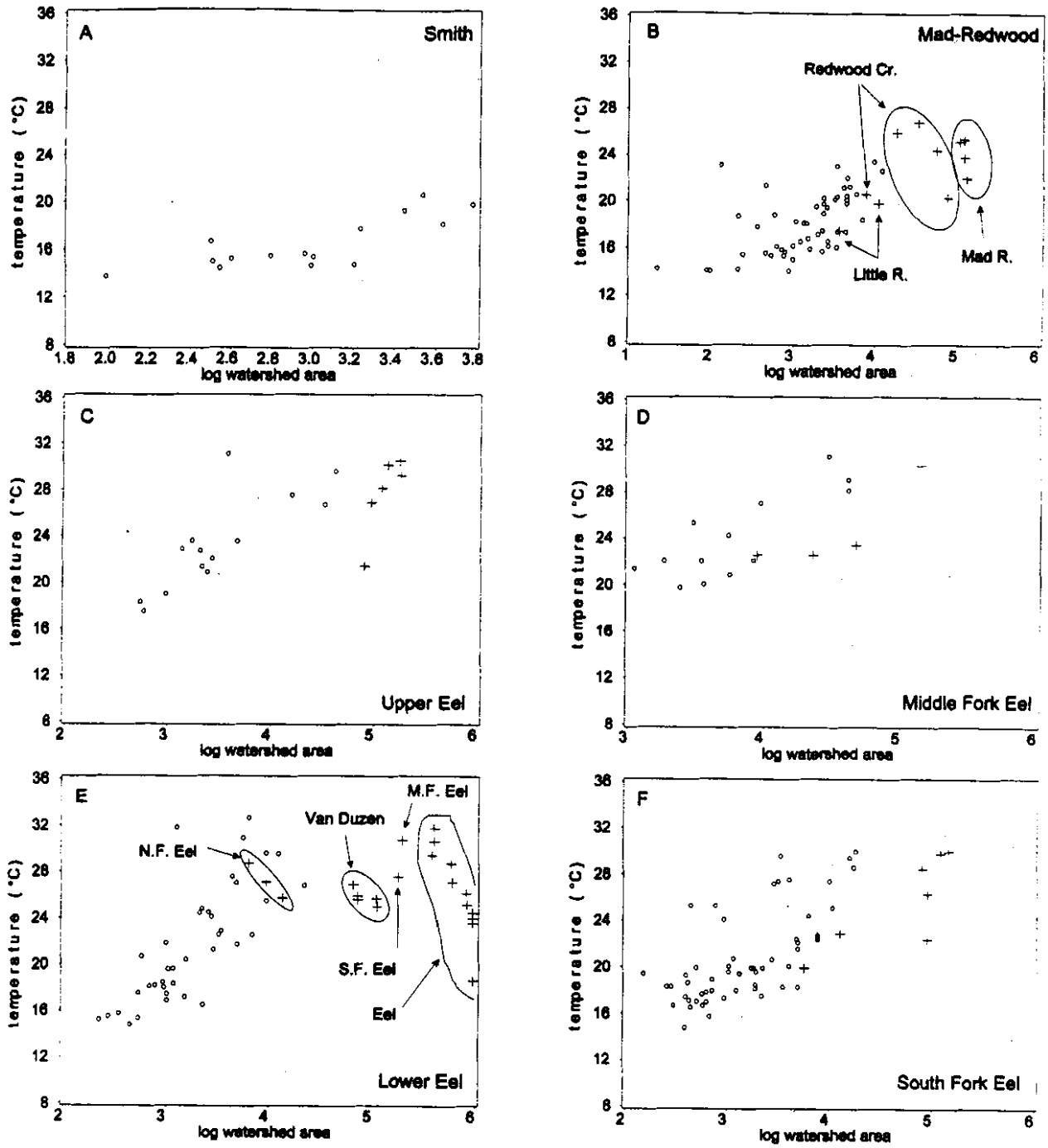

Figure D-1. The highest 1998 daily maximum stream temperature (XY1DX) versus $\log_{10}$ watershed area for HUCs comprising the range of the coho salmon in Northern California. Circles represent tributaries and crosses represent mainstems.

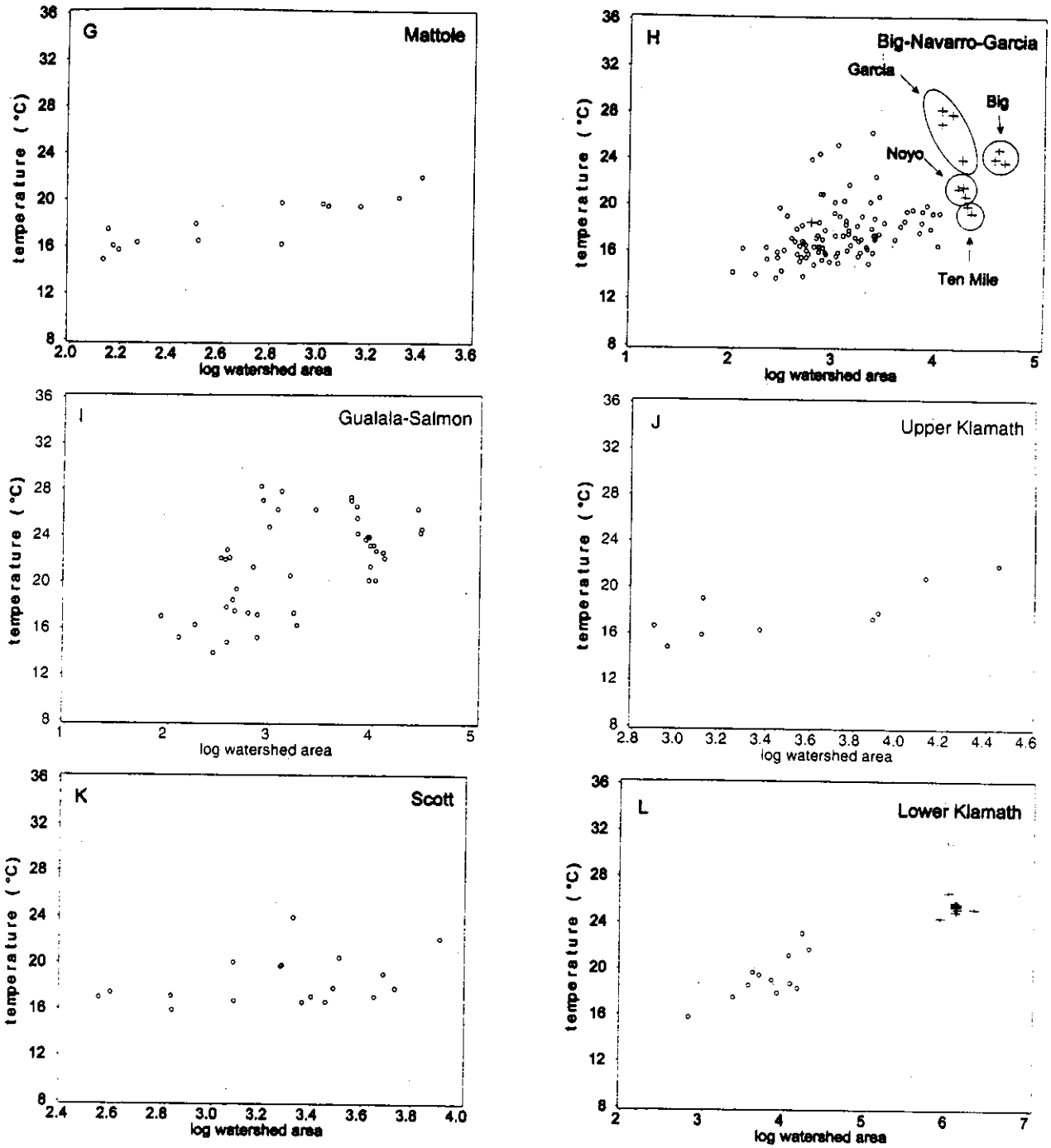

Figure D-1. (continued)

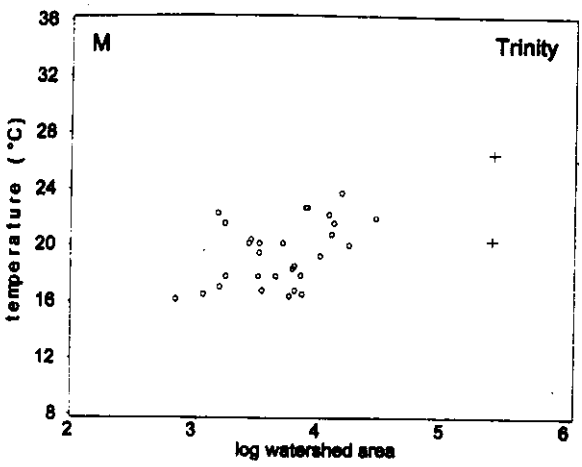

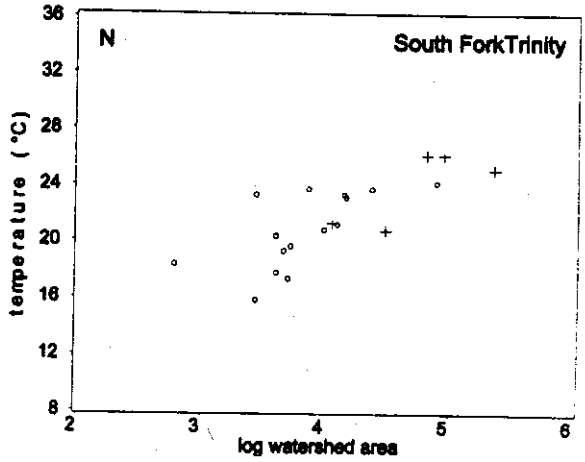

Figure D-1. (continued)

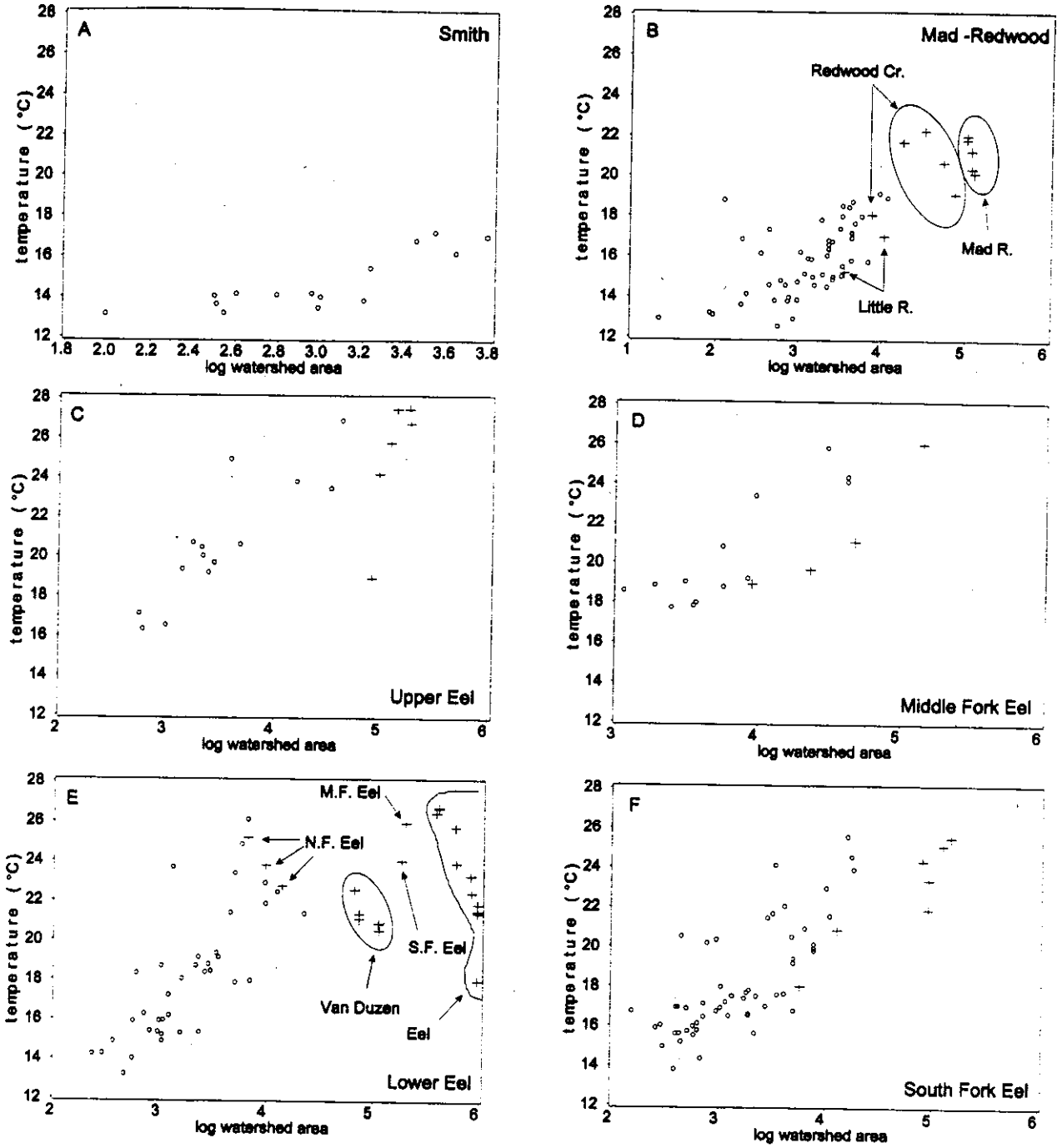

Figure D-2. The highest 1998 seven-day moving average of the daily average stream temperature (XYA7DA) versus $\log_{10}$ watershed area for HUCs comprising the range of the coho salmon in Northern California. Circles represent tributaries and crosses represent mainstems.

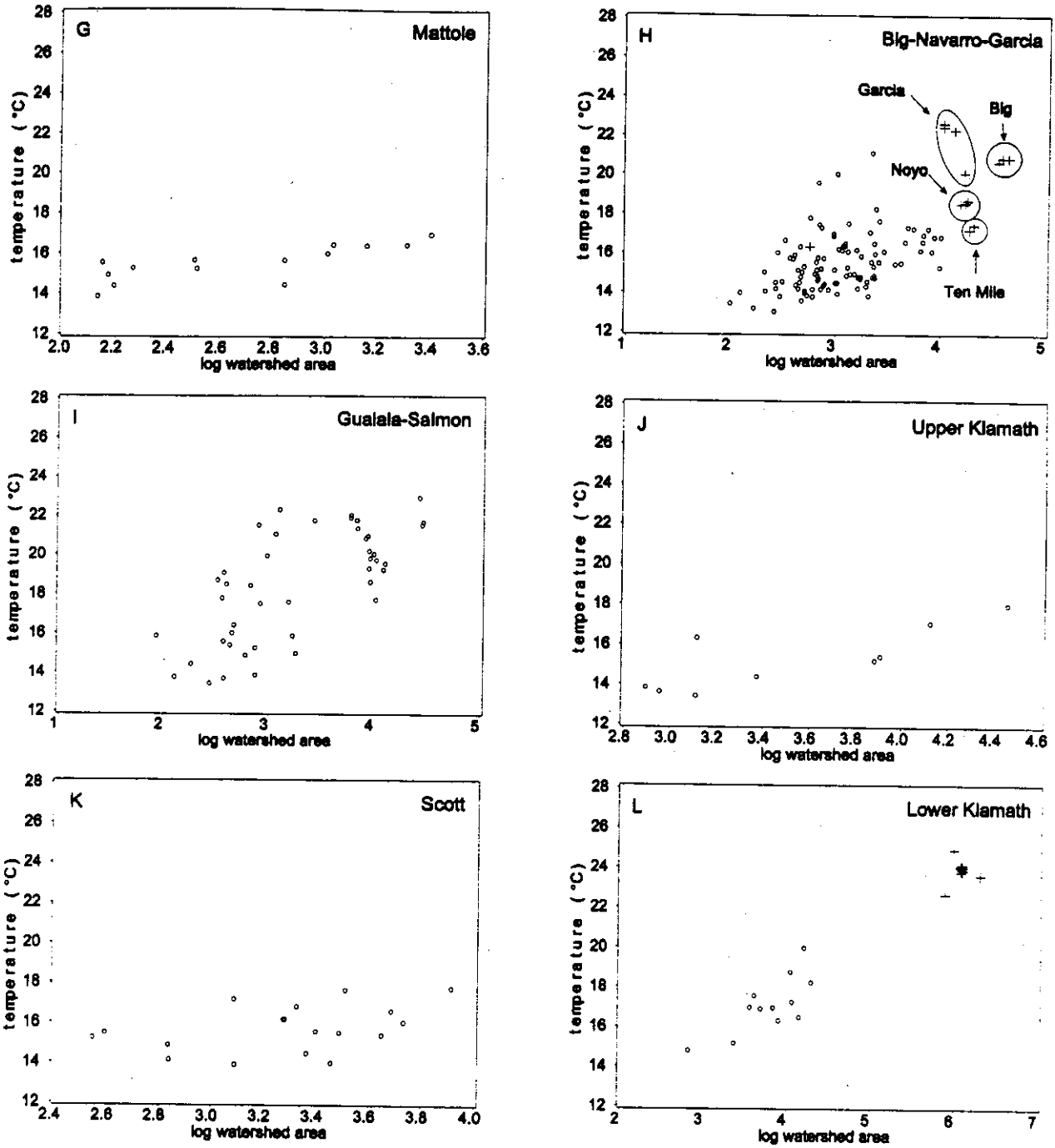

Figure D-2. (continued)

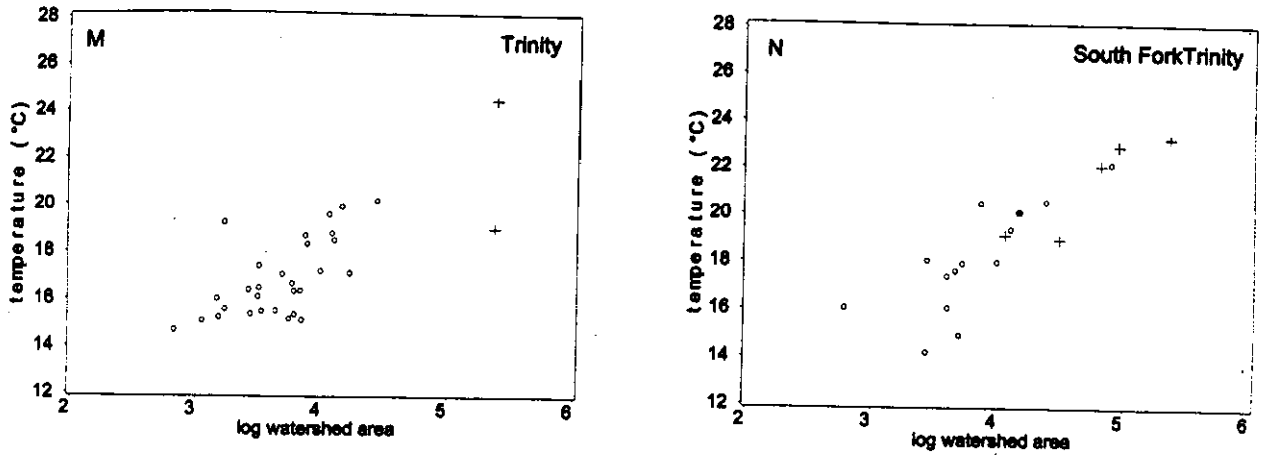

Figure D-2. (continued)

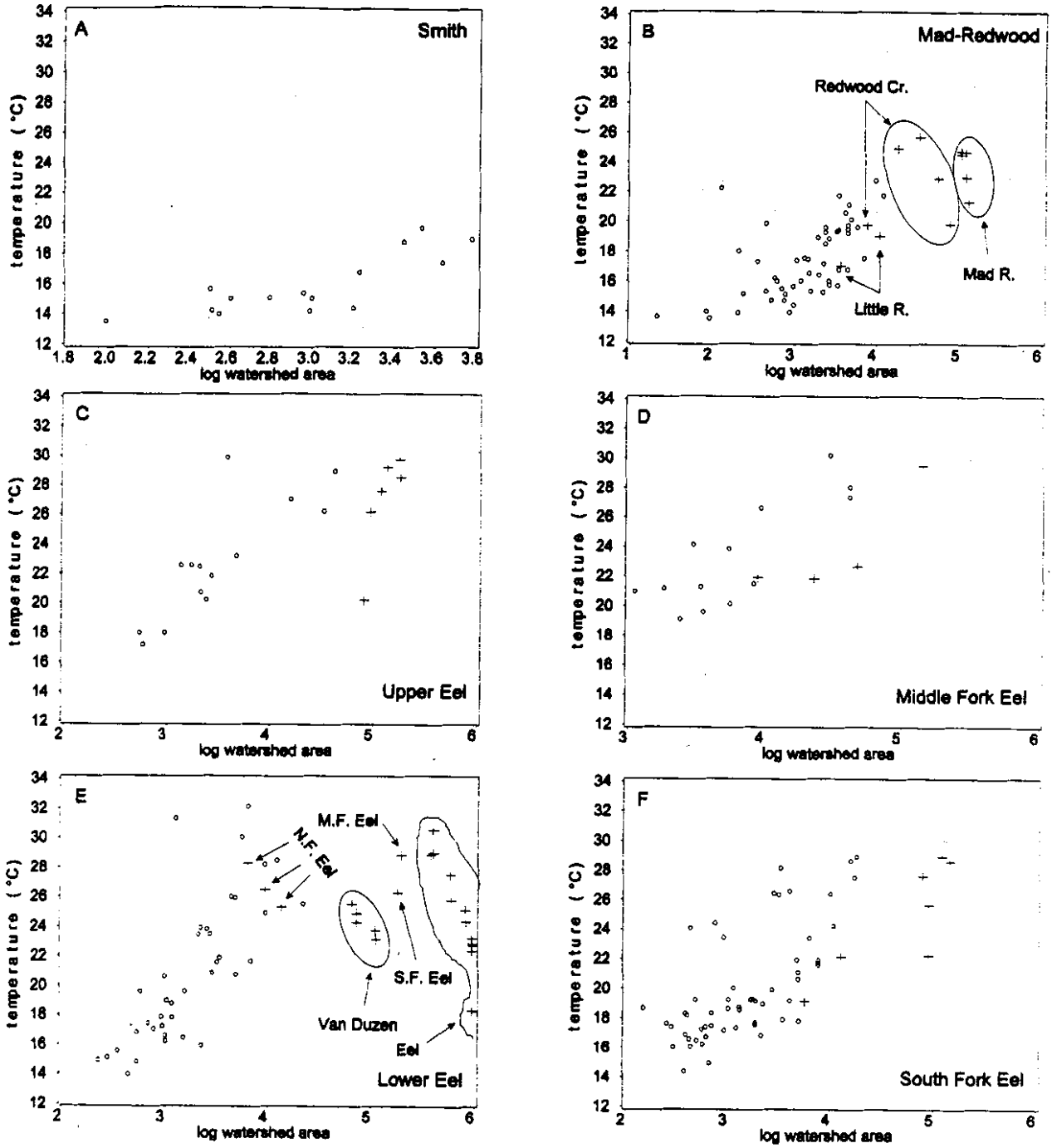

Figure D-3. The highest 1998 seven-day moving average of the daily maximum stream temperature (XYA7DX) versus $\log_{10}$ watershed area for HUCs comprising the range of the coho salmon in Northern California. Circles represent tributaries and crosses represent mainstems.

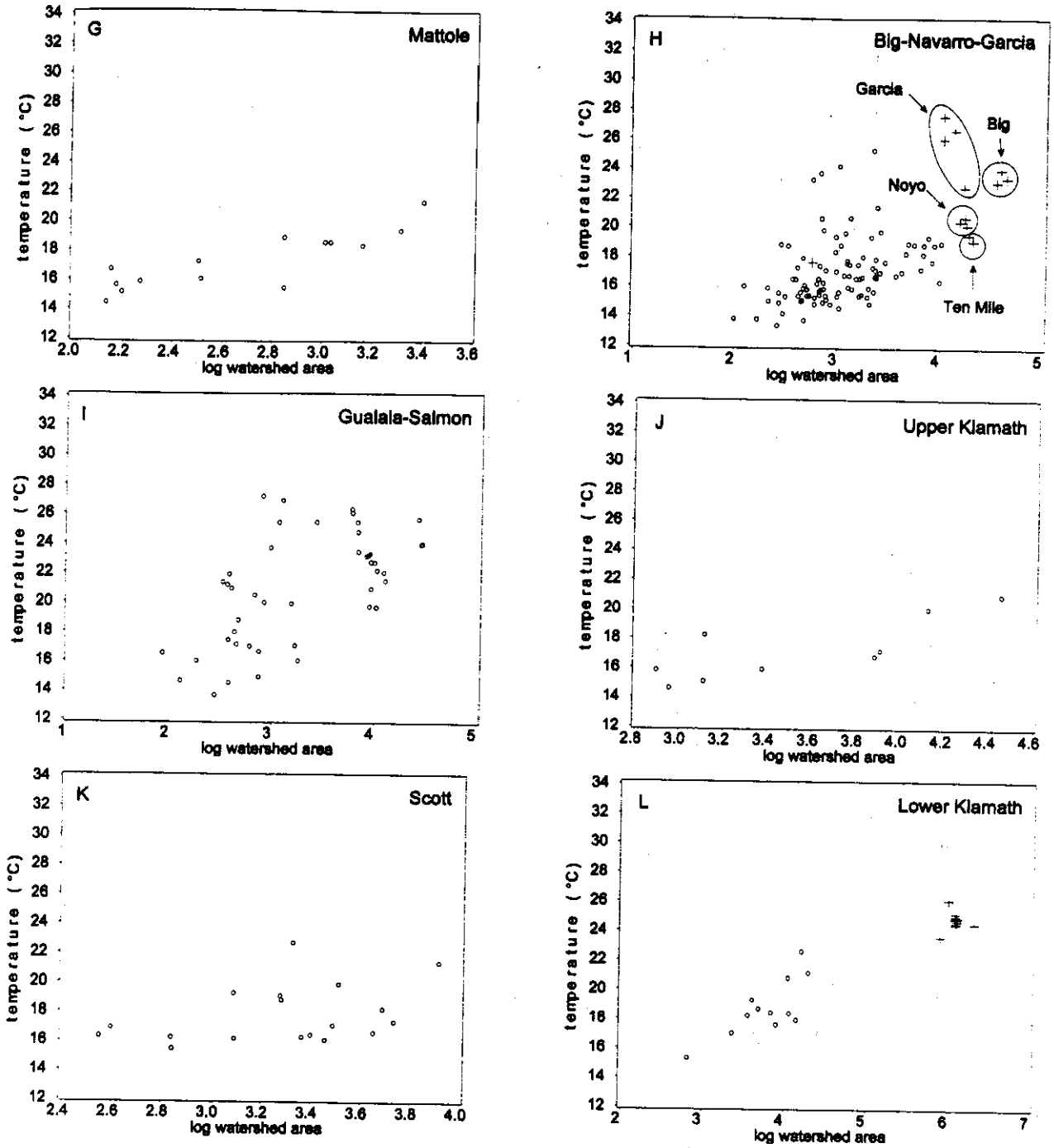

Figure D-3. (continued)

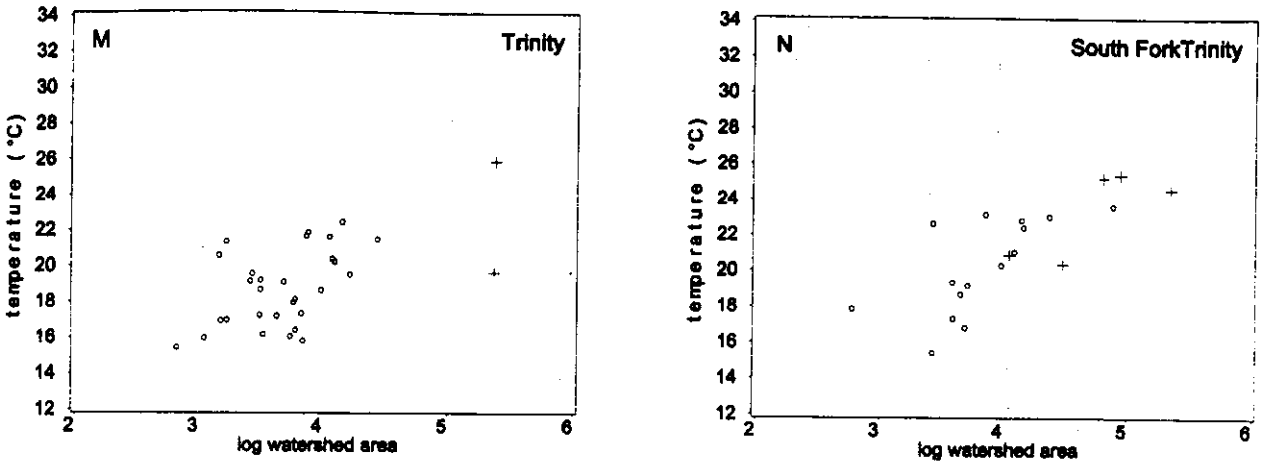

Figure D-3. (continued)

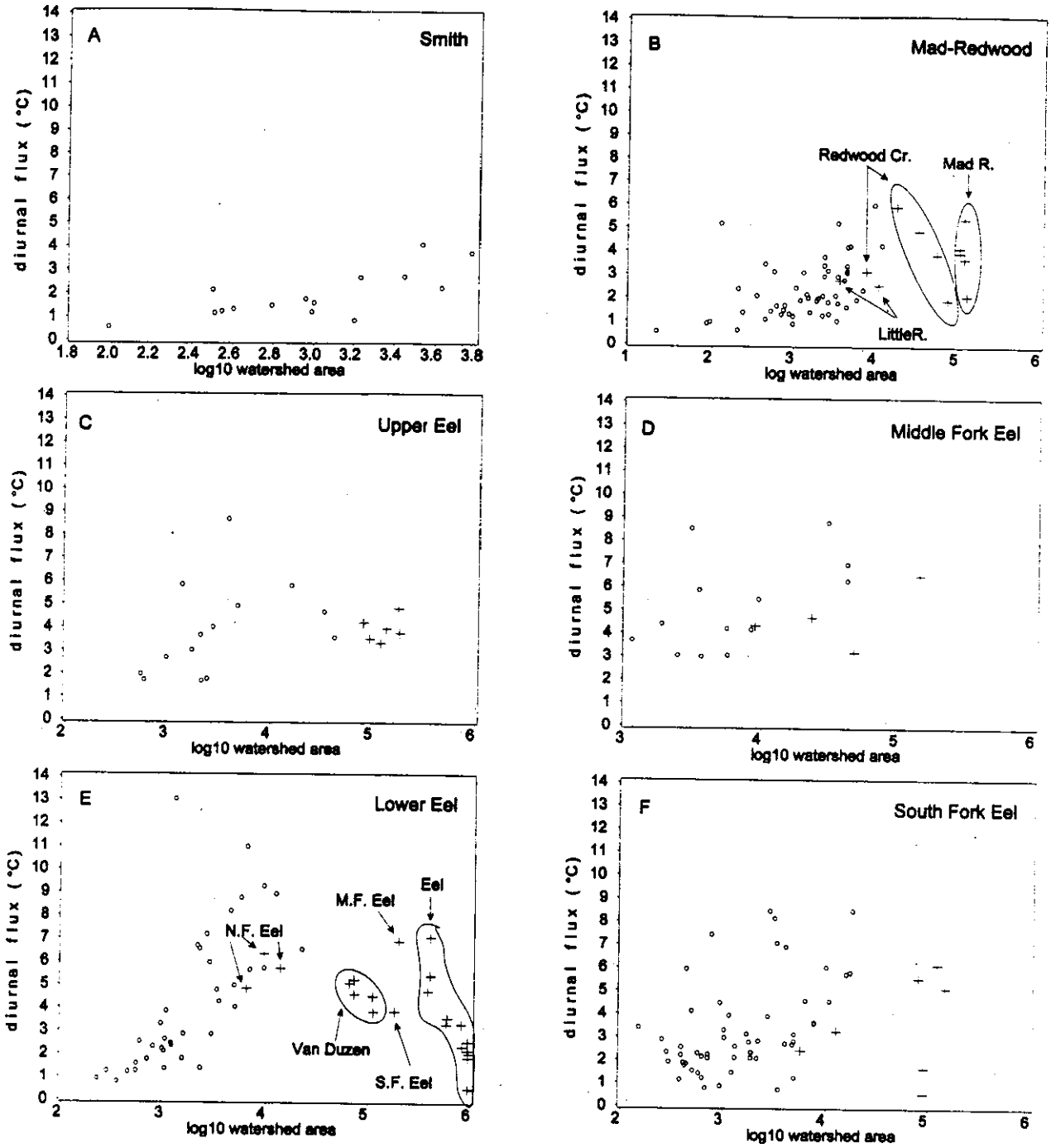

Figure D-4. The average 1998 diurnal stream temperature (AFLUX) versus $\log_{10}$ watershed area for HUCs comprising the range of the coho salmon in Northern California. Circles represent tributaries and crosses represent mainstems.

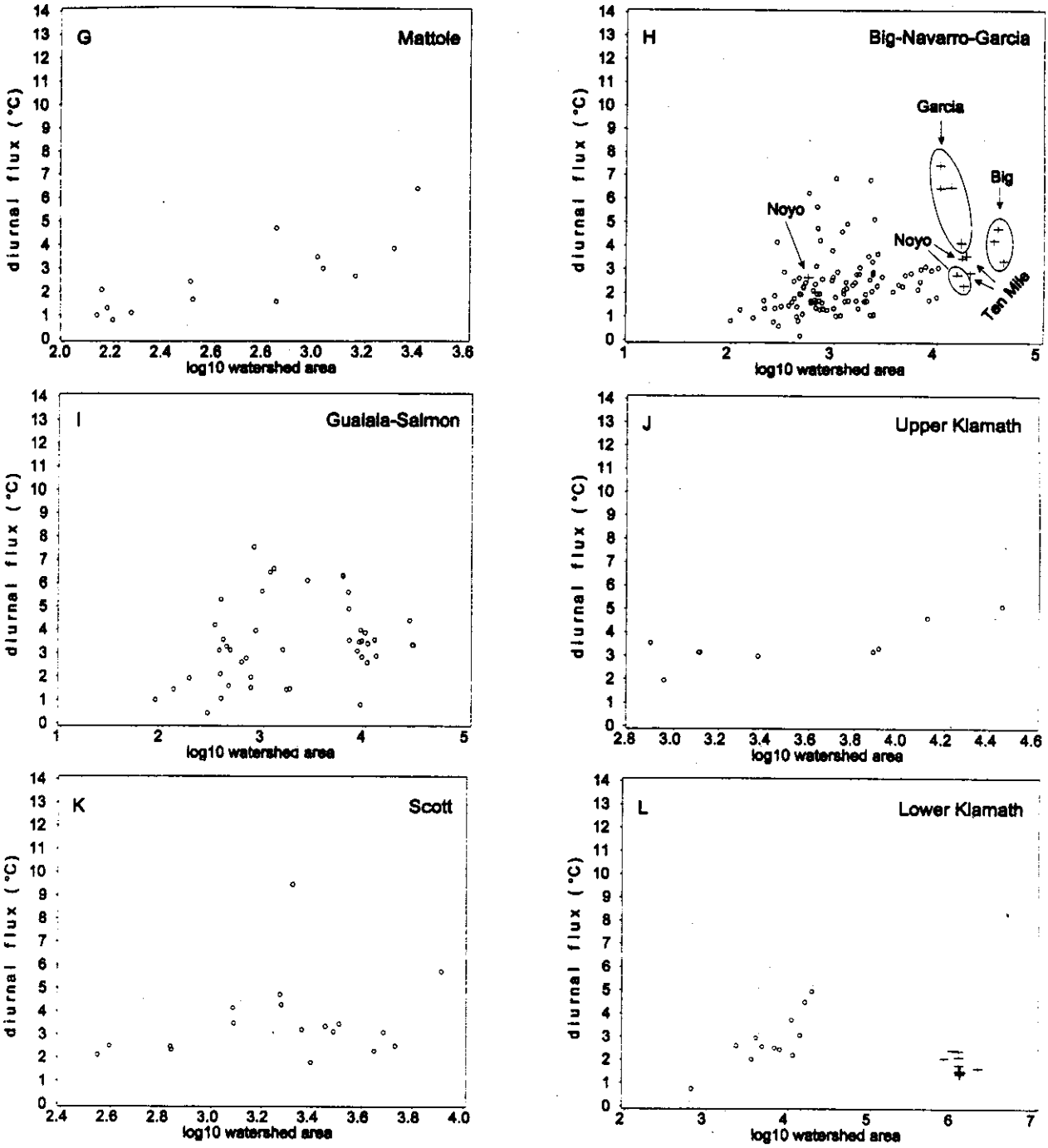

Figure D-4. (continued)

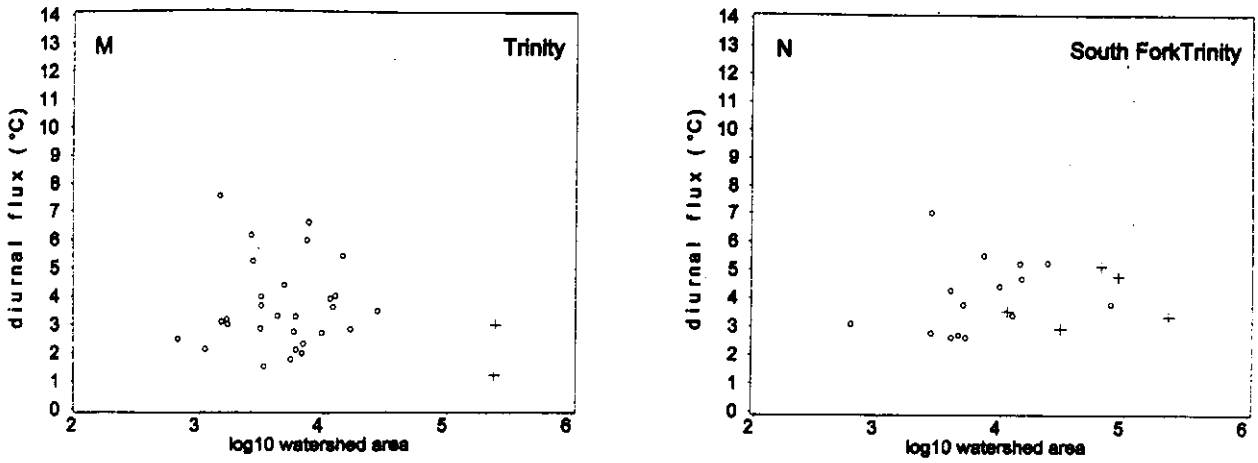

Figure D-4. (continued)

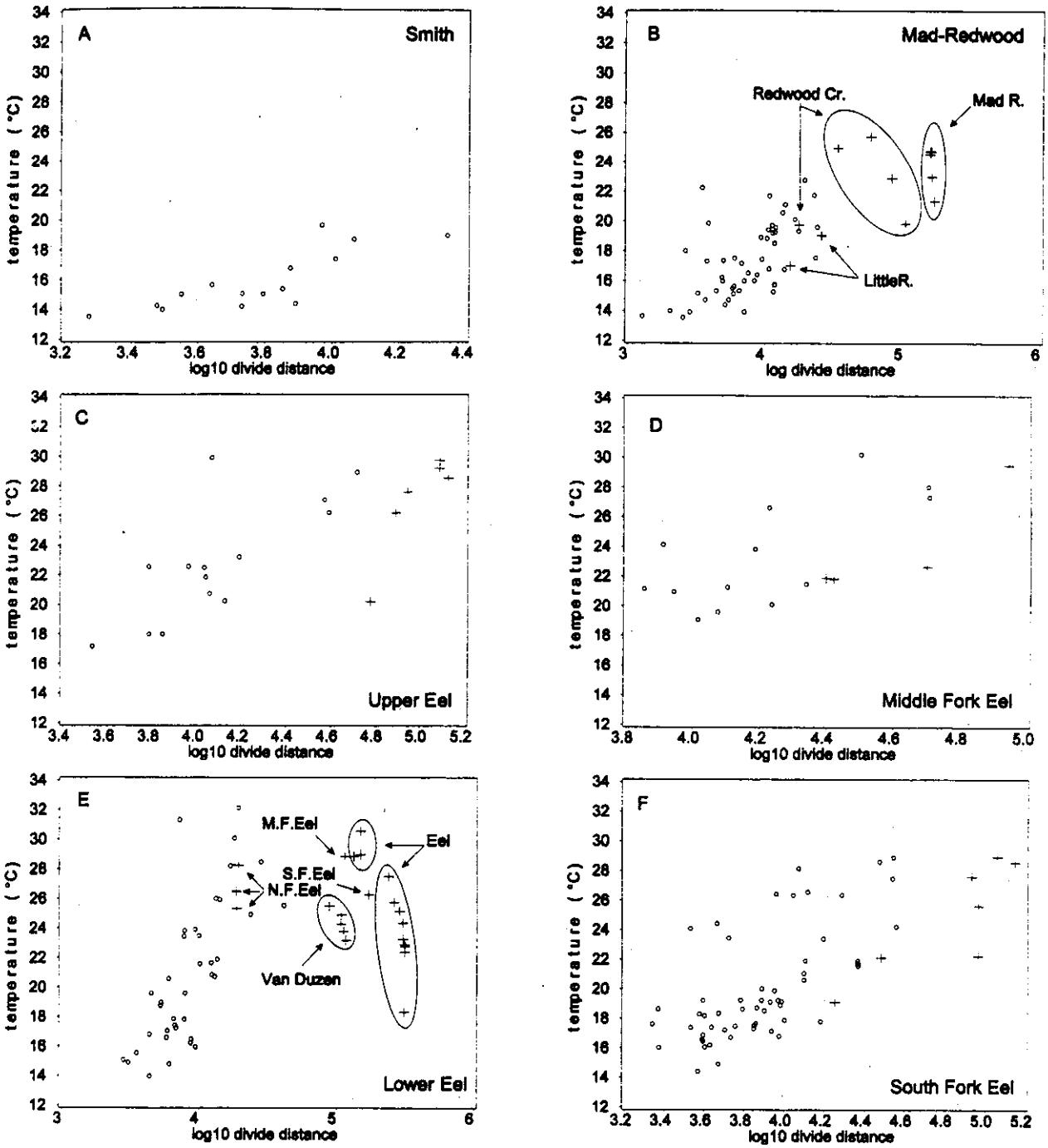

Figure D-5. The highest 1998 seven-day moving average of the daily maximum stream temperature (XYA7DX) versus $\log_{10}$ distance from watershed divide (meters) for HUCs comprising the range of the coho salmon in Northern California. Circles represent tributaries and crosses represent mainstems.

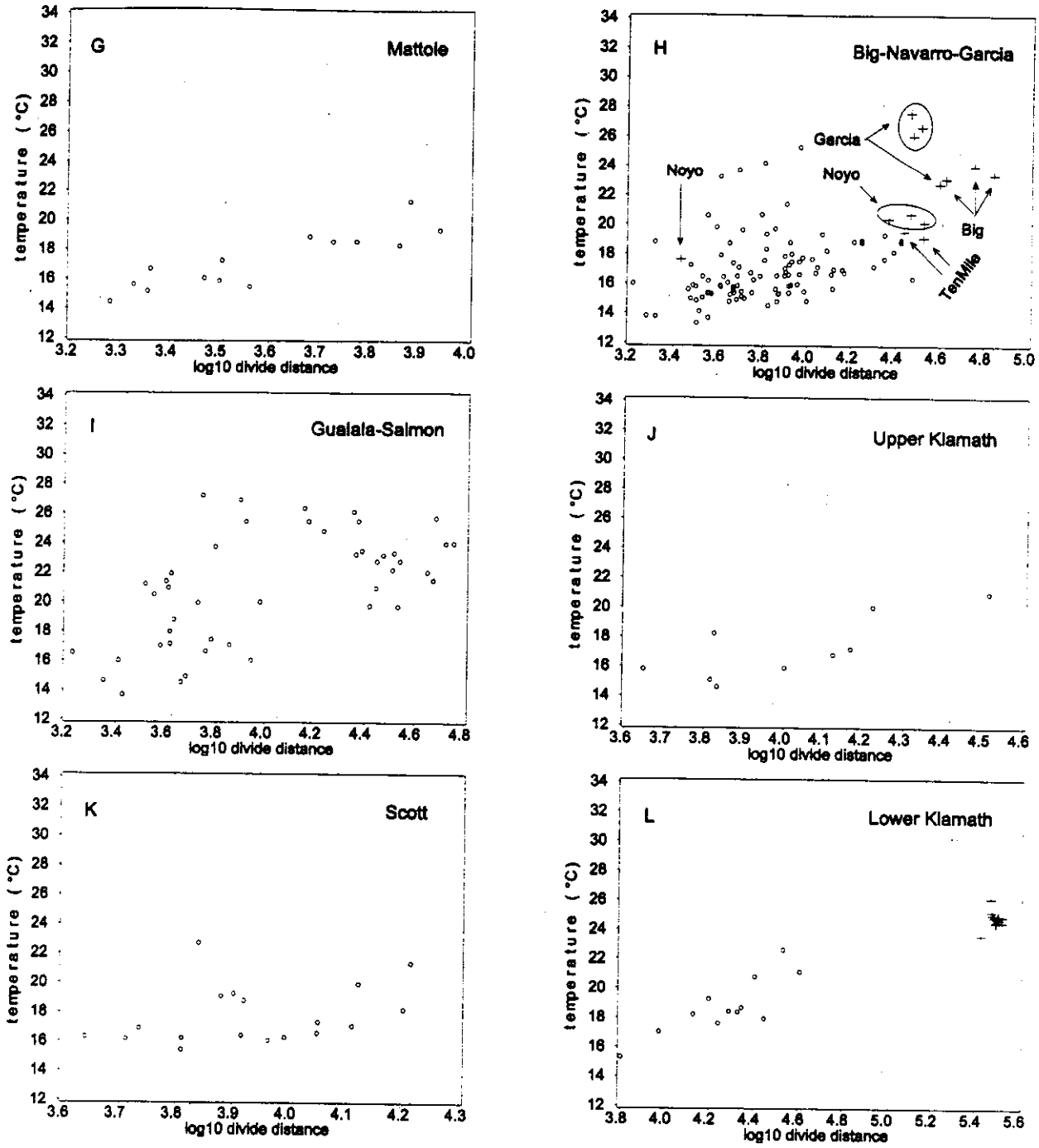

Figure D-5. (continued)

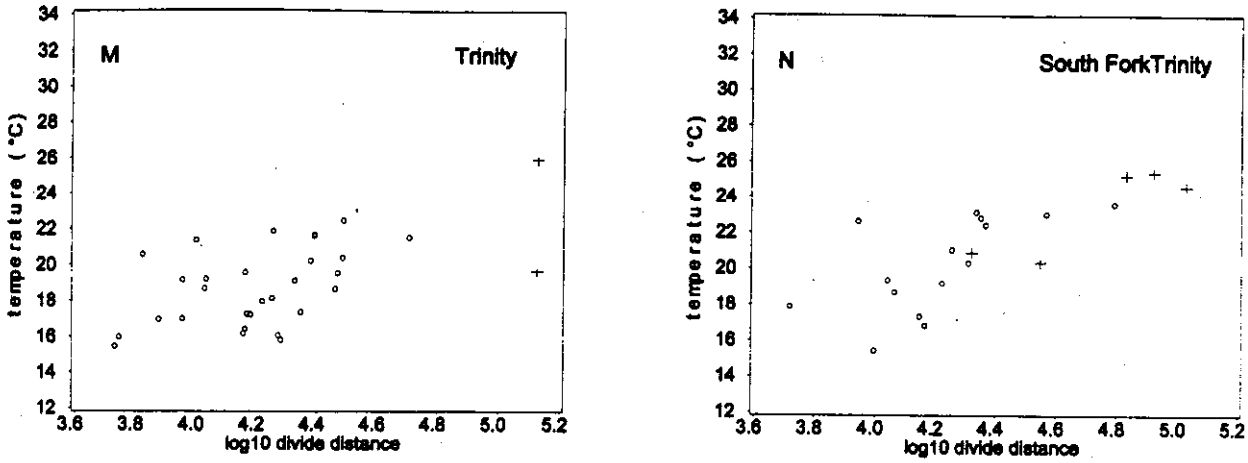

Figure D-5. (continued)

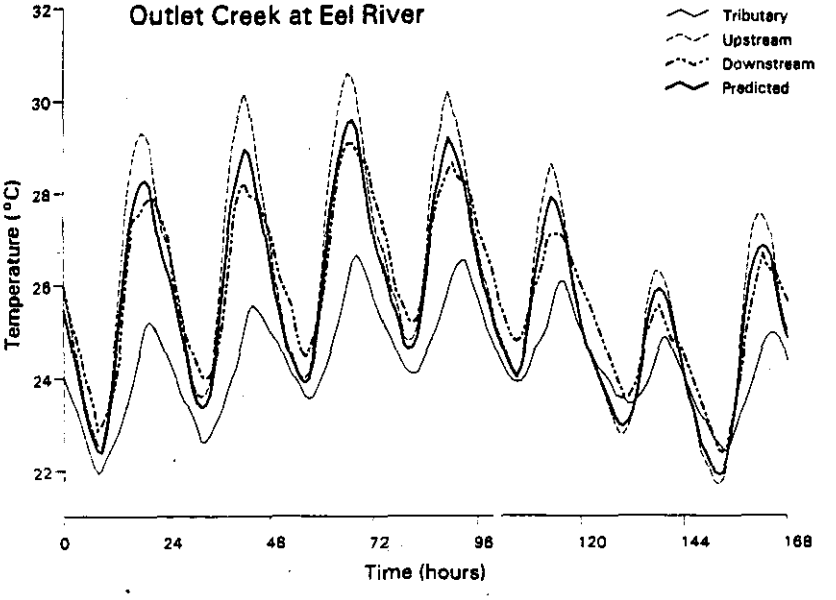

Figure D-.6. Diurnal trends in water temperature for Outlet Creek, upstream of the confluence on the Eel River, downstream of the confluence on the Eel River, and the predicted (Brown's equation) temperature downstream of the confluence. Temperatures were measured during the week of August 8, 1997.

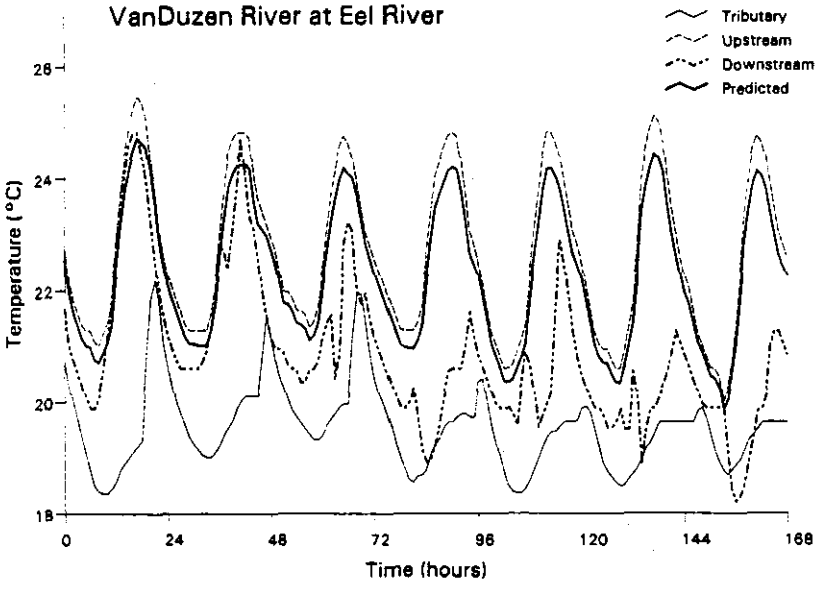

Figure D-7. Diurnal trends in water temperature for the Van Duzen River, upstream of the confluence on the Eel River, downstream of the confluence on the Eel River, and the predicted (Brown's equation) temperature downstream of the confluence. Temperatures were measured during the week of August 8, 1997.

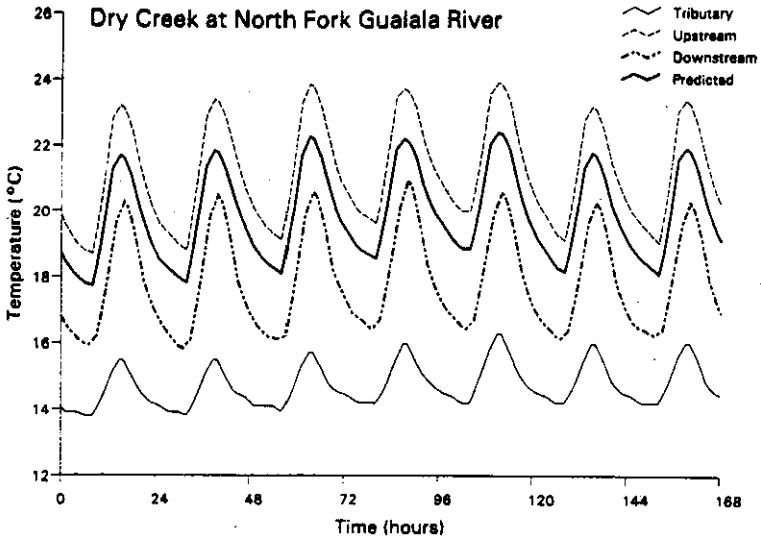

Figure D-8. Diurnal trends in water temperature for Dry Creek, upstream of the confluence on the North Fork Gualala River, downstream of the confluence on the North Fork Gualala River, and the predicted (Brown's equation) temperature downstream of the confluence. Temperatures were measured during the week of July 8, 1997.

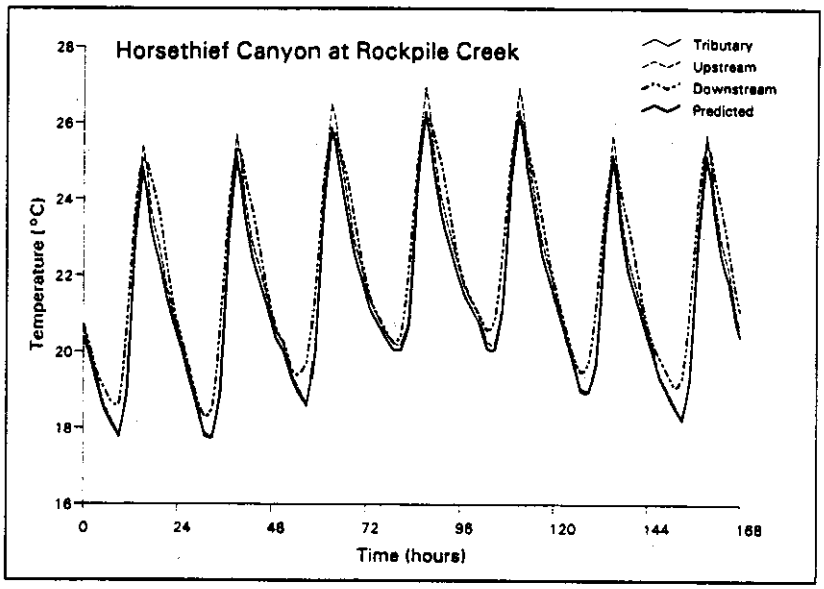

Figure D-9. Diurnal trends in water temperature for Horsethief Canyon, upstream of the confluence on Rockpile Creek, downstream of the confluence on Rockpile Creek, and the predicted (Brown's equation) temperature downstream of the confluence. Temperatures were measured during the week of July 8, 1997.

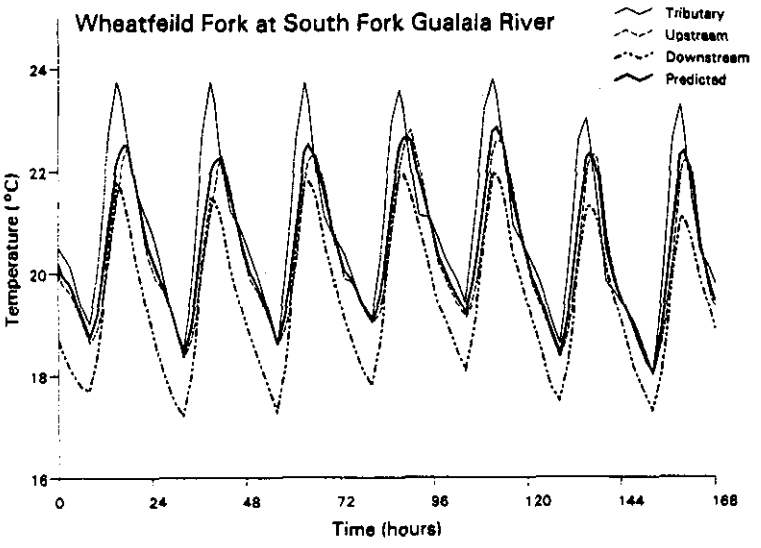

Figure D-10. Diurnal trends in water temperature for Wheatfield Fork, upstream of the confluence on South Fork Gualala River, downstream of the confluence on the South Fork Gualala River, and the predicted (Brown's equation) temperature downstream of the confluence. Temperatures were measured during the week of July 8, 1997.

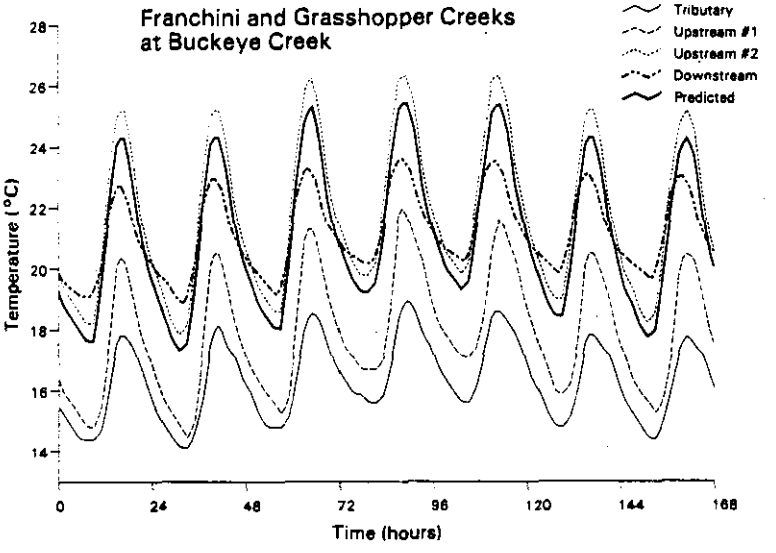

Figure D-11. Diurnal trends in water temperature for Grasshopper Creek (tributary #1), Franchini Creek (tributary #2), upstream of the confluence on Buckeye Creek, downstream of the confluence on Buckeye Creek, and the predicted (Brown's equation) temperature downstream of the confluence. Temperatures were measured during the week of August 8, 1997.

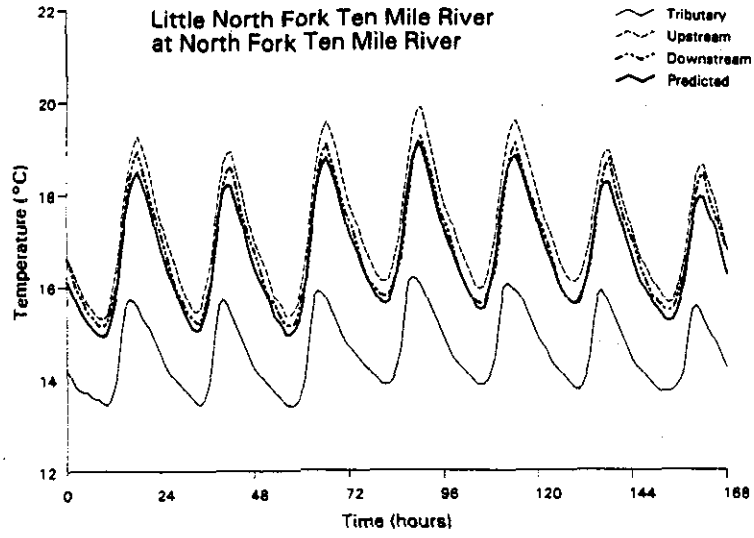

Figure D-12. Diurnal trends in water temperature for Little North Fork Ten Mile River, upstream of the confluence on the North Fork Ten Mile River, downstream of the confluence on the North Fork Ten Mile River, and the predicted (Brown's equation) temperature downstream of the confluence. Temperatures were measured during the week of August 4, 1998.

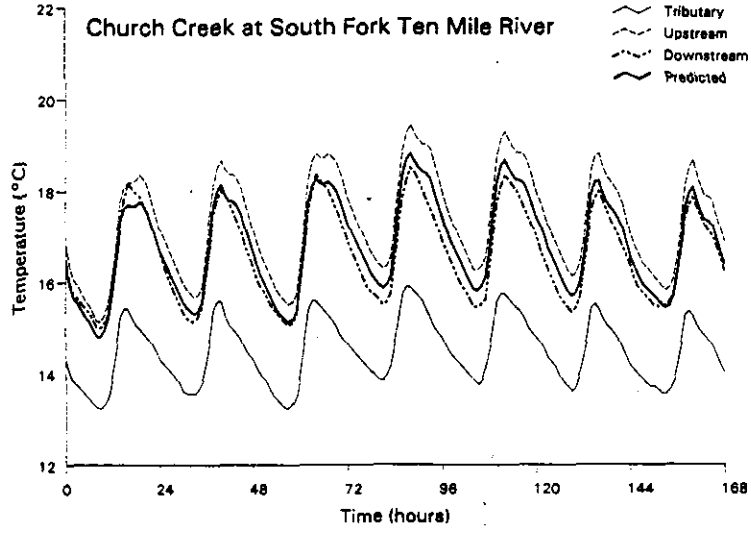

Figure D-13. Diurnal trends in water temperature for Church Creek, upstream of the confluence on the South Fork Ten Mile River, downstream of the confluence on the SF Ten Mile River, and the predicted (Brown's equation) temperature downstream of the confluence. Temperatures were measured during the week of August 4, 1997.

APPENDIX E

Influence of Site-Specific Attributes on Stream Temperatures

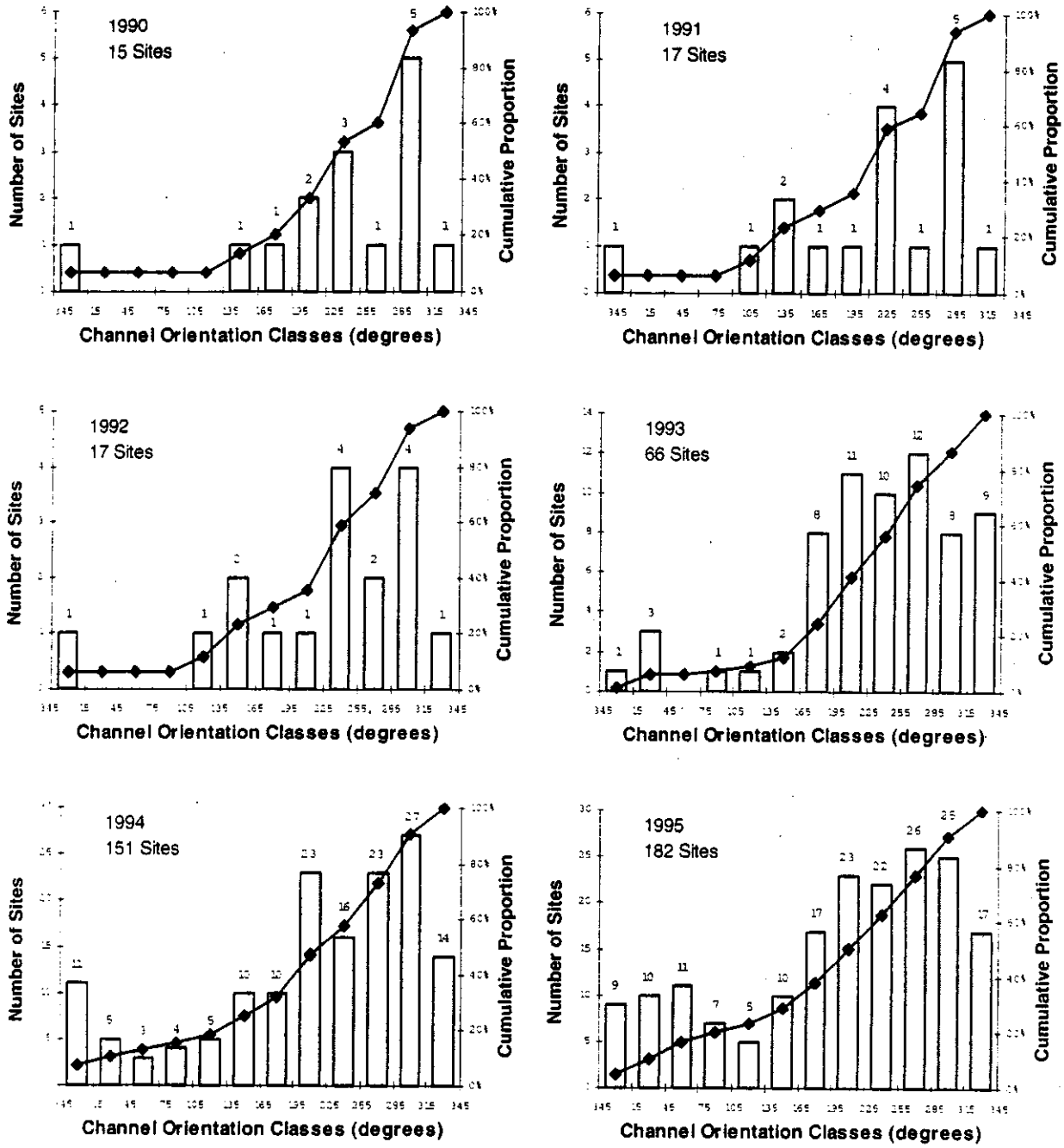

Figure E-1. Distribution of stream temperature monitoring sites by channel orientation classes. Orientation was derived in GIS at a point ~600 meters upstream from the stream temperature monitoring site.

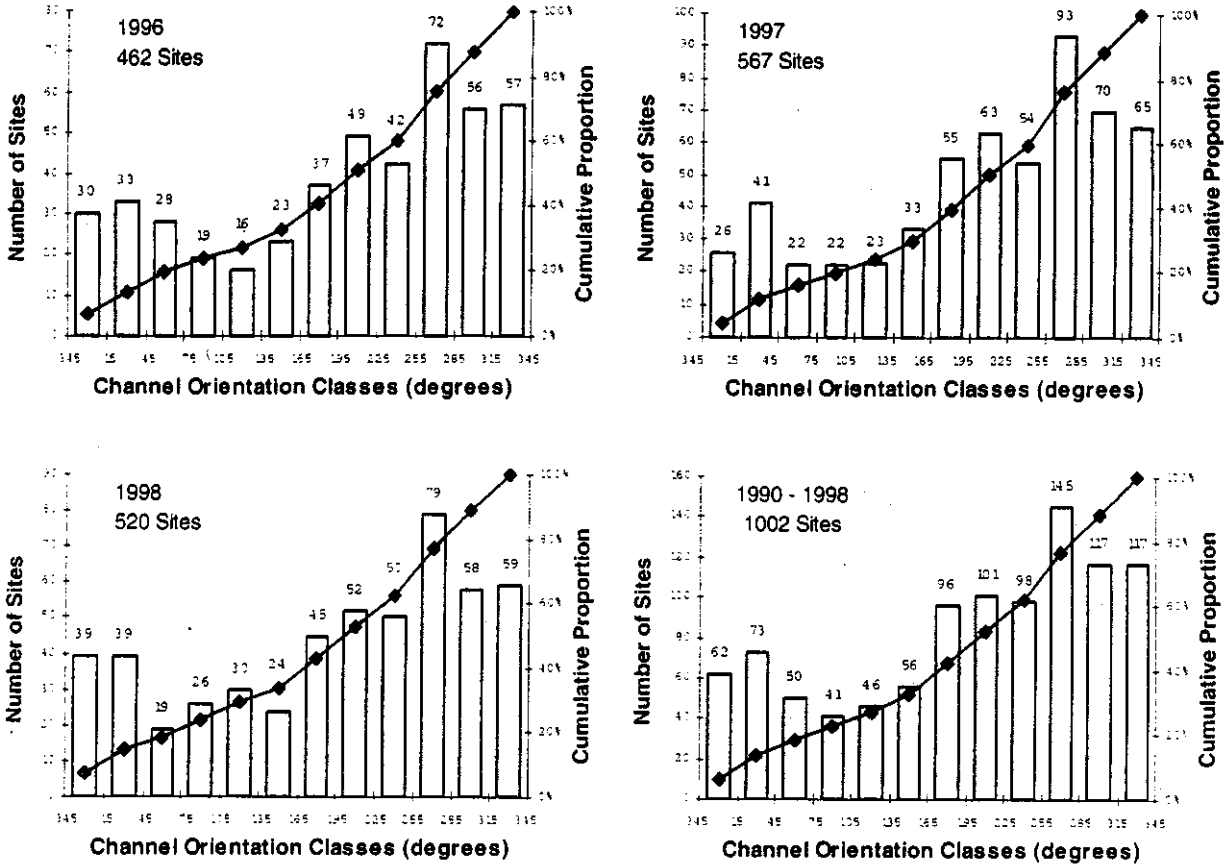

Figure E-1. (continued)

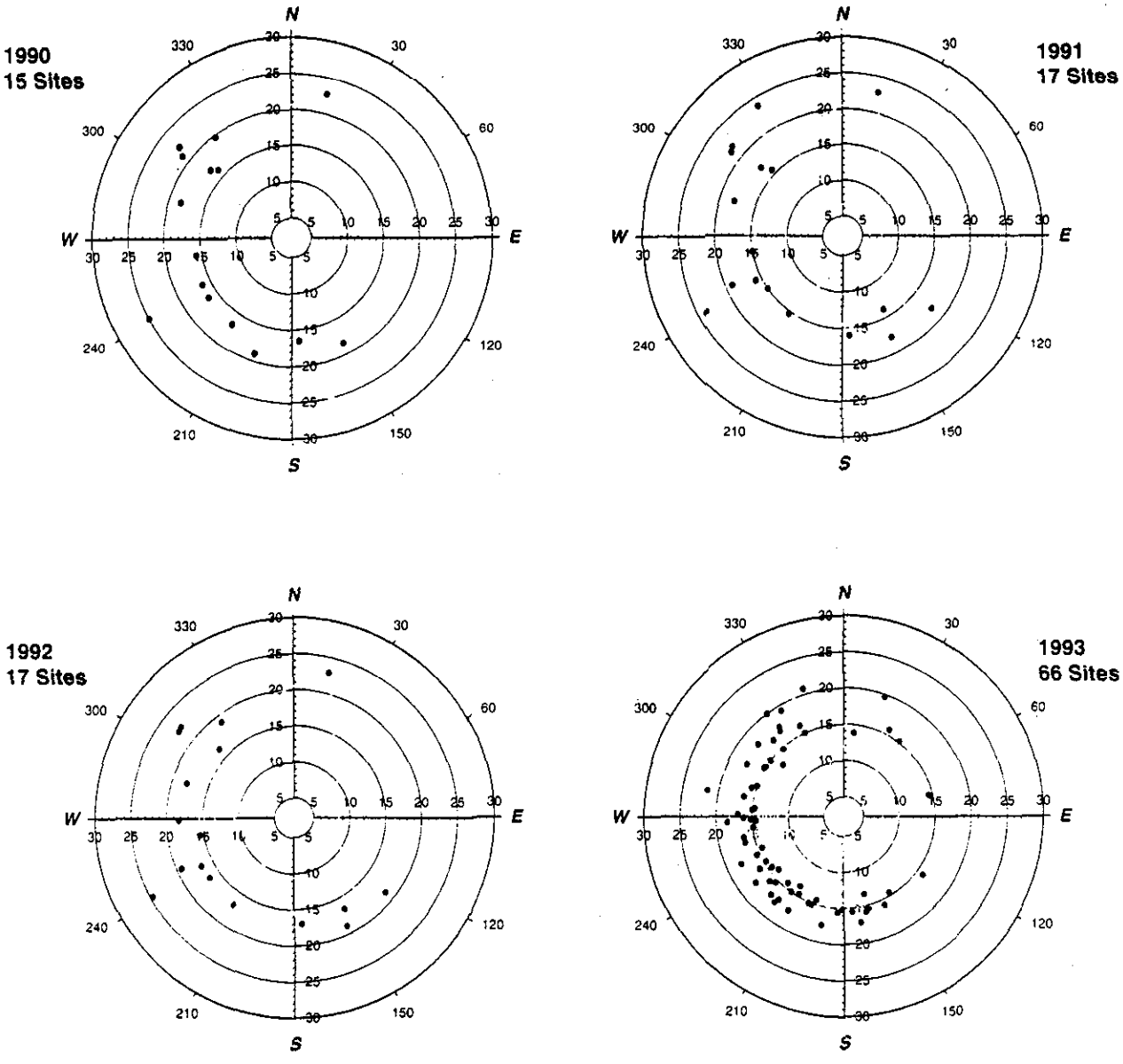

Figure E-2. Highest 7-day moving average of the daily mean (°C) with respect to channel orientation (degrees) for years 1990 - 1998. Orientation was derived in GIS over the reach ~600 meters upstream from the stream temperature monitoring location. Orientation was determined in a downstream direction along the 600-m reach.

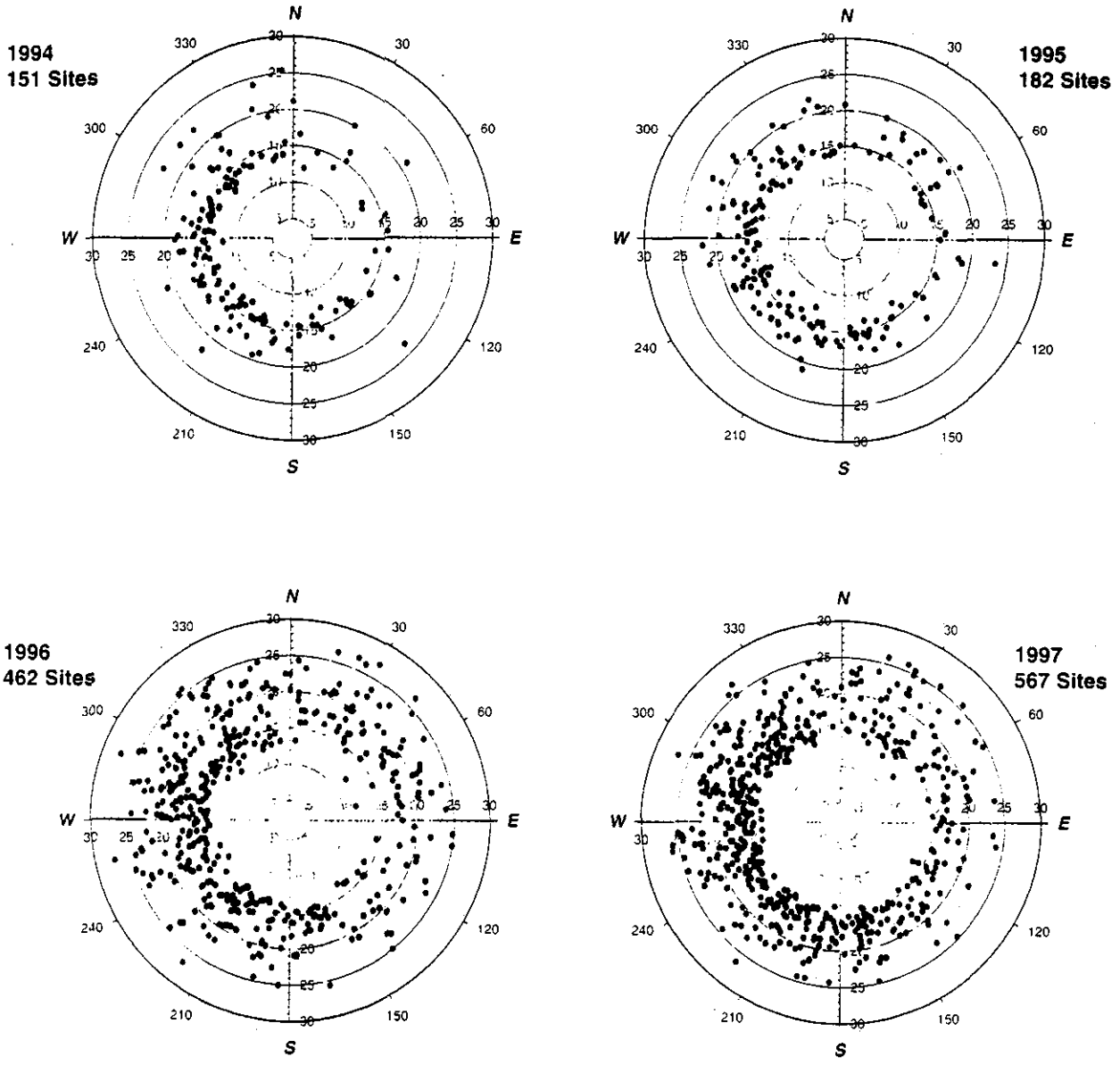

Figure E-2. (continued)

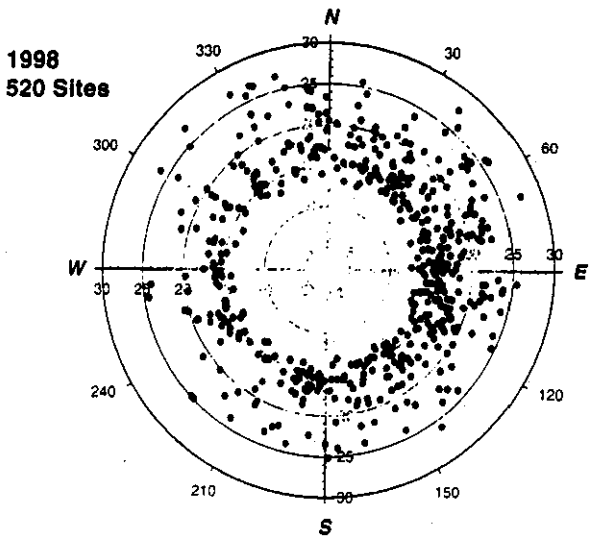

Figure E-2. (continued)